2nd February 2018– San Francisco

Analysis and Design of Diffractive and Micro-optical Systems with VirtualLab Fusion Software

Huiying Zhong and Prof. Frank Wyrowski

Applied Computational Optics Group in Friedrich Schiller University Jena

LightTrans International UG

Jena, Germany

Jena, Germany

Three Teams …

- **Applied Computational Optics Group** at Friedrich Schiller University of Jena
  - R&D in optical modeling and design with emphasis on **fast physical optics**
- **Wyrowski Photonics**
  - Development of fast physical optics software VirtualLab Fusion
- **LightTrans International UG**
  - Distribution of VirtualLab, together with distributors worldwide
  - Optical engineering, technical support, seminars, and trainings

LightTrans - Products

- **VirtualLab Fusion** – software for optical modeling and design.
- **Optical design** and engineering, consulting.
- **Training** and support for VirtualLab including software and design courses.
- **Prototyping** of optical components, especially micro-optics.

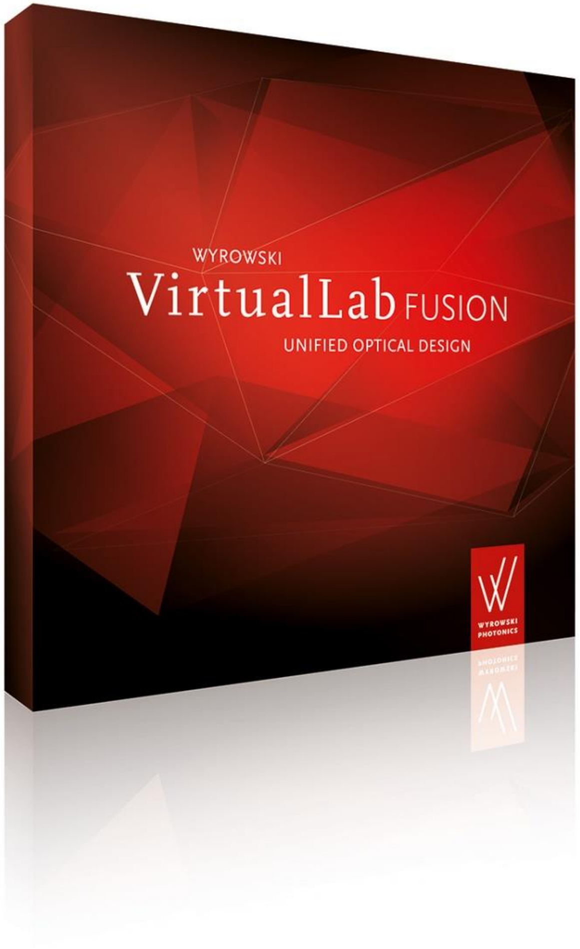

LightTrans – A Short Overview

- Founded in 1999
- About 20 employees
- Distributors world-wide

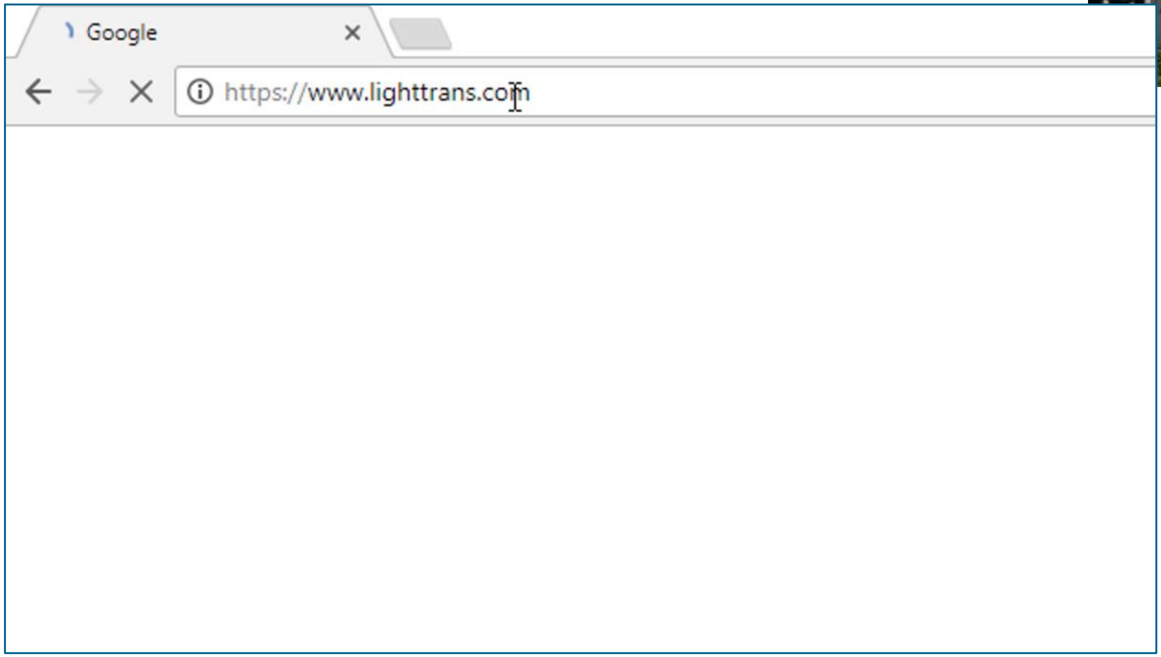

Aim of this Seminar

- Overview of ray&field tracing techniques in VirtualLab Fusion, both implemented and forthcoming
- Overview of application examples, ability of model and design
- Note that this is not a hand-on training. If you are interested in more details of one specific topics, please contact LightTrans/distributor for training/courses

Trail Version and Getting Started

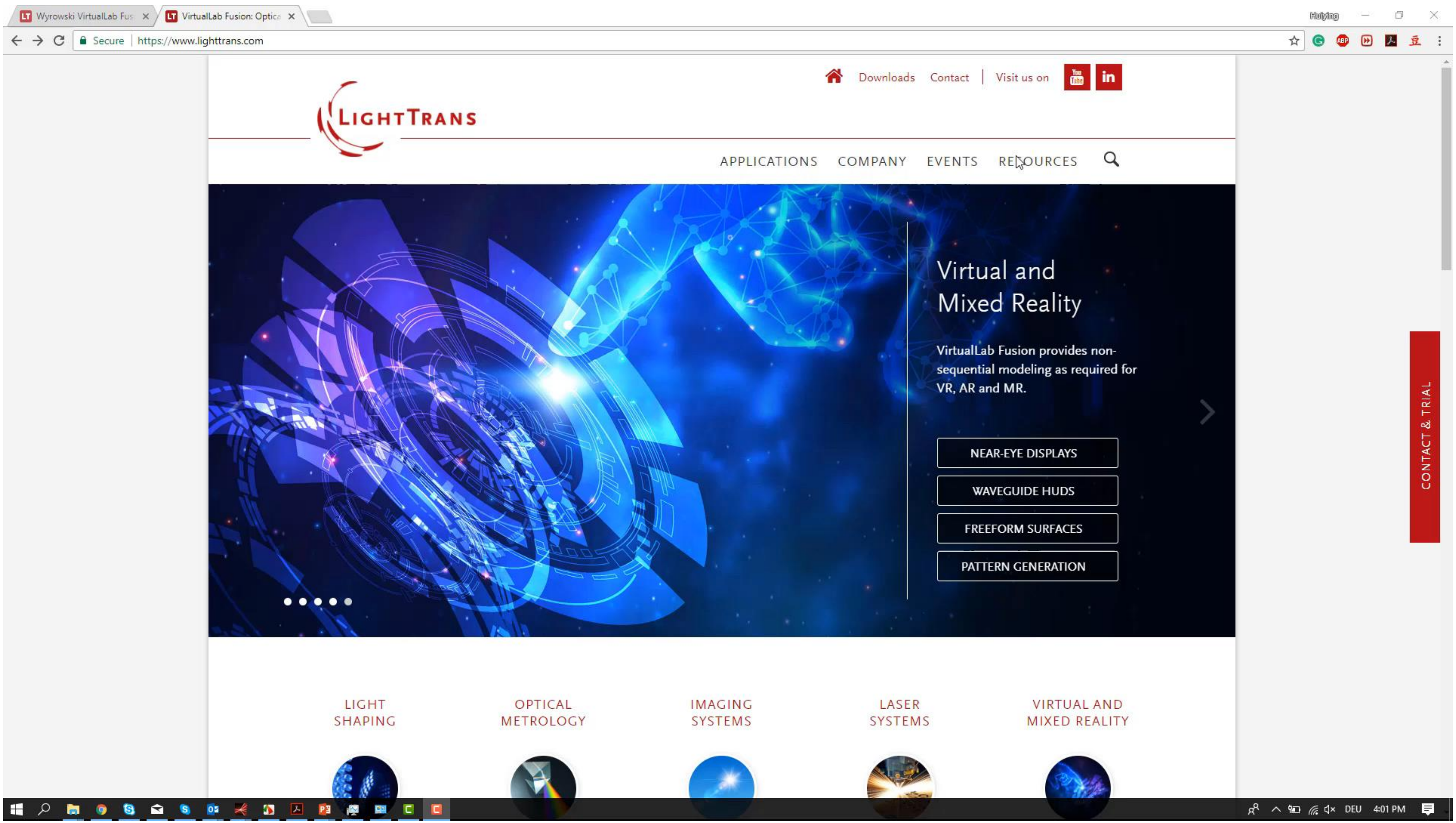

Program

Detailed Schedule

09:30 – 10:45 Sequential and non-sequential modeling. In VirtualLab Fusion light is represented by vectorial fields (physical optics) and rays (ray optics). Fields and rays are propagated from the source through the components and to the detectors in a sequential or non-sequential way. Physical optics propagation to components and detectors encompasses fast implementations of diffraction integrals like Debye, Richards-Wolf, Rayleigh-Huygens, Fresnel and Fraunhofer and generalizations of them with a fully automatized selection by VirtualLab Fusion.

10:45 – 11:00 Coffee break

11:00 – 12:30 Propagation techniques. For a vectorial physical-optics propagation through lenses, freeform surfaces, lens arrays, crystals, gratings, etalons, waveplates, microstructures, gratings, scattering surfaces, GRIN media, and diffractive optical elements VirtualLab provides a bundle of techniques like local boundary operators (LPIA), coating matrix, Fourier Modal Method (FMM), perfectly matched layer, split-step-type solvers, Mie scattering, Thin Element Approximation (TEA), and GRIN media propagation.

12:30 – 13:30 Lunch (included in the free seminar)

Program

13:30 – 14:00 Source and detector modeling. The modeling of sources like cw and pulsed laser sources, laser diodes, VCSEL's, and LED's in VirtualLab Fusion is presented. The unsurpassed flexibility of the definition of detector functions is demonstrated at examples like radiometry and photometry detectors, wavefront analysis, Stokes vector, polarization, and pulse duration.

14:00 – 14:30 Imaging and laser systems. Importing lens systems into VirtualLab Fusion enables sequential and non-sequential ray and physical optics analysis and optimization, including a sophisticated investigation of the PSF and MTF and of the appearance of ghost images by internal reflections. The inclusion of gratings, diffractive lenses and HOEs is shown together with its analysis by FMM.

14:30 – 14:45 Coffee break

14:45 – 15:30 Light shaping. The design of DOEs by established algorithms is demonstrated for the design of a diffractive beam splitter and a diffuser for light shaping. The specific challenges for the design of non-paraxial beam splitters for pattern generation of mobile devices are addressed. Laser beam shaping by diffractive and refractive elements is presented. The use of SLMs alongside VirtualLab is shown.

15:30 – 16:15 Waveguides for HUD and NED displays. The usage of waveguide plates in combination with gratings seems to be a very promising candidate in mixed reality devices. The design and analysis of such waveguide layouts requires the electromagnetic analysis of surface and volume gratings together with a

Overview of VirtualLab Fusion

Simulation?

Simulation Technology

Simulation* is the imitation of the operation of a real-world process or system …

* Reference: Wikipedia

From Real Lab to VirtualLab

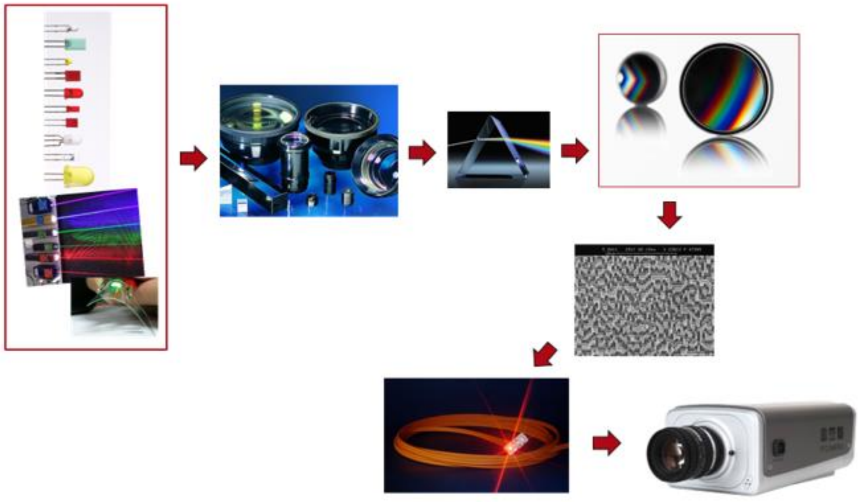

Pictures from http://de.wikipedia.org/

From
real lab
to
virtual lab
(VirtualLab)

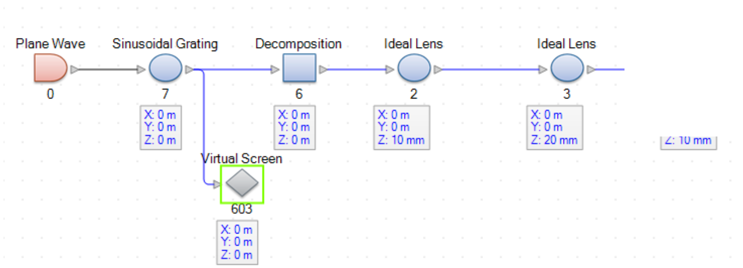

Video of build up an LPD

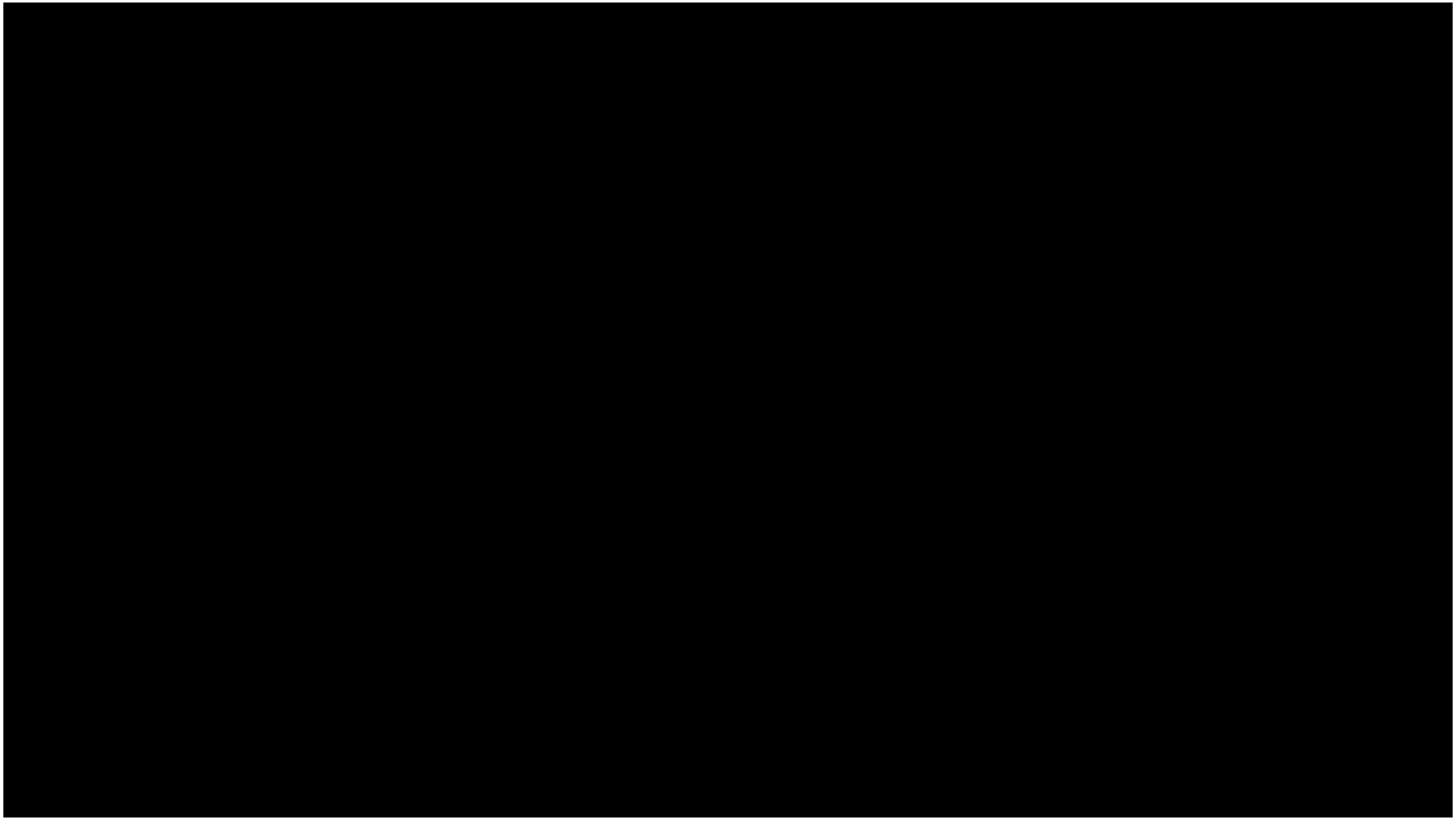

Simulation Technology – Digital Twins

Simulation* is the imitation of the operation of a real-world process or system …

→ Evaluation

Inverse process

→ Design

Photonics technology demands for the development!

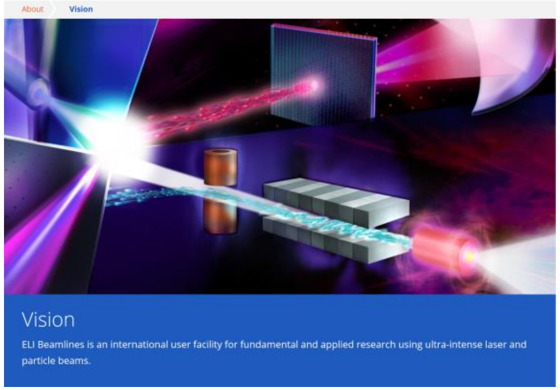

Modern computer technology enables significant progress in optical simulation technology!

* Reference: Wikipedia

VLF is a software for simulation and design

- Optical simulation technology is indispensable for R&D and innovative products in optics and photonics.

Simulation* is the imitation of the operation of a real-world process or system … The act of simulating something first **requires that a model be developed**; …

Optical Modeling Task?

Optical Modeling Task: Sources

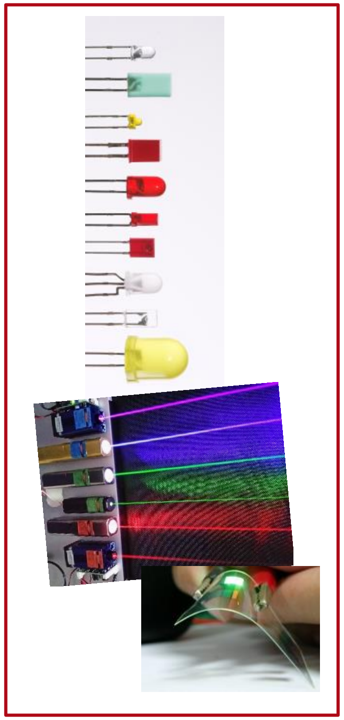

- Coherent, partially coherent (spatial modes or multi-wavelength)
- Stationary or pulse (spatiotemporal distribution)
- Physical quantities, e.g., polarization, beam size.
- …

Pictures from http://de.wikipedia.org/

Optical Modeling Task: Components

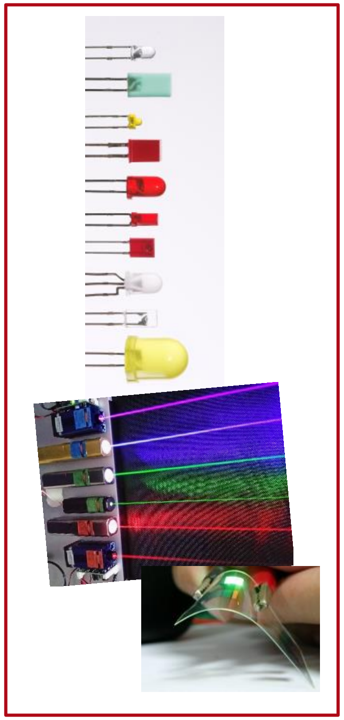

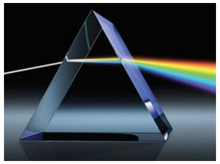

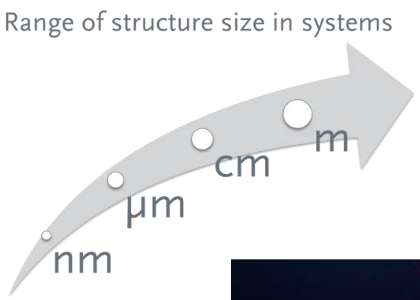

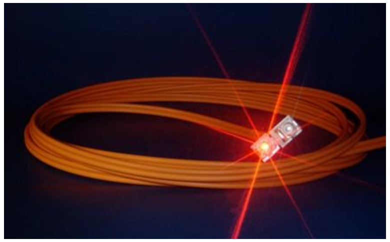

- Three dimentional shape and size
- Feature size
- Applications

Pictures from http://de.wikipedia.org/

Optical Modeling Task: Detector

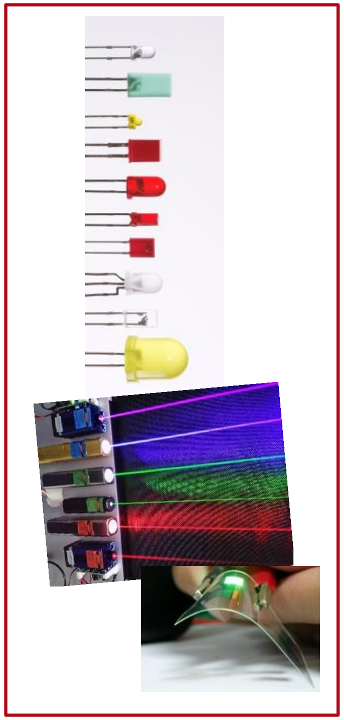

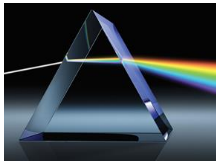

- Physical quantities, e.g., radiometric and photometric quantities, polarization, wavefront, pulse duration
- Merit functions

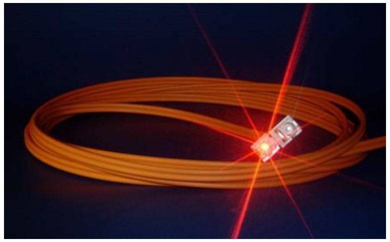

Optical Modeling Task: Light Propagation

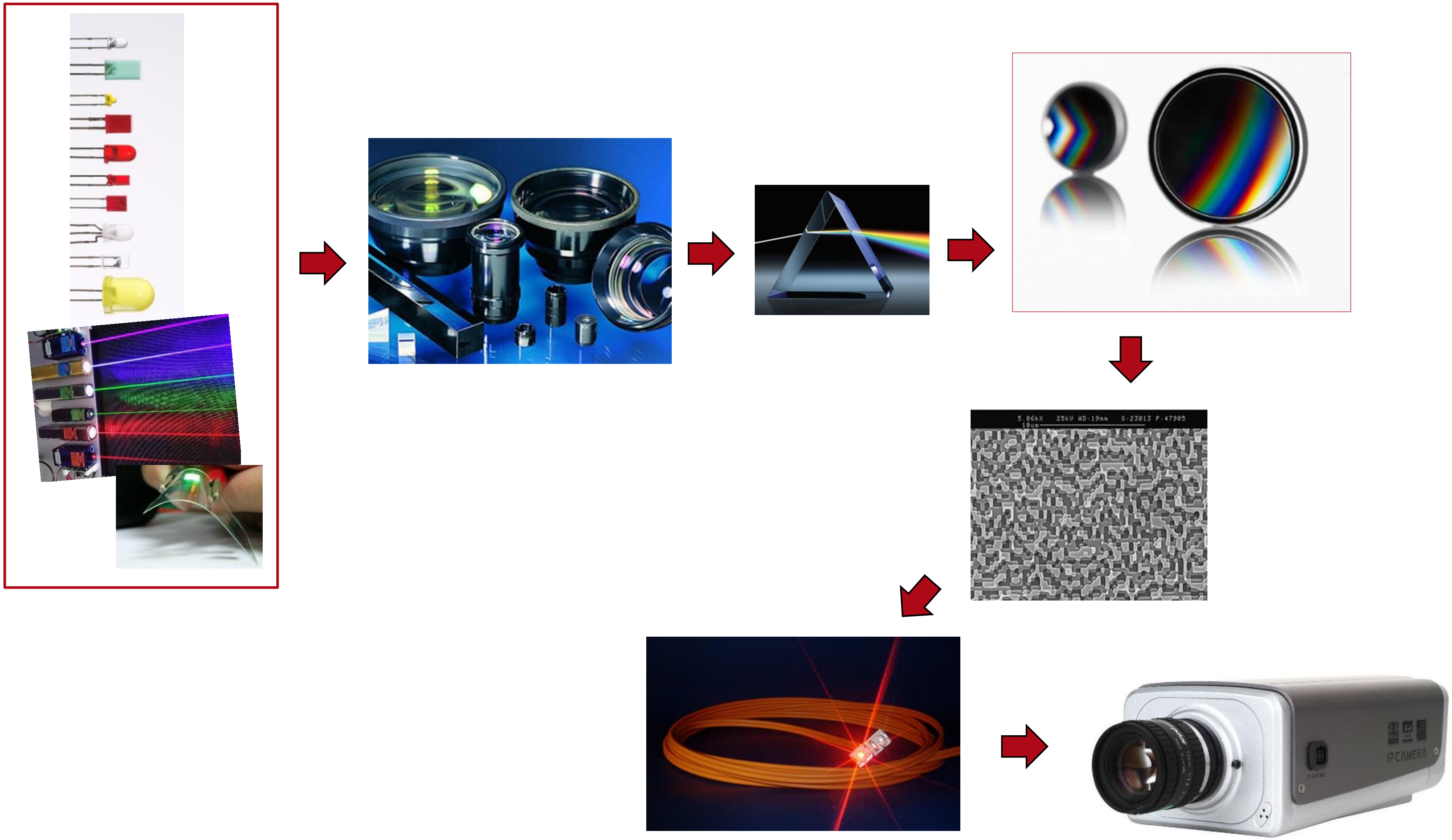

Optical Modeling Task

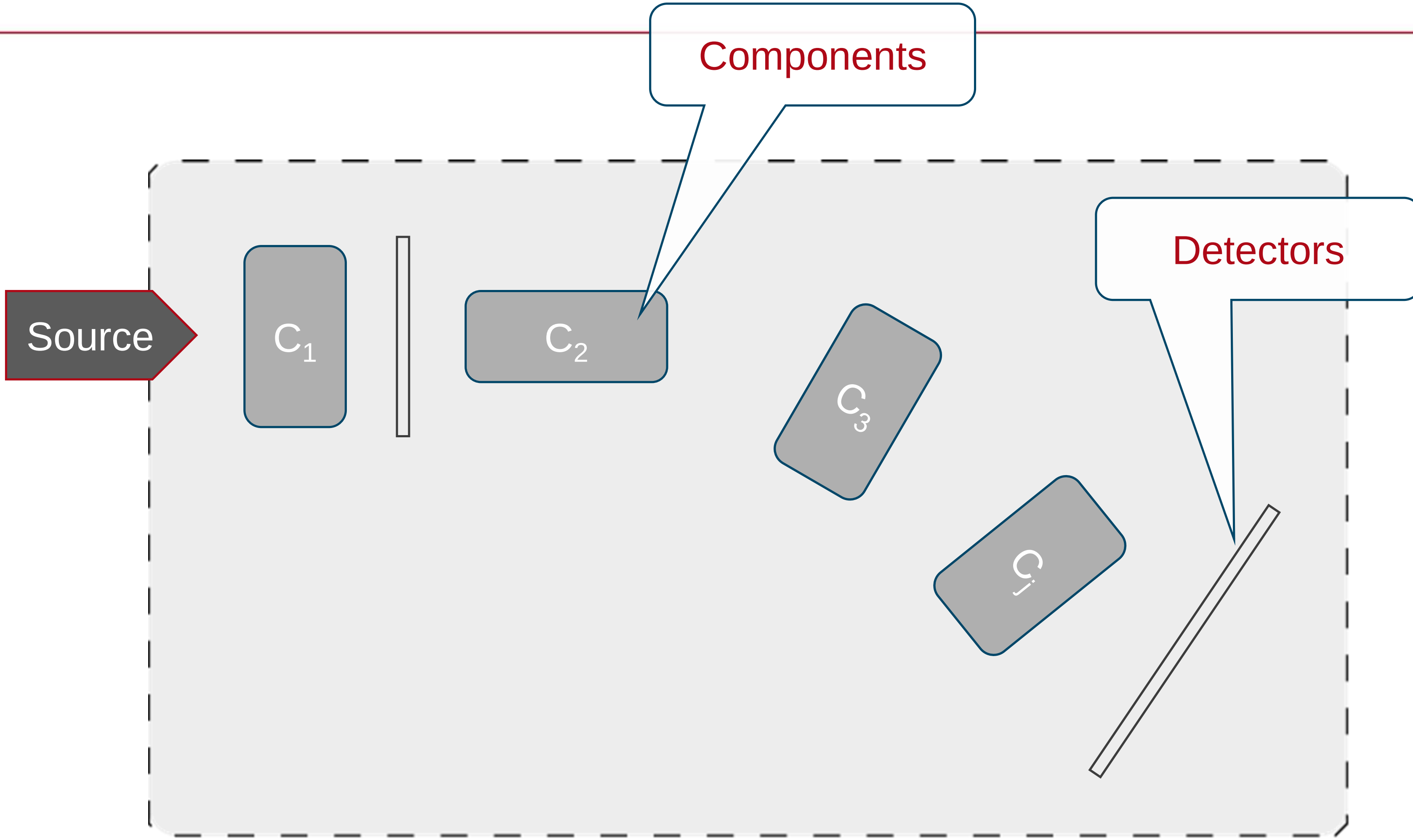

Optical Modeling: Sequential

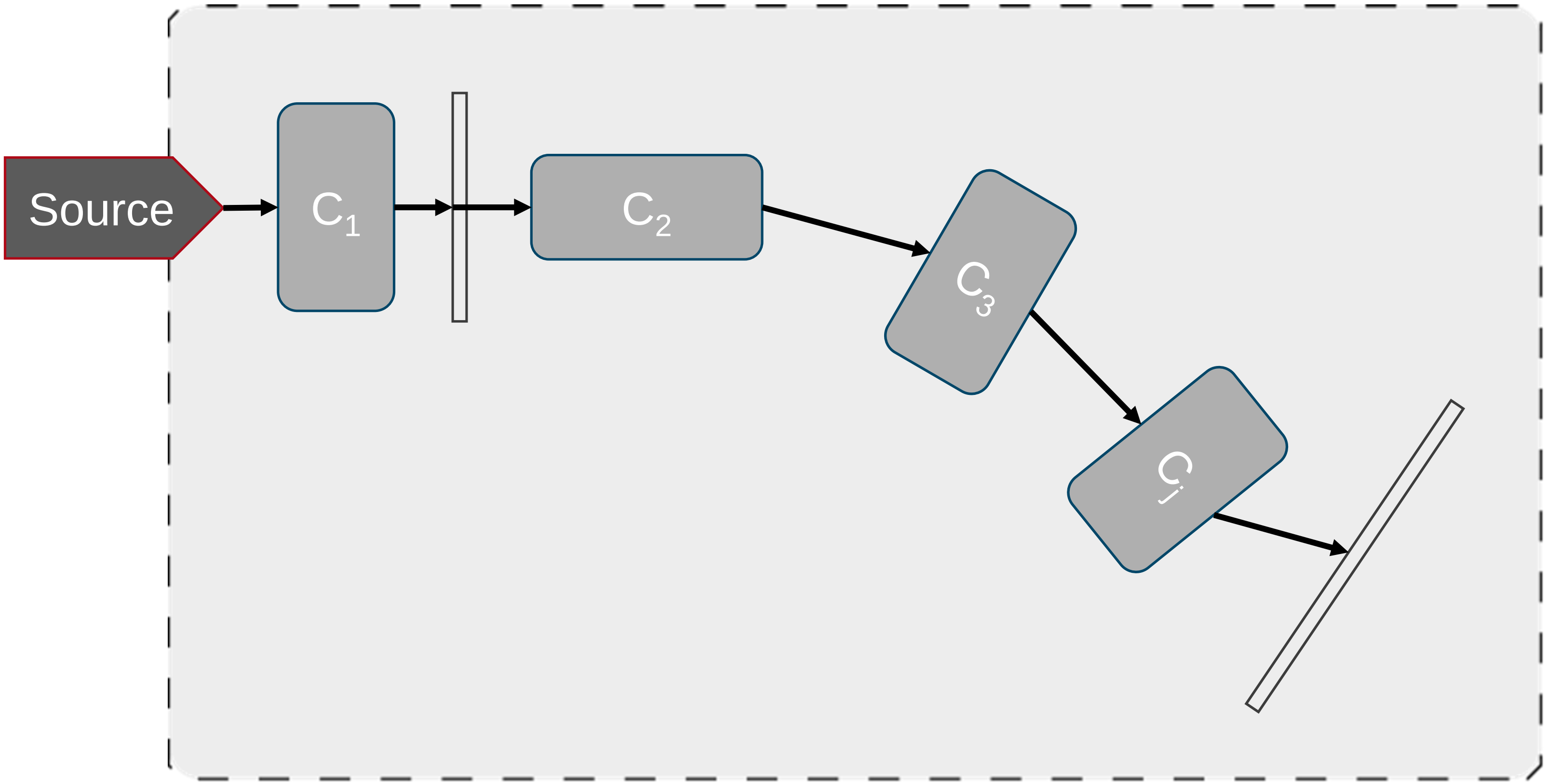

Task/System Illustration

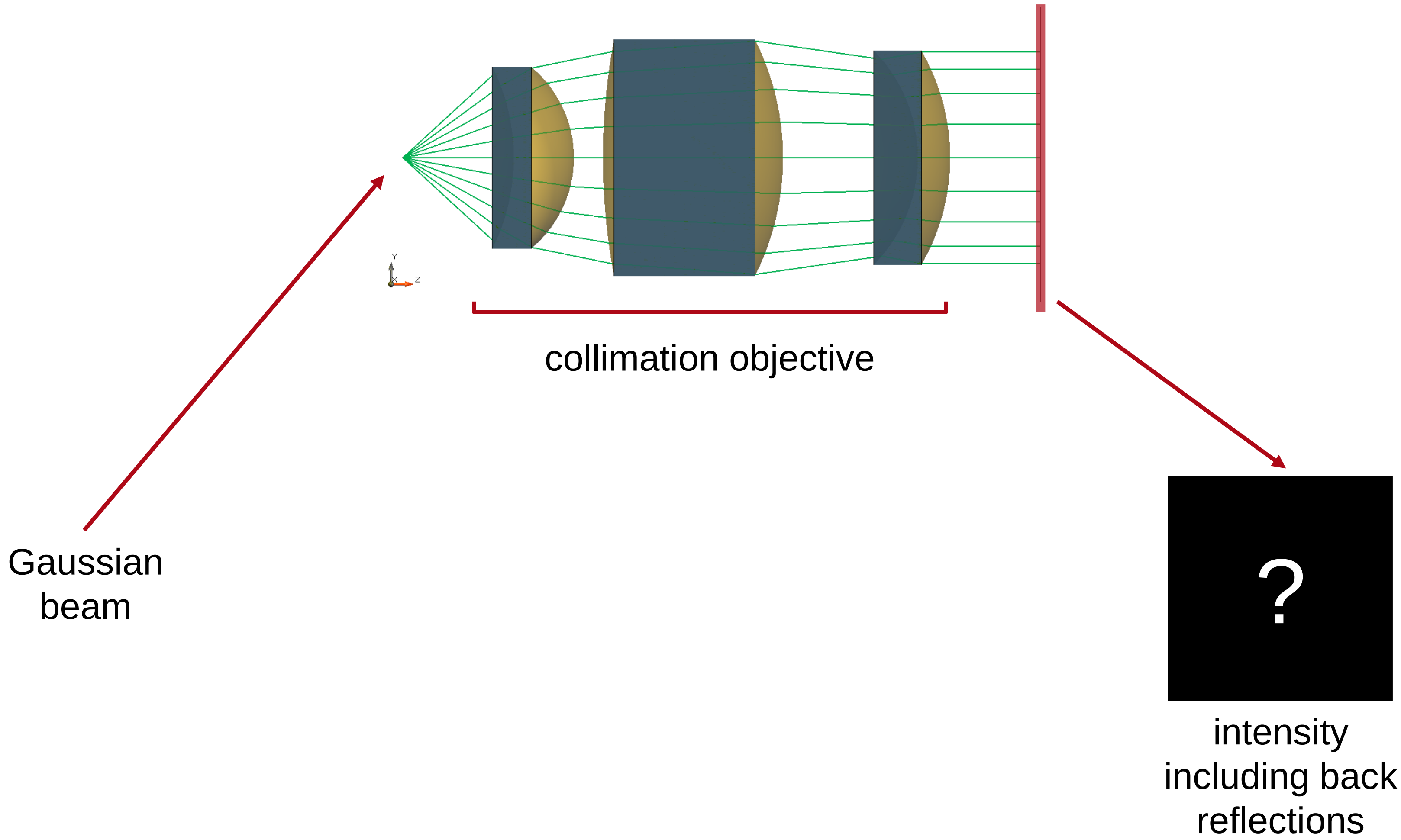

Result: Field Tracing Sequential

sequential overview (without ghost imaging)

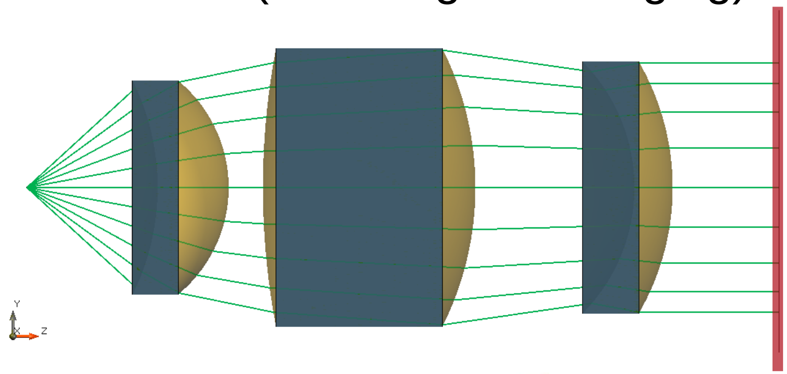

Interface	+/+	+/-	-/-	-/+
	☑	☐	☐	☐
Interface #1 (Conical Interface)	☑	☐	☐	☐
Interface #2 (Conical Interface)	☑	☐	☐	☐
Interface #3 (Conical Interface)	☑	☐	☐	☐
Interface #4 (Conical Interface)	☑	☐	☐	☐
Interface #5 (Conical Interface)	☑	☐	☐	☐
Interface #6 (Conical Interface)	☑	☐	☐	☐

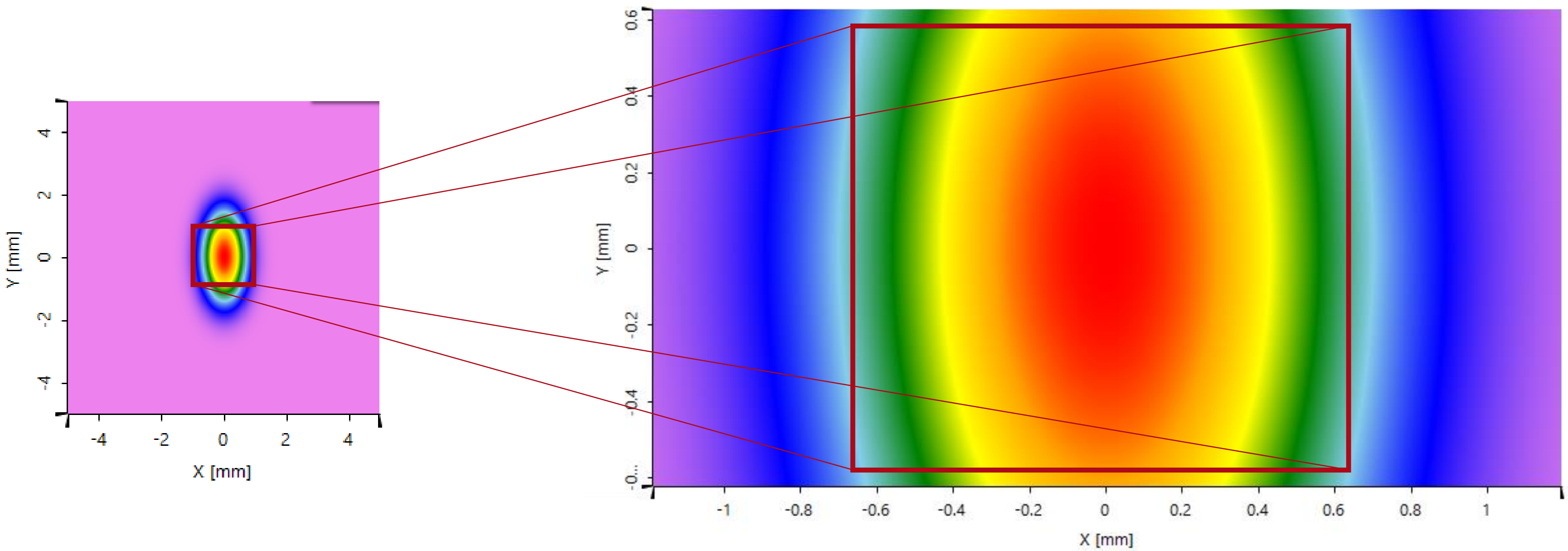

Optical Modeling: Non-sequential

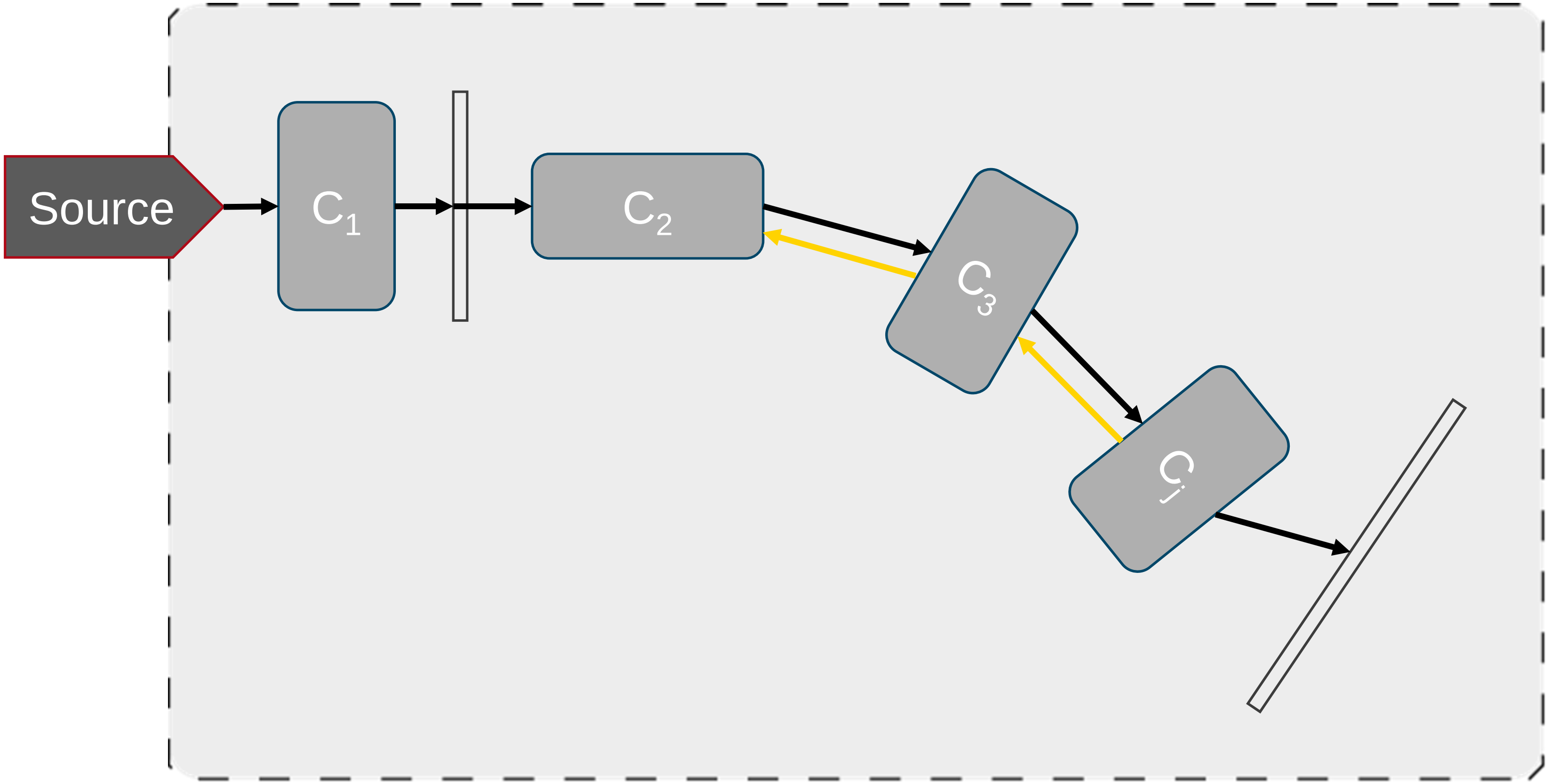

Result: Field Tracing Sequential

sequential overview (without ghost imaging)

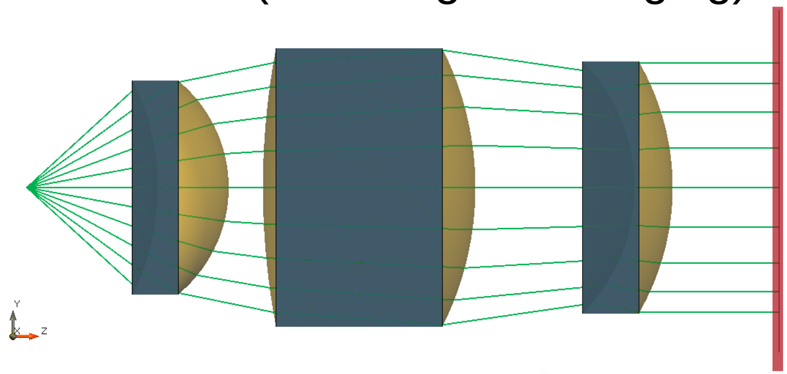

Interface	+/+	+/-	-/-	-/+
	☑	☐	☐	☐
Interface #1 (Conical Interface)	☑	☐	☐	☐
Interface #2 (Conical Interface)	☑	☐	☐	☐
Interface #3 (Conical Interface)	☑	☐	☐	☐
Interface #4 (Conical Interface)	☑	☐	☐	☐
Interface #5 (Conical Interface)	☑	☐	☐	☐
Interface #6 (Conical Interface)	☑	☐	☐	☐

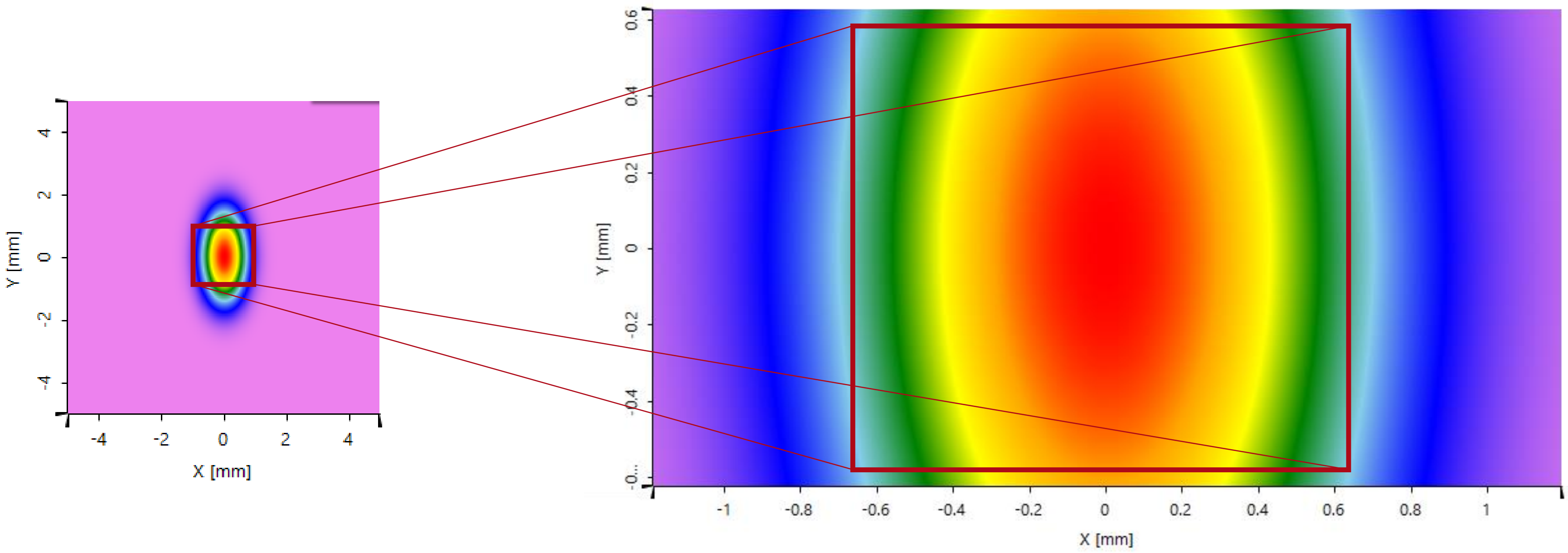

Result: Field Tracing Full Non-sequential

allowing reflection at all surfaces at all lenses (full non-sequential)

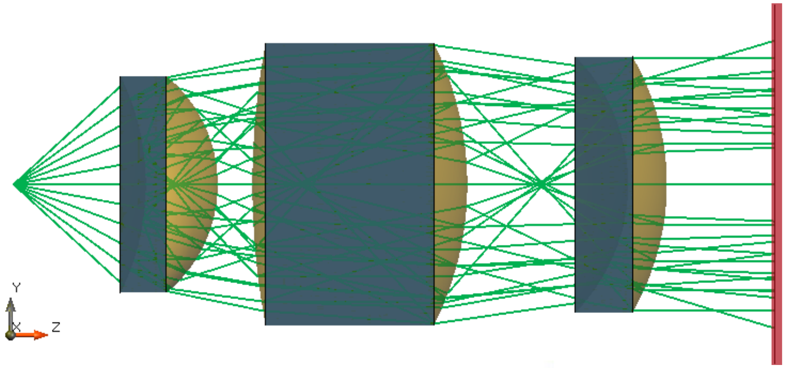

Interface	+/+	+/-	-/-	-/+
	☑	☑	☑	☑
Interface #1 (Conical Interface)	☑	☑	☑	☑
Interface #2 (Conical Interface)	☑	☑	☑	☑
Interface #3 (Conical Interface)	☑	☑	☑	☑
Interface #4 (Conical Interface)	☑	☑	☑	☑
Interface #5 (Conical Interface)	☑	☑	☑	☑
Interface #6 (Conical Interface)	☑	☑	☑	☑

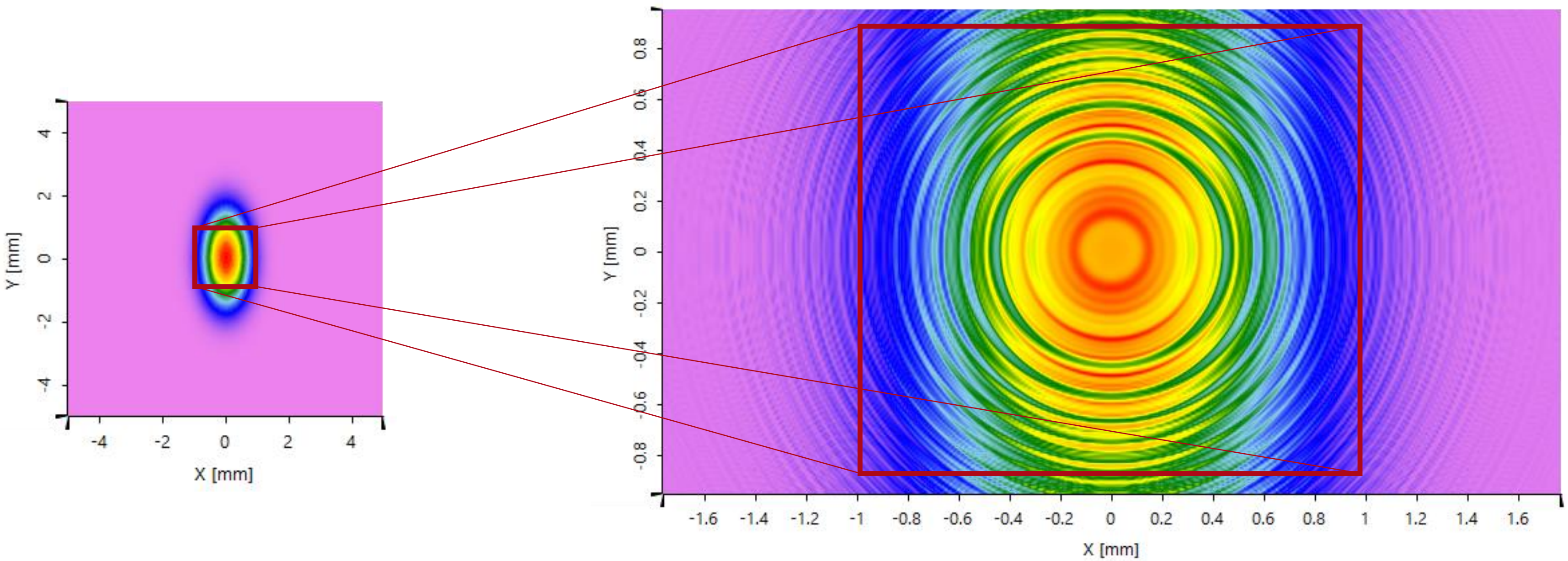

Ray Optics or Physical Optics?

Ray and Physical Optics

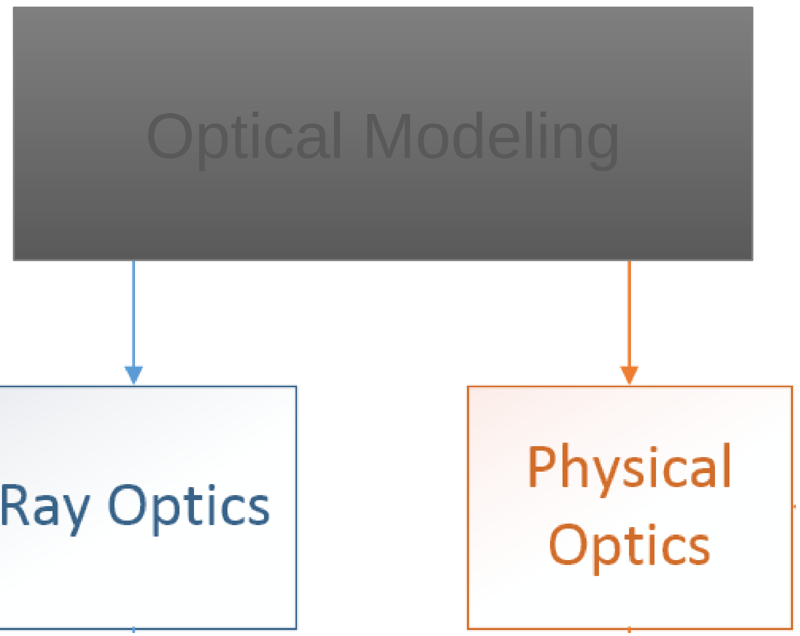

Pierre de Fermat
(1601 - 1665)

James Clerk Maxwell
(1831-1879)

Ray Optics and Physical Optics

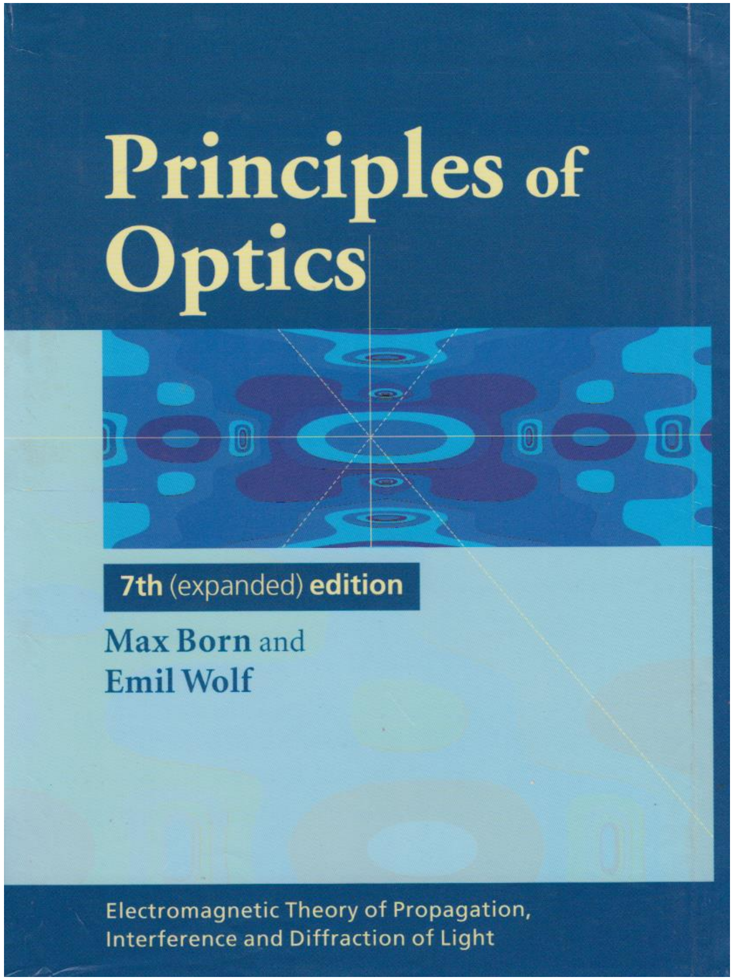

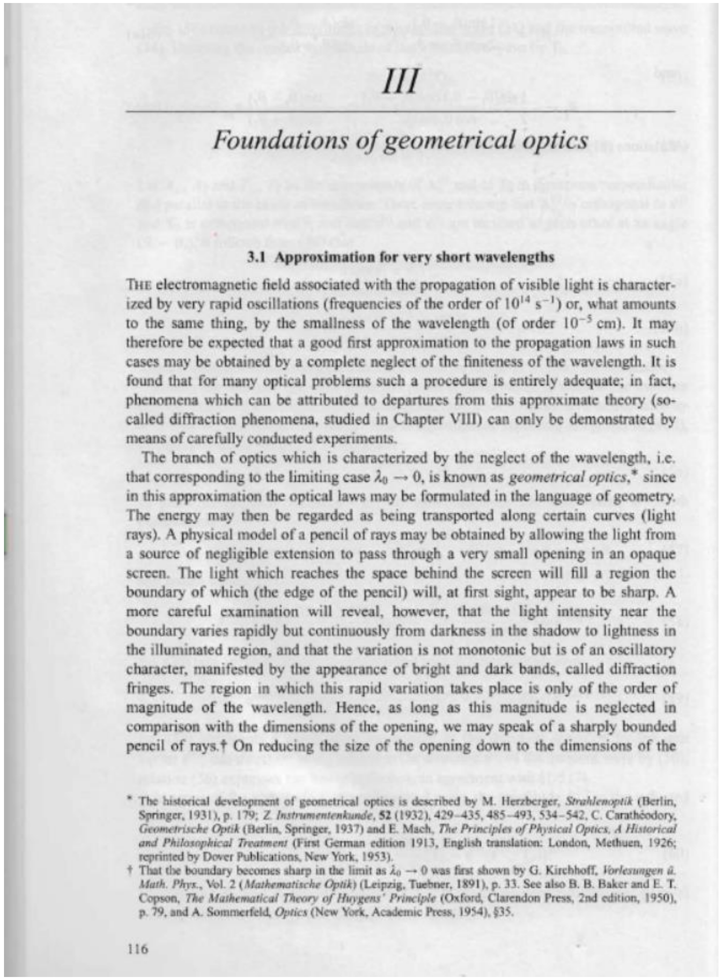

III

Foundations of geometrical optics

3.1 Approximation for very short wavelengths

THE electromagnetic field associated with the propagation of visible light is characterized by very rapid oscillations (frequencies of the order of 10^{14} s^{-1}) or, what amounts to the same thing, by the smallness of the wavelength (of order 10^{-5} cm). It may therefore be expected that a good first approximation to the propagation laws in such cases may be obtained by a complete neglect of the finiteness of the wavelength. It is found that for many optical problems such a procedure is entirely adequate; in fact, phenomena which can be attributed to departures from this approximate theory (so-called diffraction phenomena, studied in Chapter VIII) can only be demonstrated by means of carefully conducted experiments.

The branch of optics which is characterized by the neglect of the wavelength, i.e. that corresponding to the limiting case $\lambda_0 \rightarrow 0$, is known as *geometrical optics*,* since in this approximation the optical laws may be formulated in the language of geometry. The energy may then be regarded as being transported along certain curves (light rays). A physical model of a pencil of rays may be obtained by allowing the light from a source of negligible extension to pass through a very small opening in an opaque screen. The light which reaches the space behind the screen will fill a region the boundary of which (the edge of the pencil) will, at first sight, appear to be sharp. A more careful examination will reveal, however, that the light intensity near the boundary varies rapidly but continuously from darkness in the shadow to lightness in the illuminated region, and that the variation is not monotonic but is of an oscillatory character, manifested by the appearance of bright and dark bands, called diffraction fringes. The region in which this rapid variation takes place is only of the order of magnitude of the wavelength. Hence, as long as this magnitude is neglected in comparison with the dimensions of the opening, we may speak of a sharply bounded pencil of rays.† On reducing the size of the opening down to the dimensions of the

* The historical development of geometrical optics is described by M. Herzberger, *Strahlenoptik* (Berlin, Springer, 1931), p. 179; *Z. Instrumentenkunde*, **52** (1932), 429–435, 485–493, 534–542, C. Carathéodory, *Geometrische Optik* (Berlin, Springer, 1937) and E. Mach, *The Principles of Physical Optics, A Historical and Philosophical Treatment* (First German edition 1913, English translation: London, Methuen, 1926; reprinted by Dover Publications, New York, 1953).

† That the boundary becomes sharp in the limit as $\lambda_0 \rightarrow 0$ was first shown by G. Kirchhoff, *Vorlesungen ü. Math. Phys.*, Vol. 2 (*Mathematische Optik*) (Leipzig, Tuebner, 1891), p. 33. See also B. B. Baker and E. T. Copson, *The Mathematical Theory of Huygens' Principle* (Oxford, Clarendon Press, 2nd edition, 1950), p. 79, and A. Sommerfeld, *Optics* (New York, Academic Press, 1954), §35.

116

Ray Optics and Physical Optics

$$\nabla \times \boldsymbol{E}(\boldsymbol{r}) = \mathrm{i}\omega\mu_0 \boldsymbol{H}(\boldsymbol{r})$$
$$\nabla \times \boldsymbol{H}(\boldsymbol{r}) = -\mathrm{i}\omega\epsilon_0 \check{\epsilon}_\mathrm{r}(\omega) \boldsymbol{E}(\boldsymbol{r}),$$
$$\nabla \cdot \boldsymbol{E}(\boldsymbol{r}) = 0,$$
$$\nabla \cdot \boldsymbol{H}(\boldsymbol{r}) = 0.$$

$$\nabla\check{\psi}(\boldsymbol{r}) \times \tilde{\boldsymbol{E}}(\boldsymbol{r}) = \omega\mu_0 \tilde{\boldsymbol{H}}(\boldsymbol{r})$$
$$\nabla\check{\psi}(\boldsymbol{r}) \times \tilde{\boldsymbol{H}}(\boldsymbol{r}) = -\omega\epsilon_0 \check{\epsilon}_\mathrm{r}(\omega) \tilde{\boldsymbol{E}}(\boldsymbol{r})$$
$$\nabla\check{\psi}(\boldsymbol{r}) \cdot \tilde{\boldsymbol{E}}(\boldsymbol{r}) = 0$$
$$\nabla\check{\psi}(\boldsymbol{r}) \cdot \tilde{\boldsymbol{H}}(\boldsymbol{r}) = 0$$

$$(\nabla\psi(\boldsymbol{r}))^2 = k_0^2 n^2(\boldsymbol{r}).$$

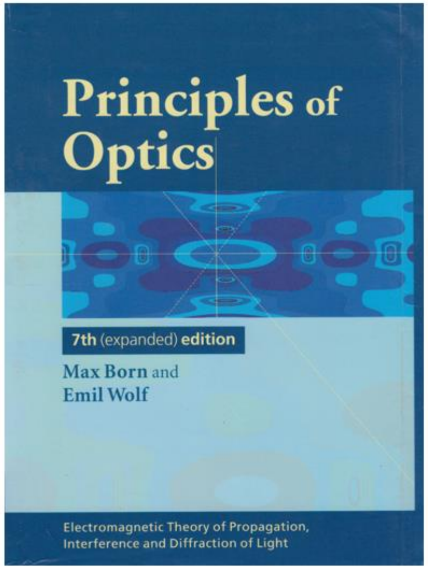

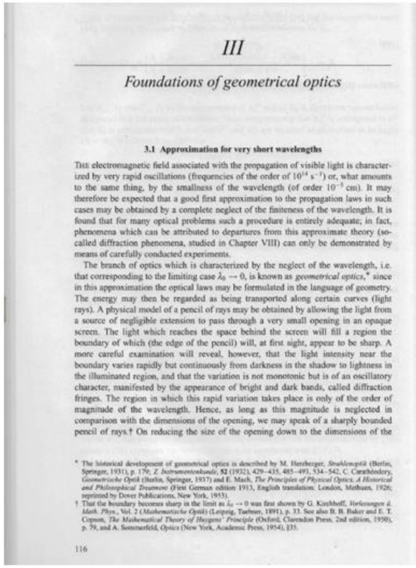

III

Foundations of geometrical optics

3.1 Approximation for very short wavelengths

The electromagnetic field associated with the propagation of visible light is characterized by very rapid oscillations (frequencies of the order of 10^{14} s^{-1}) or, what amounts to the same thing, by the smallness of the wavelength (of order 10^{-5} cm). It may therefore be expected that a good first approximation to the propagation laws in such cases may be obtained by a complete neglect of the finiteness of the wavelength. It is found that for many optical problems such a procedure is entirely adequate; in fact, phenomena which can be attributed to departures from this approximate theory (so-called diffraction phenomena, studied in Chapter VIII) can only be demonstrated by means of carefully conducted experiments.

The branch of optics which is characterized by the neglect of the wavelength, i.e. that corresponding to the limiting case $\lambda_0 \to 0$, is known as *geometrical optics*,* since in this approximation the optical laws may be formulated in the language of geometry. The energy may then be regarded as being transported along certain curves (light rays). A physical model of a pencil of rays may be obtained by allowing the light from a source of negligible extension to pass through a very small opening in an opaque screen. The light which reaches the space behind the screen will fill a region the boundary of which (the edge of the pencil) will, at first sight, appear to be sharp. A more careful examination will reveal, however, that the light intensity near the boundary varies rapidly but continuously from darkness in the shadow to lightness in the illuminated region, and that the variation is not monotonic but is of an oscillatory character, manifested by the appearance of bright and dark bands, called diffraction fringes. The region in which this rapid variation takes place is only of the order of magnitude of the wavelength. Hence, as long as this magnitude is neglected in comparison with the dimensions of the opening, we may speak of a sharply bounded pencil of rays.† On reducing the size of the opening down to the dimensions of the

* The historical development of geometrical optics is described by M. Herzberger, *Strahlenoptik* (Berlin, Springer, 1931), p. 179; *Z. Instrumentenkunde*, **52** (1932), 429–435, 485–493, 534–542. C. Carathéodory, *Geometrische Optik* (Berlin, Springer, 1937) and E. Mach, *The Principles of Physical Optics. A Historical and Philosophical Treatment* (First German edition 1913, English translation: London, Methuen, 1926; reprinted by Dover Publications, New York, 1953).

† That the boundary becomes sharp in the limit as $\lambda_0 \to 0$ was first shown by G. Kirchhoff, *Vorlesungen ü. Math. Phys.*, Vol. 2 (*Mathematische Optik*) (Leipzig, Teubner, 1891), p. 33. See also B. B. Baker and E. T. Copson, *The Mathematical Theory of Huygens' Principle* (Oxford, Clarendon Press, 2nd edition, 1950), p. 79, and A. Sommerfeld, *Optics* (New York, Academic Press, 1954), §35.

116

Physical Concept for Modeling: Ray Optics

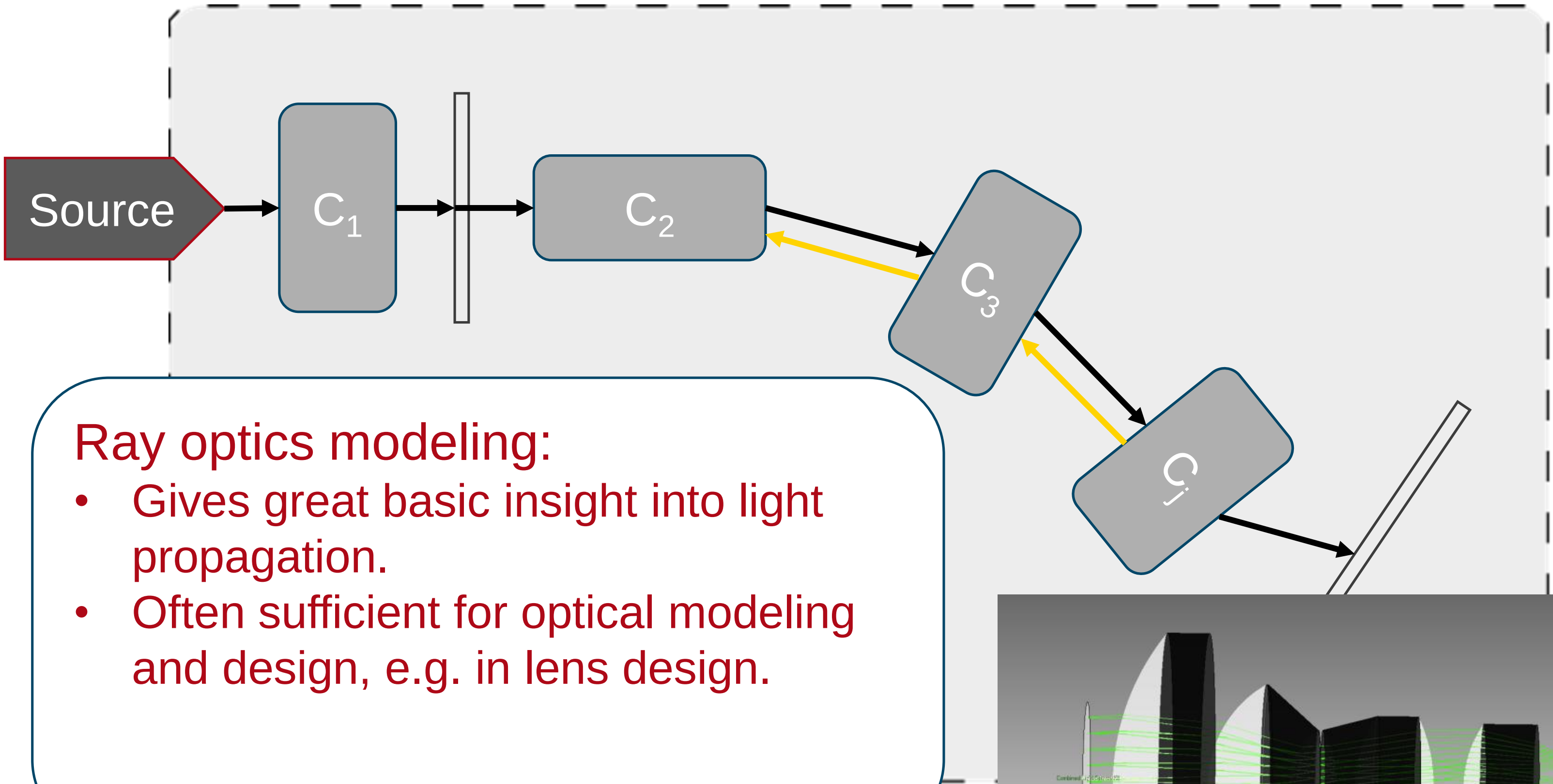

Ray optics modeling:

- Gives great basic insight into light propagation.
- Often sufficient for optical modeling and design, e.g. in lens design.

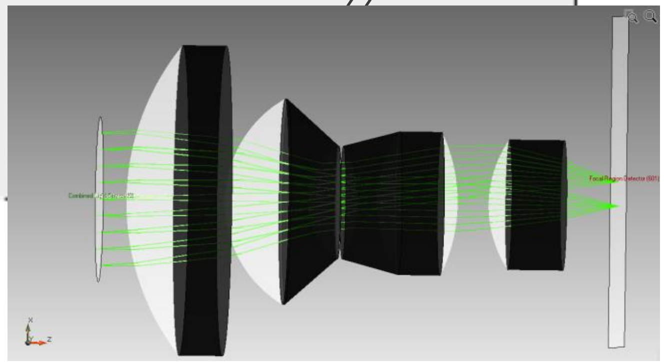

Ray Optics and Aberration Theory

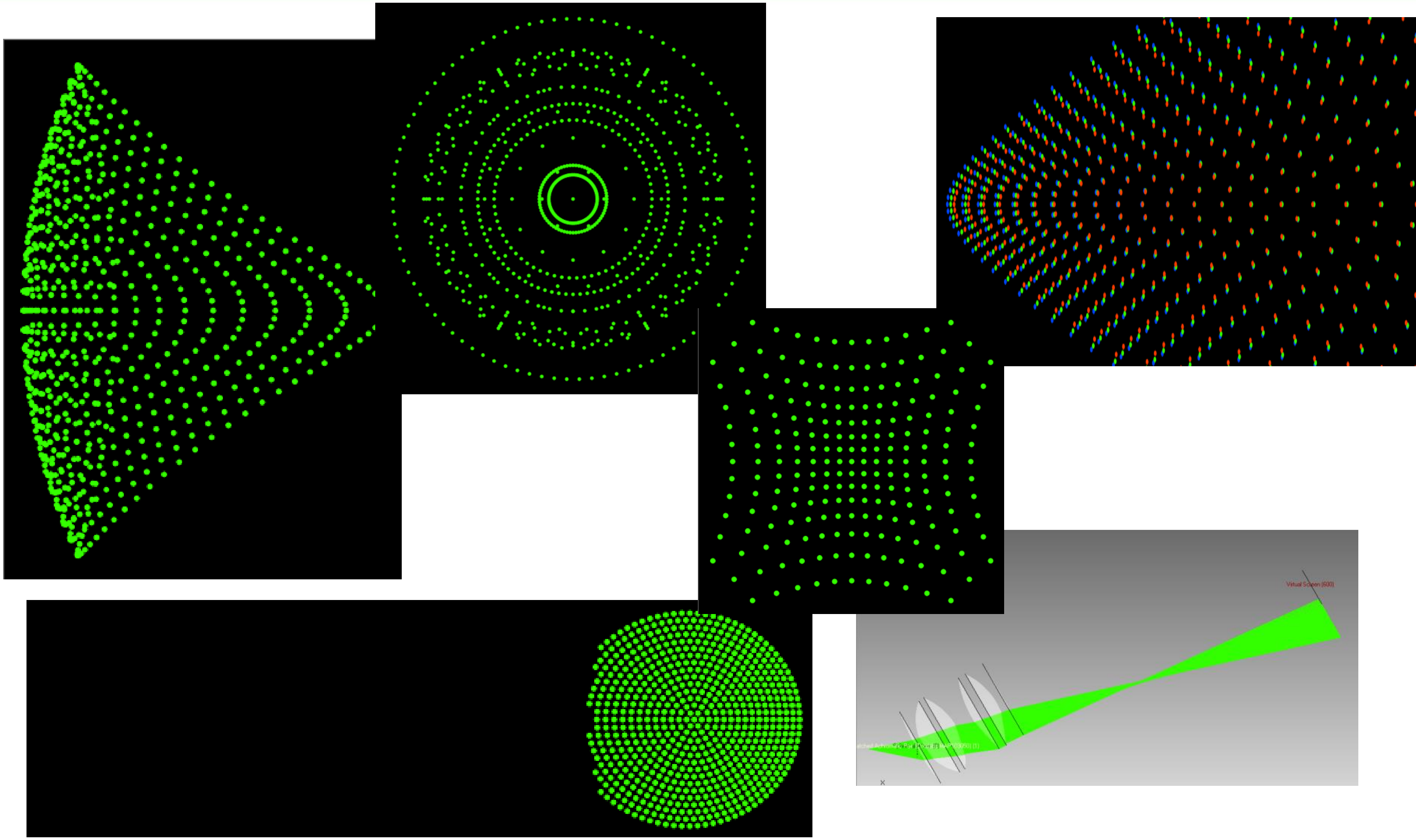

Ray and Physical Optics

Ray Optics

Physical Optics

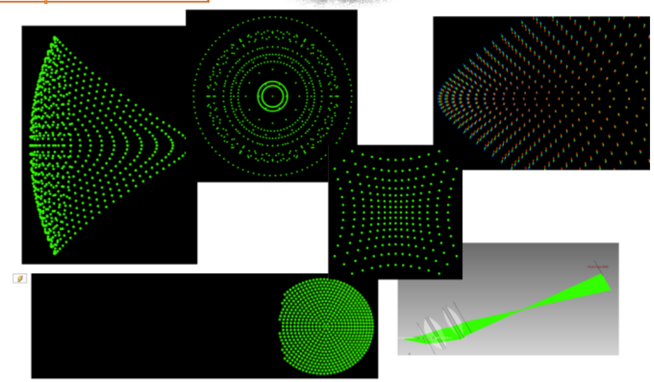

Ray optics modeling:

- Gives great basic insight into light propagation.
- Often sufficient for optical design, e.g. in standard lens design.

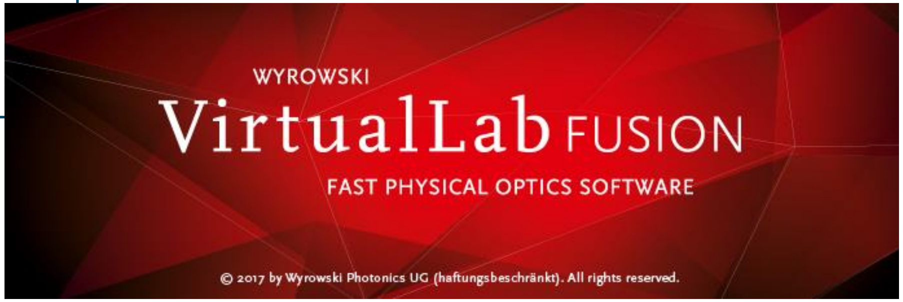

Ray Tracing in VirtualLab Fusion

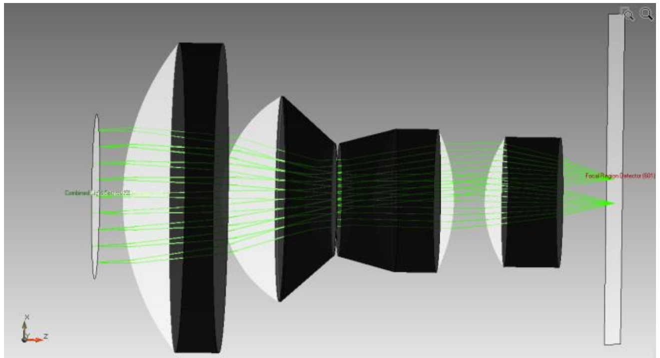

- Ray Tracing System Analyzer
- Detector
  - Spot size
  - Wavefront error (Zernike polynomials)
  - Focal length analyzer
  - …

Ray Tracing Engine Comparison: VLF vs. Code V vs. Zemax

Zongzhao Wang, Tingcheng Zhang and Irfan Badar
Date: 2017, Dec, 31th
Applied Computational Optics Group, Jena
China Aerospace Science and Technology (CAST) Corporation

System Illustration

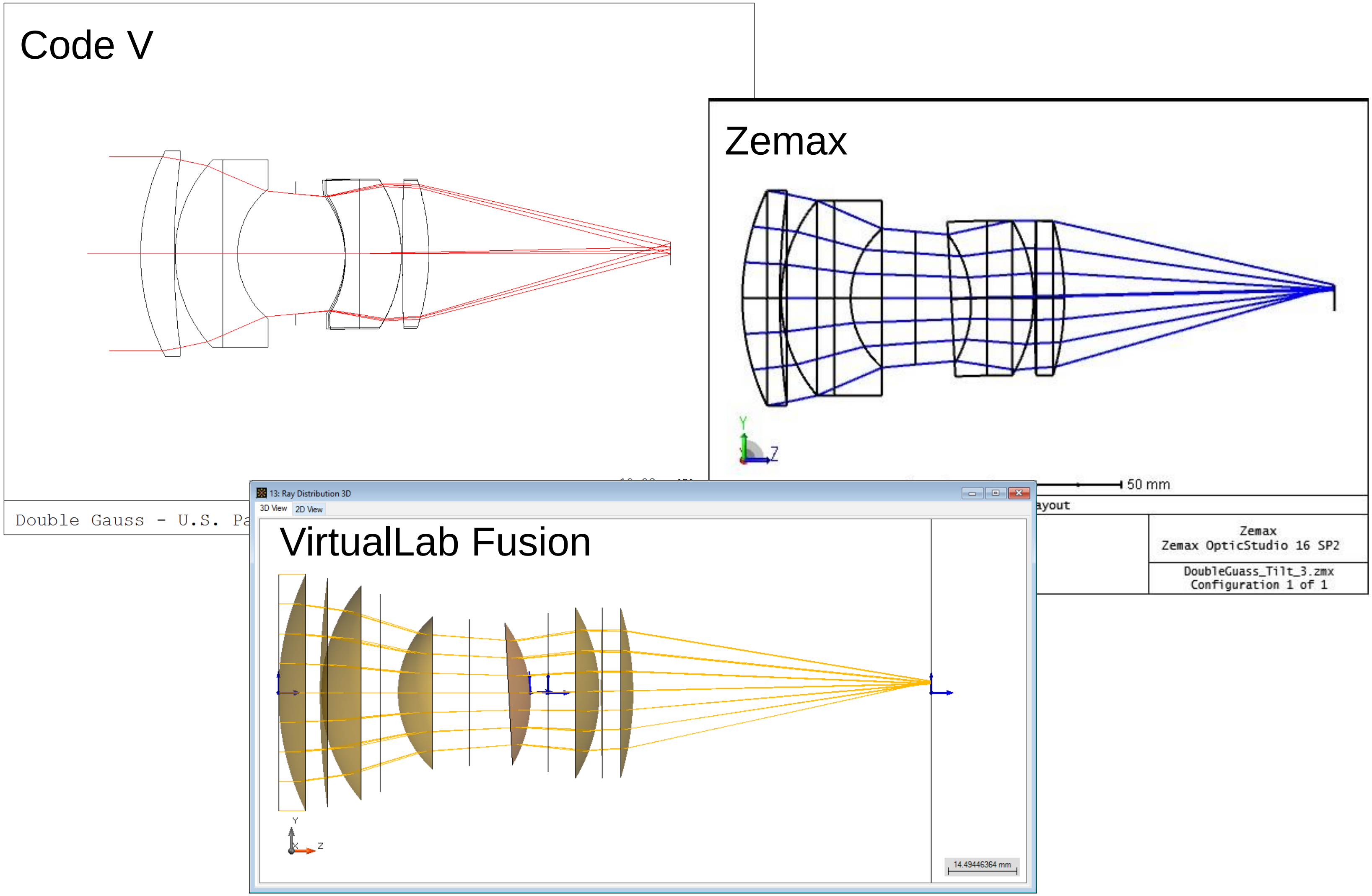

Specification of Simulation Parameters

- Working wavelength: 587 nm
- Polarization: E_x-polarized
- Effective focal length:
  - CODE V: 100.00049 mm
  - VLF: (*Focal Length Analyzer* can‘t calculate lens pair)
  - Zemax: 100.000487205913 mm
- NA of System: 0.2499
- Beam Diameter (Entrance Pupil): 50 mm
- Field of View: 0°
- Vignetting: 0

Dot Diagram Comparison: Target Plane

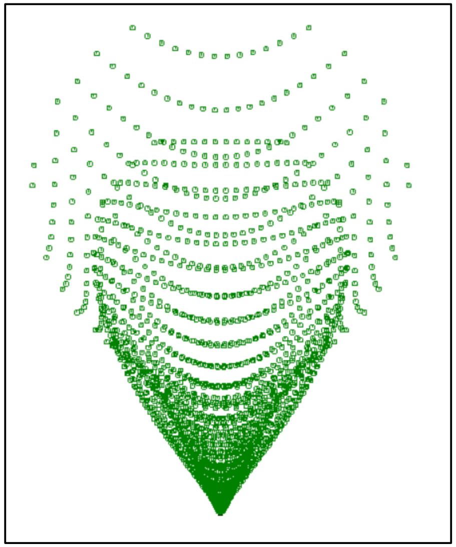

Code V

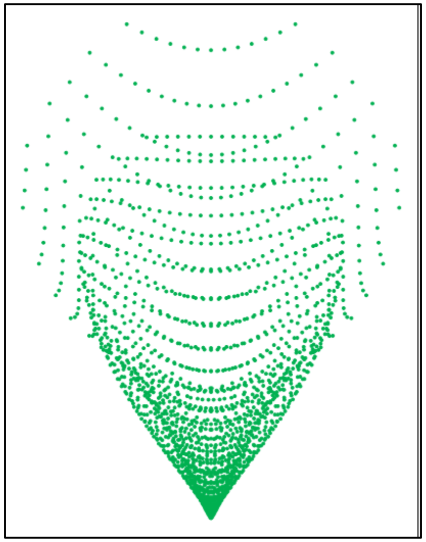

VLF

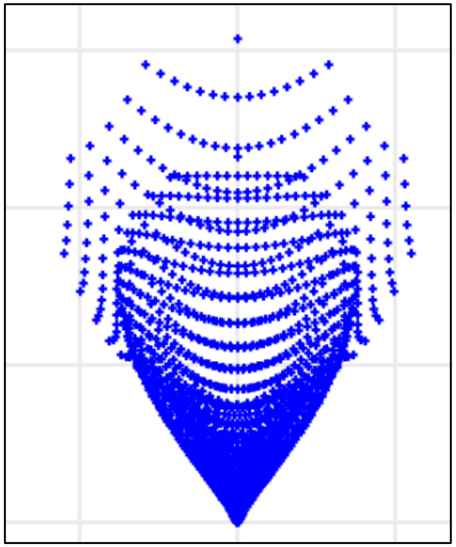

Zemax

Precise Comparison: Position

Ray position at initial plane			
No.	Lateral coordinates	No.	Lateral coordinates
1	(0, 15 mm)	4	(0, 7.5 mm)
2	(0, -15 mm)	5	(0, -7.5 mm)
3	(7.5 mm, 7.5 mm)	6	(7.5 mm, -7.5 mm)

Ray position at imaging plane			
No.	VLF	Code V	Zemax
1	(0, 2.1524 mm)	(0, 2.1524 mm)	(0, 2.1524 mm)
2	(0, 2.1536 mm)	(0, 2.1536 mm)	(0, 2.1536 mm)
3	(52.07 µm, 1.927 mm)	(52.07 µm, 1.927 mm)	(52.07 µm, 1.927 mm)
4	(0, 1.905 mm)	(0, 1.905 mm)	(0, 1.905 mm)
5	(0, 1.8825 mm)	(0, 1.8825 mm)	(0, 1.8825 mm)
6	(-56.77 µm, 1.9162 mm)	(56.77 µm, 1.9162 mm)	(56.77 µm, 1.9162 mm)

Ray Tracing in VirtualLab Fusion

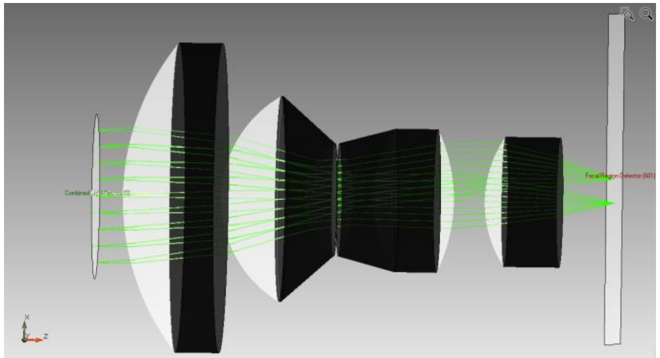

- Ray Tracing System Analyzer
- Detector
  - Spot size
  - Wavefront error (Zernike polynomials)
  - Focal length analyzer
  - …
- Parametric optimization

Parametric Optimization of An Achromatic Doublet

Schematic and Light Path Diagram

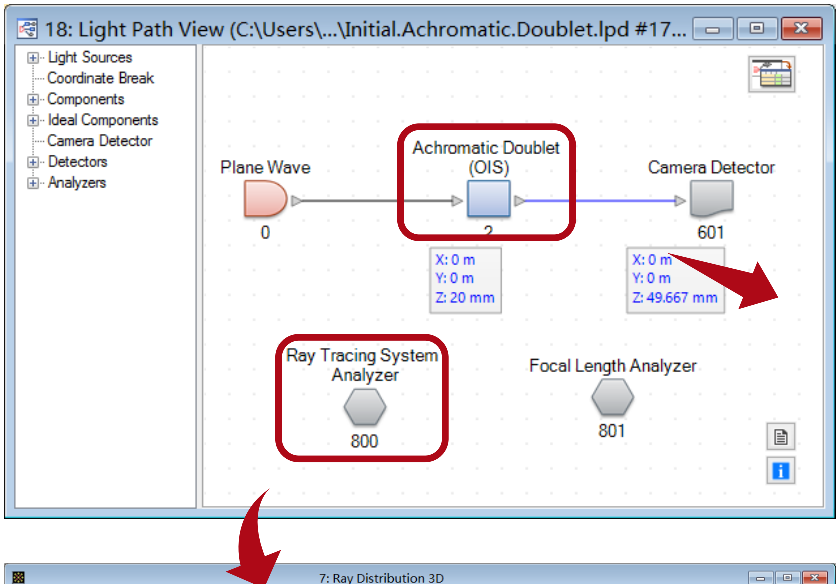

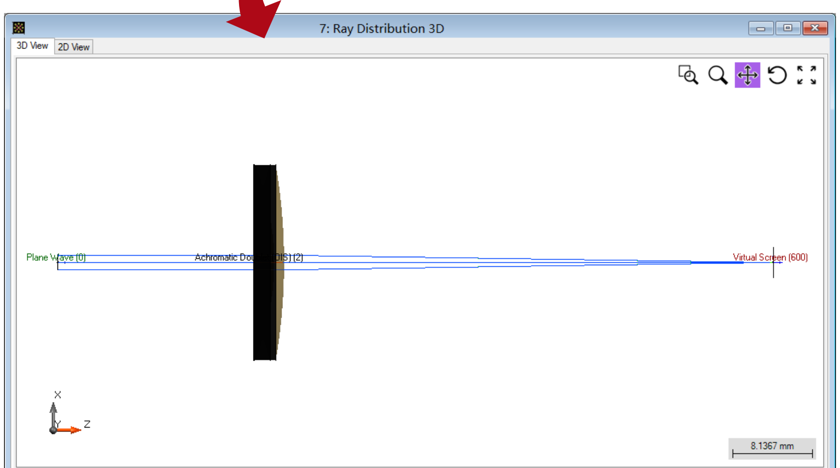

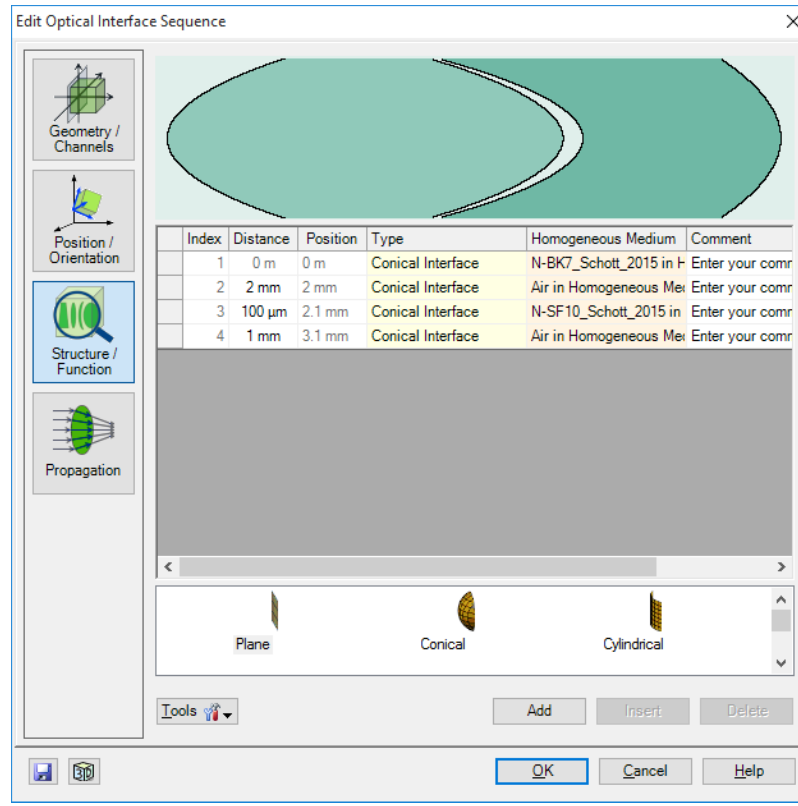

Set Optimization Target

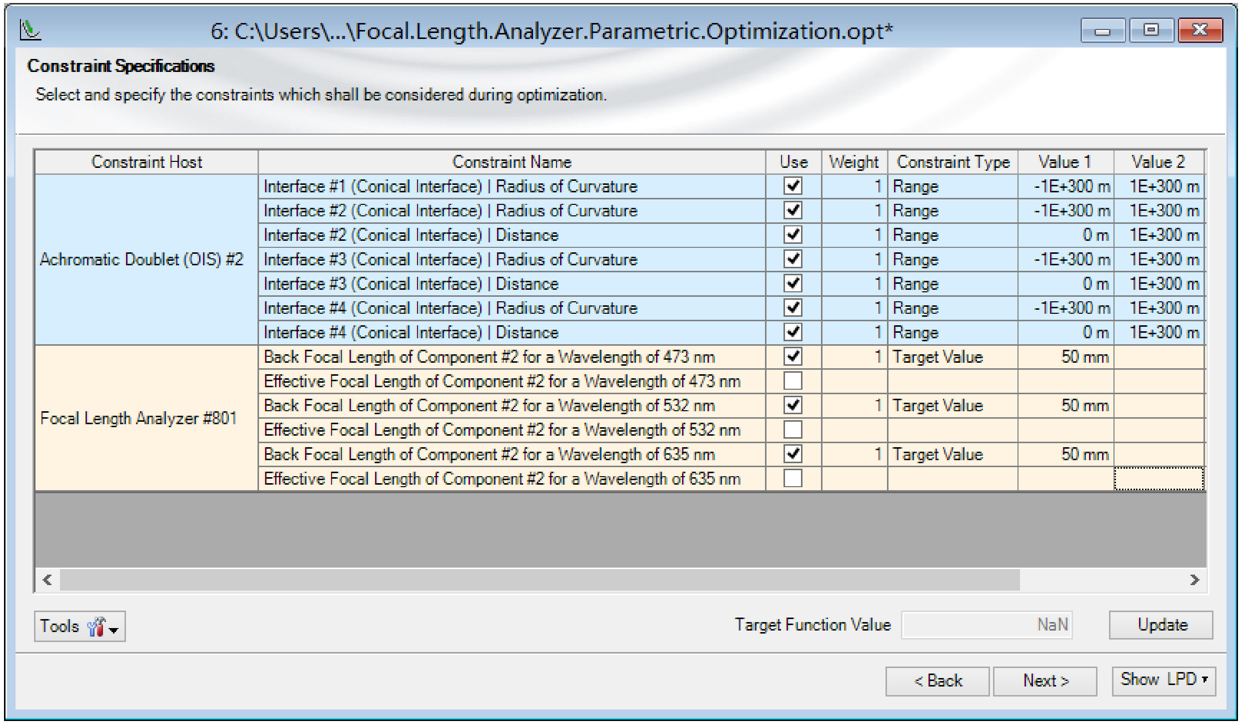

Constraint Host	Constraint Name	Use	Weight	Constraint Type	Value 1	Value 2
Achromatic Doublet (OIS) #2	Interface #1 (Conical Interface) | Radius of Curvature	✓	1	Range	-1E+300 m	1E+300 m
	Interface #2 (Conical Interface) | Radius of Curvature	✓	1	Range	-1E+300 m	1E+300 m
	Interface #2 (Conical Interface) | Distance	✓	1	Range	0 m	1E+300 m
	Interface #3 (Conical Interface) | Radius of Curvature	✓	1	Range	-1E+300 m	1E+300 m
	Interface #3 (Conical Interface) | Distance	✓	1	Range	0 m	1E+300 m
	Interface #4 (Conical Interface) | Radius of Curvature	✓	1	Range	-1E+300 m	1E+300 m
	Interface #4 (Conical Interface) | Distance	✓	1	Range	0 m	1E+300 m
Focal Length Analyzer #801	Back Focal Length of Component #2 for a Wavelength of 473 nm	✓	1	Target Value	50 mm	
	Effective Focal Length of Component #2 for a Wavelength of 473 nm	☐				
	Back Focal Length of Component #2 for a Wavelength of 532 nm	✓	1	Target Value	50 mm	
	Effective Focal Length of Component #2 for a Wavelength of 532 nm	☐				
	Back Focal Length of Component #2 for a Wavelength of 635 nm	✓	1	Target Value	50 mm	
	Effective Focal Length of Component #2 for a Wavelength of 635 nm	☐				

- Focal Length Analyzer
  - Effective Focal Length is set to 50 mm: for all chosen wavelengths

Optimization Result

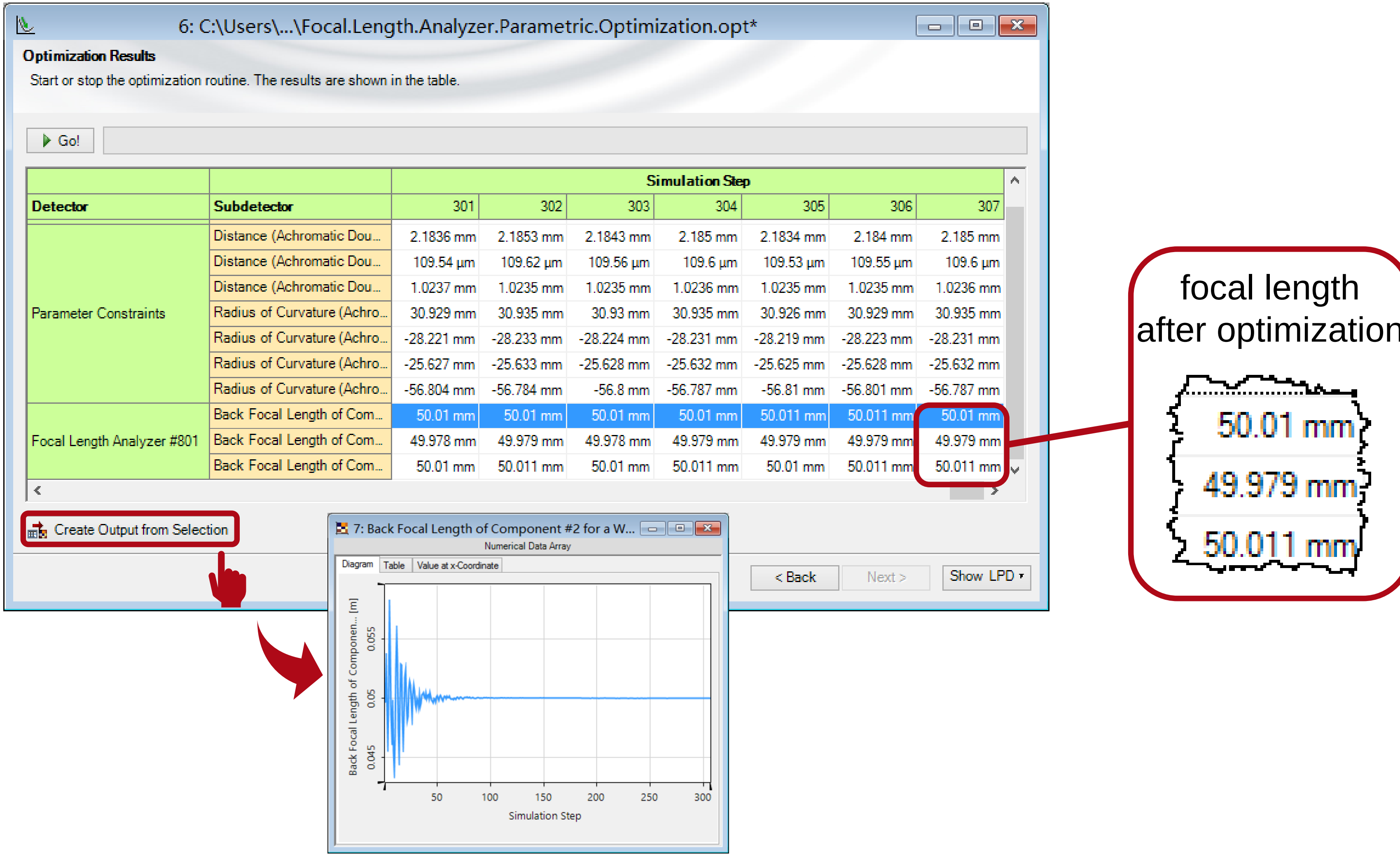

		Simulation Step						
Detector	Subdetector	301	302	303	304	305	306	307
Parameter Constraints	Distance (Achromatic Dou...	2.1836 mm	2.1853 mm	2.1843 mm	2.185 mm	2.1834 mm	2.184 mm	2.185 mm
	Distance (Achromatic Dou...	109.54 µm	109.62 µm	109.56 µm	109.6 µm	109.53 µm	109.55 µm	109.6 µm
	Distance (Achromatic Dou...	1.0237 mm	1.0235 mm	1.0235 mm	1.0236 mm	1.0235 mm	1.0235 mm	1.0236 mm
	Radius of Curvature (Achro...	30.929 mm	30.935 mm	30.93 mm	30.935 mm	30.926 mm	30.929 mm	30.935 mm
	Radius of Curvature (Achro...	-28.221 mm	-28.233 mm	-28.224 mm	-28.231 mm	-28.219 mm	-28.223 mm	-28.231 mm
	Radius of Curvature (Achro...	-25.627 mm	-25.633 mm	-25.628 mm	-25.632 mm	-25.625 mm	-25.628 mm	-25.632 mm
	Radius of Curvature (Achro...	-56.804 mm	-56.784 mm	-56.8 mm	-56.787 mm	-56.81 mm	-56.801 mm	-56.787 mm
Focal Length Analyzer #801	Back Focal Length of Com...	50.01 mm	50.01 mm	50.01 mm	50.01 mm	50.011 mm	50.011 mm	50.01 mm
	Back Focal Length of Com...	49.978 mm	49.979 mm	49.978 mm	49.979 mm	49.979 mm	49.979 mm	49.979 mm
	Back Focal Length of Com...	50.01 mm	50.011 mm	50.01 mm	50.011 mm	50.01 mm	50.011 mm	50.011 mm

Comparison of Results

Dot Diagram (initial setup)

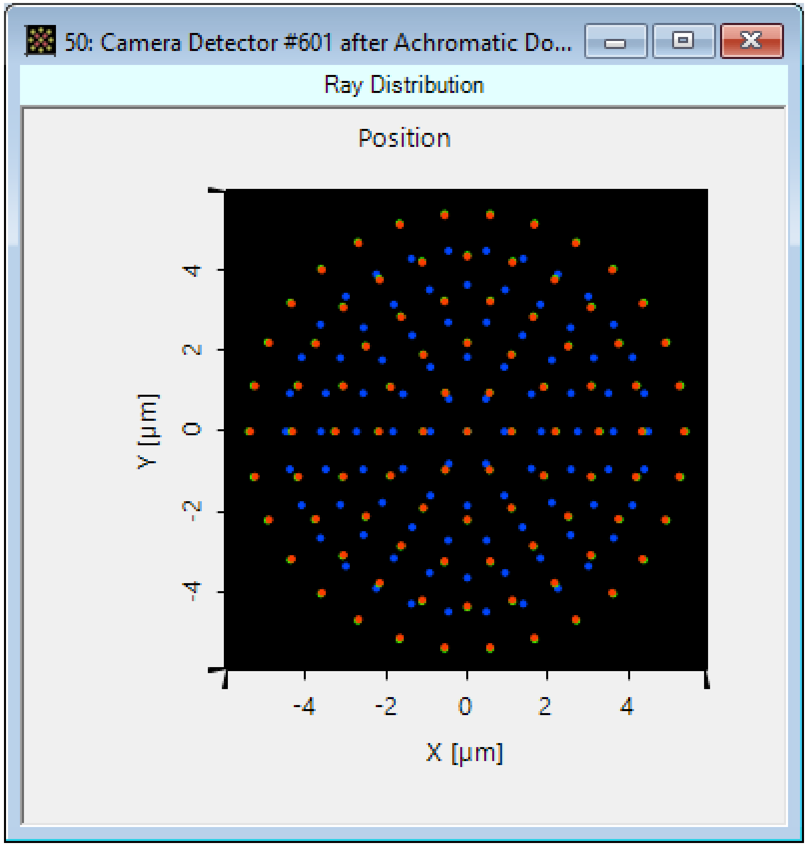

Dot Diagram (optimized)

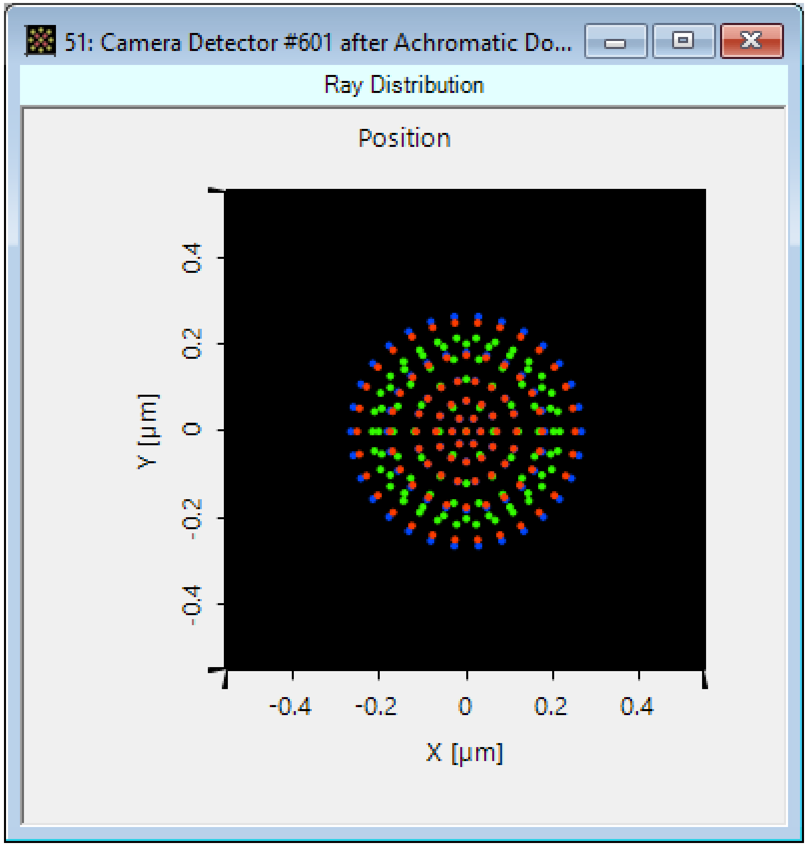

Ray and Physical Optics

Ray Optics

Physical Optics

Ray optics modeling:

- Gives great basic insight into light propagation.
- Often sufficient for optical design, e.g. in standard lens design.
- **Suffers from serious limitations.**

Ray Tracing Concept and Limitations

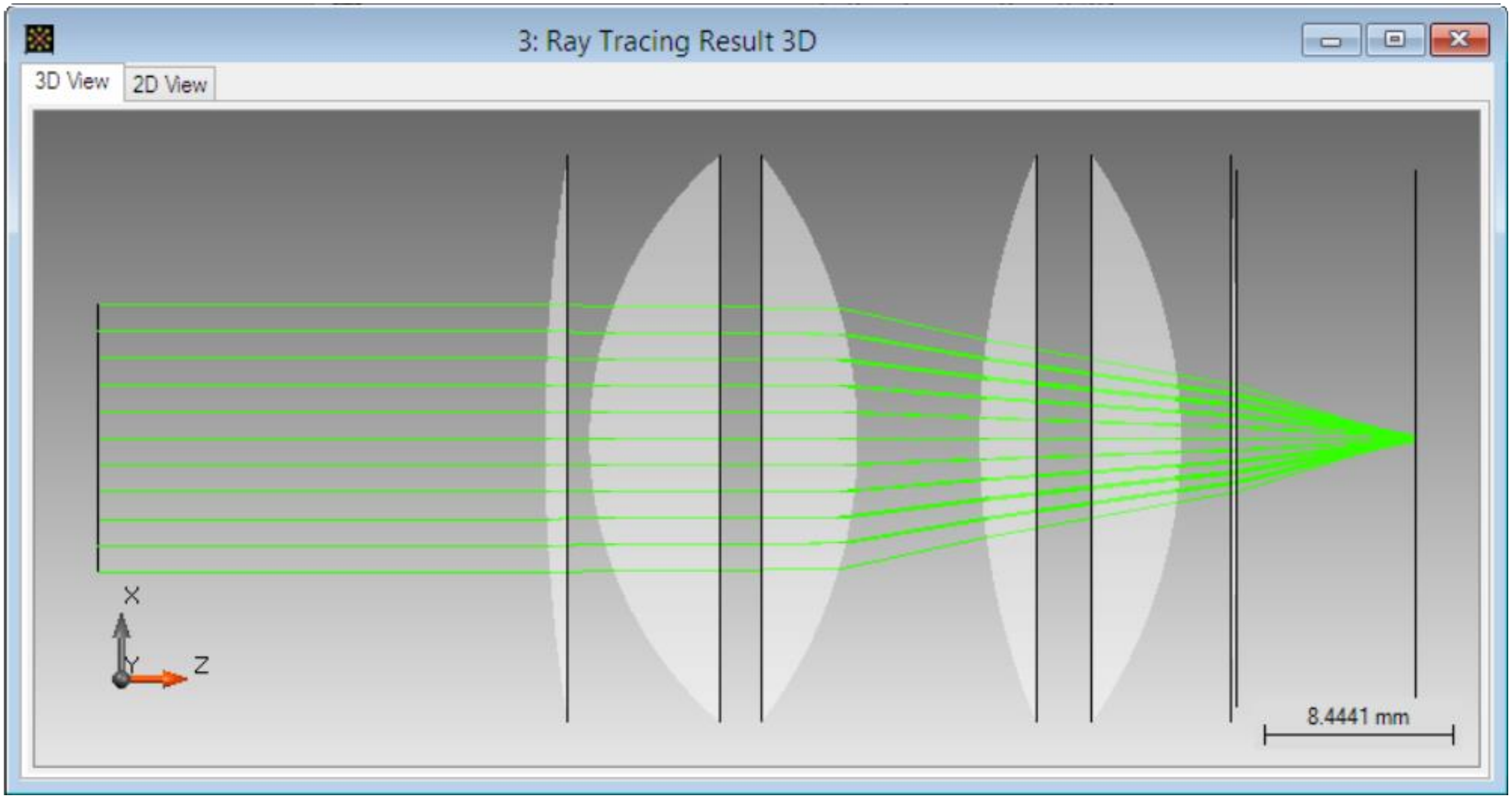

Ray Tracing Concept and Limitations

Source modeled by a suitable ray bundle.

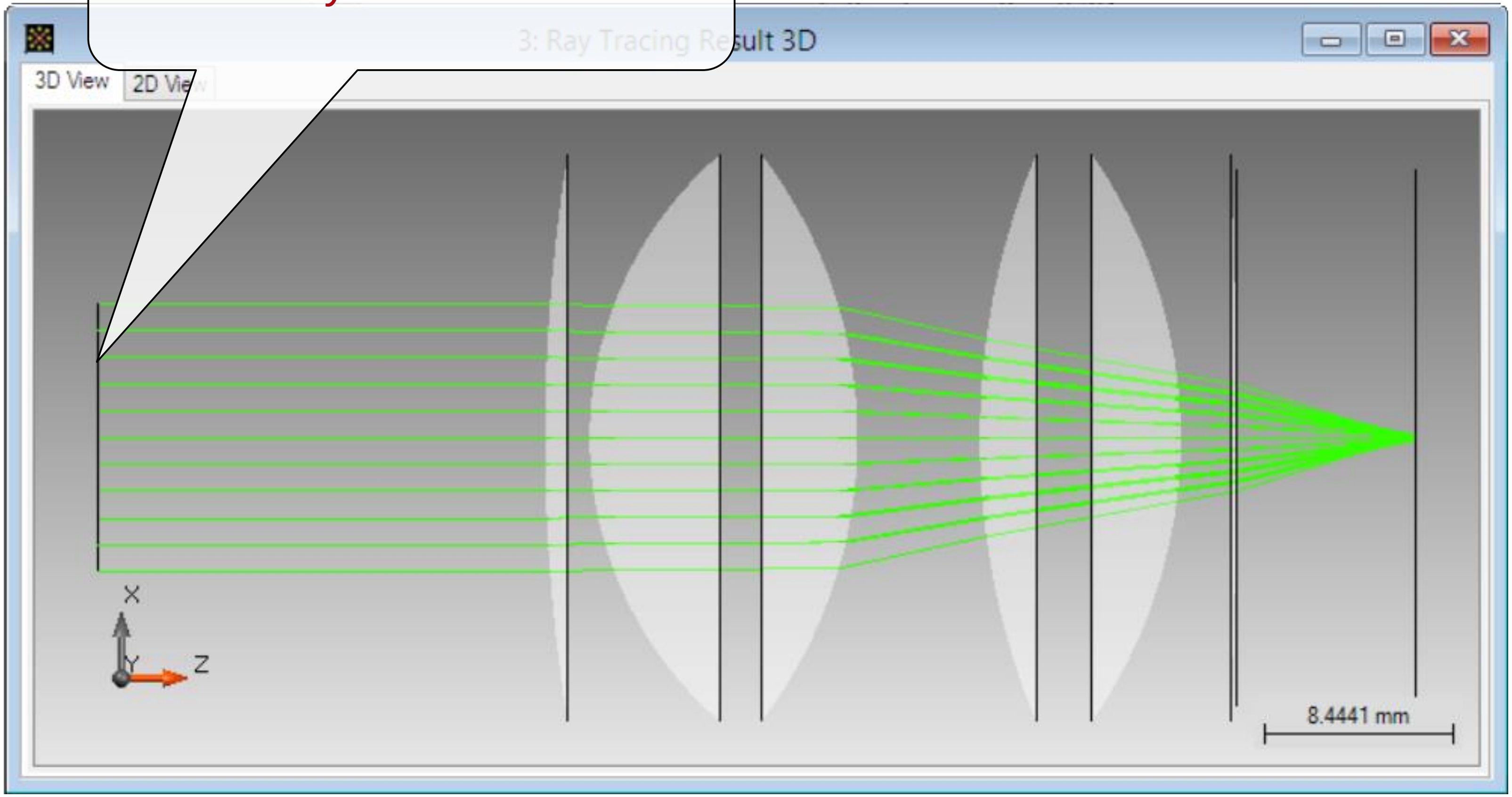

Ray Tracing Limitations: Gaussian Source

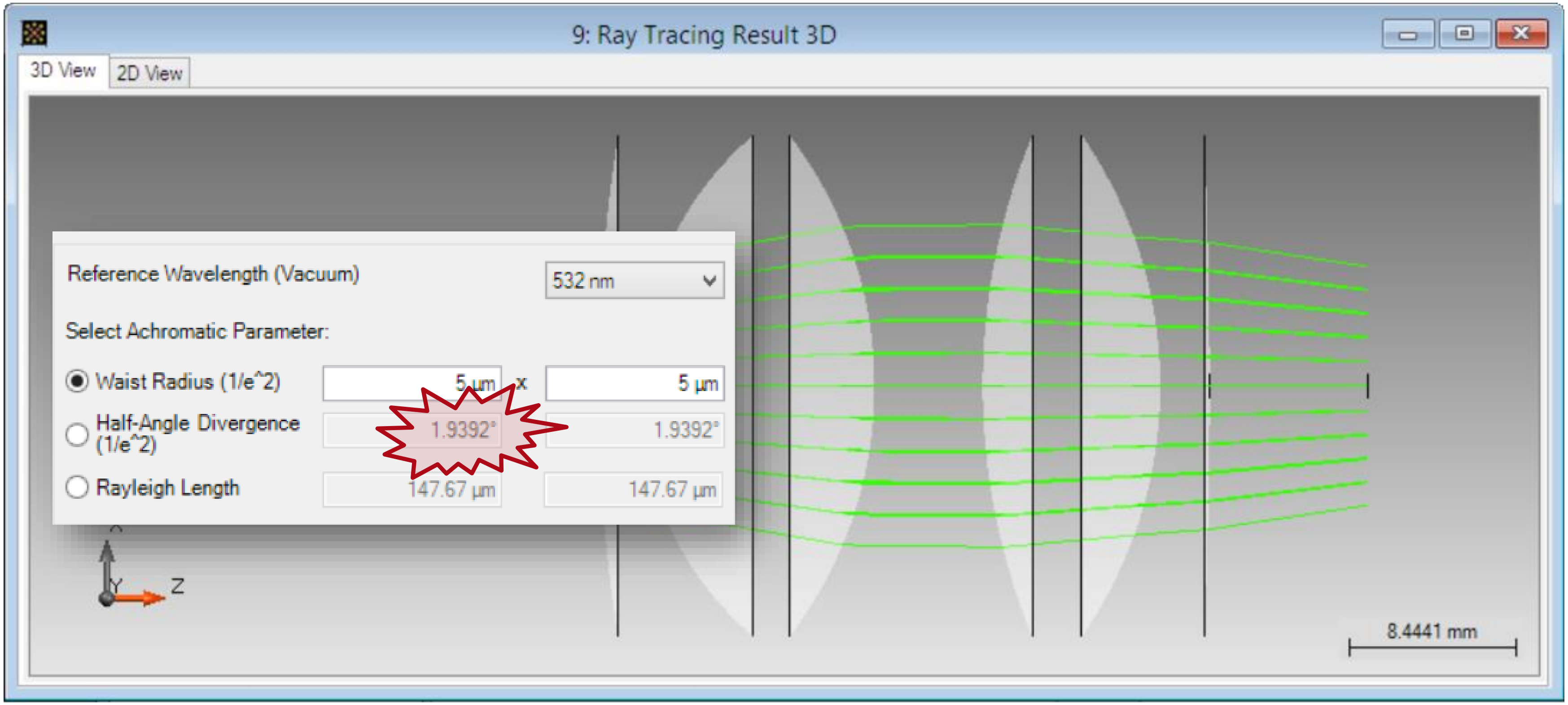

Ray Tracing Limitations: Gaussian Source

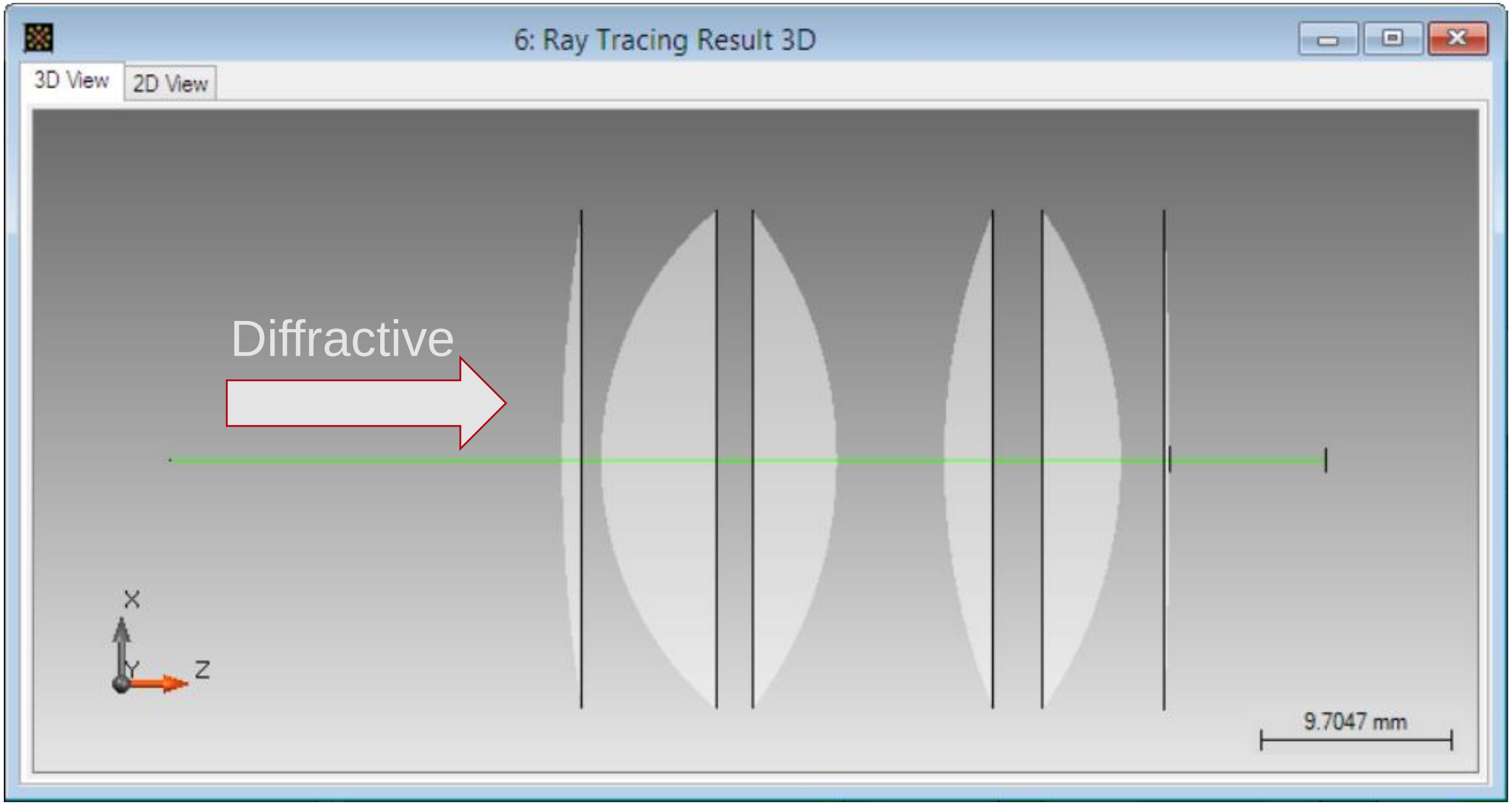

Ray Tracing Limitations: Gaussian Source

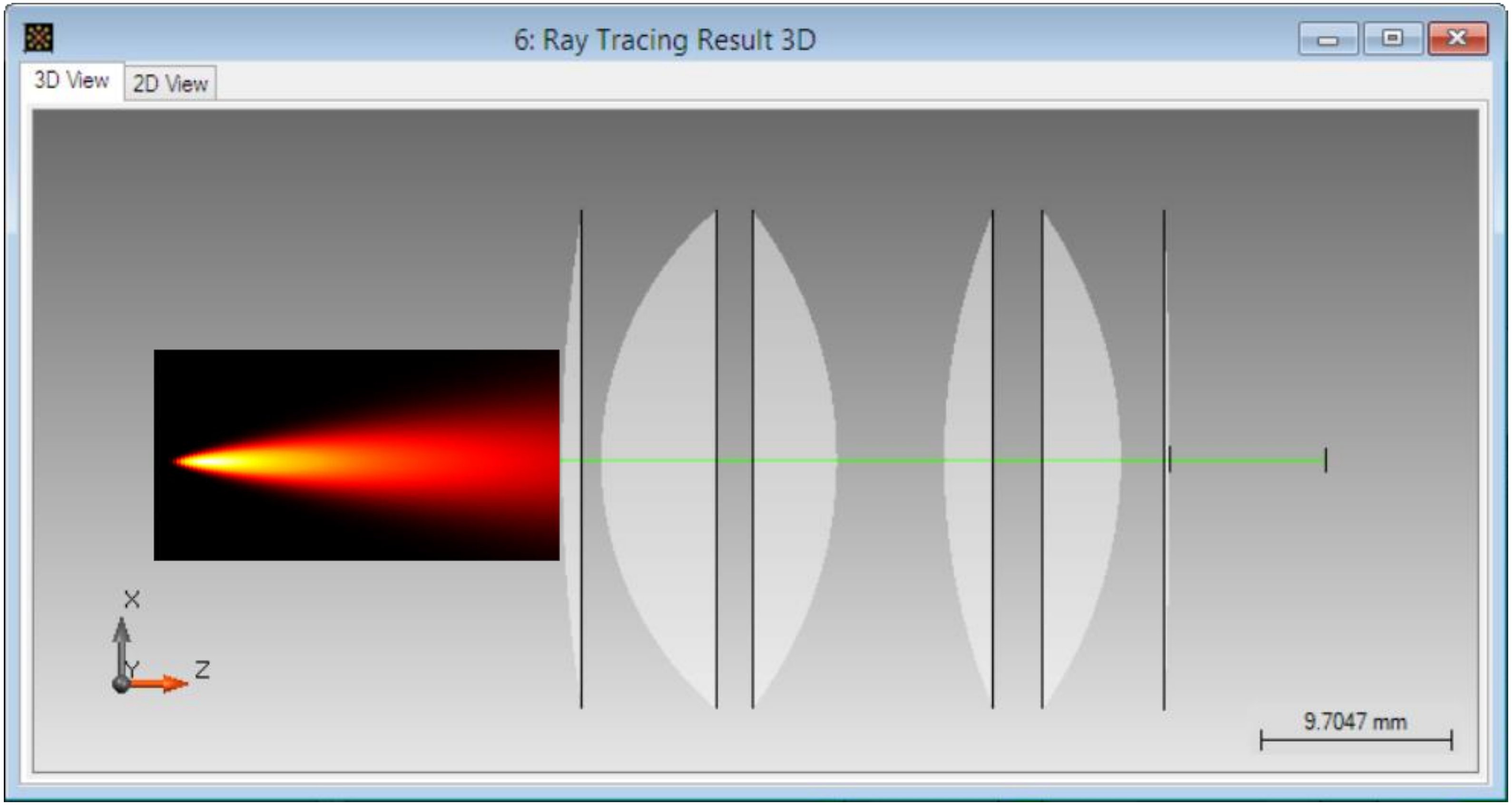

Ray Tracing Limitations: Gaussian Source

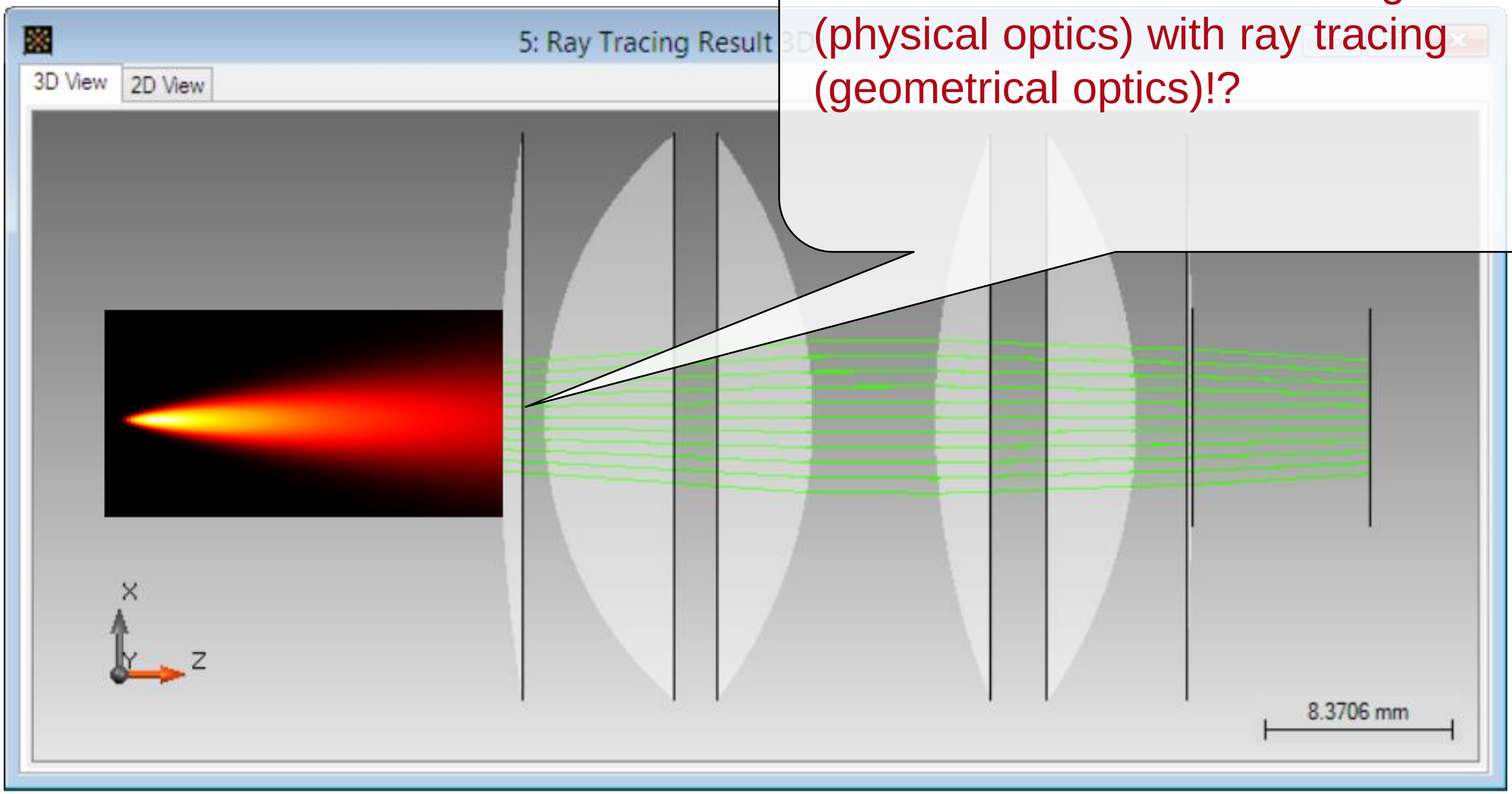

Connection of diffraction integral (physical optics) with ray tracing (geometrical optics)!?

Ray Tracing Limitations: Focusing

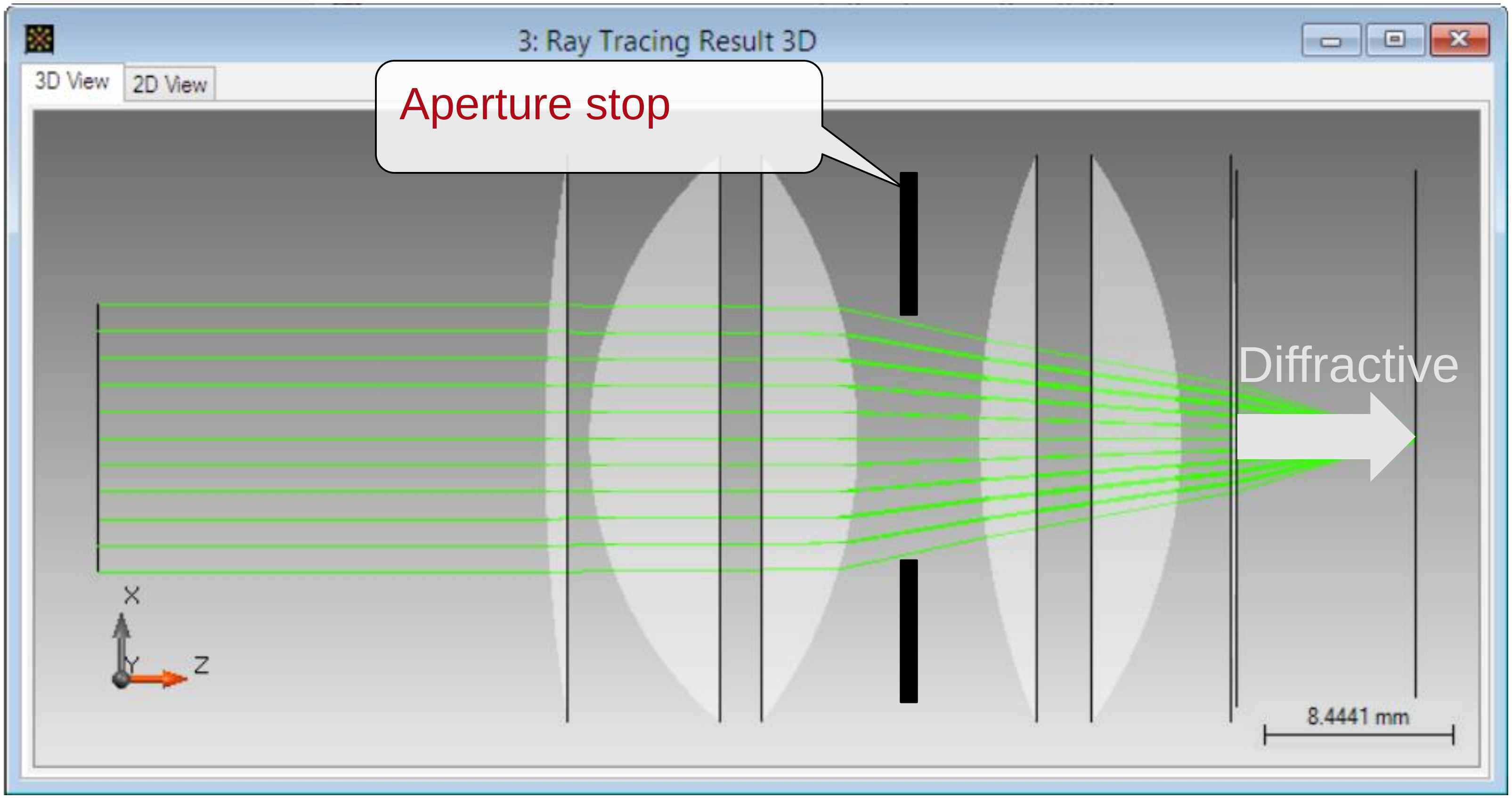

Ray Tracing Limitations: Focusing

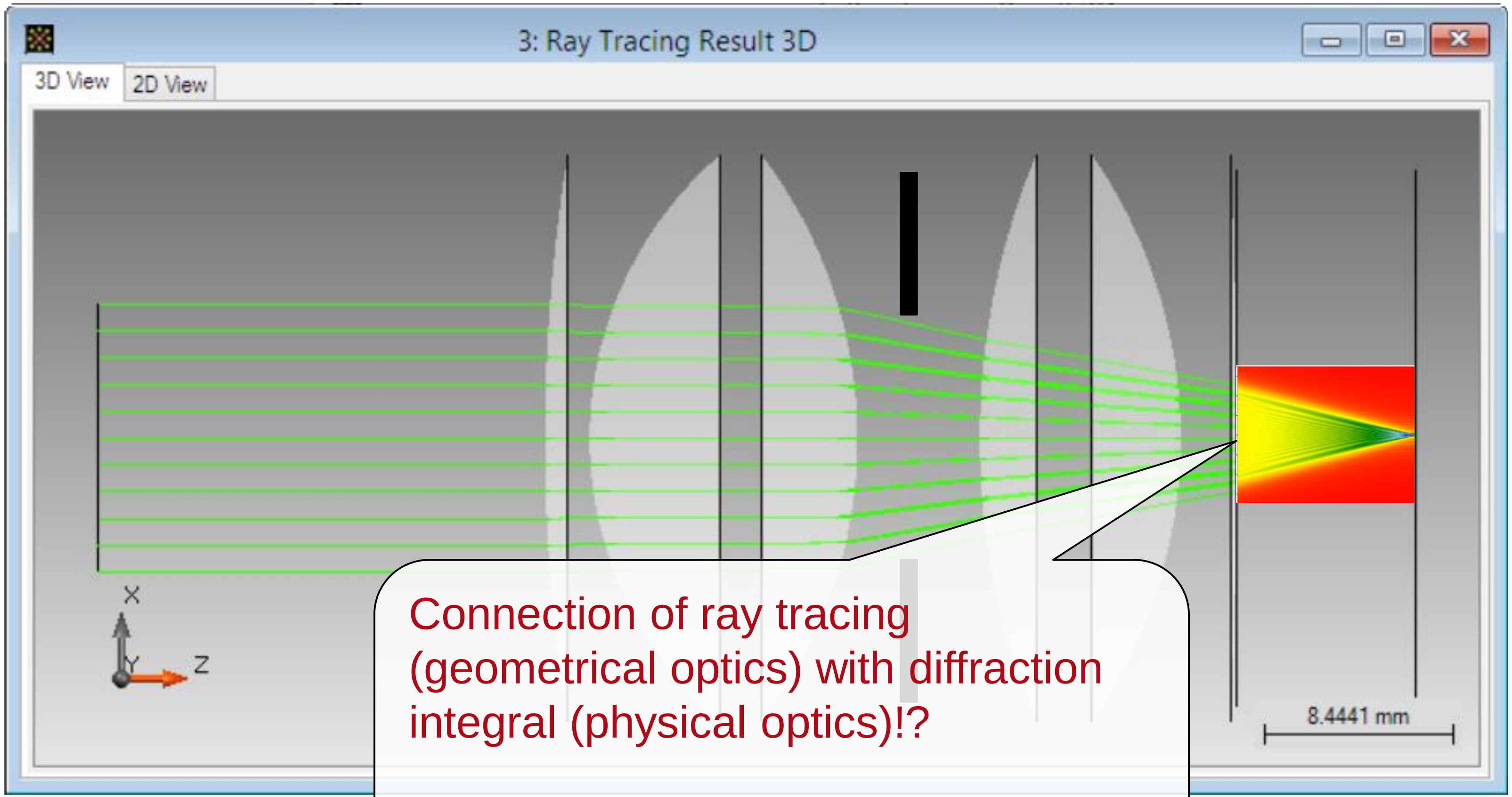

Connection of ray tracing (geometrical optics) with diffraction integral (physical optics)!?

Ray Tracing Limitations: Vectorial Modeling

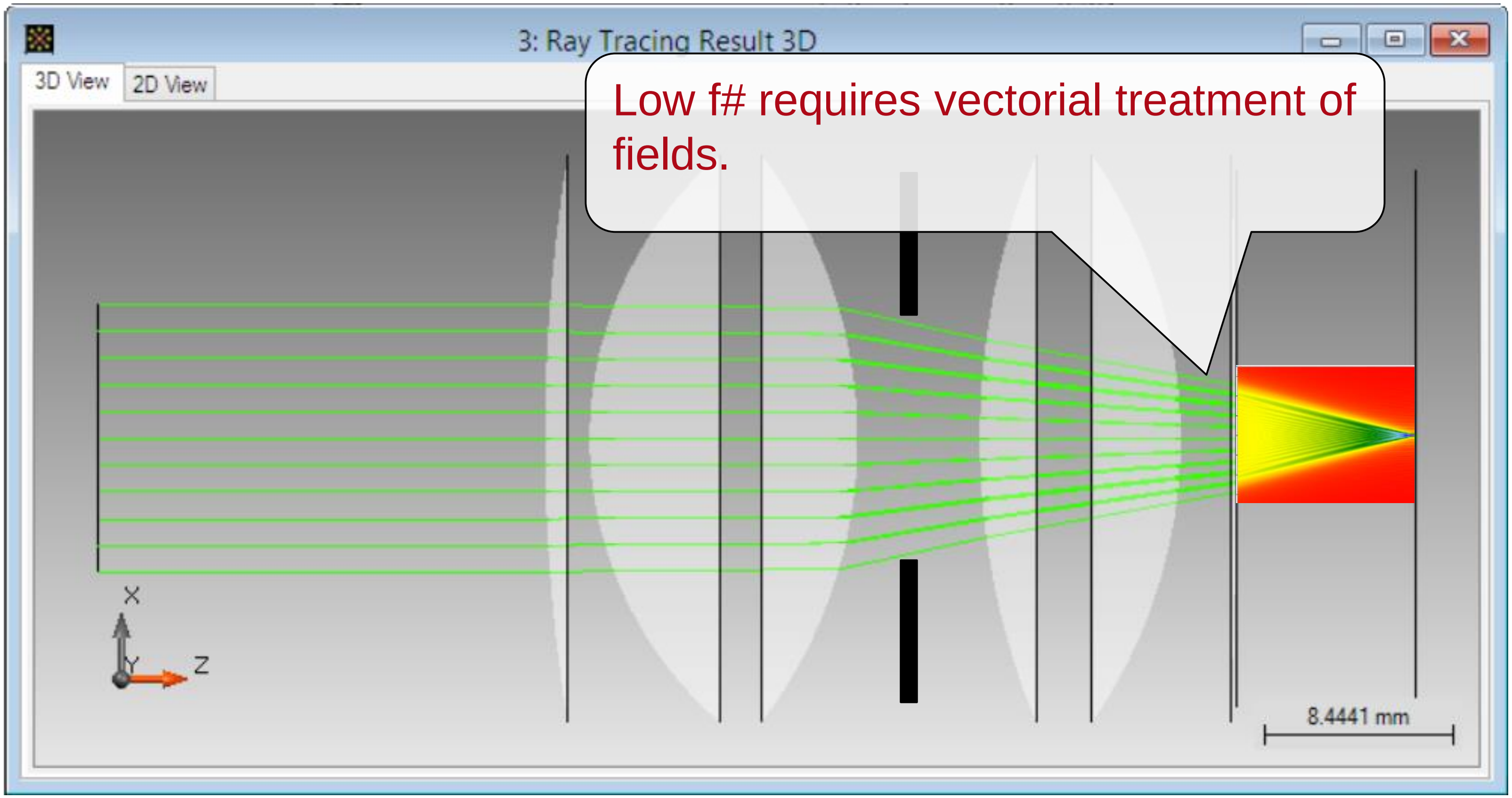

Ray Tracing Limitations: Vectorial Modeling

Energy losses and polarization effects at surfaces must be taken into account!

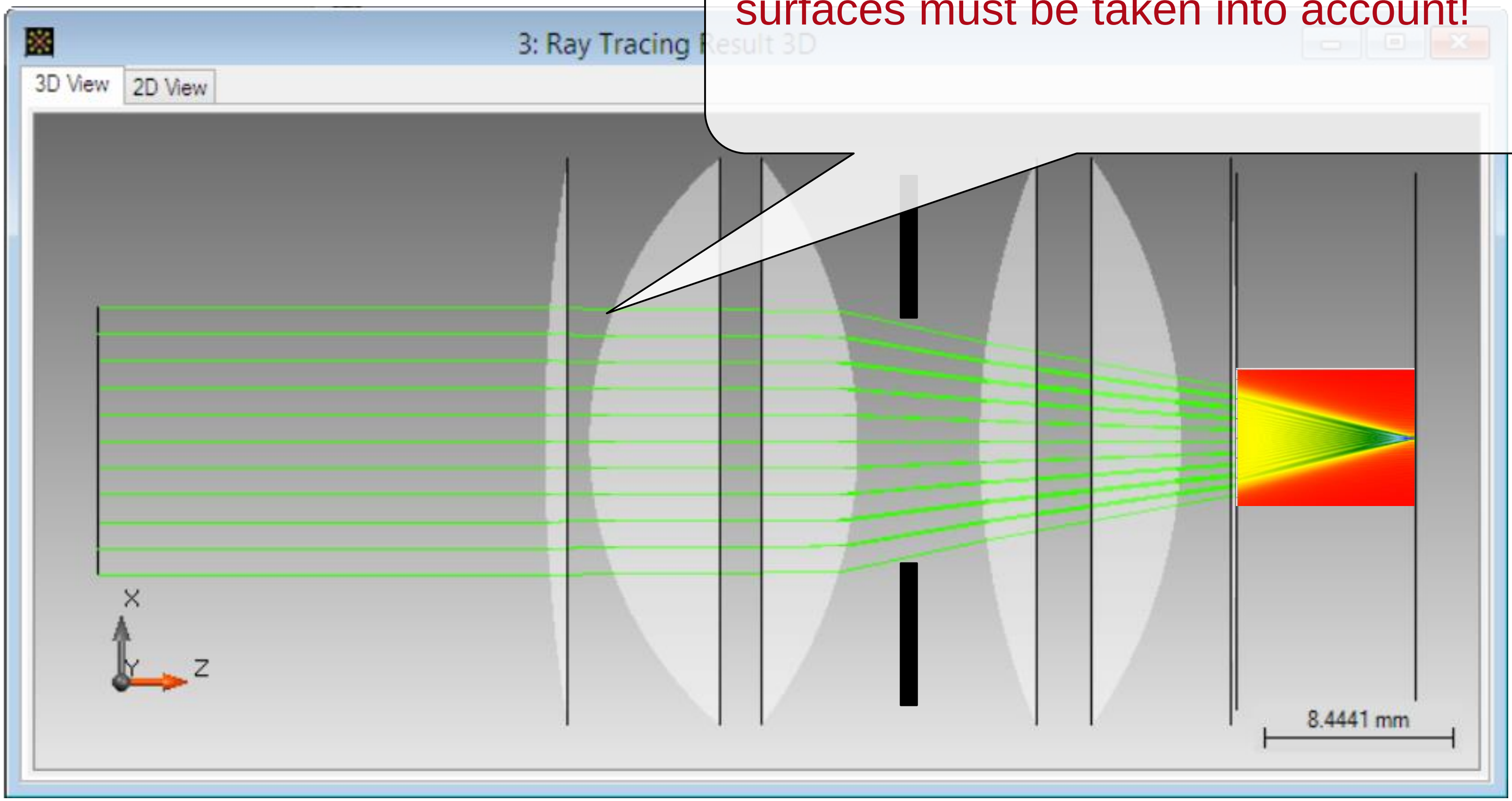

Fresnel Effect: Reflectance for TE/TM

Air vs. BK7 glass

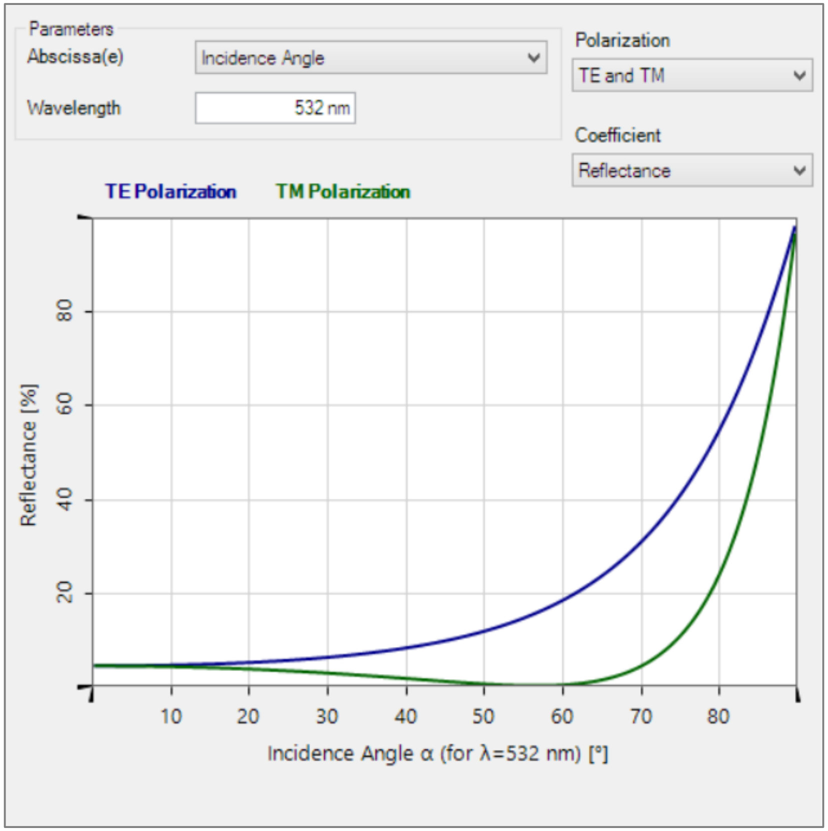

Air vs. silver

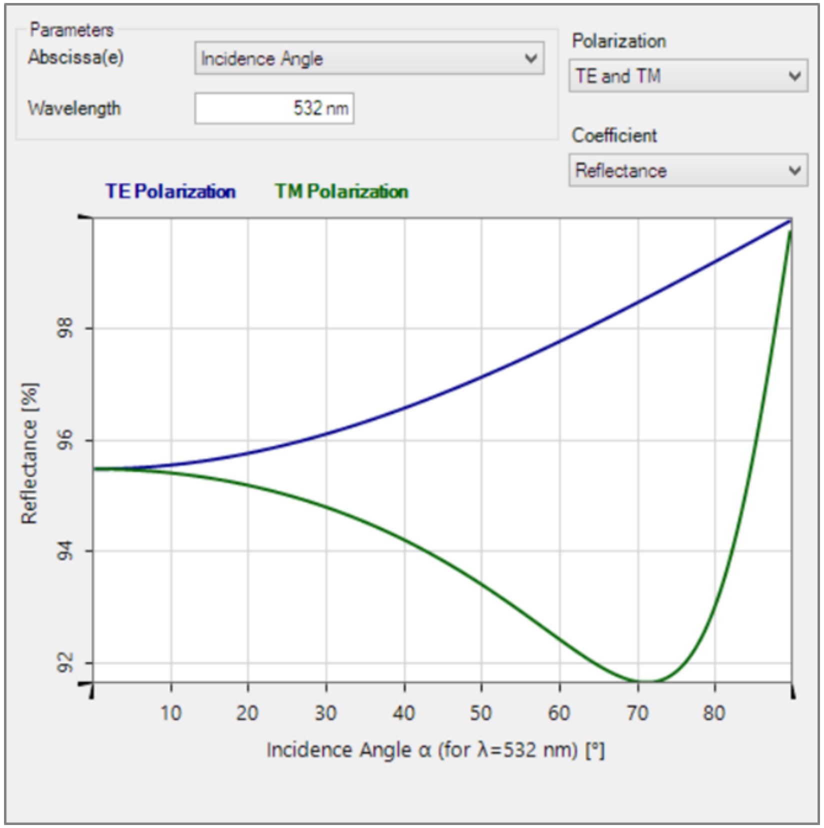

Fresnel Effect: Reflectance for TE/TM

Air vs. BK7 glass

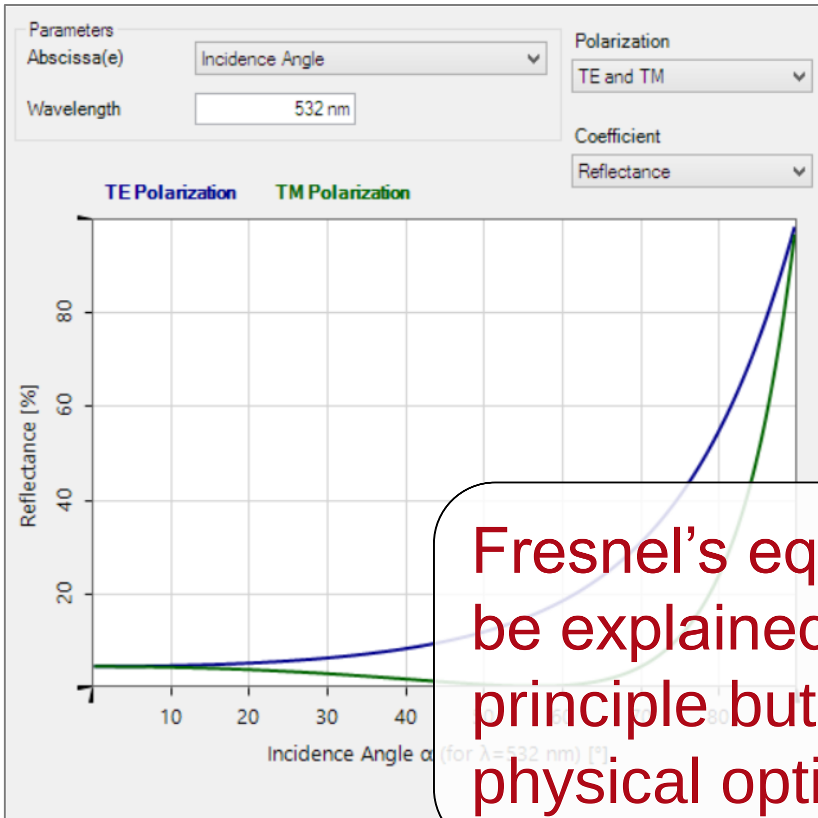

Air vs. silver

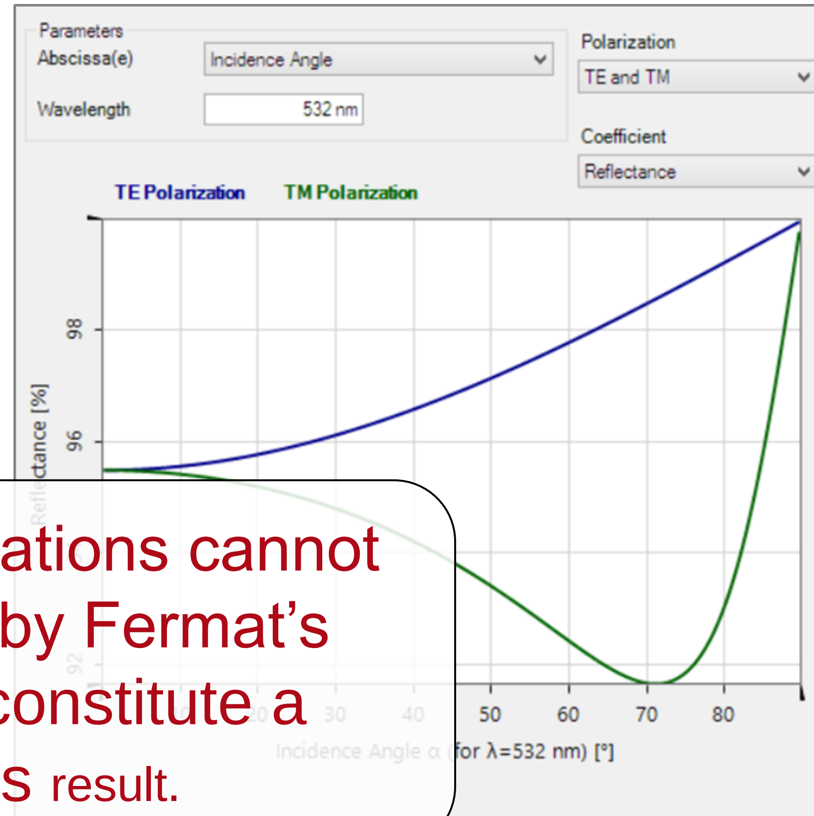

Fresnel's equations cannot be explained by Fermat's principle but constitute a physical optics result.

Ray Tracing Limitations: Gratings / DOE

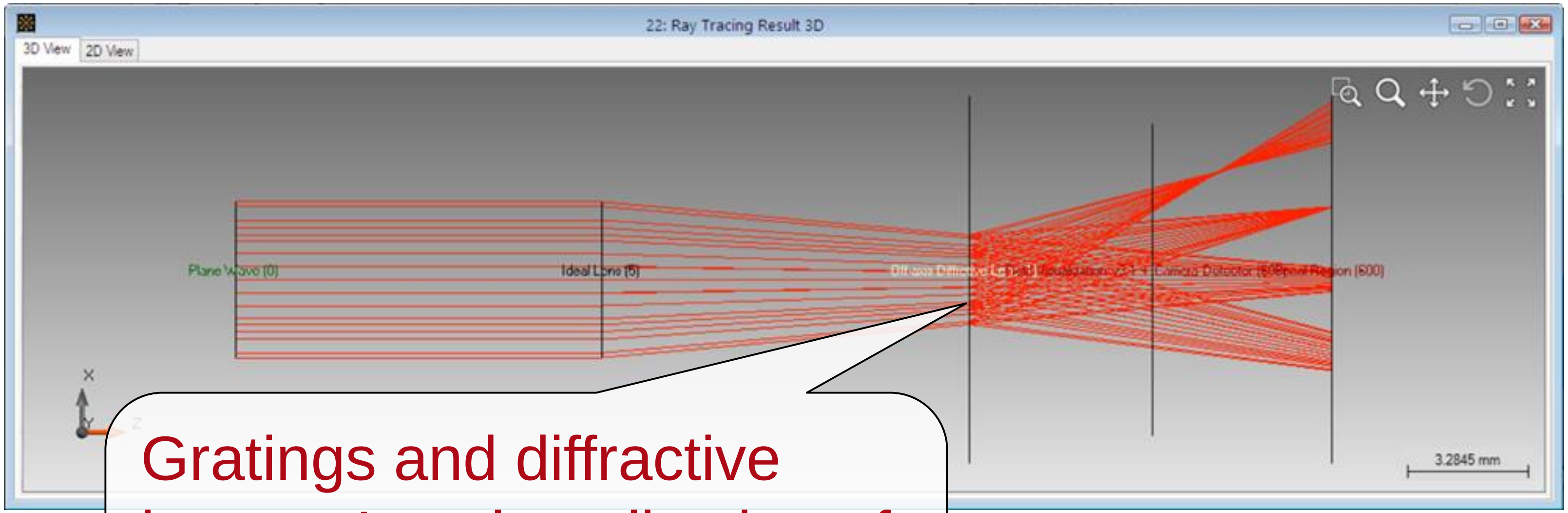

Gratings and diffractive lenses: Local application of vectorial grating response by grating theory.

Ray and Physical Optics

Ray Optics

Physical Optics

Ray optics modeling:

- Gives great basic insight into light propagation.
- Often sufficient for optical design, e.g. in standard lens design.
- **Suffers from serious limitations.**

Demand for physical optics modeling and design!

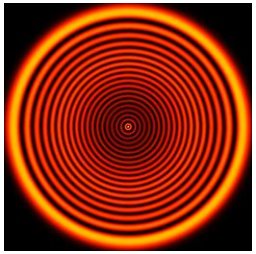

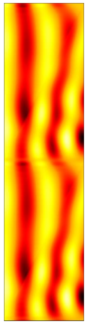

Optical Modeling: The Common Understanding

Ray Optics

Physical Optics

Universal Maxwell solver, e.g., FMM and FEM

Universal, Rigorous Maxwell Solver

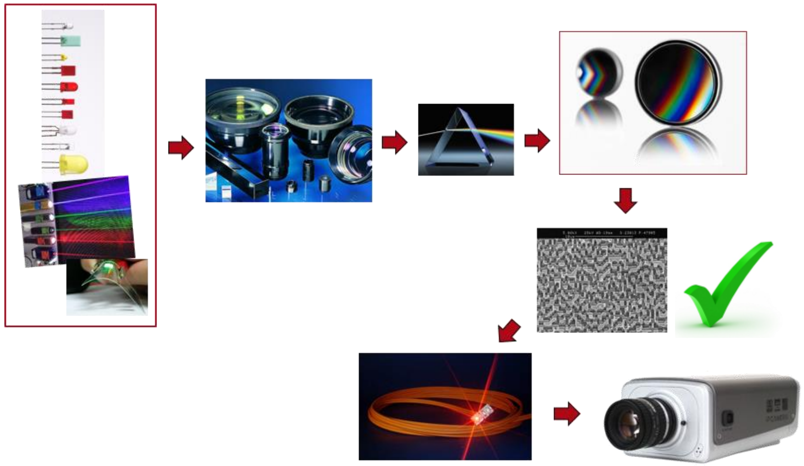

- Fourier Modal Method

Fourier Modal Method

- Sawtooth grating
  - Diffraction angle and efficiency

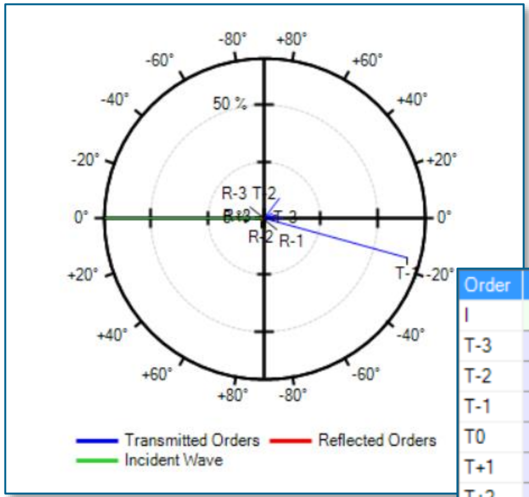

Order	Angle	Efficiency
I	0°	100 %
T-3	-52.919°	0.12312 %
T-2	-32.131°	0.2671 %
T-1	-15.422°	65.654 %
T0	0°	9.2988 %
T+1	15.422°	5.6679 %
T+2	32.131°	4.1998 %
T+3	52.919°	11.072 %
R-3	52.919°	0.17409 %
R-2	32.131°	1.7735 %
R-1	15.422°	0.49041 %
R0	0°	0.19224 %
R+1	-15.422°	0.094539 %
R+2	-32.131°	0.099558 %
R+3	-52.919°	0.89336 %

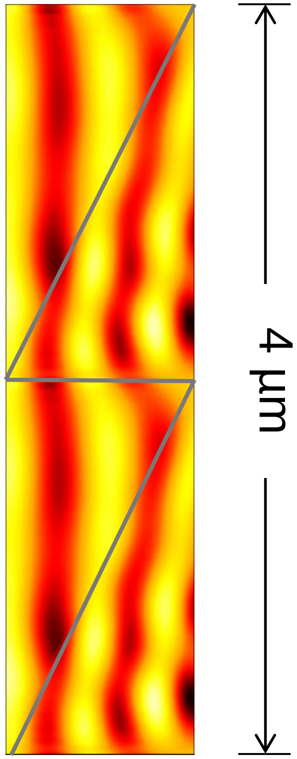

Universal, Rigorous Maxwell Solver

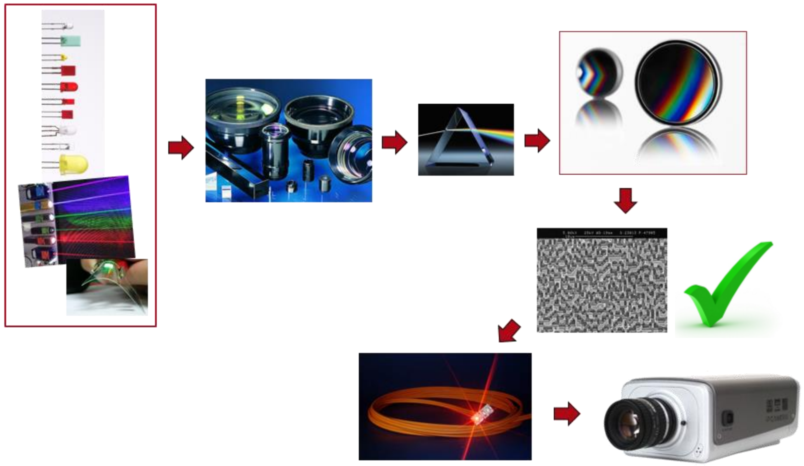

- Fourier Modal Method
- Integral Method (WIAS Berlin)

Universal, Rigorous Maxwell Solver

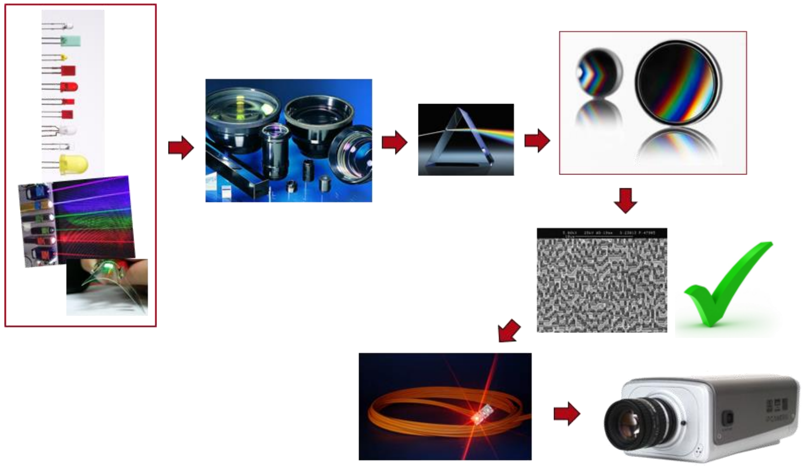

- Fourier Modal Method
- Integral Method (WIAS Berlin)
- Finite Element Method (Interface to JCMWave; Zuse Institut Berlin)

Universal, Rigorous Maxwell Solver

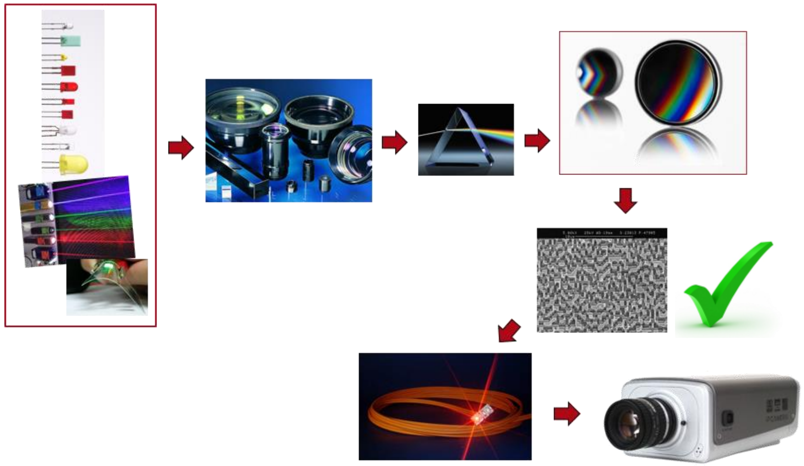

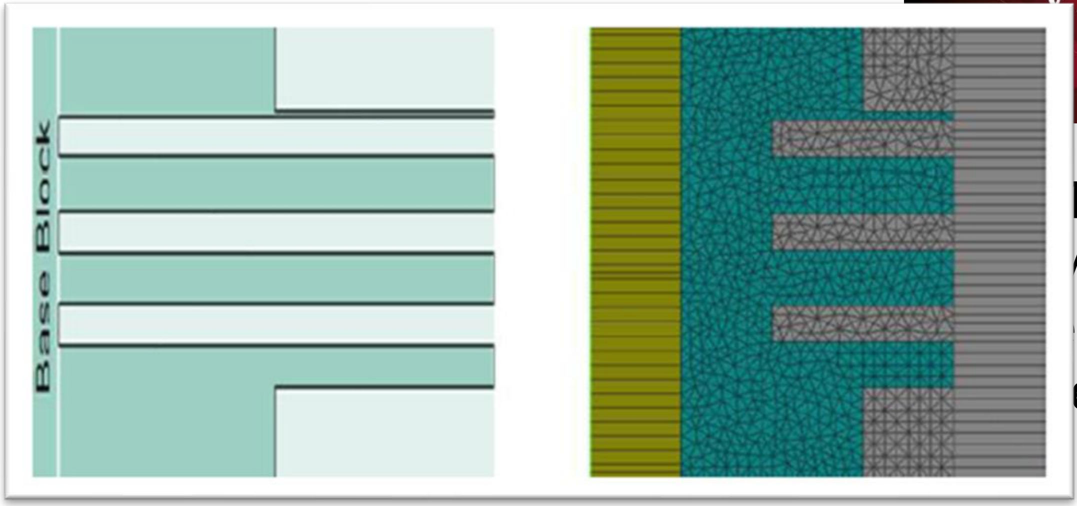

lodal Method
lethod (WIAS Berlin)
ment Method (Interface to
e; Zuse Institut Berlin)

Universal, Rigorous Maxwell Solver

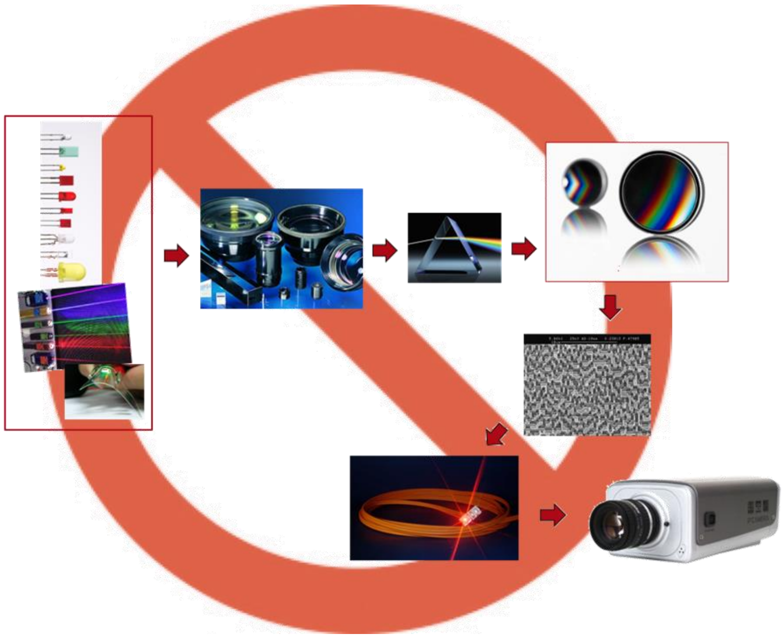

- Fourier Modal Method
- Integral Method (WIAS Berlin)
- Finite Element Method (Interface to JCMWave; Zuse Institut Berlin)

Fast Physical Optics

Tearing: Regional Decomposition

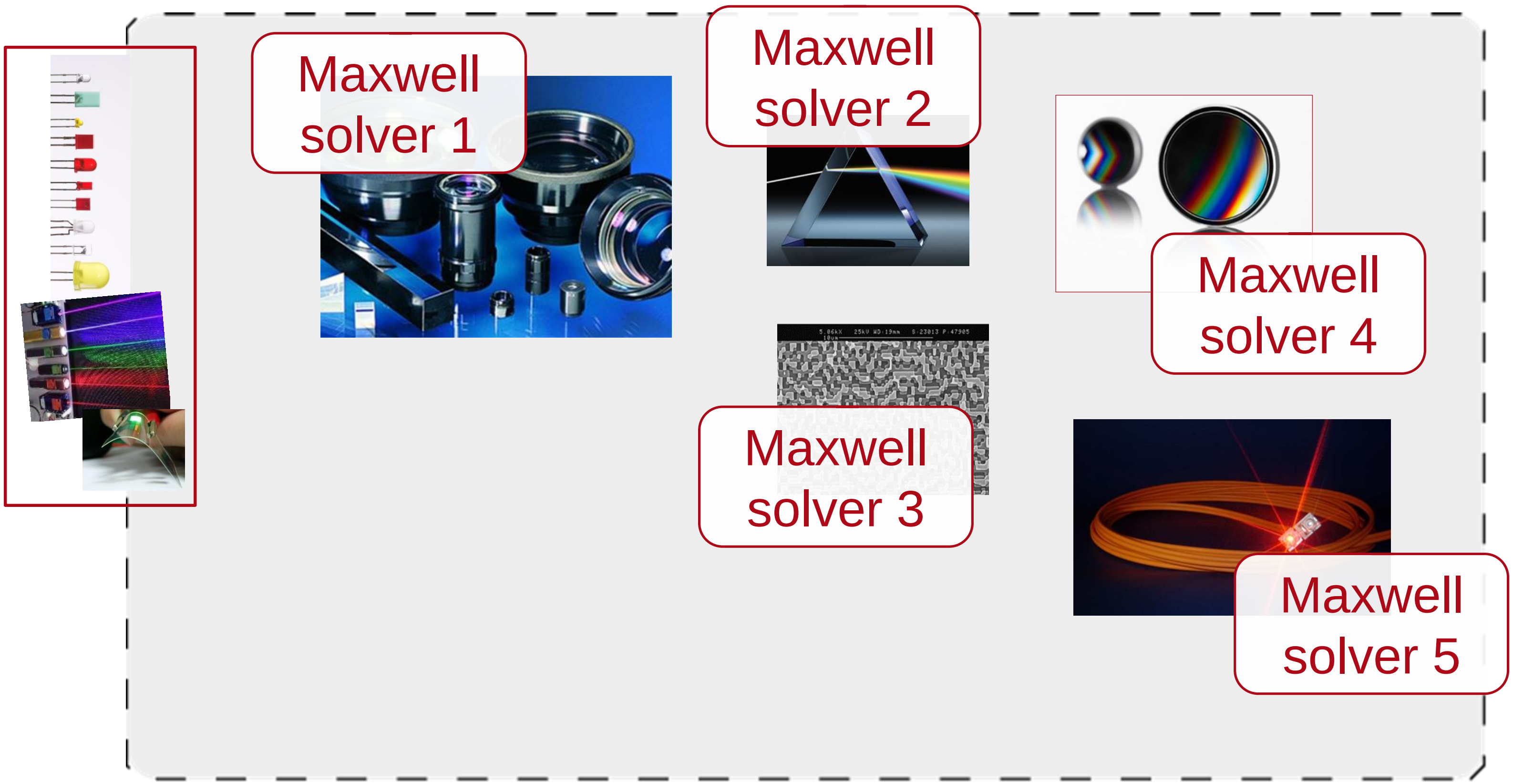

Fast Physical Optics by Field Tracing

In **Fast Physical Optics** we comply with the following strategies:

1. Tearing: The optical system is decomposed into various regions in which different types of specialized Maxwell solvers are applied.

Example

- Field tracing concept

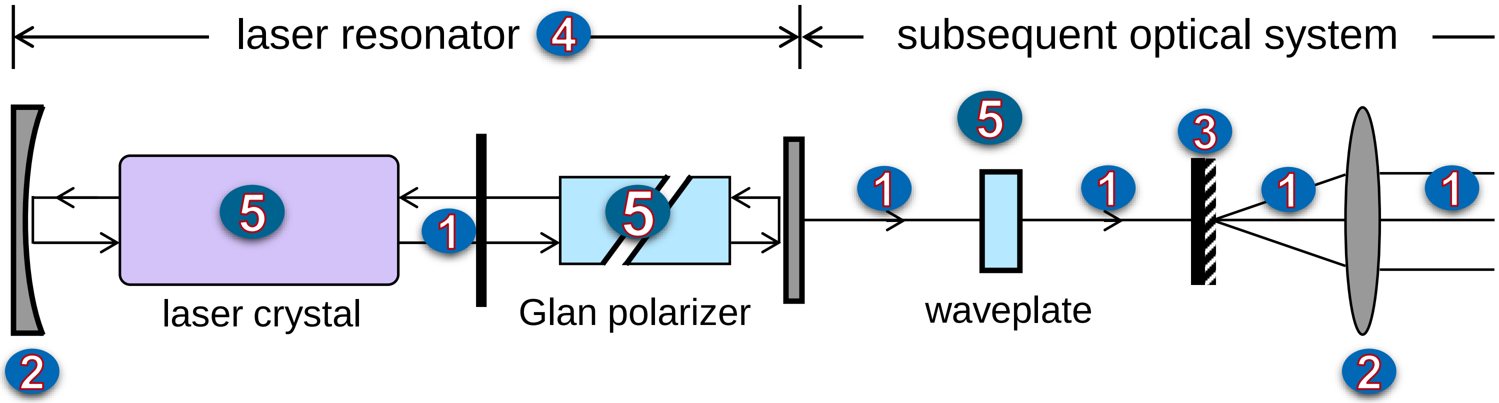

1 Free space: Diffraction integral

2 Lens & mirror: Geometrical optics

11:00 – 12:30 Propagation techniques. For a vectorial physical-optics propagation through lenses, freeform surfaces, lens arrays, crystals, gratings, etalons, waveplates, microstructures, gratings, scattering surfaces, GRIN media, and diffractive optical elements VirtualLab provides a bundle of techniques like local boundary operators (LPIA), coating matrix, Fourier Modal Method (FMM), perfectly matched layer, split-step-type solvers, Mie scattering, Thin Element Approximation (TEA), and GRIN media propagation.

12:30 – 13:30 Lunch (included in the free seminar)

Polarization Conversion

[Izdebskaya 2009] Izdebskaya *et al.*, "**Dynamics of linear polarization conversion in uniaxial crystals**," Opt. Express **17**, 18196-18208 (2009)

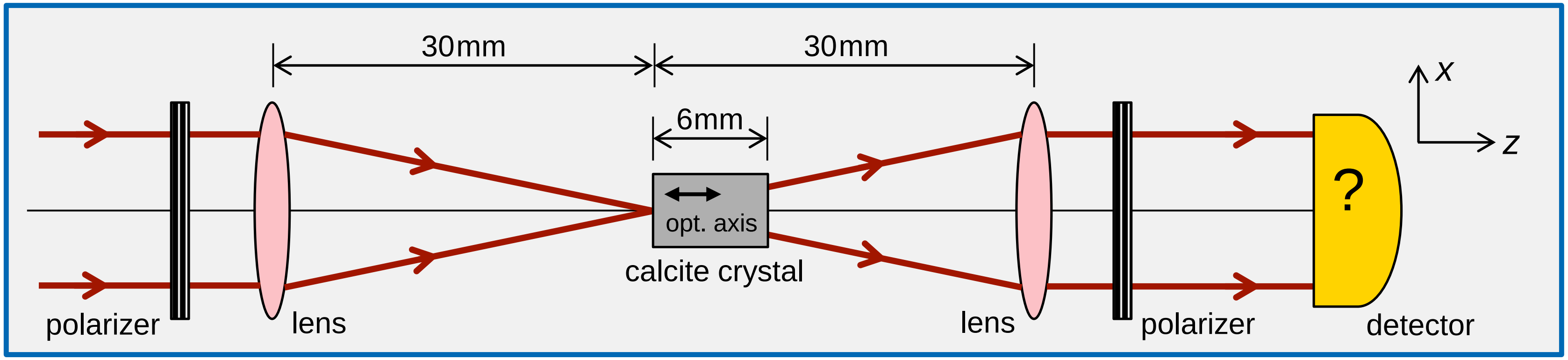

- input field type: Gaussian Hermite mode (0,0)
- waist radius: 1.5×1.5 mm
- wavelength: 633 nm
- polarization: linear in *x*
- focal length: 30 mm
- crystal length: 6 mm
- crystal type: calcite (uniaxial) with n_o= 1.6558, n_e= 1.4852

Polarization Conversion

topological quadrupole [simulation]

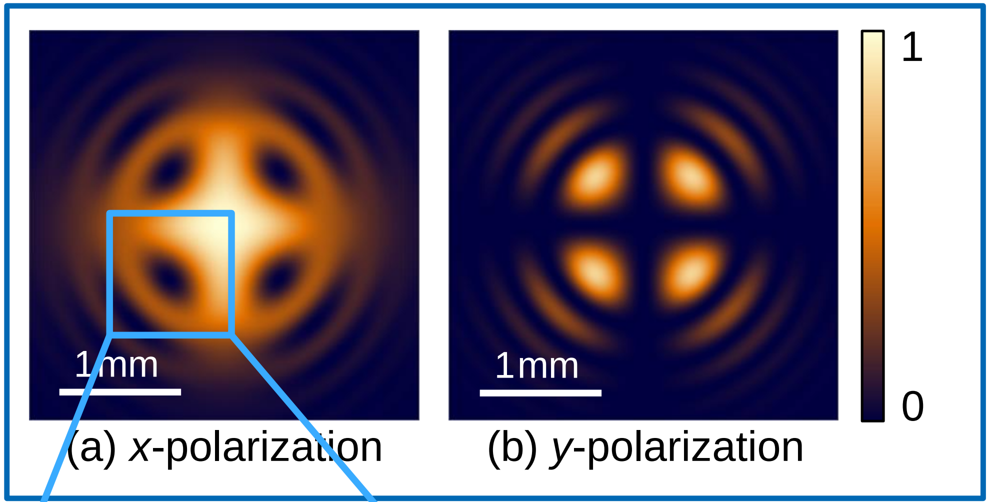

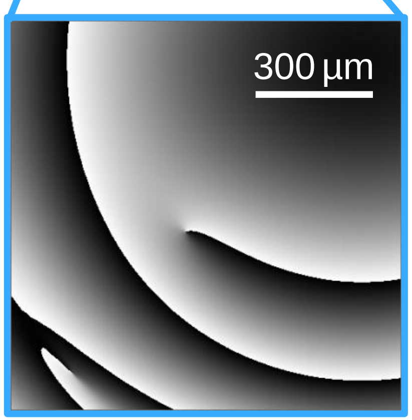

phase in
selected region

experimental measurements

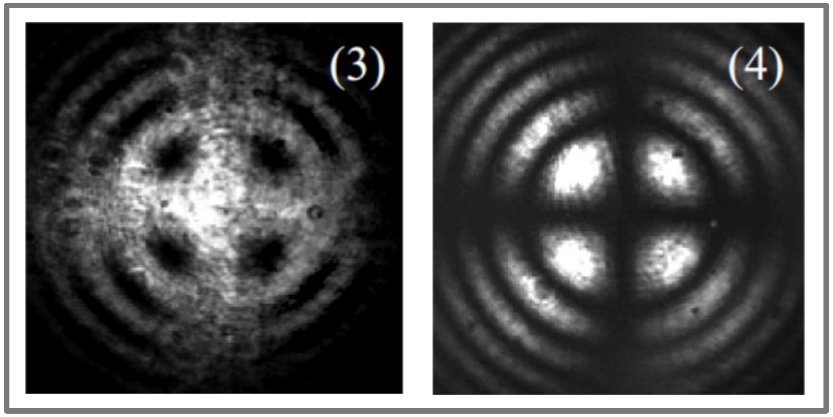

Fig. 4 from [Izdebskaya 2009]

Fast Physical Optics by Field Tracing

In **Fast Physical Optics** we comply with the following strategies:

1. Tearing: The optical system is decomposed into various regions in which different types of specialized Maxwell solvers are applied.

2. Interconnection: The solutions per region are connected through non-sequential field tracing to solve Maxwell's equations in the entire system.

Interconnection of Regional Maxwell Solvers

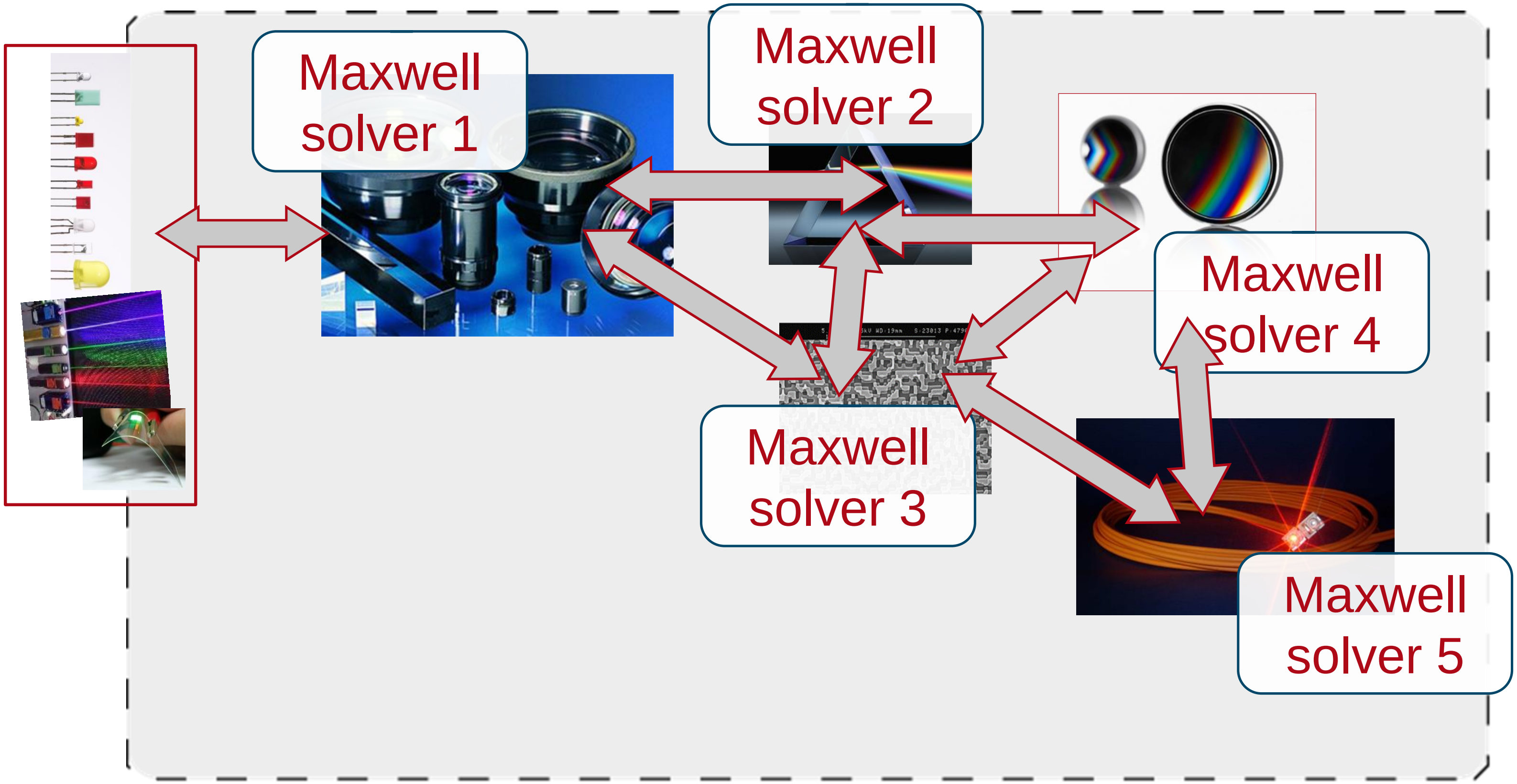

Fast Physical Optics by Field Tracing

In **Fast Physical Optics** we comply with the following strategies:

1. Tearing: The optical system is decomposed into various regions in which different types of specialized Maxwell solvers are applied.

2. Interconnection: The solutions per region are connected through non-sequential field tracing to solve Maxwell's equations in the entire system.

Non-Sequential Optical Field Tracing

Michael Kuhn, Frank Wyrowski, and Christian Hellmann

Kuhn, M.; Wyrowski, F. & Hellmann, C. (2012), Non-sequential optical field tracing, *in* T. Apel & O. Steinbach, ed., 'Finite Element Methods and Applications', Springer-Verlag, Berlin, , pp. 257-274.

Fast Physical Optics by Field Tracing

In **Fast Physical Optics** we comply with the following strategies:

1. Tearing: The optical system is decomposed into various regions in which different types of specialized Maxwell solvers are applied.

2. Interconnection: The solutions per region are connected through non-sequential field tracing to solve Maxwell's equations in the entire system.

Surface Channels

- Setting A

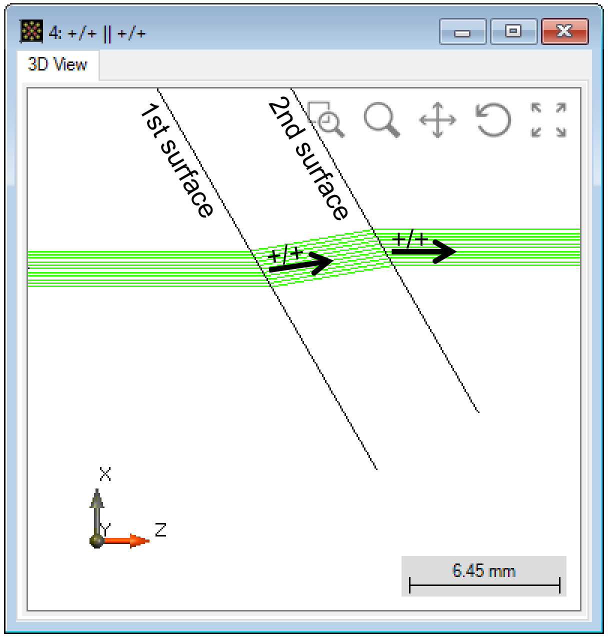

Surface	+/+	+/-	-/-	-/+
1st	×			
2nd	×			

- Setting B

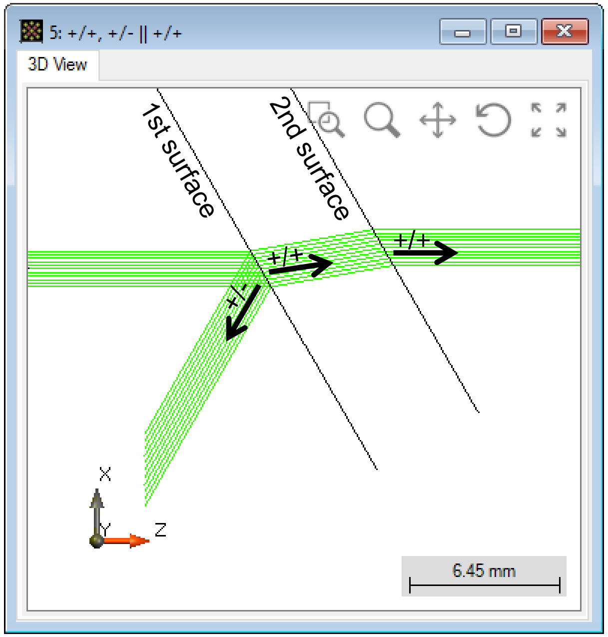

Surface	+/+	+/-	-/-	-/+
1st	×	×		
2nd	×			

Surface Channels

- Setting C

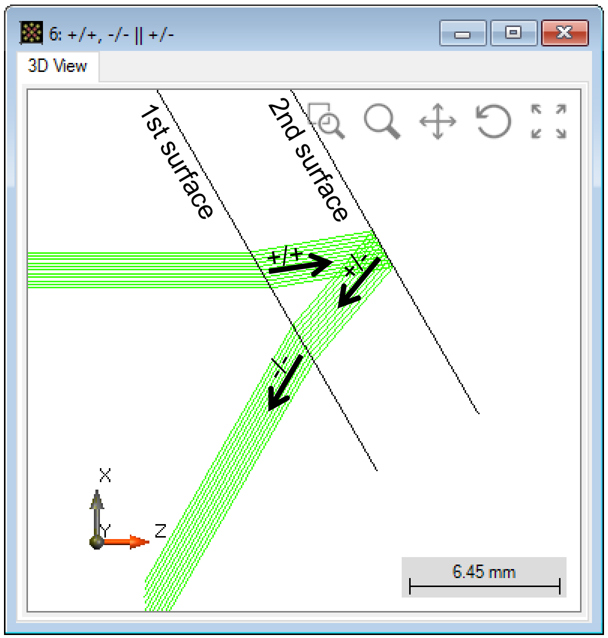

Surface	+/+	+/-	-/-	-/+
1st	×		×	
2nd		×		

- Setting D

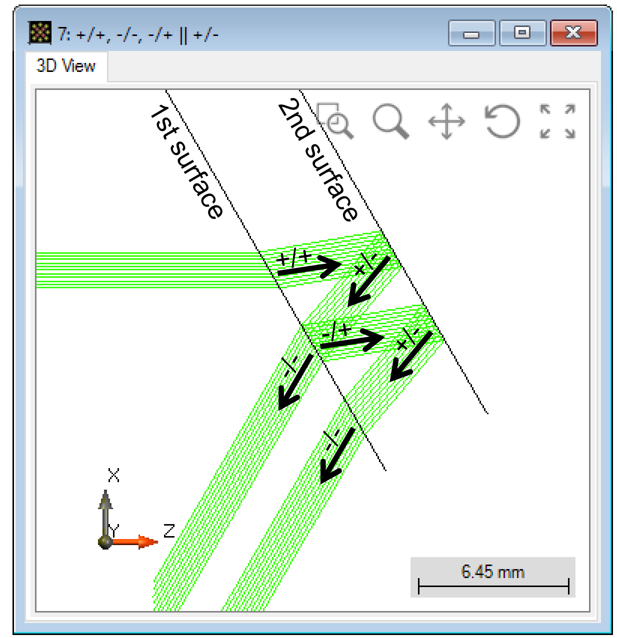

Surface	+/+	+/-	-/-	-/+
1st	×		×	×
2nd		×		

Surface Channels

- Setting E

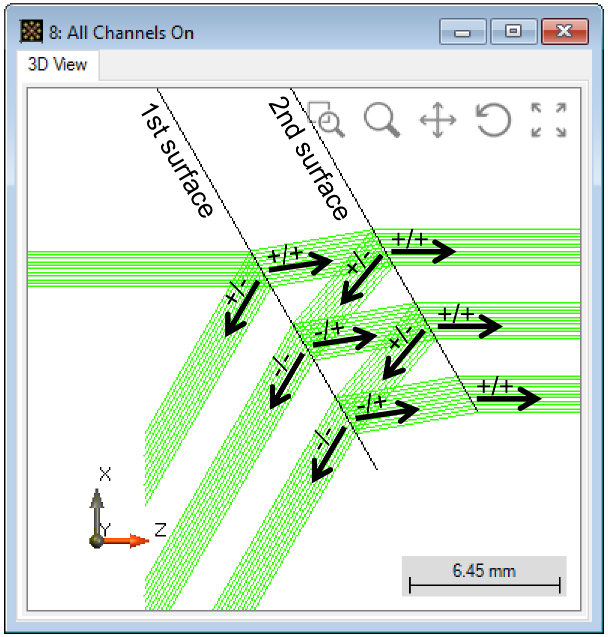

Surface	+/+	+/-	-/-	-/+
1st	×	×	×	×
2nd	×	×	×	×

Note: an activated channel does not necessarily lead to corresponding light path(s). E.g., the -/- and -/+ channel of 2nd interface do not influence the tracing, because there is no backward incidence.

Imaging Systems > Ghost Imaging

Investigation of Ghost Imaging at a Collimation Objective

LightTrans International UG

Task/System Illustration

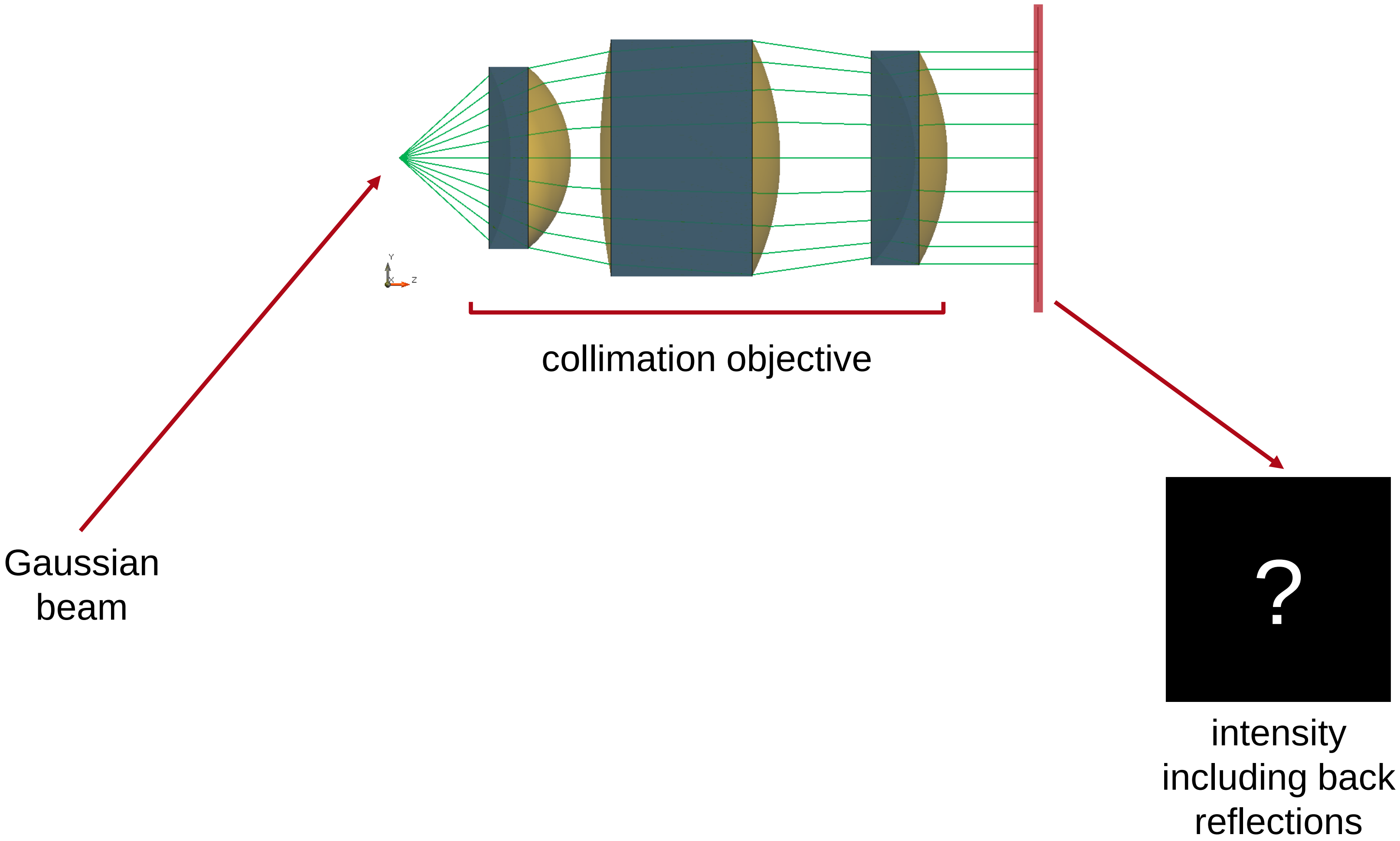

Result: Field Tracing Sequential

sequential overview (without ghost imaging)

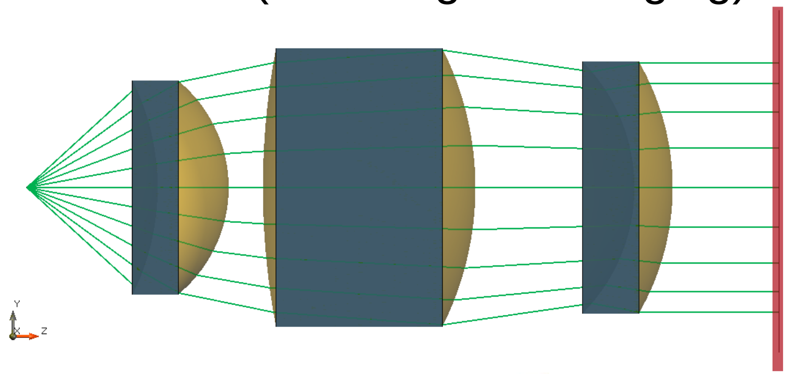

Interface	+/+	+/-	-/-	-/+
	☑	☐	☐	☐
Interface #1 (Conical Interface)	☑	☐	☐	☐
Interface #2 (Conical Interface)	☑	☐	☐	☐
Interface #3 (Conical Interface)	☑	☐	☐	☐
Interface #4 (Conical Interface)	☑	☐	☐	☐
Interface #5 (Conical Interface)	☑	☐	☐	☐
Interface #6 (Conical Interface)	☑	☐	☐	☐

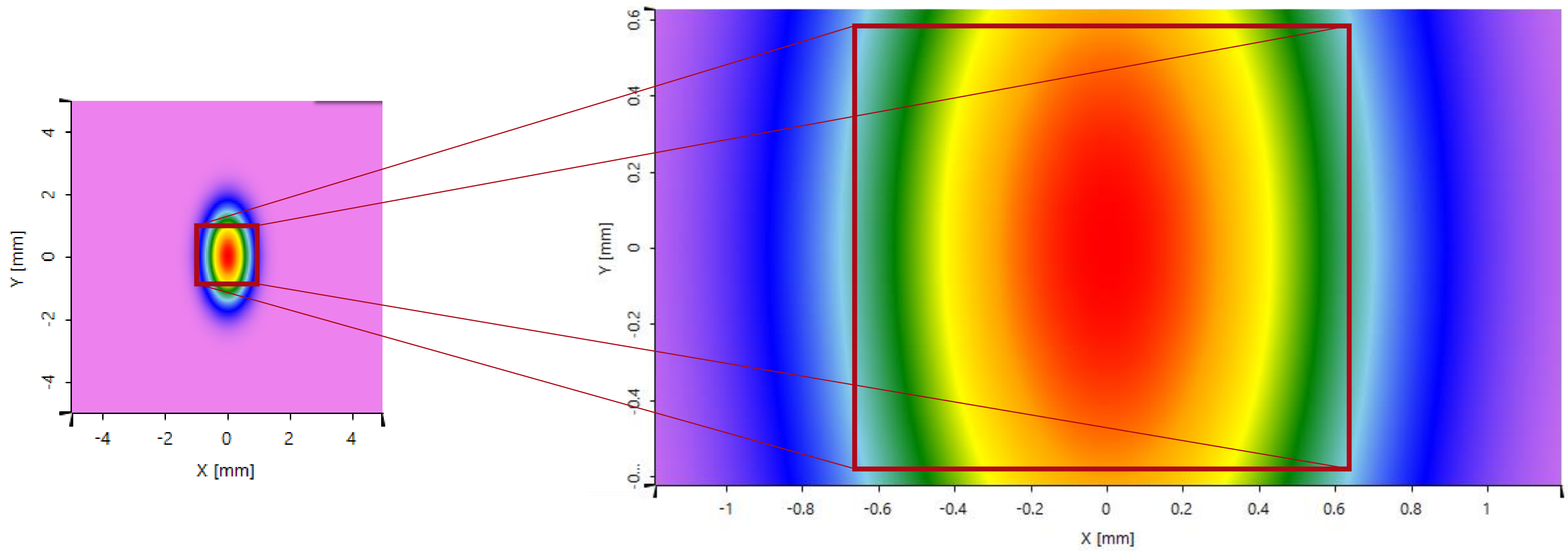

Result: 3D Ray Tracing

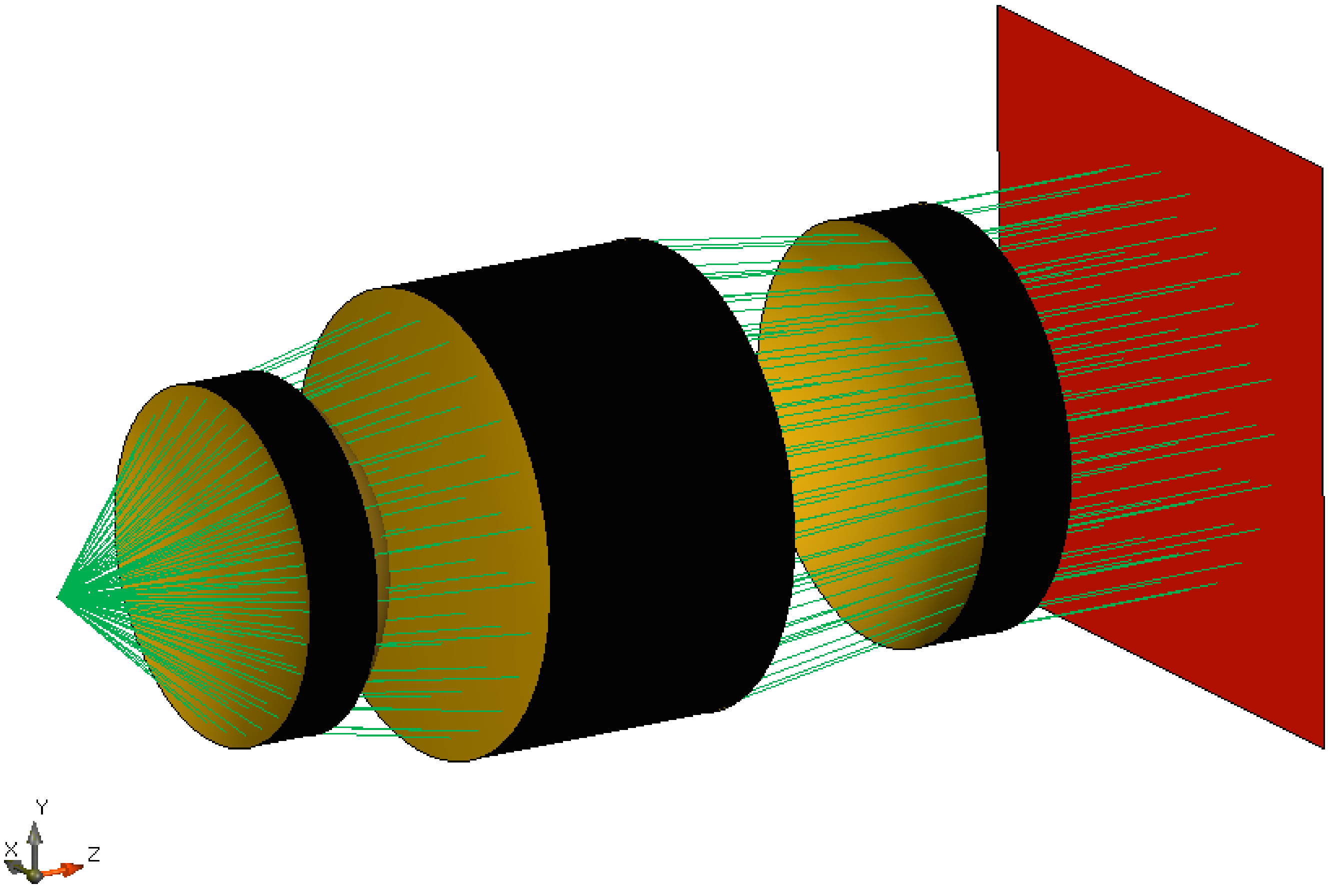

Result: Field Tracing Non-sequential

allowing reflection at first surface of last lens

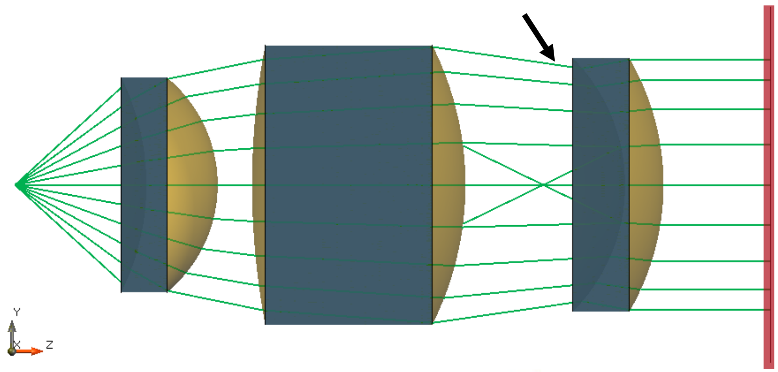

Interface	+/+	+/-	-/-	-/+
	☑	■	☐	■
Interface #1 (Conical Interface)	☑	☐	☐	☐
Interface #2 (Conical Interface)	☑	☐	☐	☐
Interface #3 (Conical Interface)	☑	☐	☐	☐
Interface #4 (Conical Interface)	☑	☐	☐	☑
Interface #5 (Conical Interface)	☑	☑	☐	☐
Interface #6 (Conical Interface)	☑	☐	☐	☐

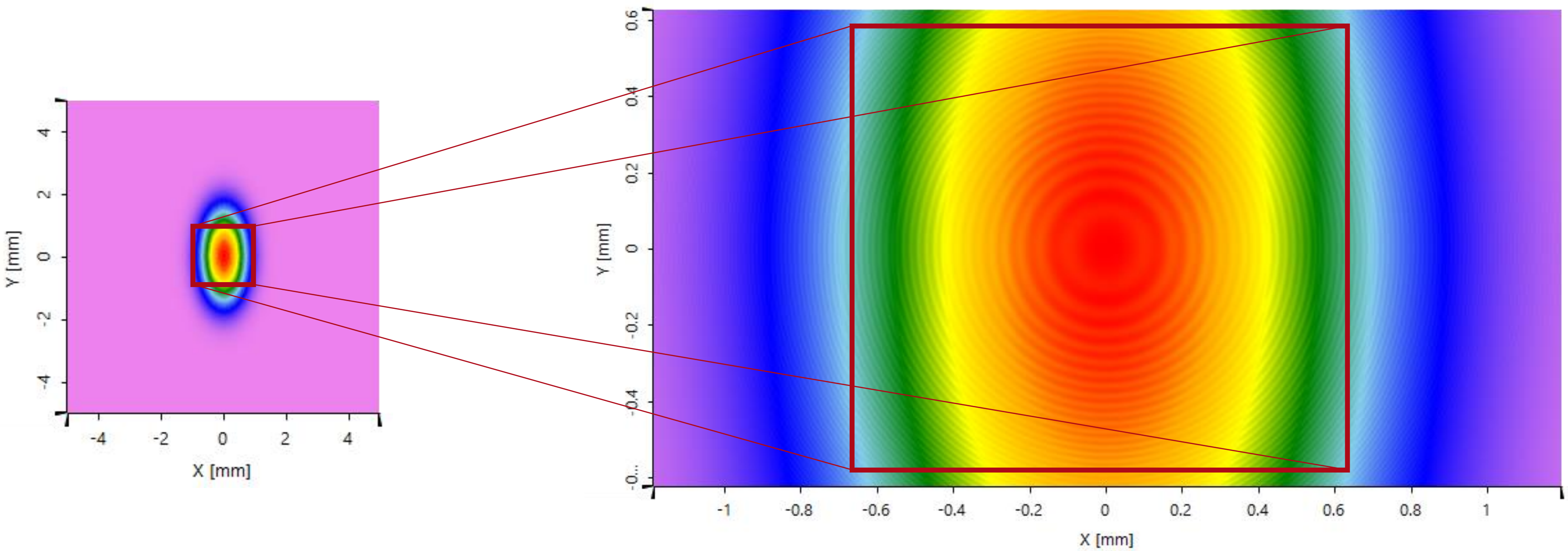

Result: 3D Ray Tracing Non-sequential

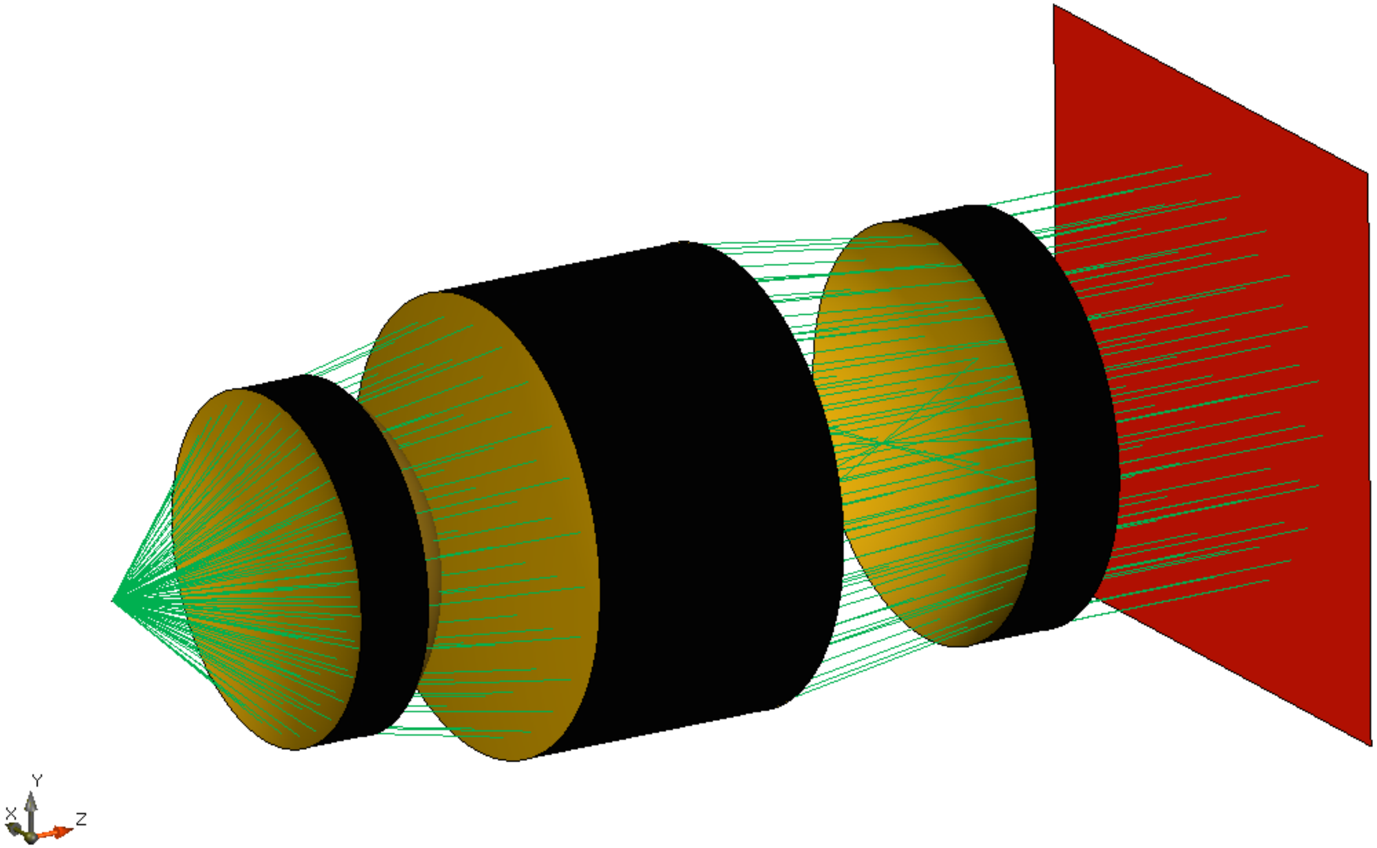

Result: Field Tracing Full Non-sequential

allowing reflection at all surfaces at all lenses (full non-sequential)

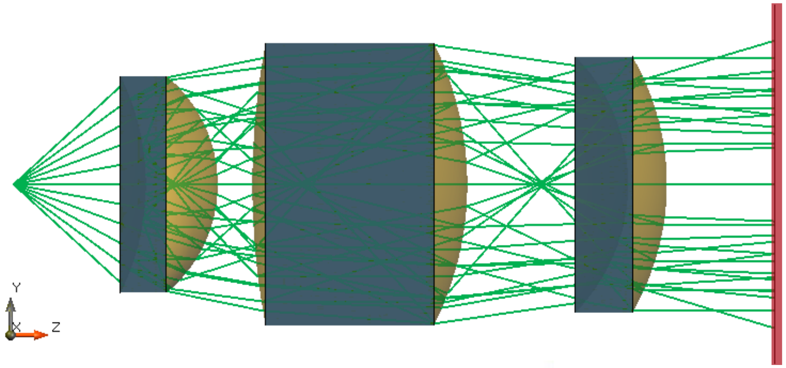

Interface	+/+	+/-	-/-	-/+
	☑	☑	☑	☑
Interface #1 (Conical Interface)	☑	☑	☑	☑
Interface #2 (Conical Interface)	☑	☑	☑	☑
Interface #3 (Conical Interface)	☑	☑	☑	☑
Interface #4 (Conical Interface)	☑	☑	☑	☑
Interface #5 (Conical Interface)	☑	☑	☑	☑
Interface #6 (Conical Interface)	☑	☑	☑	☑

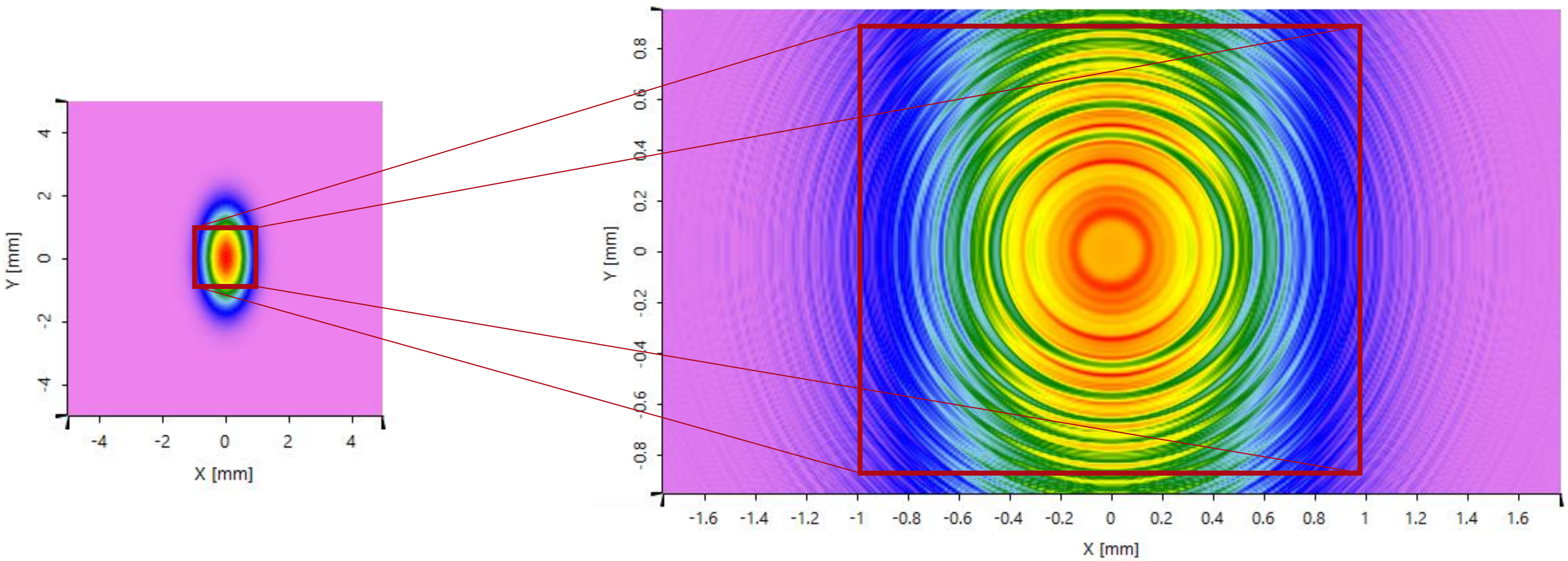

Non-sequential Field Tracing

Coupled Surfaces Analysis by Using Non-sequential Field Tracing

Theory Background

- Global S matrix

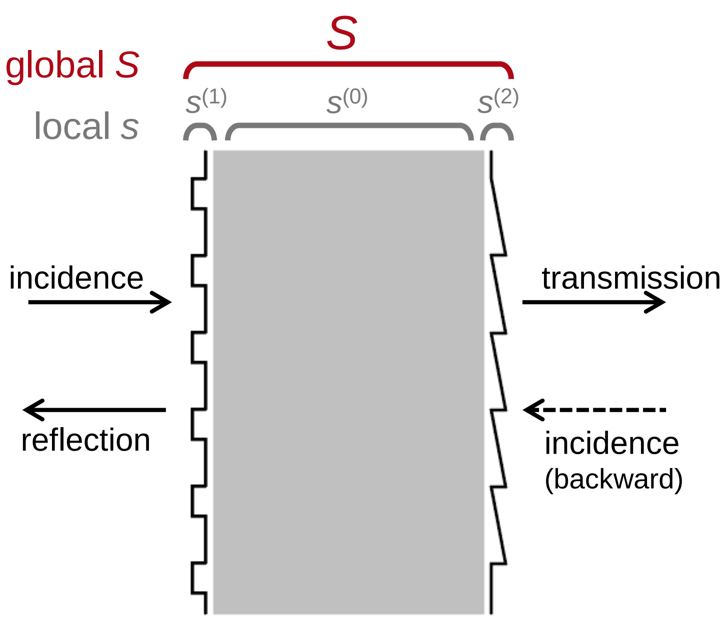

  - Recursion with respect to number of regions / layers

- Non-sequential field tracing

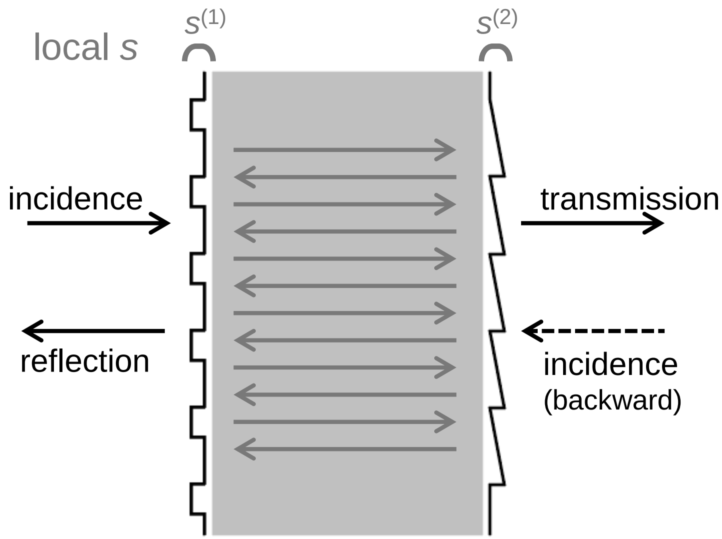

  - Recursion with respect to number of light paths

Planar Surface + Planar Surface

- Structure

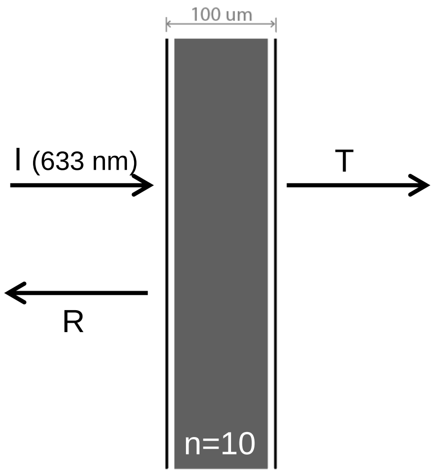

Global S matrix

Eff. (T)	Eff. (R)
4.04%	96%

- Non-sequential field tracing

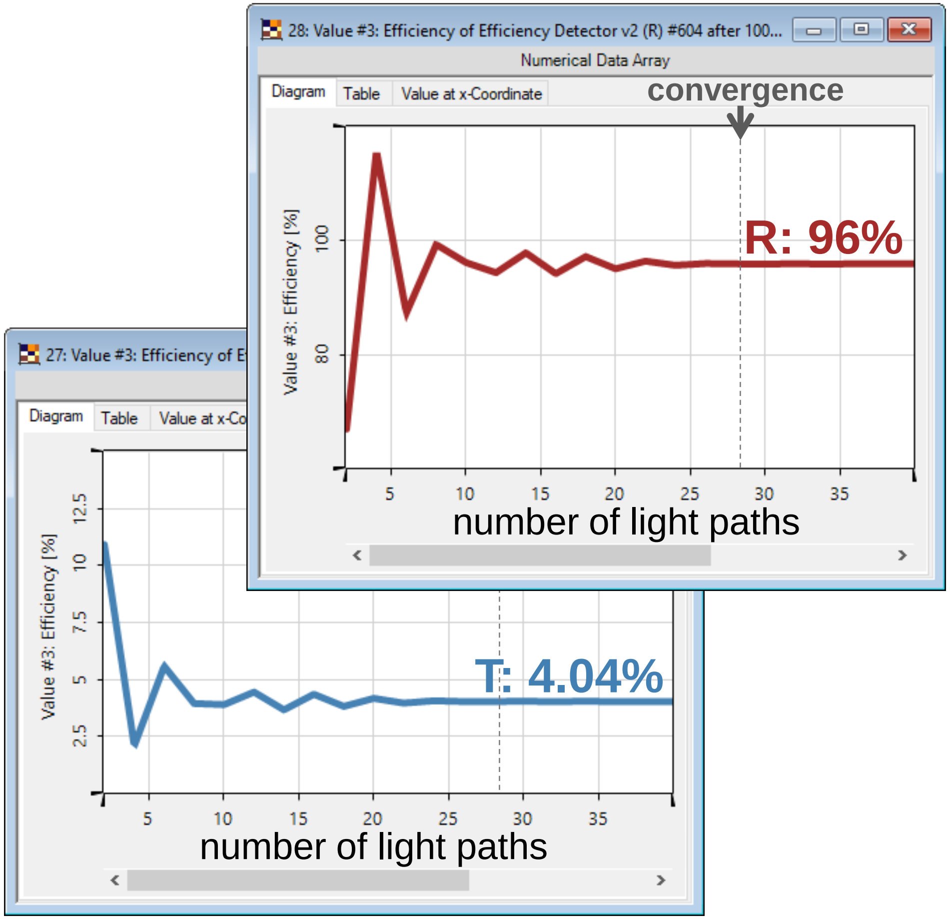

Rectangular + Sawtooth Grating (parallel)

- Single grating

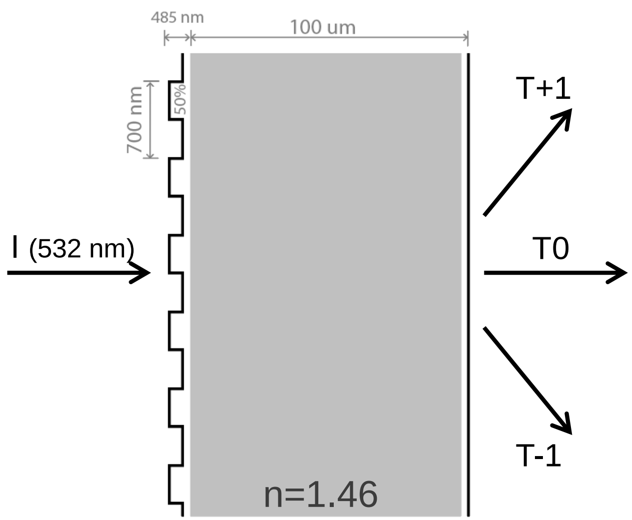

Global S matrix (TM)

T	Eff.	R	Eff.
±1	31.9%	±1	1.26%
0	30.6%	0	3.03%

- ... with sawtooth coating

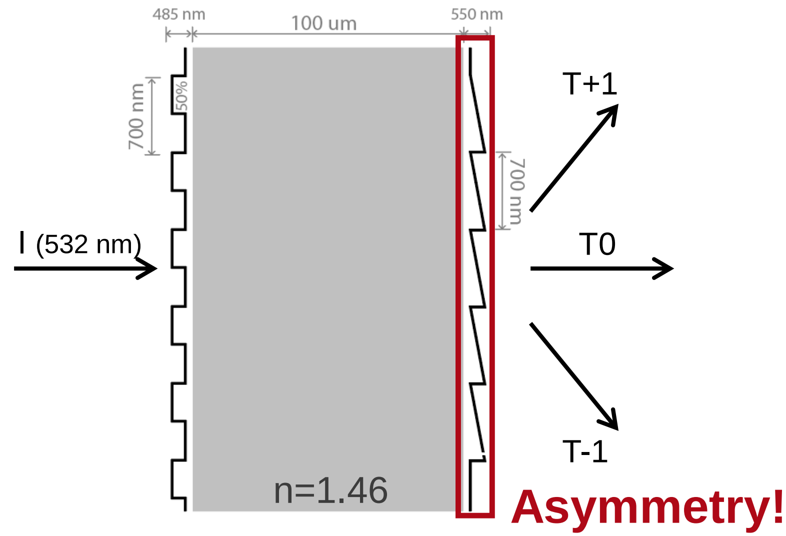

Global S matrix (TM)

T	Eff.	R	Eff.
-1	28.1%	-1	0.65%
0	18.2%	0	0.923%
+1	51.4%	+1	0.74%

Rectangular + Sawtooth Grating (parallel)

- Non-sequential field tracing

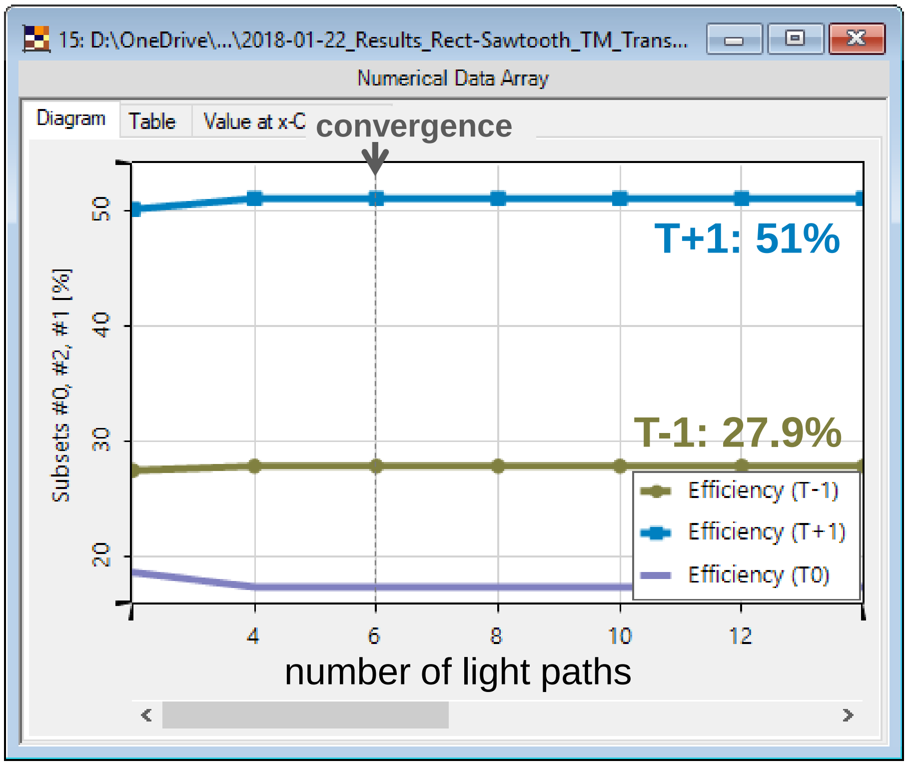

- ... with sawtooth coating

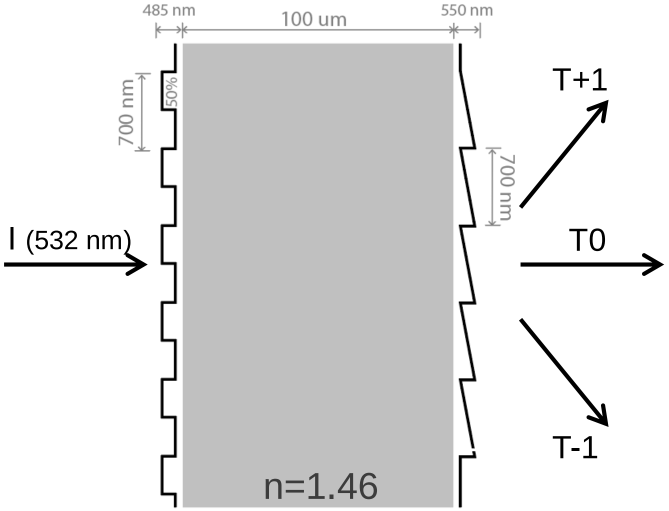

Global S matrix (TM)

T	Eff.	R	Eff.
-1	28.1%	-1	0.65%
0	18.2%	0	0.923%
+1	51.4%	+1	0.74%

Rectangular + Sawtooth Grating (parallel)

- Non-sequential field tracing

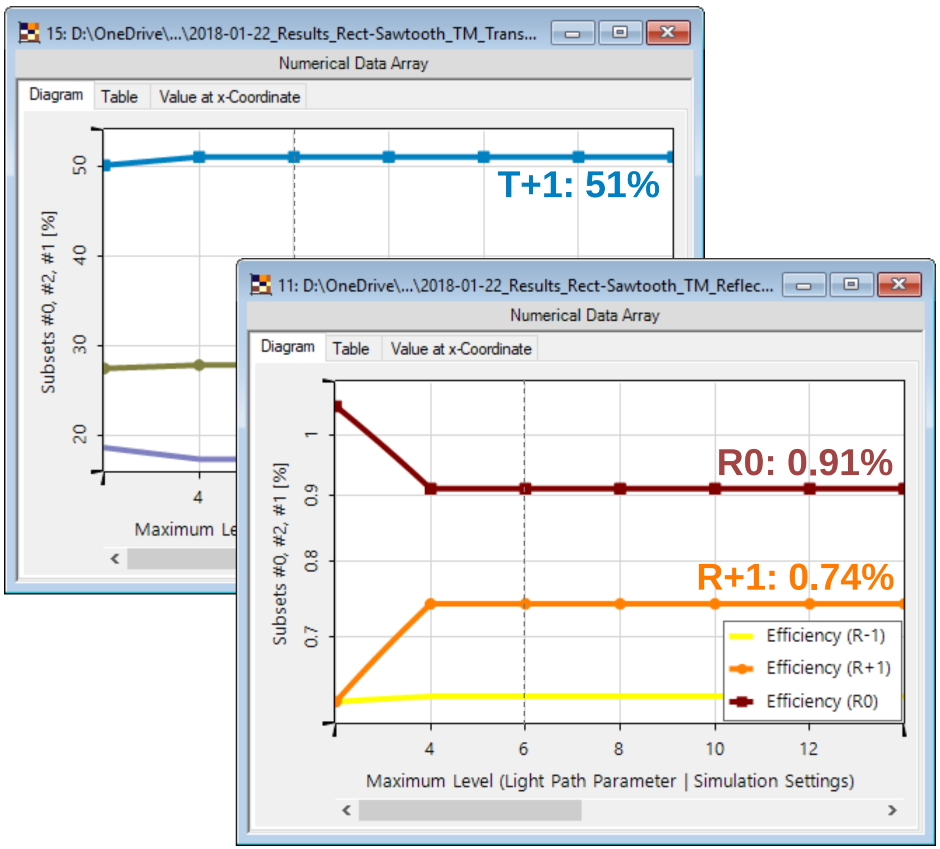

- ... with sawtooth coating

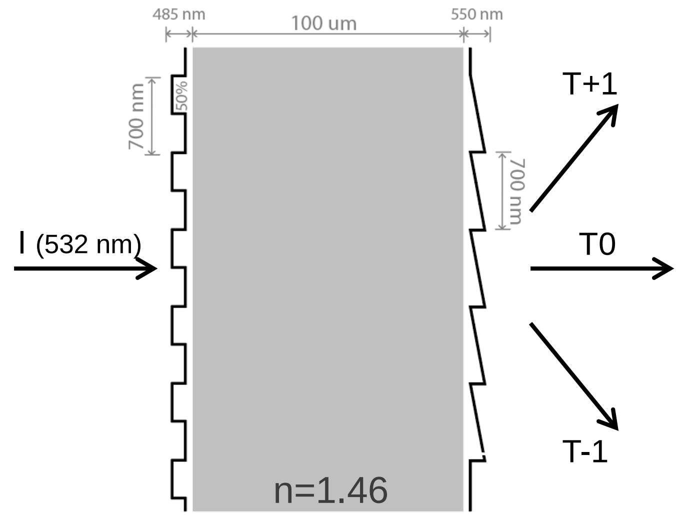

Global S matrix (TM)

T	Eff.	R	Eff.
-1	28.1%	-1	0.65%
0	18.2%	**0**	**0.923%**
+1	51.4%	**+1**	**0.74%**

Computational Effort

- Parallel gratings

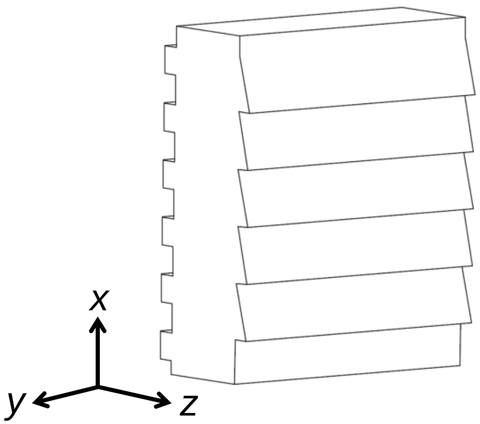

Global S matrix	Non-sequential field tracing
$\sim M^3$ (scaling with number of layers)	$\sim M^3$ (scaling with number of light paths)

with M as the number of diffraction (evanescent included) orders used in calculation

- Crossed gratings

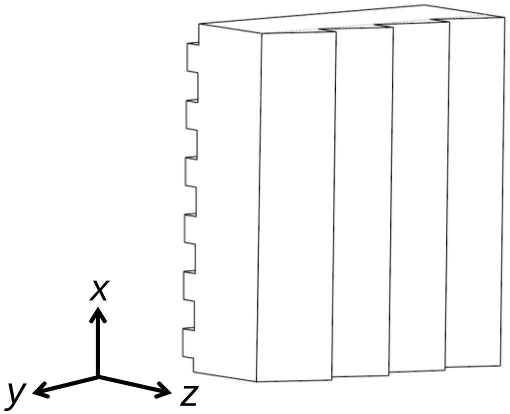

Global S matrix	Non-sequential field tracing
$\sim(M_x \times M_y)^3$ (scaling with number of layers)	$\sim(M_x^3 + M_y^3)$ (scaling with number of light paths)

with M_x and M_y as the number of diffraction (evanescent included) orders in both directions

Rectangular + Sawtooth Grating (crossed)

- Structure
  - Front: rectangular grating
    (along *x* direction)
  - Back: sawtooth grating
    (along *y* direction)

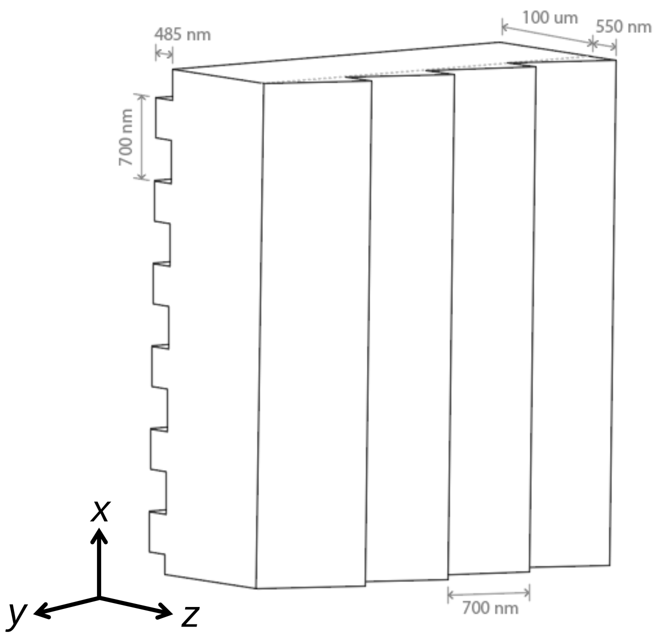

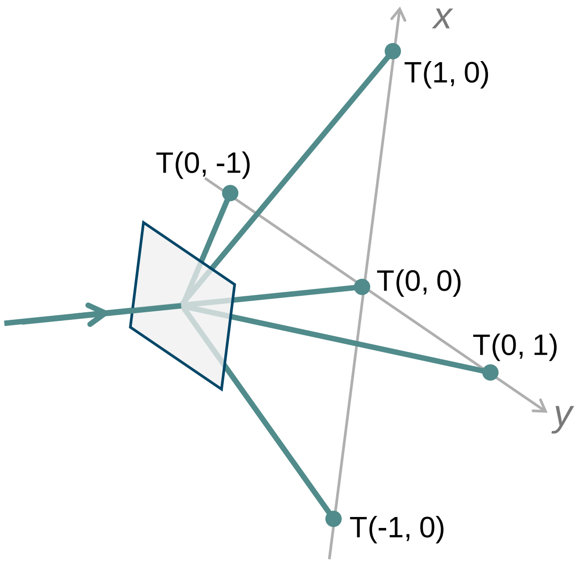

Global S matrix (TM)

T	Eff.	R	Eff.
-1, 0	5.4%	-1, 0	5.7%
0, -1	4.2%	0, -1	5.8%
0, 0	4.5%	0, 0	13.8%
0, 1	44.9%	0, 1	4.6%
1, 0	5.4%	1, 0	5.7%

Rectangular + Sawtooth Grating (crossed)

- Non-sequential field tracing (TM)

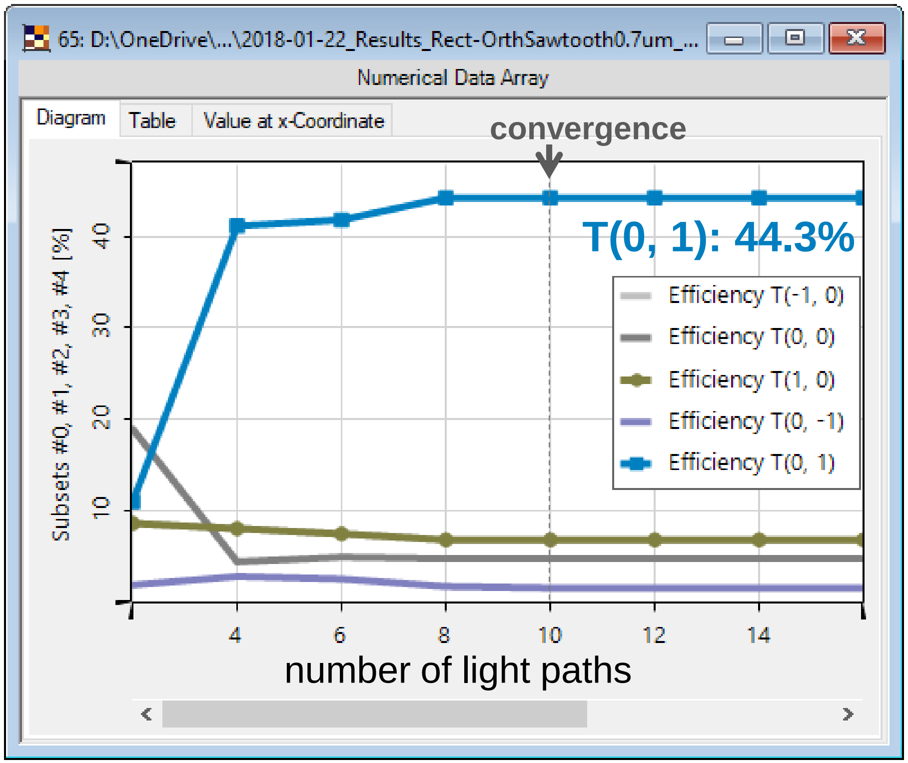

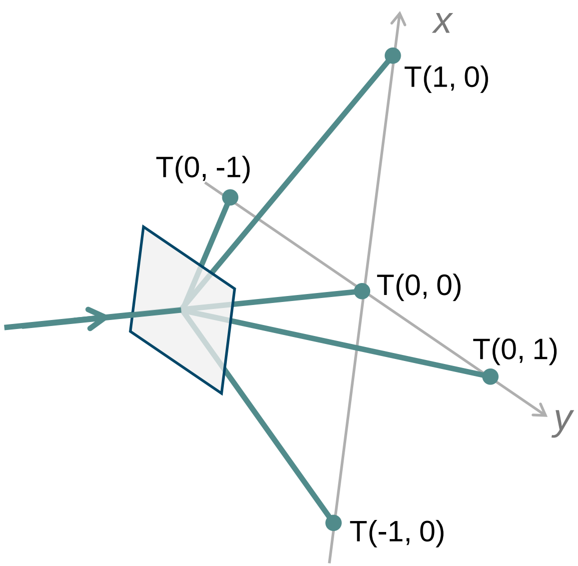

Global S matrix (TM)

T	Eff.	R	Eff.
-1, 0	5.4%	-1, 0	5.7%
0, -1	4.2%	0, -1	5.8%
0, 0	4.5%	0, 0	13.8%
0, 1	**44.9%**	0, 1	4.6%
1, 0	5.4%	1, 0	5.7%

Rectangular + Sawtooth Grating (crossed)

- Non-sequential field tracing (TE) **Polarization included!**

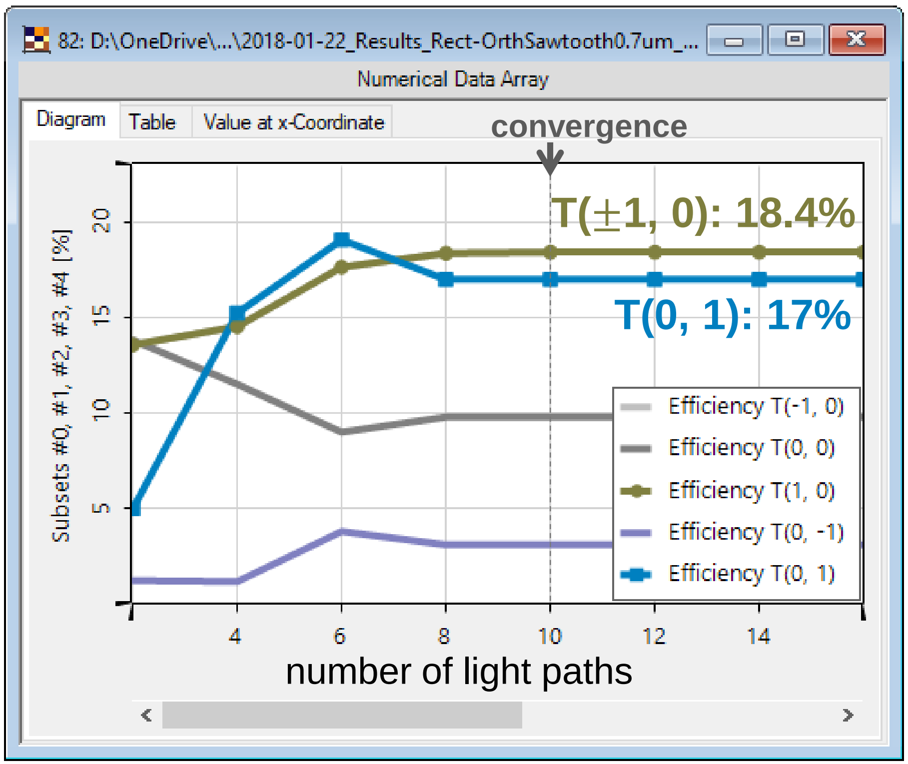

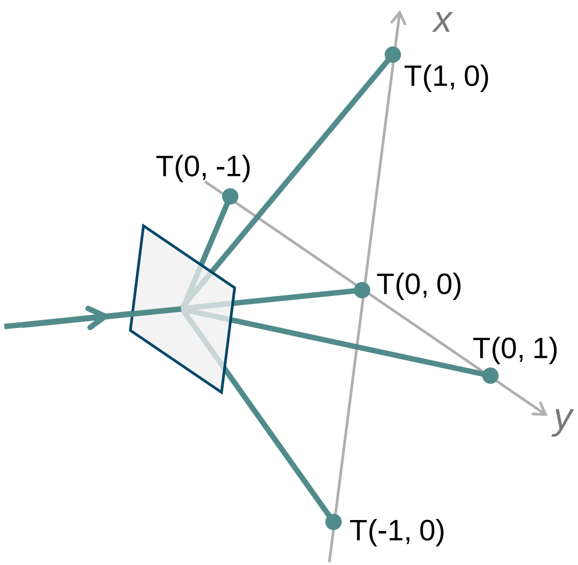

Global S matrix (TE)

T	Eff.	R	Eff.
-1, 0	**18%**	-1, 0	1.1%
0, -1	2.8%	0, -1	0.46%
0, 0	11.9%	0, 0	22.6%
0, 1	**17.1%**	0, 1	6.89%
1, 0	**18%**	1, 0	1.1%

Rectangular + Sawtooth Grating (45° rotated)

- Structure
  - Front: rectangular grating
    (along *x* direction)
  - Back: sawtooth grating
    (along *x*-*y* diagonal direction)

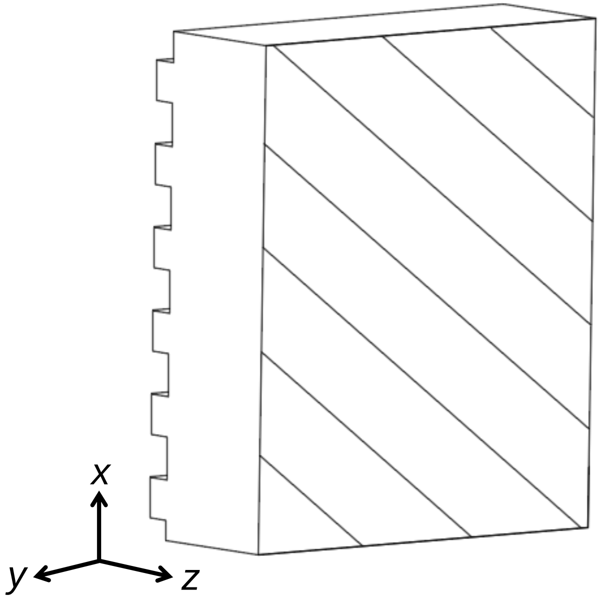

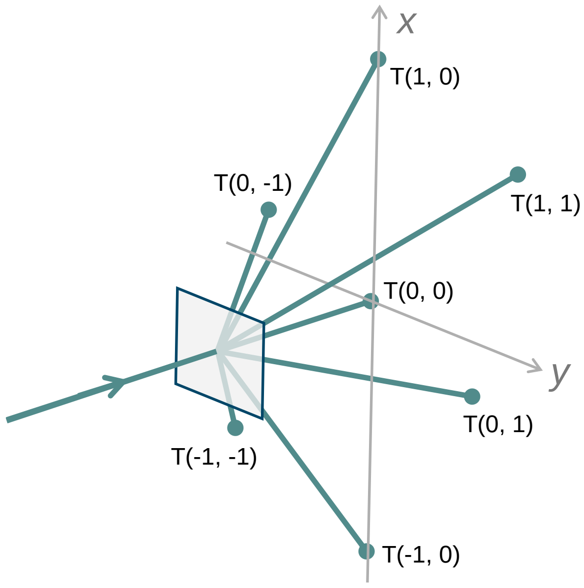

Global S matrix (TM)
➔ No common period!
➔ Huge computational effort even with approximated common period

Rectangular + Sawtooth Grating (45° rotated)

- Non-sequential field tracing (TM)

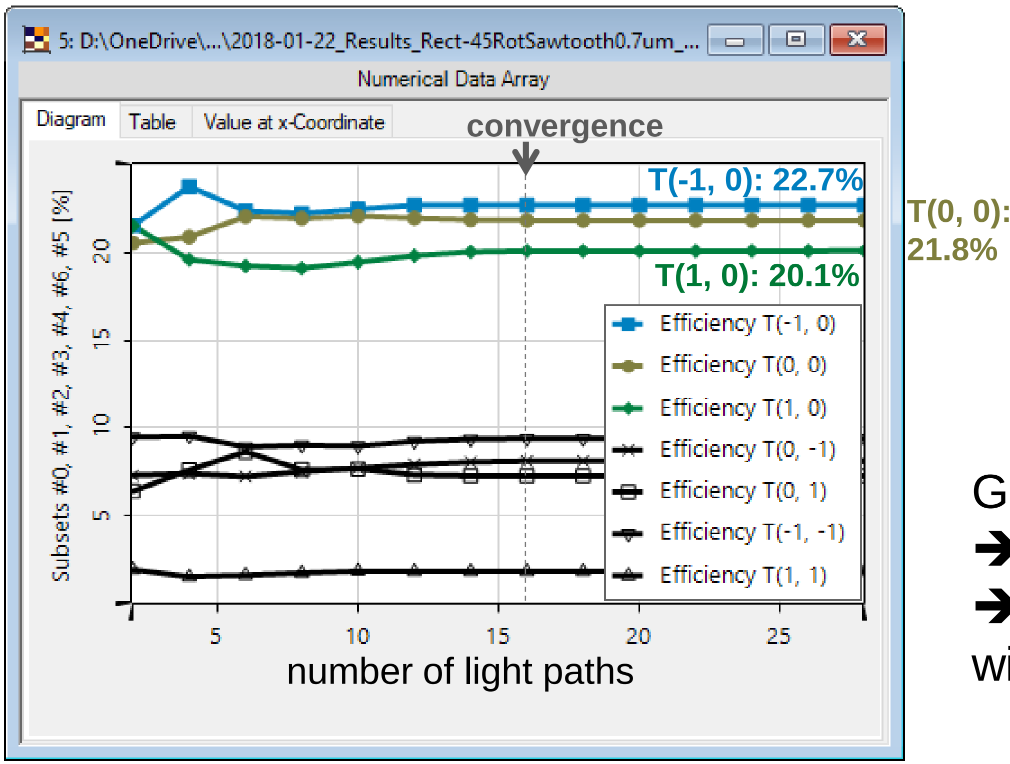

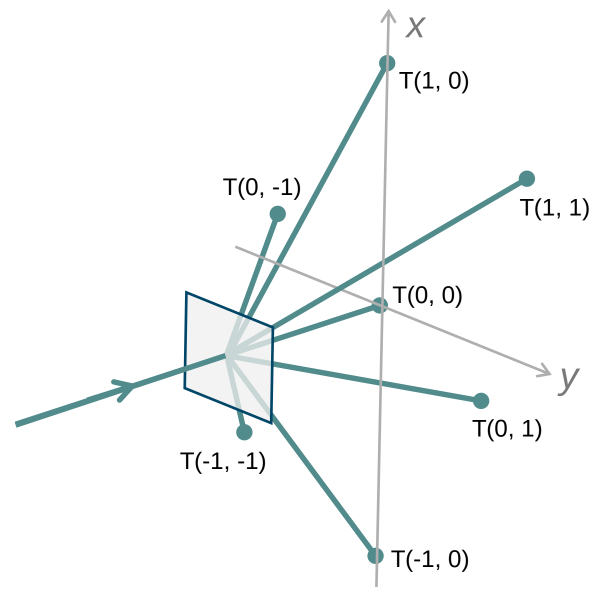

Global S matrix ***NOT*** possible!
➔ No common period
➔ Huge computational effort even with approximated common period

Document & Technical Info

code	
version of document	1.0
title	Coupled Surfaces Analysis by Using Non-sequential Field Tracing
category	Non-sequential Field Tracing
author	Site Zhang (LightTrans)
used VL version	7.2.0.2

Specifications of PC Used for Simulation	
Processor	i7-4910MQ (4 CPU cores)
RAM	32 GB
Operating System	Windows 10

Fast Physical Optics by Field Tracing

In **Fast Physical Optics** we comply with the following strategies:

1. Tearing: The optical system is decomposed into various regions in which different types of specialized Maxwell solvers are applied.

2. Interconnection: The solutions per region are connected through non-sequential field tracing to solve Maxwell's equations in the entire system.

3. Field operations should be linear in the number of field samples N.

Rigorous Propagation in Homogeneous Media

Maxwell's equations in x-domain:

$$\nabla \times \boldsymbol{E}(\boldsymbol{r},\omega) = \mathrm{i}\omega\mu_0 \boldsymbol{H}(\boldsymbol{r},\omega)$$
$$\nabla \times \boldsymbol{H}(\boldsymbol{r},\omega) = -\mathrm{i}\omega\epsilon_0\check{\epsilon}_{\mathrm{r}}(\omega)\boldsymbol{E}(\boldsymbol{r},\omega)$$
$$\nabla \cdot \boldsymbol{E}(\boldsymbol{r},\omega) = 0$$
$$\nabla \cdot \boldsymbol{H}(\boldsymbol{r},\omega) = 0$$

Intergal operator is a N^2 operation!

Rigorous propagation in x-domain (Rayleigh-Sommerfeld integral):

$$V^{\mathrm{out}}(\boldsymbol{\rho},z) \propto \int\int_{-\infty}^{\infty} V^{\mathrm{in}}(\boldsymbol{\rho}',z_0)\frac{\exp(\mathrm{i}k_0\check{n}R)}{R}\left(\mathrm{i}k_0\check{n}-\frac{1}{R}\right)\frac{\Delta z}{R}\,\mathrm{d}^2\rho'$$

with $R = \sqrt{(x-x')^2+(y-y')^2+(\Delta z)^2}$.

Rigorous Propagation in Homogeneous Media

Maxwell's equations in x-domain:

$$\nabla \times \boldsymbol{E}(\boldsymbol{r},\omega) = \mathrm{i}\omega\mu_0 \boldsymbol{H}(\boldsymbol{r},\omega)$$

$$\nabla \times \boldsymbol{H}(\boldsymbol{r},\omega) = -\mathrm{i}\omega\epsilon_0\check{\epsilon}_{\mathrm{r}}(\omega)\boldsymbol{E}(\boldsymbol{r},\omega)$$

$$\nabla \cdot \boldsymbol{E}(\boldsymbol{r},\omega) = 0$$

$$\nabla \cdot \boldsymbol{H}(\boldsymbol{r},\omega) = 0$$

Maxwell's equations in k-domain:

$$\check{\boldsymbol{k}} \times \tilde{\boldsymbol{E}}(\boldsymbol{\kappa},z,\omega) = \omega\mu_0\tilde{\boldsymbol{H}}(\boldsymbol{\kappa},z,\omega)$$

$\check{\boldsymbol{k}}$ … $)\tilde{\boldsymbol{E}}(\boldsymbol{\kappa},z,\omega)$

Simple product is
a *N* operation!

Rigorous propaga n in k-domain:

$$\tilde{V}^{\mathrm{out}}(\boldsymbol{\kappa},z) = \tilde{V}^{\mathrm{in}}(\boldsymbol{\kappa},z_0) \times \exp\left(\mathrm{i}\check{k}_z(\kappa)\Delta z\right)$$

Can be extended to propagation between tilted planes.

Field Tracing in Different Domains

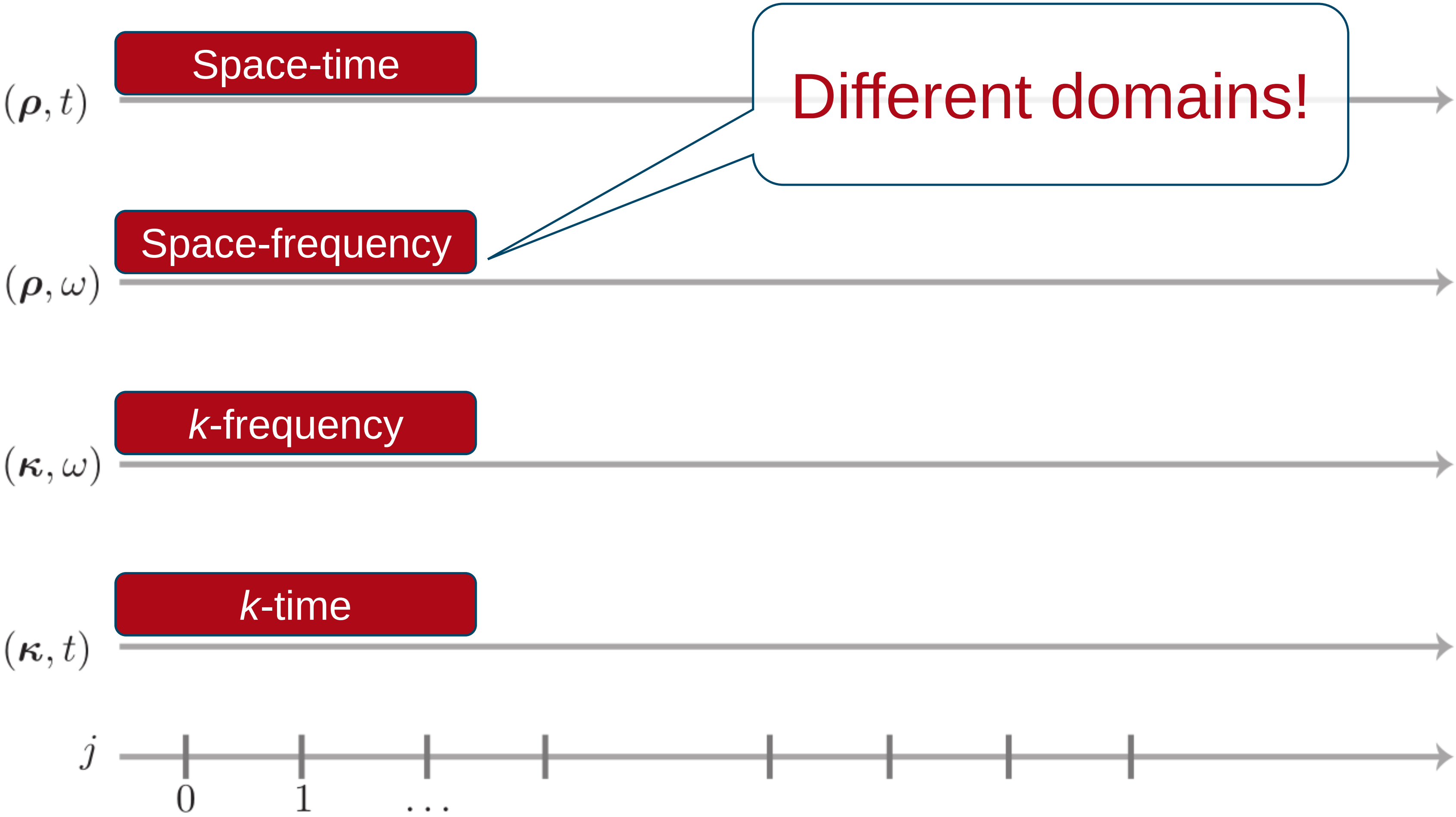

Field Tracing in Different Domains

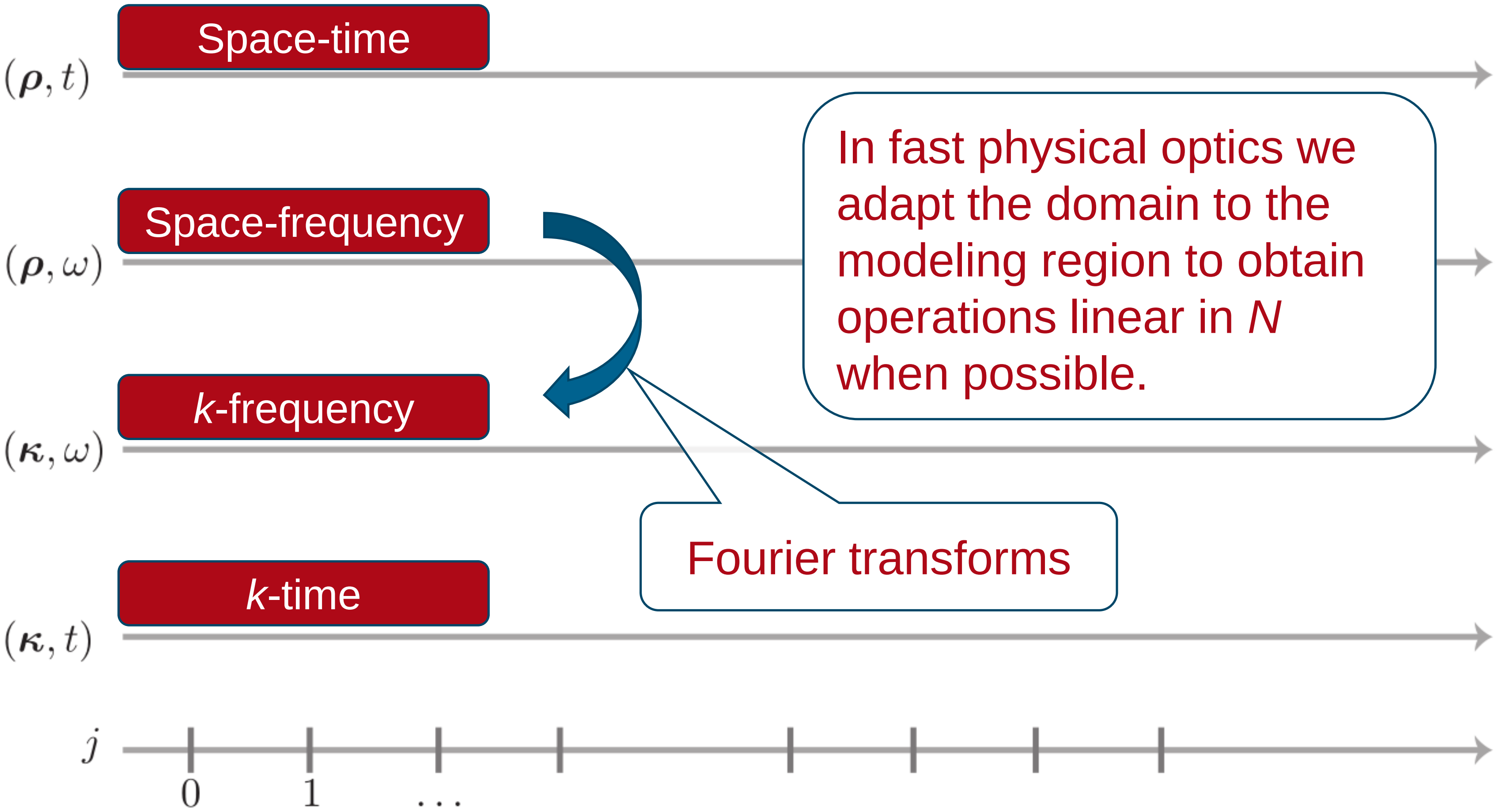

Fast Physical Optics by Field Tracing

In **Fast Physical Optics** we comply with the following strategies:

1. Tearing: The optical system is decomposed into various regions in which different types of specialized Maxwell solvers are applied.

2. Interconnection: The solutions per region are connected through non-sequential field tracing to solve Maxwell's equations in the entire system.

3. Field operations should be linear in the number of field samples N.

Fast Physical Optics by Field Tracing

In **Fast Physical Optics** we comply with the following strategies:

1. Tearing: The optical system is decomposed into various regions in which different types of specialized Maxwell solvers are applied.

2. Interconnection: The solutions per region are connected through non-sequential field tracing to solve Maxwell's equations in the entire system.

3. Field operations should be linear in the number of field samples N.

4. The number of field parameters N should be minimized.

What does it mean for the Fourier transform?

General Example with Aberrations

$$V_\ell(\boldsymbol{\rho},z,\omega) = |V_\ell(\boldsymbol{\rho},z,\omega)|\exp\left(\mathrm{i}\varphi_\ell(\boldsymbol{\rho},z,\omega)\right)\exp\left(\mathrm{i}\psi(\boldsymbol{\rho},z,\omega)\right)$$

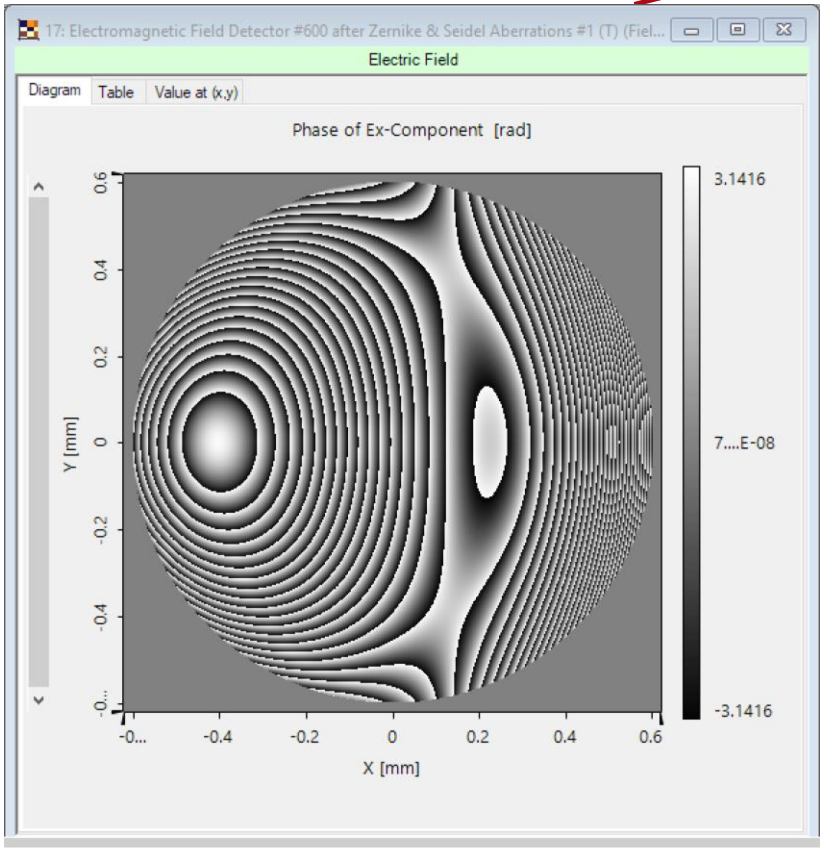

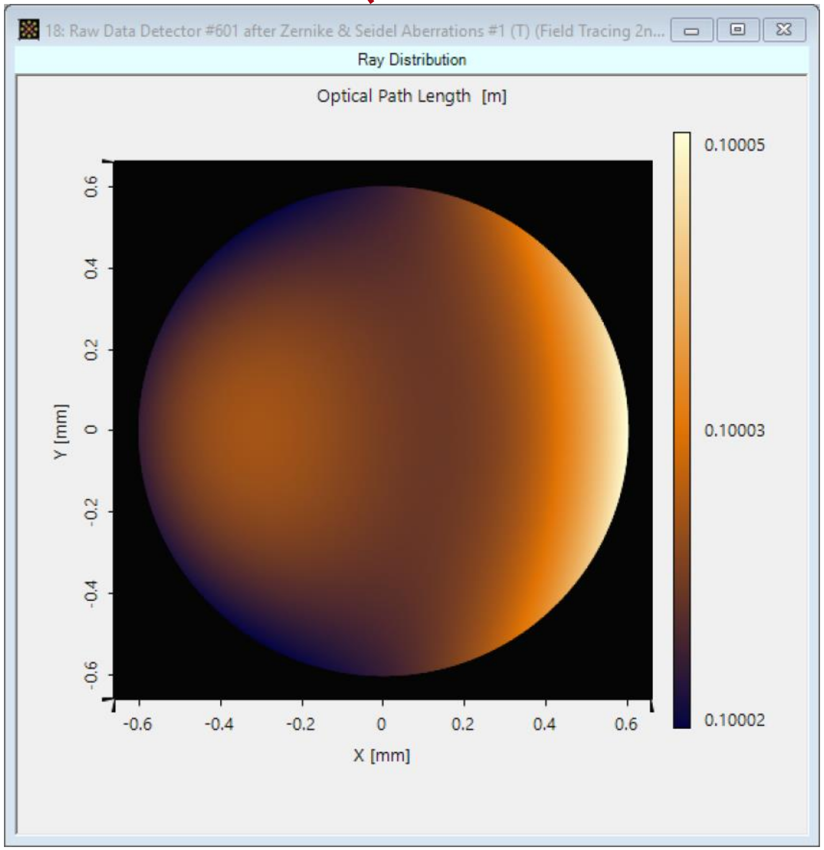

Example Spherical Field with Stop

$$V_\ell(\boldsymbol{\rho},z,\omega) = |V_\ell(\boldsymbol{\rho},z,\omega)| \exp\left(\mathrm{i}\varphi_\ell(\boldsymbol{\rho},z,\omega)\right) \exp\left(\mathrm{i}\psi(\boldsymbol{\rho},z,\omega)\right)$$

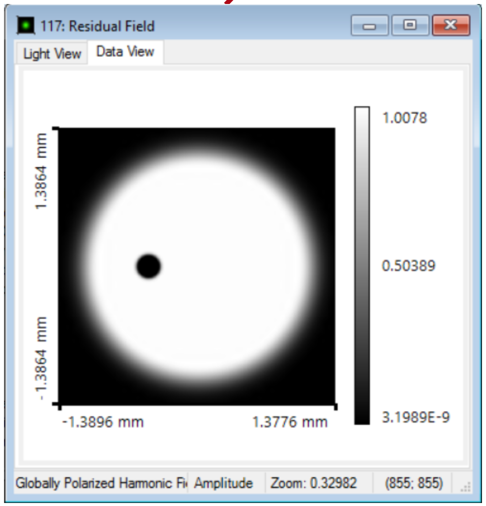

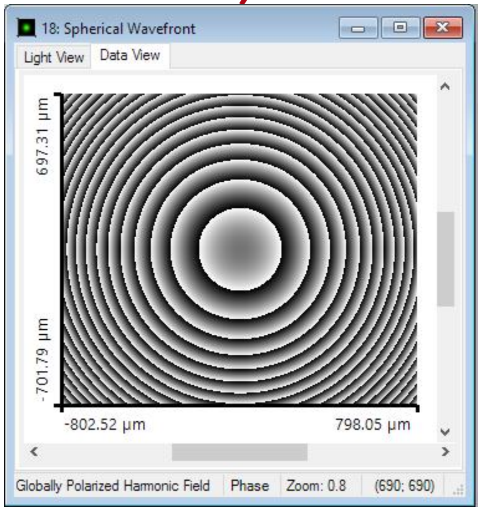

Simulation for Spherical Field with Stop

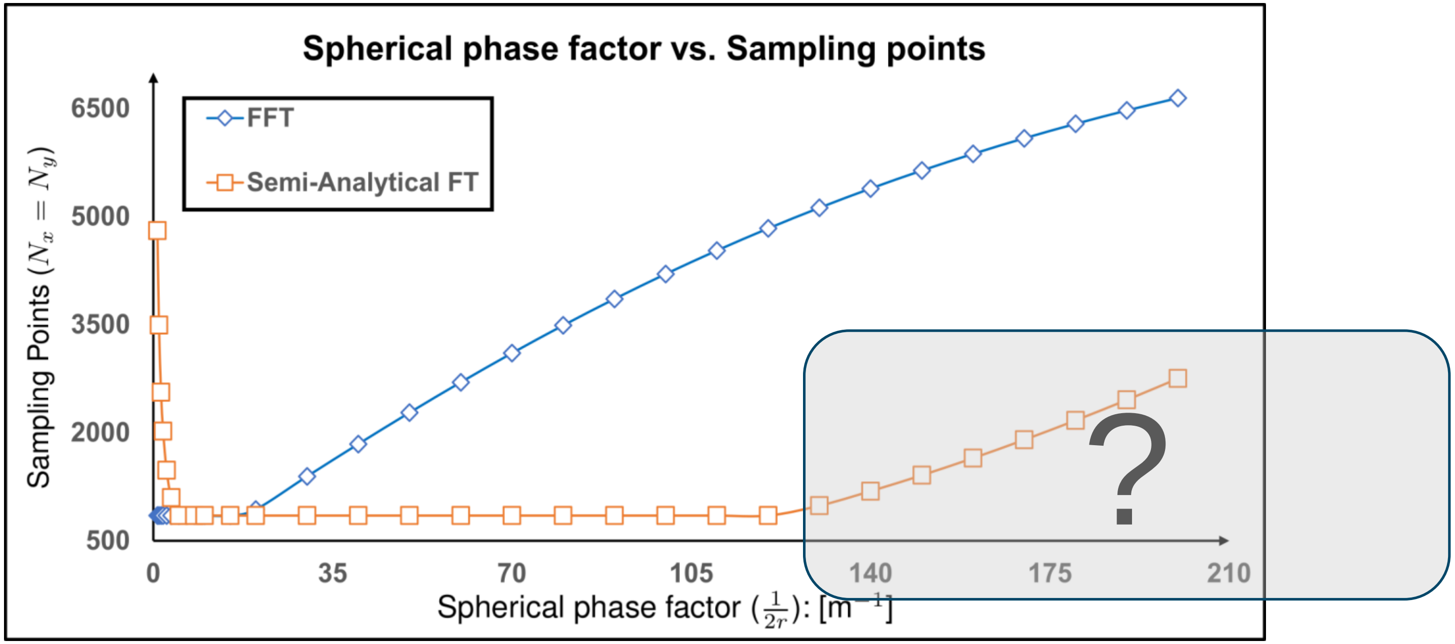

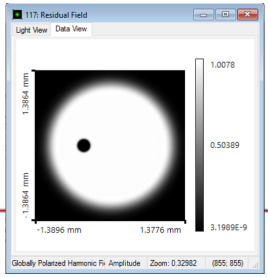

Example Spherical Field with Stop

$$V_\ell(\boldsymbol{\rho},z,\omega) = |V_\ell(\boldsymbol{\rho},z,\omega)| \exp\left(\mathrm{i}\varphi_\ell(\boldsymbol{\rho},z,\omega)\right) \exp\left(\mathrm{i}\psi(\boldsymbol{\rho},z,\omega)\right)$$

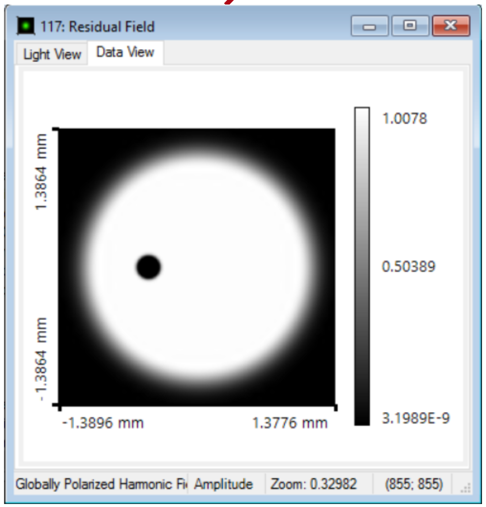

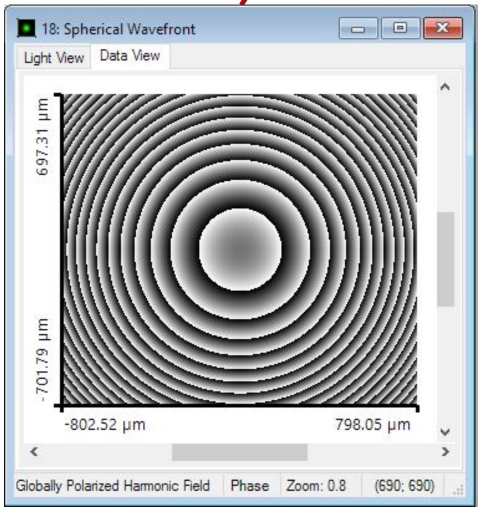

Results of Fourier Transform

$$V_\ell(\boldsymbol{\rho},z,\omega) = |V_\ell(\boldsymbol{\rho},z,\omega)|\exp(\mathrm{i}\varphi_\ell(\boldsymbol{\rho},z,\omega))\boxed{\exp(\mathrm{i}\psi(\boldsymbol{\rho},z,\omega))}$$

Spherical wavefront with decreasing radius of curvature; increasing NA

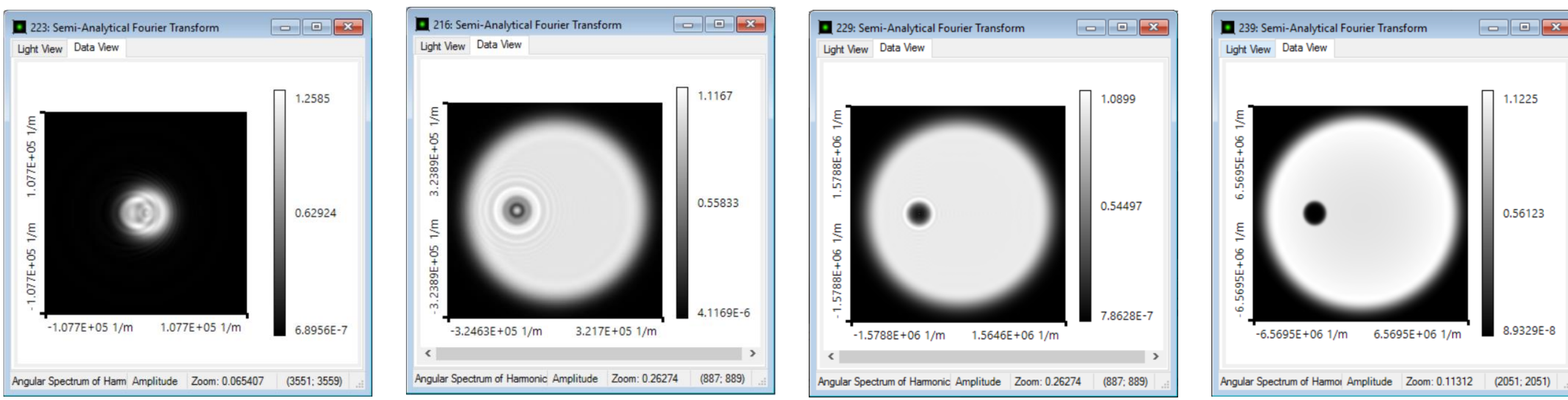

Results of Fourier Transform

$$V_\ell(\boldsymbol{\rho},z,\omega) = |V_\ell(\boldsymbol{\rho},z,\omega)|\exp(i\varphi_\ell(\boldsymbol{\rho},z,\omega))\exp(i\psi(\boldsymbol{\rho},z,\omega))$$

Spherical wavefront with decreasing radius of curvature; increasing NA

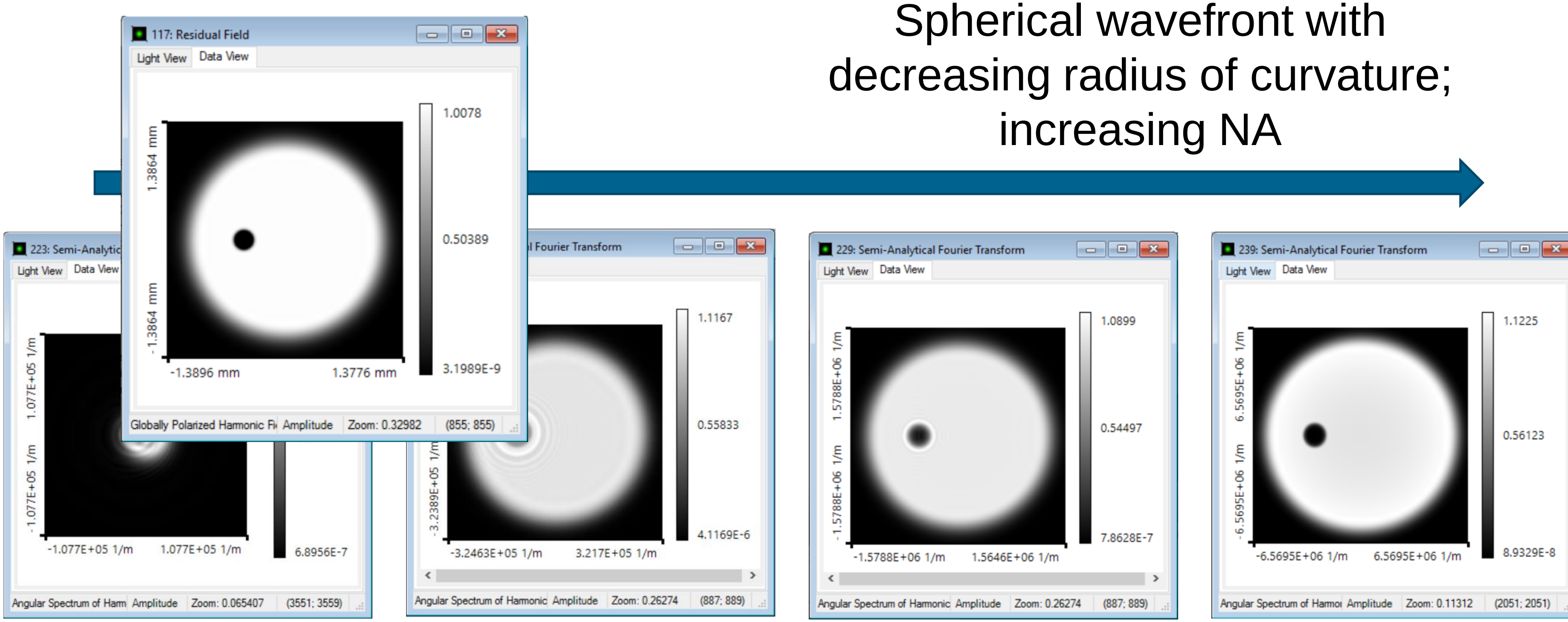

Types of Fourier Transforms

Classical FFT: Requires sampling with $N^{\mathsf{nyq}}(V)$ and thus it is practical for weak wavefront phases only.

Semi-analytical FFT: Can analytically handle wavefront phase $\psi_{\mathsf{q}}(\boldsymbol{\rho}) = A + \boldsymbol{B} \cdot \boldsymbol{\rho} + C\,xy + \boldsymbol{D} \cdot (x^2, y^2)$. Thus it requires sampling with $N^{\mathsf{nyq}}(U_{\mathrm{q}}^{\mathrm{res}})$ and thus it is practical for weak to moderate wavefront phases.

Types of Fourier Transforms

Classical FFT: Requires sampling with $N^{\text{nyq}}(V)$ and thus it is practical for weak wavefront phases only.

Semi-analytical FFT: Can analytically handle wavefront phase $\psi_{\text{q}}(\boldsymbol{\rho}) = A + \boldsymbol{B} \cdot \boldsymbol{\rho} + C\,xy + \boldsymbol{D} \cdot (x^2, y^2)$. Thus it requires sampling with $N^{\text{nyq}}(U_{\text{q}}^{\text{res}})$ and thus it is practical for weak to moderate wavefront phases.

Geometric Fourier Transform: Enables calculation of Fourier transform with $N^{\text{nyq}}(U)$ sampling points. Technique is suitable for fields with strong wavefront phase ψ, which is parametrized by $N(\psi)$ parameters.

⇒ Minimization of *N* enables fast physical optics!

Triad of Fourier Transform Techniques

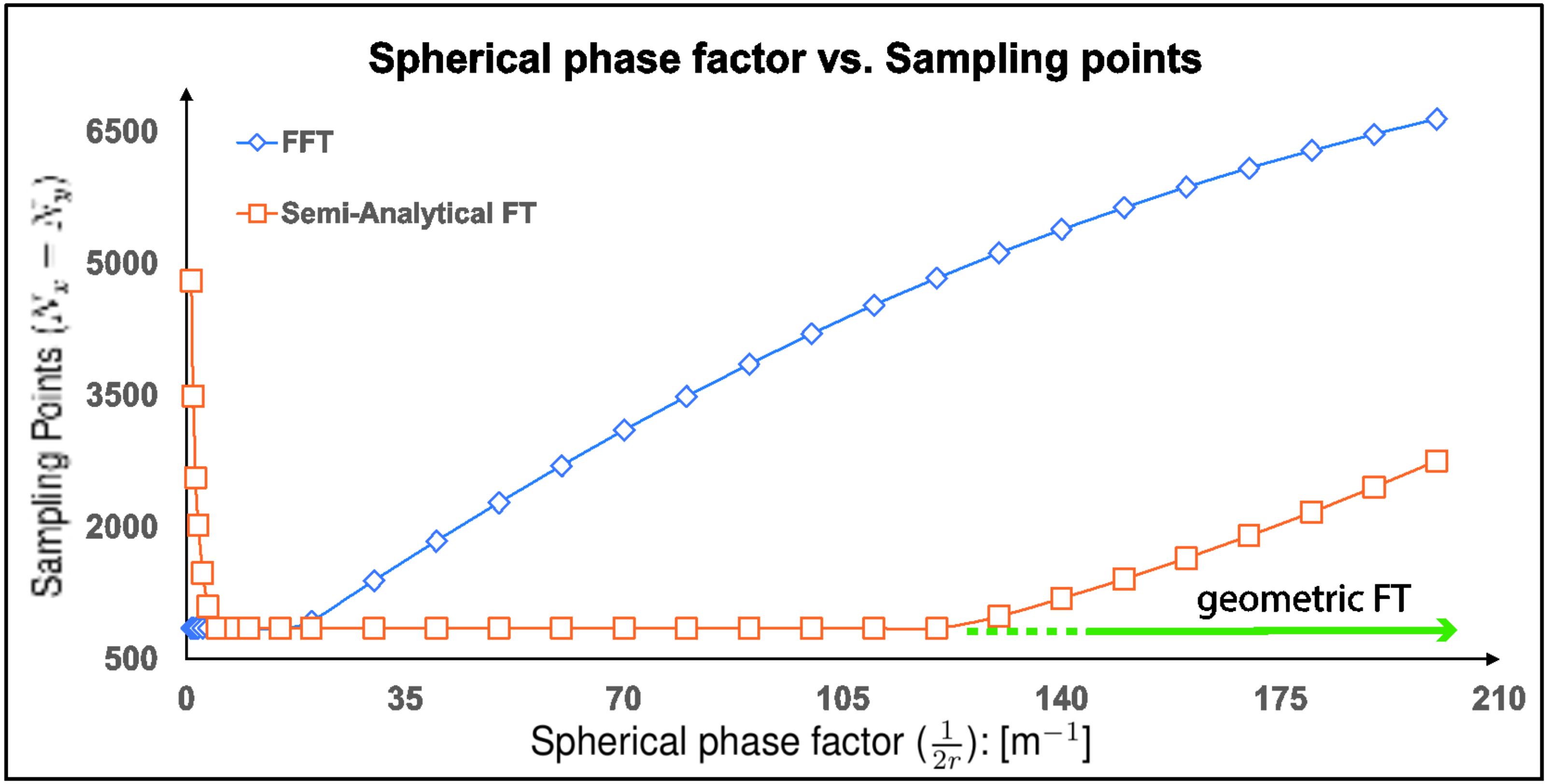

Triad of Fourier Transform Techniques

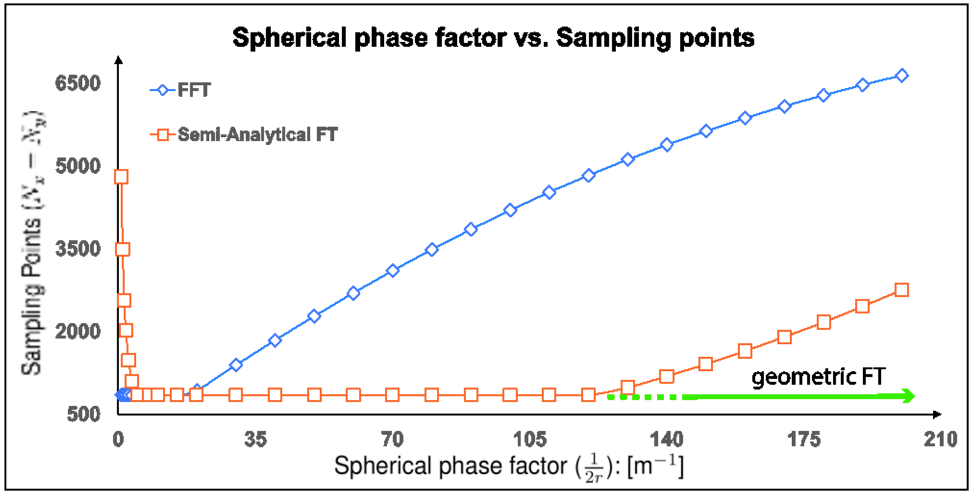

- Techniques have been implemented in 2nd generation field tracing engine in VirtualLab Fusion.
- Algorithm is based on a hybrid sampling: combination of equidistant sampling, non-equidistant sampling, analytical expressions.
- Automatic selection of techniques per operation.

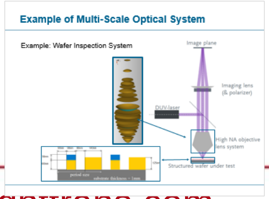

Fast Physical Optics Modeling Zones

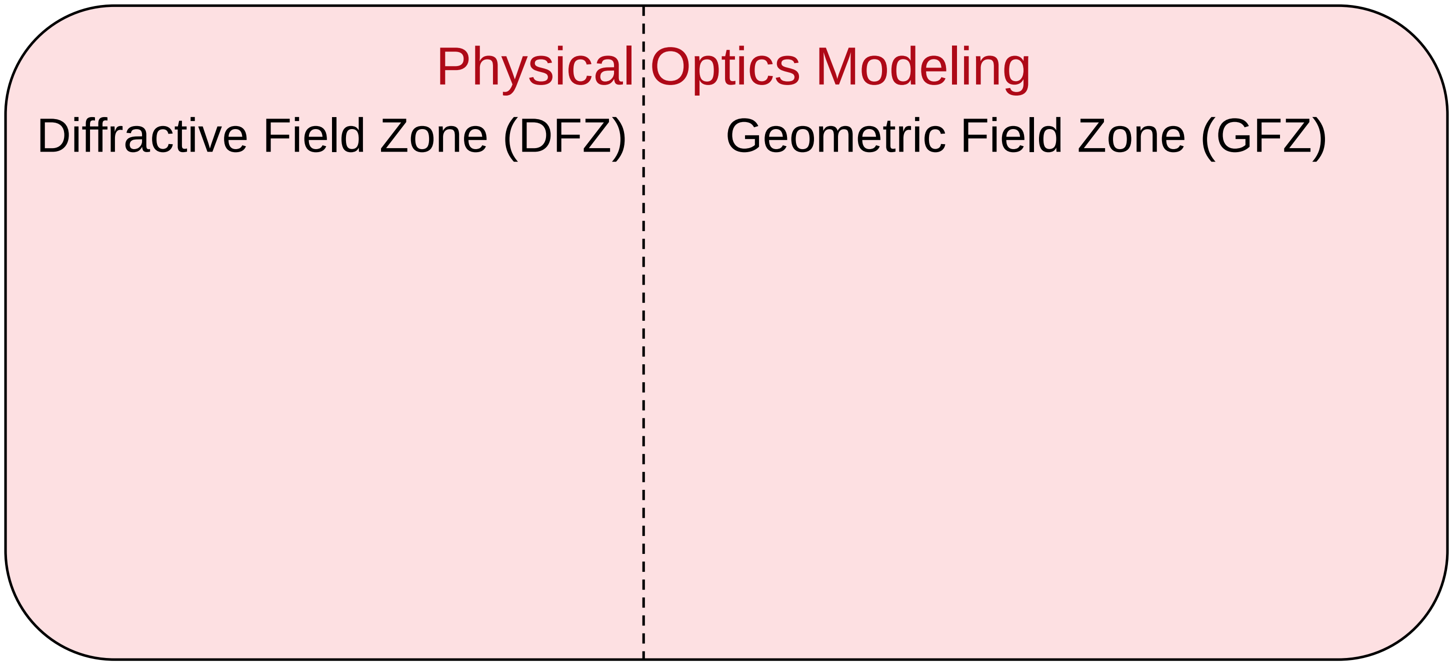

Fast Physical Optics Modeling Zones

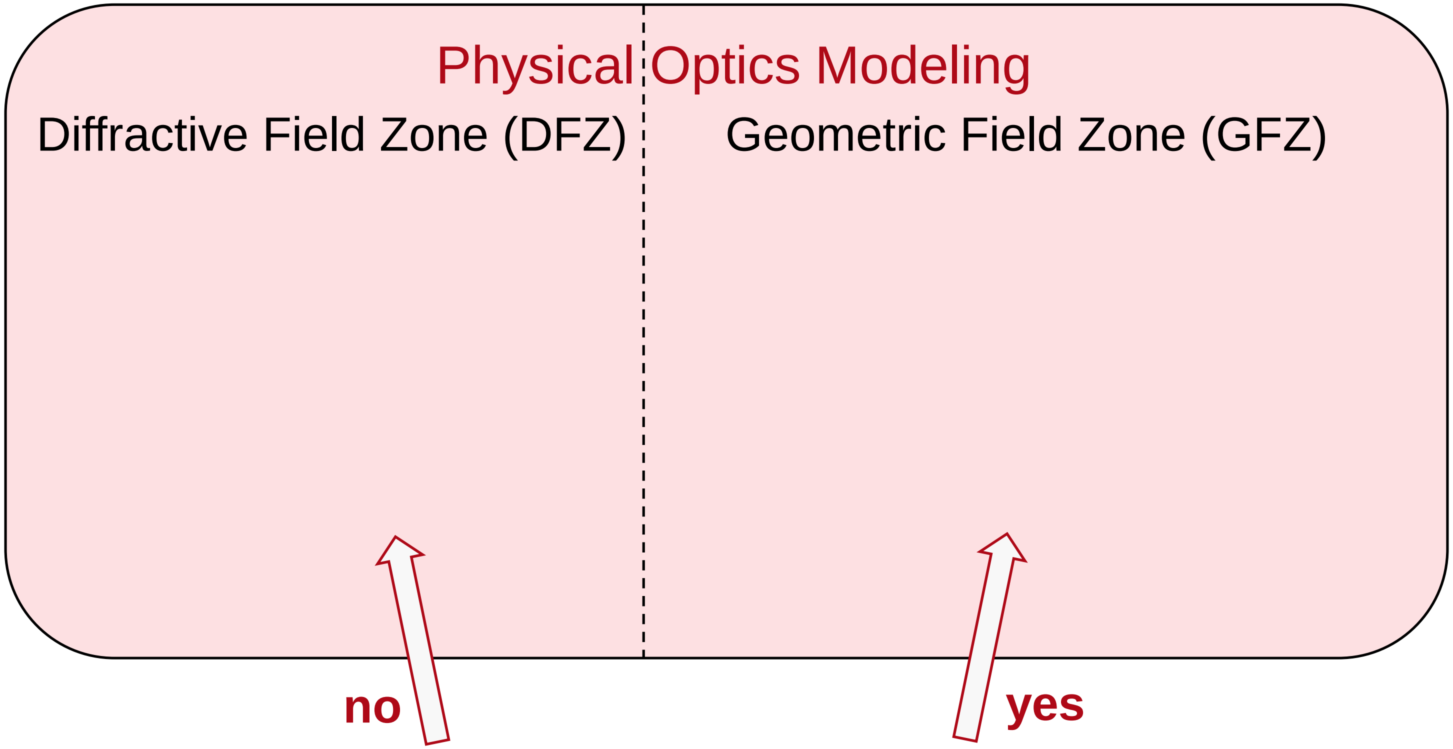

Is the geometric Fourier Transform
accurate enough for application?

Fast Physical Optics: Numerical Effort

Physical Optics Modeling

Diffractive Field Zone (DFZ)	Geometric Field Zone (GFZ)
Modeling governed by $N^{\text{nyq}}(U)$	Modeling governed by $N(\psi)$
Semi-analytical FFT	Geometric FT

$$N(\psi) \ll N^{\text{nyq}}(U) \ll N^{\text{nyq}}(V)$$

Fast Physical Optics: Numerical Effort

Physical Optics Modeling

Diffractive Field Zone (DFZ)	Geometric Field Zone (GFZ)
Modeling governed by $N^{\text{nyq}}(U)$	Modeling governed by $N(\psi)$
Semi-analytical FFT	Geometric FT

$$N(\psi) \ll N^{\text{nyq}}(U) \ll N^{\text{nyq}}(V)$$

$$100 \ll 100^2 \ll 1000^2$$

$$1 \ll 100 \ll 10000$$

1st generation technology

Fast Physical Optics: Numerical Effort

Physical Optics Modeling

Diffractive Field Zone (DFZ)

Modeling governed by $N^{\text{nyq}}(U)$

Semi-analytical FFT

Geometric Field Zone (GFZ)

Modeling governed by $N(\psi)$

Geometric FT

$$N(\psi) \ll N^{\text{nyq}}(U) \ll N^{\text{nyq}}(V)$$

$$100 \ll 100^2 \ll 1000^2$$

2nd generation technology $1 \ll 100 \ll 10000$

Geometric and Diffractive Maxwell Solver

Physical Optics Modeling

Diffractive Field Zone (DFZ)

Geometric Field Zone (GFZ)

We connect diffractive and geometric solvers of Maxwell’s equations.

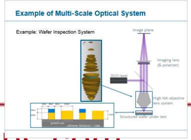

Field Zones in Fast Physical Optics

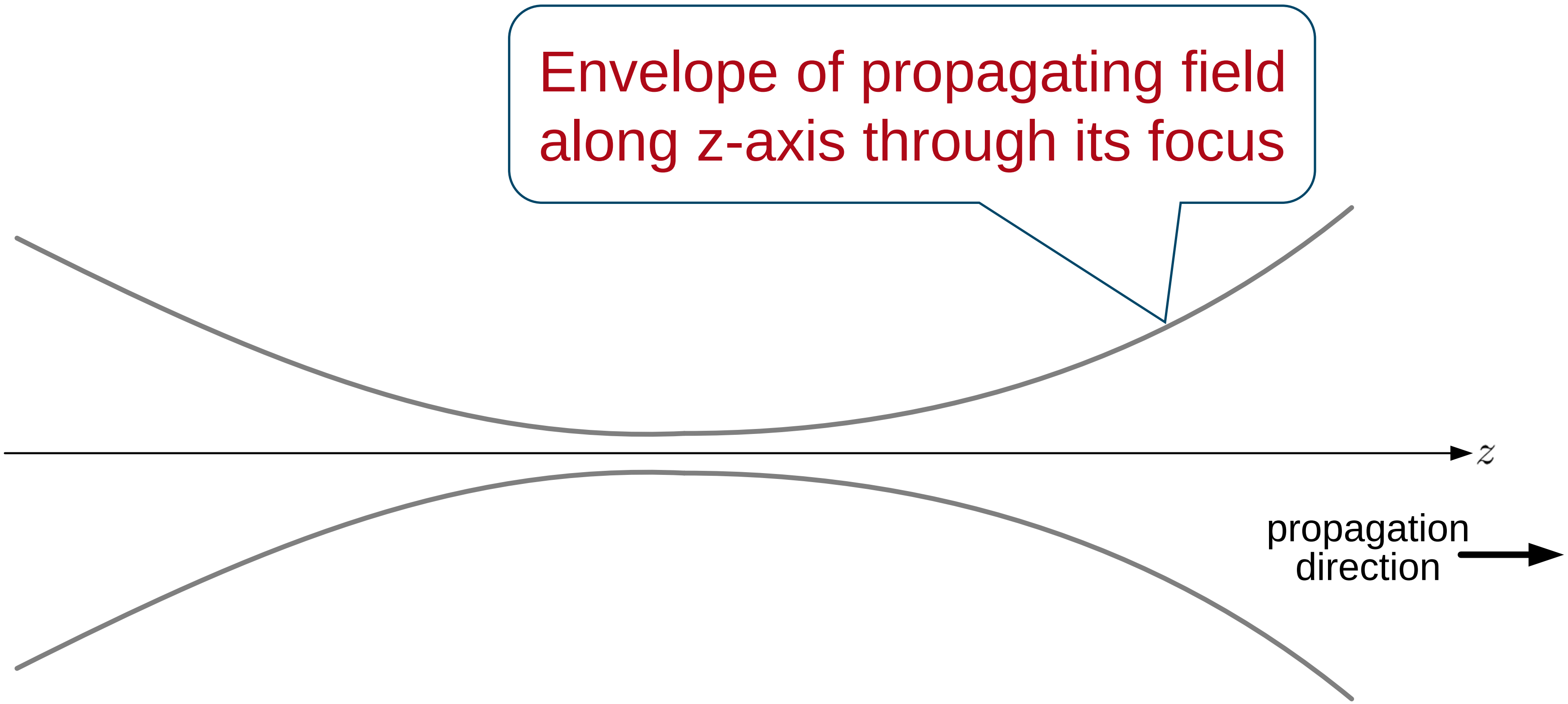

Field Zones in Fast Physical Optics

Envelope of propagating field along z-axis through its focus

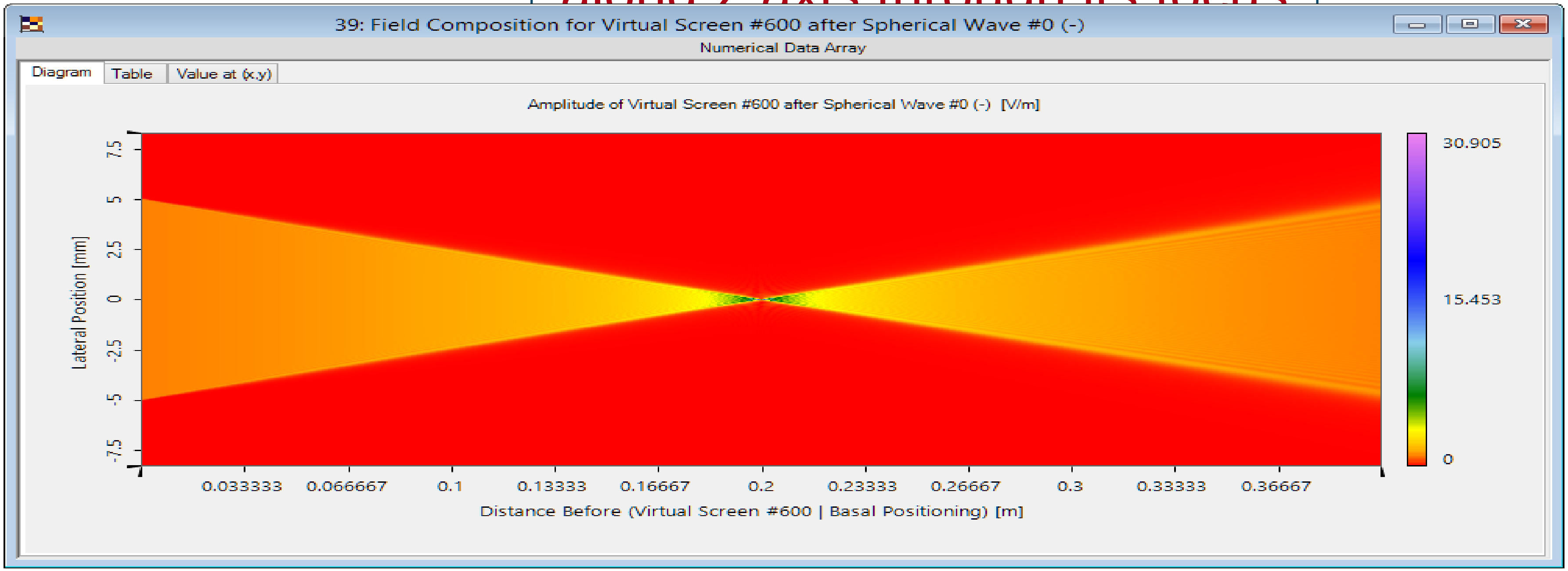

Field Zones in Fast Physical Optics

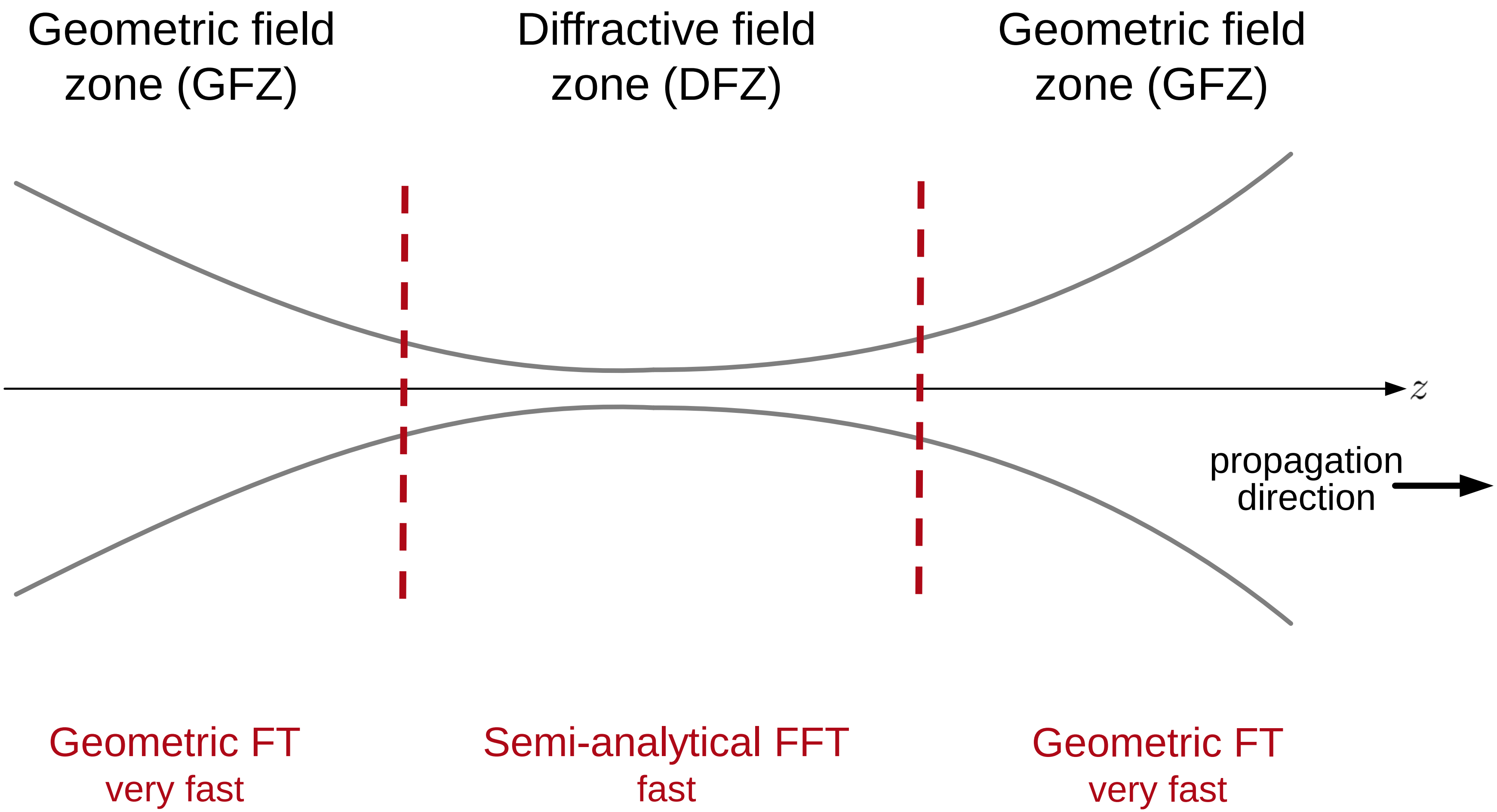

Field Zones in Fast Physical Optics

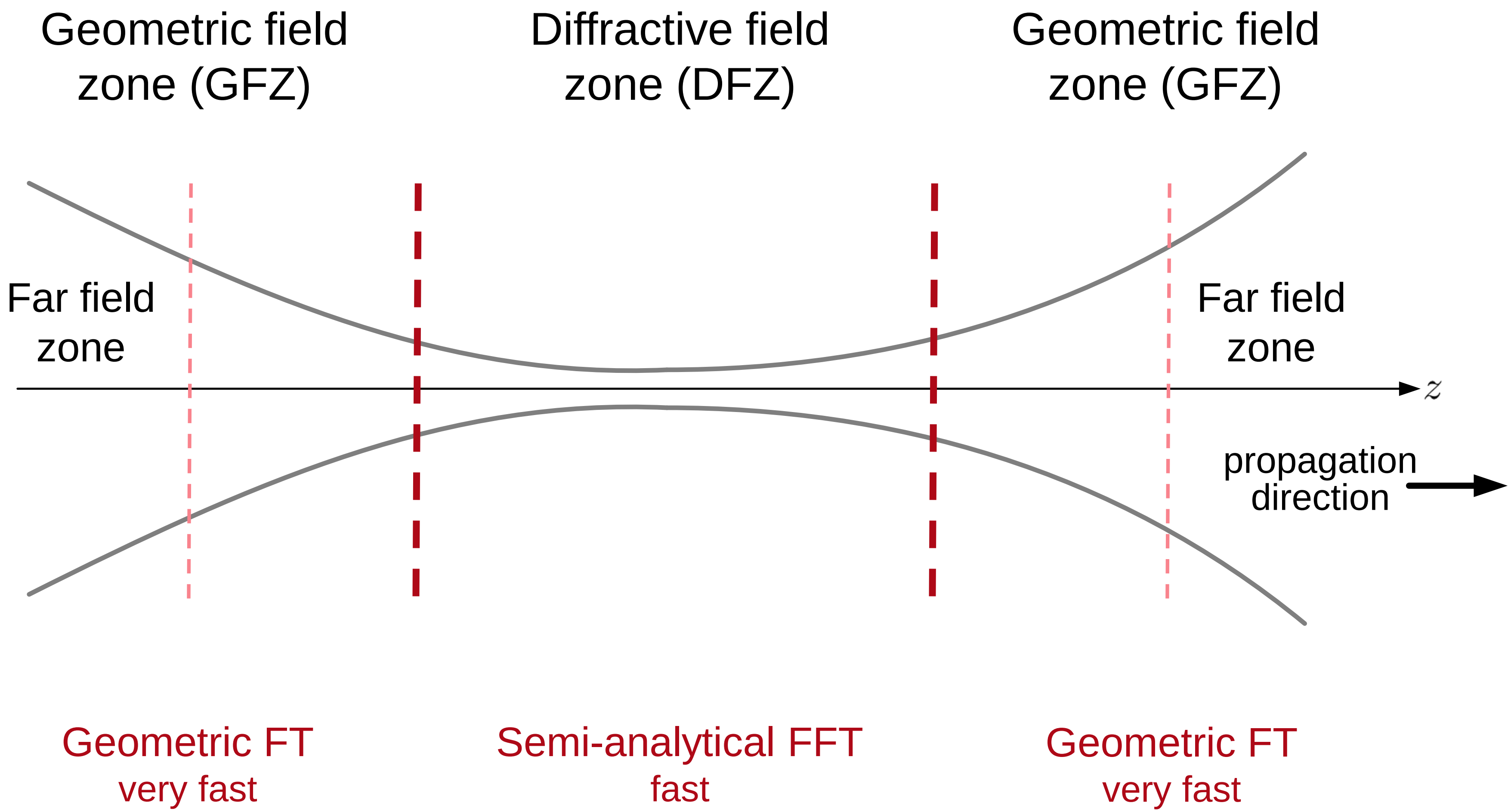

Field Zones in Fast Physical Optics

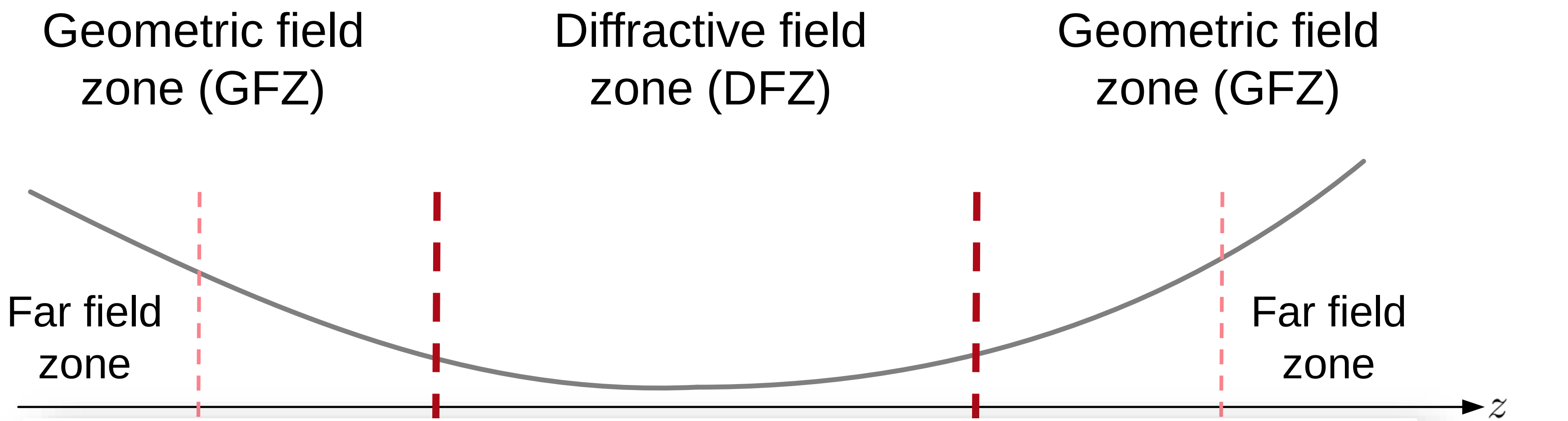

Zone	Geometric FT	Phase ψ
diffractive zone	No	—
geometric zone	Yes	general
far zone	Yes	spherical

Geometric FT
very fast

Semi-analytical FFT
fast

Geometric FT
very fast

Example: Free-Space Propagation

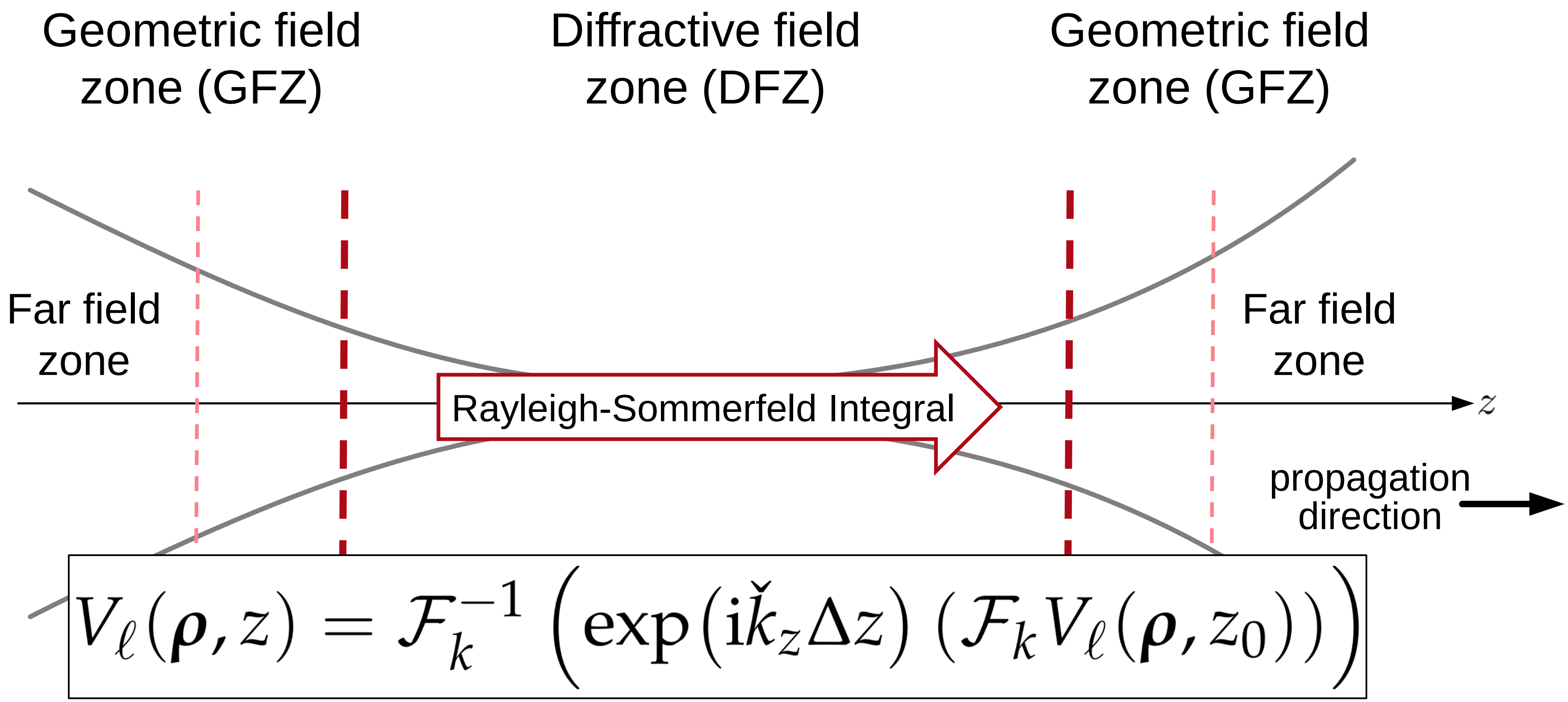

$$V_\ell(\boldsymbol{\rho}, z) = \mathcal{F}_k^{-1}\left(\exp\left(\mathrm{i}\check{k}_z \Delta z\right)\left(\mathcal{F}_k V_\ell(\boldsymbol{\rho}, z_0)\right)\right)$$

Geometric FT
very fast

Semi-analytical FFT
fast

Geometric FT
very fast

Example: Free-Space Propagation

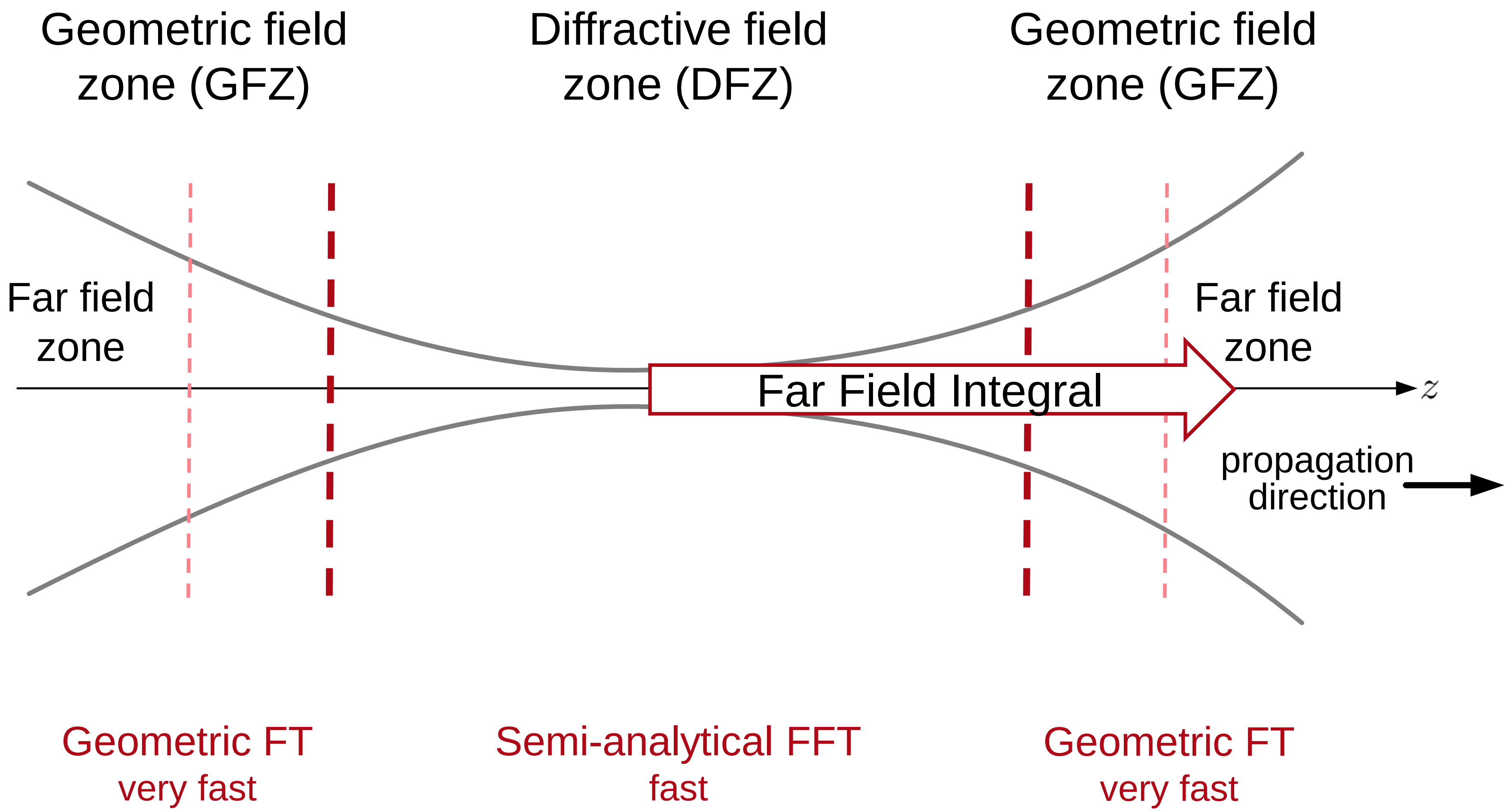

Example: Free-Space Propagation

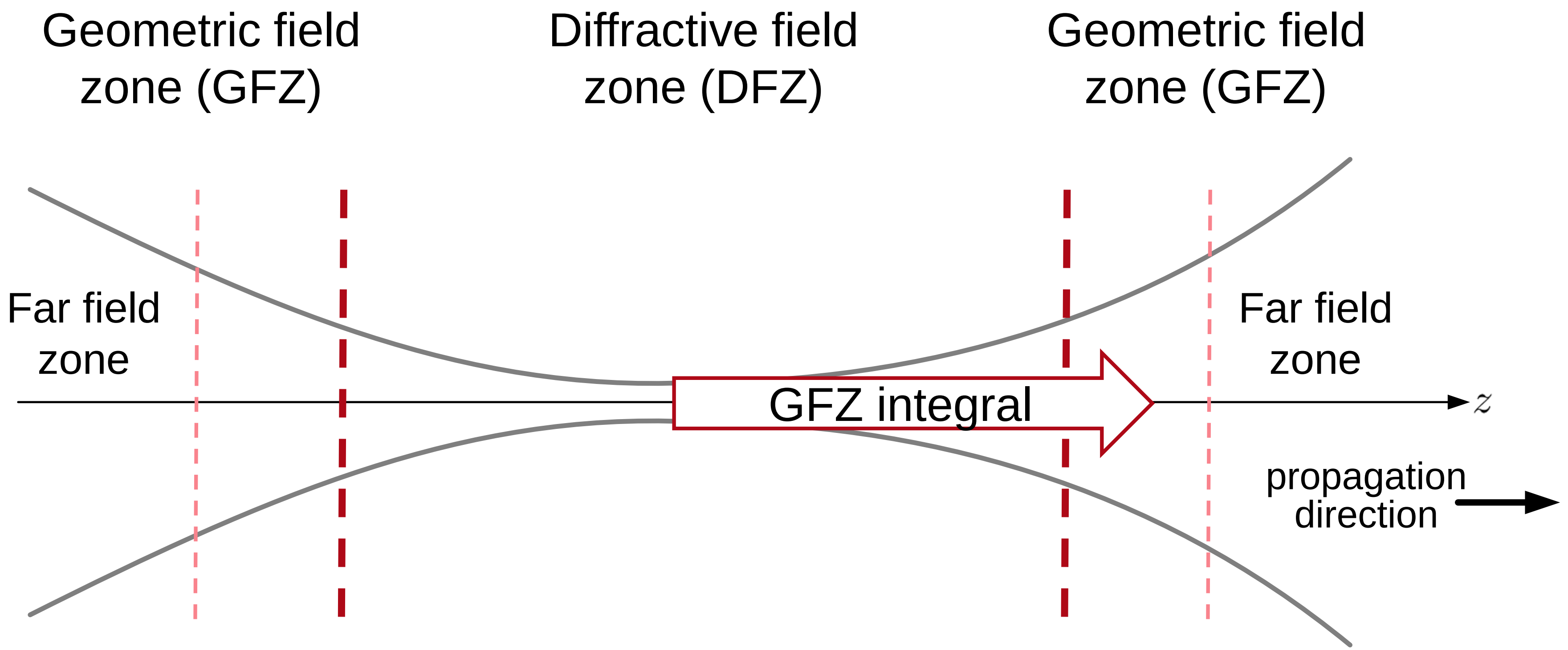

Geometric FT
very fast

Semi-analytical FFT
fast

Geometric FT
very fast

Example: Free-Space Propagation

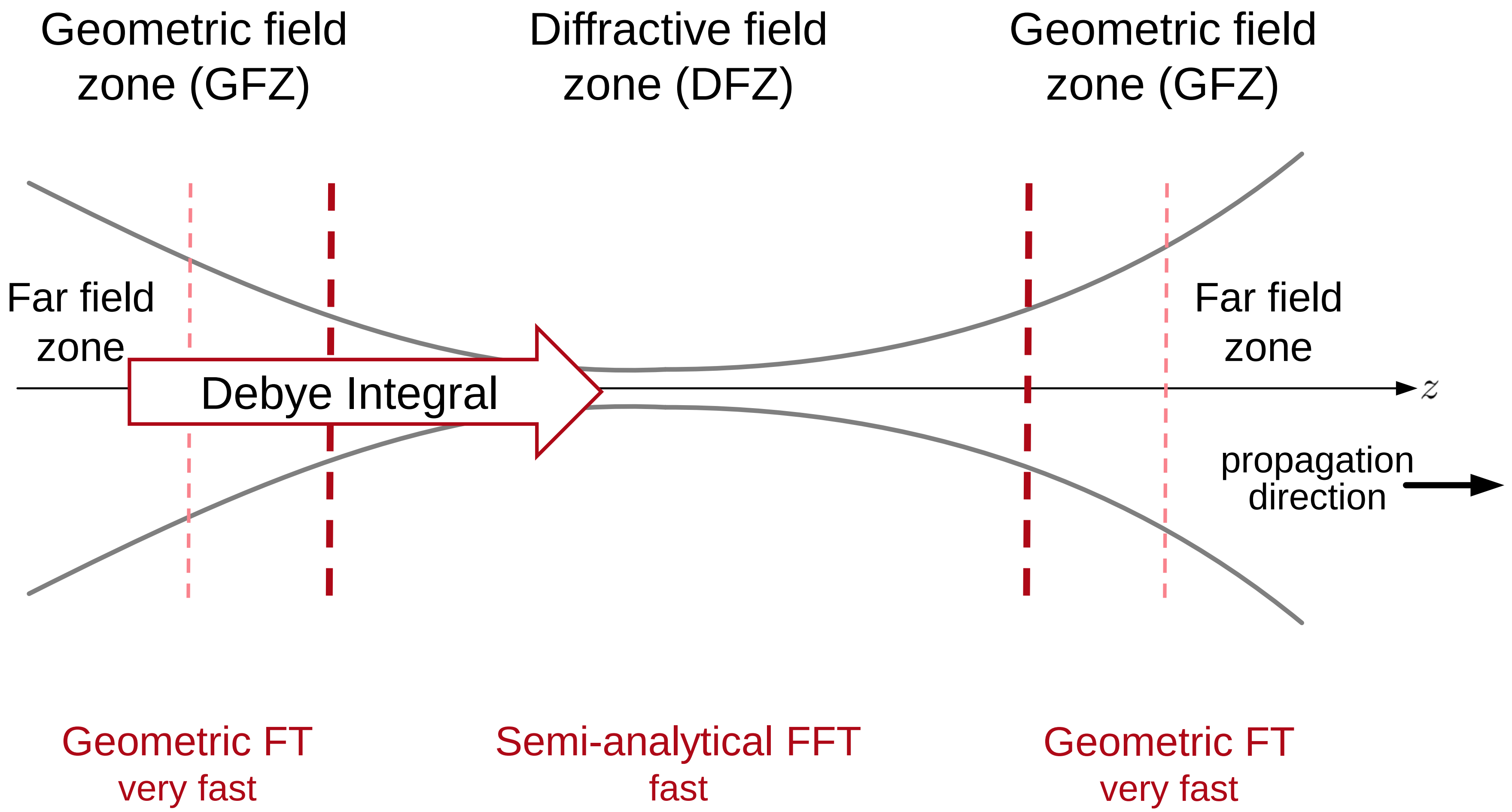

Example: Free-Space Propagation

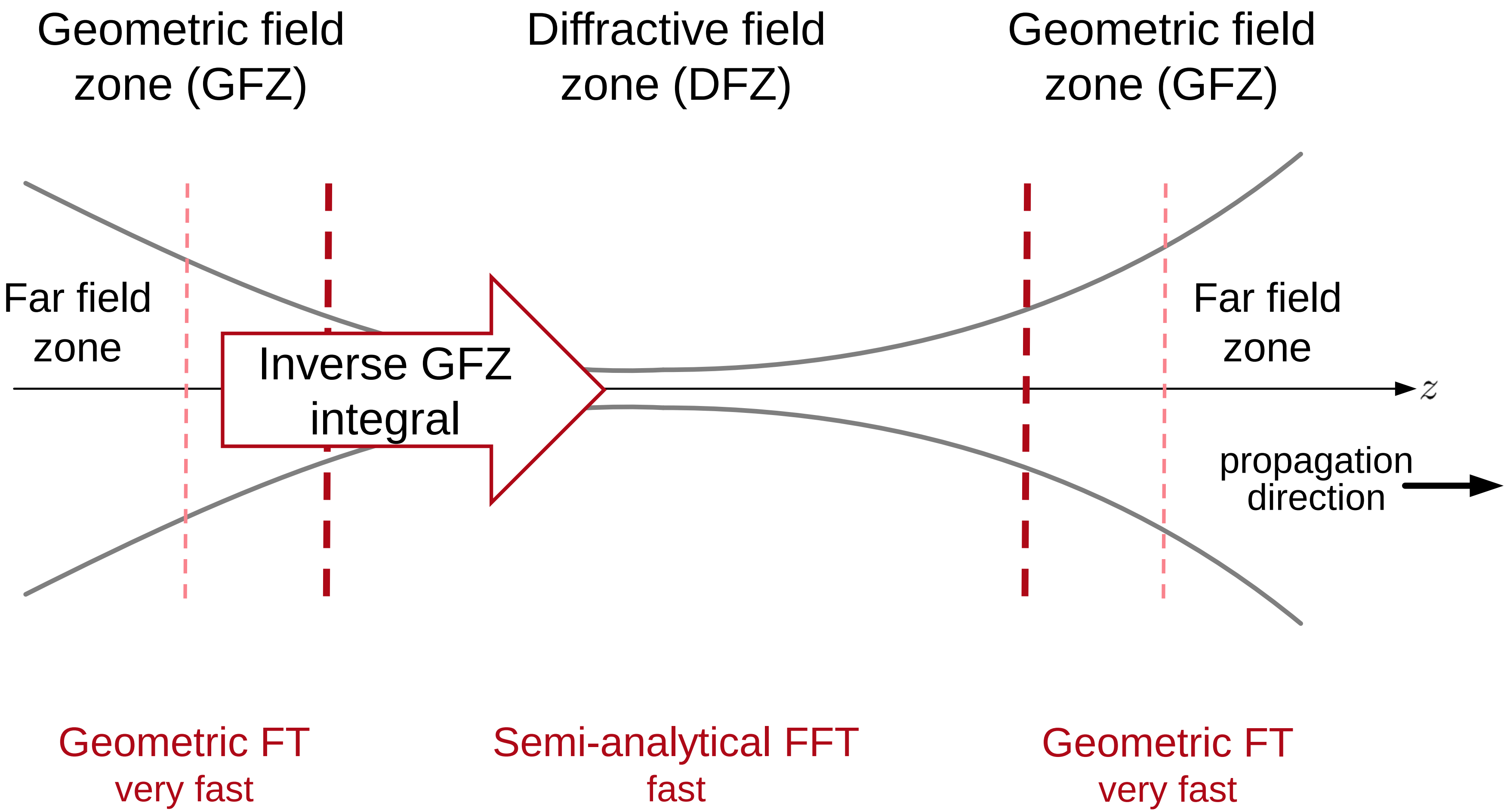

Example: Free-Space Propagation

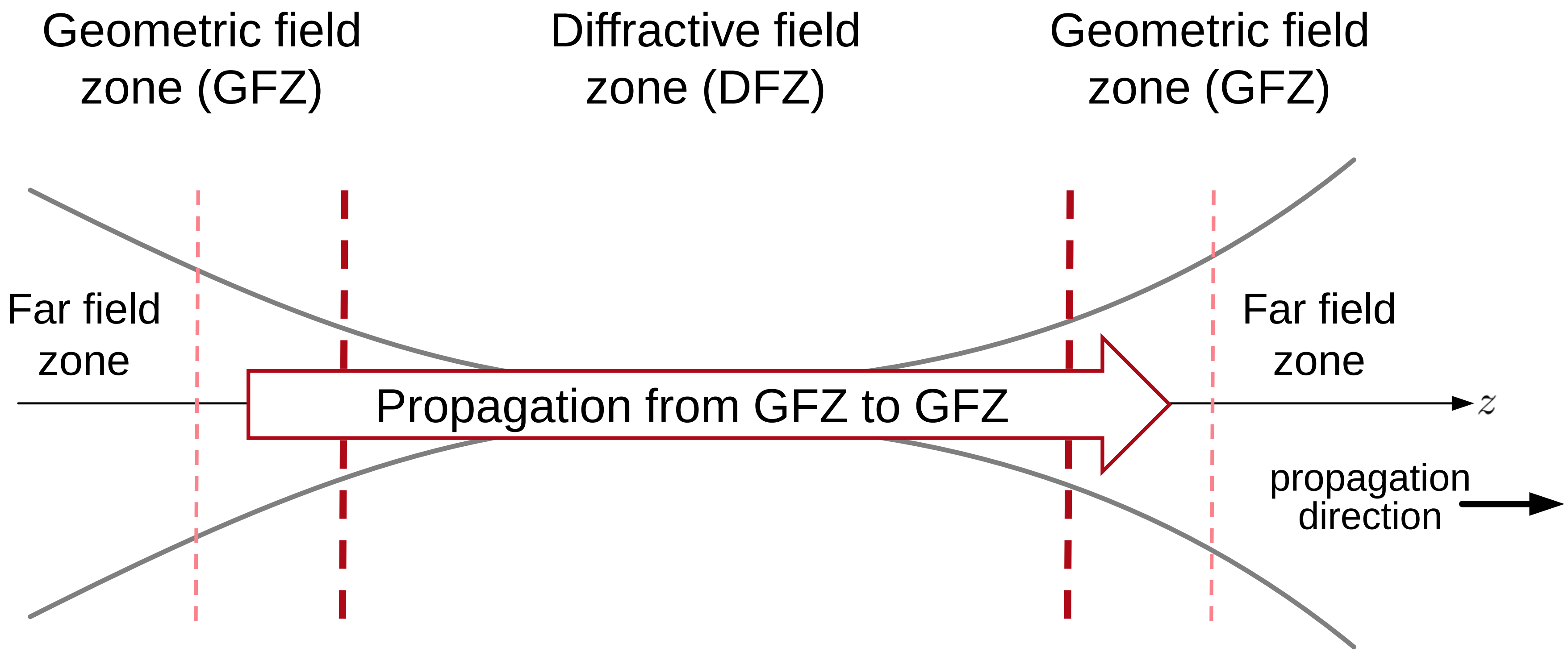

Geometric FT
very fast

Semi-analytical FFT
fast

Geometric FT
very fast

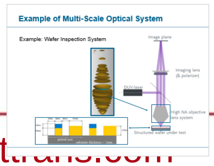

Propagation Operator in VirtualLab

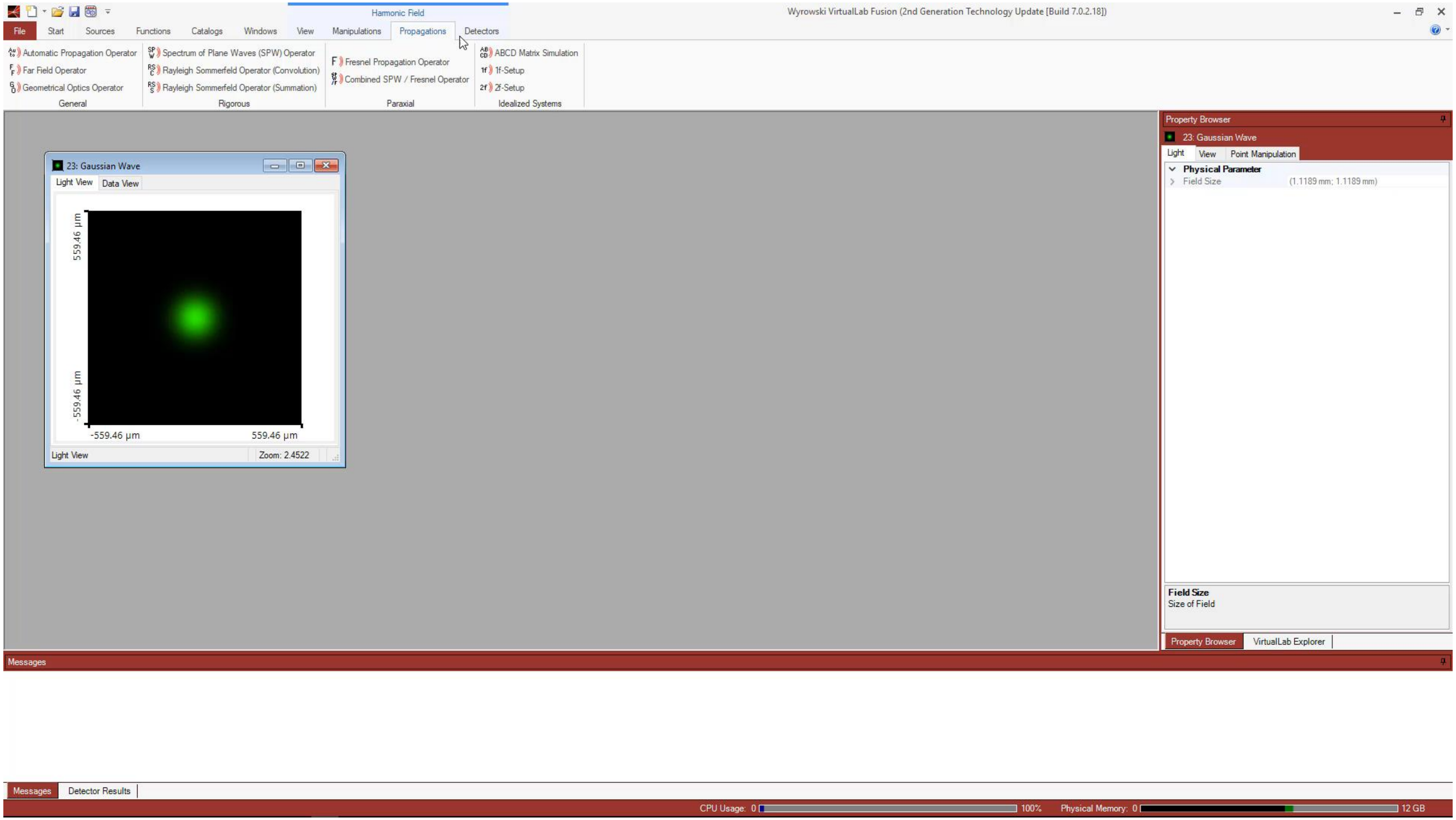

11:00-12:30

Propagation techniques

Components

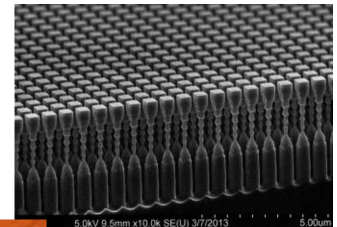

[1] IMS-Mechatronics Lab

[2] ISUZU GLASS

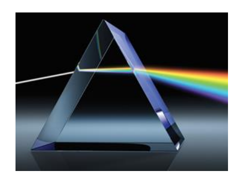

Components with Planer Interfaces

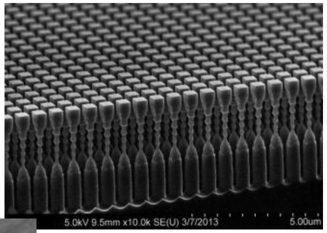

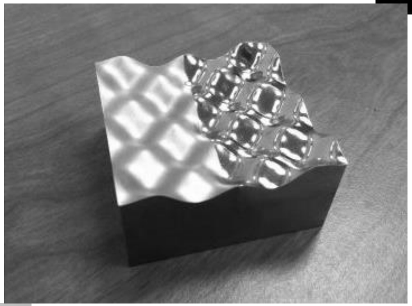

[1] IMS-Mechatronics Lab

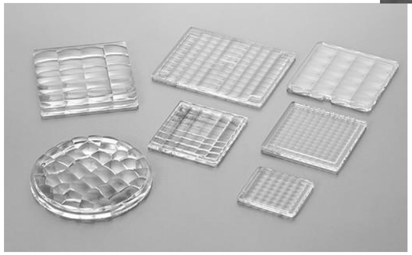

[2] ISUZU GLASS

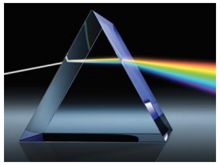

Fresnel Effects

- Fresnel effects calculator with different diagram, and possibilities to include coatings

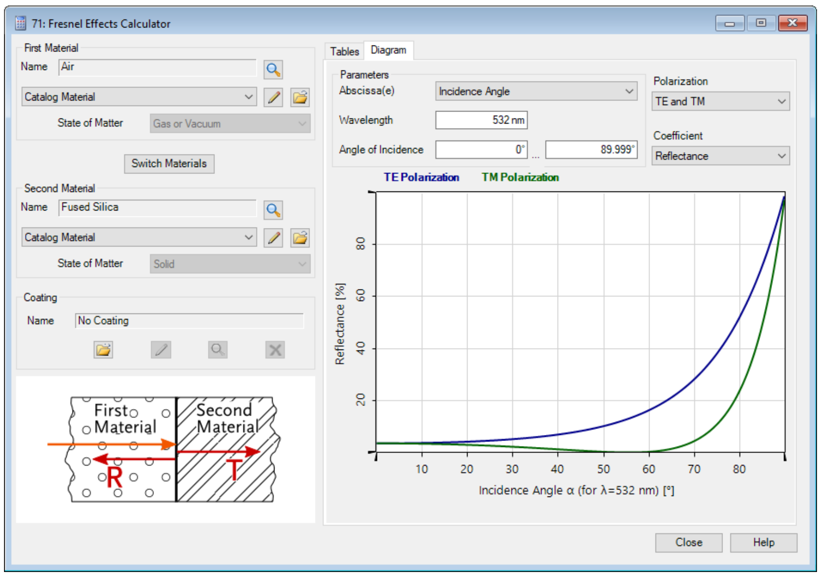

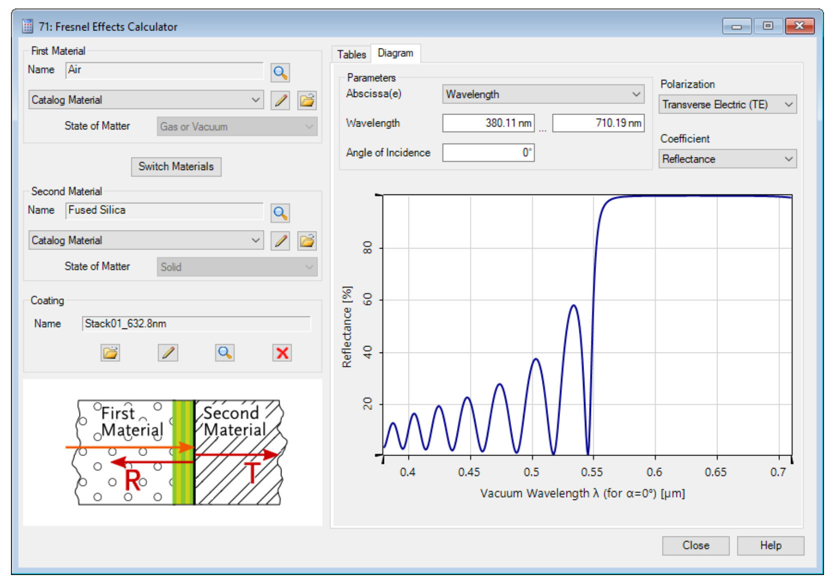

Lens

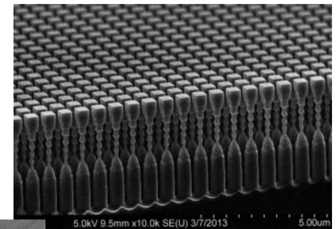

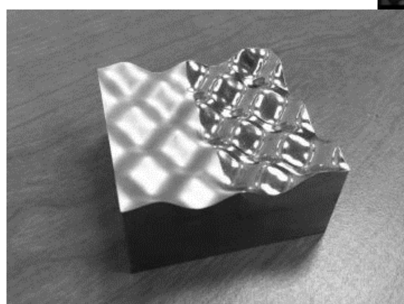

[1] IMS-Mechatronics Lab

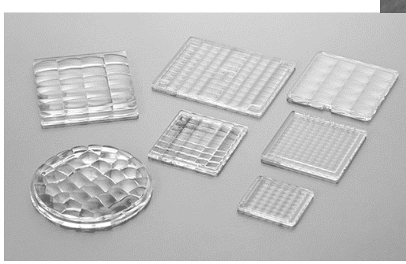

[2] ISUZU GLASS

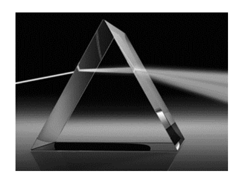

10 nm

Ex-amplitude

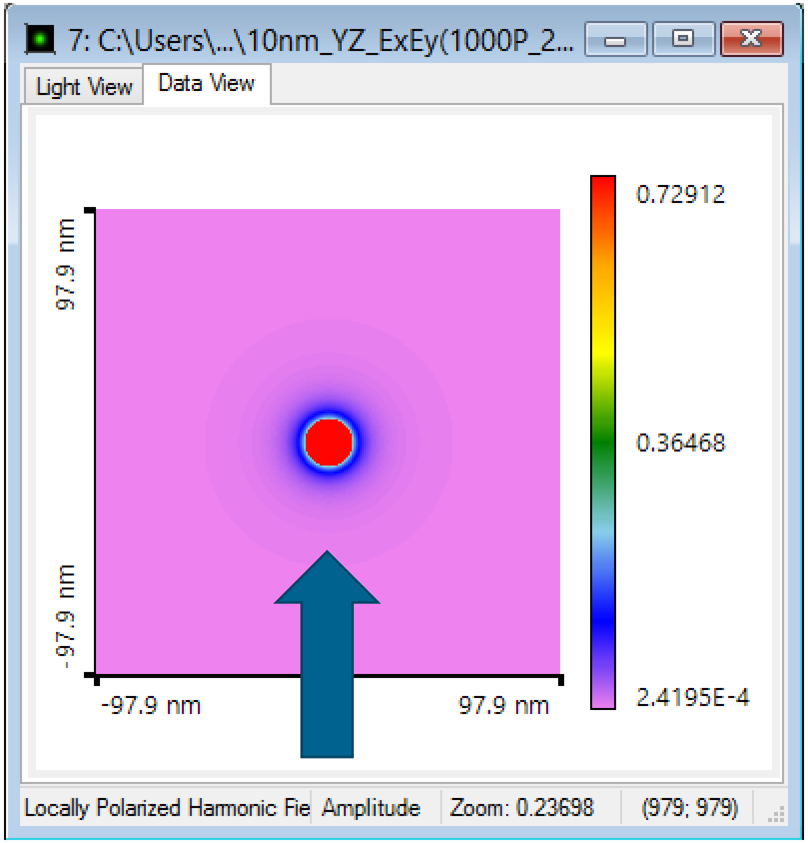

Ex-phase

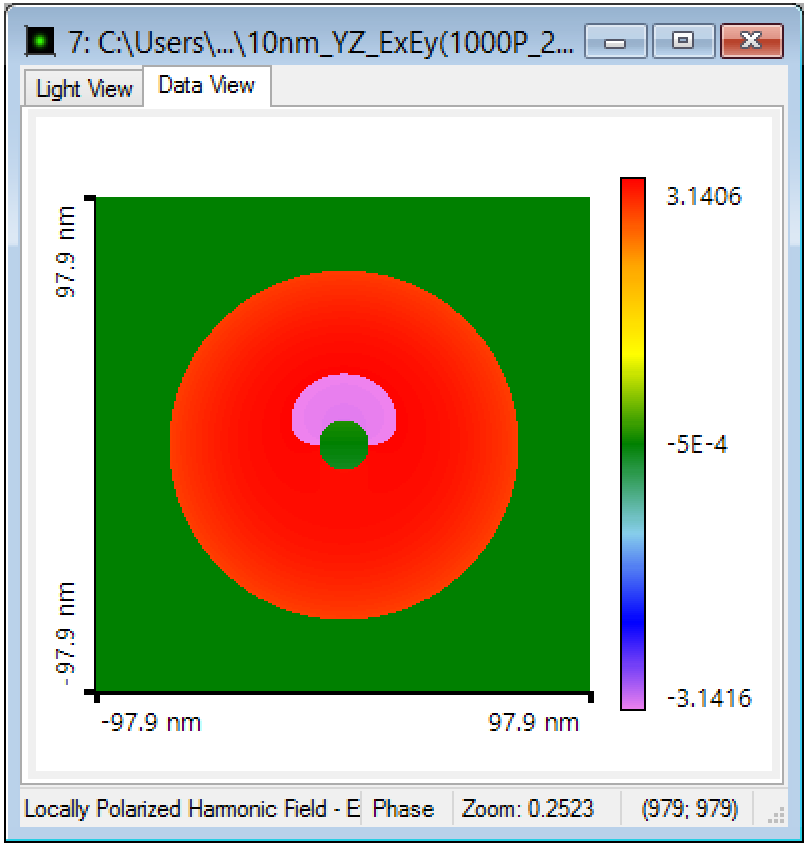

100 nm

Ex-amplitude

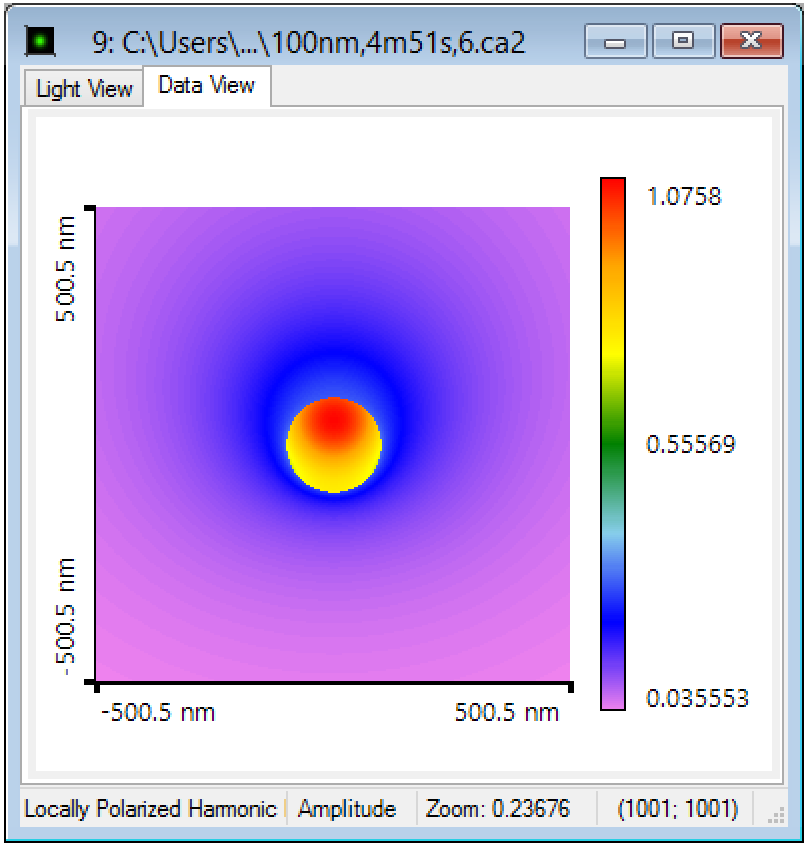

Ex-phase

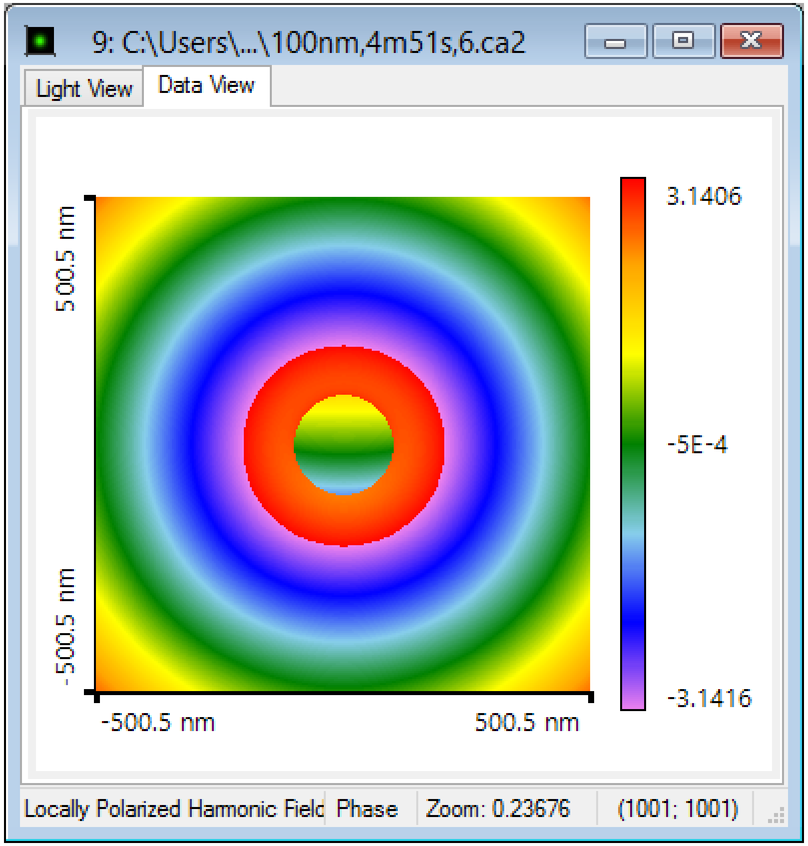

300 nm

Ex-amplitude

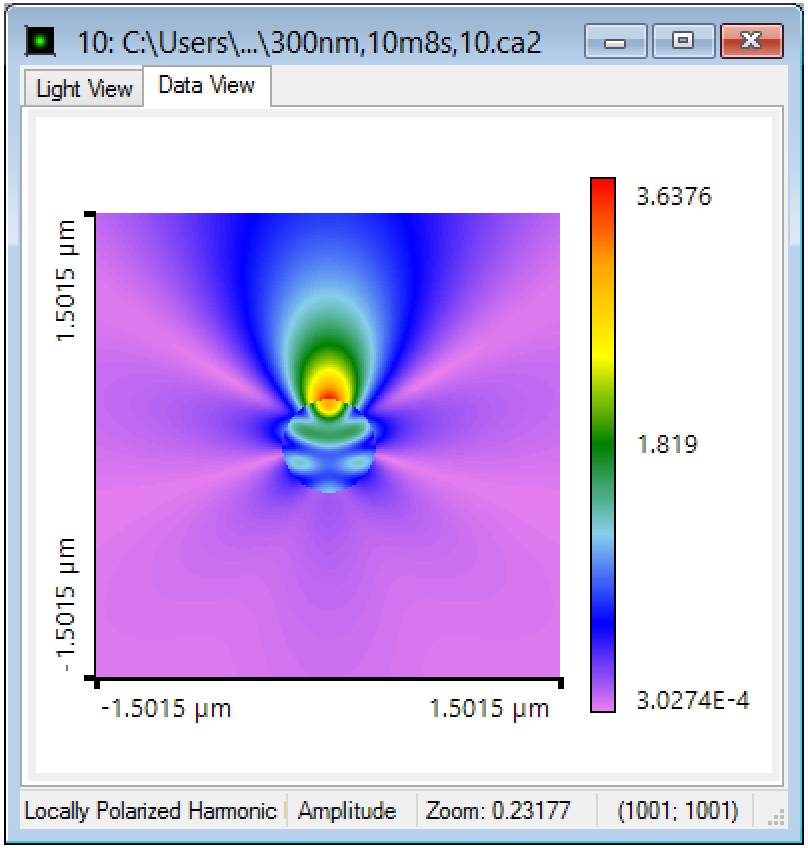

Ex-phase

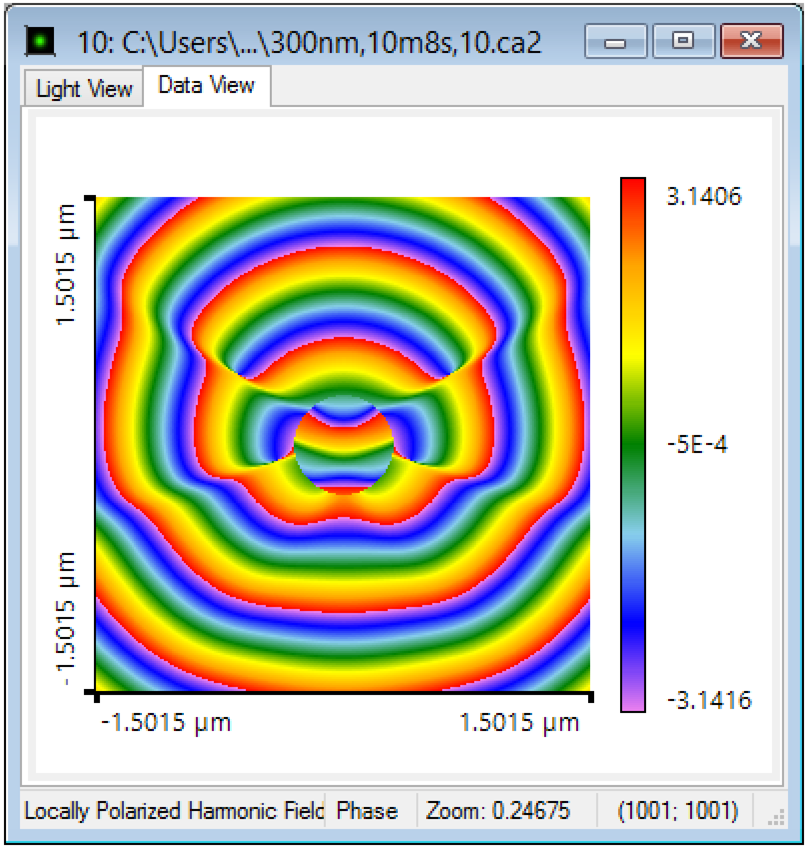

5 um

Ex-amplitude

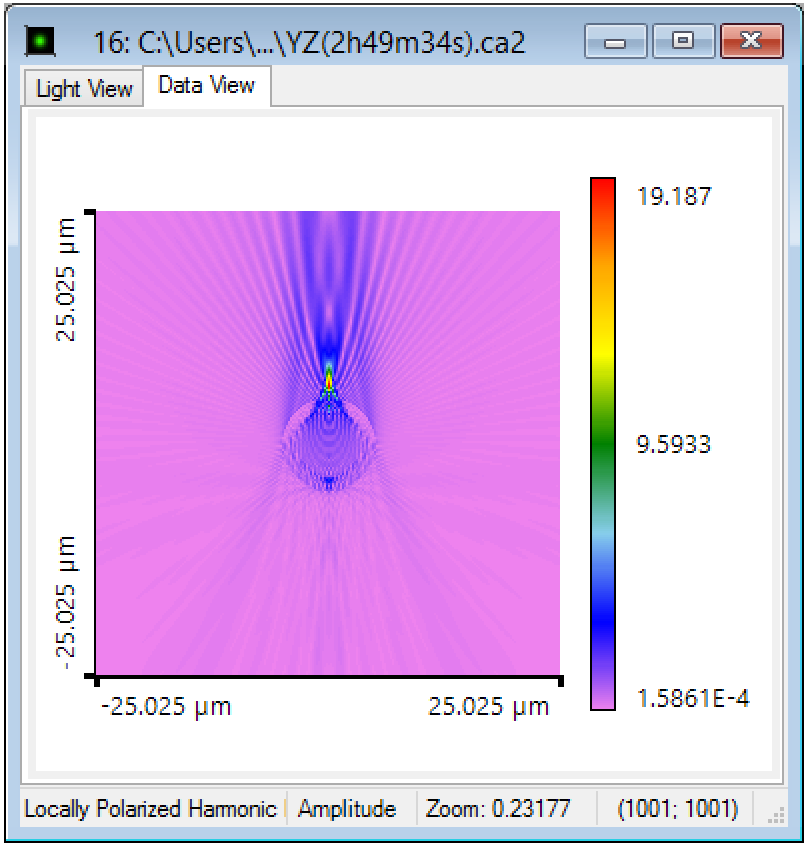

Ex-phase

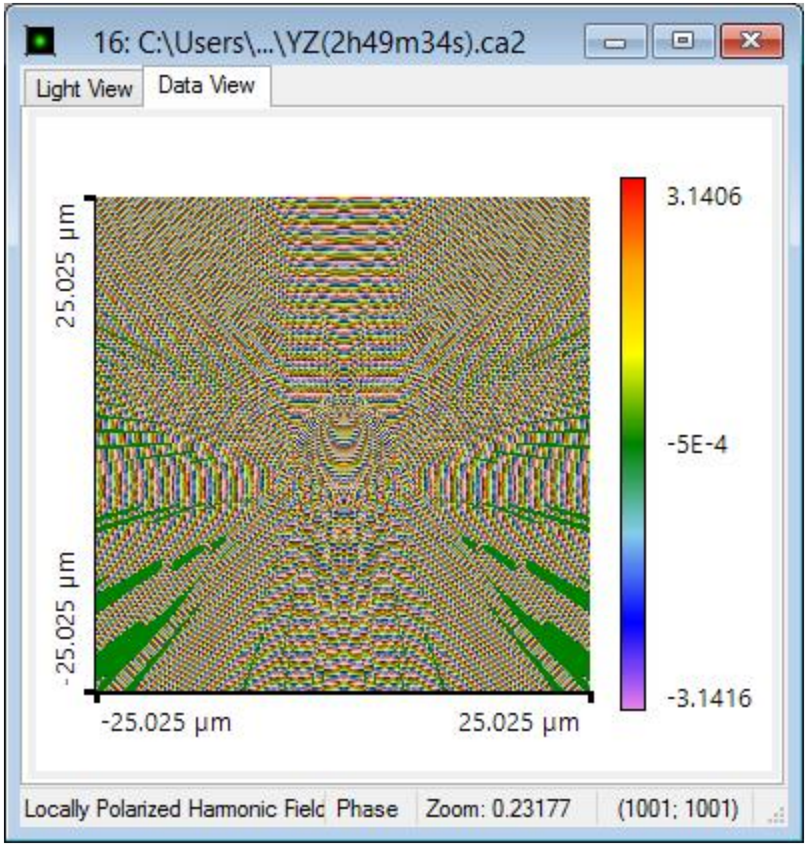

8 um

Ex-amplitude

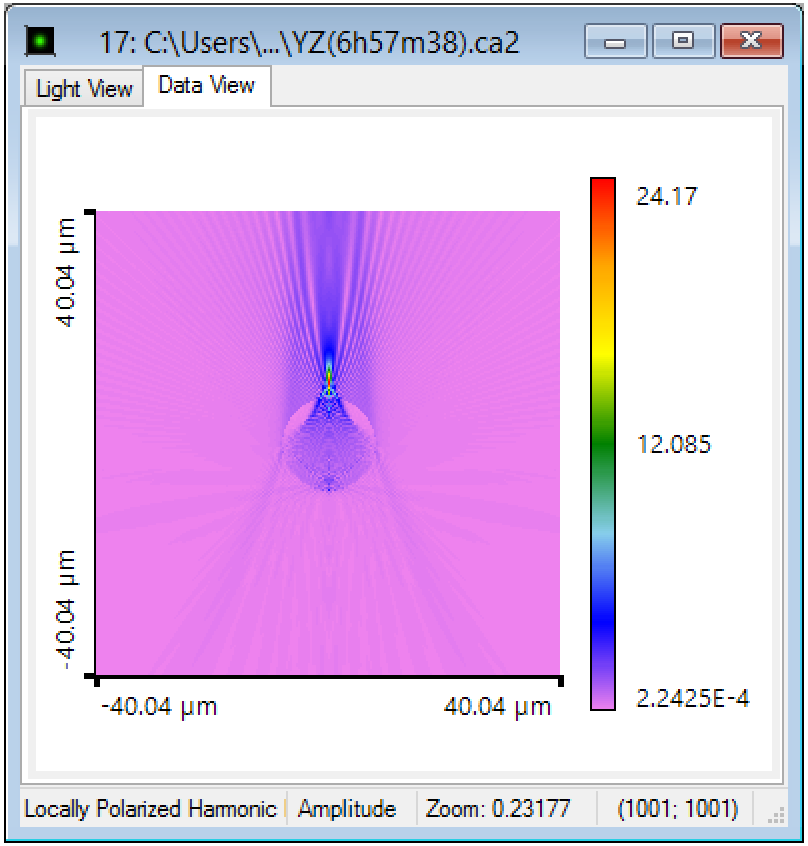

Ex-phase

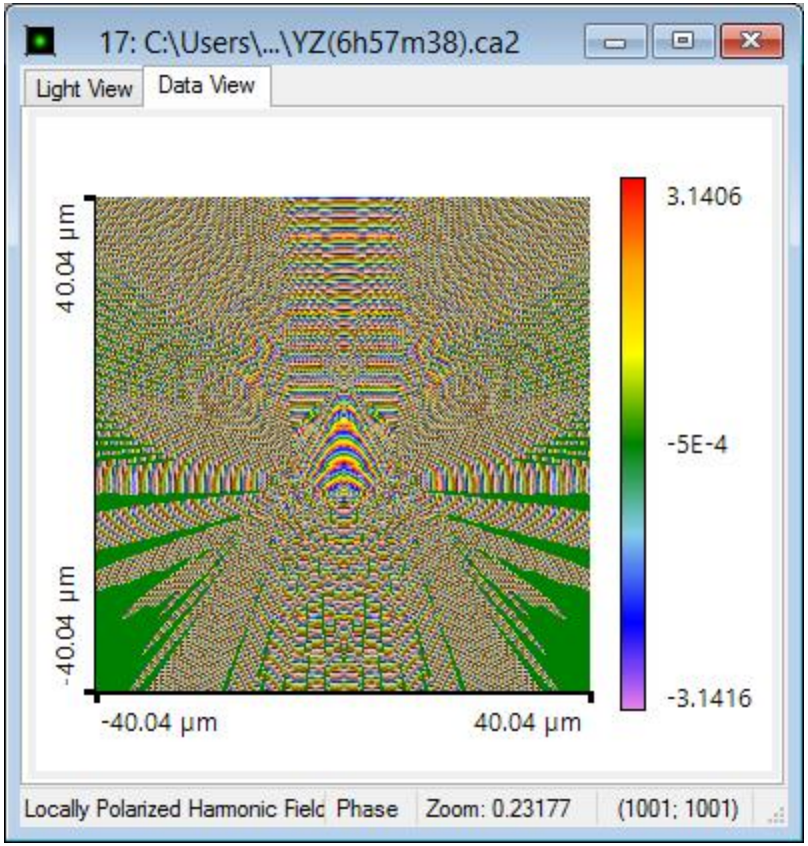

10 um

Ex-amplitude

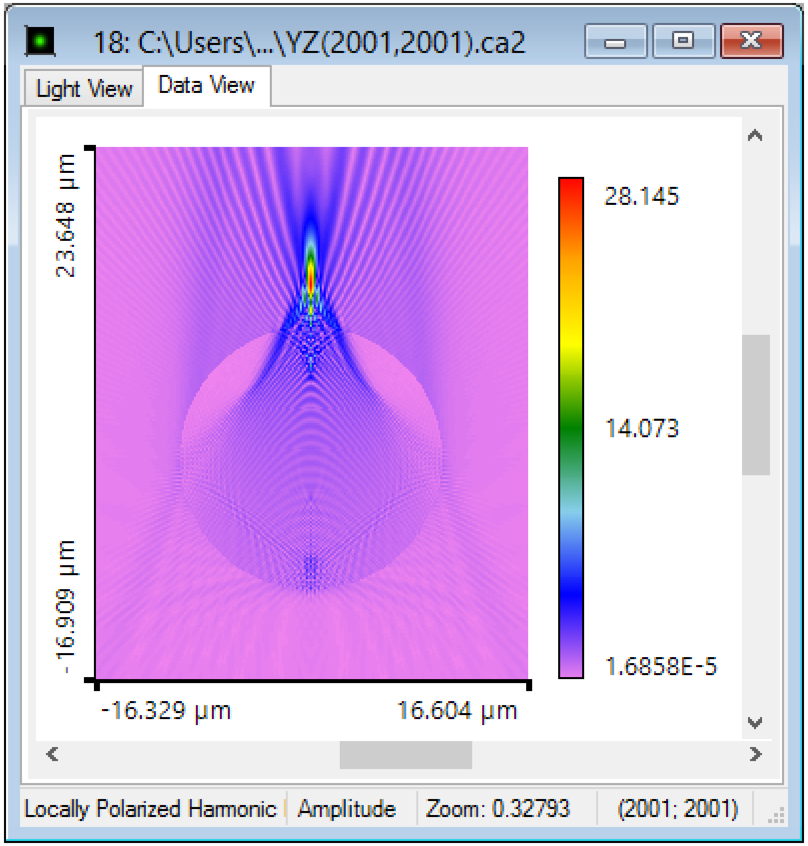

Ex-phase

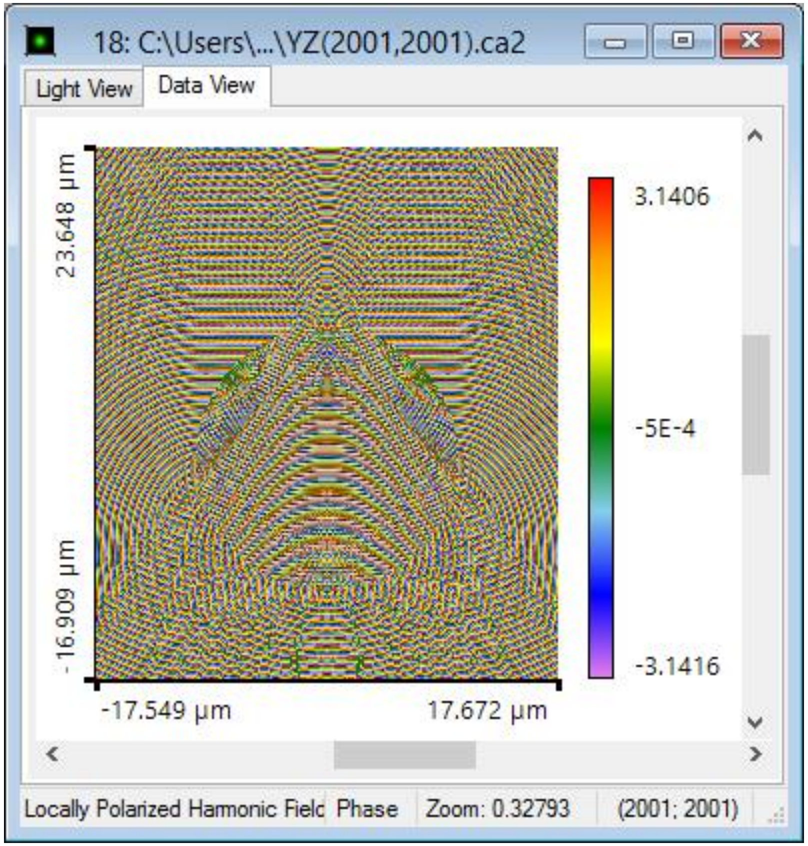

100 um

Ex-amplitude

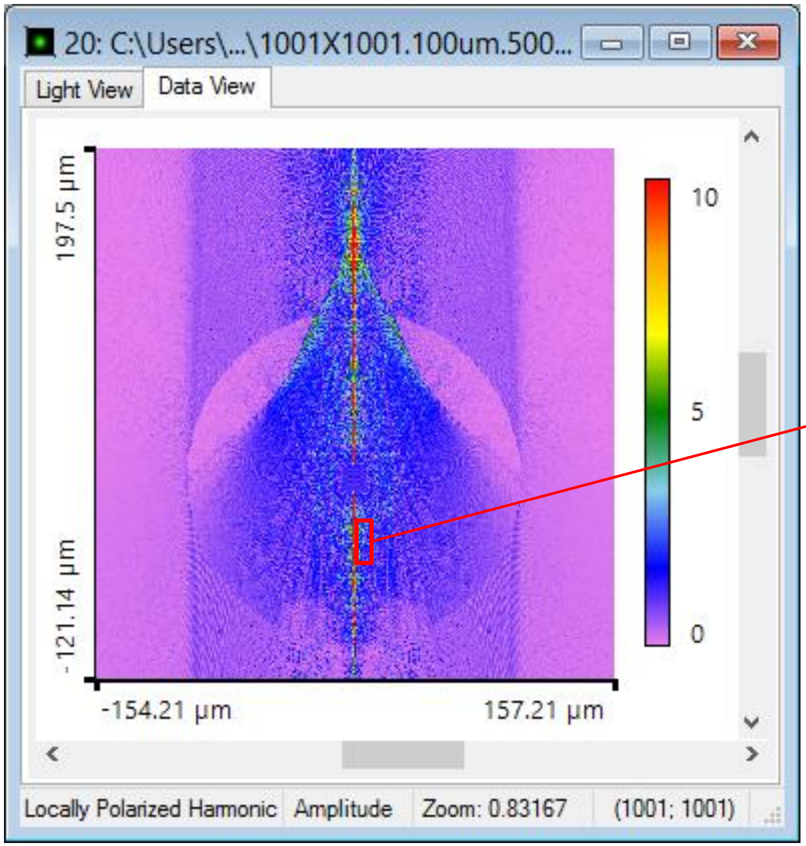

Ex-amplitude

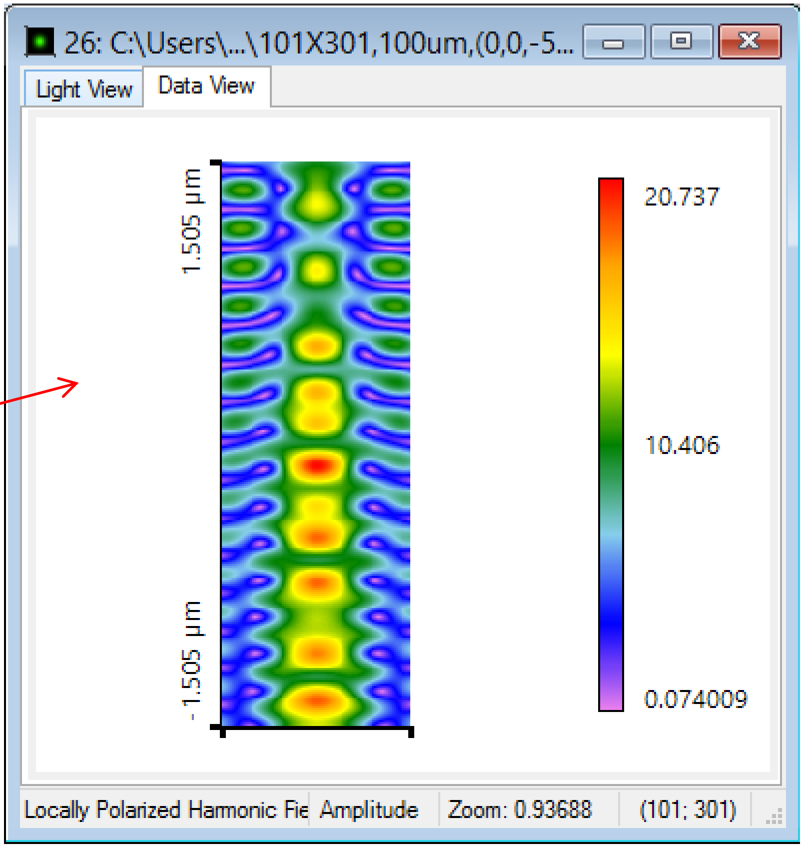

Truncate order vs. computation time

SPs	Nt	Time
(2000, 2000)	2200	?
(1000, 1000)	1150	4d10h
(2000, 2000)	150	1d 14h 40m
(1000, 1000)	125	7h12m
(1000, 1000)	80	2h 50m
(1000, 1000)	30	21m
(1000, 1000)	10	8m11s

For large sphere, Mie theory is numerically time consuming.
For lens without high symmetry, Mie theory is not valid.

Further Tearing

- Field propagation through a curved surface
- Free space propagation
- Field propagation through a curved surface
- Further non-sequentially propagation

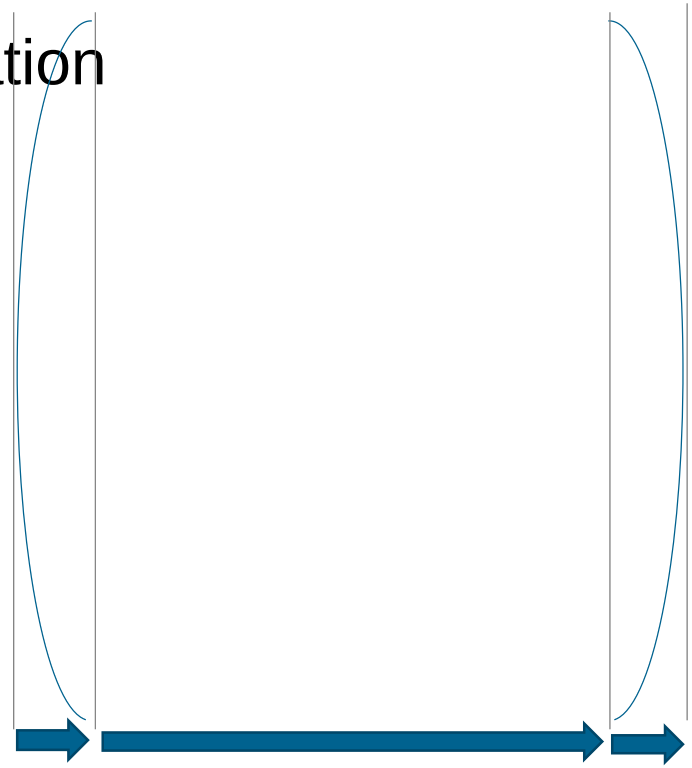

Further Tearing

- Field propagation through a curved surface
- Free space propagation
- Field propagation through a curved surface
- Further non-sequentially propagation

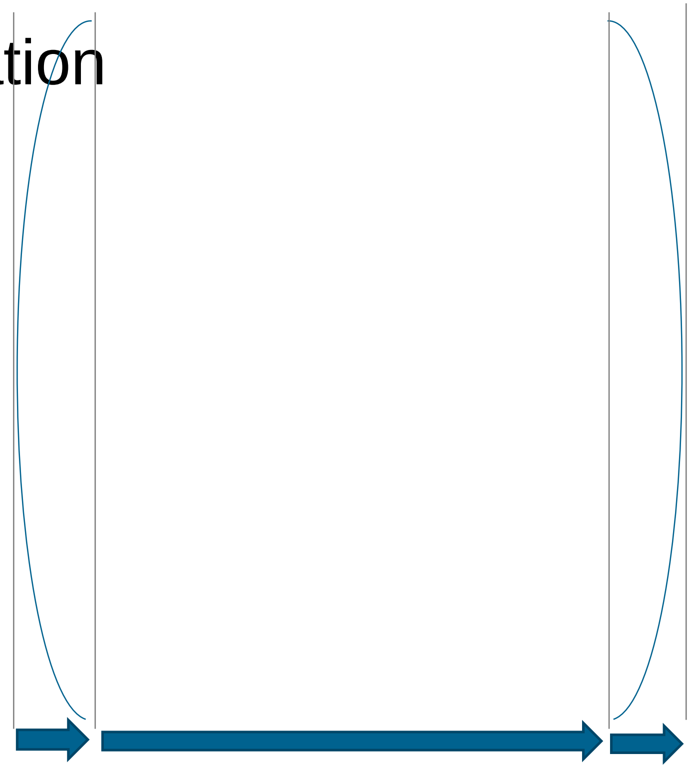

Local Plane Interface Approximation (LPIA)

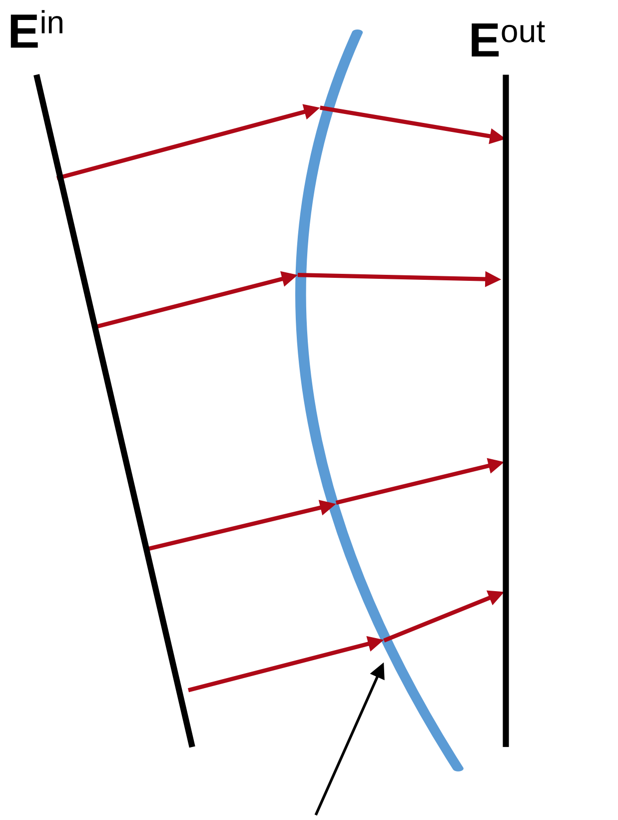

- For each k-value the bidirectional operator in space domain is the response of the surface on a plane wave.
- Response is obtained by local satisfaction of boundary condition.

LPIA: FEM Reference Sinusoidal Grating

Structure: single interface with air and fused silica

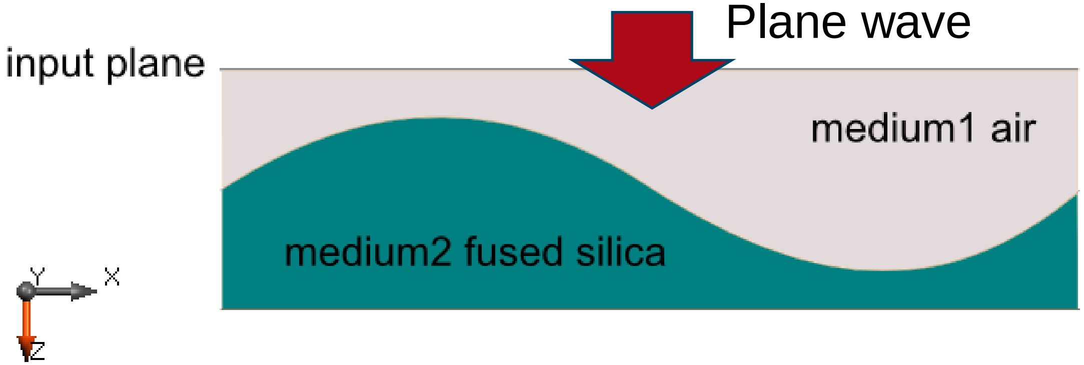

LPIA: FEM Reference Sinusoidal Grating

Structure: single interface with air and fused silica

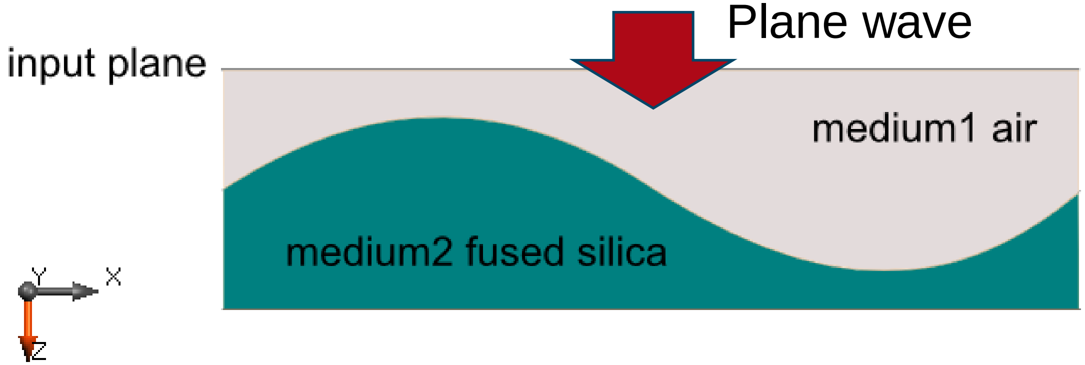

Field amplitude calculated by FEM

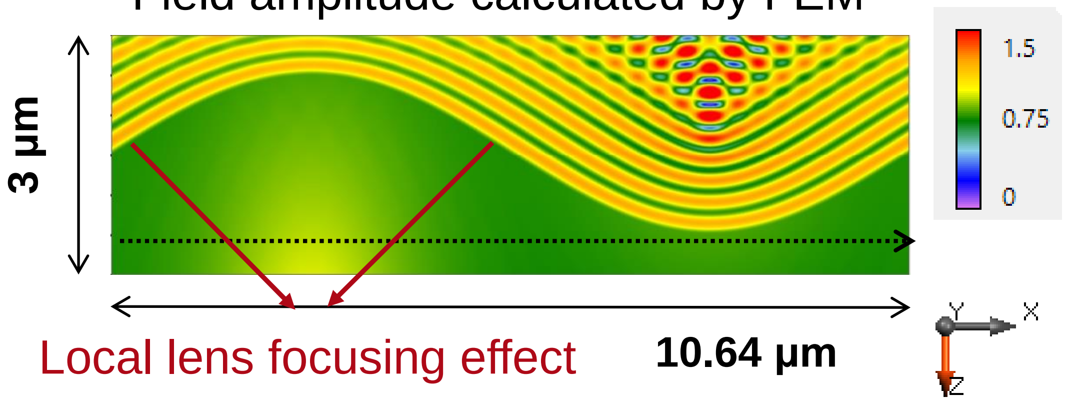

Comparison of Near Field: LPIA vs. FEM

[depth: 2 μm]

- Incident field:
  - TE polarized plane wave;
  - Wavelength: 532 nm;
  - Normal incidence;
- Structure:
  - Sinusoidal grating 2D;
  - Air/Fused silica;
  - Period: 10.64 um= 20λ;
- Output:
  - Amplitude of the electric field behind the grating(LPIA);
  - Amplitude of the electric field behind the grating(FEM);

LPIA: Normalized Amplitude

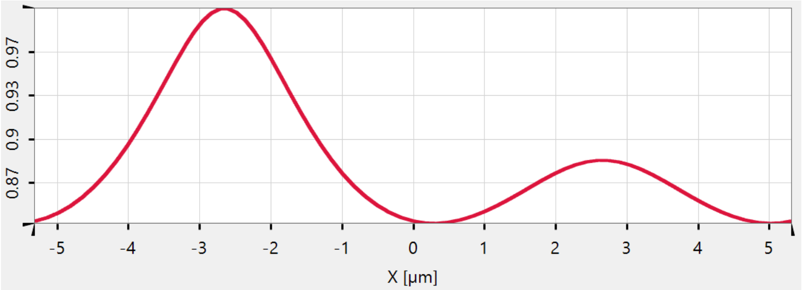

FEM: Normalized Amplitude

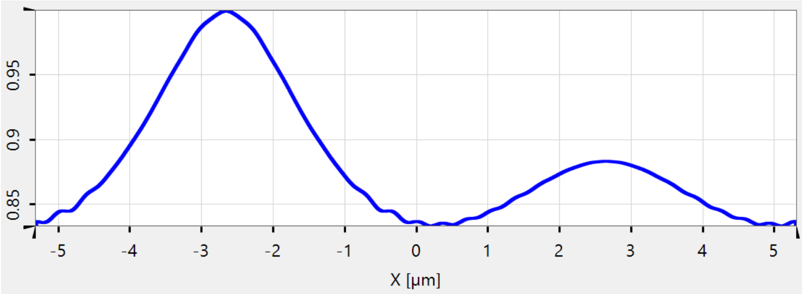

LPIA vs. FEM: Normalized Amplitude

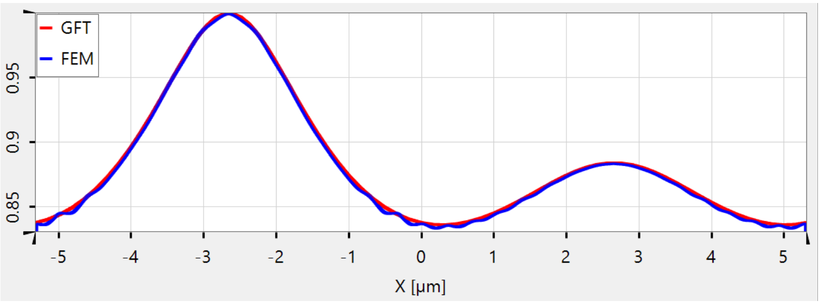

Import Zemax File

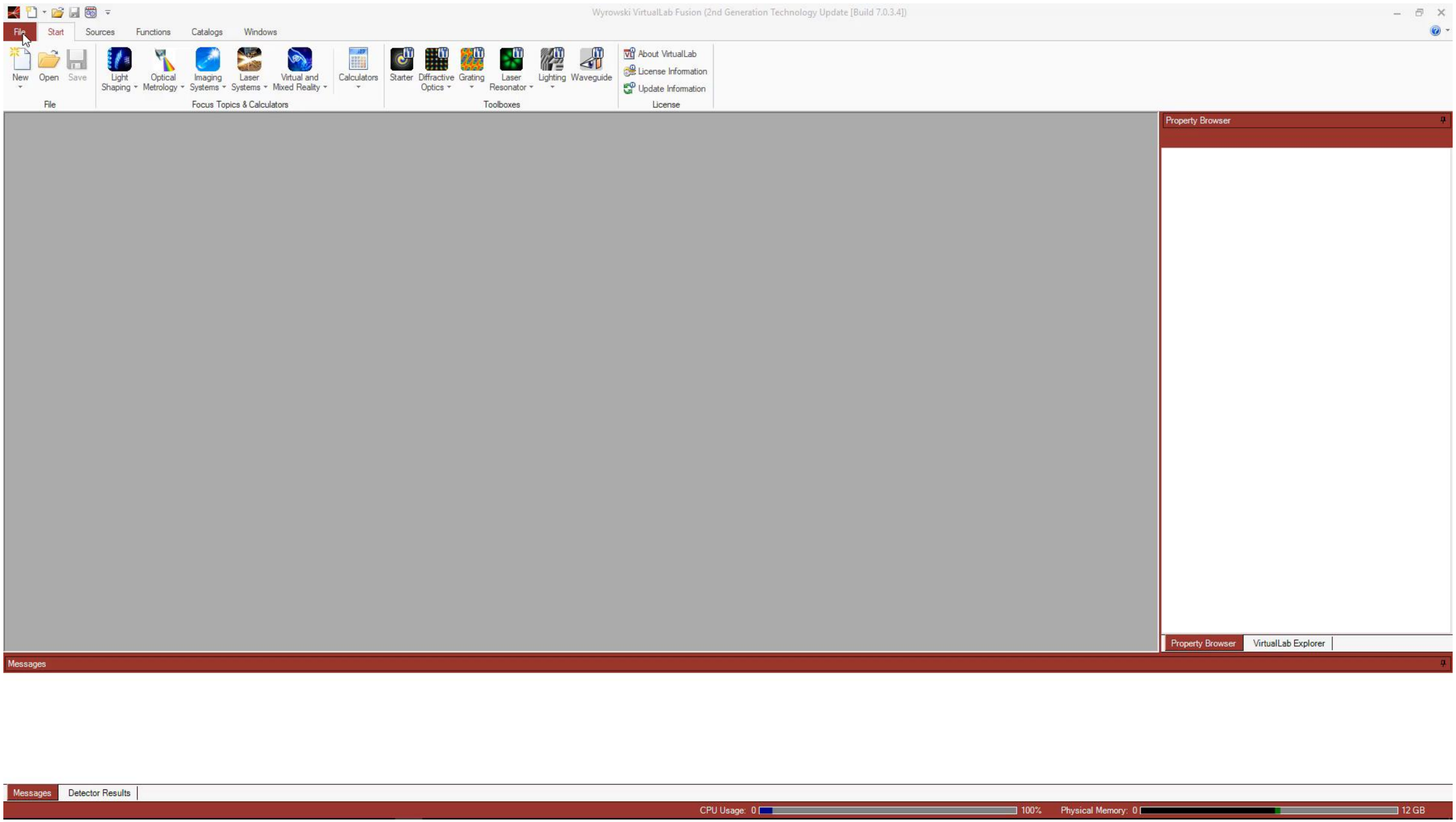

Components

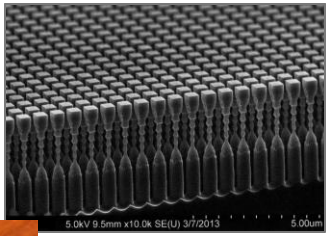

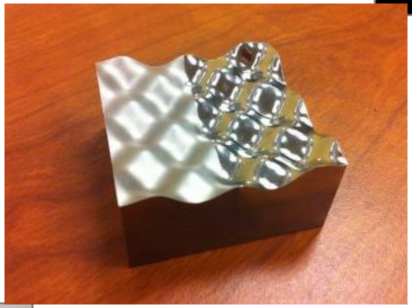

[1] IMS-Mechatronics Lab

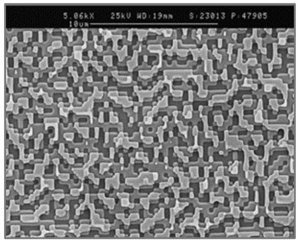

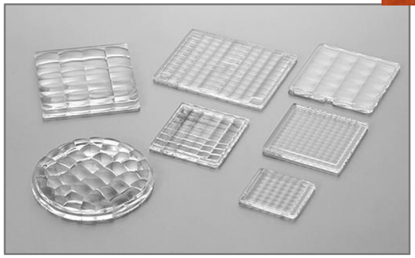

[2] ISUZU GLASS

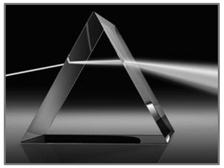

Freeform

Beam Shaping by Freeform Interface

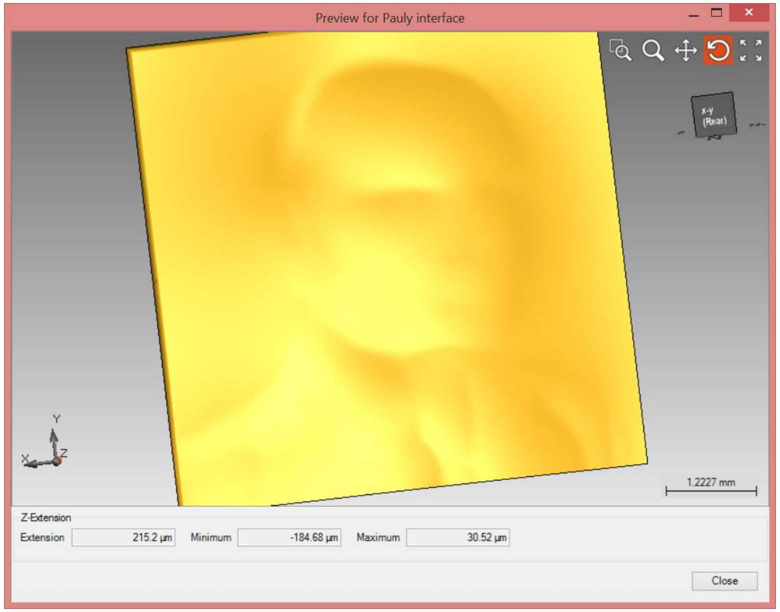

Yuliy Schwartzburg, Romain Testuz, Andrea Tagliasacchi, Mark Pauly

École Polytechnique Fédérale de Lausanne, Computer Graphics and Geometry Laboratory

High-contrast Computational Caustic Design

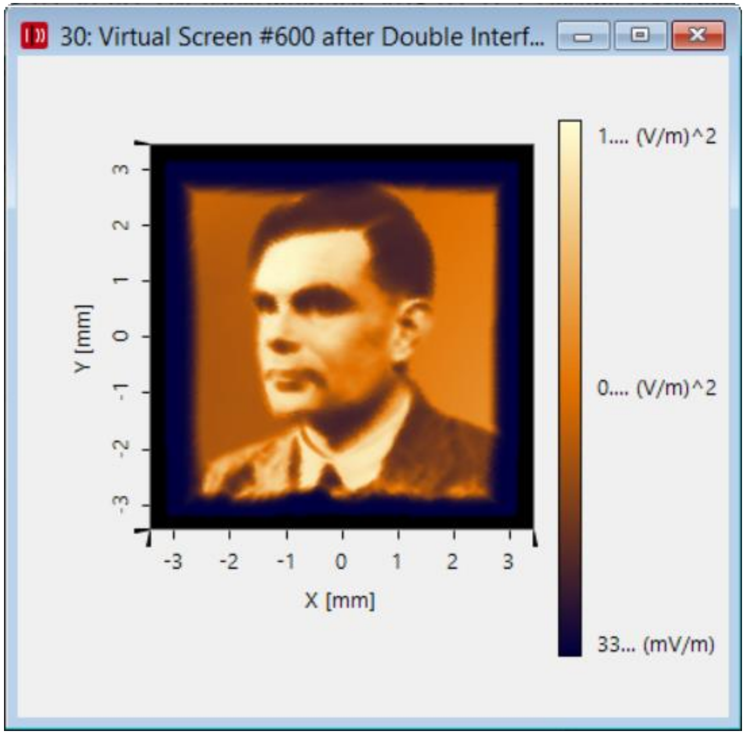

Results

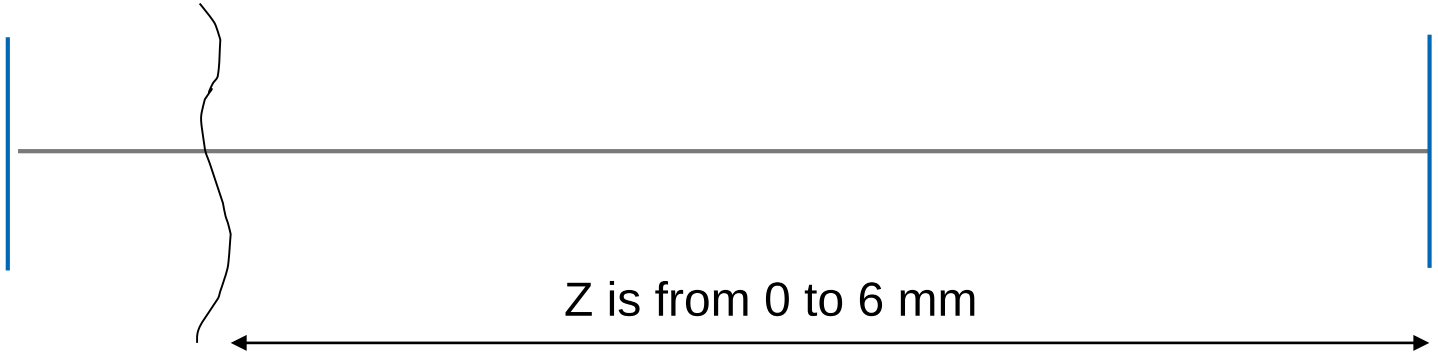

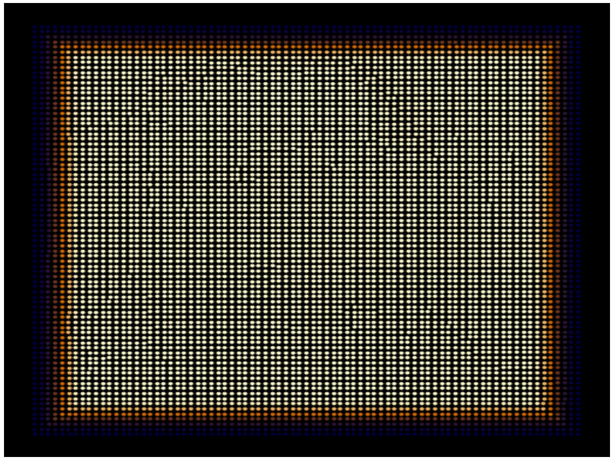

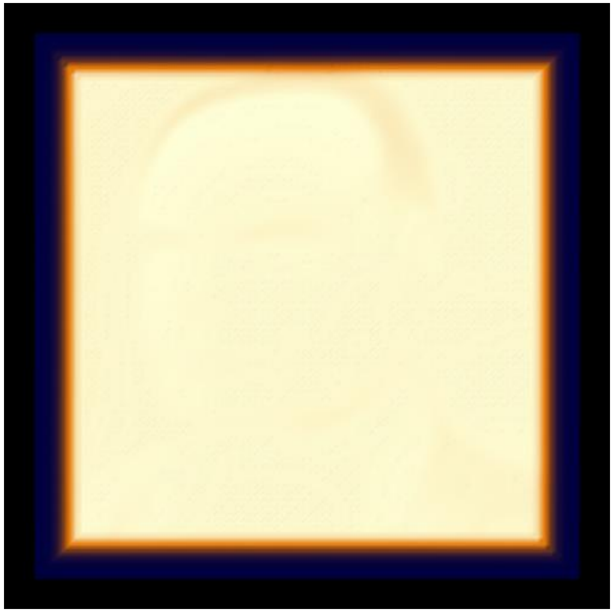

Measurement of Orbital Angular Momentum

Martin P. J. Lavery, *et al*., "Refractive elements for the measurement of the orbital angular momentum of a single photon," Opt. Express 20, 2110-2115 (2012)

Simulation in VirtualLab Fusion

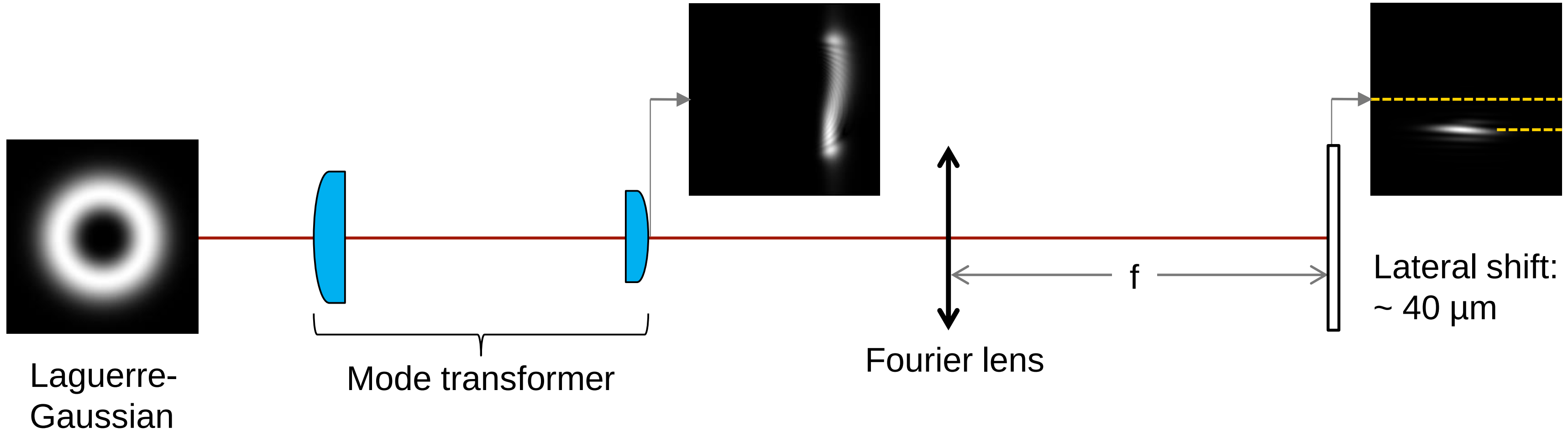

Laguerre-Gaussian

- Light source

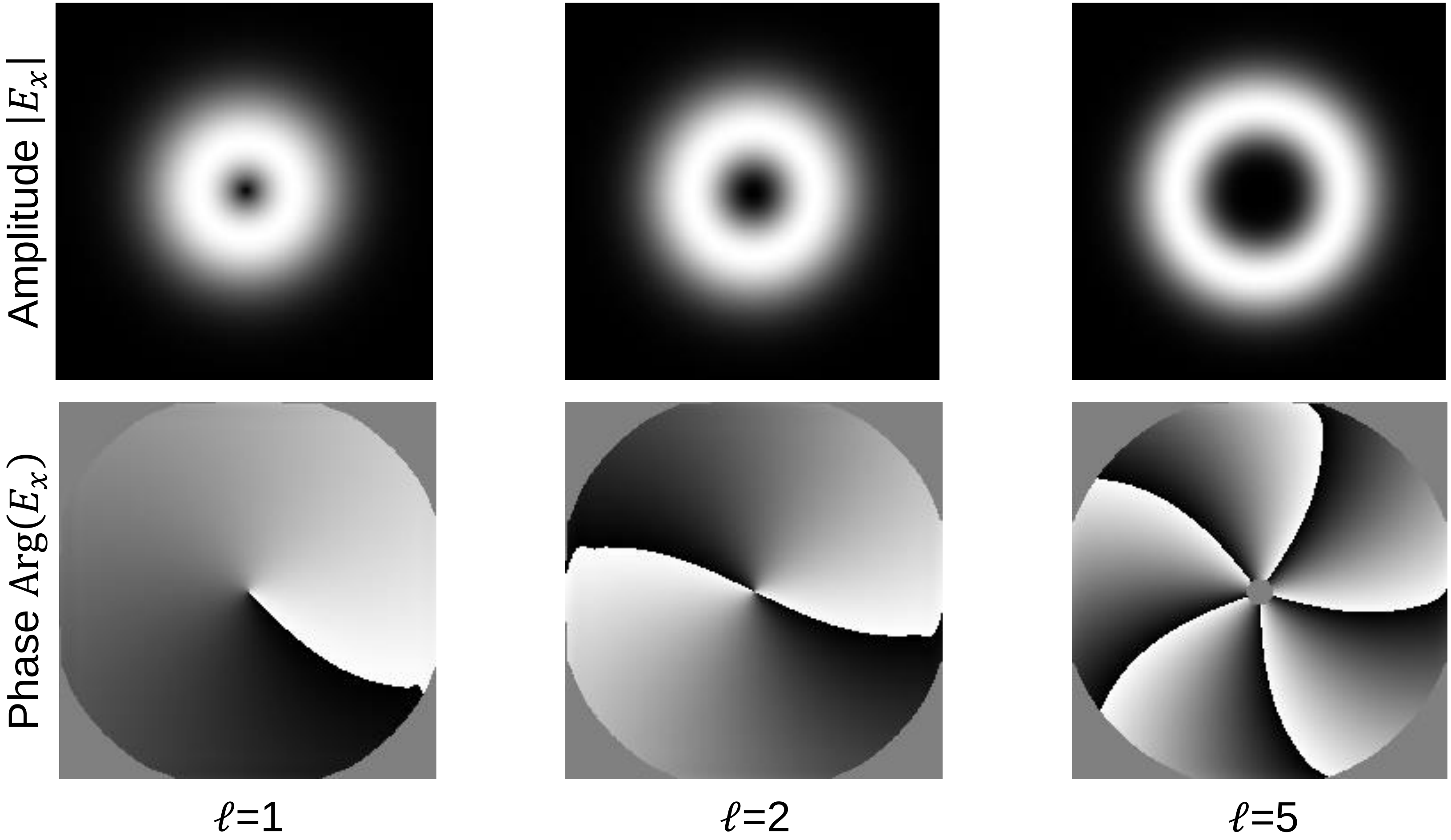

Mode Transformer

$$Z_1(x,y) = \frac{a}{f(n-1)}\left[y\arctan\left(\frac{y}{x}\right) - x\ln\left(\frac{\sqrt{x^2+y^2}}{b}\right) + x - \frac{1}{a}\underbrace{\left(\frac{1}{2}(x^2+y^2)\right)}_{lens\ term}\right]$$

$$Z_2(x,y) = -\frac{ab}{f(n-1)}\left[\exp\left(-\frac{u}{a}\right)\cos\left(\frac{v}{a}\right) - \frac{1}{ab}\underbrace{\left(\frac{1}{2}(u^2+v^2)\right)}_{lens\ term}\right]$$

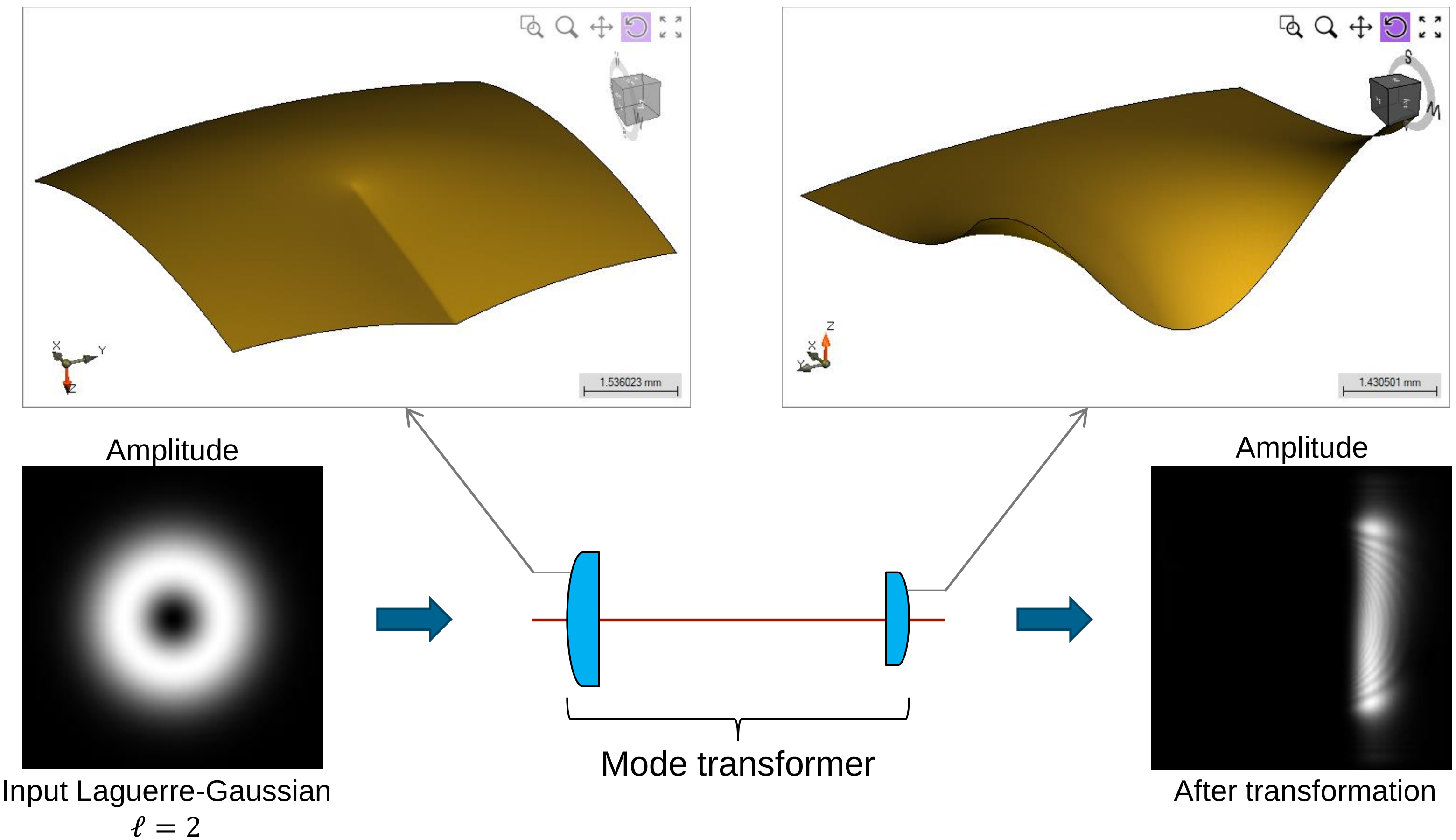

Mode Transformer

$$Z_1(x,y) = \frac{a}{f(n-1)}\left[y\arctan\left(\frac{y}{x}\right) - x\ln\left(\frac{\sqrt{x^2+y^2}}{b}\right) + x - \underbrace{\frac{1}{a}\left(\frac{1}{2}(x^2+y^2)\right)}_{\textit{lens term}}\right]$$

$$Z_2(x,y) = -\frac{ab}{f(n-1)}\left[\exp\left(-\frac{u}{a}\right)\cos\left(\frac{v}{a}\right) - \underbrace{\frac{1}{ab}\left(\frac{1}{2}(u^2+v^2)\right)}_{\textit{lens term}}\right]$$

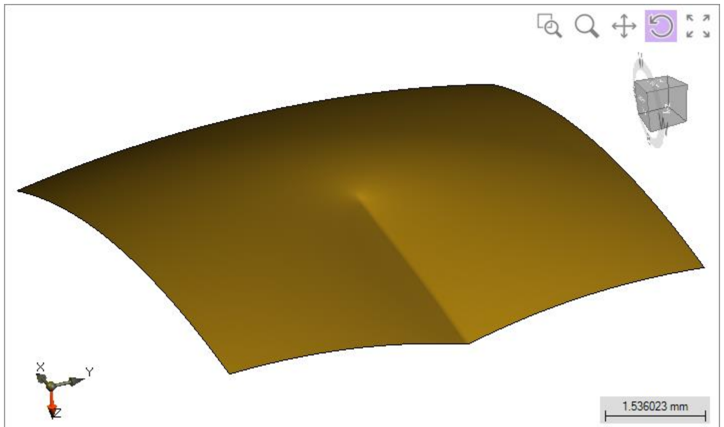

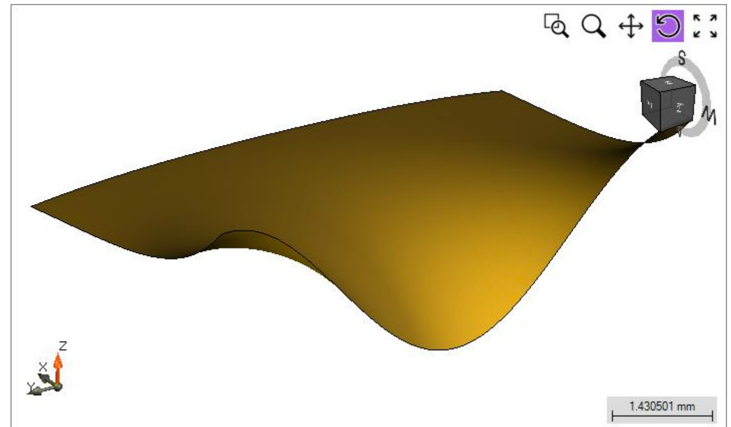

Phase

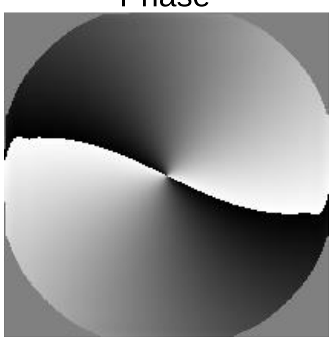

Input Laguerre-Gaussian
$\ell = 2$

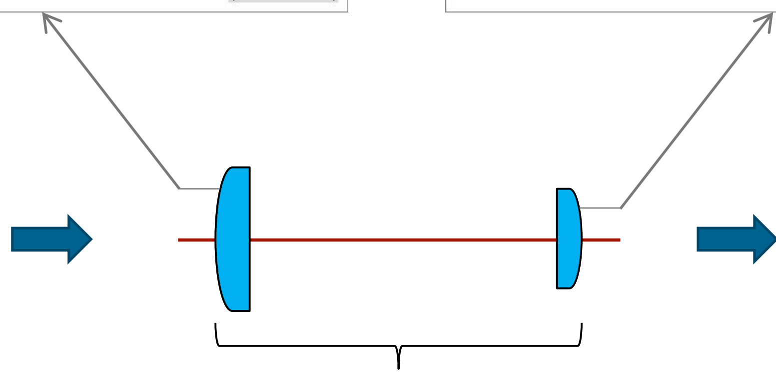

Mode transformer

Phase

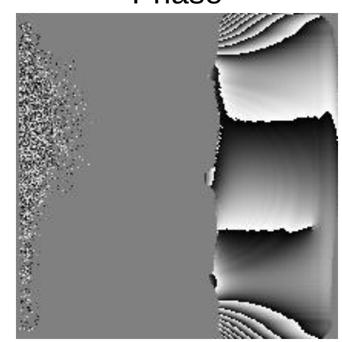

After transformation

Mode Transformer

- Amplitude distributions before and after transformation

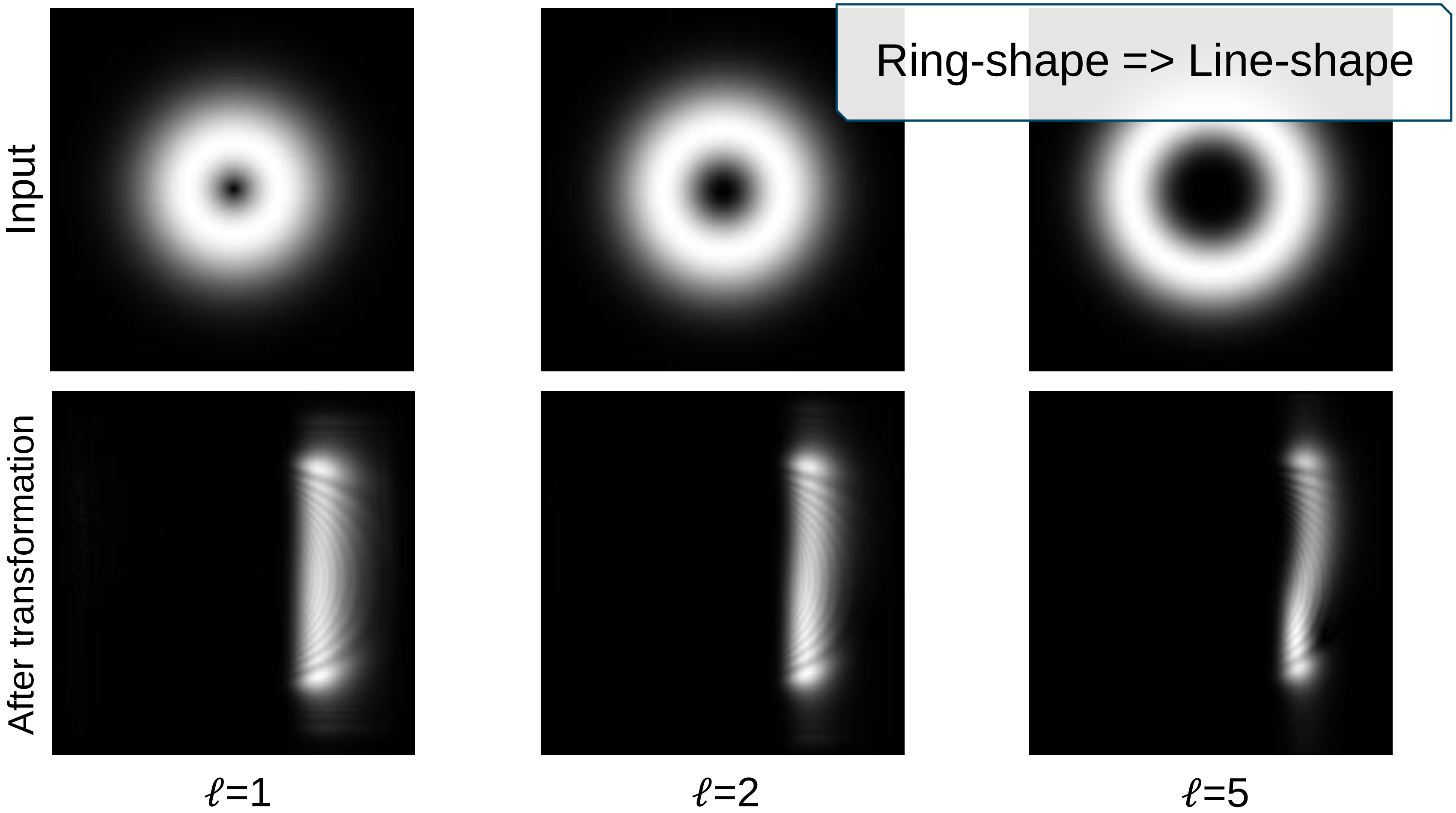

Mode Transformer

- Phase distribution before and after transformation

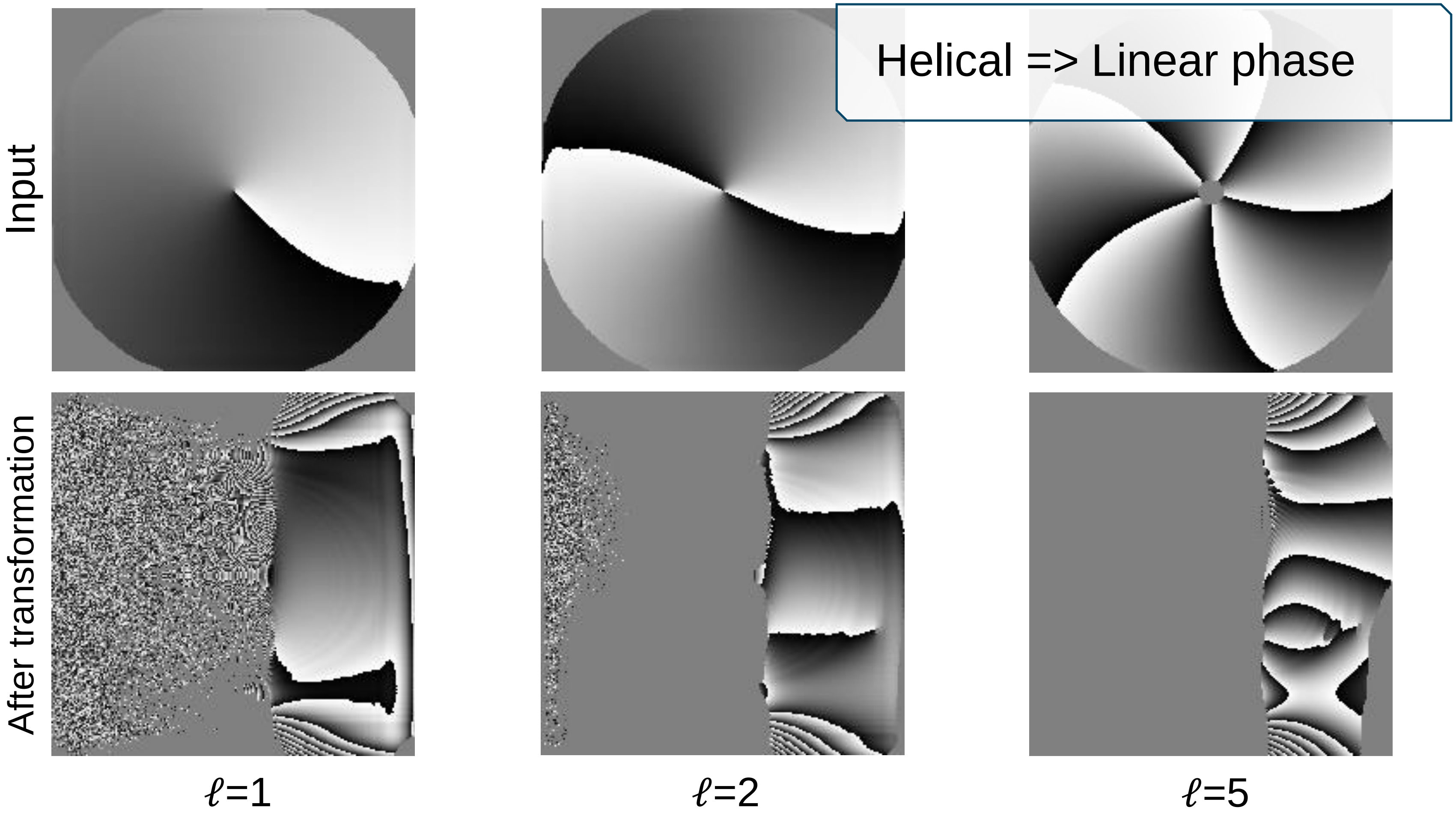

Detection Part

- Shift theorem
  - A linear phase in one domain leads to a lateral shift in the other domain according to Fourier transformation

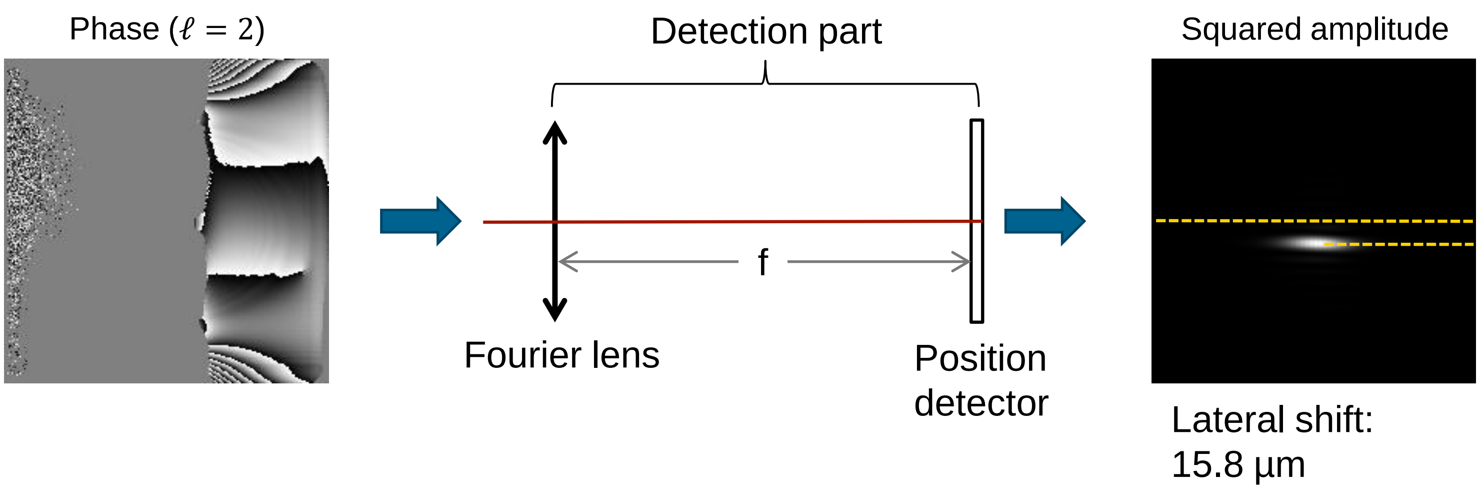

Detection Part

- Shift theorem
  - A linear phase in one domain leads to a lateral shift in the other domain according to Fourier transformation

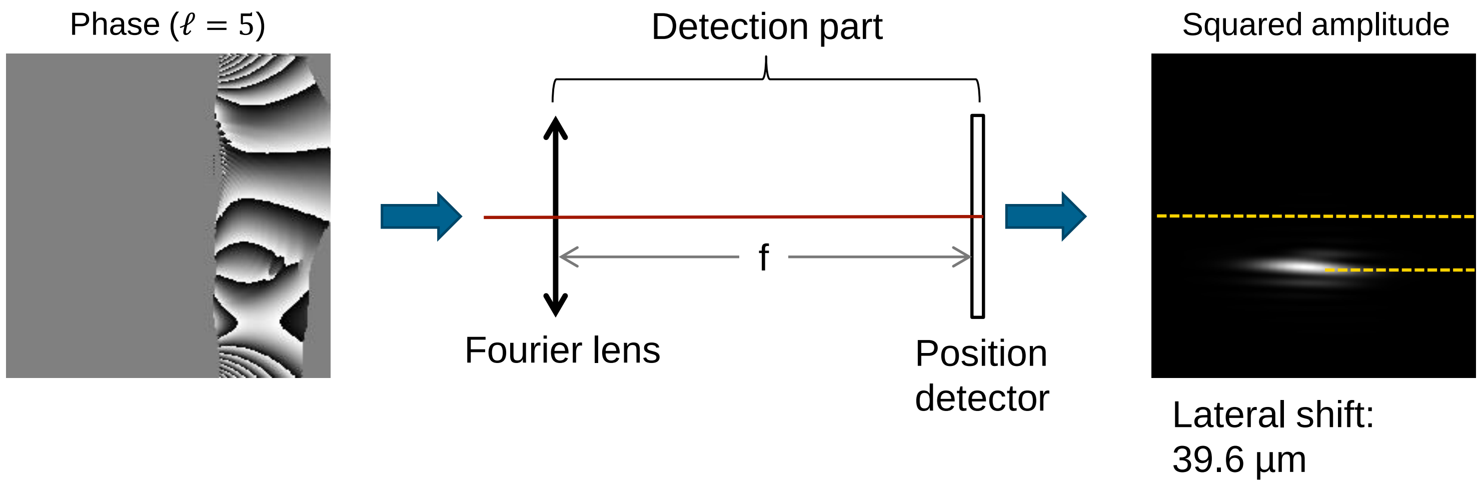

System Functioning

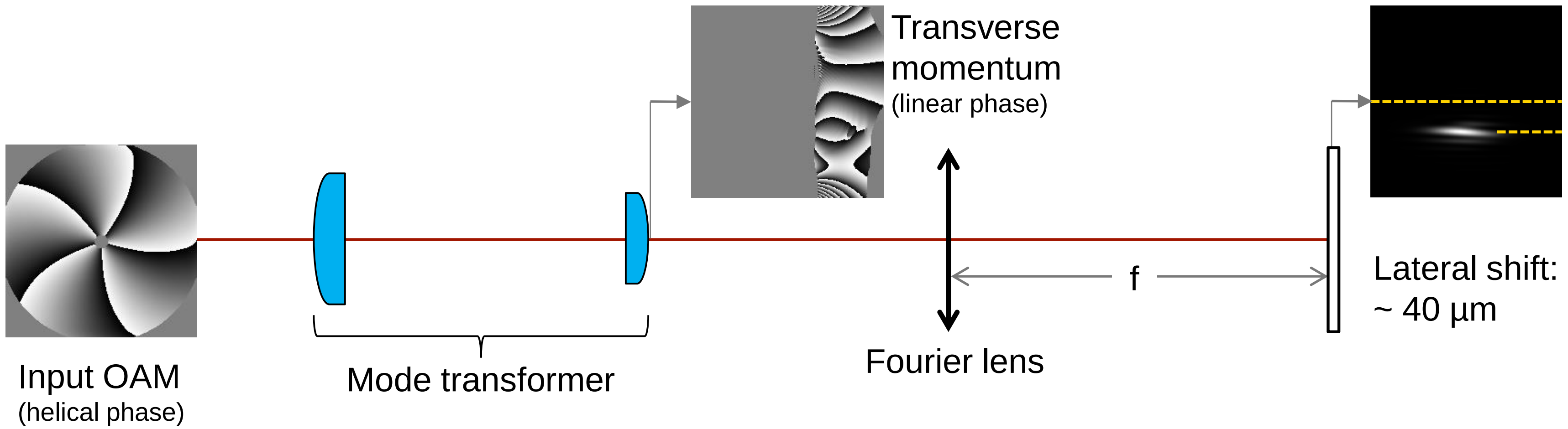

- An input OAM is firstly transformed to transverse momentum by the mode transformer, which is composed of two freeform refractive optical elements
- The transverse momentum is then transformed into lateral position shift by a Fourier lens
- By precise measurement of the lateral shift, one reads the OAM state i.e. the encoded information

System Functioning

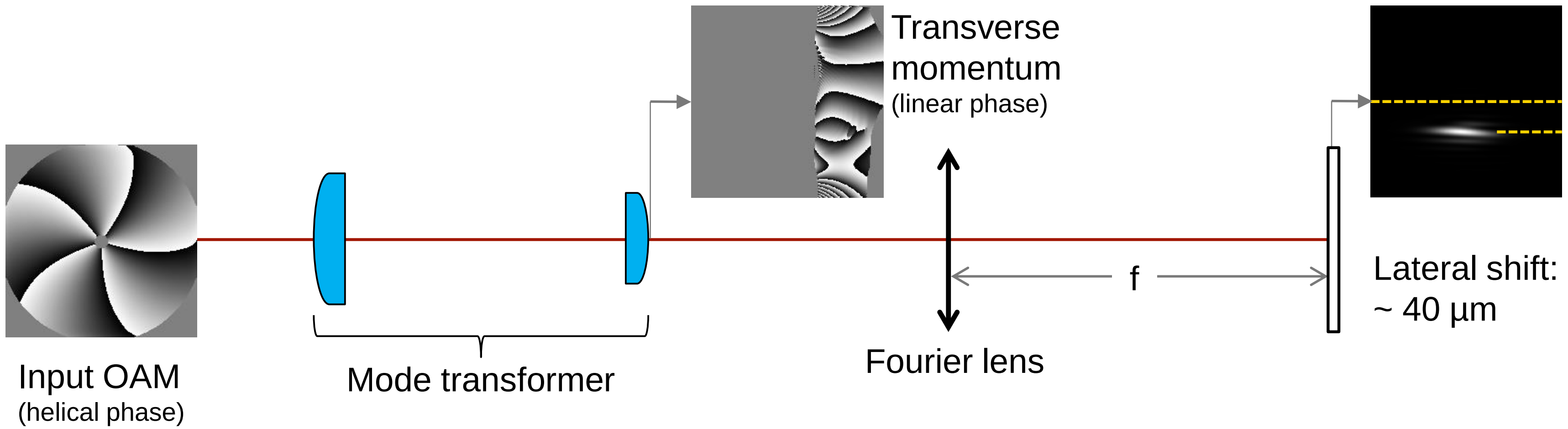

- Testing
  - Using ParameterRun and set the angular order of input OAM from 1 to 15, and measure the detected lateral position

Visualization of Surface Profiles in 1D, 2D and 3D

Task: Visualization of Surface Profiles

- To define the structure of any optical system it is pretty typical to define components, which are oriented within the system.
- Each component can by typically defined by combining optical surfaces and media.
- The visualization of these building blocks is very important.
- VirtualLab provides several options to visualize surfaces in 1D and 3D.
- In addition a 2D visualization of surfaces I possible.

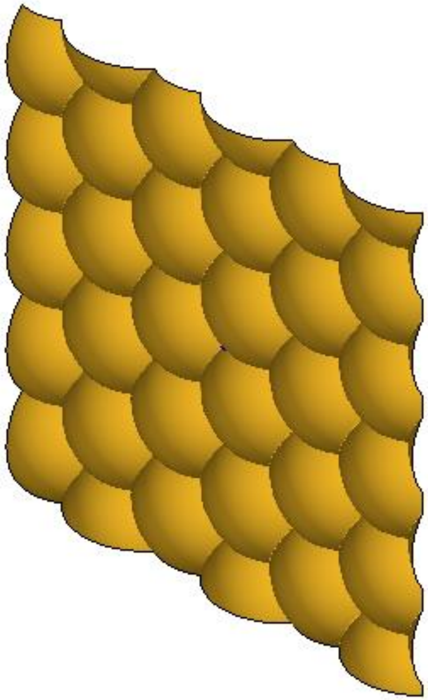

Standard Surface Visualization

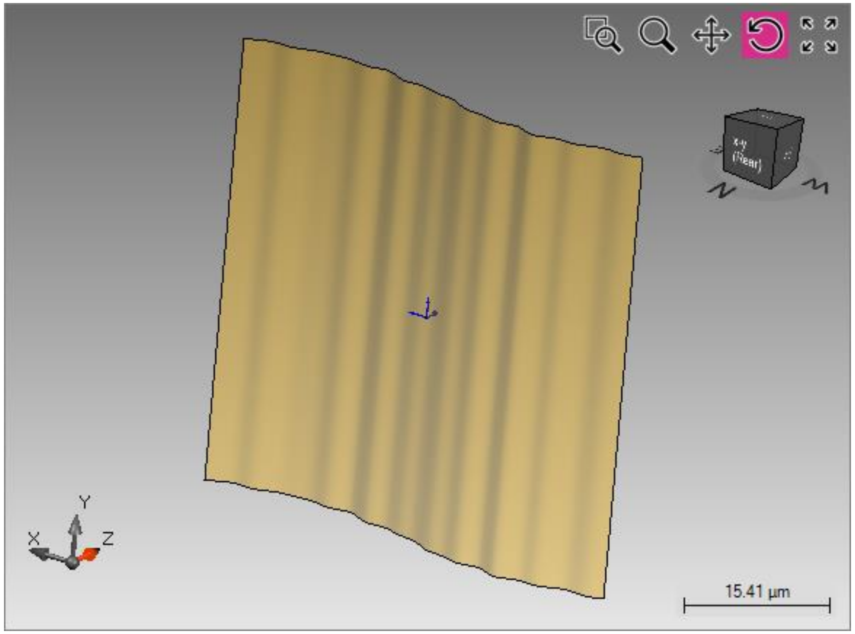

3D view of optical surfaces

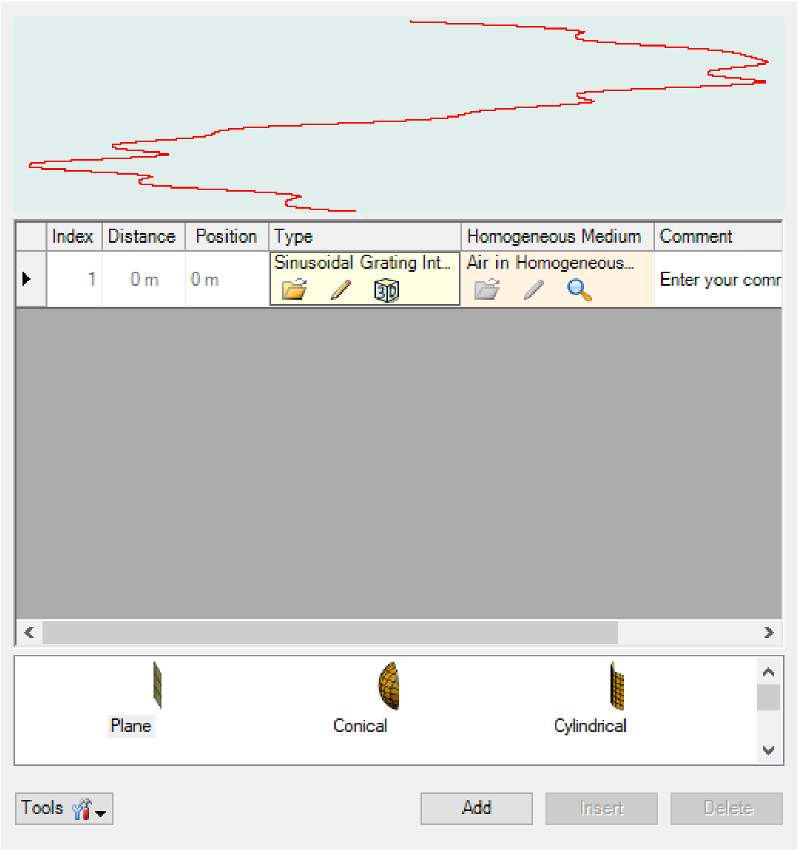

Edit dialog of optical interface sequence including 1D profile

Customized Surface Visualization

1D

2018-01-30_Christian_Hellmann_DisplayOfSurfaceSagInVirtualLab

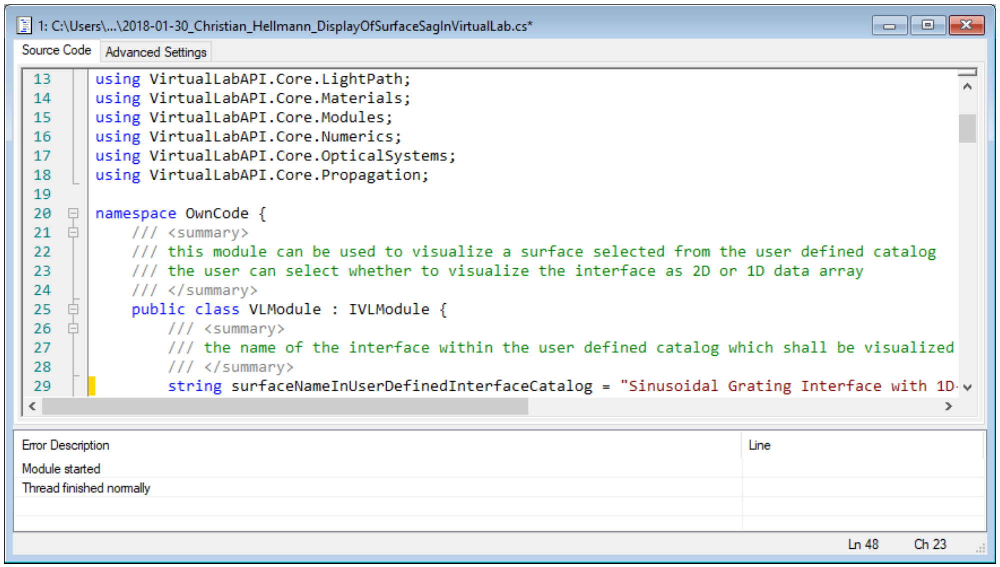

Select name of surface which should be load from user defined catalog.

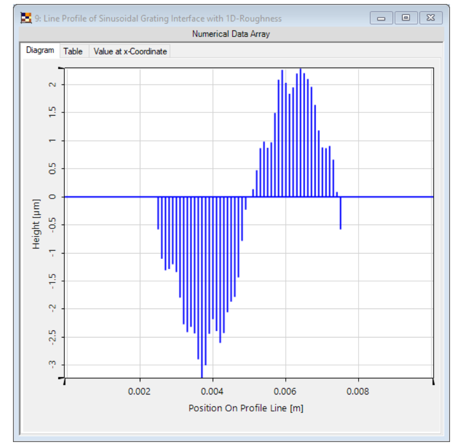

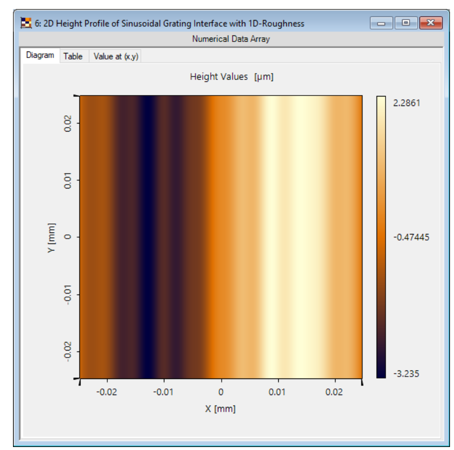

2D

Gratings

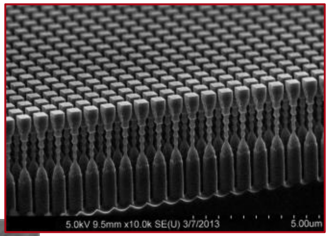

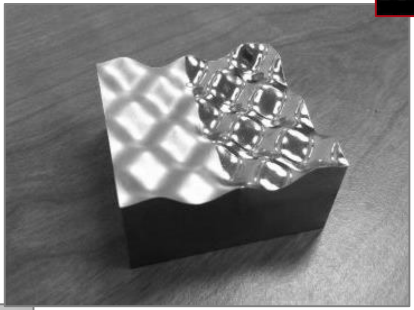

[1] IMS-Mechatronics Lab

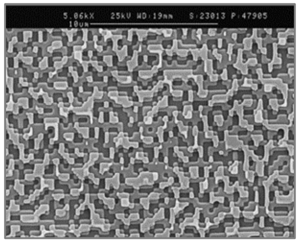

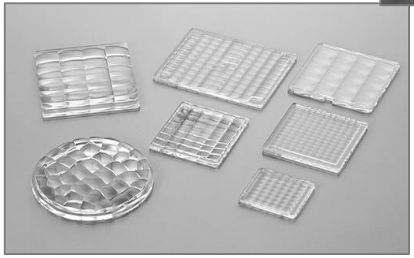

[2] ISUZU GLASS

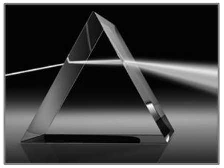

Modeling Technologies

- Electromagnetic analysis of gratings by
  - Fourier Modal Method (FMM)
  - (also called) Rigorous Coupled Wave Analysis (RCWA)
  - Integral Method
- Approximated analysis by Thin Element Approximation
- Merit functions:
  - Diffraction efficiency
  - Near field
  - Far field
  - Field inside grating
  - Polarization analysis
  - Customized merit functions.

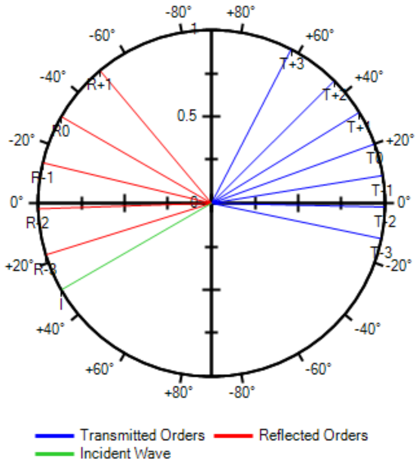

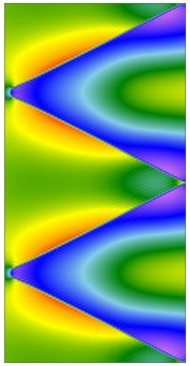

- Grating analysis for plane and general incident waves
- Analysis include degree of coherence, color, polarization.

Grating analysis for general incident waves.

- Typically gratings are only a part of an entire optical system
- In addition to the grating there are e.g. illumination and detector optics
- Simulation of multi-scale optical systems including macroscopic optical components and gratings.
- Fourier Modal Method for general incident waves in combination with other field tracing techniques (like e.g. geometrical optics, diffraction integrals and physical optics) enables the simulation of such multi-scale optical setups

Micro- / nano-structures

Ultrasparse Dielectric Nanowire Grid Polarizer

LightTrans International UG

Simulation Results

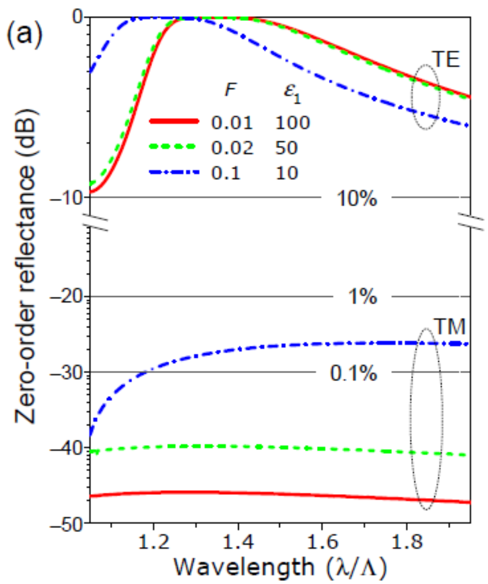

Figure from J. W. Yoon *et al.*, Opt. Express **23**, 28849-28856 (2015)

VirtualLab simulation

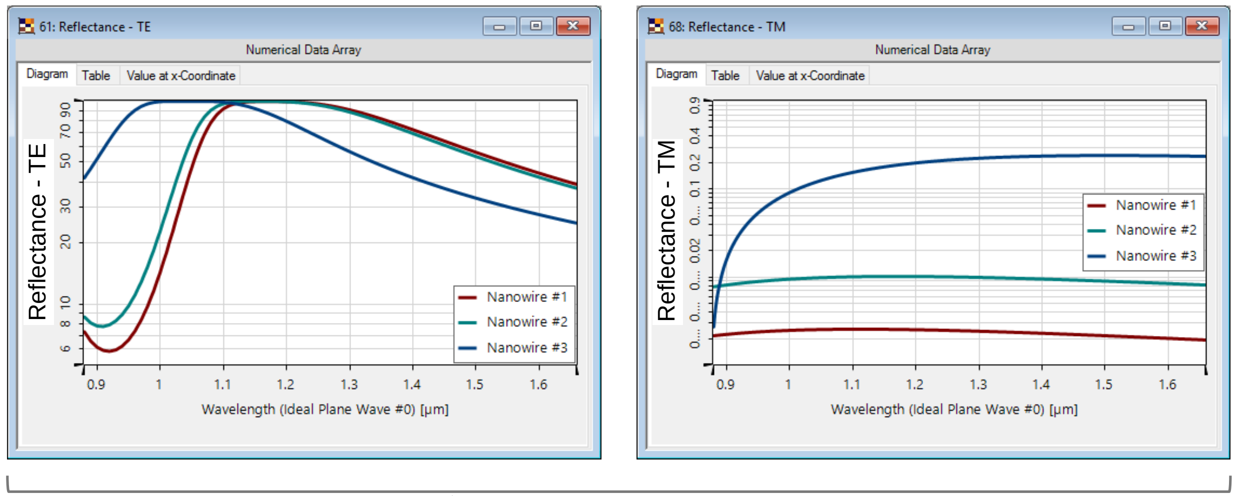

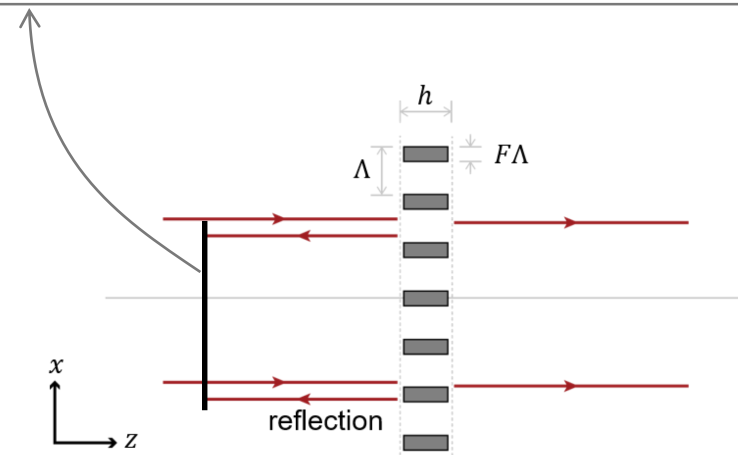

Simulation Results

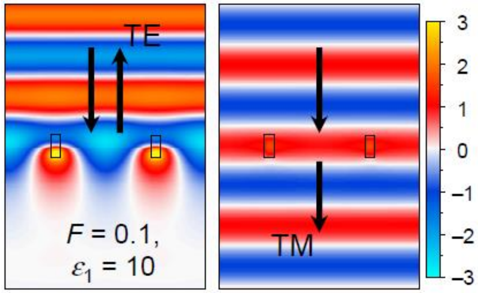

Figure from J. W. Yoon *et al.*, Opt. Express **23**, 28849-28856 (2015)

VirtualLab simulation

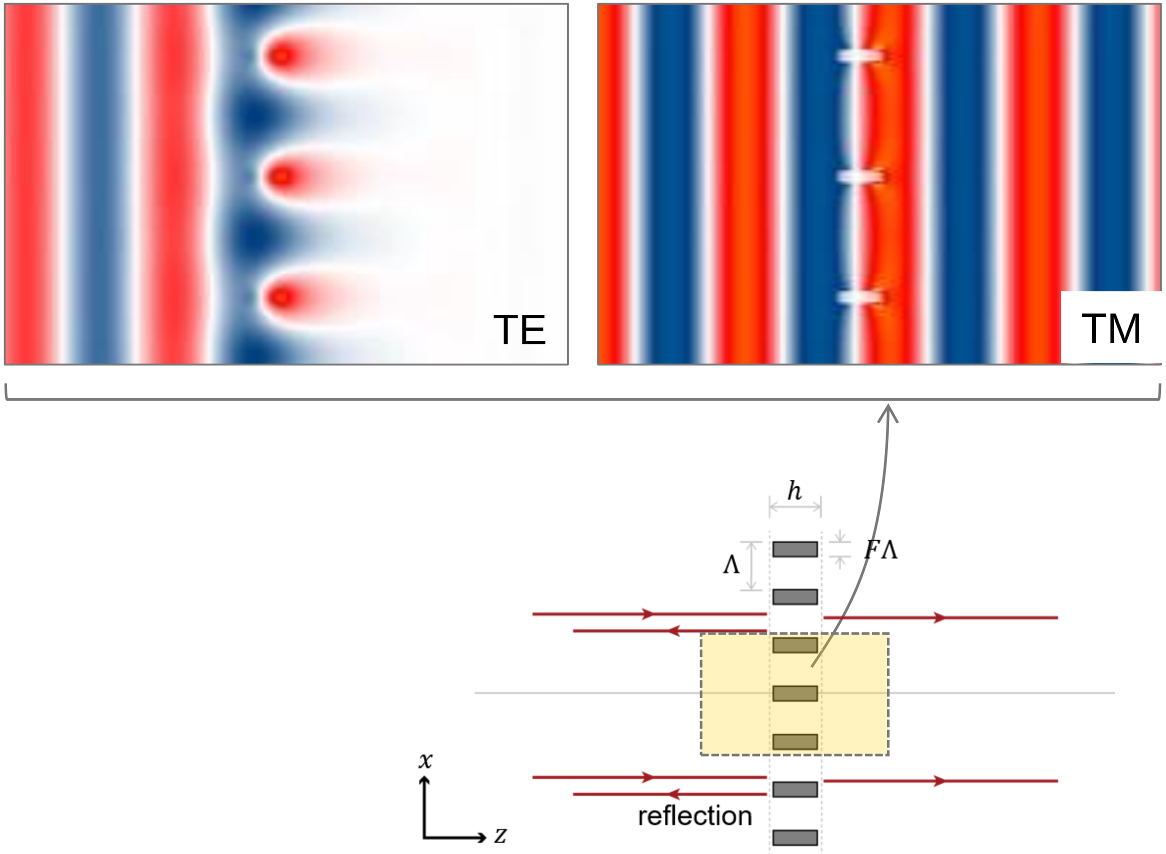

Simulation Results

Highlights

- fast calculation for periodic structures using Fourier modal method (FMM)
- easy access to full field information within nano-structures

VirtualLab simulation

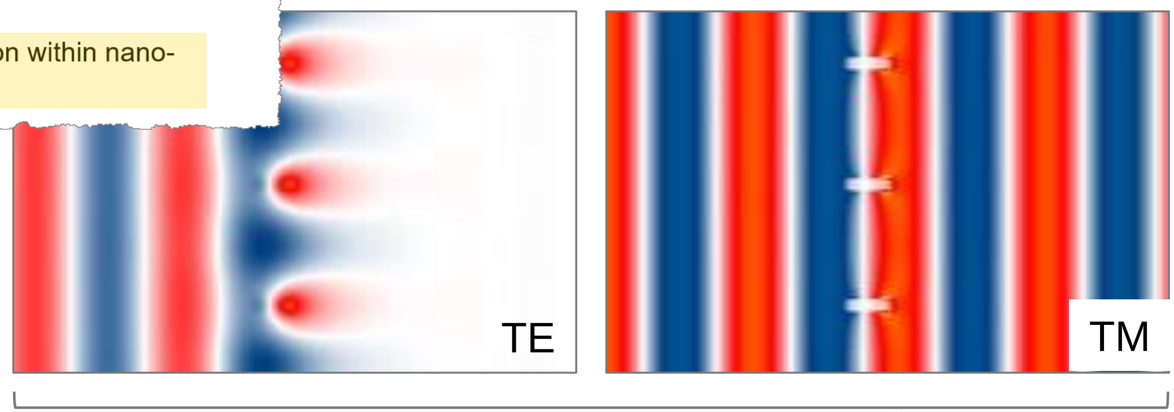

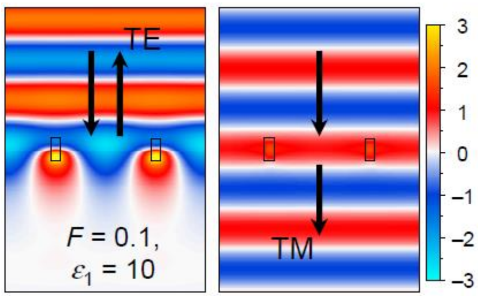

Figure from J. W. Yoon *et al.*, Opt. Express **23**, 28849-28856 (2015)

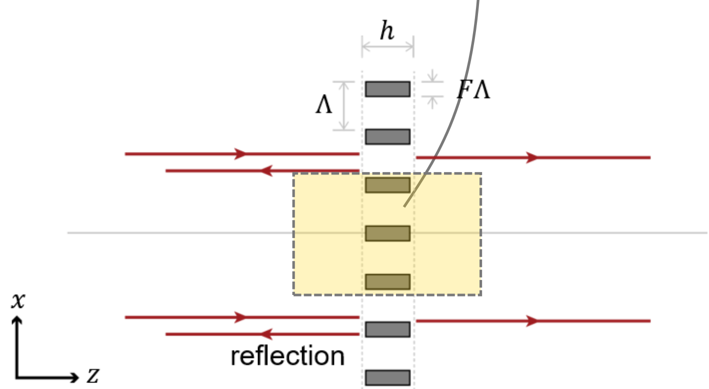

Imaging Systems > Inclusion of Gratings

Rigorous Simulation of Holographic generated Volume Grating

Task/System Illustration

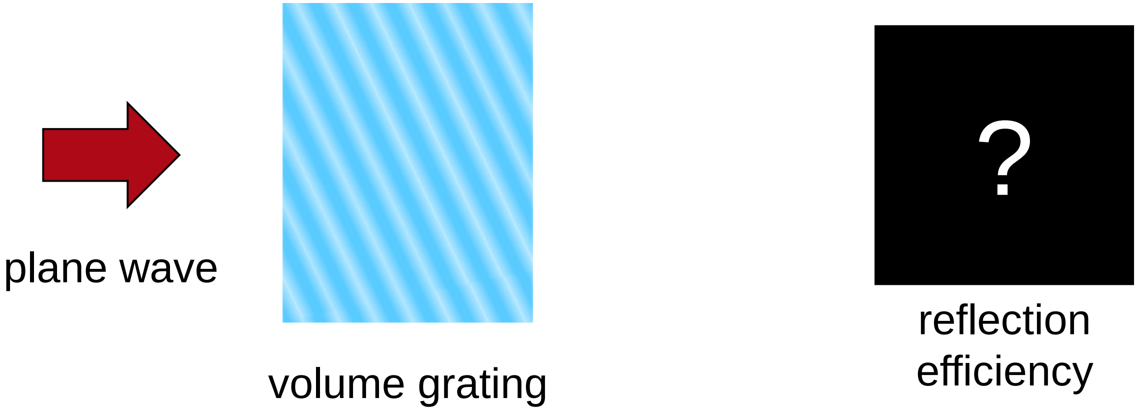

Specification: Volume Grating

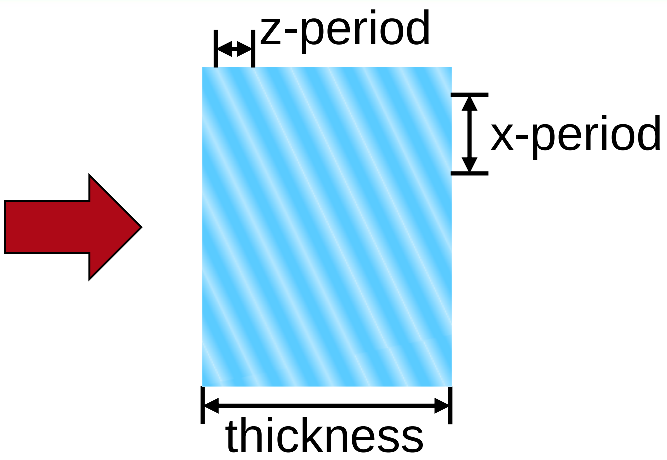

Parameter	Description / Value & Unit
type	holographic generated
index modulation	0.01 (increased due to exposure)
thickness	70 µm
period in x-direction	507.6 nm
period in z-direction	292.5 nm
tilt of modulation	59.9°

Result: Angular Dependency of Reflection

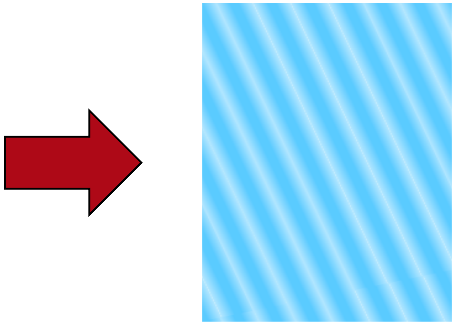

Reflection, -1st order

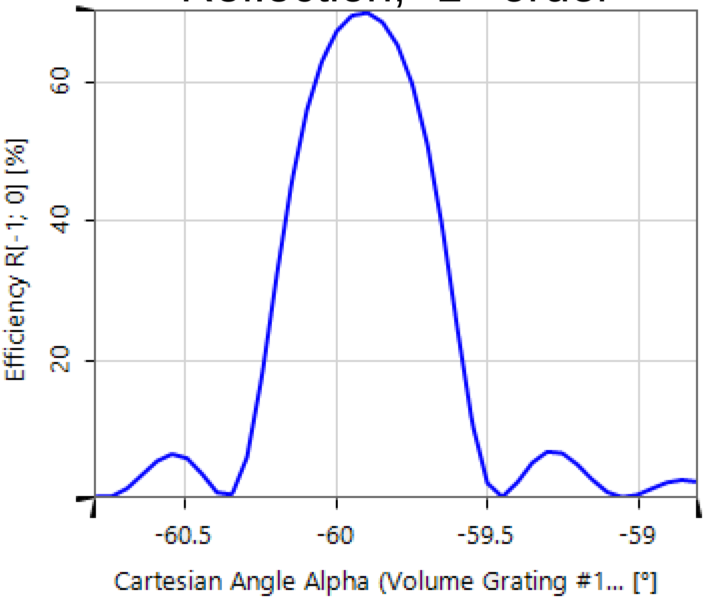

shift of angular dependent reflection due to holographic interference angle of 59.9°

Result: Wavelength Dependency of Reflection

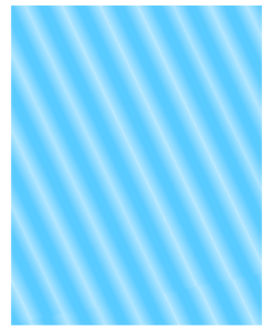

Reflection, -1^{st} order

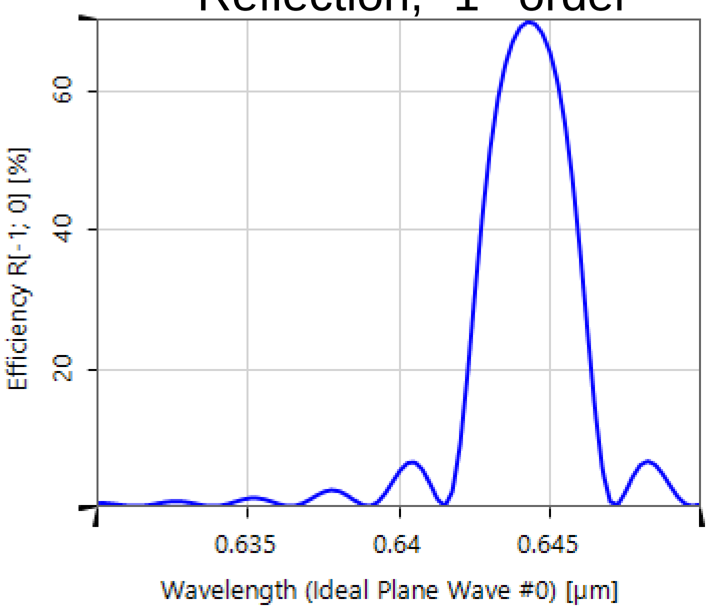

shift of wavelength dependent reflection due to locally increased effective refraction index

Fields in Focal Regions

Example Wafer inspection system

Example of Multi-scale Optical System

Example: Wafer Inspection System

Complex macroscopic high NA imaging lens system and microscopic grating structure (integrated circuit wafer structure) in one optical setup. Simulation results can be found in Scenario 515

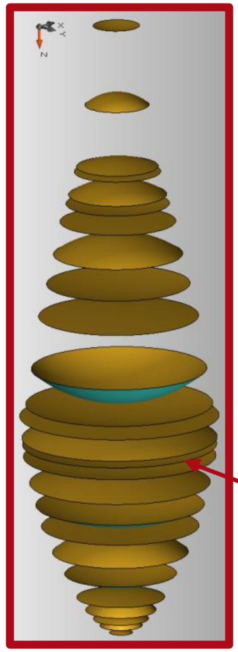

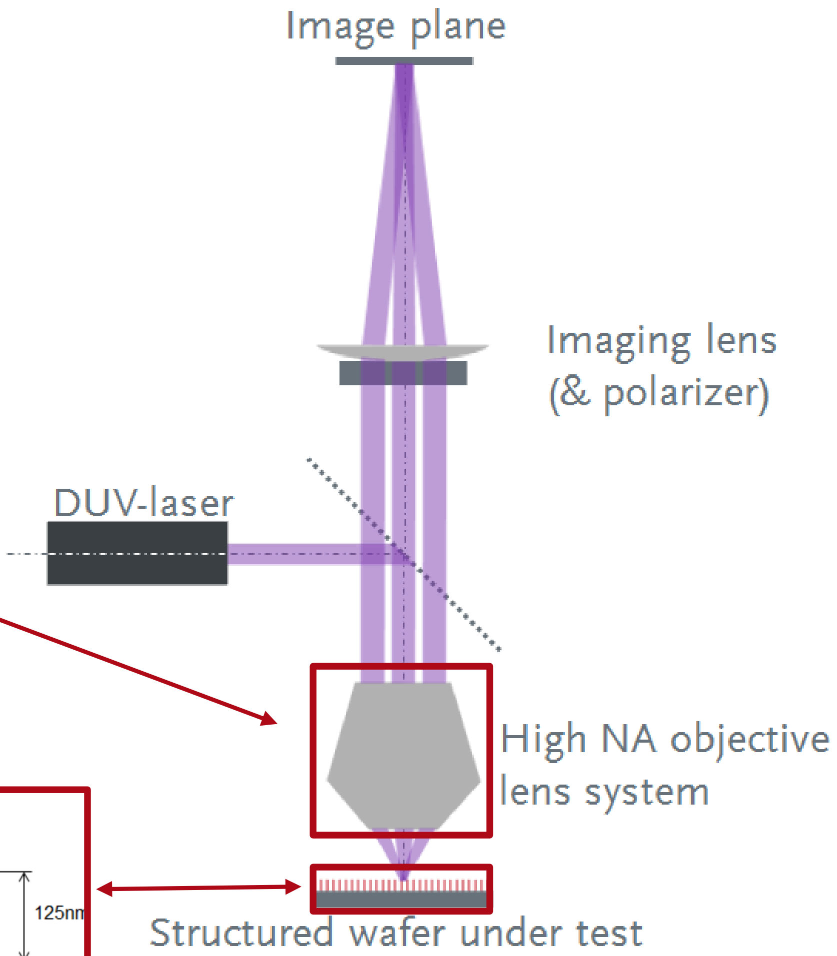

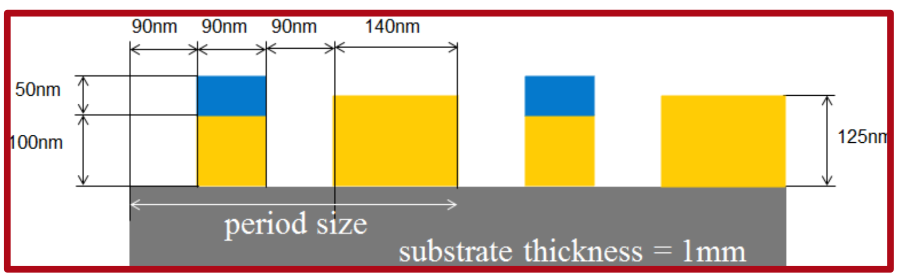

Base Grating Structure

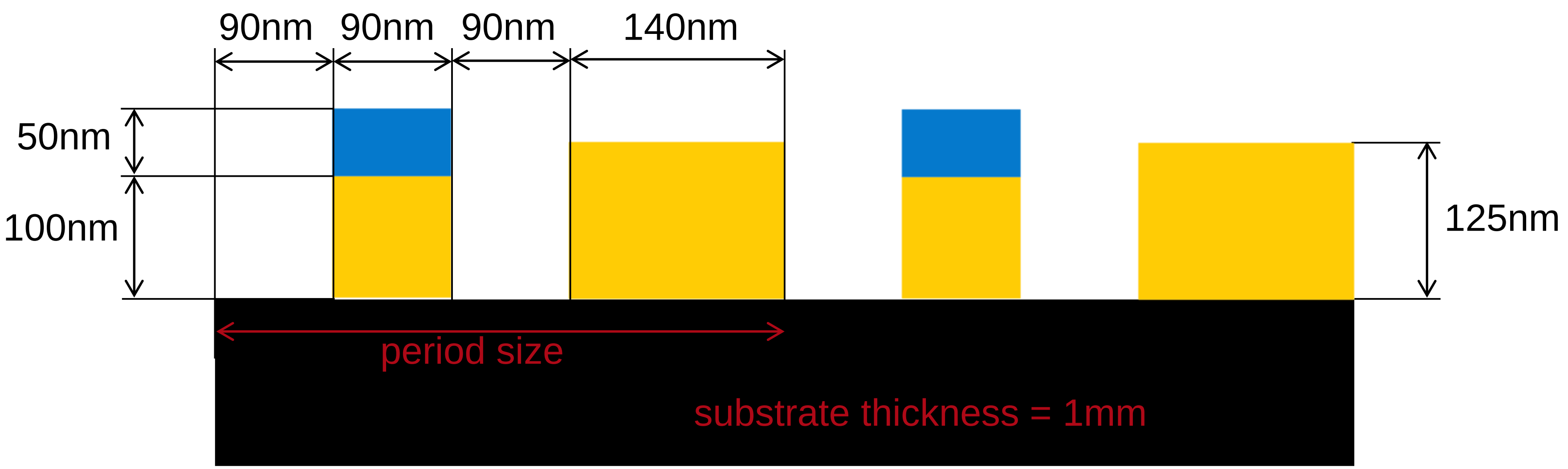

Base Structure Analysis

Intensity Image of Grating after Polarizer in X-Direction

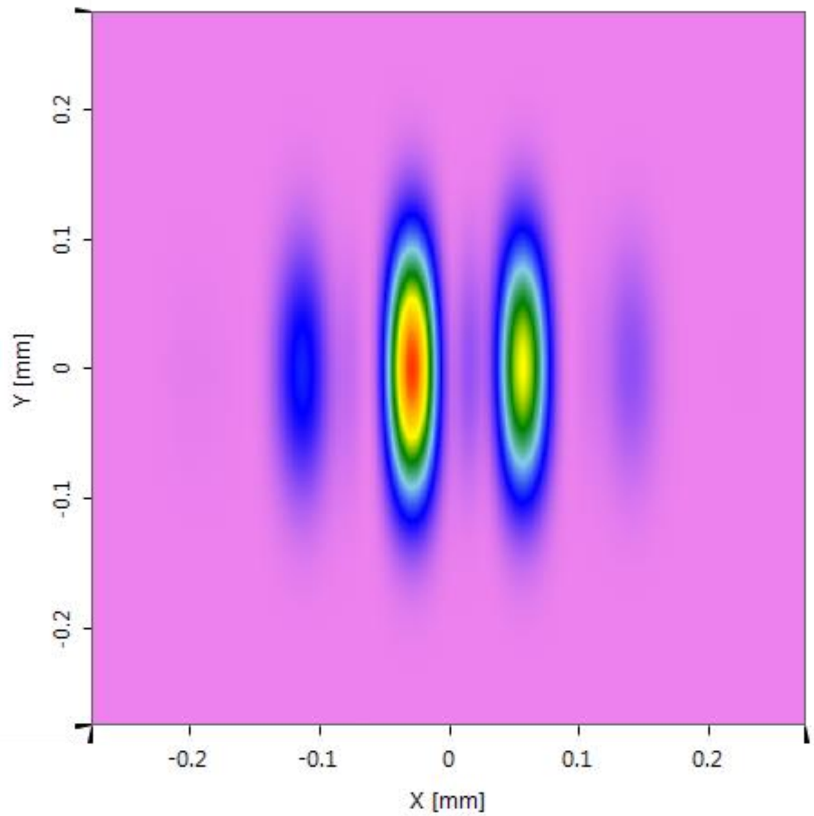

Intensity Image of Grating after Polarizer in Y-Direction

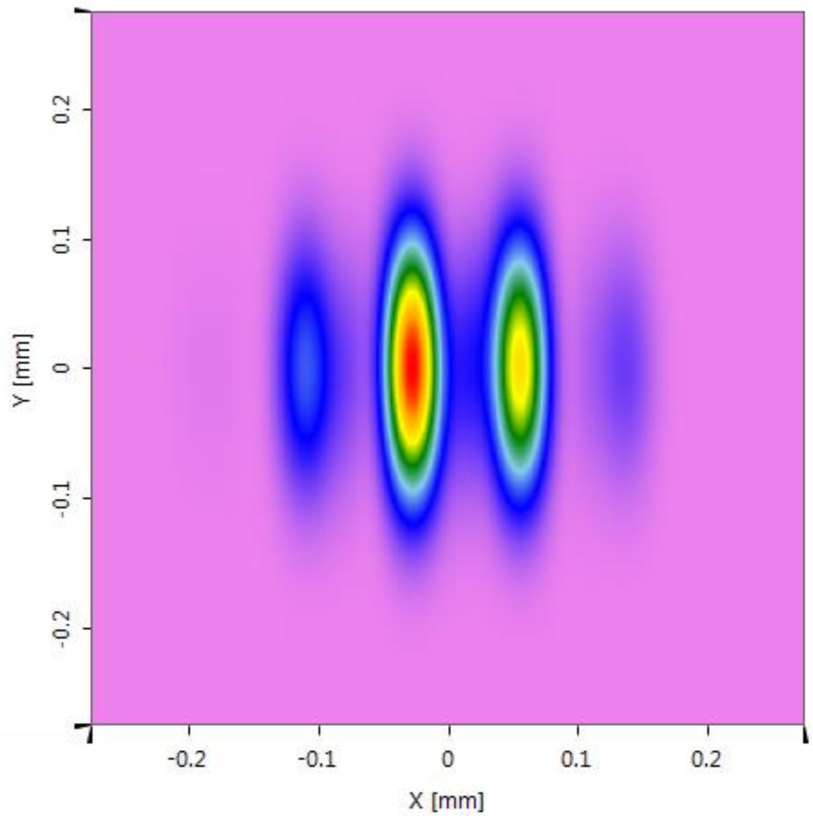

Modified Grating Structure

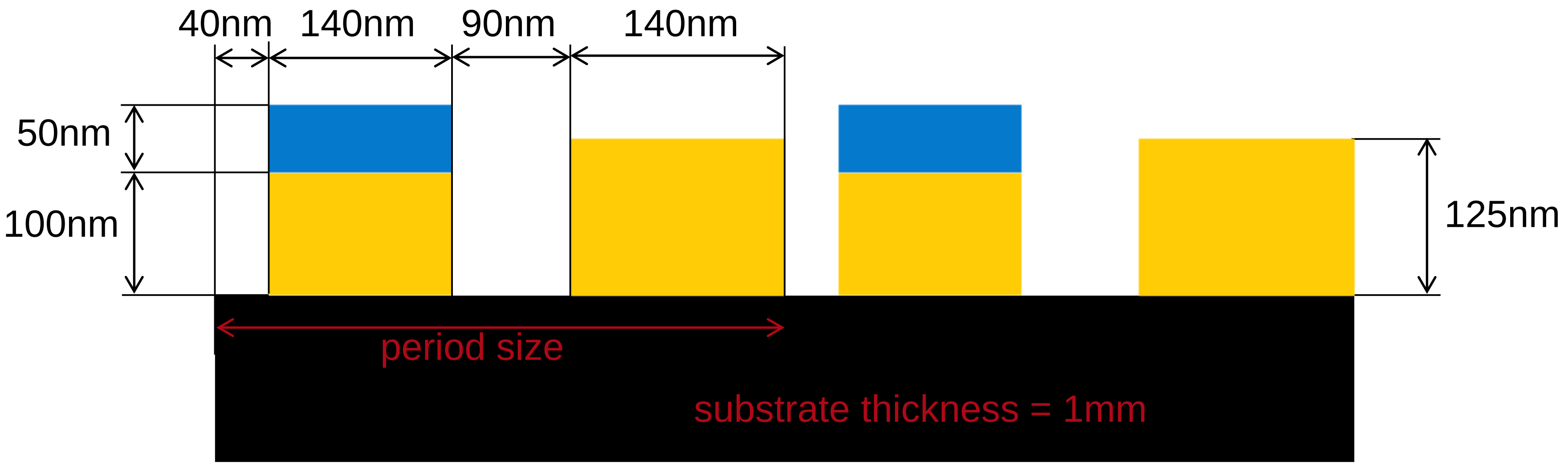

Modified Structure Analysis

Intensity Image of Grating after Polarizer in X-Direction

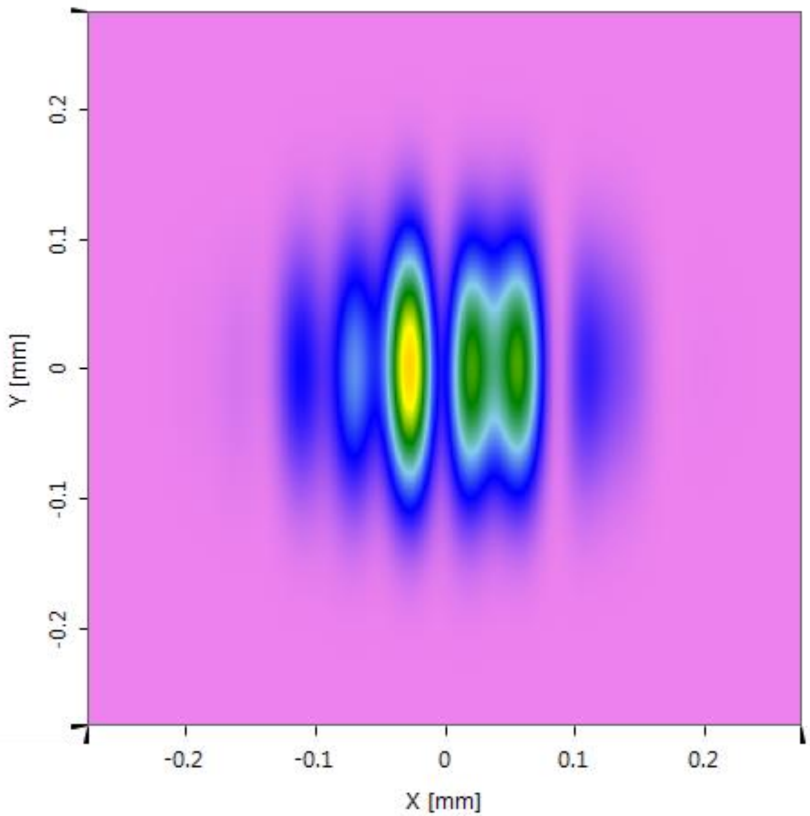

Inte
Pol

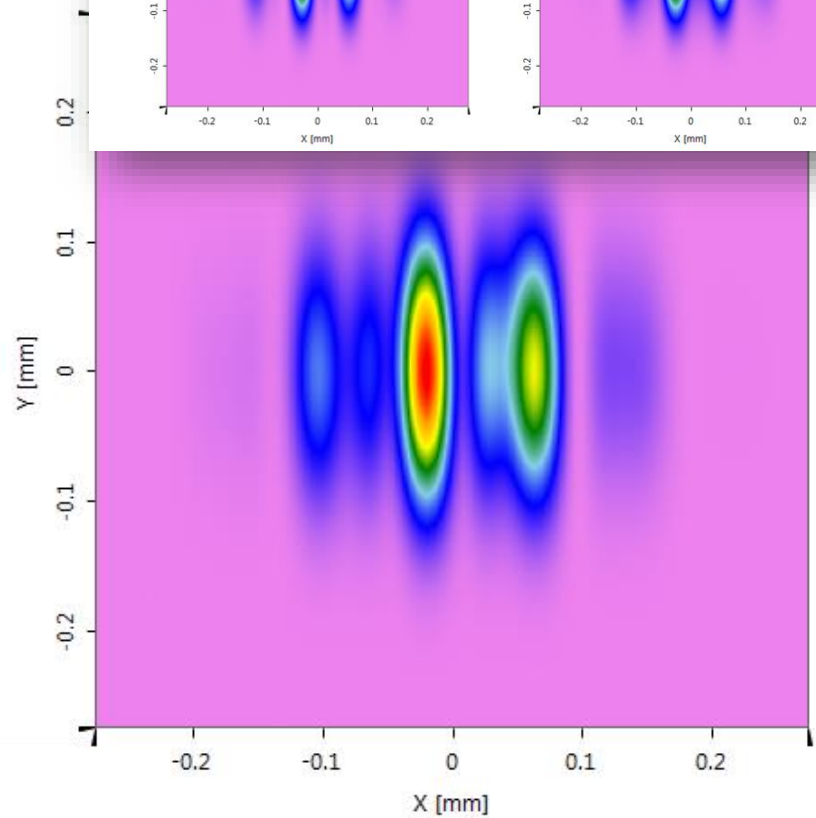

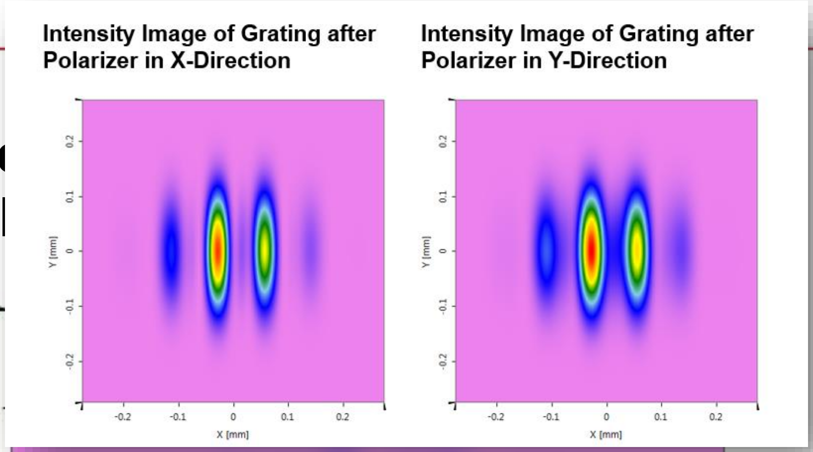

Diffractive optical element / Diffractive lens

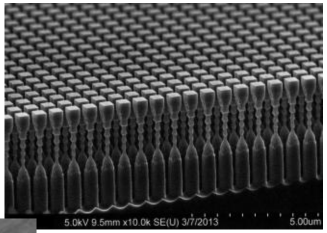

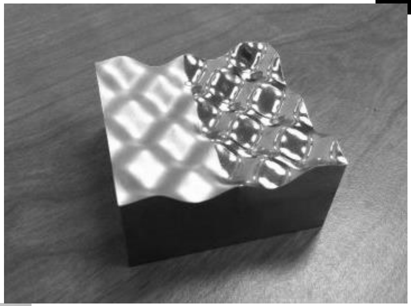

[1] IMS-Mechatronics Lab

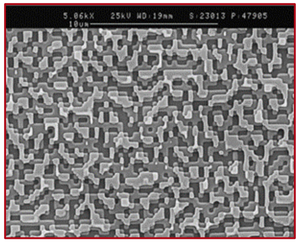

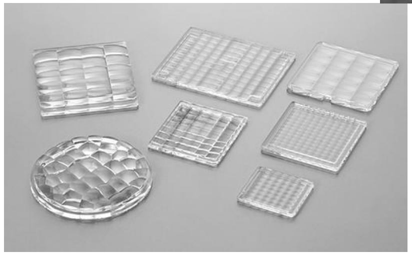

[2] ISUZU GLASS

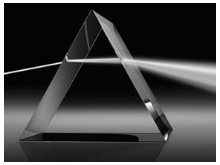

Nutshell (Hartwig Crailsheim v0.2)

Analysis of Sub-Wavelength Beam Splitter Structure with Approximated, Rigorous and Semi-Rigorous Method

Light, Structure & Analysis Methods

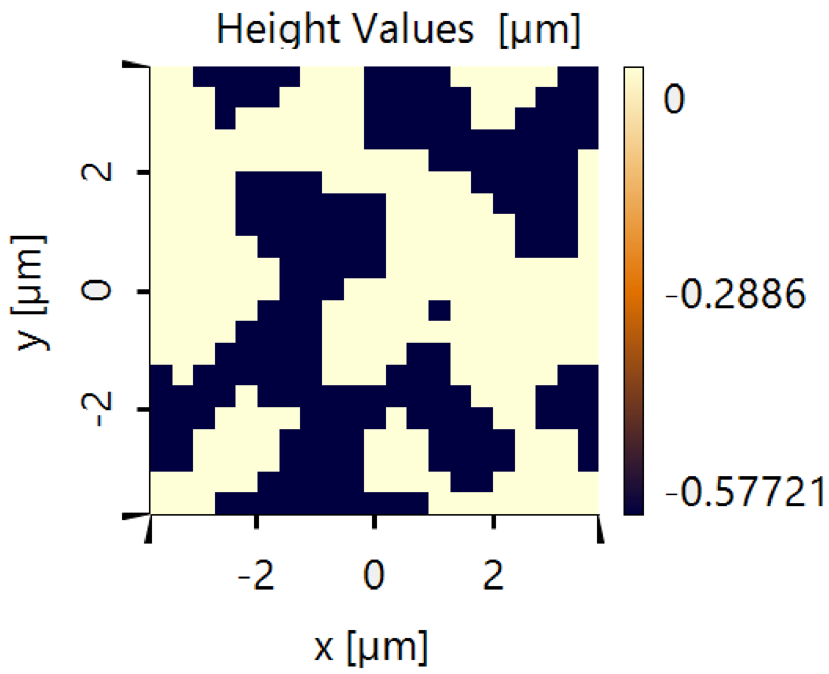

wavelength: 532 nm

Diffractive 1 : 7 × 7 Splitter

period: 7.56 µm

smallest feature size: 360 nm

on-axis order separation: ~4°

Analysis Methods

- Thin Element Approximation (**TEA**)
- Rigorous Fourier Modal Method (**FMM**)
- Semi Rigorous **Split Step** Method (with Periodic Boundary Conditions?)

Analysis Results

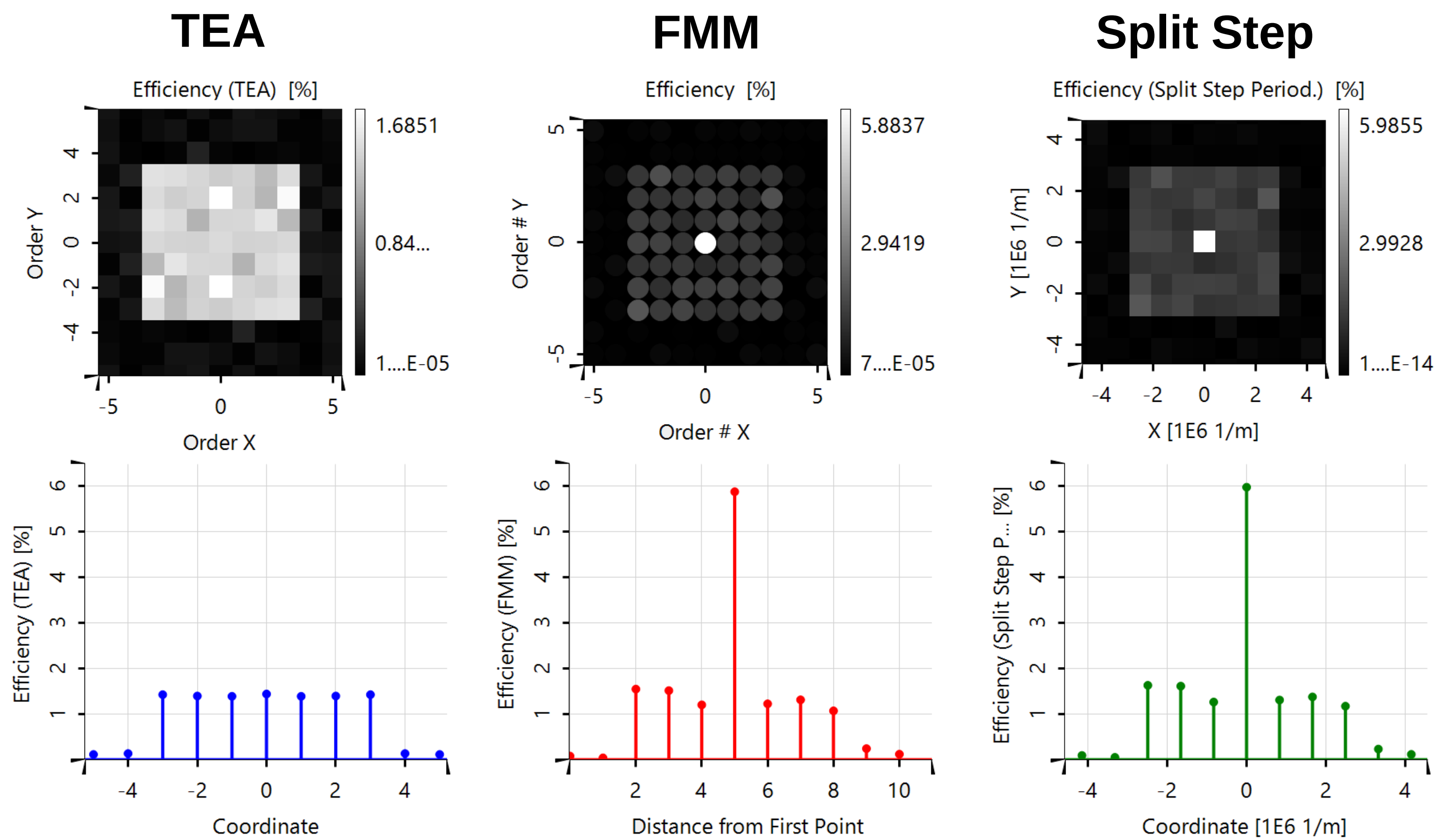

Computation Time of Efficiencies	instantaneous	~6min	~15s

Result Compilation

Field Inside

> Split Step & FMM

> Amplitudes

Period = 50µm; Smallest Feature = 4.7410µm

Structure Height Profile

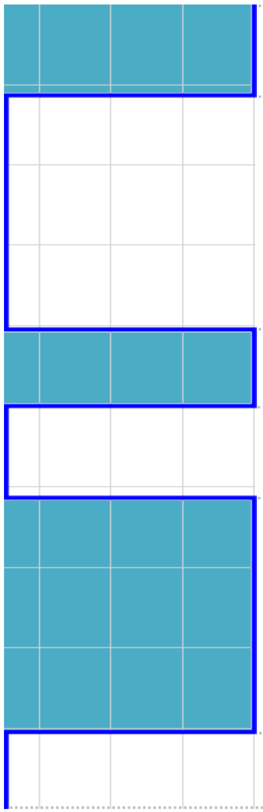

Split Step

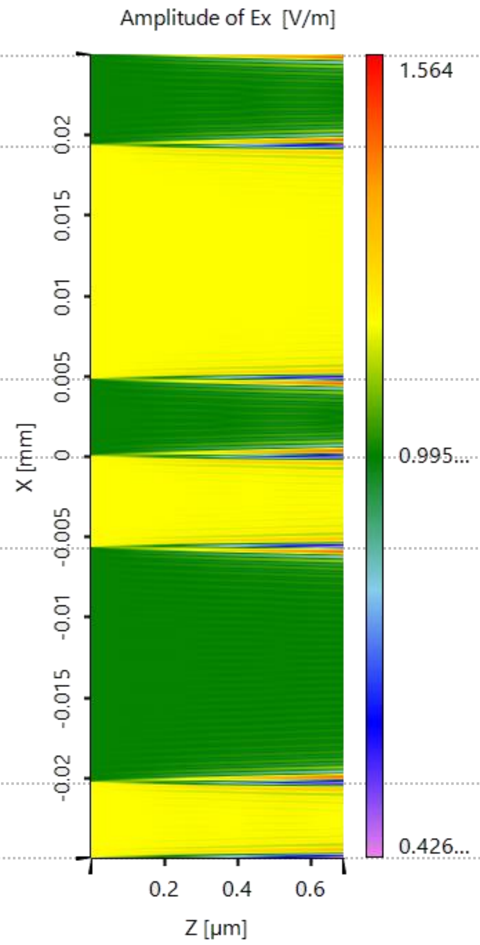

FMM

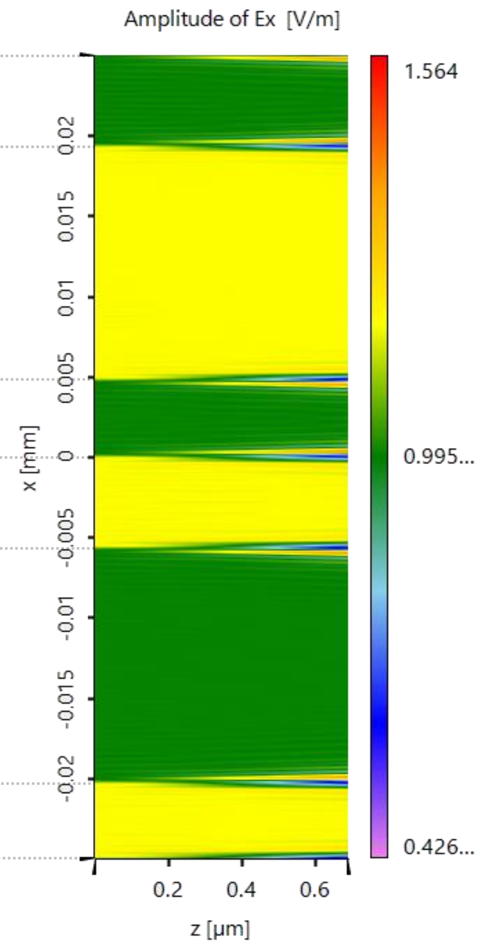

Period = 20µm; Smallest Feature = 1.8964µm

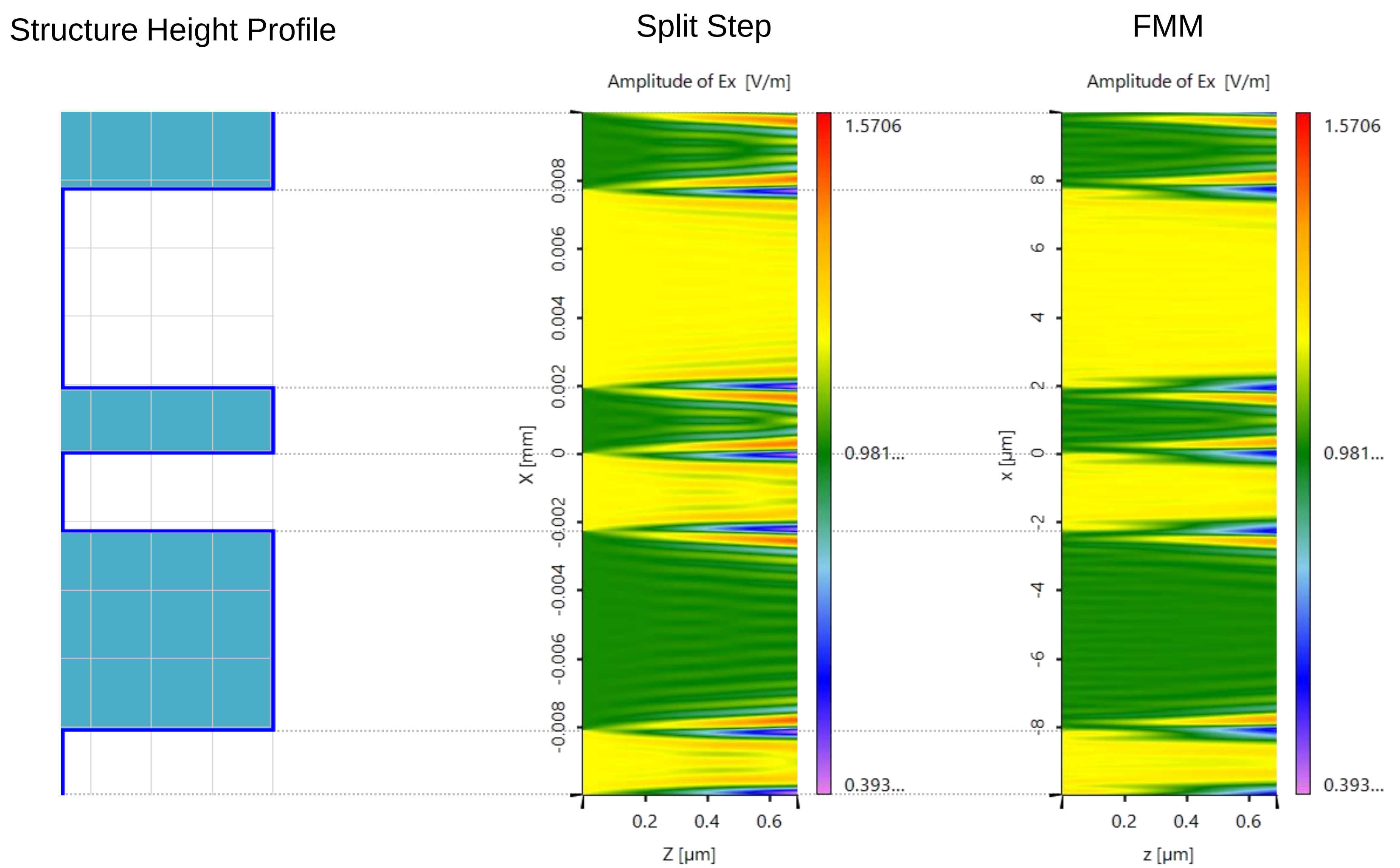

Period = 10µm; Smallest Feature = 0.9482µm

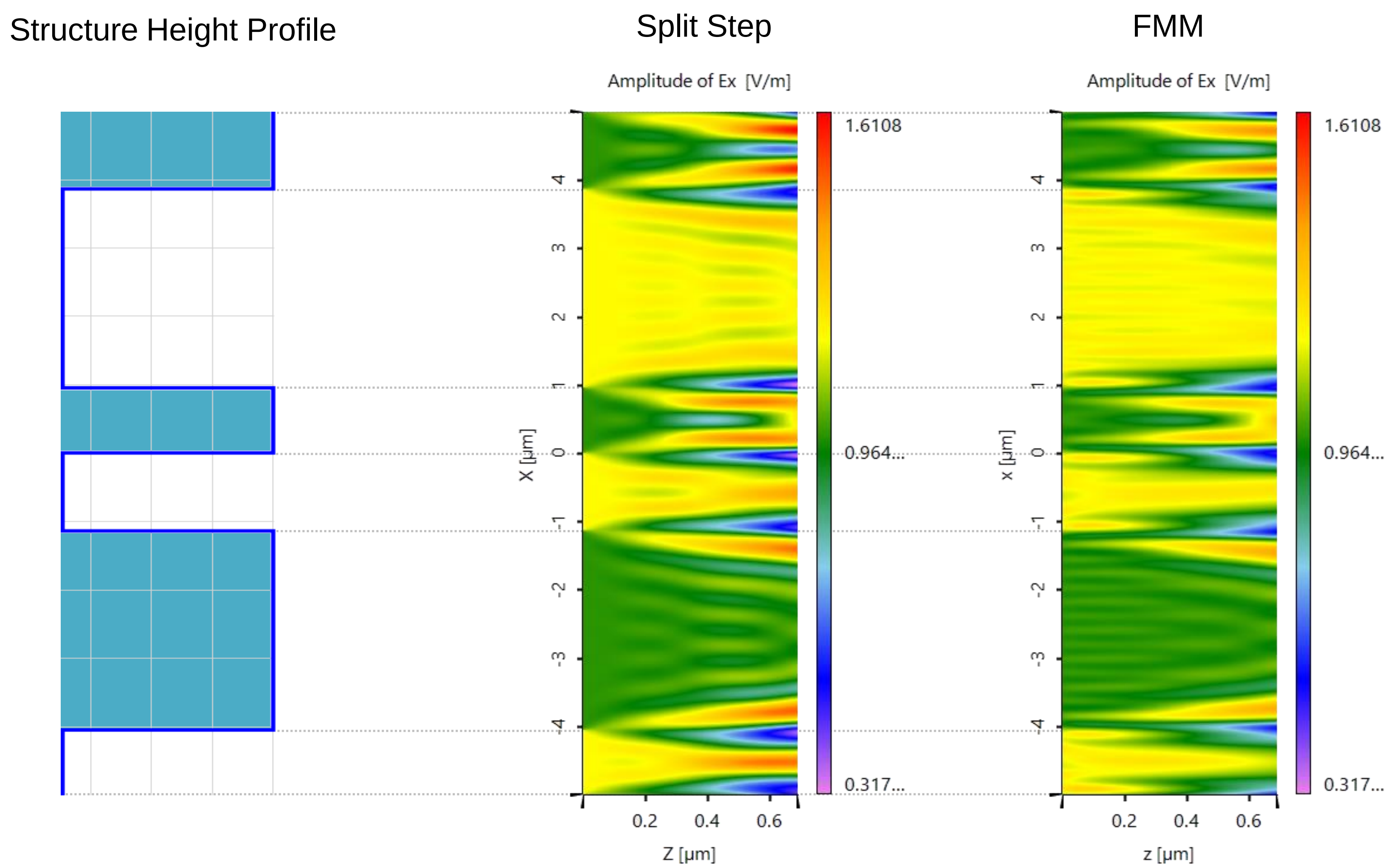

Period = 5µm; Smallest Feature = 0.4741 µm

Structure Height Profile

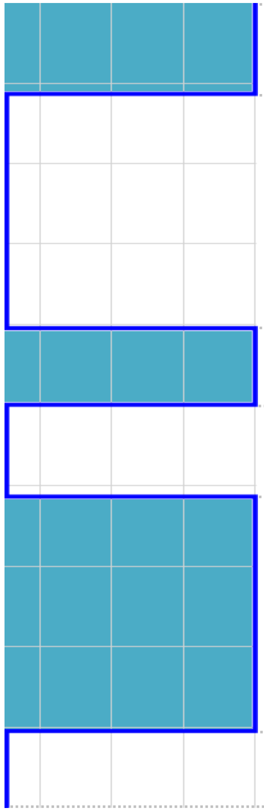

Split Step

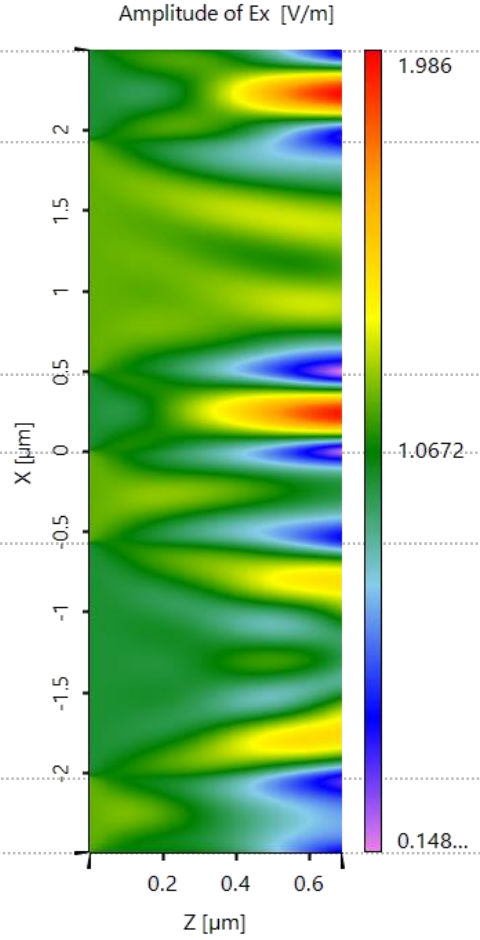

FMM

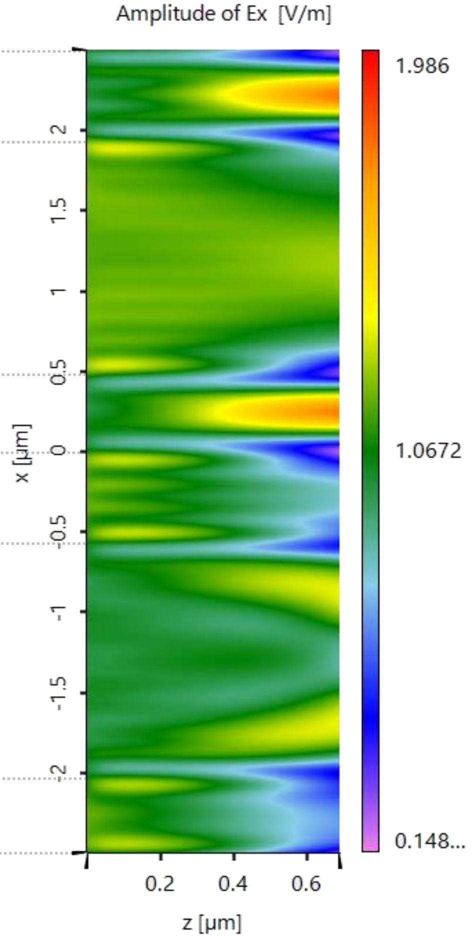

Result Compilation

Field Inside

> Split Step & FMM

> Phases

Period = 50µm; Smallest Feature = 4.7410µm

Structure Height Profile

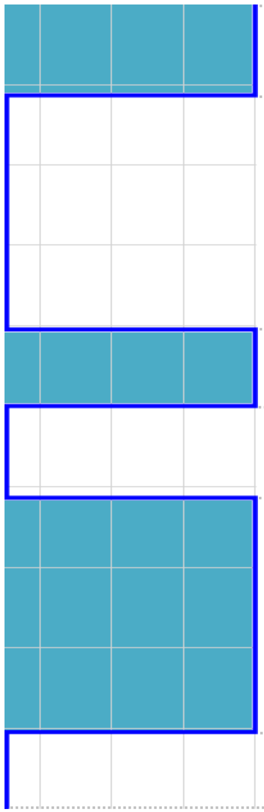

Split Step

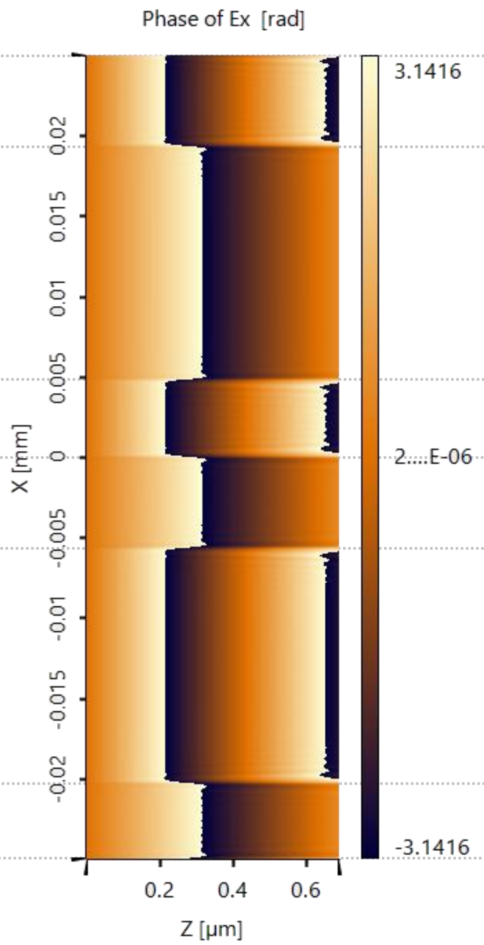

FMM

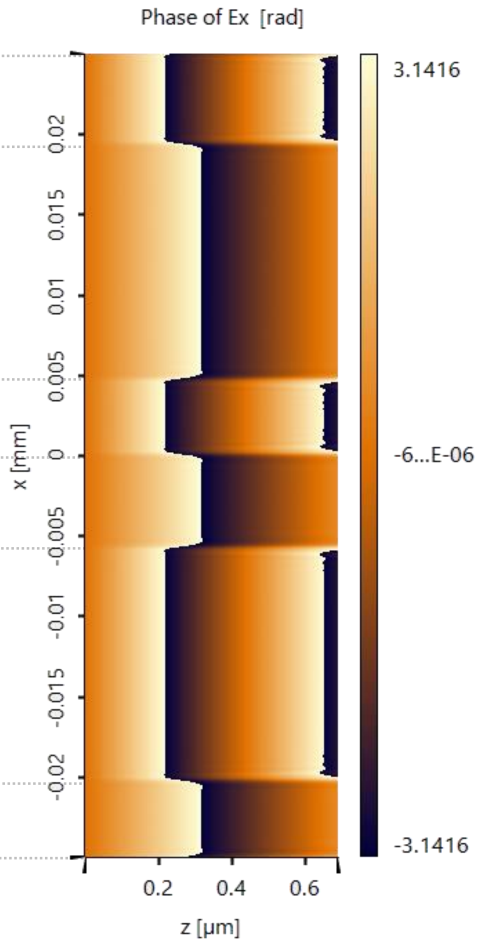

Period = 20µm; Smallest Feature = 1.8964µm

Structure Height Profile

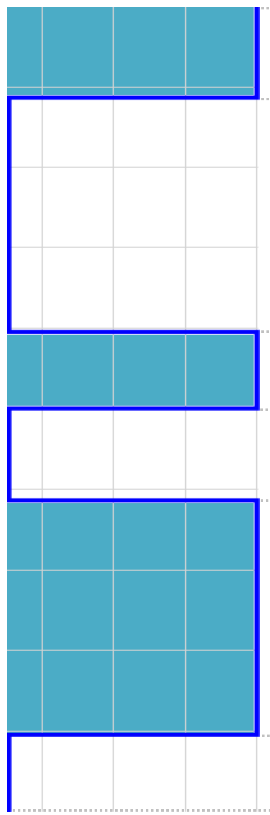

Split Step

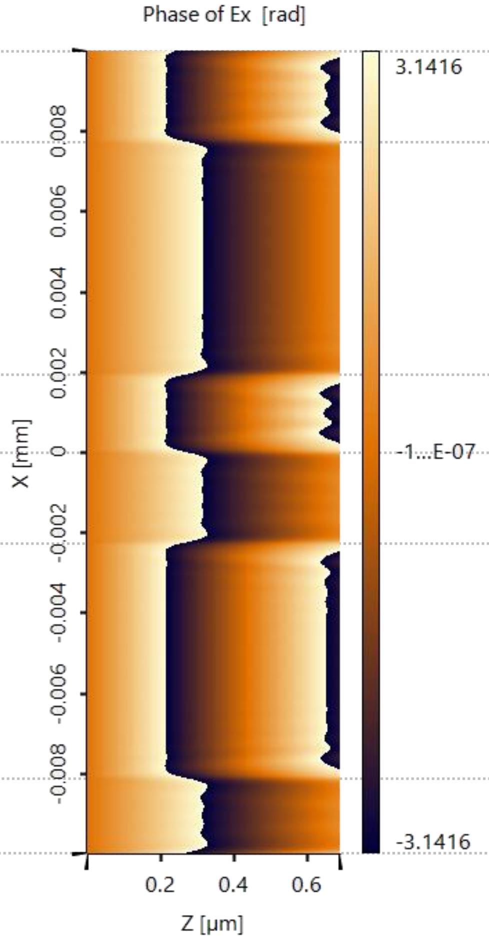

FMM

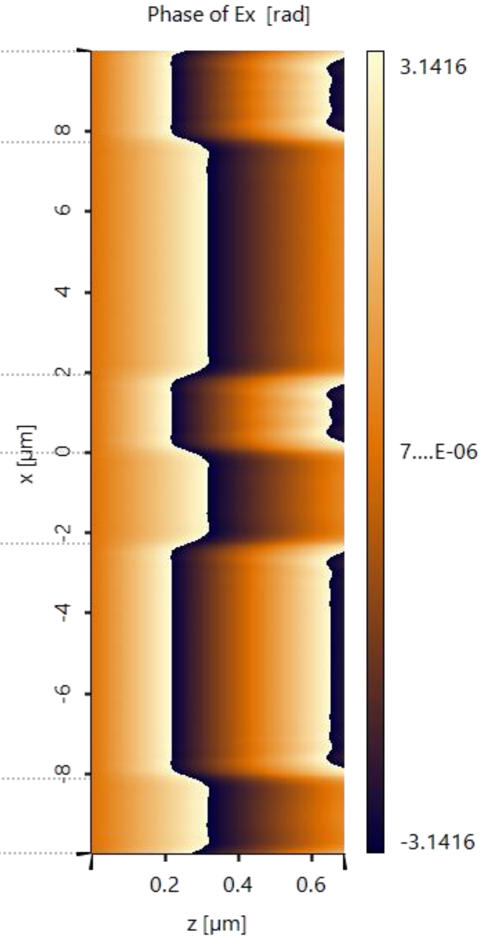

Period = 10µm; Smallest Feature = 0.9482µm

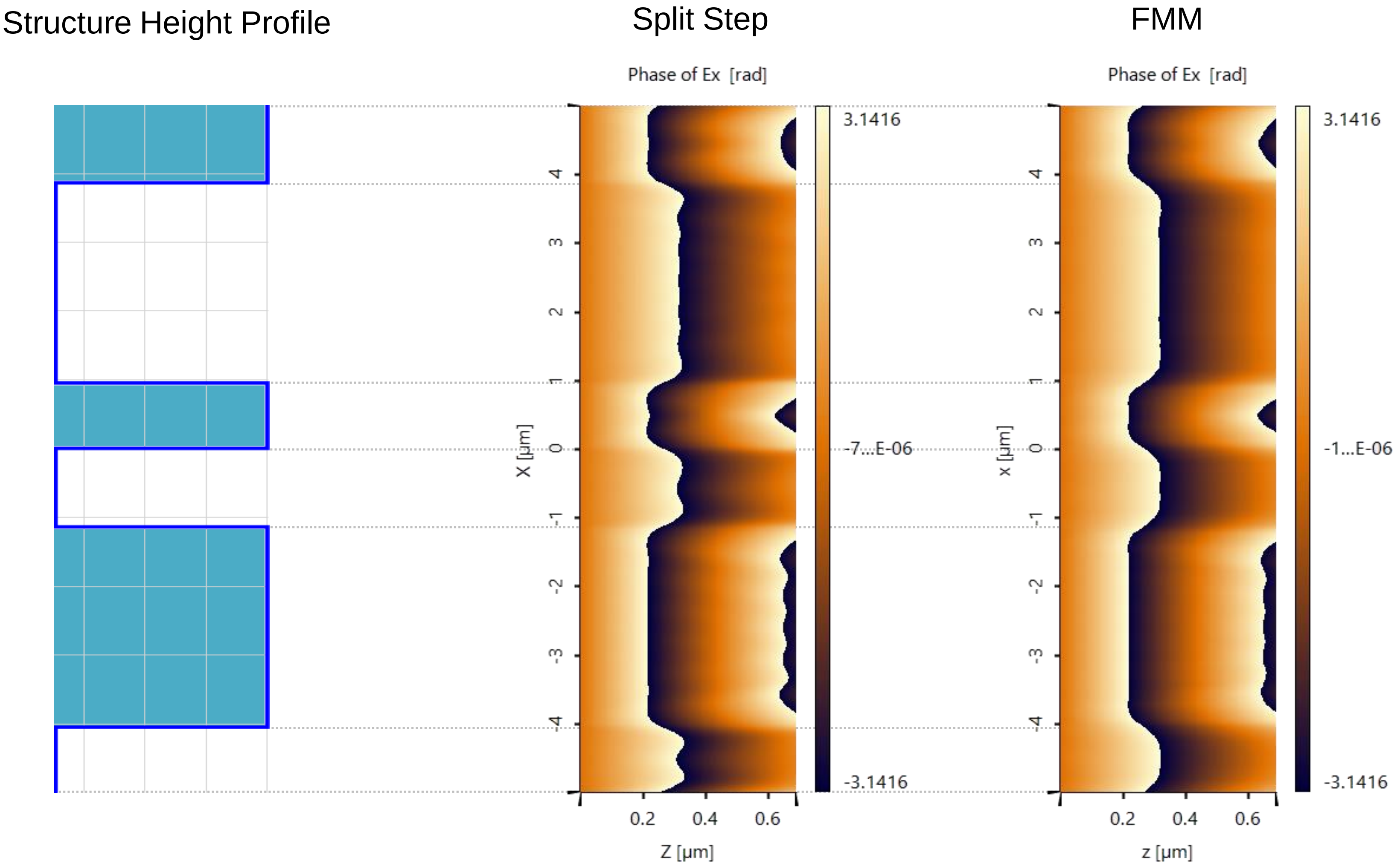

Period = 5µm; Smallest Feature = 0.4741 µm

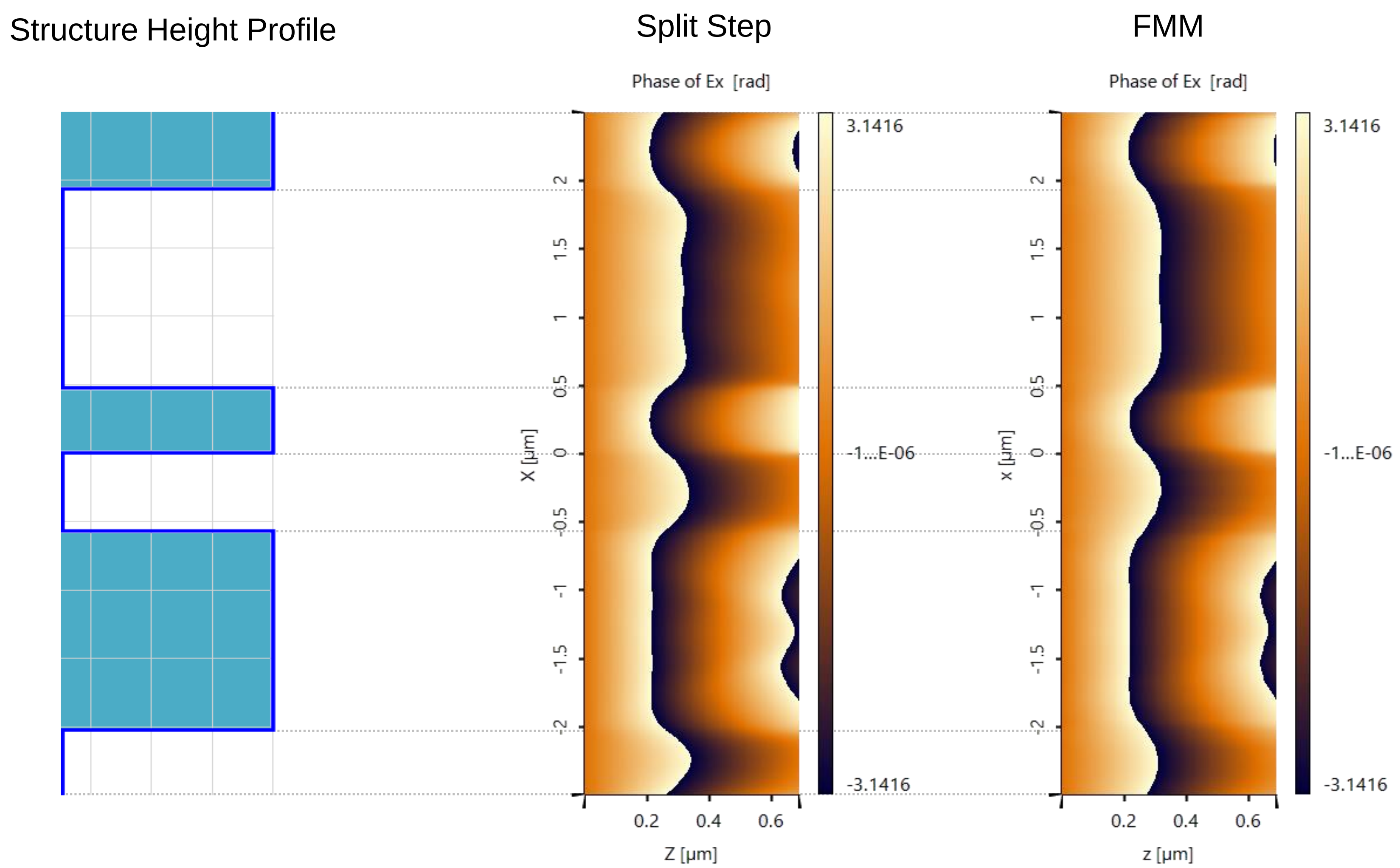

Result Compilation

Field Inside + Efficiencies

> Split Step & FMM

> Phases

Efficiency Calculation

- For the calculation based on TEA and FMM, the Grating Toolbox was used.

- In case of the Split Step method the following procedure is applied for the near field of one period's size in order to get values that might be interpreted as the efficiencies:
  - Fourier transform
  - normalizing
  - dividing by the square root of the full field's summed norm for Ex

  → regarding the squared amplitudes

The calculation for the Split Step method should be reconsidered.

Period = 50µm; Smallest Feature = 4.7410µm

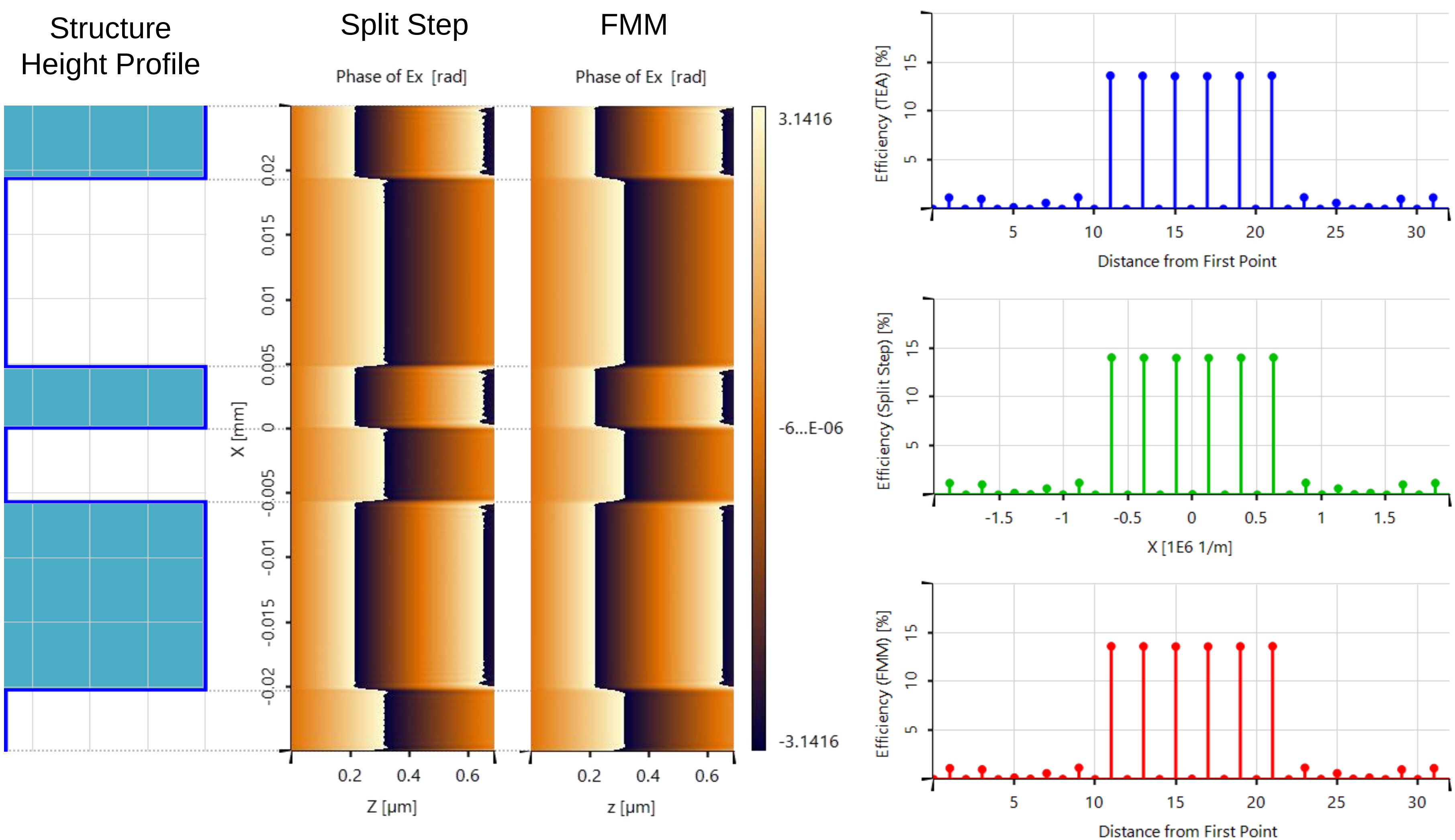

Period = 20µm; Smallest Feature = 1.8964µm

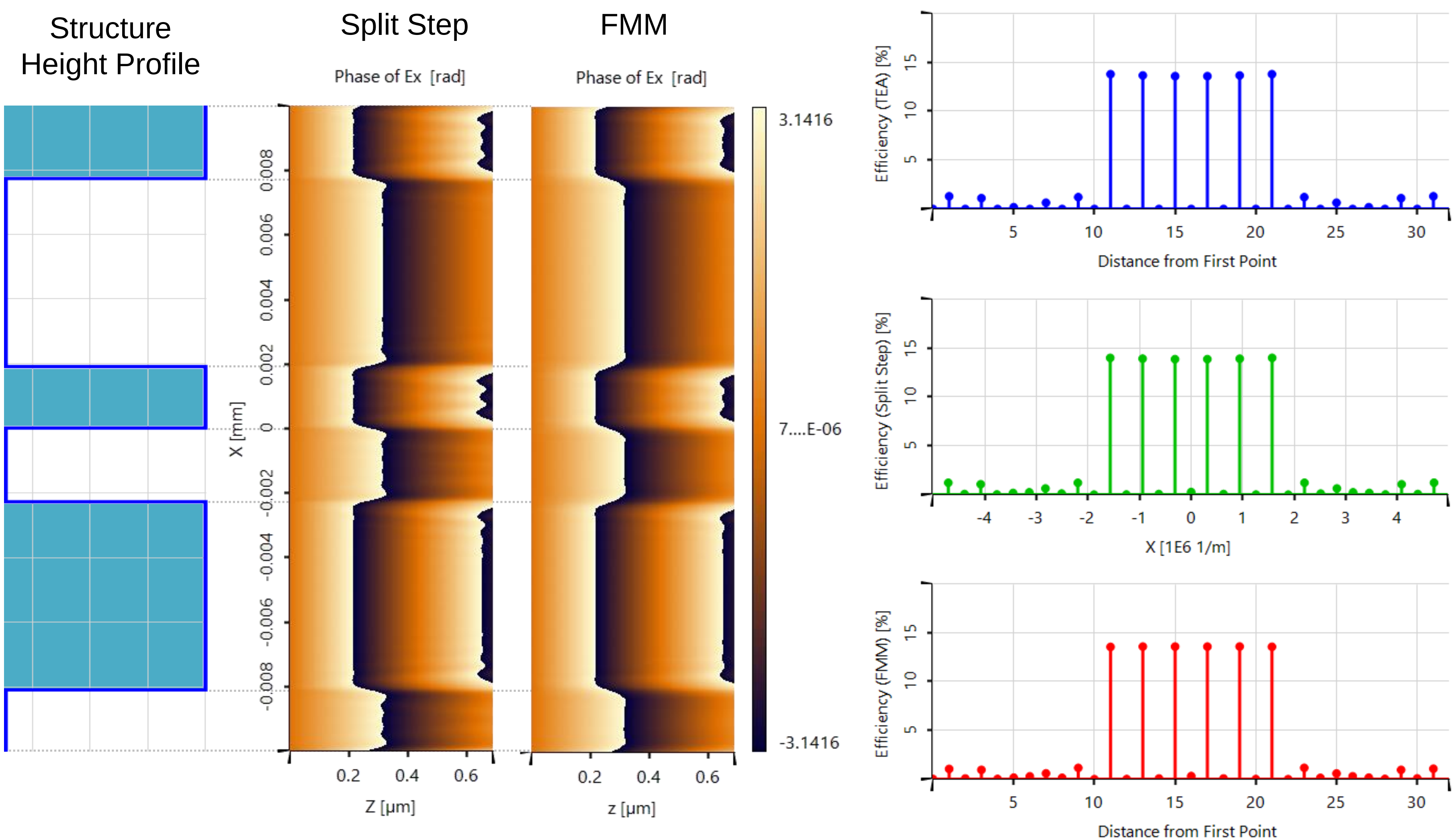

Period = 10µm; Smallest Feature = 0.9482µm

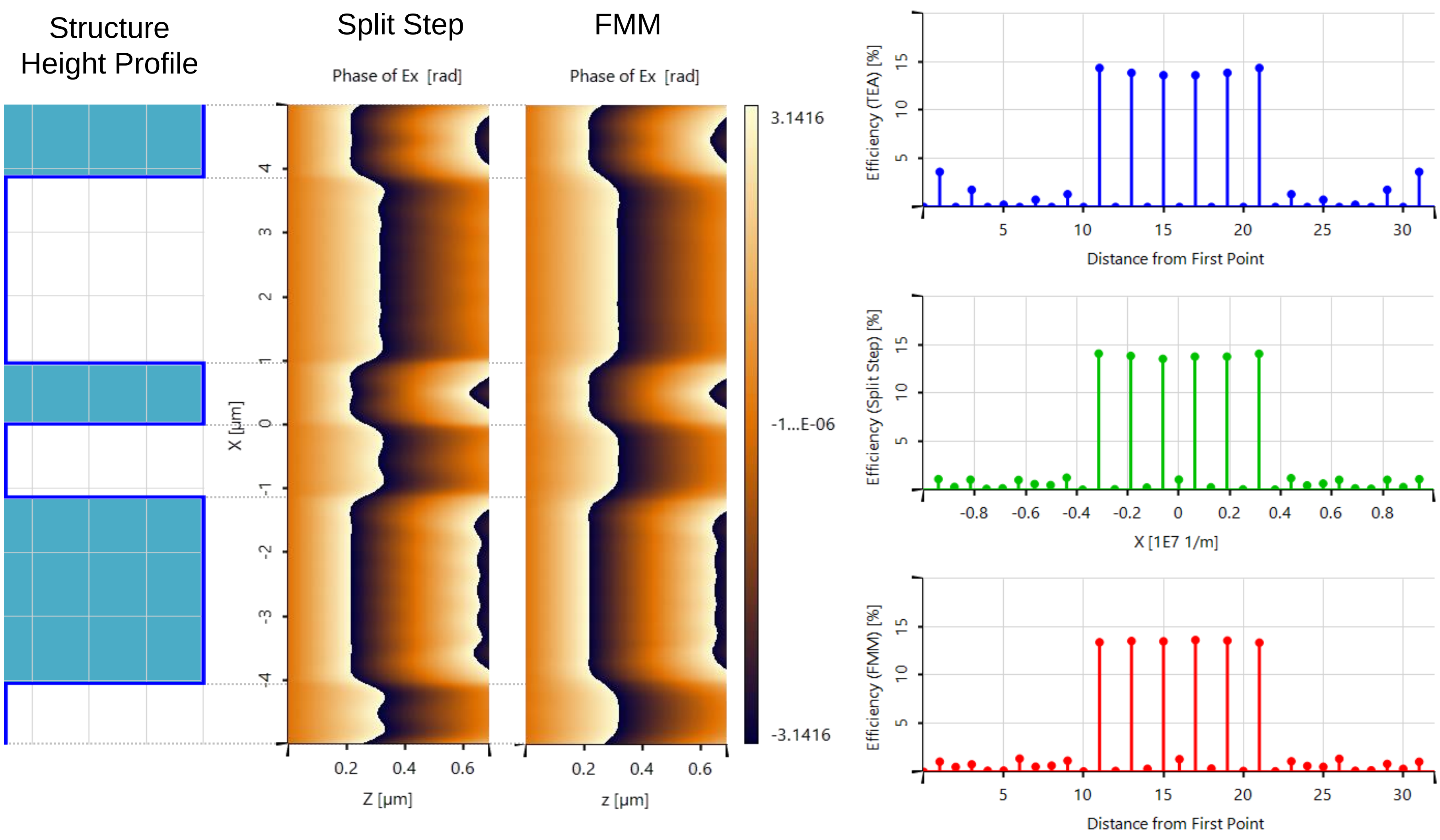

Period = 5µm; Smallest Feature = 0.4741 µm

Structure Height Profile | Split Step | FMM

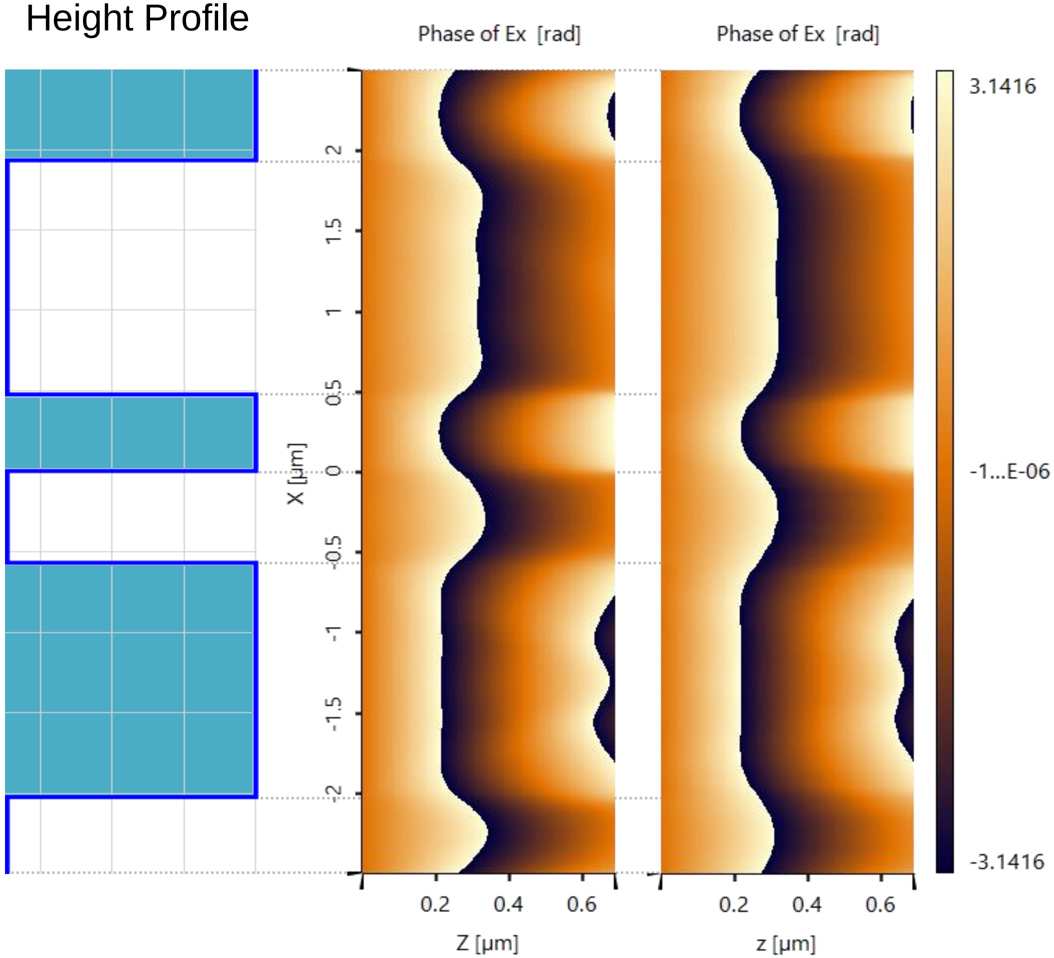

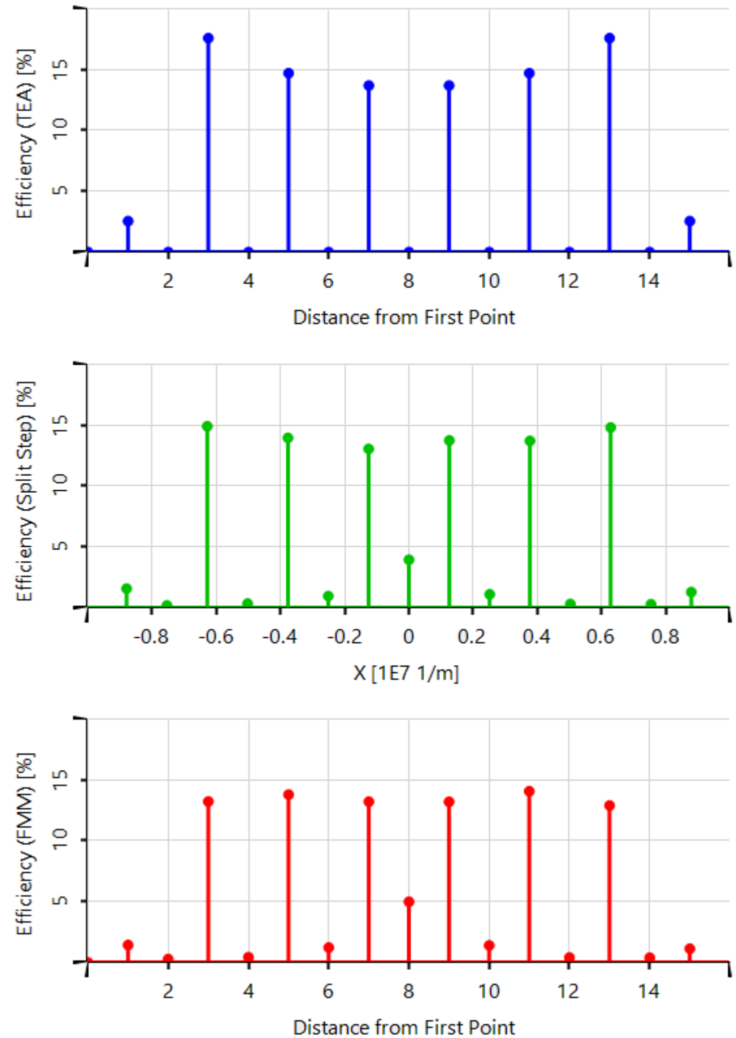

Design and Modeling of a Diffractive Lens

Task Description

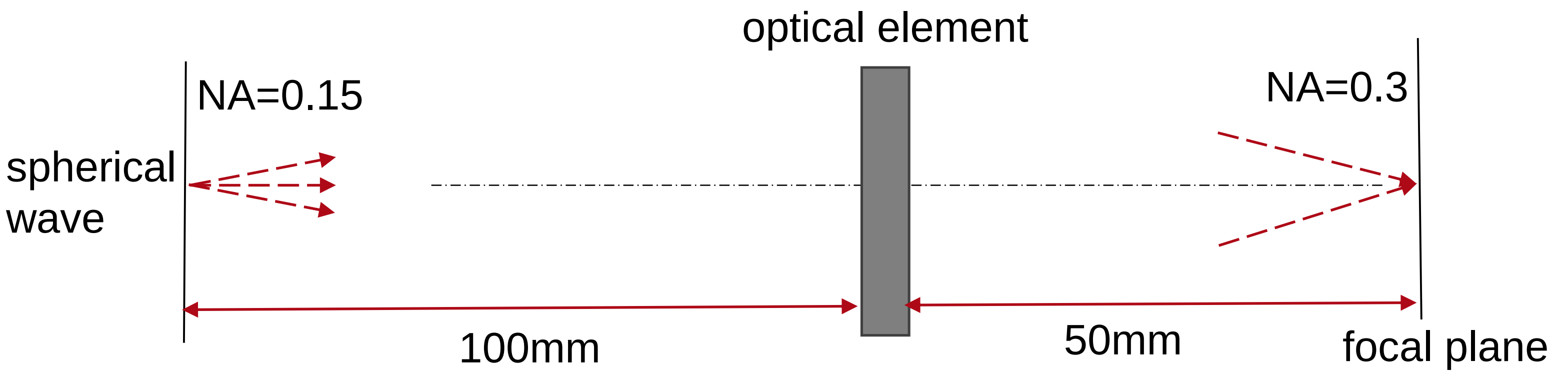

- For a given input spherical wave, to design an optical element to focus the input beam with a specific numerical aperture (NA=0.3) and a required working distance (50mm).

Design Process: Functional Embodiment

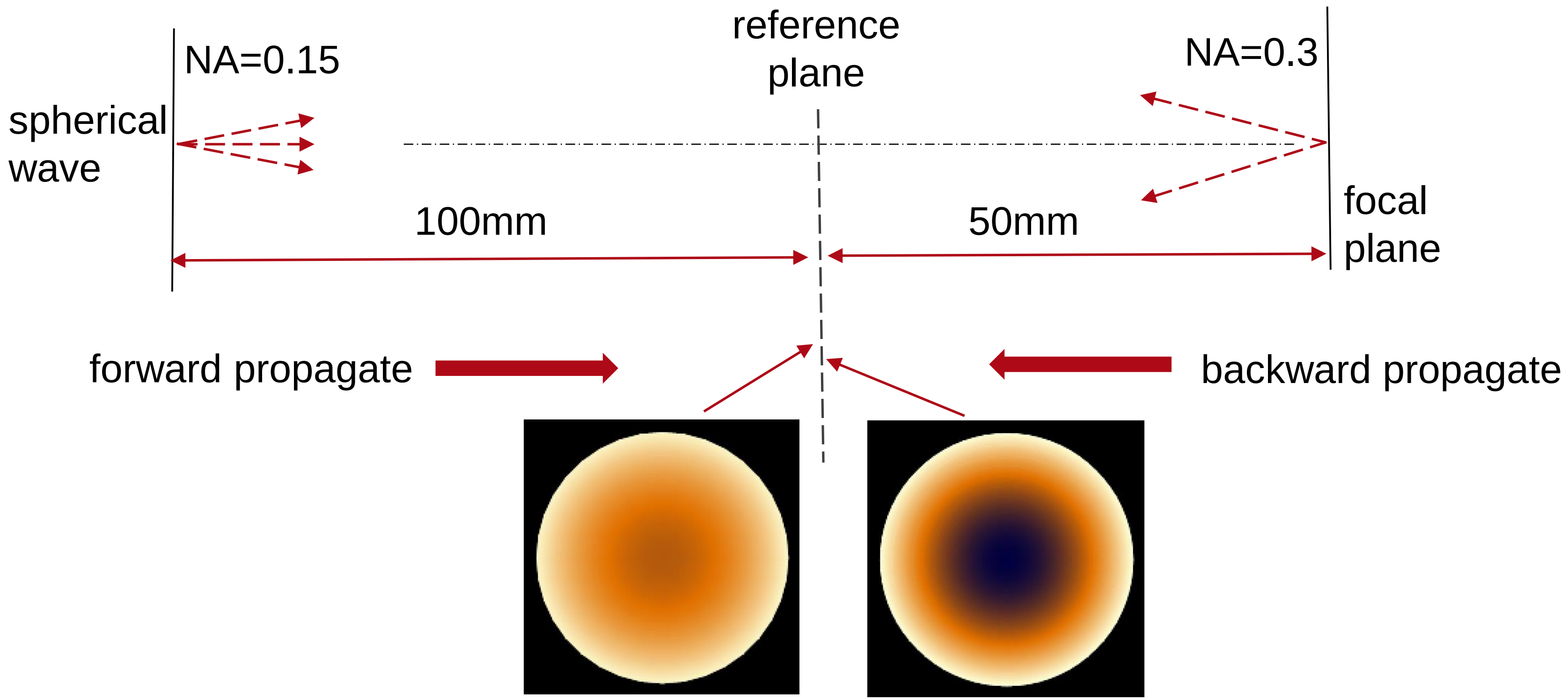

φ^{in}: phase from input field

φ^{out}: phase from output field

The element is consider as a phase only function, which is the subtraction of the phase from input and output field: $\varphi(x, y) = \varphi^{\mathrm{out}}(x, y) - \varphi^{\mathrm{in}}(x, y)$

Design Process: Structure Embodiment

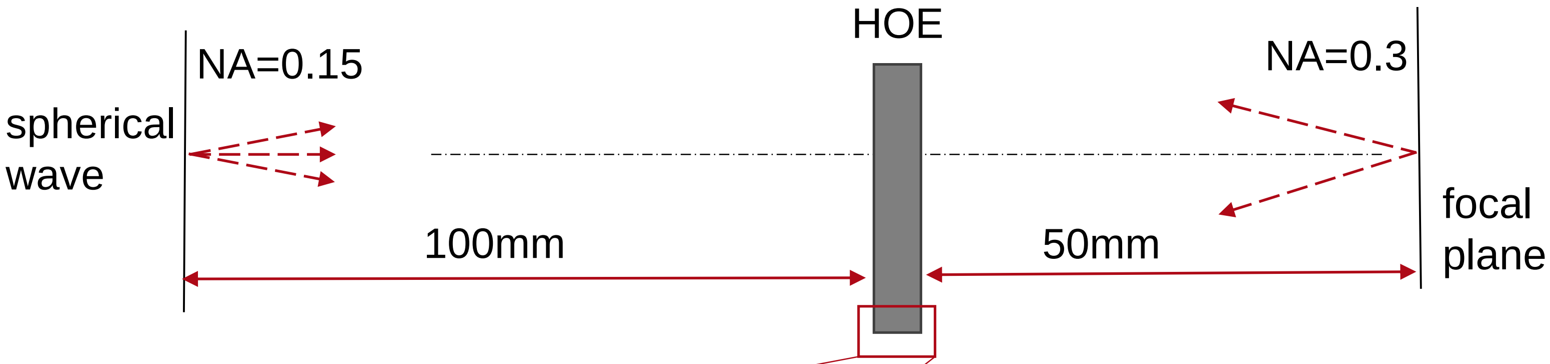

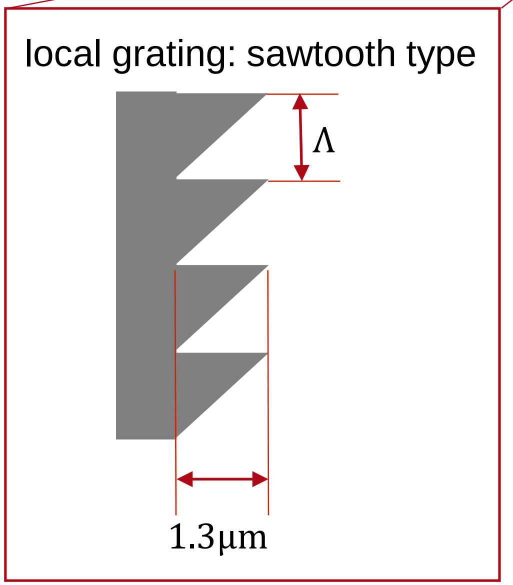

- The local grating of the HOE is chosed as sawtooth type.
- The 1st order is selected as working order.
- Local grating period $\Lambda(x,y)$ of the HOE is obtained with the phase function.

$$\Lambda(x,y) = \frac{2\pi}{|\nabla\varphi(x,y)|}$$

Simulation with Designed Result

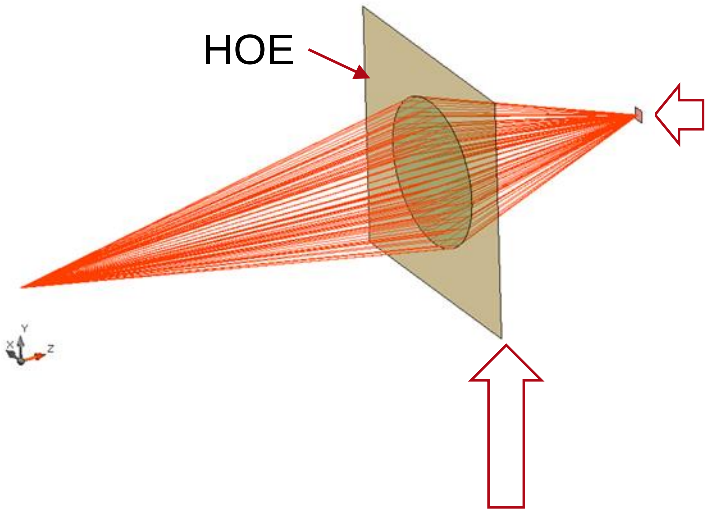

dot diagram

$(RMS \approx 100nm)$

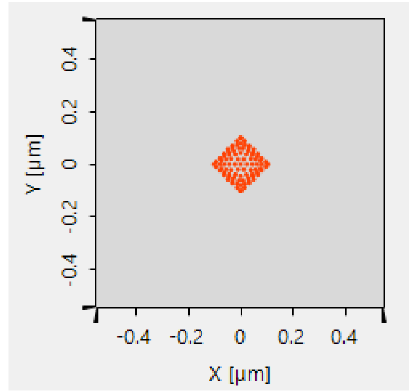

PSF

(Airy disk diameter $\approx 2.5\mu m$)

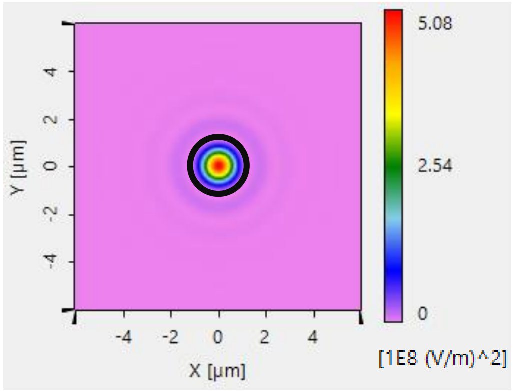

Intensity After the HOE

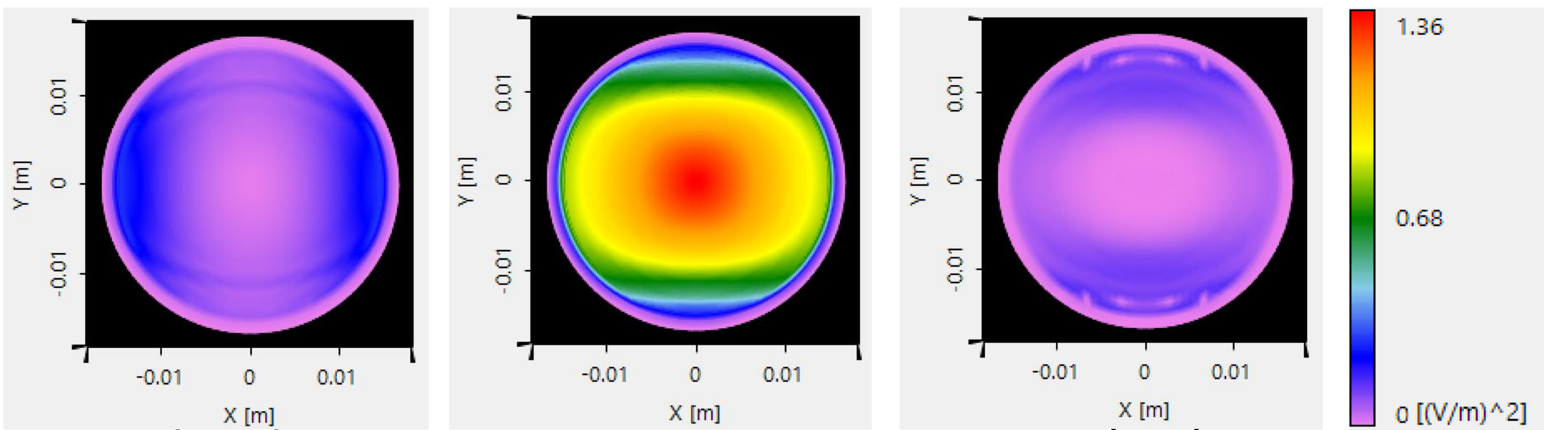

0th order 1st order 2nd order

Scenario 90 (3.0)

Simulation of Scattering at Rough Surface

Surfaces in VirtualLab are usually smooth. In contrast, real surfaces are always rough to a certain degree.

This application scenario demonstrates the simulation of a Gauss beam that passes a glass plate with a rough surface according to measured height profile data. In 1m distance the scattered light is analyzed.

Modeling Task

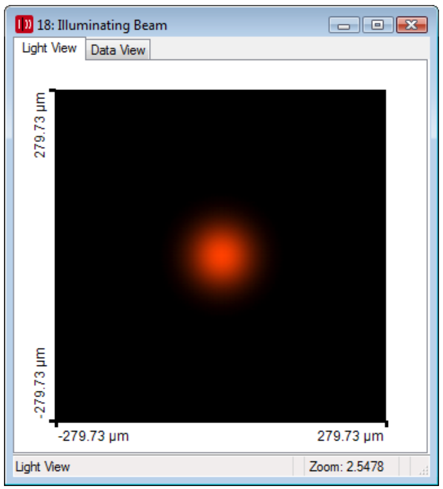

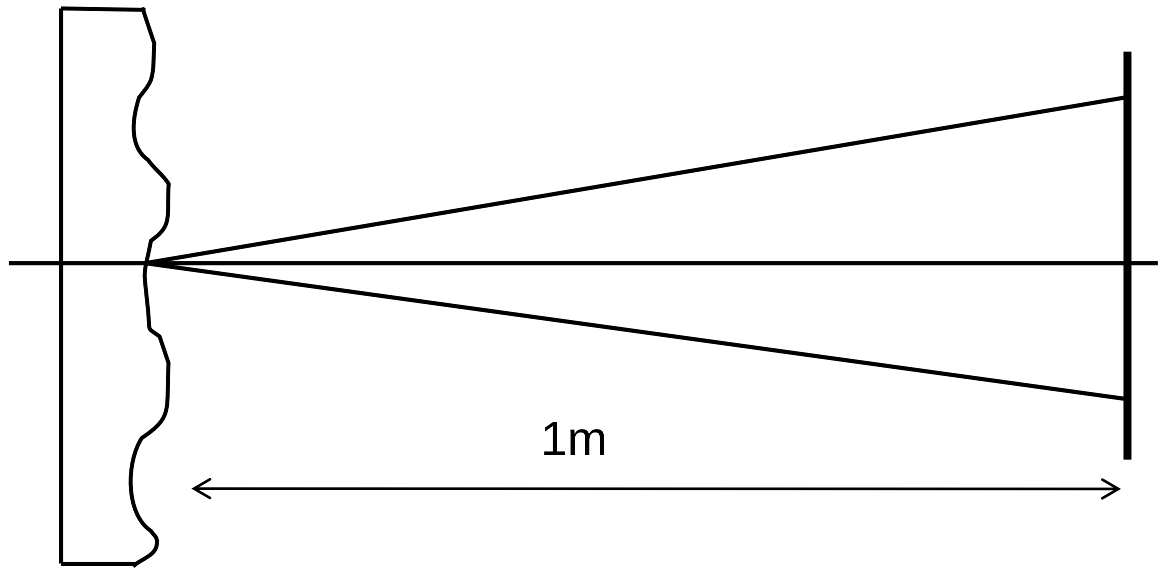

Gaussian laser beam
λ: 632nm
($1/e^2$) diameter: 100µm

Glass Plate
(Fused Silica)
with rough
2nd surface

Scatterd Light Field
on Screen=?

Measured Surface Profile Data

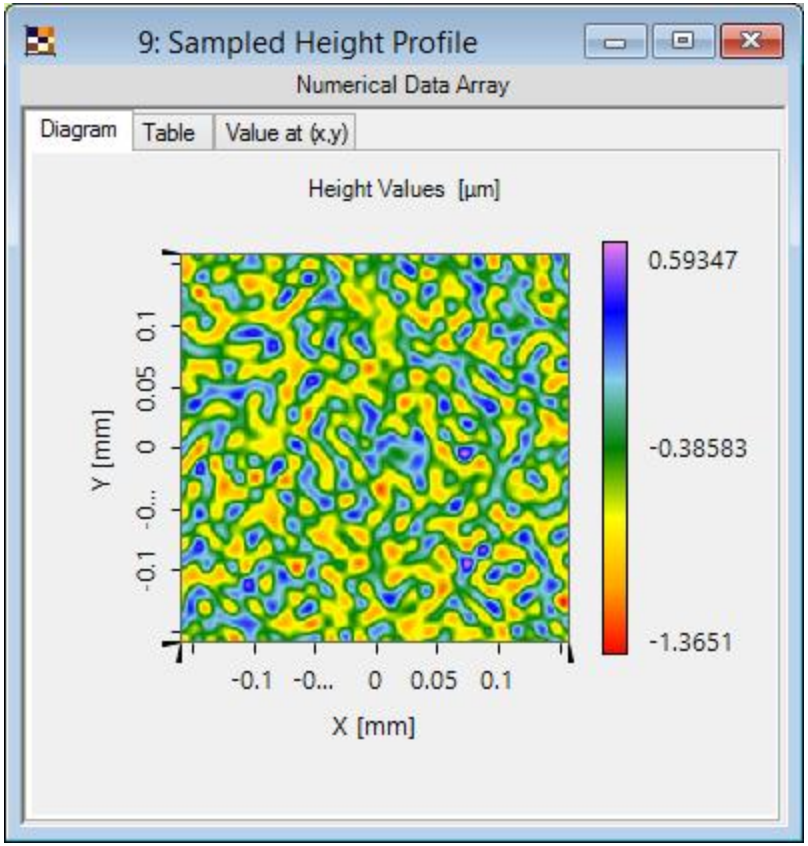

Result: Diffraction Pattern

in real colors

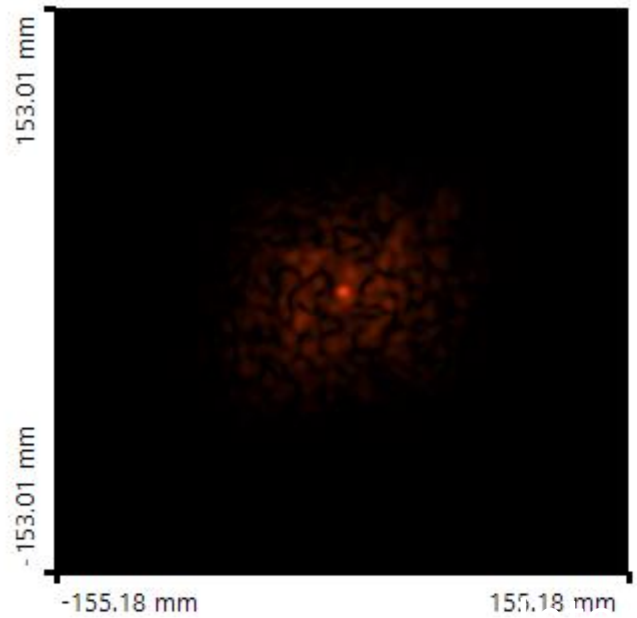

in false (reverse rainbow) colors

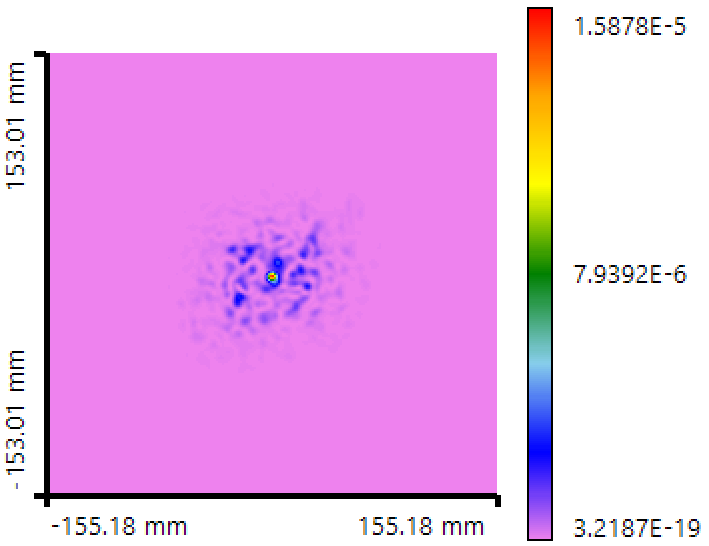

Exercise (v0.9.1)

Analysis of System with Binary Lens

Modeling Task

round
∅ 3mm

PSF & MTF calculation

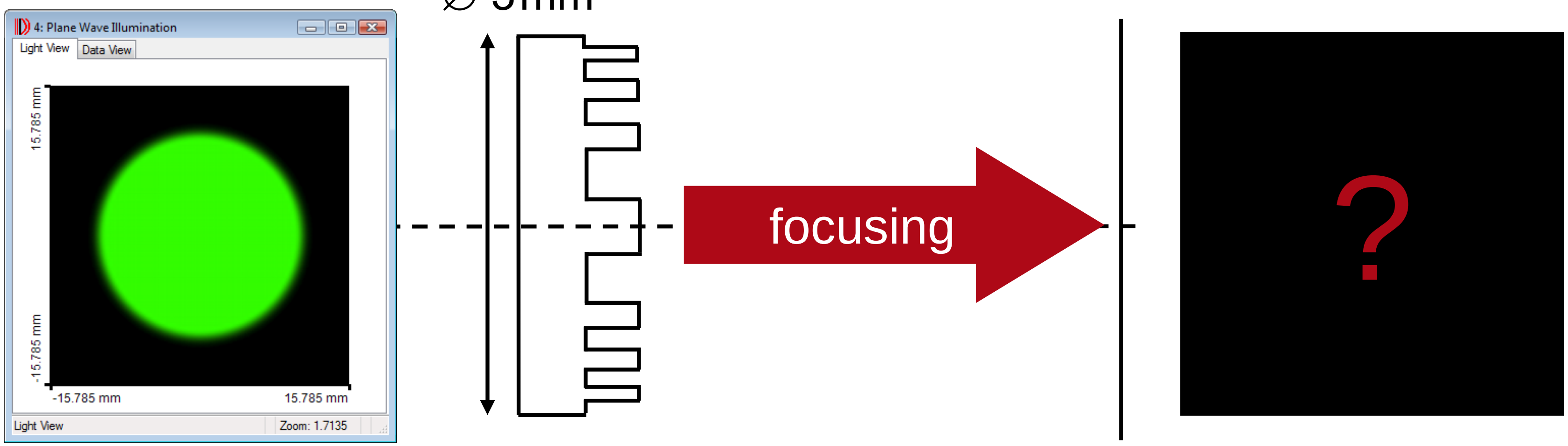

plane wave
wavelength: 532 nm
∅ 2.5 mm
with 5 % edge width

- diffractive lens (based on conical surface)
- 2 levels

focal plane

effective focal length f=200 mm

Expected Result: Phase Directly after Lens

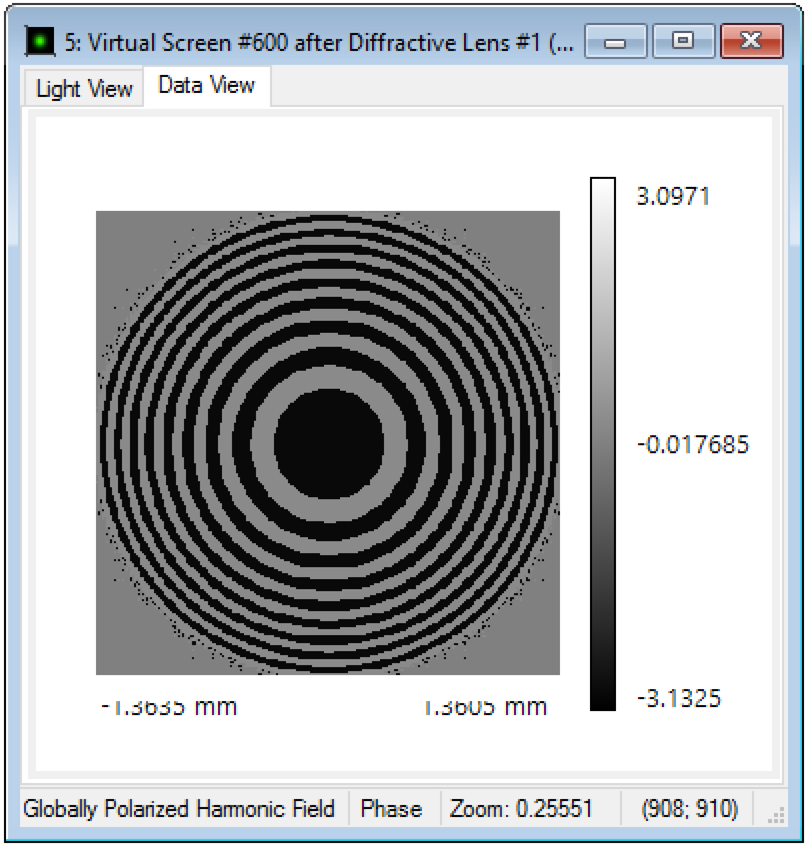

phase of field after lens

Expected Result: PSF & MTF

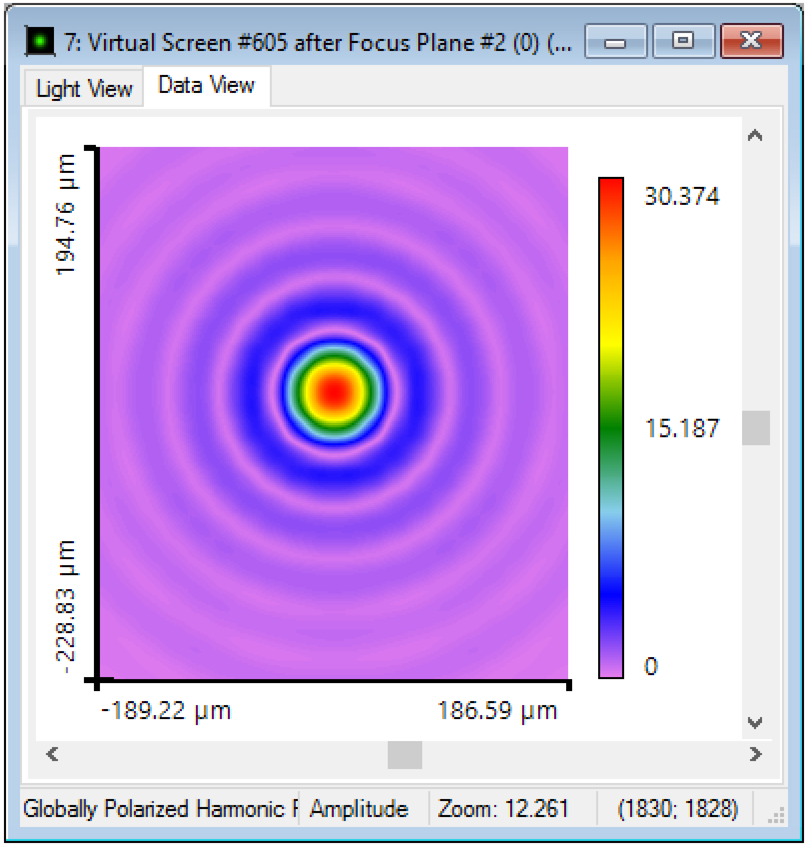

PSF

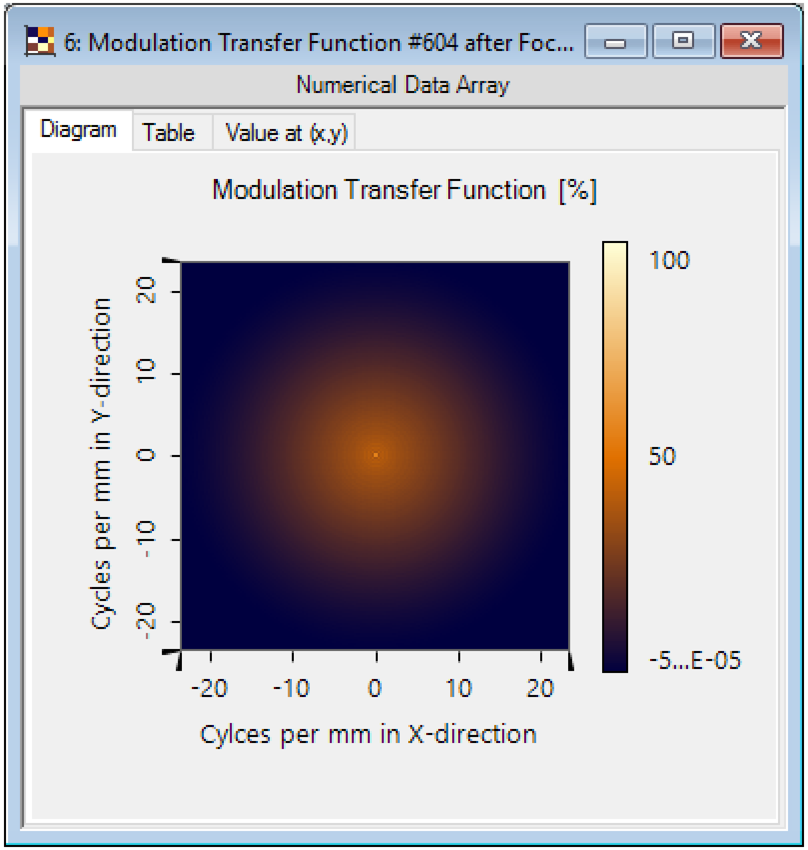

2D MTF

AppS.0009 (1.1)

Simulation of a Bifocal Hybrid Lens

Keywords: bifocal Lens, combined Interface, hybrid lens, multifocal lens, multifocal, bifocal

Task Description

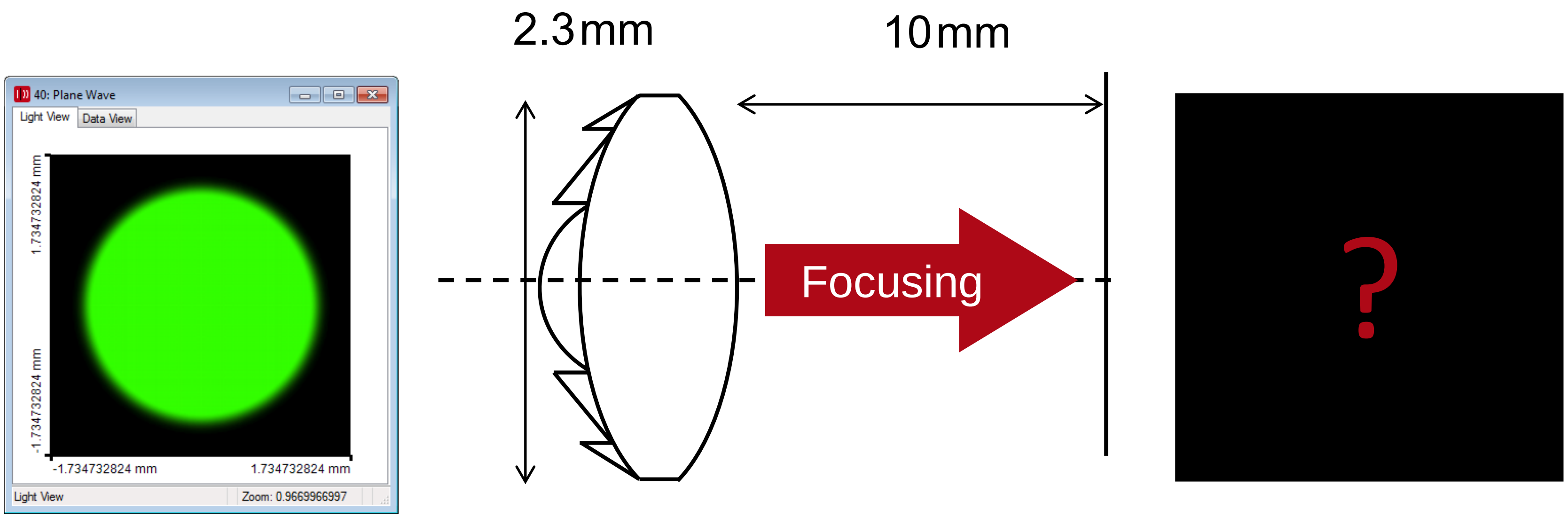

plane wave

bifocal lens with hybrid surface

target plane

Task Description

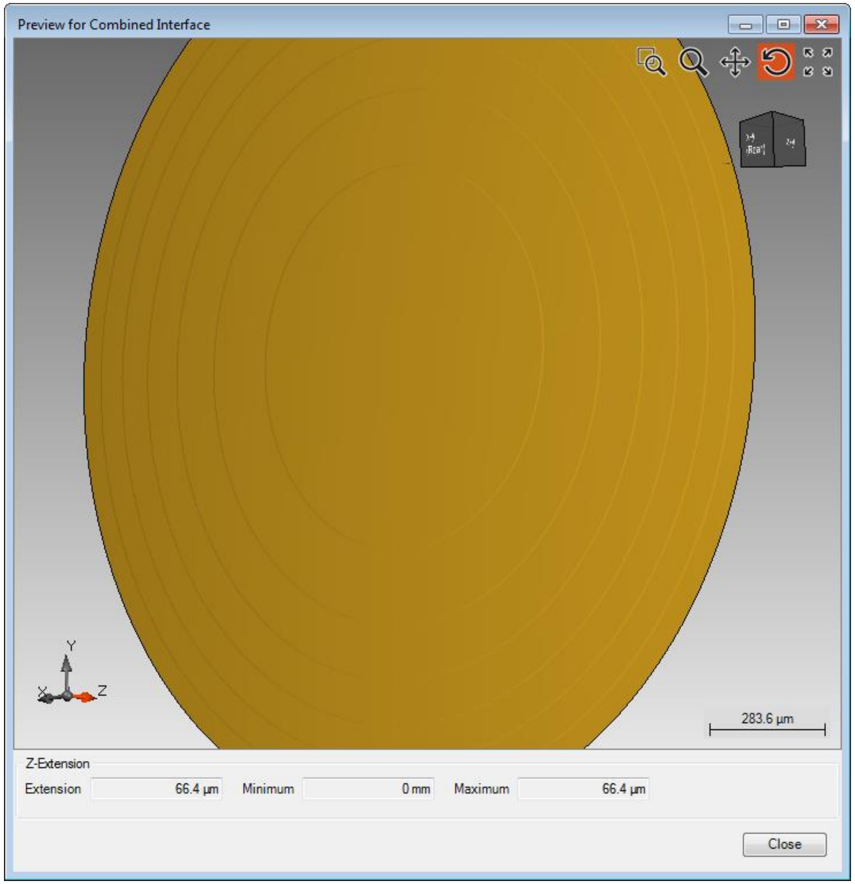

- Center thickness of lens: 1 mm.
- Diameter: 2.3 mm
- Radius of curvature of the spherical surface: 10 mm
- Hybrid surface modeled as a superposition of a spherical and a diffractive lens surface.
- Superposition of surface profiles by combined interface of VirtualLab.
- Diffractive lens parameters:
  - Radius: Infinity
  - A2: 0.0022608
  - A4: 0.00038131
  - A6: 2.74E-06

On-Axis Intensity

The **intensity along the optical axis** can be taken as indicator for the focal positions. Via **parameter run** the position behind the lens is varied. **To speed up** the simulation, a **separate LPD** with the light distribution 9.37 mm behind the lens as input field is used. Hence, the **muliple propagation through this hybrid lens is avoided**.

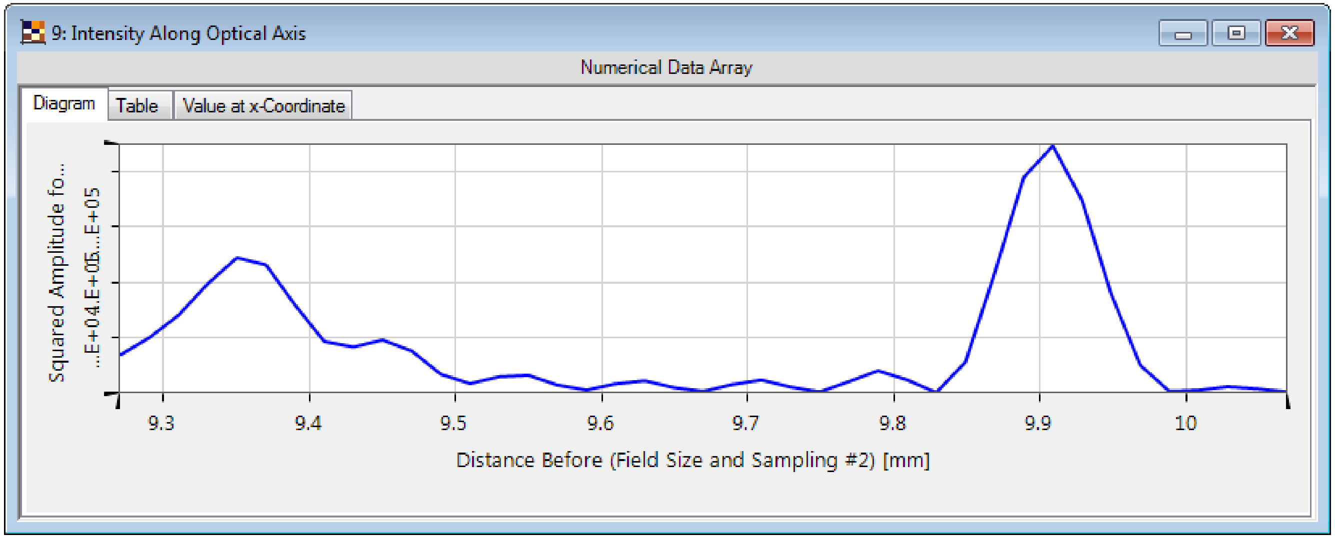

On-axis intensity depending on distance from lens. The two focal points in a distance of 550 µm (at 9.37 mm and 9.91 mm) are visible.

Ray Tracing System Analyzer: Results

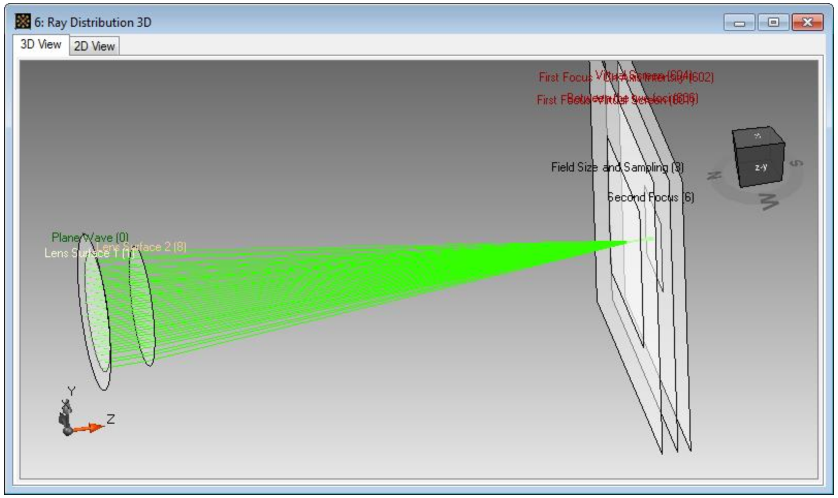

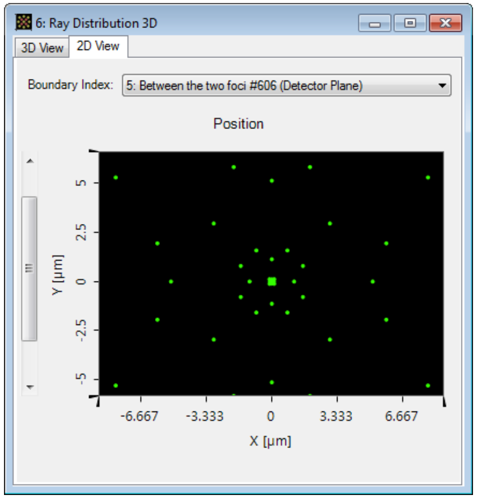

Left figure: 3D ray tracing result

Right figure: Spot diagram somewhere between the intended two focal planes.

The **position of the two focal planes** and the **point spread function (PSF)** can only be analyzed by classic **field tracing** which includes the consideration of **diffraction effects** due to the microstructured surface part of the hybrid lens (diffractive lens surface).

 file used: AppS.0009_Bifocal_Hybrid_Lens_1.lpd

Field Tracing: Point Spread Functions

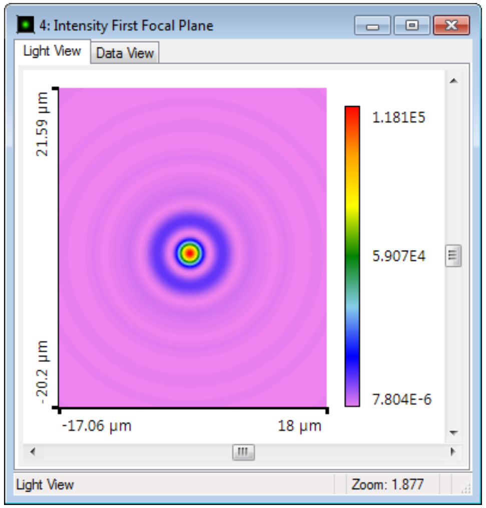

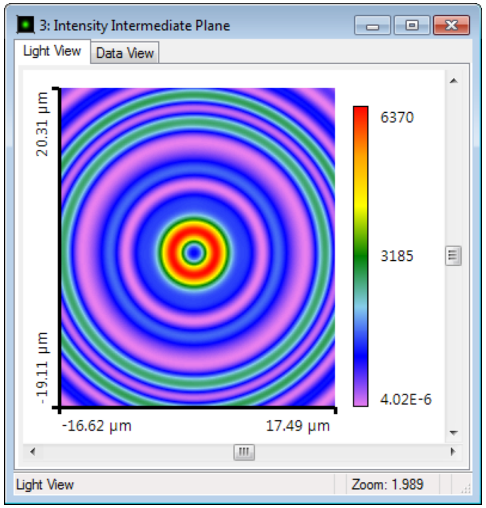

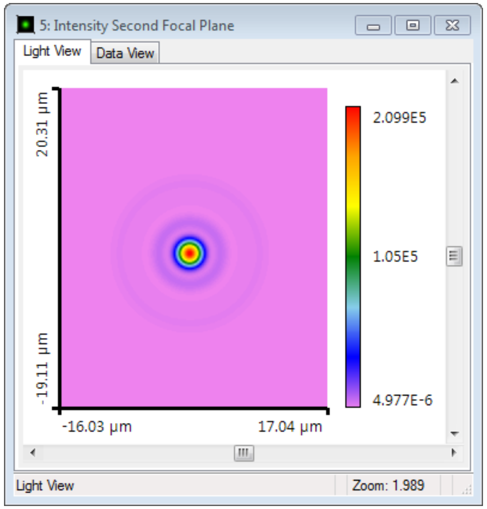

PSF in 1st focal plane, 9.37 mm after lens

PSF between focal planes, 9.67 mm after lens

PSF in focal plane 2, 9.92 mm after lens

file used: AppS.0009_Bifocal_Hybrid_Lens_1.lpd

Components

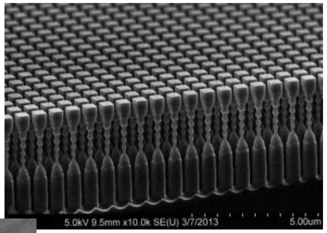

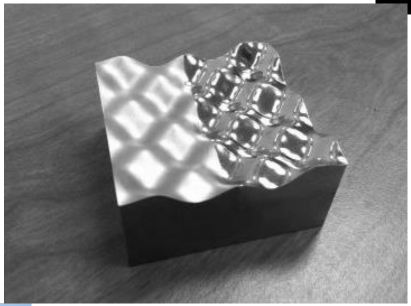

[1] IMS-Mechatronics Lab

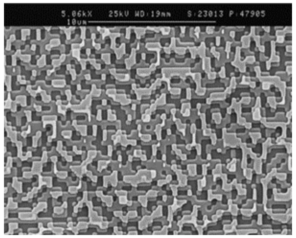

[2] ISUZU GLASS

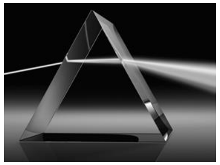

Light Shaping > Aperiodic Microlens Array

LED Top Hat Generation using Aperiodic Refractive Beam Shaper Array

Task/System Illustration

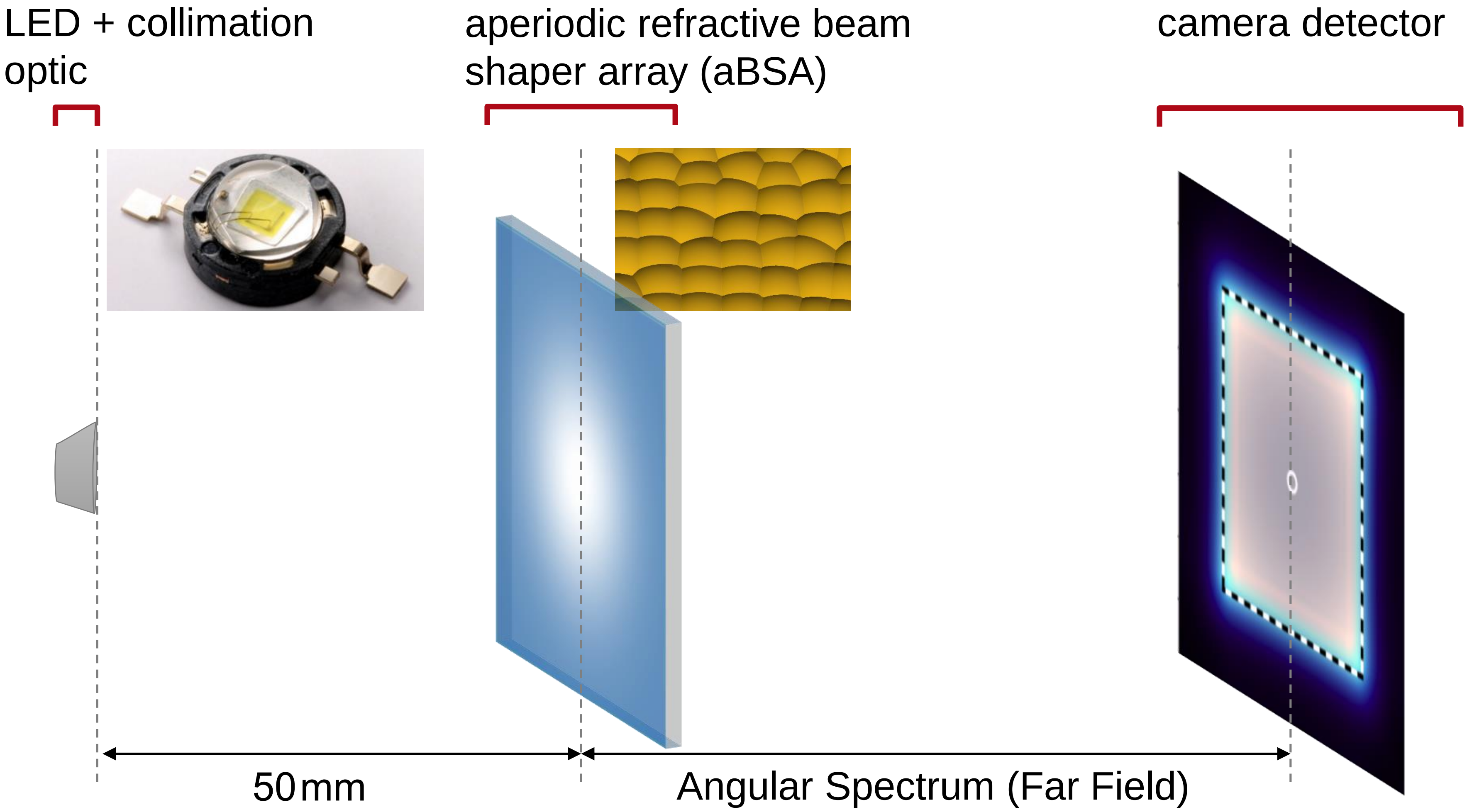

Specs: Light Source

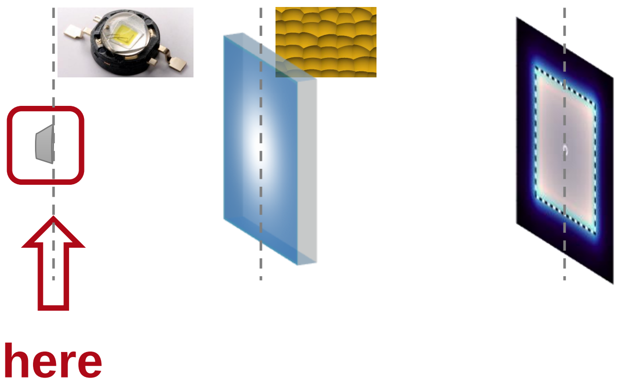

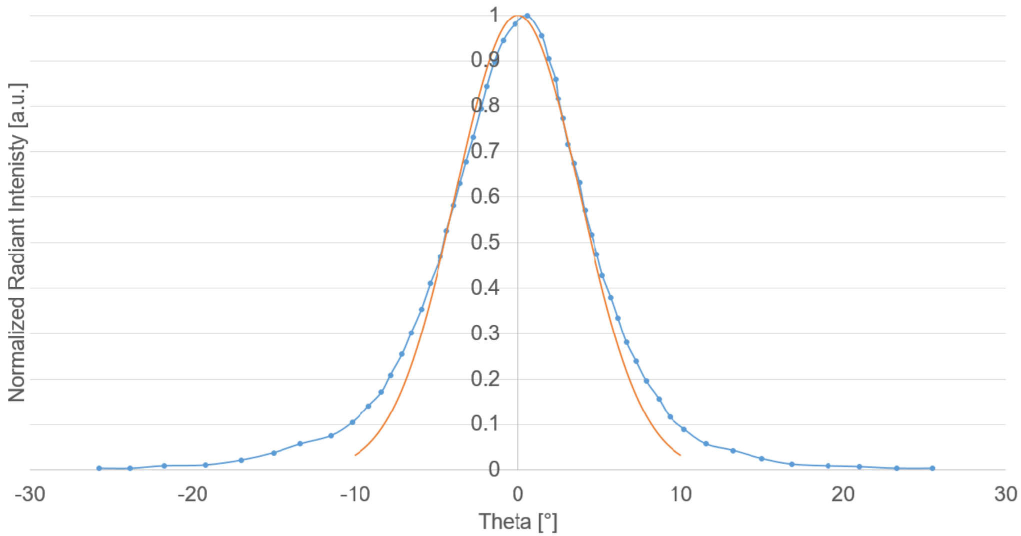

Parameter	Description / Value & Unit
name/type	Seoul Z-LED P4 from Seoul Semiconductors
partially coherent source type	Gaussian type planar source
collimation	TIR lens from Carclo Optics (part no. 10003)
spectrum	pure white light spectrum
FWHM radiant intensity	9°

Specs: Light Source

here

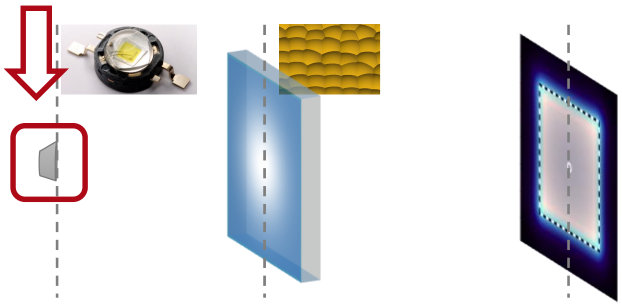

Highlights

- fast and accurate modeling of a white light LED
- design and analysis an aperiodic refractive beam shaper array to optimize a top hat intensity pattern

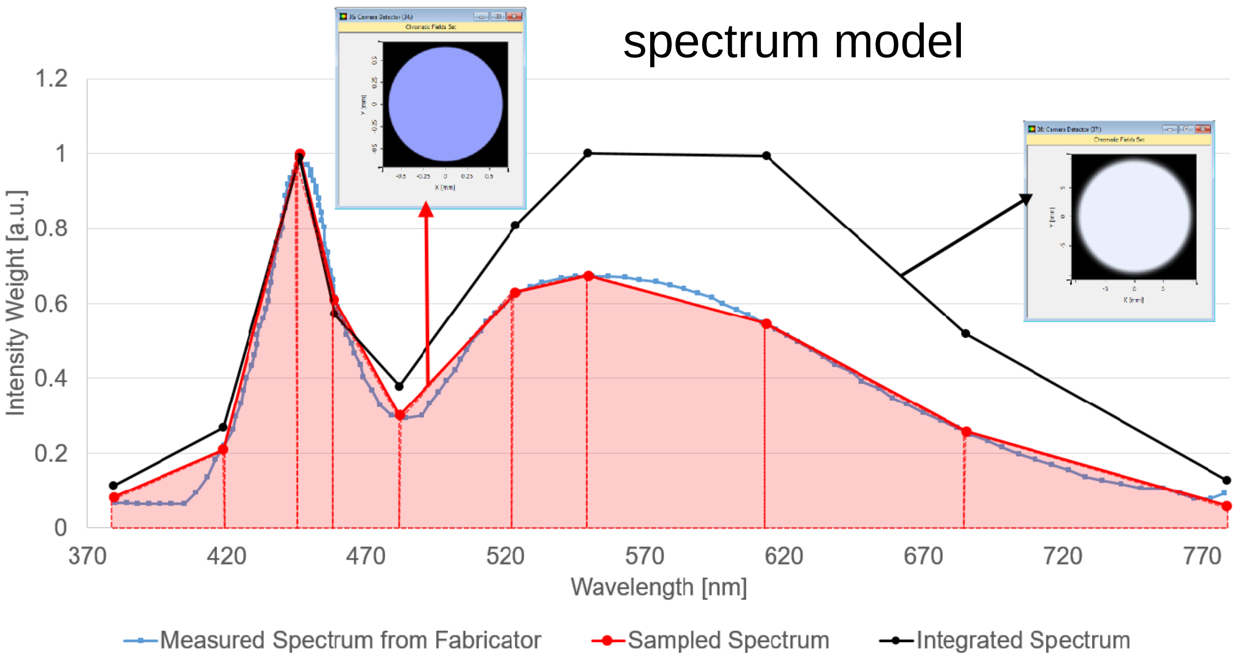

significant performance improvement
non-equidistant sampling of the spectrum

Specs: Aperiodic Refractive Beam Shaper Array

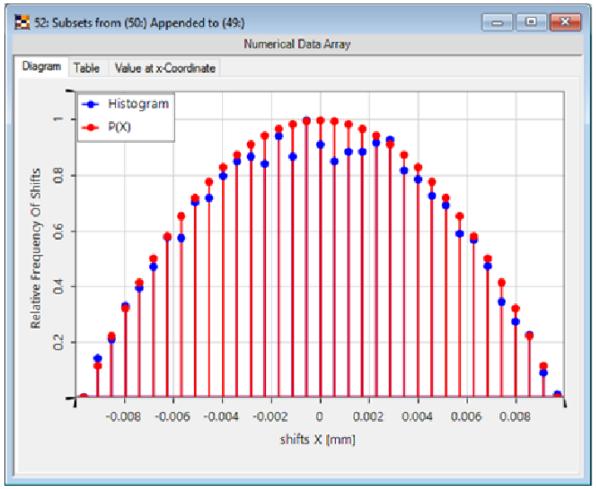

Histogram of Cell Distribution Function

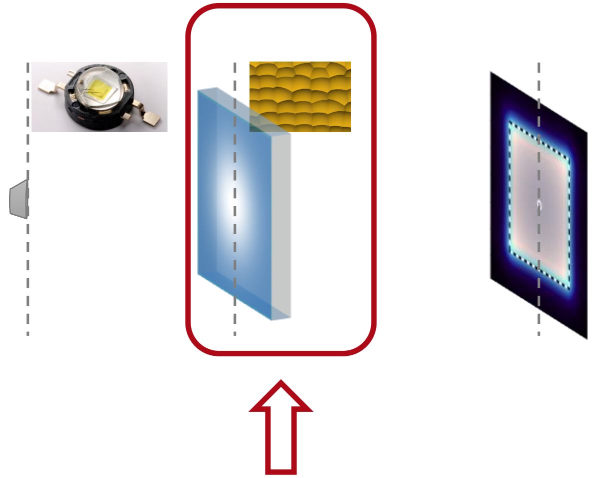

here

Highlights

- fast and accurate modeling of a white light LED
- design and analysis an aperiodic refractive beam shaper array to optimize a top hat intensity pattern

parametrization of the distribution function allows optimization regarding a desired target pattern

Parameter	**Description / Value & Unit**
cell array aperture	20x20mm
number of cells	124x124
cell distribution function	quadratic polynomial
substrate thickness	1mm
substrate material	fused silica

Specs: Evaluation

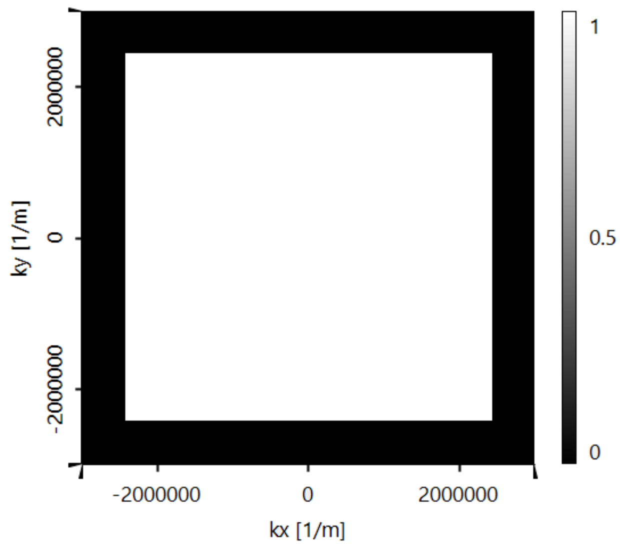

Desired Target Pattern

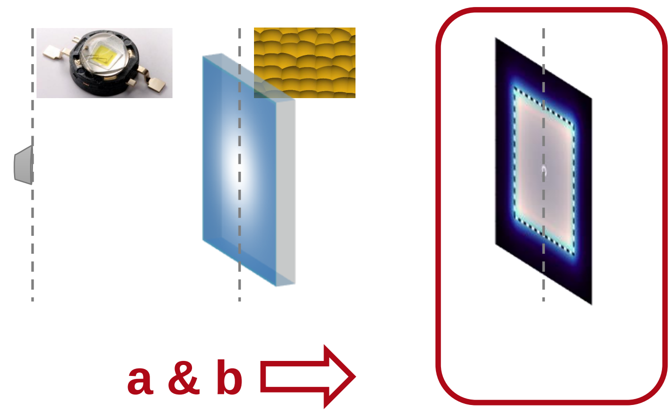

Position	Type of Evaluation	Description / Value & Unit
a	camera detector	evaluates intensity pattern
b	performance criteria evaluation	evaluates conversion & window efficiency and uniformity error regarding the desired target pattern

Results: Intensity Pattern (real color view)

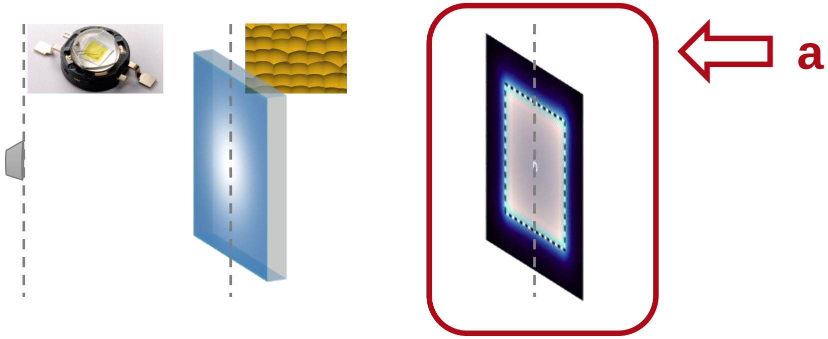

Highlights
- fast and accurate modeling of a white light LED
- design and analysis an aperiodic refractive beam shaper array to optimize a top hat intensity pattern

aperiodic beam shaper array

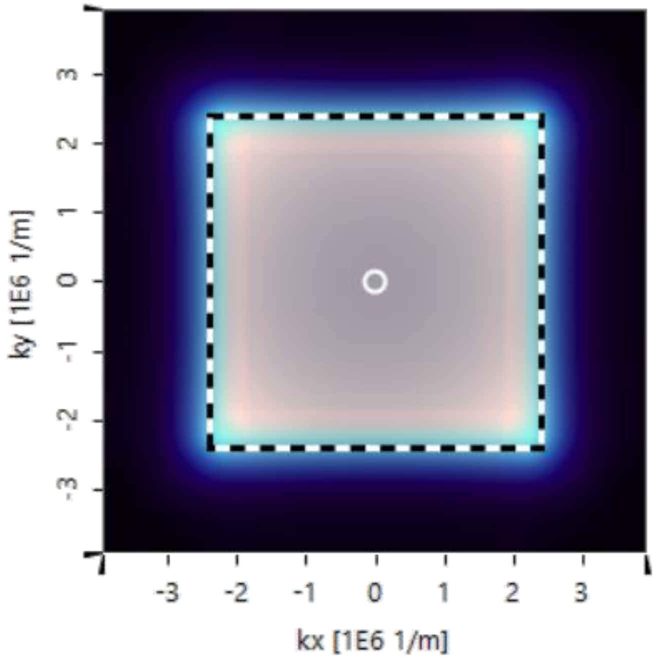

periodic microlens array

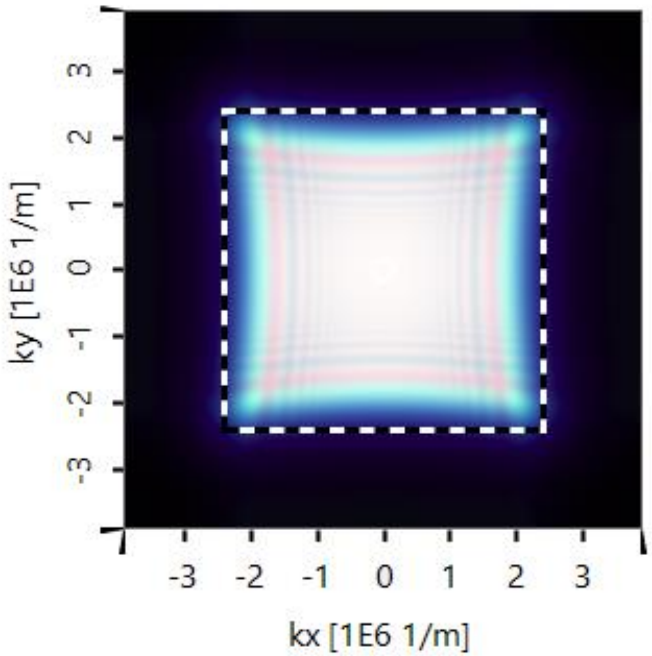

Results: Performance Criteria Evaluation

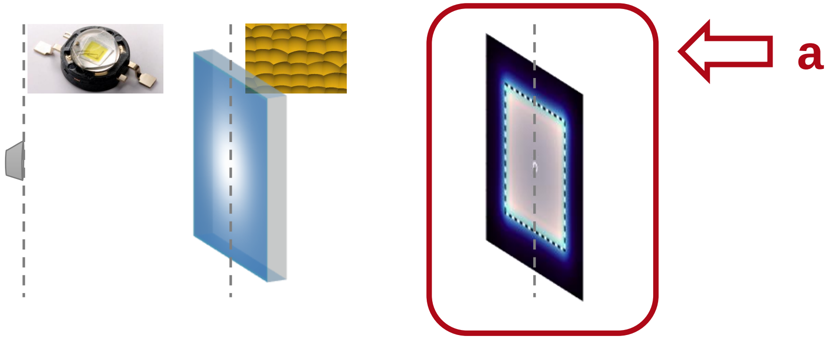

Highlights

- fast and accurate modeling of a white light LED
- design and analysis an aperiodic refractive beam shaper array to optimize a top hat intensity pattern

Parameter	Value & Unit Aperiodic Beam Shaper Array	Value & Unit Microlens Array
window efficiency	92.23 %	99.93 %
conversion efficiency	89.34 %	80.18 %
uniformity error	17.92 %	49.08 %

Crystal

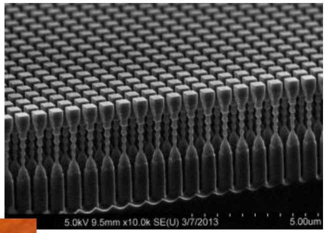

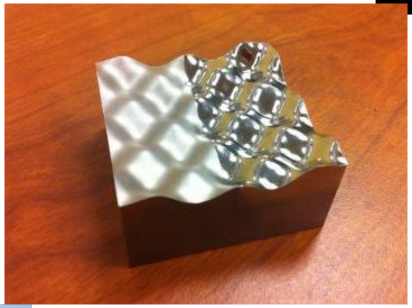

[1] IMS-Mechatronics Lab

[2] ISUZU GLASS

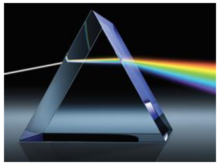

Example – Stress Birefringence

- Laser-based soldering
  - Contact free heating, versatile to use
  - Localized and minimized input of energy
  - Flux-free processing, no contamination

P. Ribes-Pleguezuelo *et al*., Opt. Express **25**, 5927-5940 (2017)

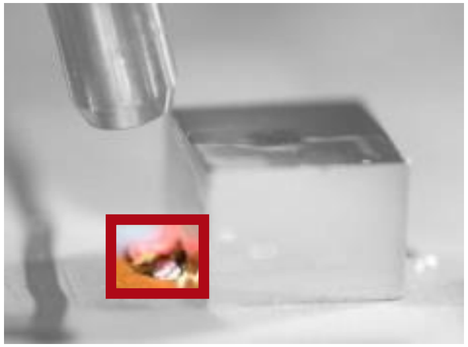

Photo from Fraunhofer IOF

- ANSYS
  - Structural/material definition
  - Transient thermal analysis
  - Stress simulation inside crystal component
- VirtualLab
  - Convert stress into optical permittivity data
  - Simulation of field propagation through birefringent materials

From Stress to Birefringence

- Convert stress to optical permittivity
  (for each layer inside stratified medium)

Stress tensor $\rightarrow$? $\rightarrow$ Permittivity tensor

$$\begin{pmatrix} \sigma_1 & \sigma_6 & \sigma_5 \\ \sigma_6 & \sigma_2 & \sigma_4 \\ \sigma_5 & \sigma_4 & \sigma_3 \end{pmatrix} \xrightarrow{\quad ? \quad} \begin{pmatrix} \epsilon_1 & \epsilon_6 & \epsilon_5 \\ \epsilon_6 & \epsilon_2 & \epsilon_4 \\ \epsilon_5 & \epsilon_4 & \epsilon_3 \end{pmatrix}$$

From Stress to Birefringence

- Convert stress to optical permittivity
  (for each layer inside stratified medium)

Stress tensor

$$\begin{pmatrix} \sigma_1 & \sigma_6 & \sigma_5 \\ \sigma_6 & \sigma_2 & \sigma_4 \\ \sigma_5 & \sigma_4 & \sigma_3 \end{pmatrix}$$

Piezo-optic constant

$$\Delta B_m = \pi_{mn} \sigma_n$$

Changes in impermeability tensor

$$\begin{pmatrix} \Delta B_1 & \Delta B_6 & \Delta B_5 \\ \Delta B_6 & \Delta B_2 & \Delta B_4 \\ \Delta B_5 & \Delta B_4 & \Delta B_3 \end{pmatrix}$$

From Stress to Birefringence

- Convert stress to optical permittivity
  (for each layer inside stratified medium)

Stress tensor

$$\begin{pmatrix} \sigma_1 & \sigma_6 & \sigma_5 \\ \sigma_6 & \sigma_2 & \sigma_4 \\ \sigma_5 & \sigma_4 & \sigma_3 \end{pmatrix}$$

Piezo-optic constant

$$\Delta B_m = \pi_{mn} \sigma_n$$

Changes in impermeability tensor

$$\begin{pmatrix} \Delta B_1 & \Delta B_6 & \Delta B_5 \\ \Delta B_6 & \Delta B_2 & \Delta B_4 \\ \Delta B_5 & \Delta B_4 & \Delta B_3 \end{pmatrix}$$

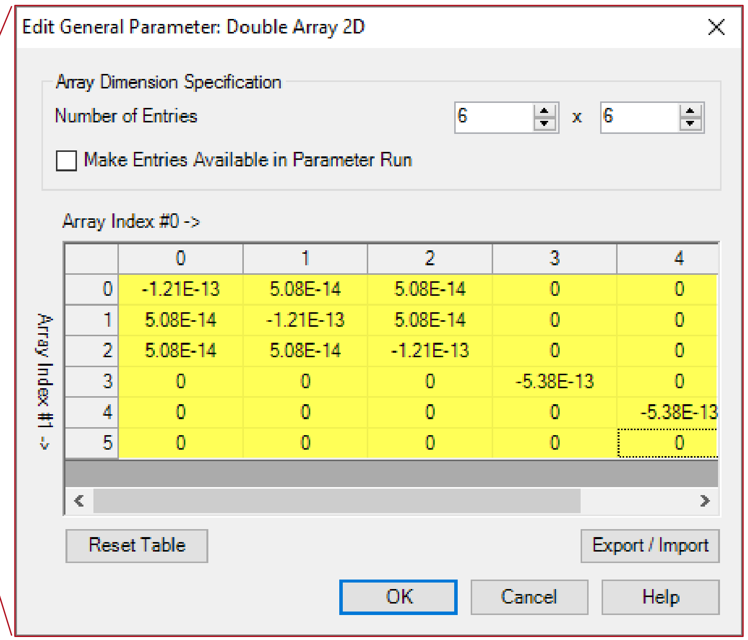

	0	1	2	3	4
0	-1.21E-13	5.08E-14	5.08E-14	0	0
1	5.08E-14	-1.21E-13	5.08E-14	0	0
2	5.08E-14	5.08E-14	-1.21E-13	0	0
3	0	0	0	-5.38E-13	0
4	0	0	0	0	-5.38E-13
5	0	0	0	0	0

Example: piezo-optic constant tensor for YAG crystal

From Stress to Birefringence

- Convert stress to optical permittivity
  (for each layer inside stratified medium)

Stress tensor

$$\begin{pmatrix} \sigma_1 & \sigma_6 & \sigma_5 \\ \sigma_6 & \sigma_2 & \sigma_4 \\ \sigma_5 & \sigma_4 & \sigma_3 \end{pmatrix}$$

$$\Delta B_m = \pi_{mn}\sigma_n$$

Changes in impermeability tensor

$$\begin{pmatrix} \Delta B_1 & \Delta B_6 & \Delta B_5 \\ \Delta B_6 & \Delta B_2 & \Delta B_4 \\ \Delta B_5 & \Delta B_4 & \Delta B_3 \end{pmatrix}$$

$$B_m = \boxed{B_{0,m}} + \Delta B_m$$

Stress-free values (related to refractive index/indicies)

Impermeability tensor

$$\begin{pmatrix} B_1 & B_6 & B_5 \\ B_6 & B_2 & B_4 \\ B_5 & B_4 & B_3 \end{pmatrix}$$

From Stress to Birefringence

- Convert stress to optical permittivity
  (for each layer inside stratified medium)

Stress tensor

$$\begin{pmatrix} \sigma_1 & \sigma_6 & \sigma_5 \\ \sigma_6 & \sigma_2 & \sigma_4 \\ \sigma_5 & \sigma_4 & \sigma_3 \end{pmatrix}$$

$$\Delta B_m = \pi_{mn} \sigma_n$$

Changes in impermeability tensor

$$\begin{pmatrix} \Delta B_1 & \Delta B_6 & \Delta B_5 \\ \Delta B_6 & \Delta B_2 & \Delta B_4 \\ \Delta B_5 & \Delta B_4 & \Delta B_3 \end{pmatrix}$$

$$B_m = B_{0,m} + \Delta B_m$$

$$\begin{pmatrix} B_1 & B_6 & B_5 \\ B_6 & B_2 & B_4 \\ B_5 & B_4 & B_3 \end{pmatrix}$$

Example: ordinary refractive index for BBO crystal

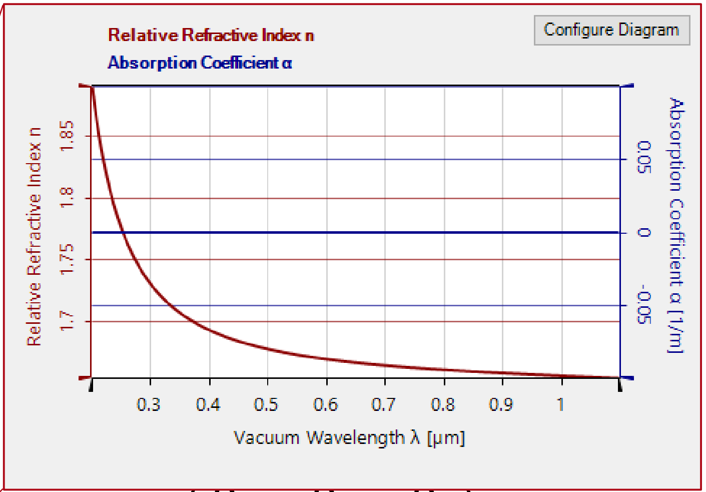

Stress-free values
(related to refractive index/indicies)

From Stress to Birefringence

- Convert stress to optical permittivity
  (for each layer inside stratified medium)

Stress tensor

$$\begin{pmatrix} \sigma_1 & \sigma_6 & \sigma_5 \\ \sigma_6 & \sigma_2 & \sigma_4 \\ \sigma_5 & \sigma_4 & \sigma_3 \end{pmatrix}$$

$$\Delta B_m = \boxed{\pi_{mn}} \sigma_n$$

Piezo-optic constant

Changes in impermeability tensor

$$\begin{pmatrix} \Delta B_1 & \Delta B_6 & \Delta B_5 \\ \Delta B_6 & \Delta B_2 & \Delta B_4 \\ \Delta B_5 & \Delta B_4 & \Delta B_3 \end{pmatrix}$$

$$B_m = \boxed{B_{0,m}} + \Delta B_m$$

Stress-free values
(related to refractive index/indicies)

Impermeability tensor

$$\begin{pmatrix} B_1 & B_6 & B_5 \\ B_6 & B_2 & B_4 \\ B_5 & B_4 & B_3 \end{pmatrix}$$

$$[\epsilon_{ij}]^{-1} = [B_{ij}]$$

Permittivity tensor

$$\begin{pmatrix} \epsilon_1 & \epsilon_6 & \epsilon_5 \\ \epsilon_6 & \epsilon_2 & \epsilon_4 \\ \epsilon_5 & \epsilon_4 & \epsilon_3 \end{pmatrix}$$

VirtualLab Simulation

- Convert stress to optical permittivity

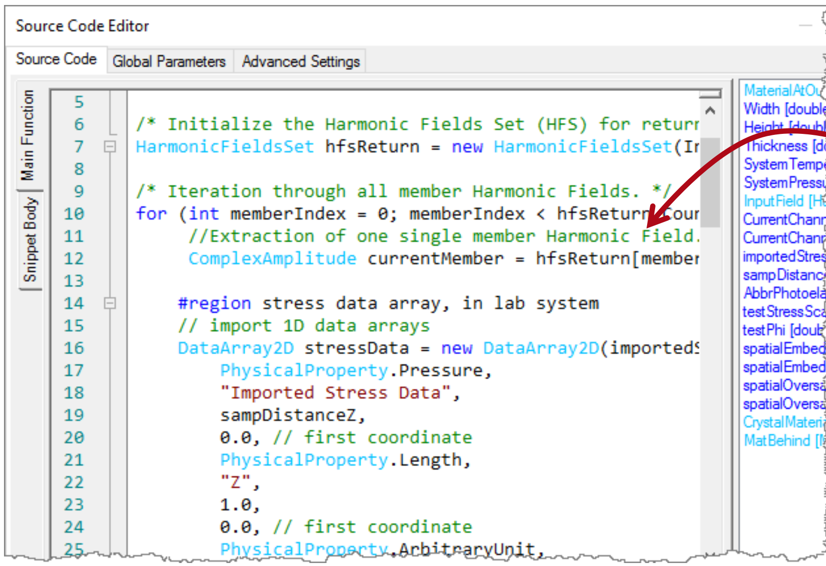

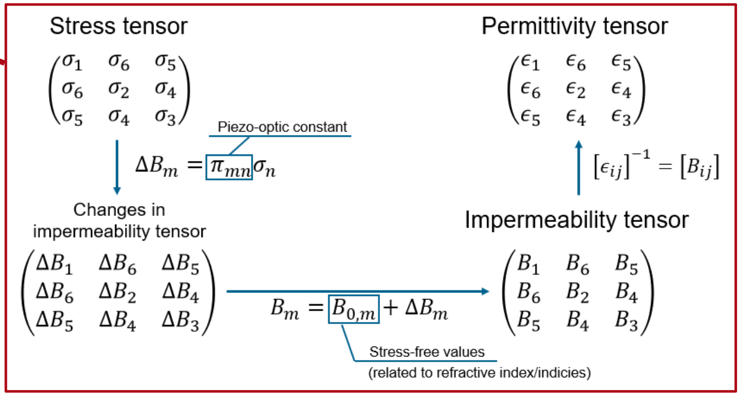

Conversion from stress tensor to the corresponding permittivity tensor is implemented by using the programmable component in VirtualLab

Simulation Results

- Input field

1) @1064 nm

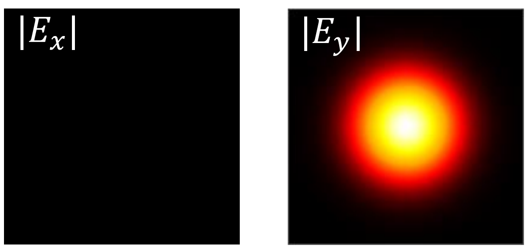

(waist radius 50 µm)

2) @532 nm

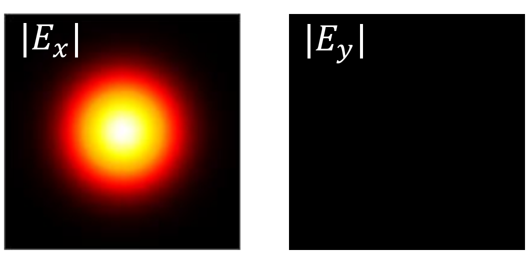

(waist radius 50 µm)

Note: we set the polarization according to the SHG configuration

- Applied stress

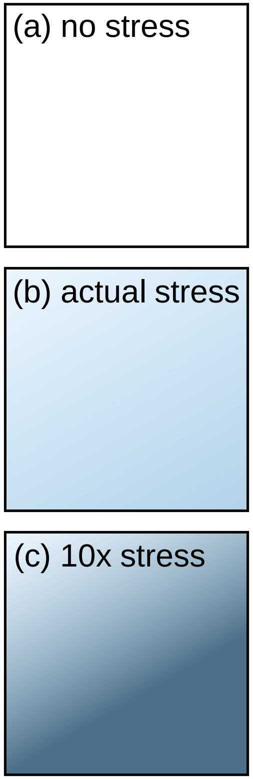

- Output field

?

Simulation Results

- YAG crystal with 1064 nm input field (Ey)

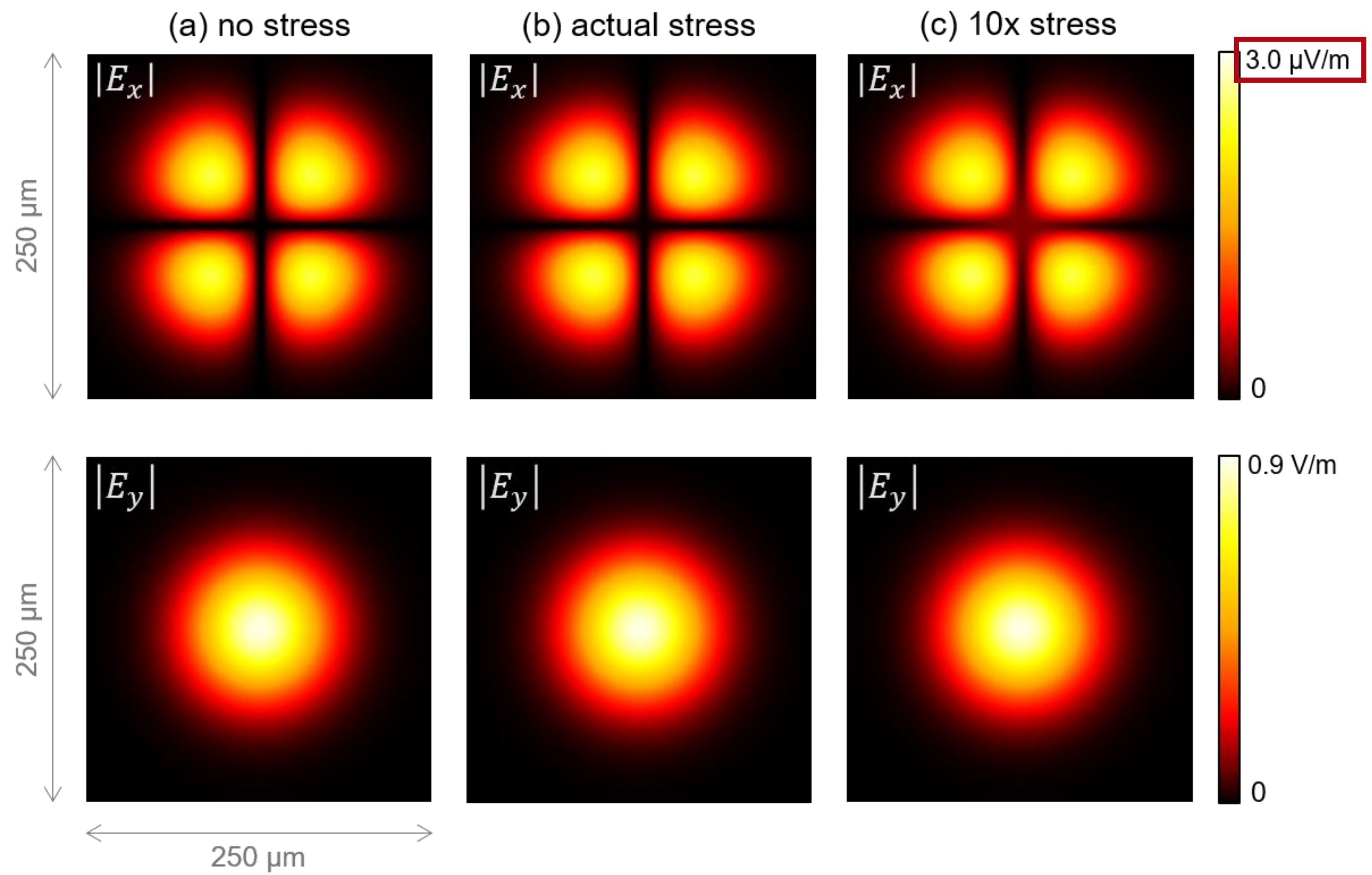

Simulation Results

- YAG crystal with 1064 nm input field (Ey)

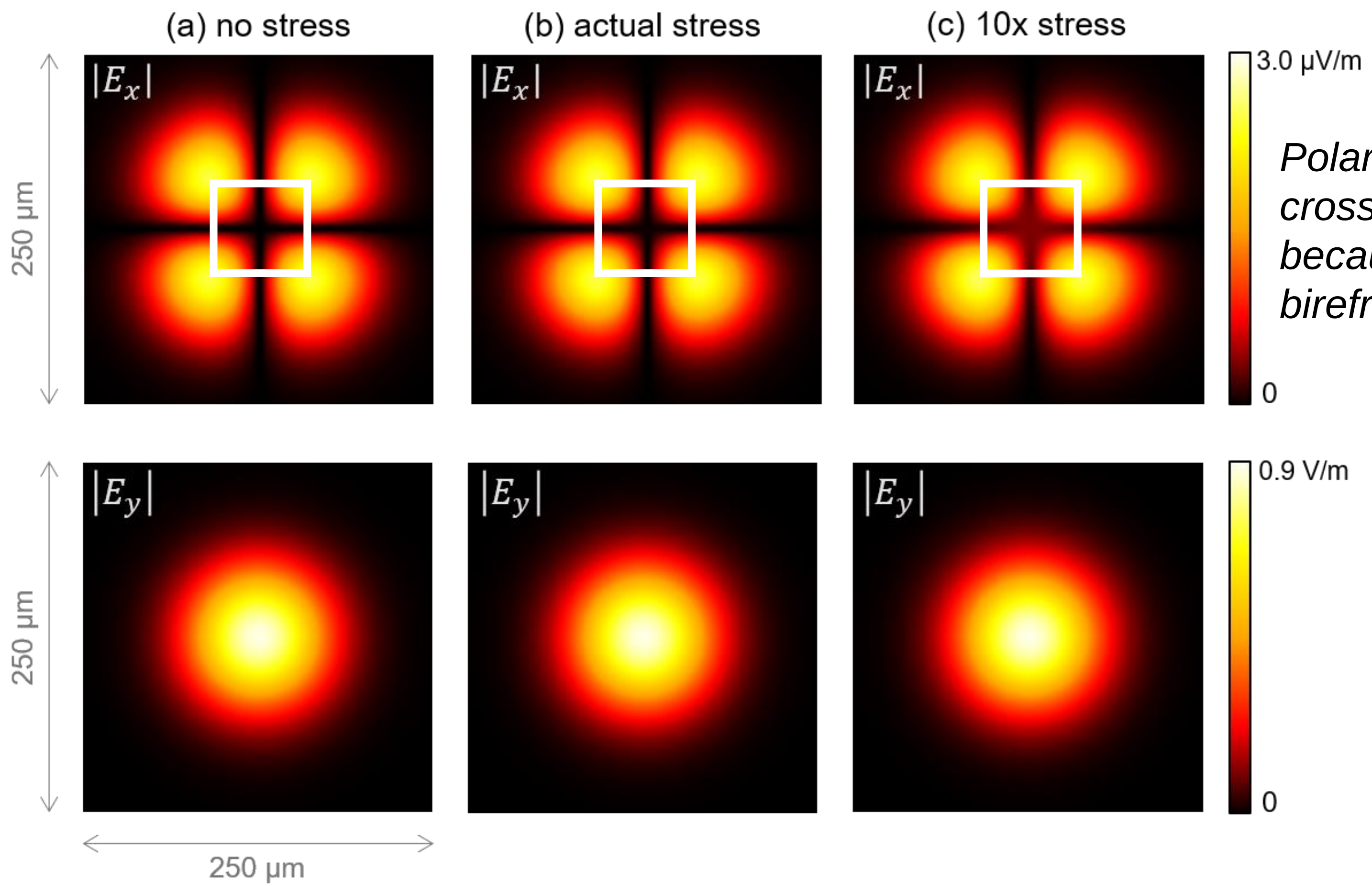

Polarization crosstalk (center) because of birefringence

Simulation Results

- YAG crystal with 1064 nm input field (Ey)
  - Further check on the influence of stress-induced birefringence, we perform parameter run from 1x to 201x stresses (with 101 steps)

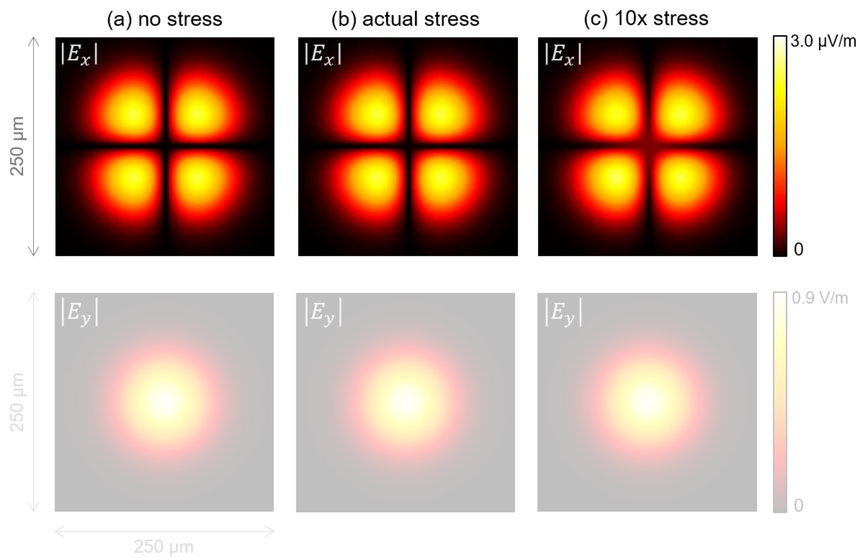

from 1x to 201x stress

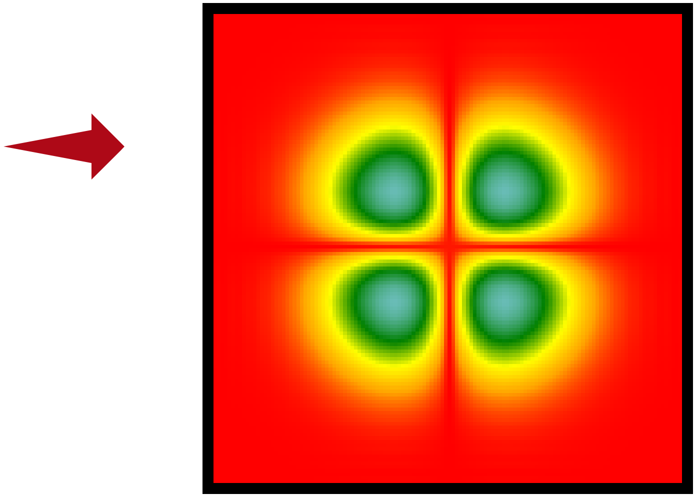

(logarithm color for better visibility)

Calculation of 101 steps: ~ **90** s
with Intel Core i7-4910MQ

Simulation Results

- YAG crystal with 532 nm input field (Ex)

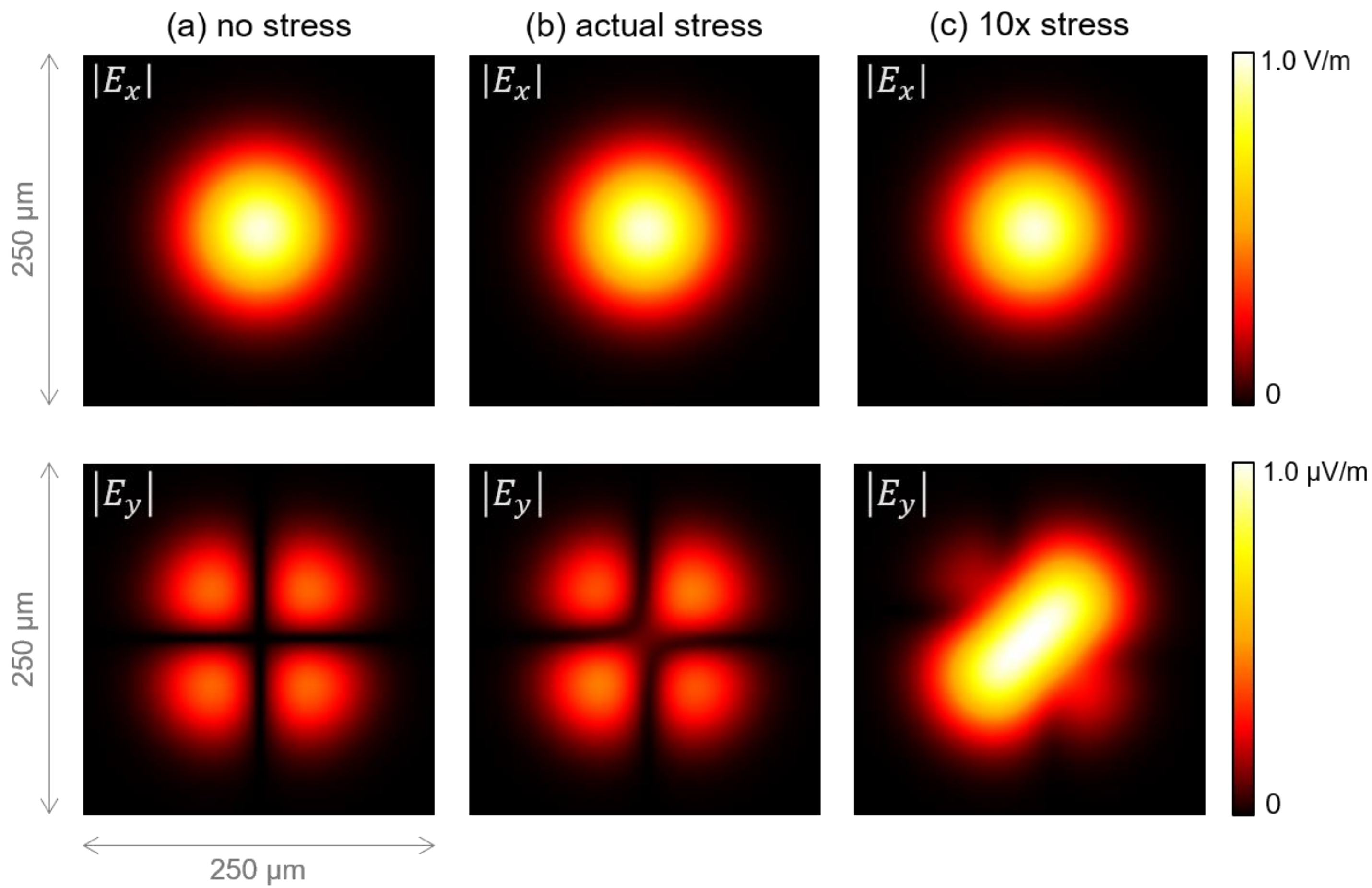

Simulation Results

- YAG crystal with 532 nm input field (Ex)
  - Further check on the influence of stress-induced birefringence, we perform parameter run from 1x to 51x stresses (with 101 steps)

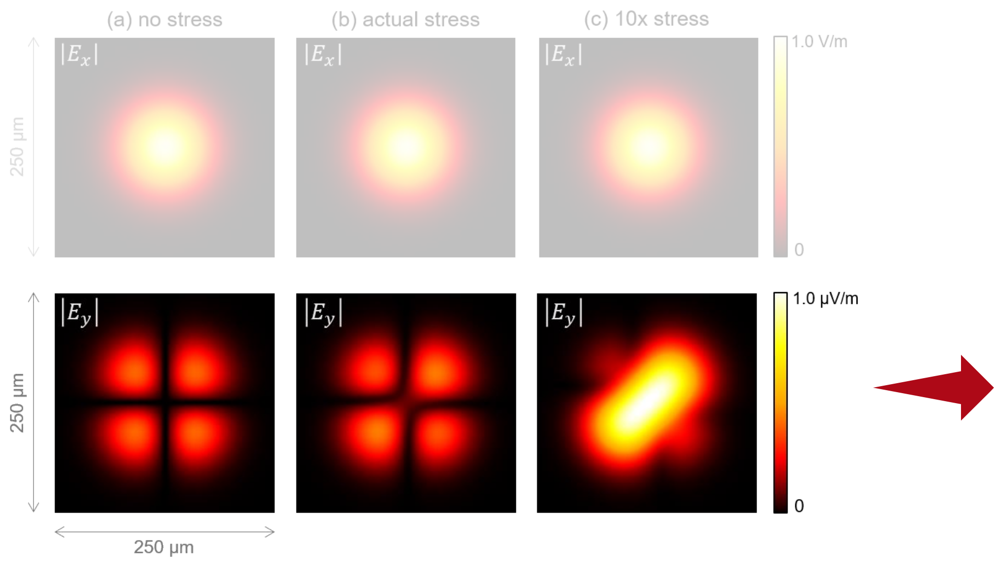

from 1x to 51x stress

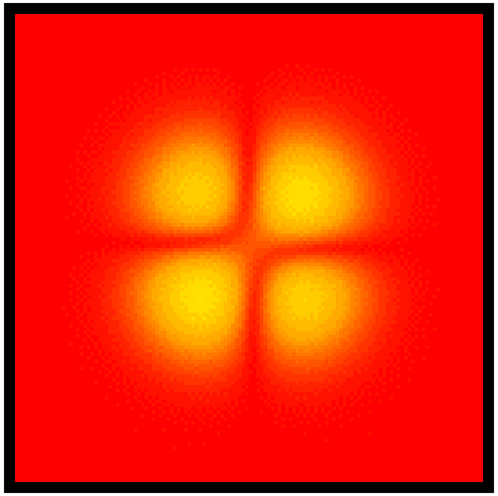

(logarithm color for better visibility)

GRIN Media

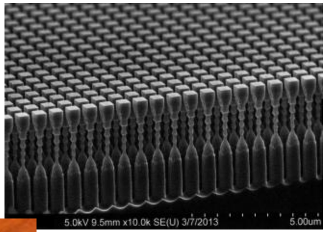

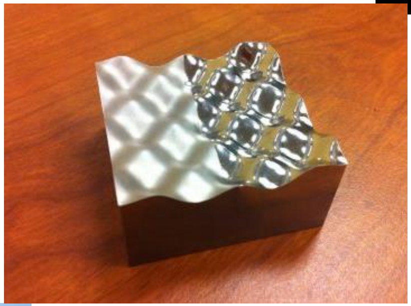

[1] IMS-Mechatronics Lab

[2] ISUZU GLASS

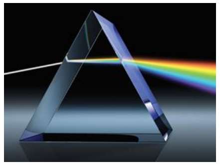

Laser Systems > Beam Delivery System

Modeling of Graded-Index (GRIN) Multimode Fiber

Task/System Illustration

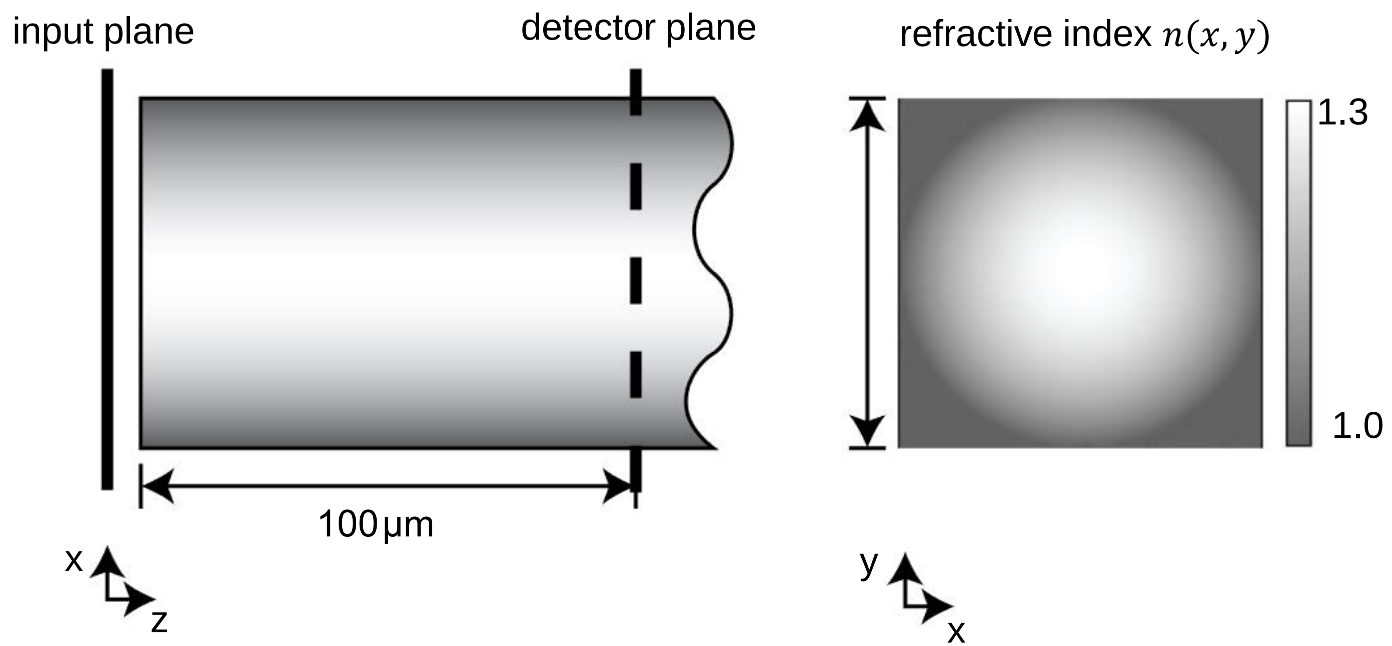

- ray propagation through a GRIN fiber
- electromagnetic field propagation through a GRIN fiber by
  - a rigorous Maxwell solver, the Fourier Modal Method (FMM) with Perfectly Matched Layers (PMLs)
  - our newly developed very fast approximated Maxwell solver

Specifications: Light Source

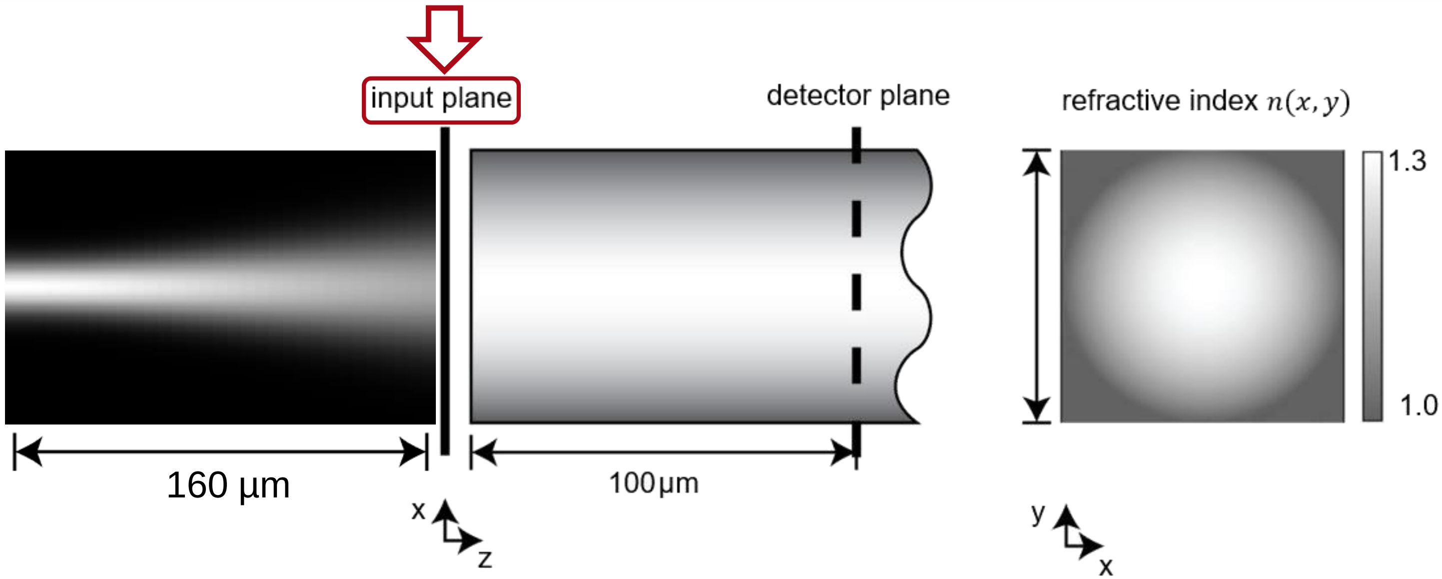

Parameter	Description / Value
coherence/mode	single Hermite Gaussian (0,0) mode
wavelength	532 nm
polarization	linear in y-direction (90°)
distance between beam waist and input plane	160 µm

Specifications: GRIN fiber

- refractive index $n(x,y)$

$$n(x,y) = n_0 \sqrt{1 - 2 \cdot \Delta \cdot \frac{r^2}{r_0^2}}$$

with $r = \sqrt{x^2 + y^2}$ and $\Delta = \frac{n_1^2 - n_2^2}{2 n_1^2}$

- in this case, $n_1 = 1.3$, $n_2 = 1.0$, $r_0 = 50\,\mu\text{m}$

Highlight

arbitrarily customizable refractive index profile

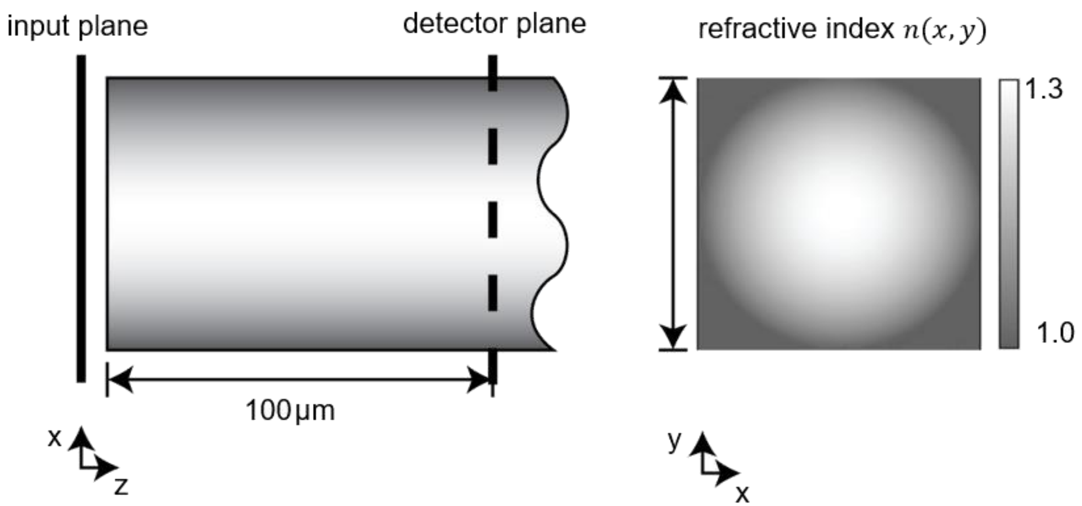

Results: 3D System Ray Tracing

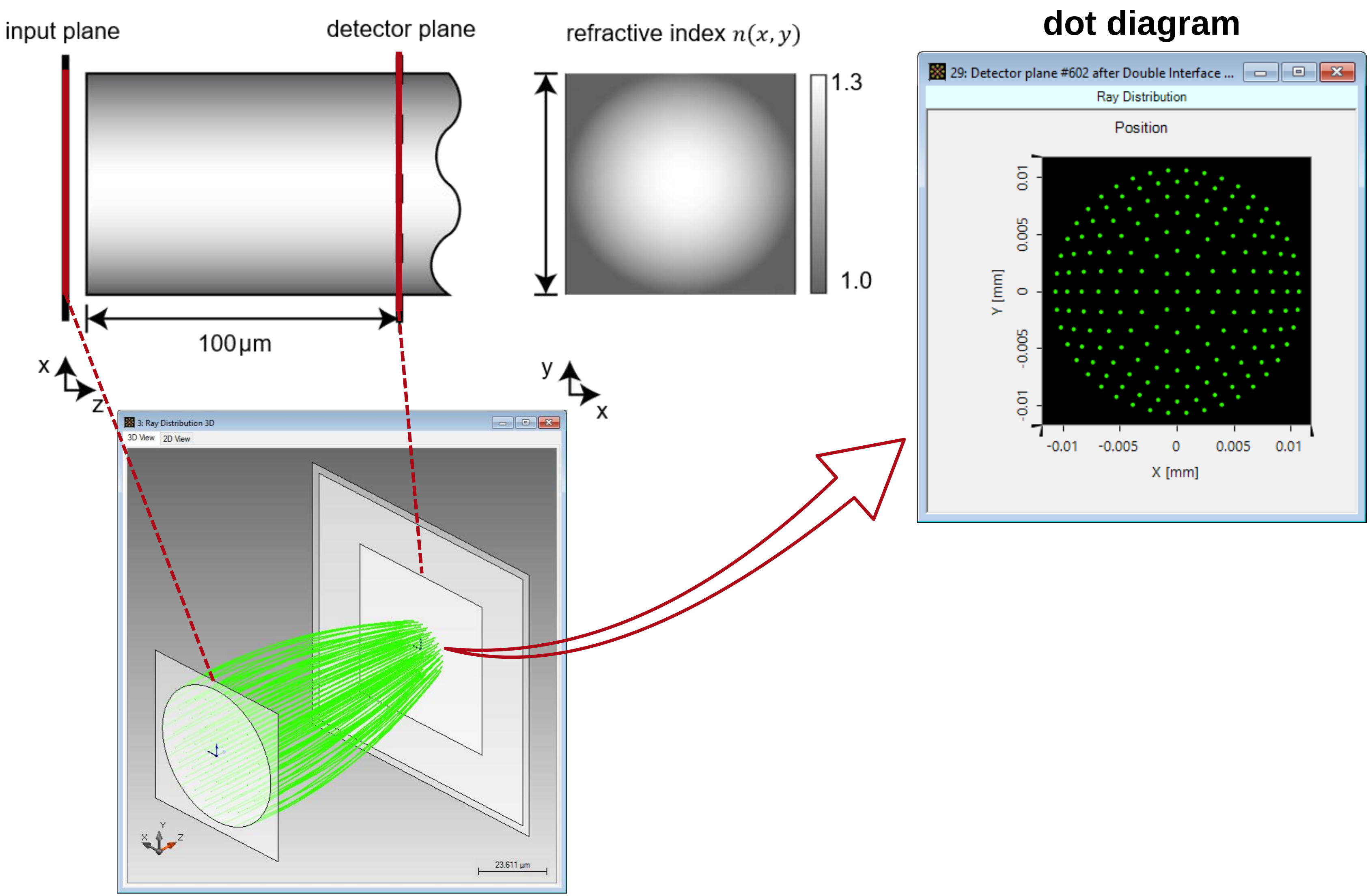

Results: Switching to Our Fast Approach

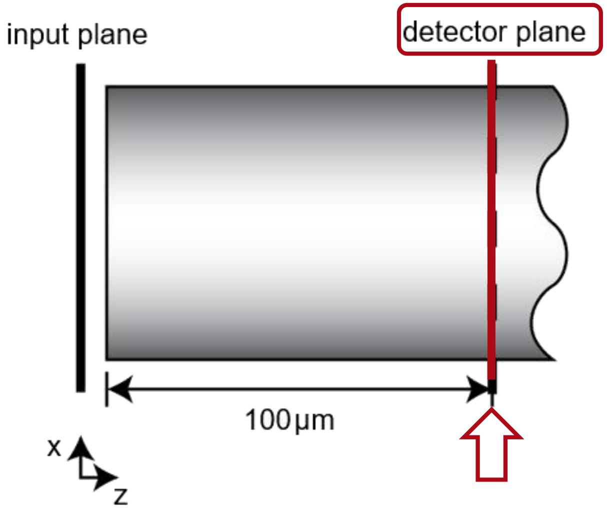

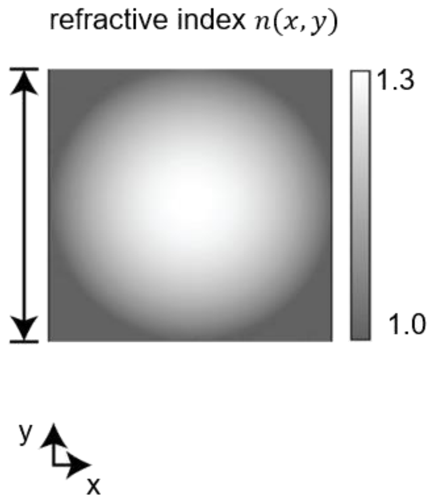

dot diagram

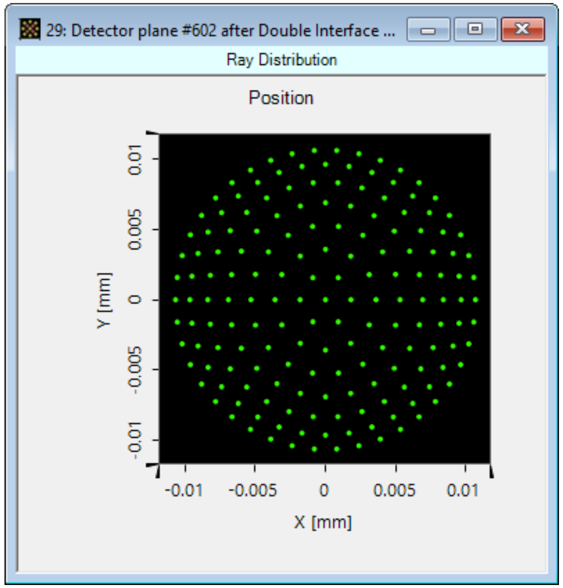

switching from ray tracing to field tracing by just one click

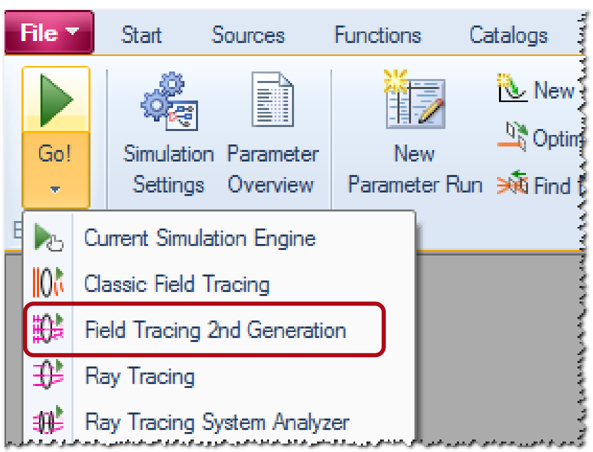

Highlights

easy switching between ray and field tracing

Results: Our Fast Approach

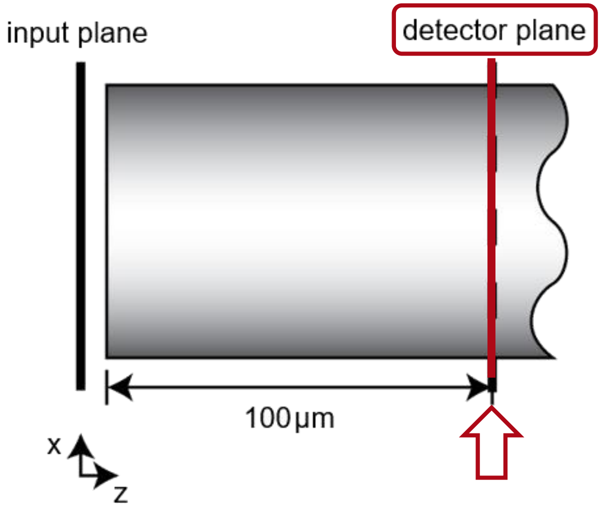

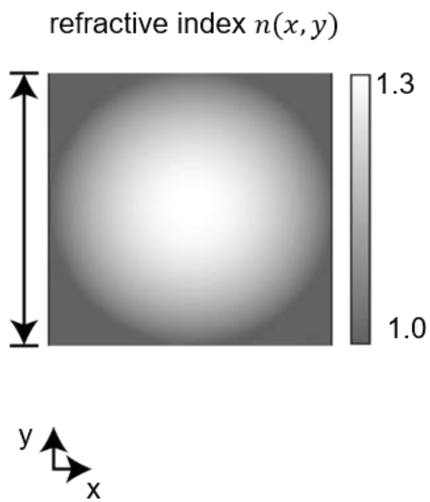

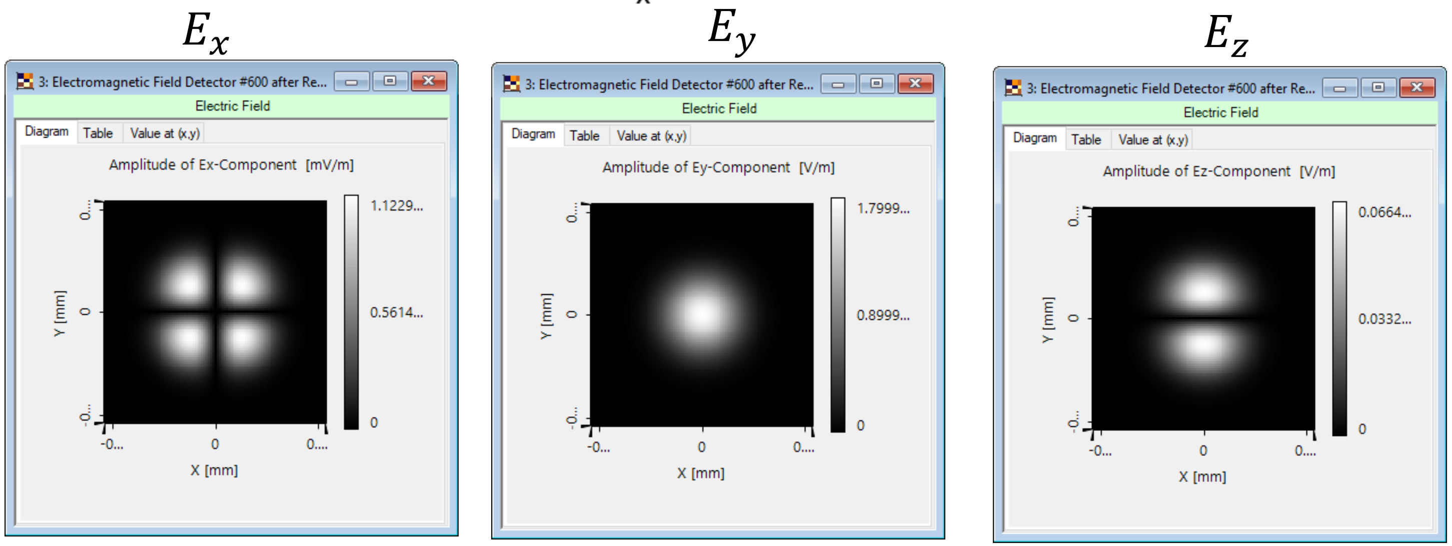

Amplitude [V/m]

Results: Our Fast Approach vs FMM

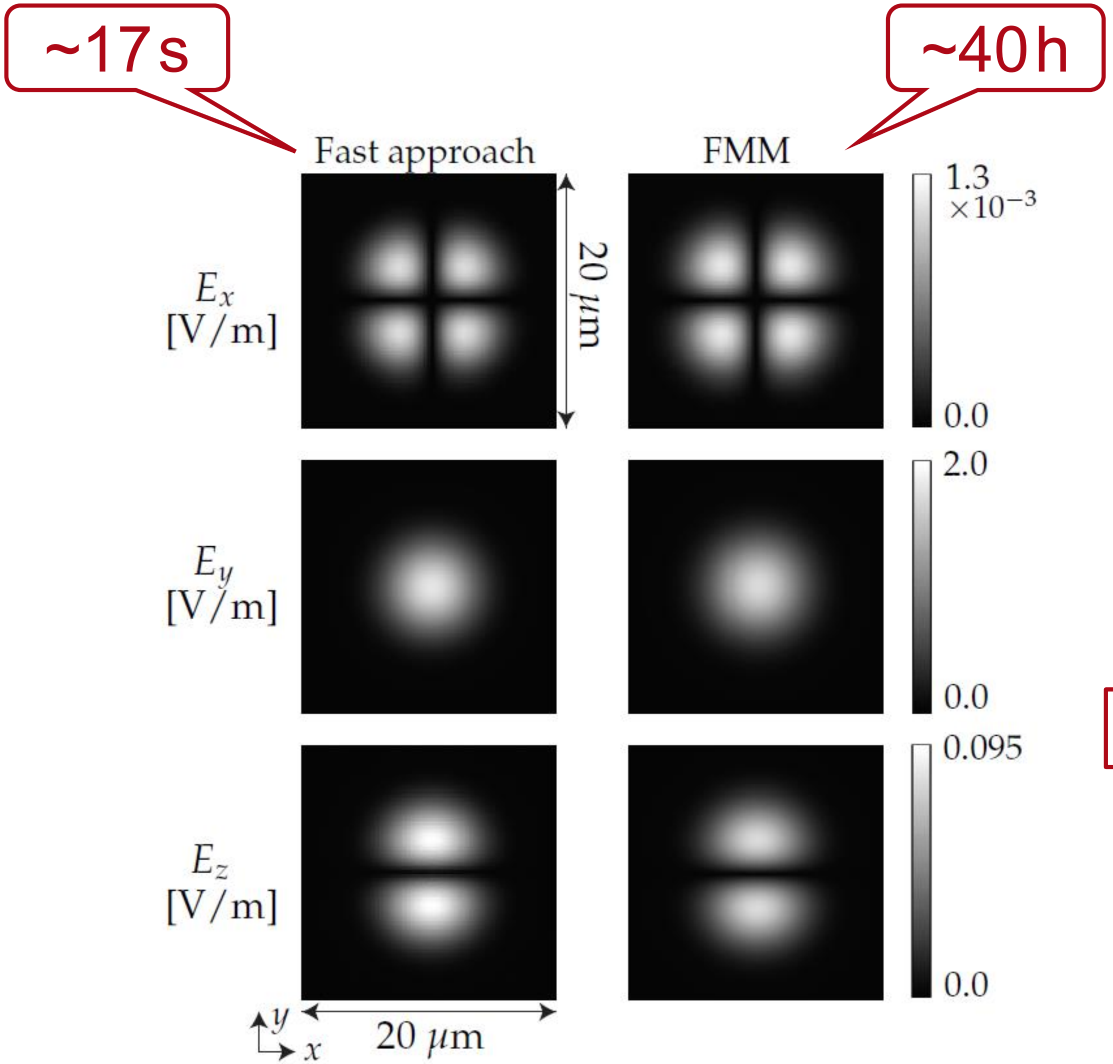

Deviation between results of both approaches is < 1%

Highlights

- high accuracy of new propagation method for multimode GRIN fibers
- consideration of polarization crosstalk

13:30-14:00

Source and detector modeling

Source

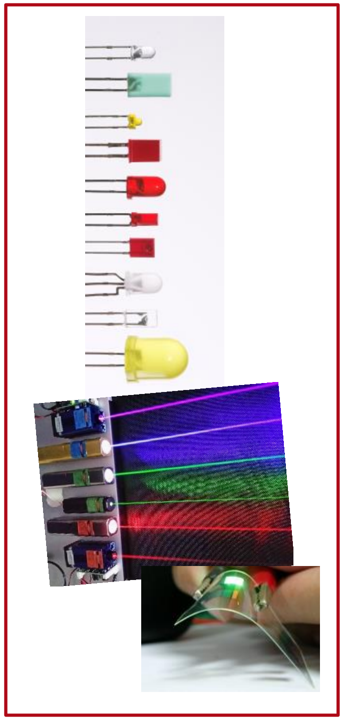

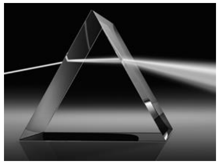

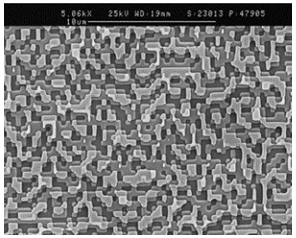

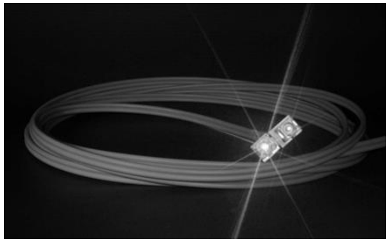

Video of sources

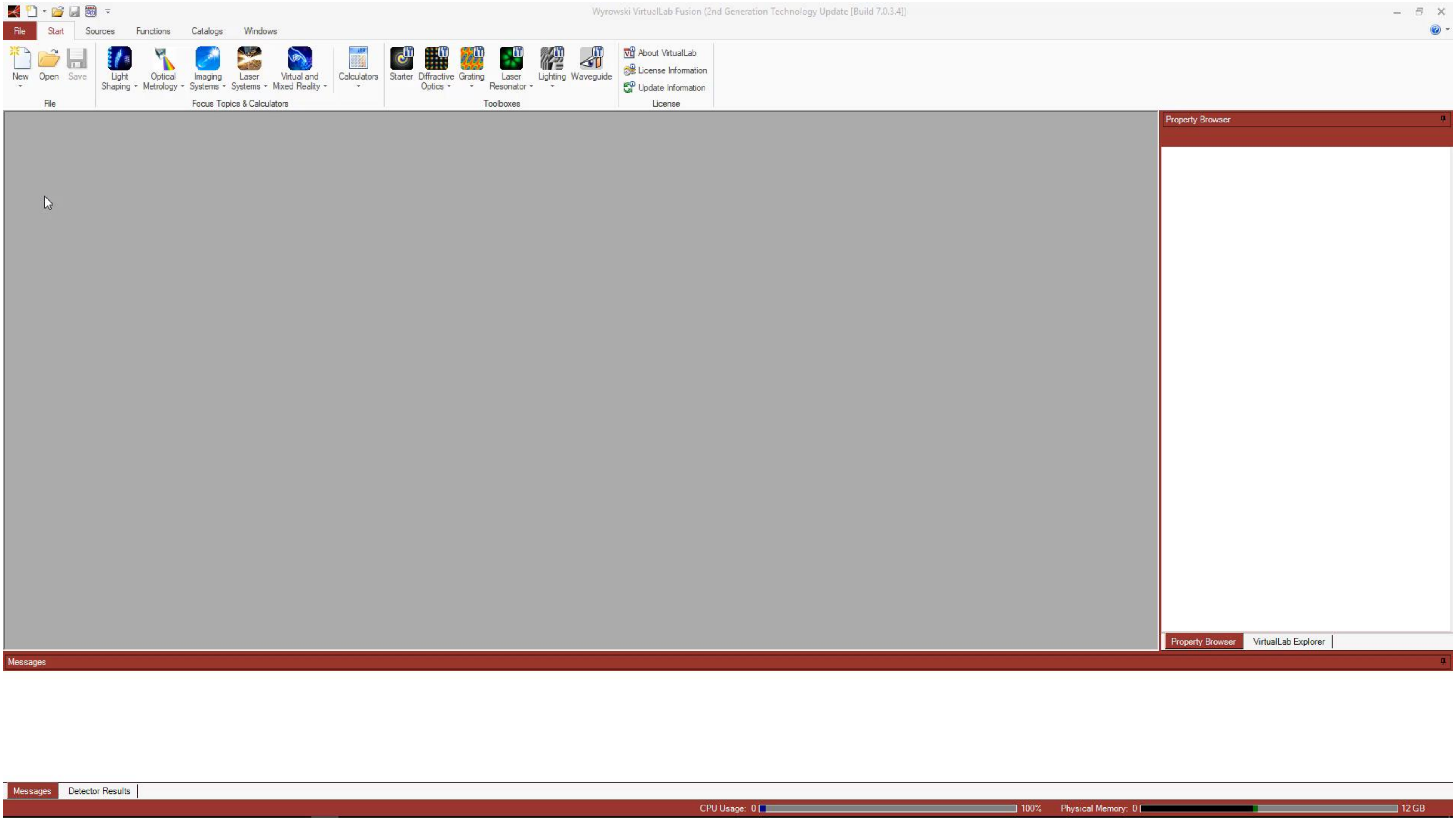

Partially Coherent Source: Lateral Modes

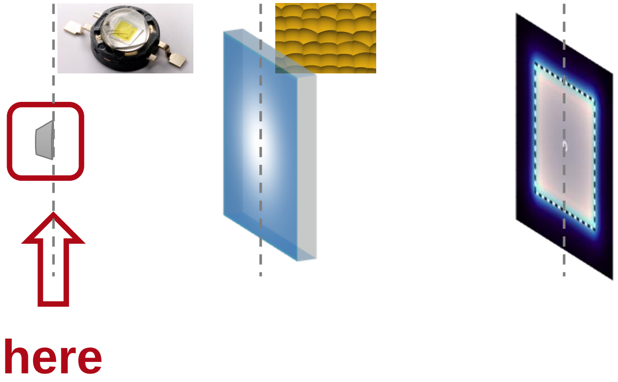

a set of point sources

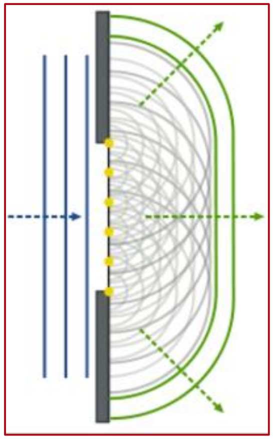

Partially Coherent Source: Lateral Modes

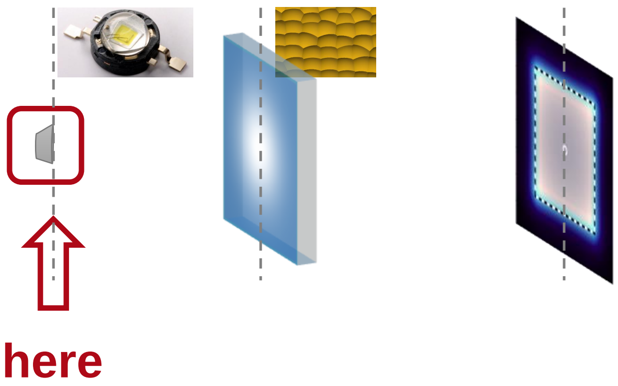

shifted- elementary-mode concept

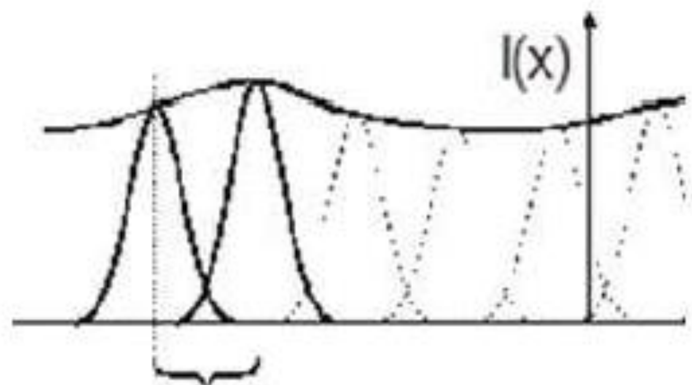

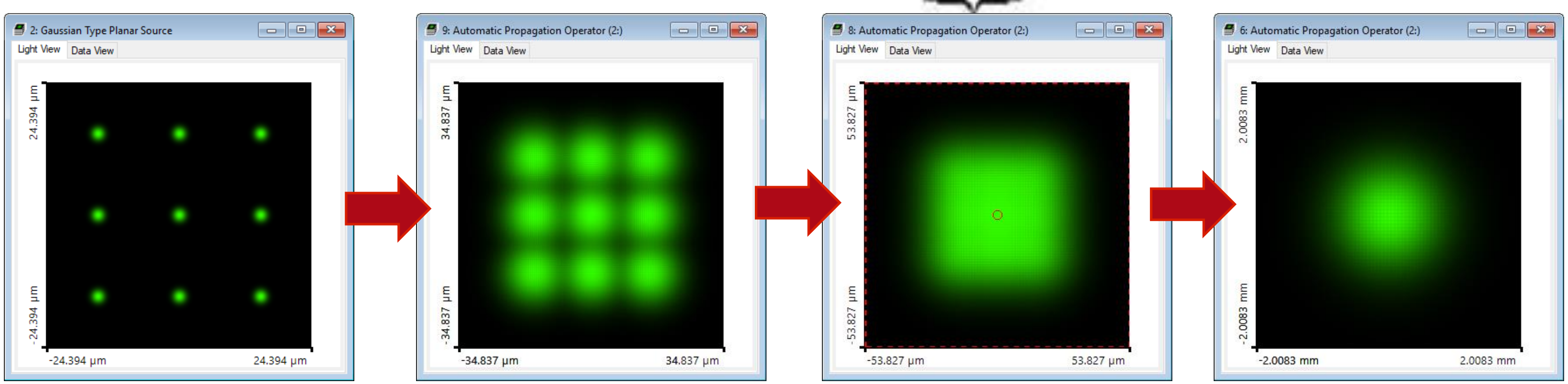

[3] Tervo, J., Turunen, J., Vahimaa, P. and Wyrowski, F. J. Opt. Soc. Am. A 27(9)(2014)

Gaussian Type Planar Source (Example)

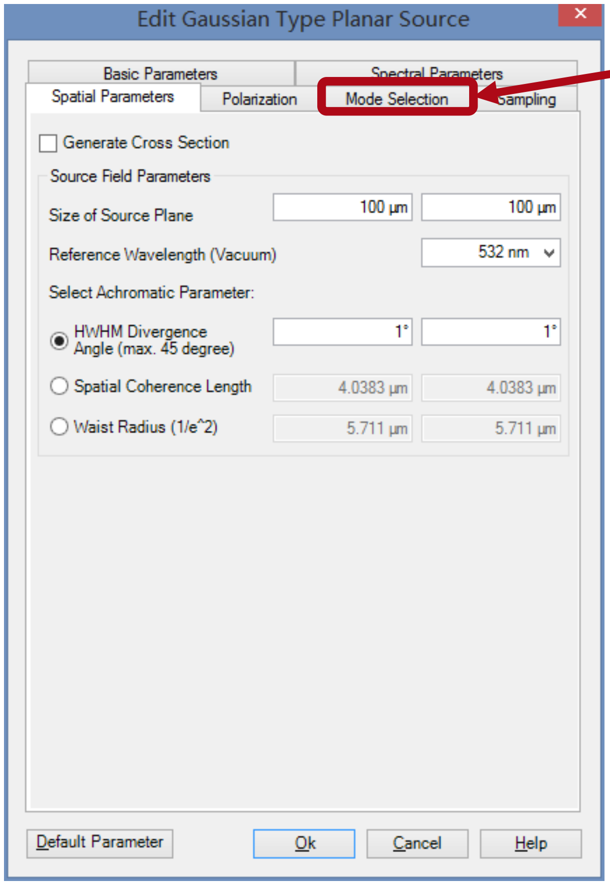

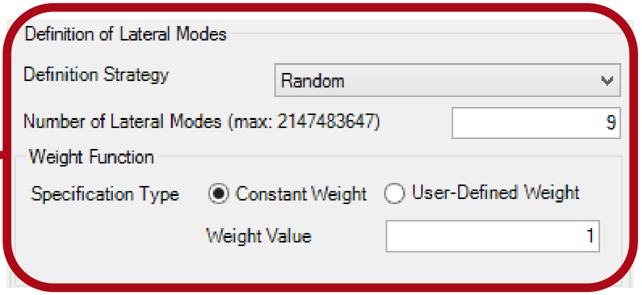

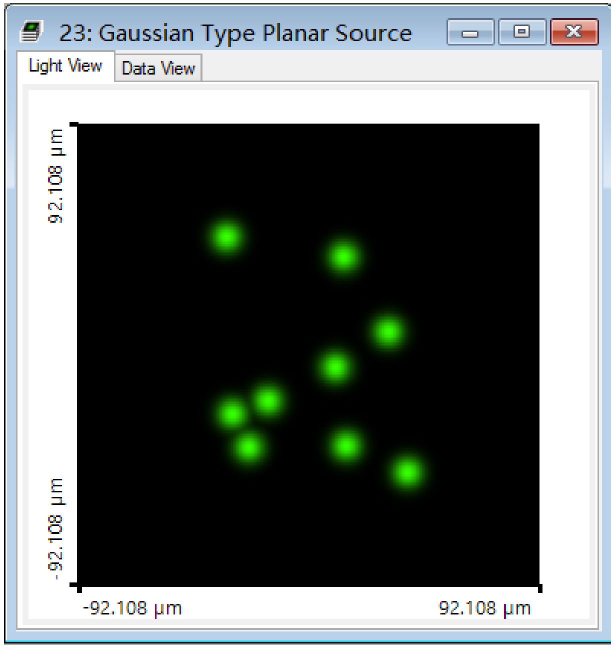

Modelling of Source

- Modelling of Source
  - Transfer the 1D data(a) into 2D field data (b)
  - Calculate the source modes by using Parametric Optimization.
    - The source contains two Gaussian Laguerre modes (d).
    - The intensity distribution is (c)

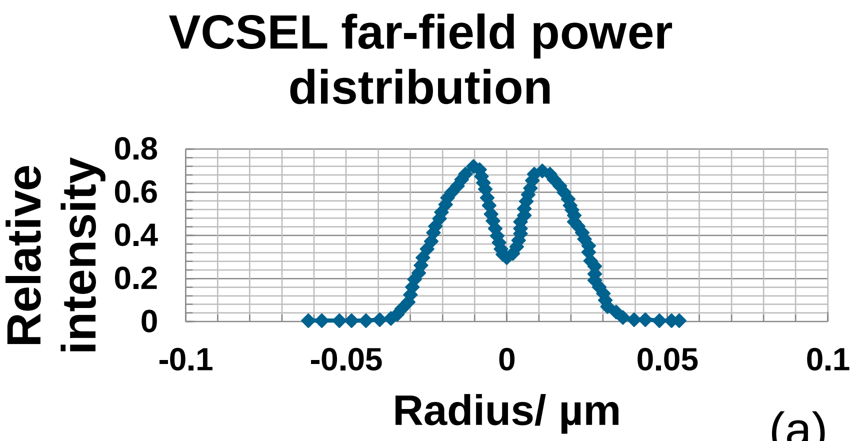

(a)

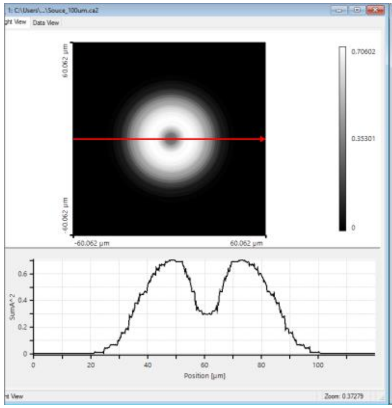

(b)

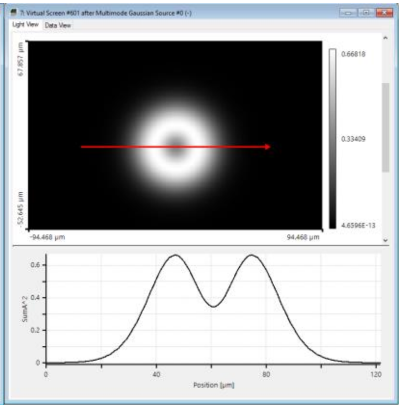

(c)

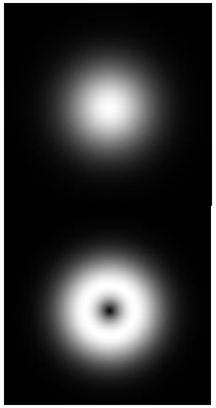

(d)

Pulse in Frequency Domain

- In frequency (wavelength) domain
  - Gaussian pulse

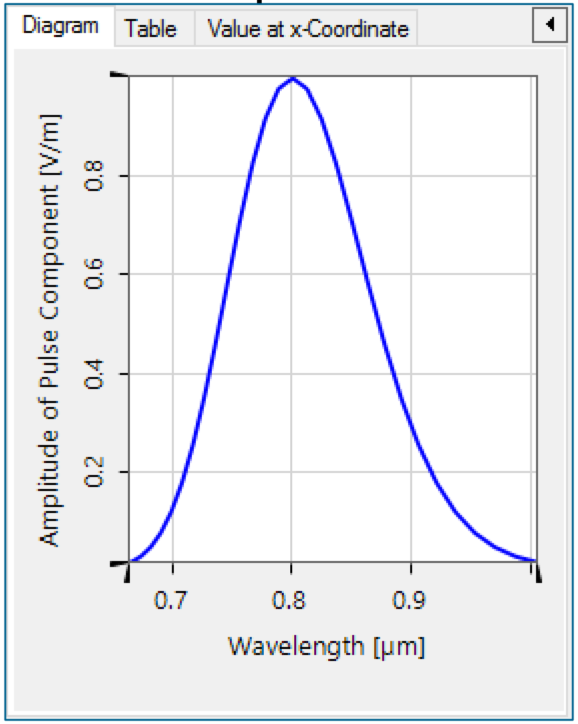

- In time domain (envelop)
  - Fourier transform

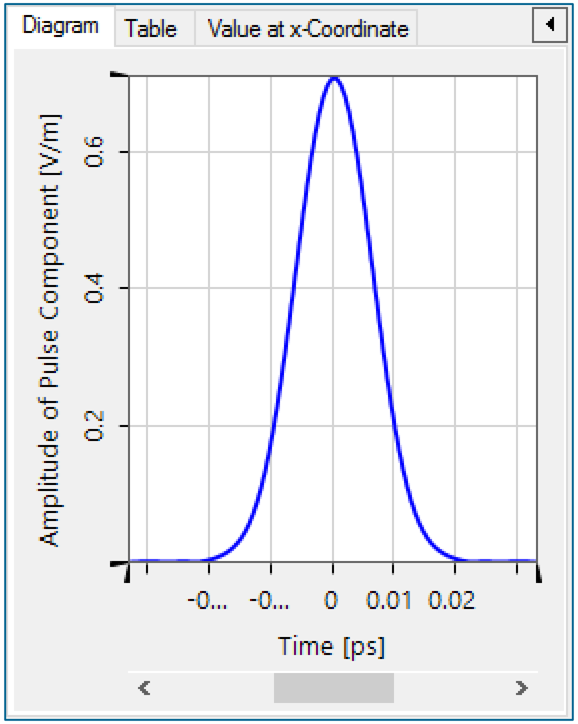

Pulse in Frequency Domain

- In frequency (wavelength) domain
  - Gaussian pulse

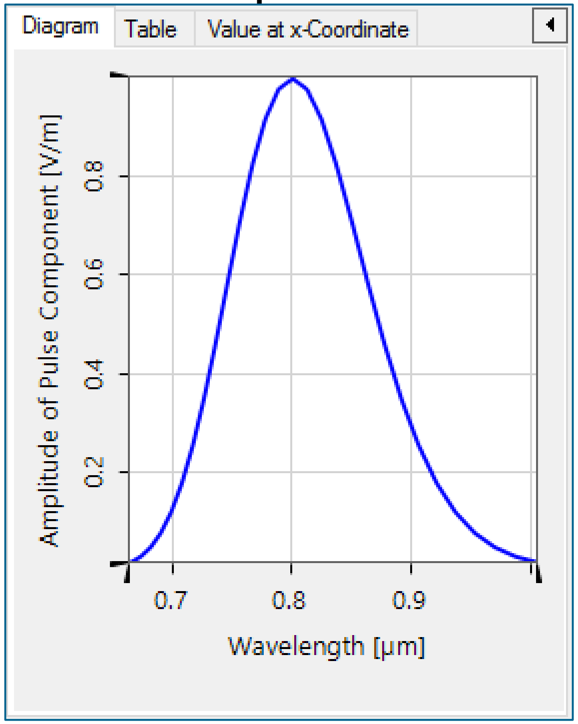

- In time domain
  - Fourier transform

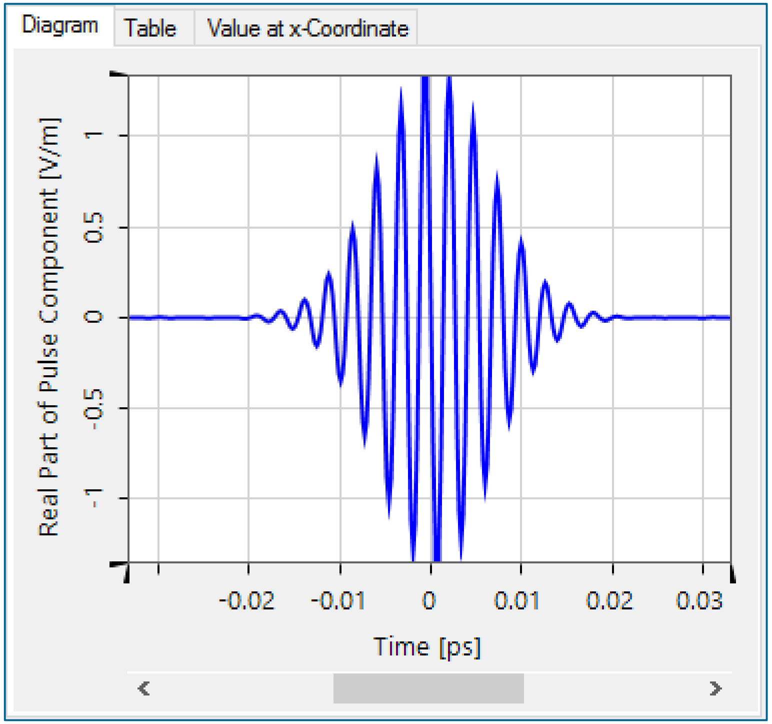

Detectors

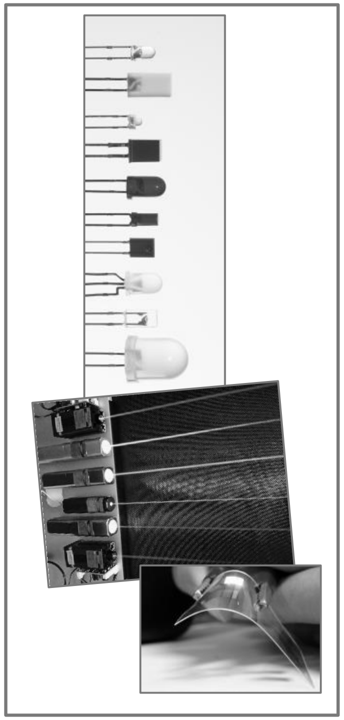

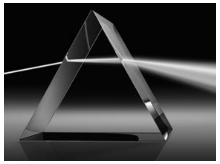

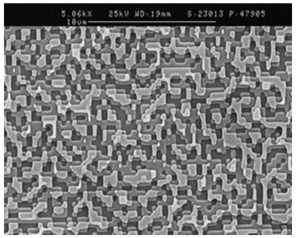

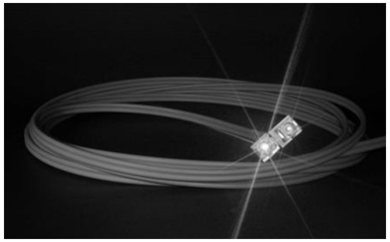

Detector of ray quantities

- Ray tracing system analyzer
- Spot diagram
- Spot size

3D Ray Tracing Analyzer: VLF

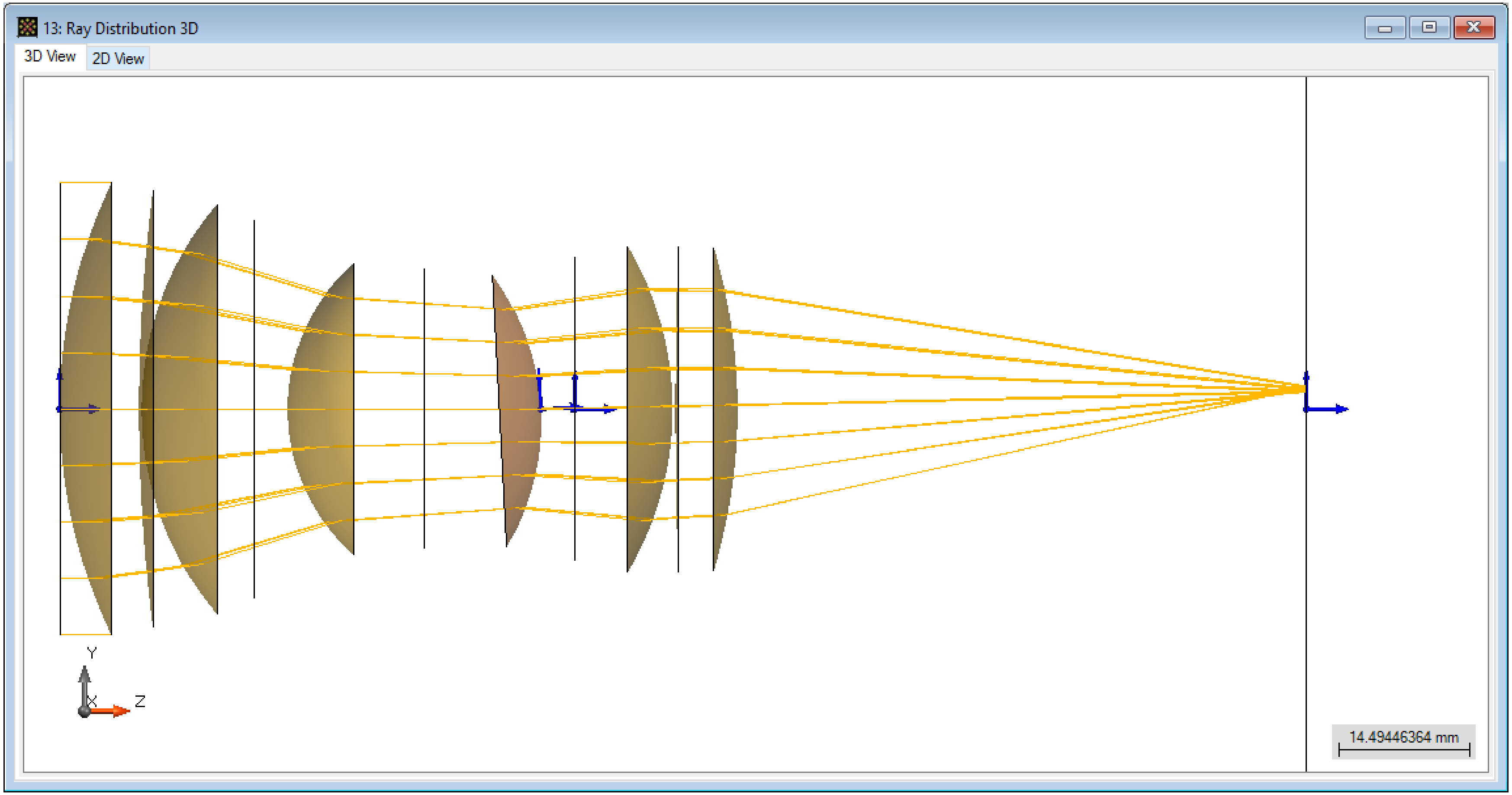

Dot Diagram Comparison: Target Plane

- **VLF** spot size (Beam diameter RMS): 581.25 µm (Centroid as reference)
- **Code V** spot size (RMS): 580.62 µm
- **VLF** spot size (Beam diameter RMS): 880.42 µm (Chief ray as reference)
- **Zemax** spot size (RMS): 880.114 µm

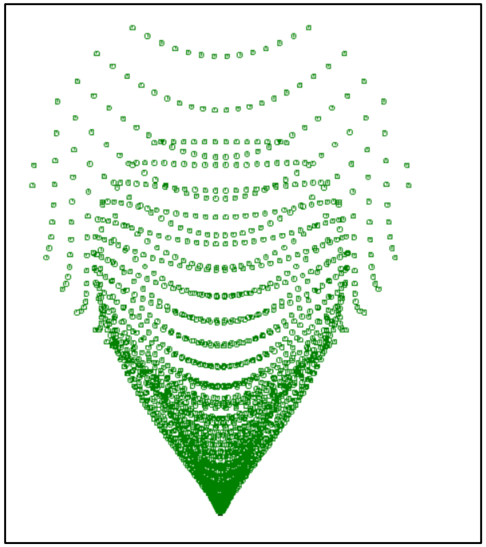

Code V

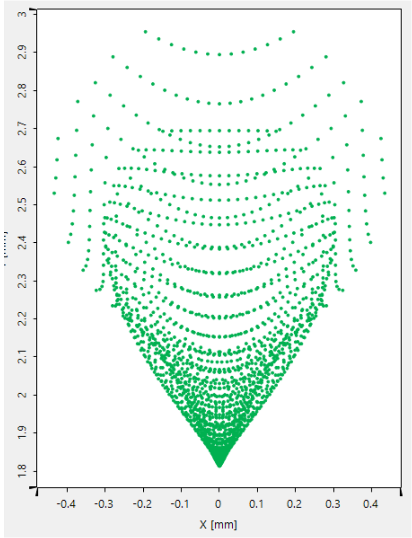

VLF

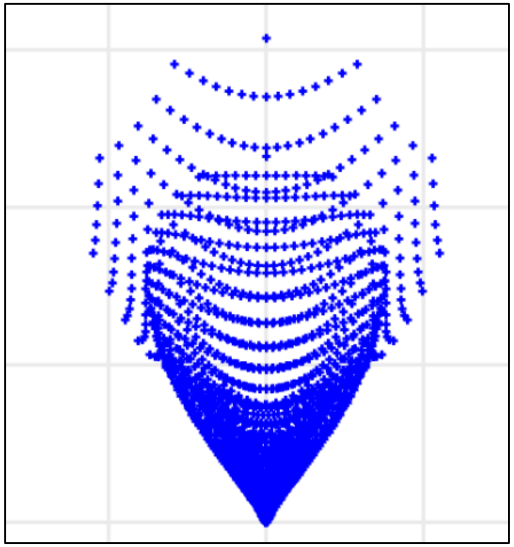

Zemax

Detector of ray quantities

- Ray tracing system analyzer
- Spot diagram
- Spot size
- Wavefront error

System Illustrations

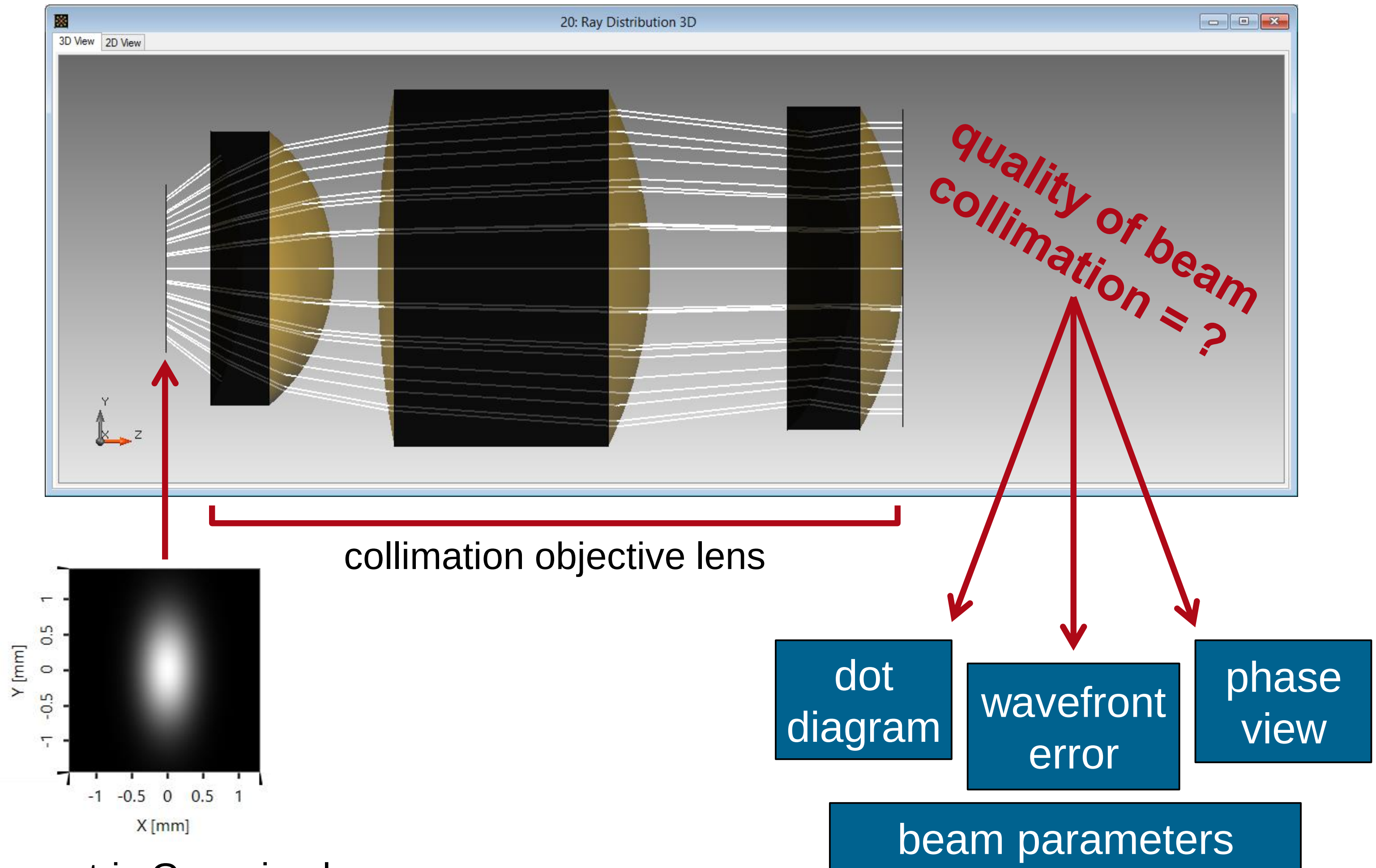

asymmetric Gaussian beam of IR laser diode ($M^2 = 1$)

Modeling & Design Results

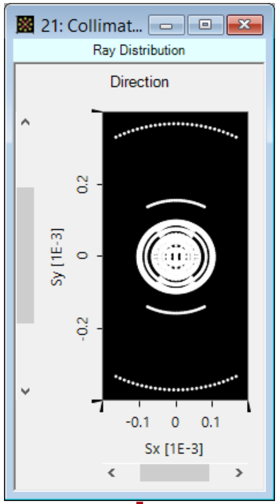

Ray Directions

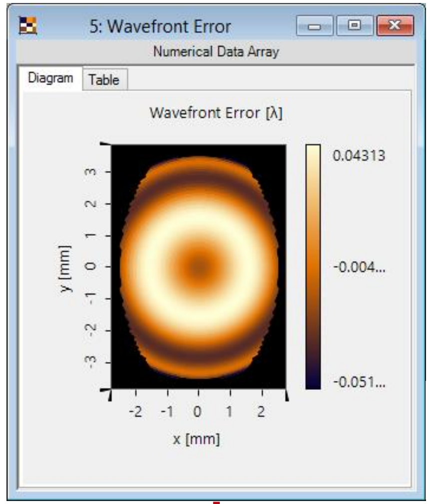

Wavefront Error

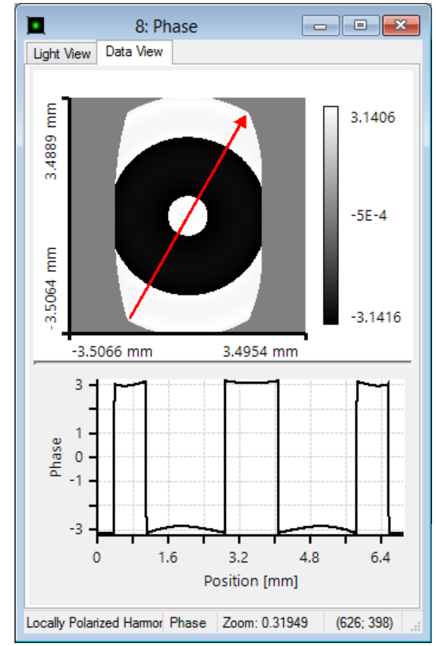

Phase Analysis

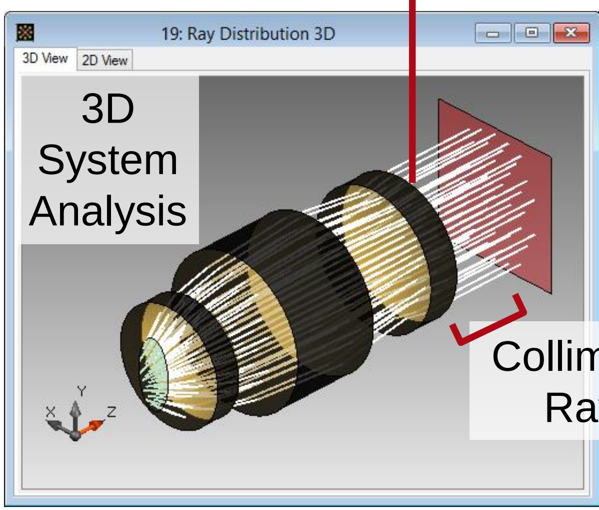

Numerical Detector Results

Quantity	Value & Unit
wavefront error (RMS)	0.03λ
divergence Angle X x Y	0.02° x 0.01°
M^2 parameter in X x Y direction	1.0180 x 1.1802

Field Detectors

- Electromagnetic field: amplitude / phase/ real and imaginary part

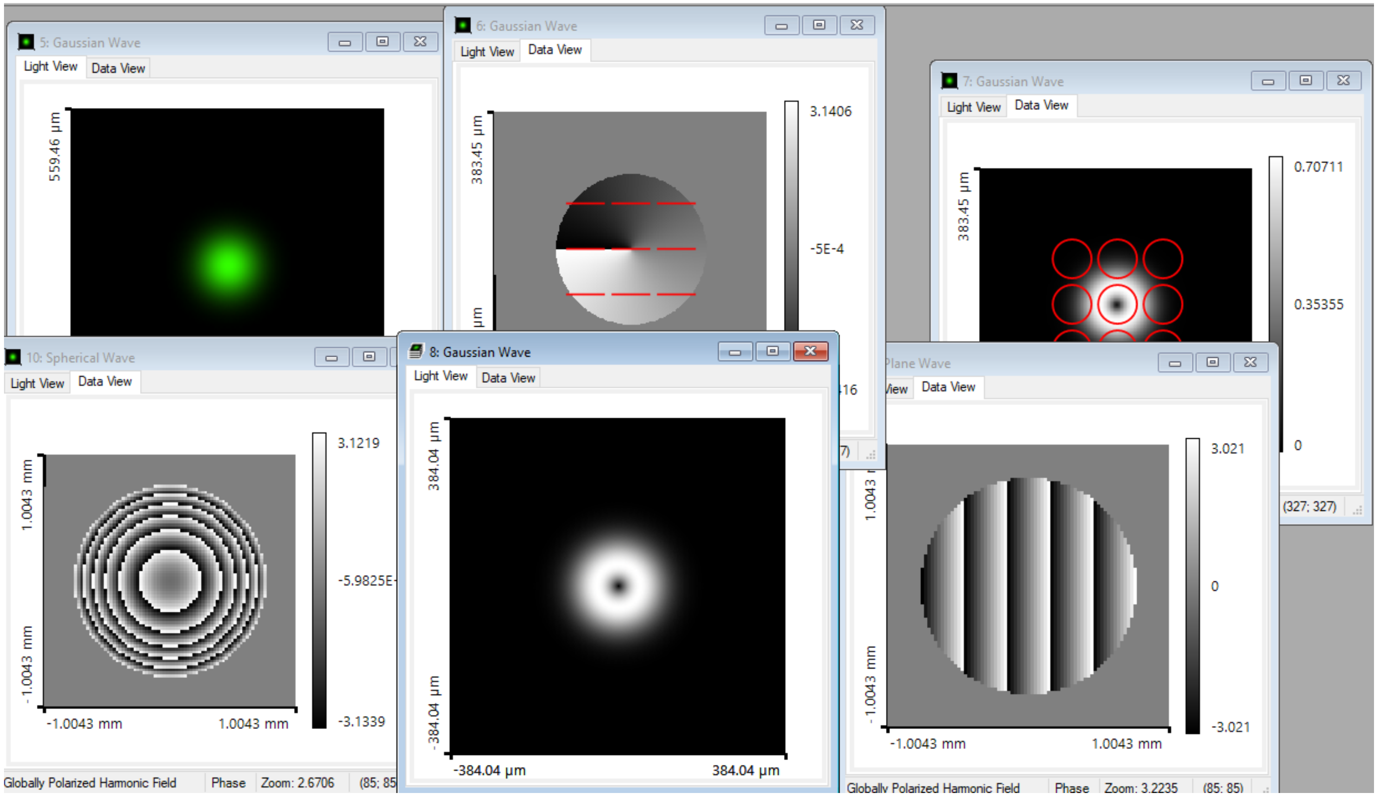

Field Detectors

- Radiometry

Theoretical Background:

- Irradiance: $E_e(\boldsymbol{\rho}) = S_z(\boldsymbol{\rho}) \quad \left[\frac{W}{m^2}\right]$
- Flux: $\Phi_e = \int\int E_e(\boldsymbol{\rho})\, dxdy \quad [W]$
- Intensity: $I(\boldsymbol{\rho}) = \|\langle \boldsymbol{S}(\boldsymbol{\rho})\rangle\| \quad \left[\frac{W}{m^2}\right]$
- Power: $P = \int\int I(\boldsymbol{\rho})\, dxdy \quad [W]$

Experiment 1: Total Reflection

- Set up

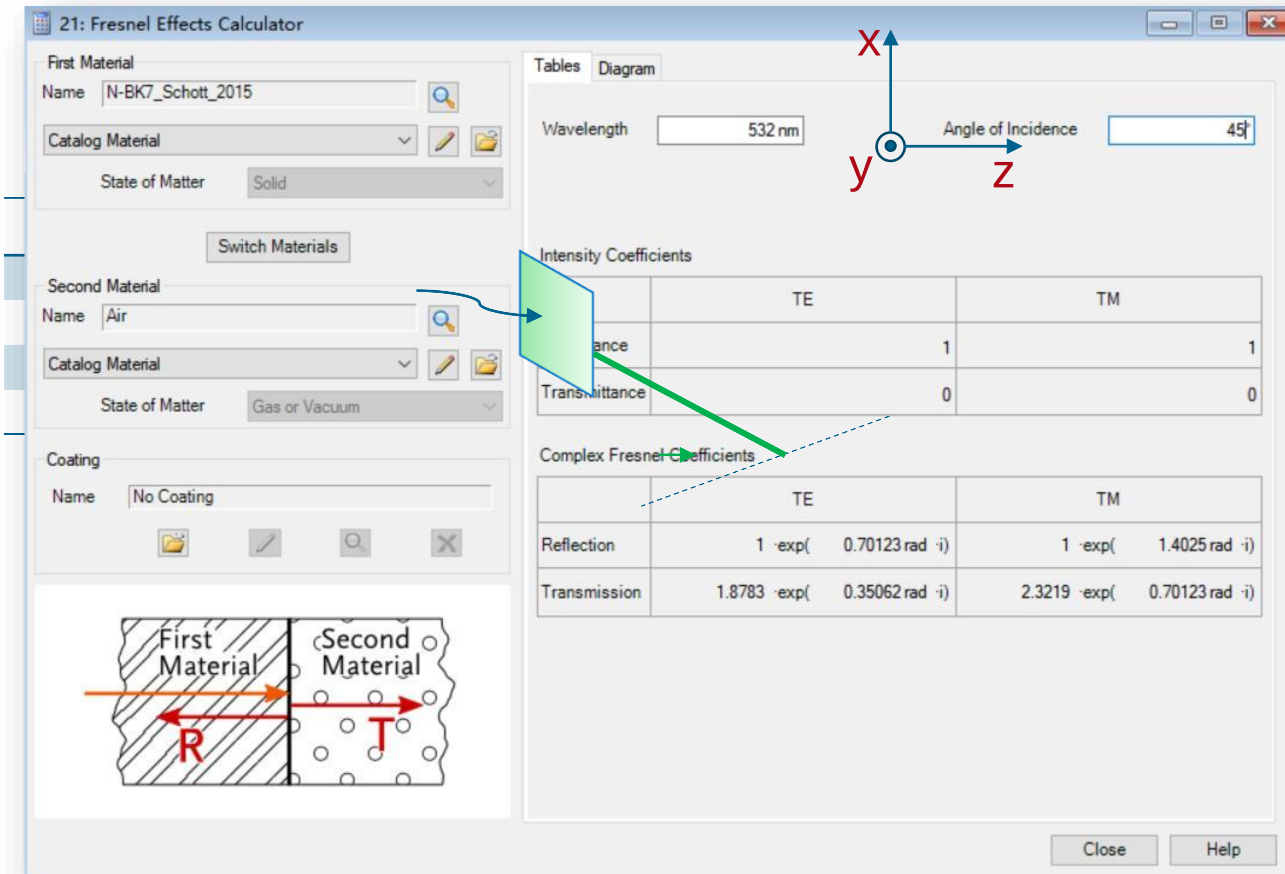

2: Air

z

ission Plane

Experiment 1: Total Reflection

- Results: Time averaged Poynting Vector

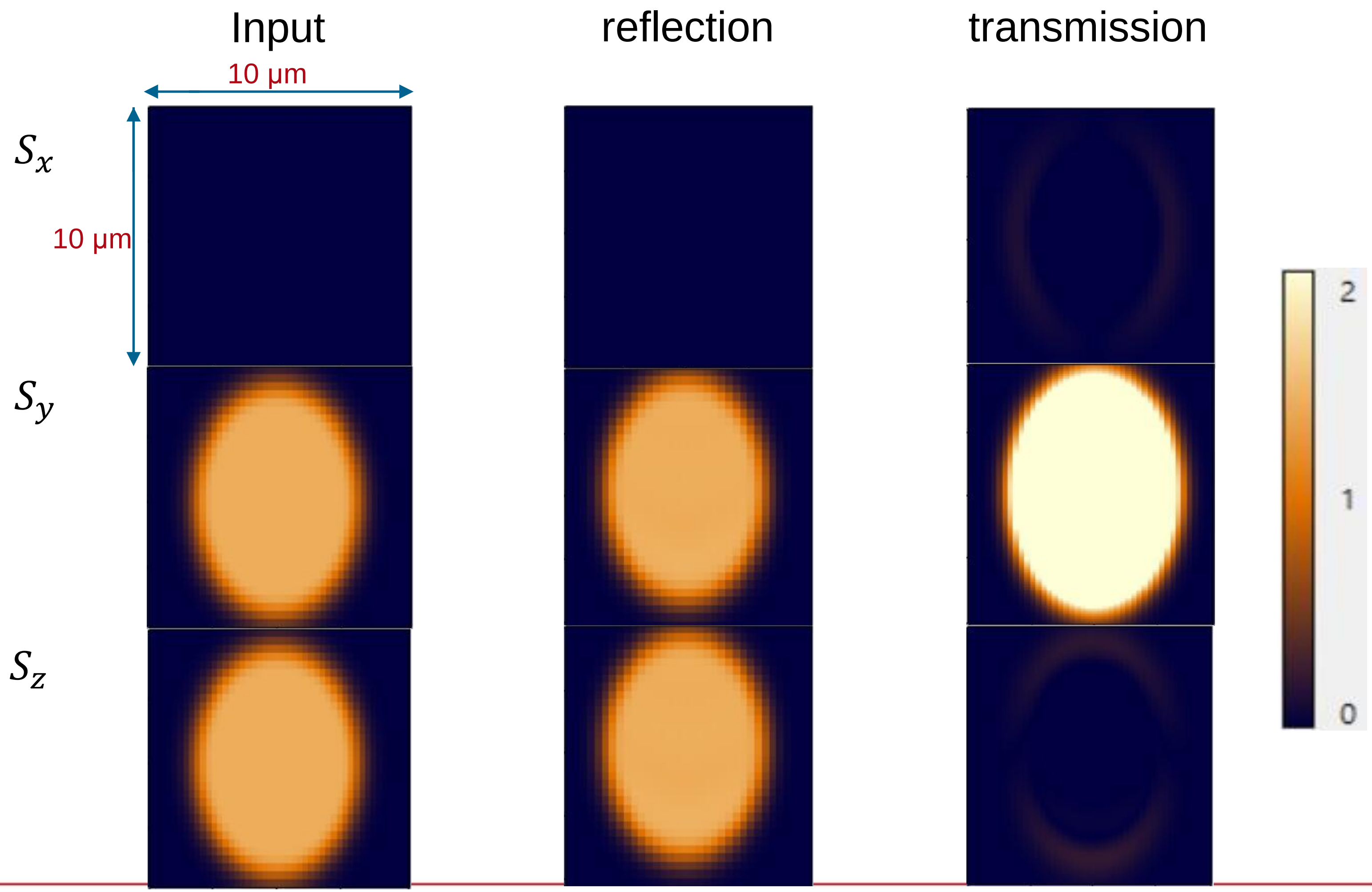

Experiment 1: Total Reflection

- Results: Irradiance

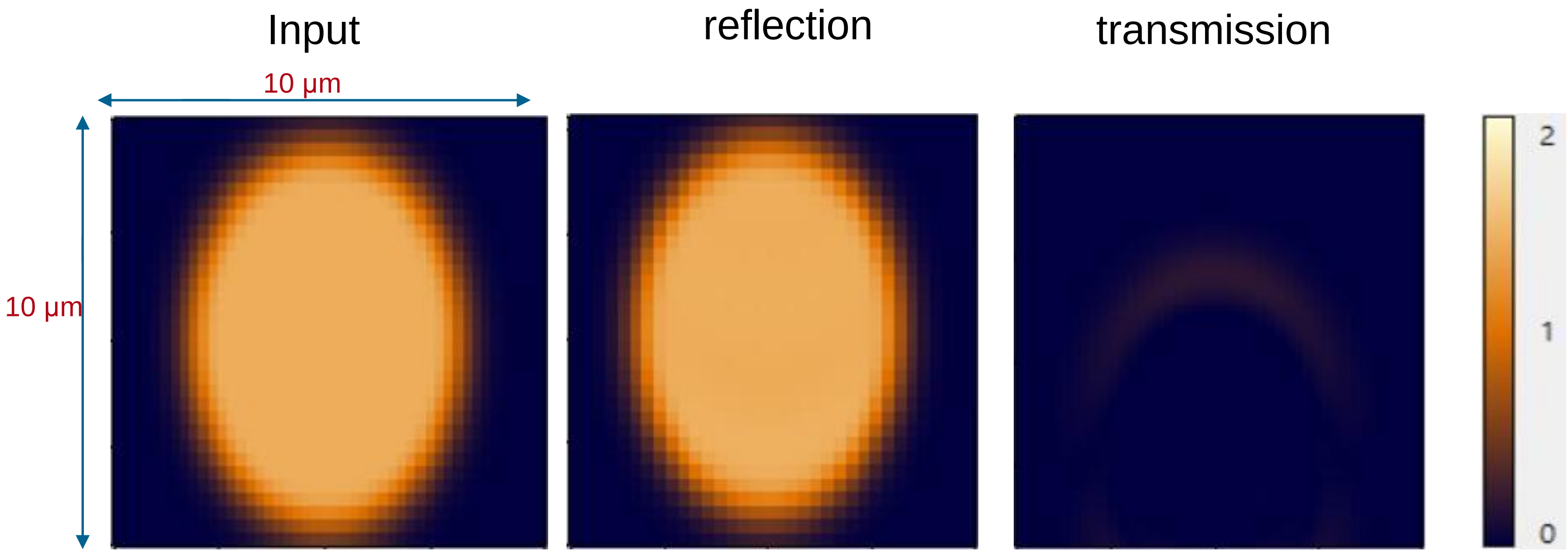

Experiment 1: Total Reflection

- Results: Flux
  - Flux

Physical Quantity	Channel	Value [W]
Flux	input	2.6760×10^{-13}
	reflection	2.6756×10^{-13}
	transmission	5.1292×10^{-17}

  - Reflectance

$$R = \frac{\Phi_{e,\mathrm{ref.}}}{\Phi_{e,\mathrm{in.}}} = 99.99\% \approx 1$$

Experiment 1: Total Reflection

- Results: Intensity

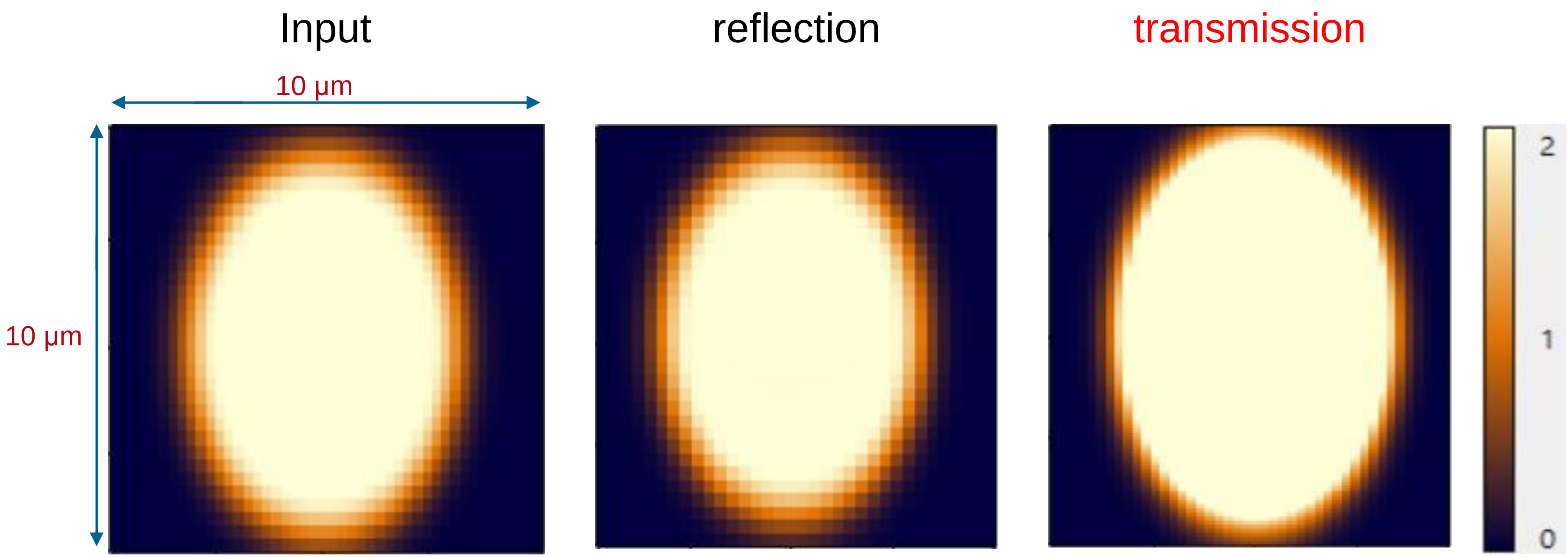

Experiment 1: Total Reflection

- Results: Power

Physical Quantity	Channel	Value [W]
Power	input	3.7871×10^{-13}
	reflection	3.7845×10^{-13}
	transmission	9.4479×10^{-13}

Experiment 2: Goos–Hänchen Shift

- Set up: Similar with experiment 1
- Only difference: Light Sourse:

Light Source: Plane Wave	
Wavelength	532nm
Polarization	E_x - polarized
Waist Radium	3 µm × 3 µm
Relative Edge Width	10%

Experiment 2: Goos–Hänchen Shift

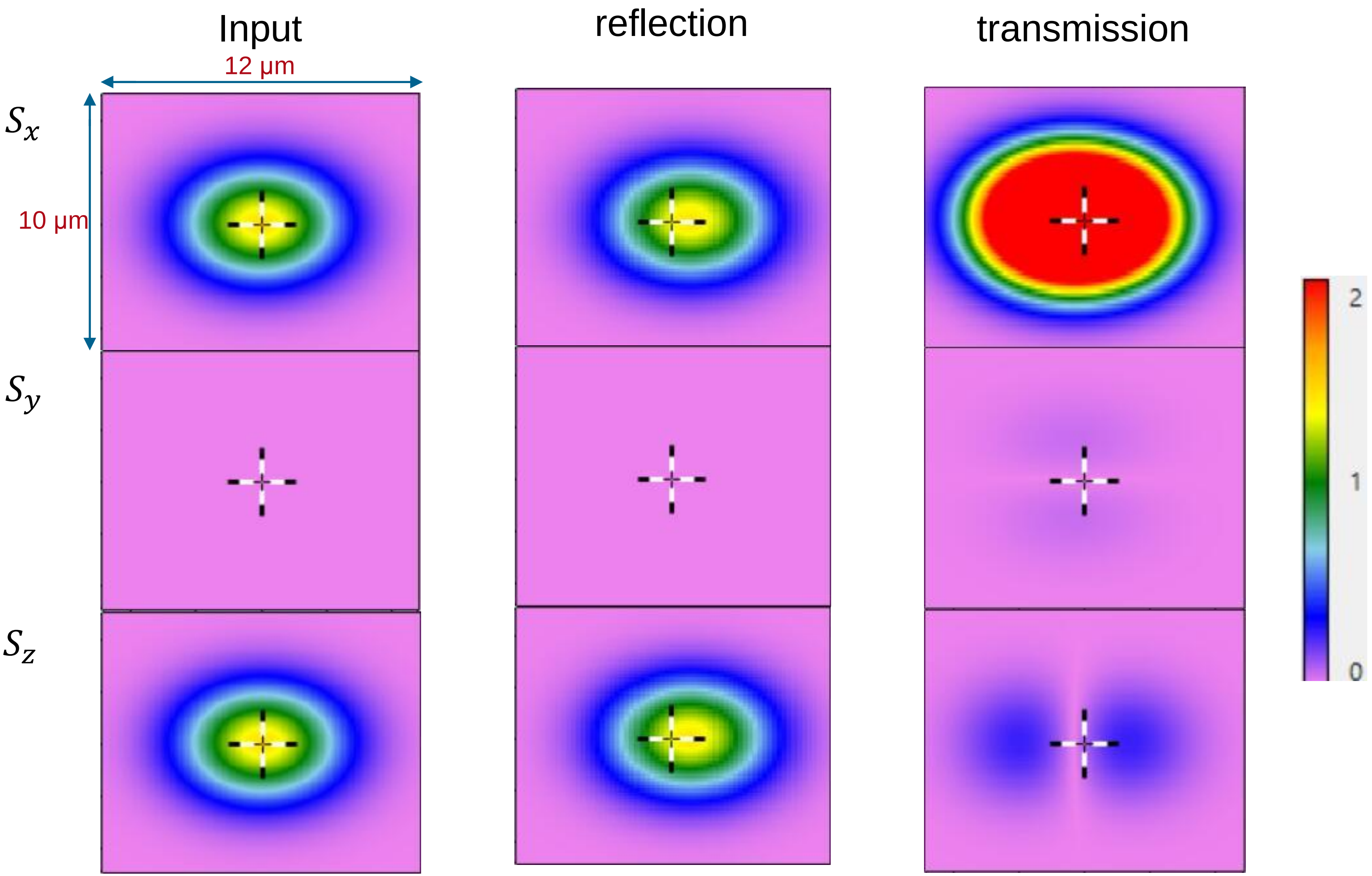

Field Detectors

- Radiometry
- Stocks parameters / polarization

Laser Systems > Crystal Modeling

Stokes Parameters Measurement behind Tilted Polarizer [Nutshell]

System Illustration

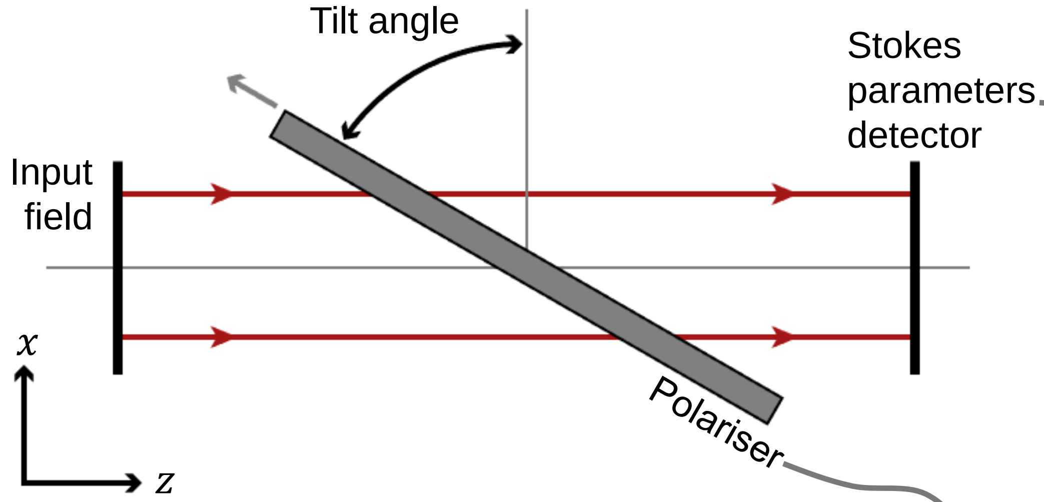

Stokes parameter calculation based on electromagnetic field information

Fully vectorial modeling of polarisers for non-paraxial situation

[S. Zhang, *et al.*, “A non-paraxial idealized polarizer model,” prepared for submission]

Simulation Results

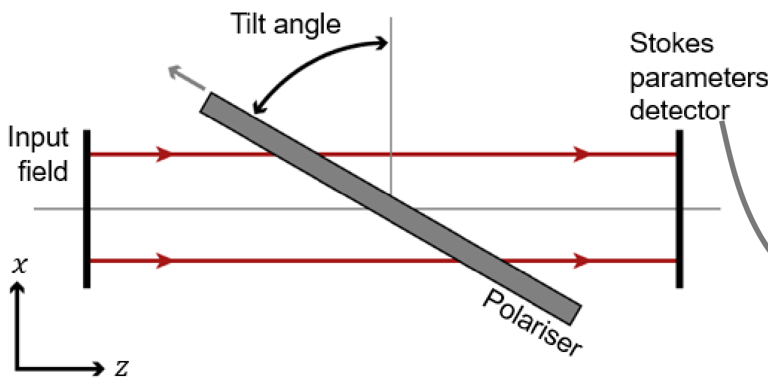

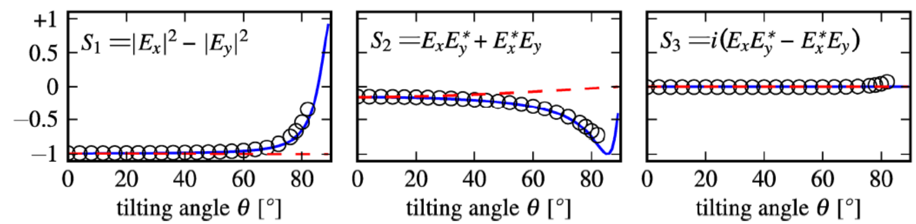

Measured and theoretical values from [J. Korger, et al., "The polarization properties of a tilted polarizer," Opt. Express 21, 27032-27042 (2013)]

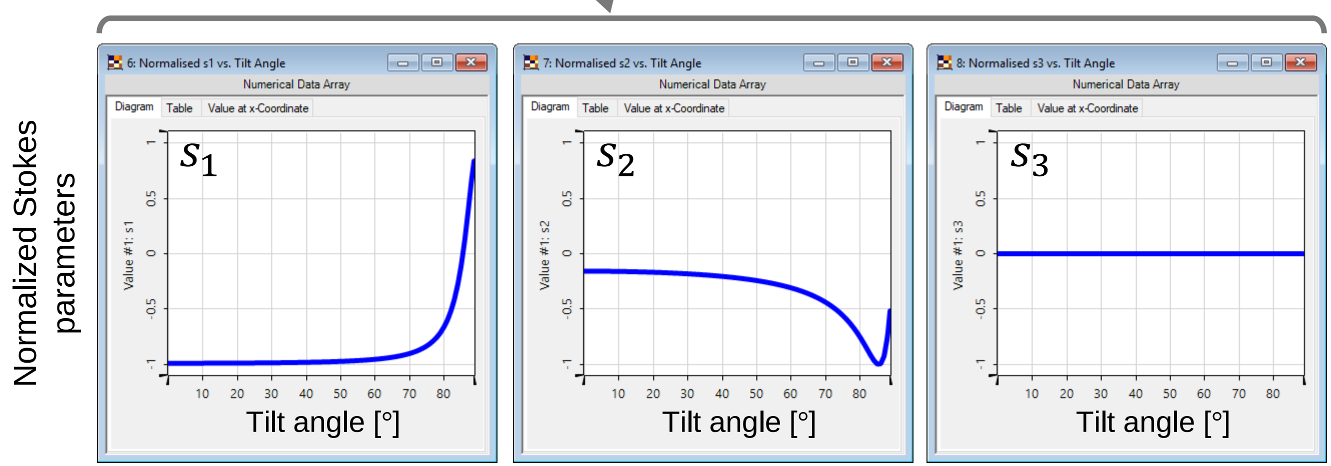

Field Detectors

- Radiometry
- Stocks parameters
- Physical quantities of pulse

Spatiotemporal Evolution of Femtosecond Pulse Focus

Overview

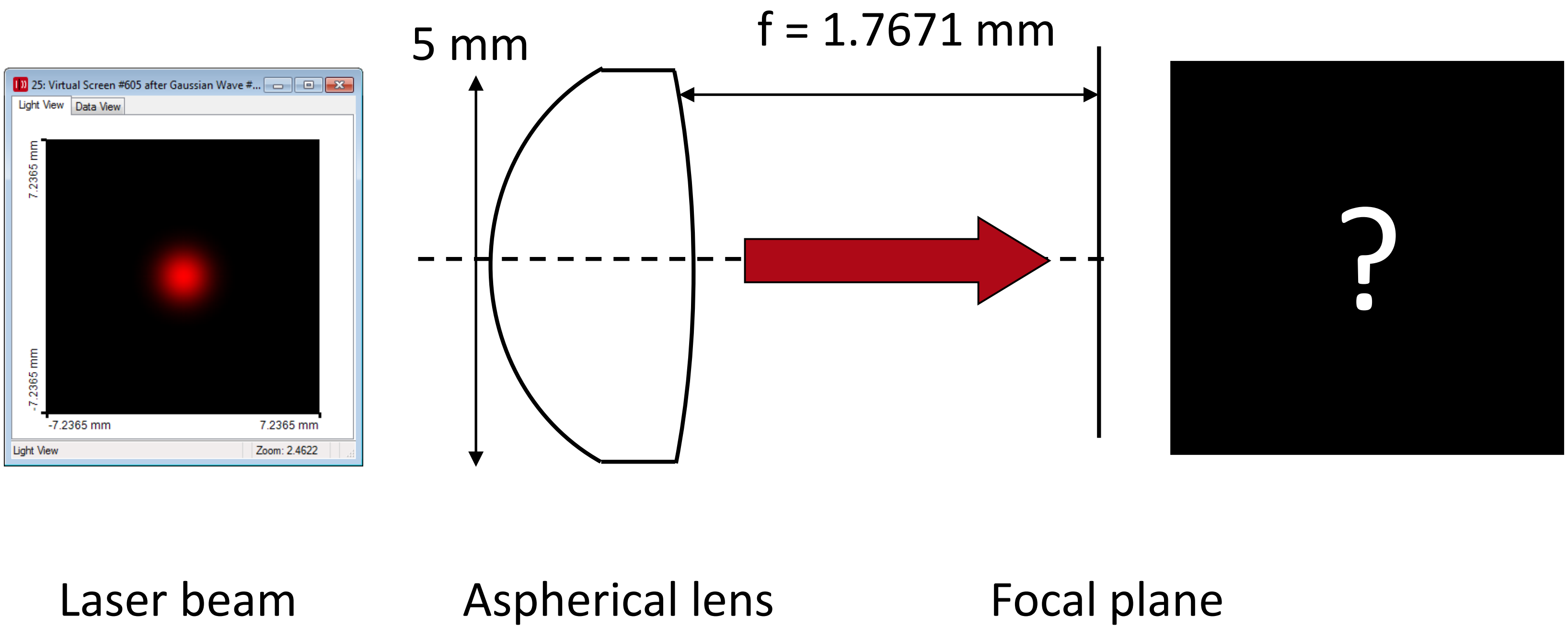

NA=0.68

Input Beam Pulse

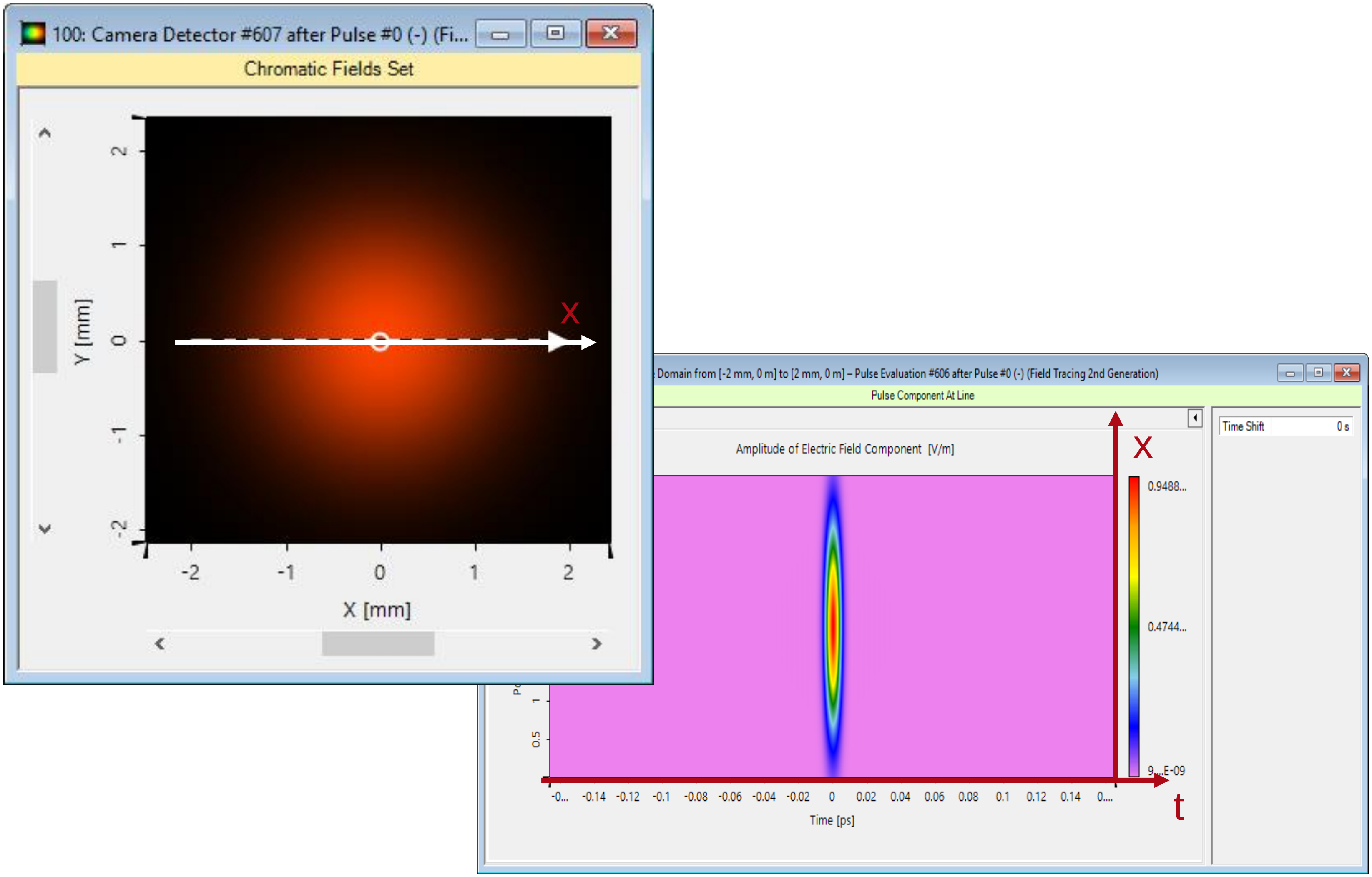

Simulation: Ex, Ey and Ez

- Enable the detectors Ex, Ey and Ez

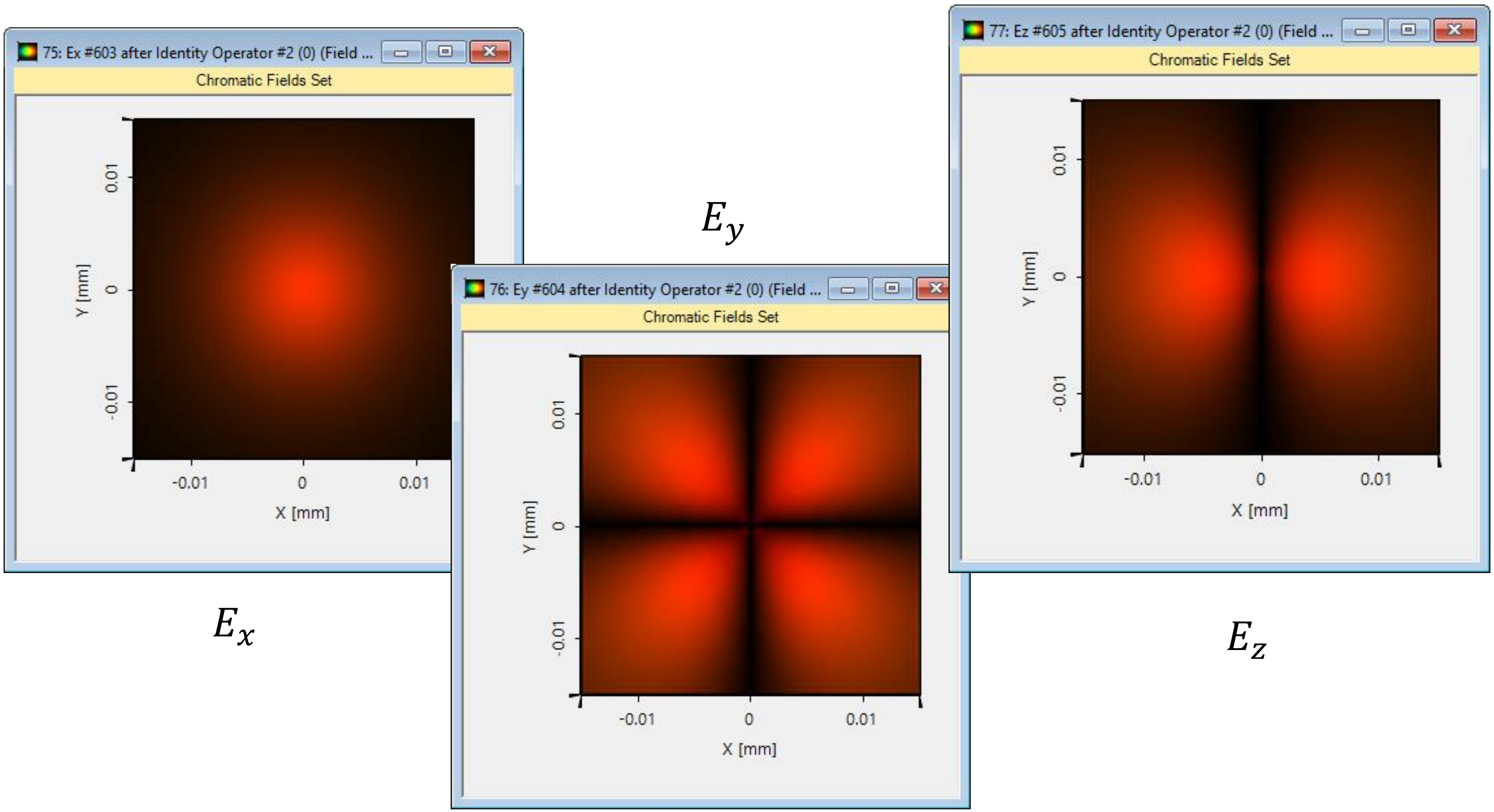

Simulation: Pulse at Point (0,0)

- Enable Detector Pulse Evaluation

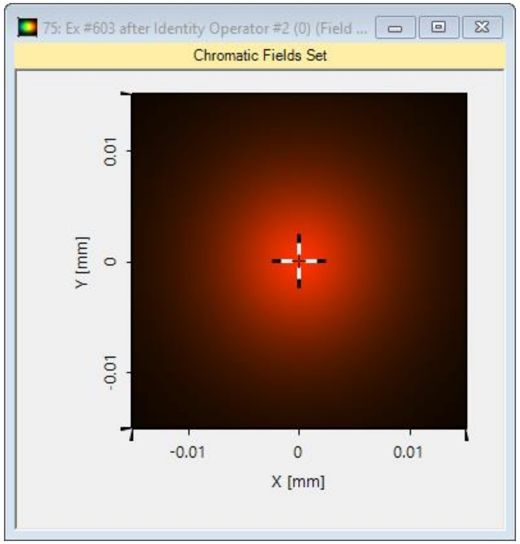

E_x

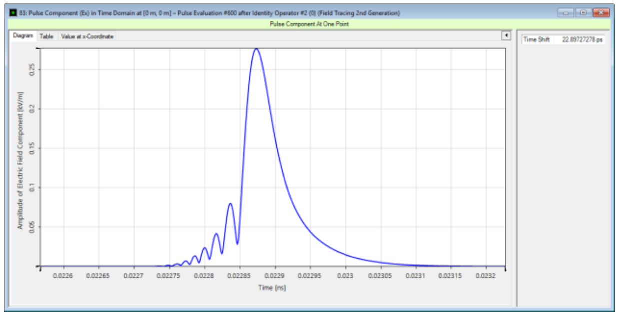

Envelope

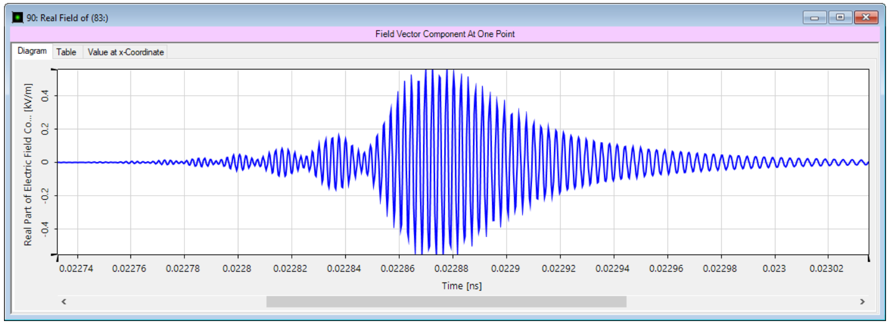

Field

Simulation: Pulse along x-Axis

Input

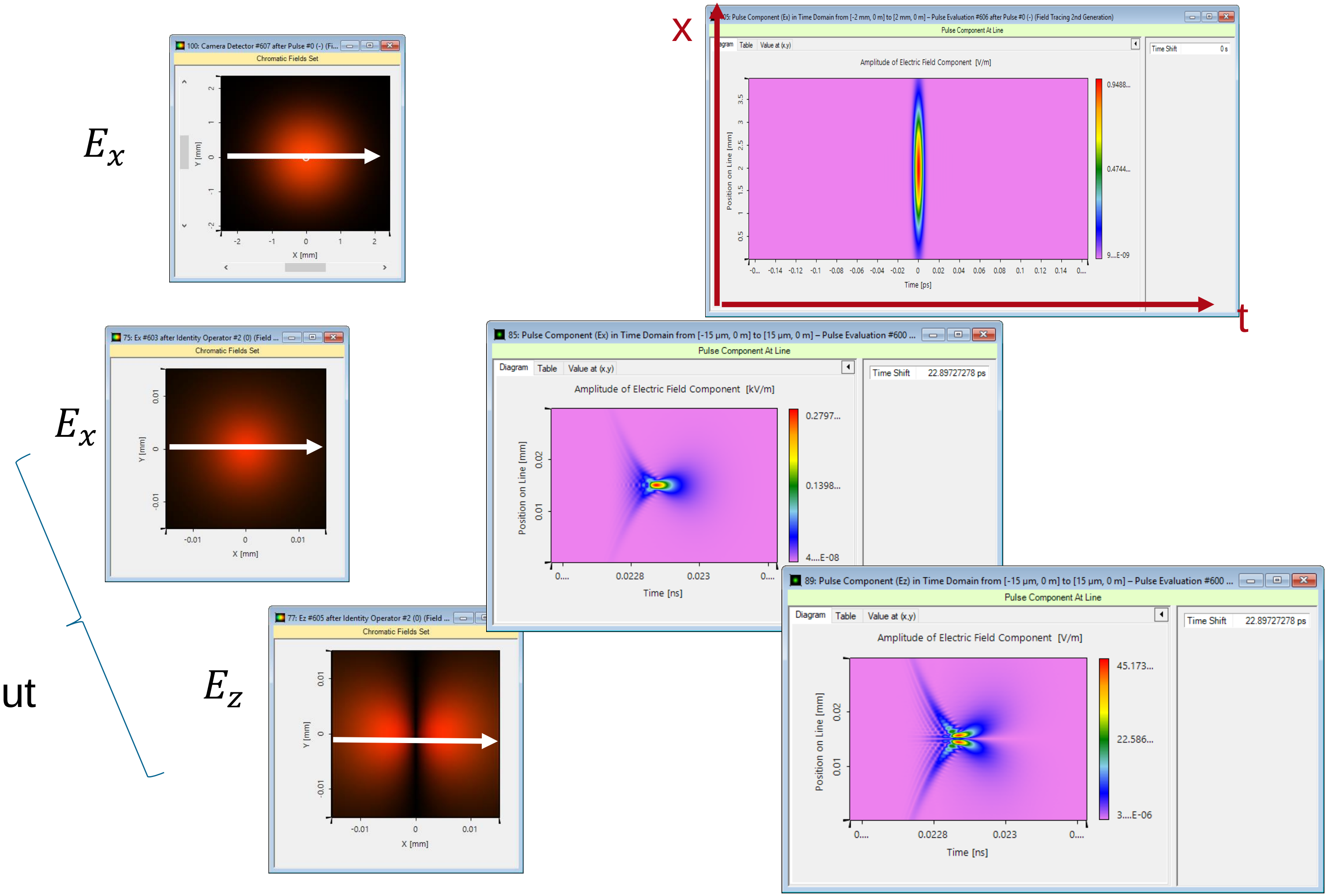

Output

Focused Topics

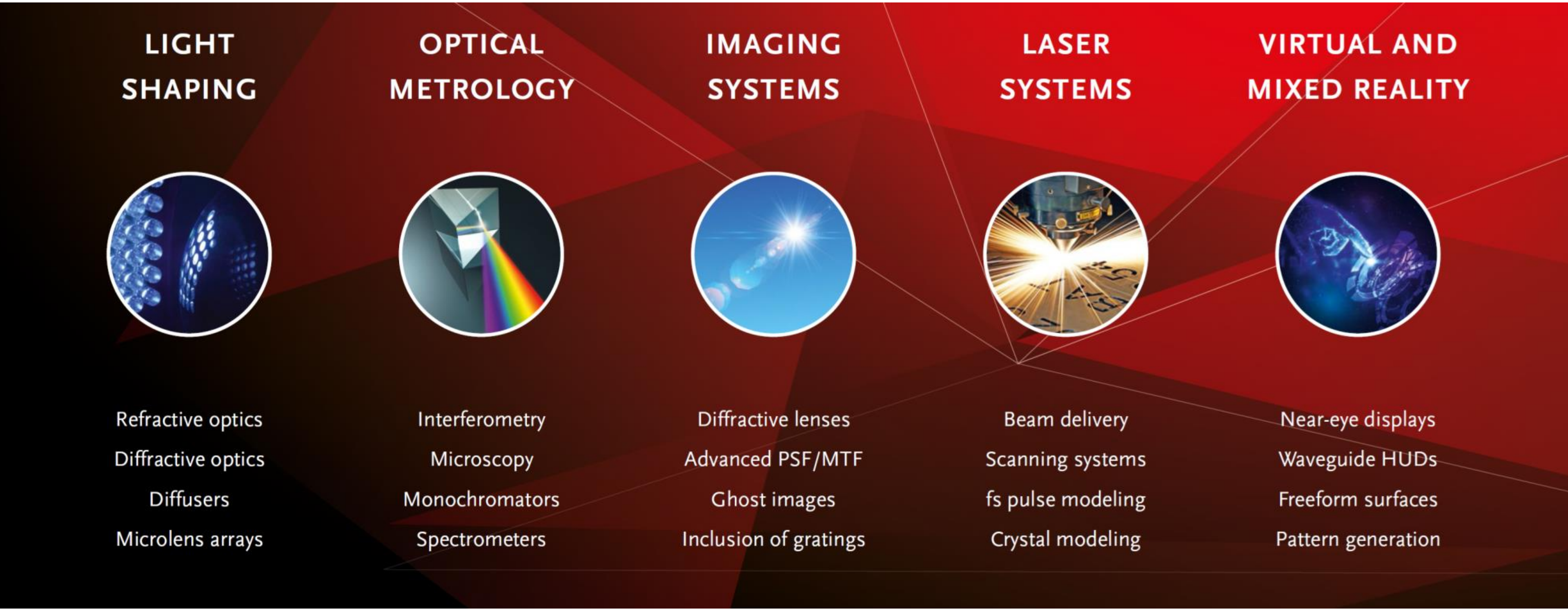

14:00-14:30

Imaging and laser systems

Specification: Collimating Lens

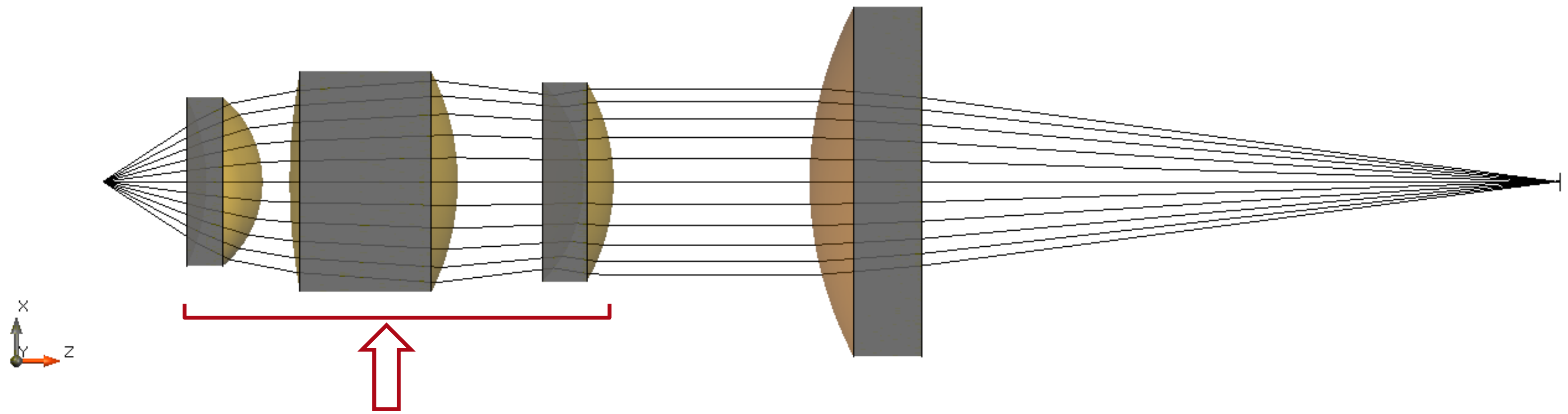

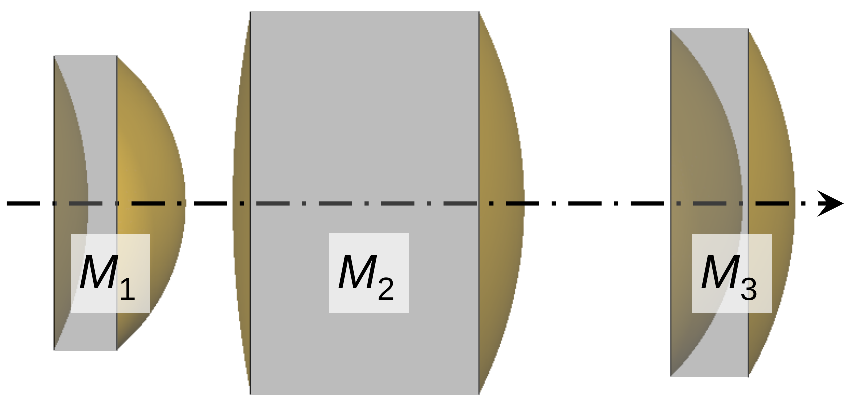

Parameter	Value & Unit
types of lens surfaces	3 lenses with 6 spherical surfaces
numerical aperture (NA)	0.63
materials	M_1: N-SF6* M_2,M_3: N-BK7*

** from catalog "Schott_2014"*

Specification: Focusing Asphere

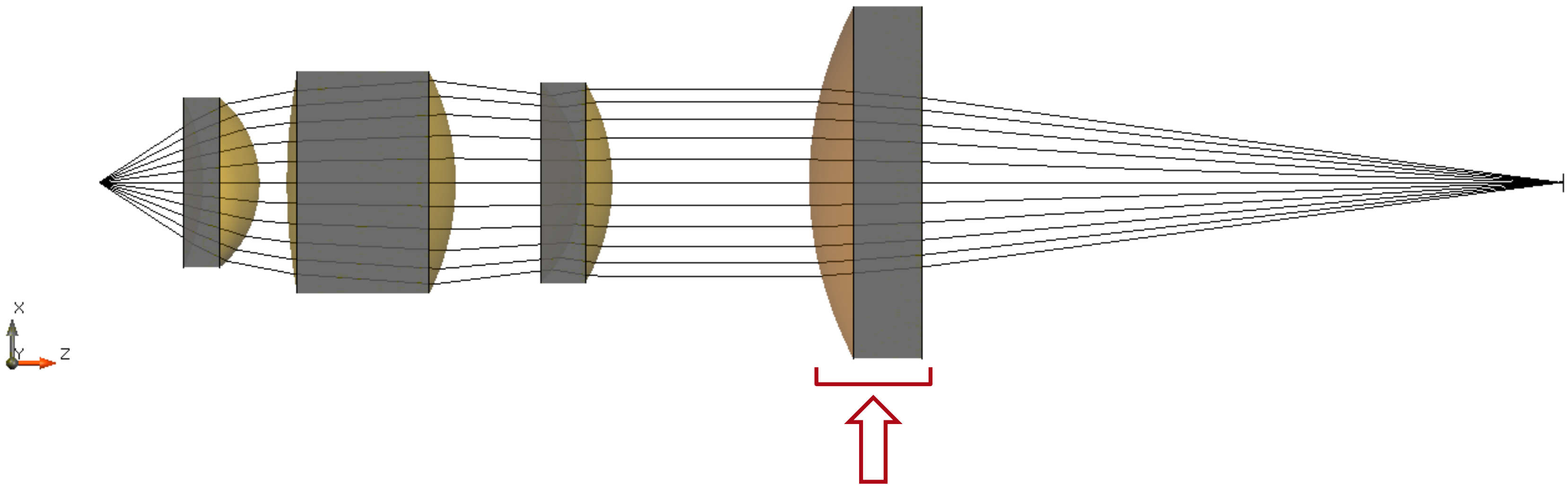

Parameter	Value & Unit
name/type	convex-plano aspherical lens from Asphericon: ALL12-25-S-U (A12-25LPX)
numerical aperture	0.23
material (M)	N-BK7

Specification: Detectors

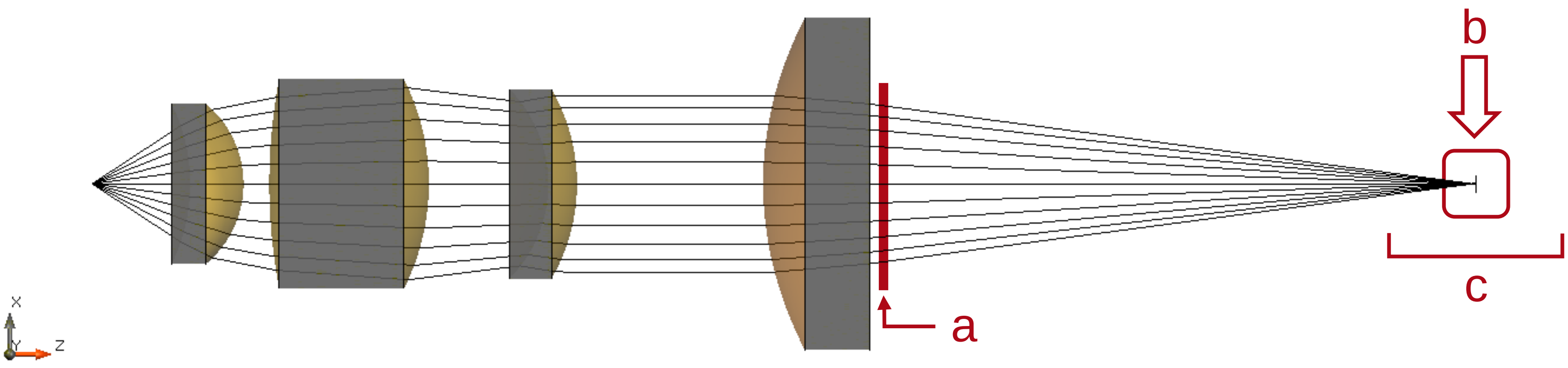

Position	Modeling Technique	Detector/Analyzer
full system	3D system ray tracing	general overview of light behavior in system
a	ray tracing	residual phase aberrations
b	ray tracing	dot diagram & focal beam size (x × y)
b	field tracing	intensity distribution
b	field tracing	focal beam size, M^2 value (x × y)
c	field tracing	focal region analysis by multiple 1D cross sections in x- & y-direction

Results: 3D System Ray Tracing

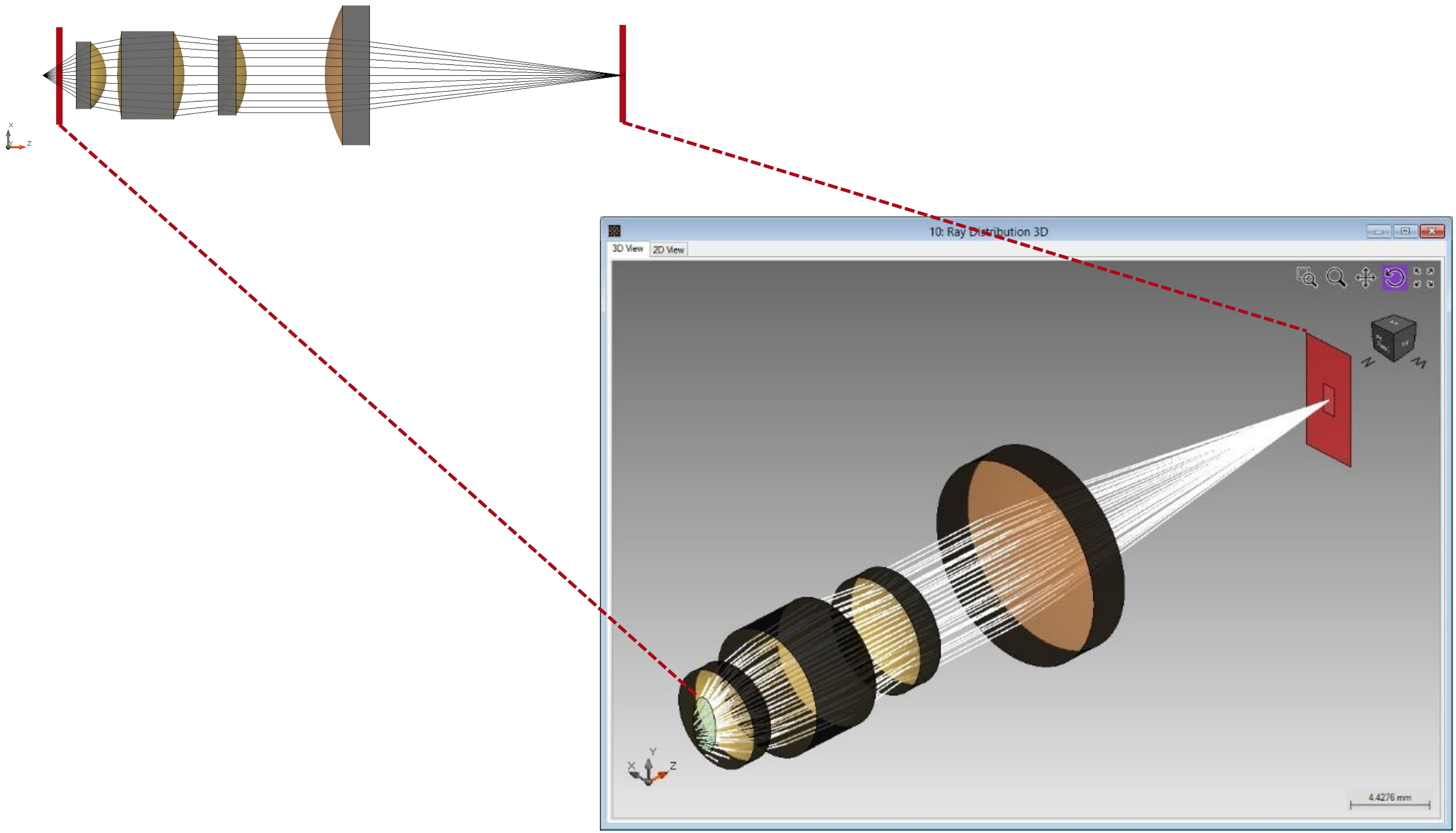

Results: Field behind Asphere

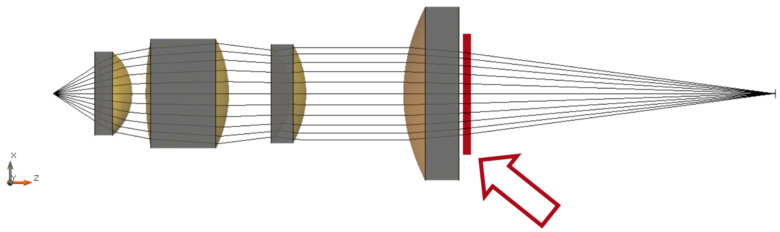

Highlights

- laser diode modeling inclusive astigmatism
- diffraction at lens apertures
- advanced focal region analysis

intensity

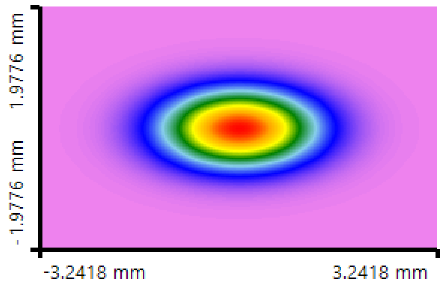

residual phase

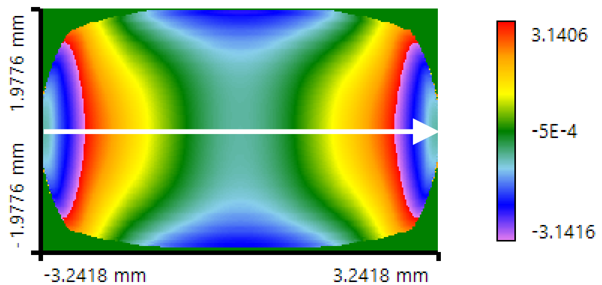

Simulation Time ~2s

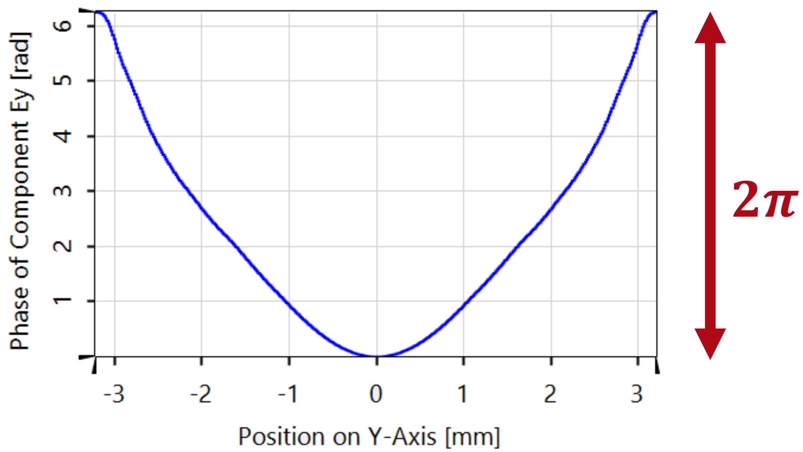

1D cross section of remaining phase

Results: Comparison with/without Astigmatisms

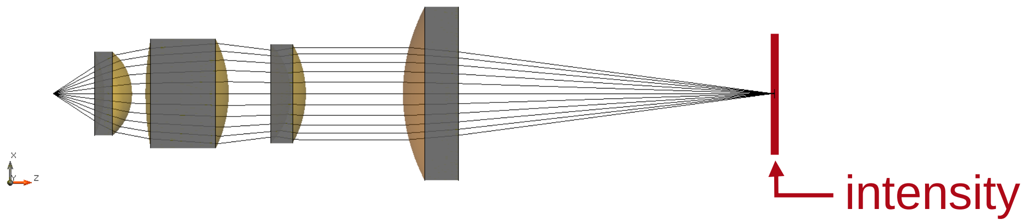

Highlights

- laser diode modeling inclusive astigmatism
- diffraction at lens apertures
- advanced focal region analysis

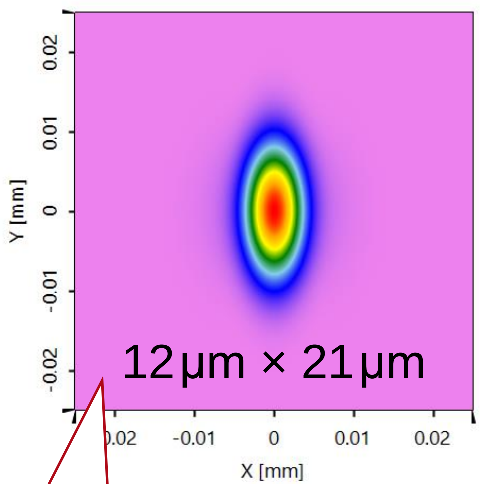

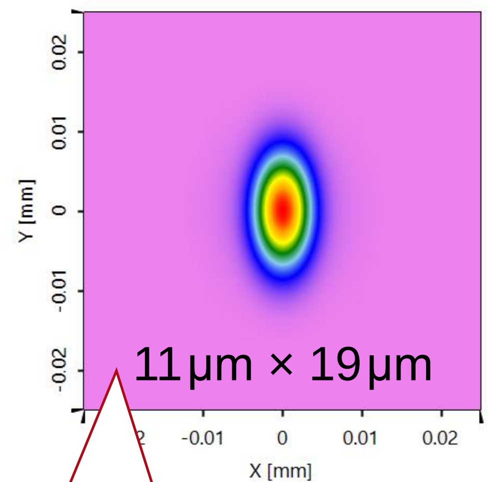

with astigmatism (11.6 µm)

without astigmatism

Results: Focus Spot (PSF) & Parameters

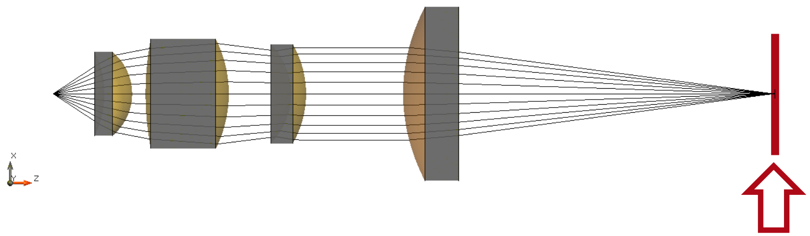

Highlights

- laser diode modeling inclusive astigmatism
- diffraction at lens apertures
- advanced focal region analysis

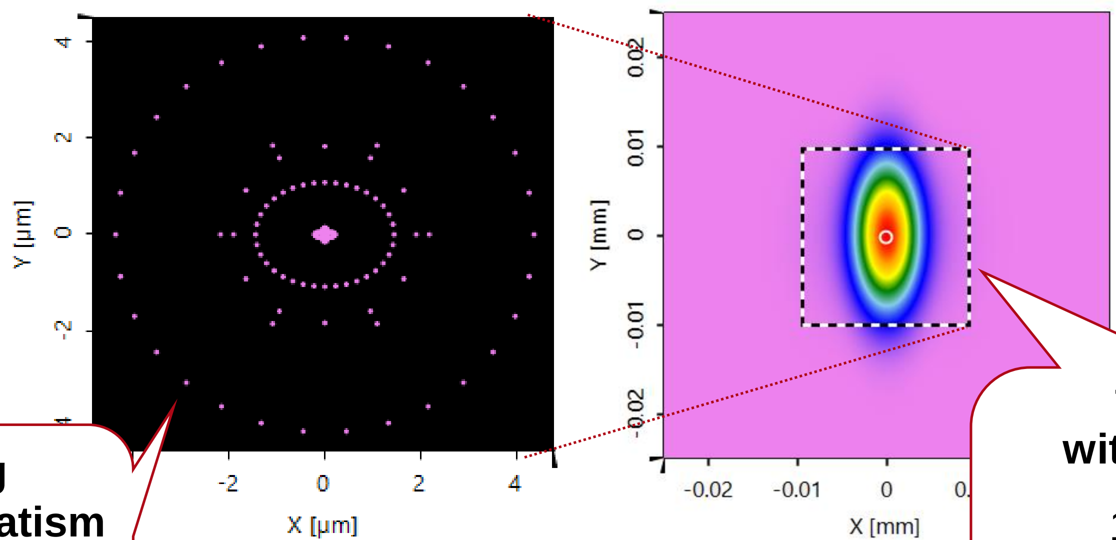

ray tracing without astigmatism

RMS diameter
(x × y) = 6 µm × 6 µm

dot diagram of ray positions

intensity

field tracing with astigmatism

$1/e^2$ diameter
(x × y) = 11 µm × 19 µm

beam quality
M2 = 1.07 × 1.01

Results: Field Analysis in Focal Region 1D

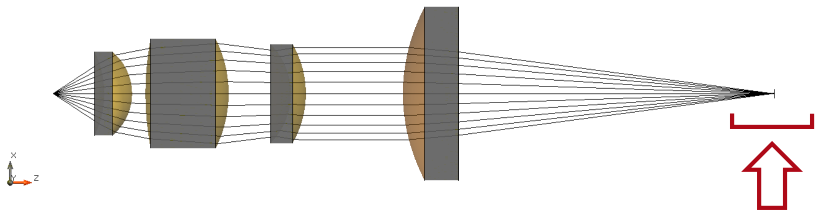

Highlights

- laser diode modeling inclusive astigmatism
- diffraction at lens apertures
- advanced focal region analysis

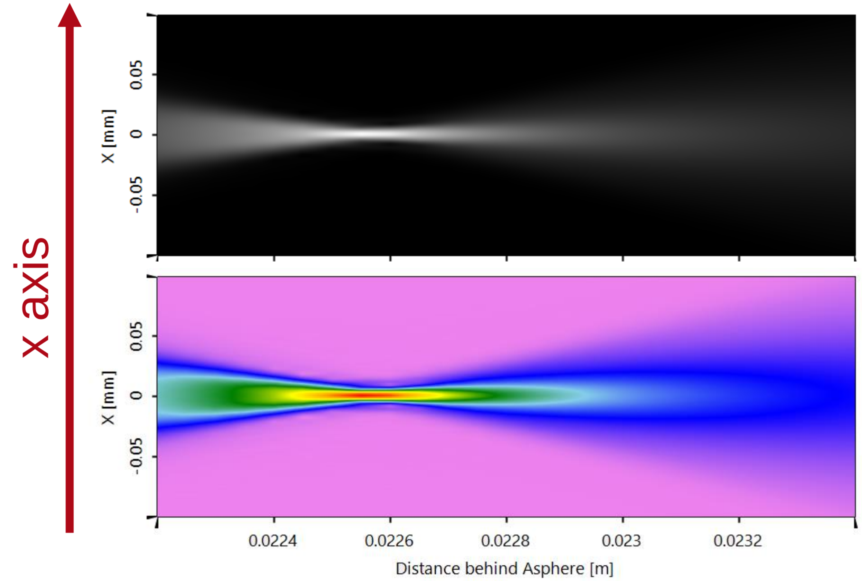

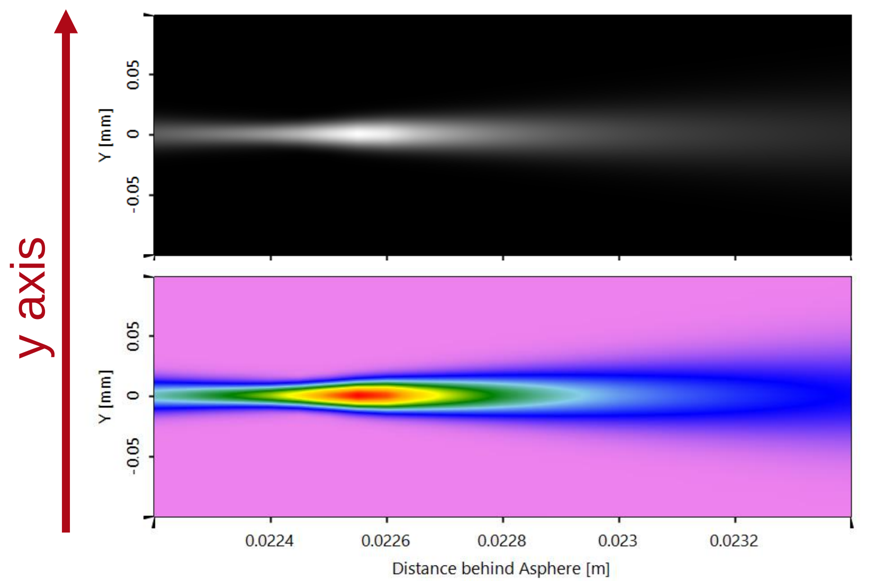

(amplitudes in grey and inverse rainbow colors)

Results: Field Development in front of Focus 2D

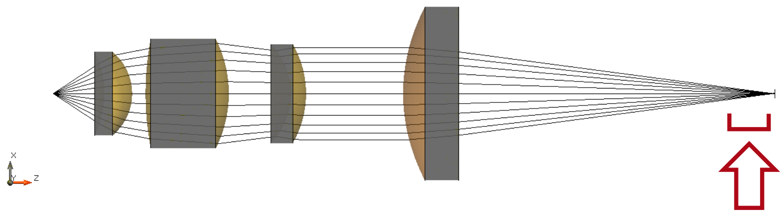

Highlights

- laser diode modeling inclusive astigmatism
- diffraction at lens apertures
- advanced focal region analysis

principal axis of beam ellipse changes from y- to x-direction.

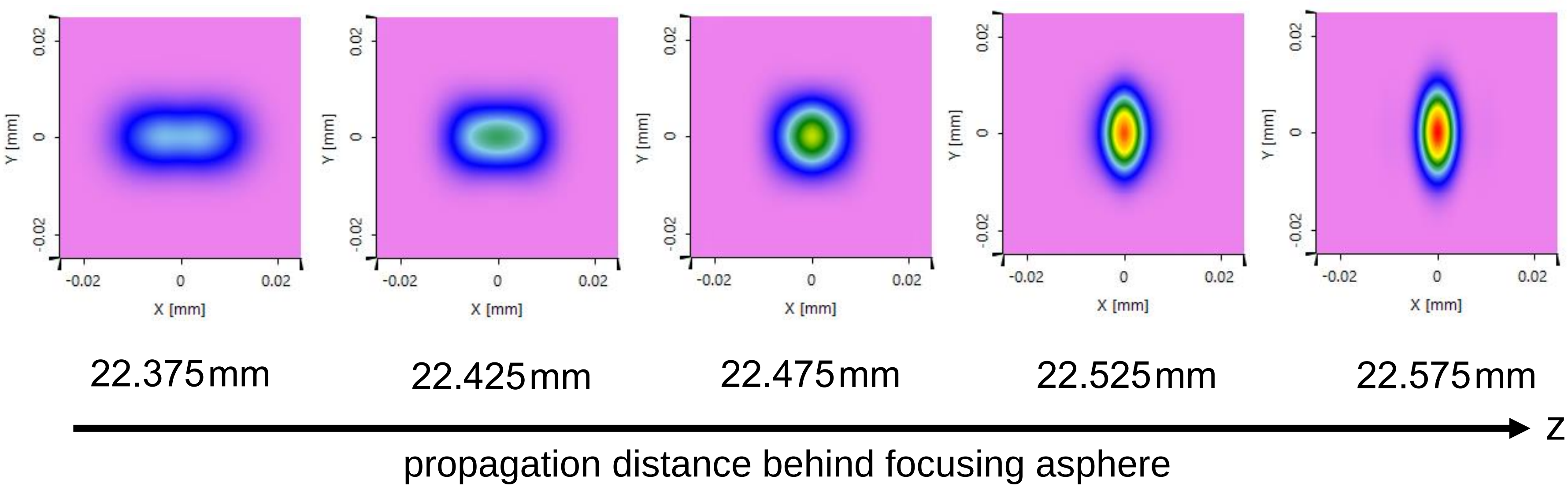

Results: Focus Position in X vs Y Direction

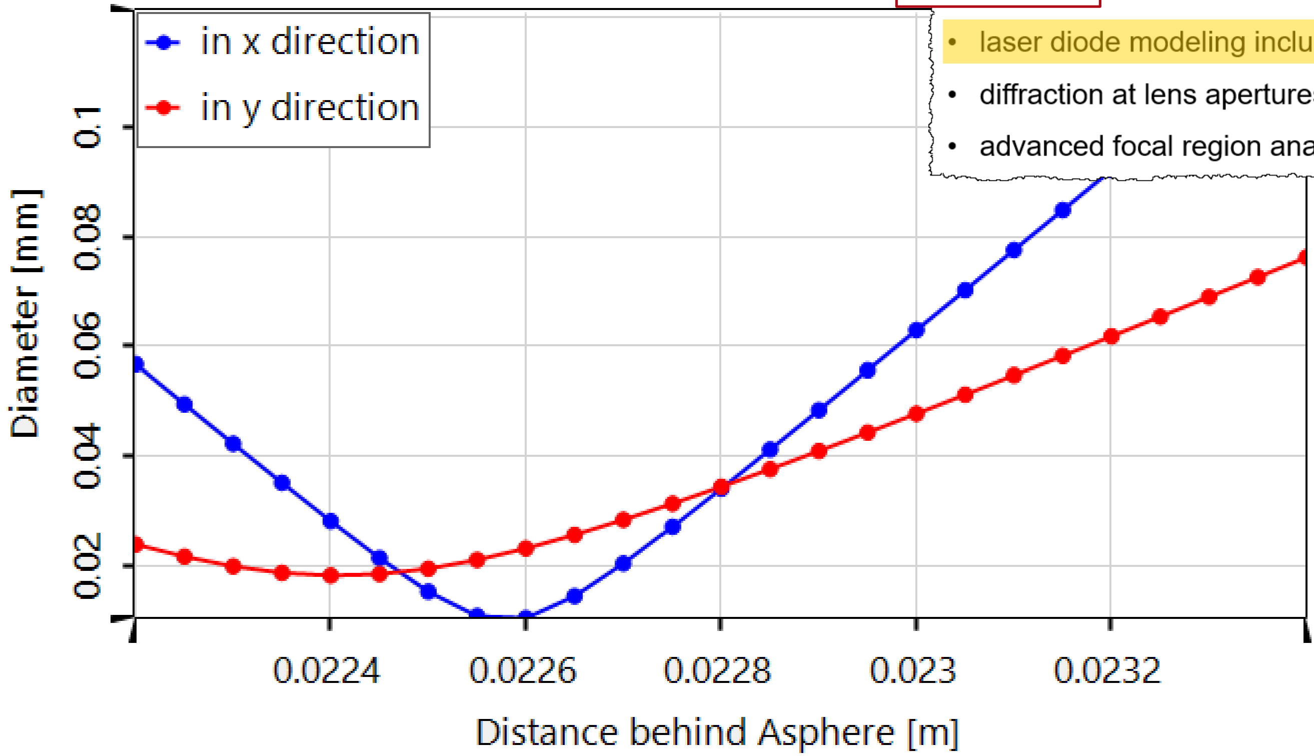

Highlights

- laser diode modeling inclusive astigmatism
- diffraction at lens apertures
- advanced focal region analysis

z-position of smallest spot diameter
is different for x- and y-direction

Document & Technical Info

code	BD.0002
version of document	1.0
title	Focus Investigation behind Aspherical Lens
category	Laser Systems > Beam Delivery (BD)
author	Hartwig Crailsheim (LightTrans)
used VL version	7.0.0.29

Specifications of PC Used for Simulation	
Processor	i7-4910MQ (4 CPU cores)
RAM	32 GB
Operating System	Windows 10

Mach-Zehnder Interferometer Using Coherent Light

Task/System Illustration

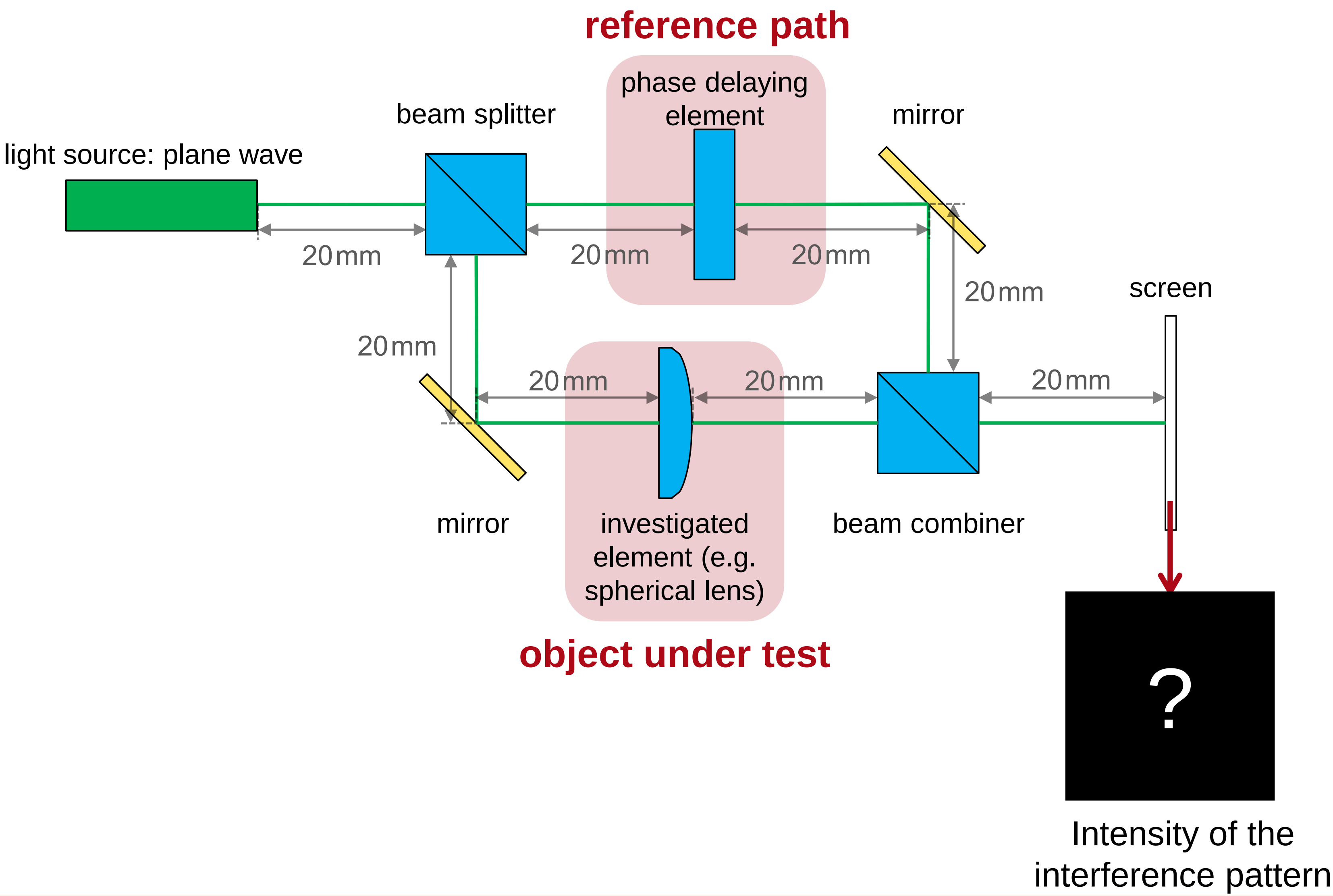

Results: 3D System Ray Tracing

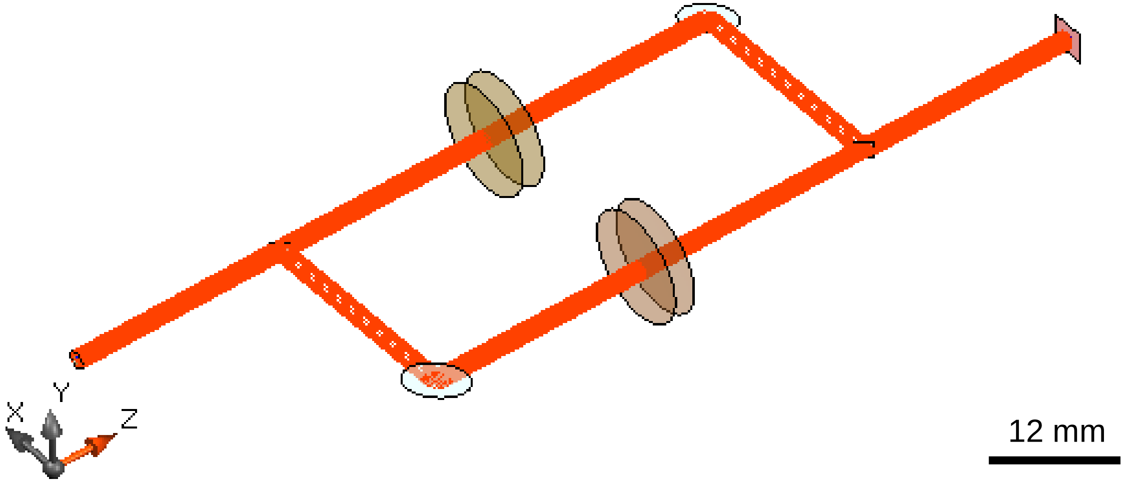

Results: Field Tracing with Tilt of the Object

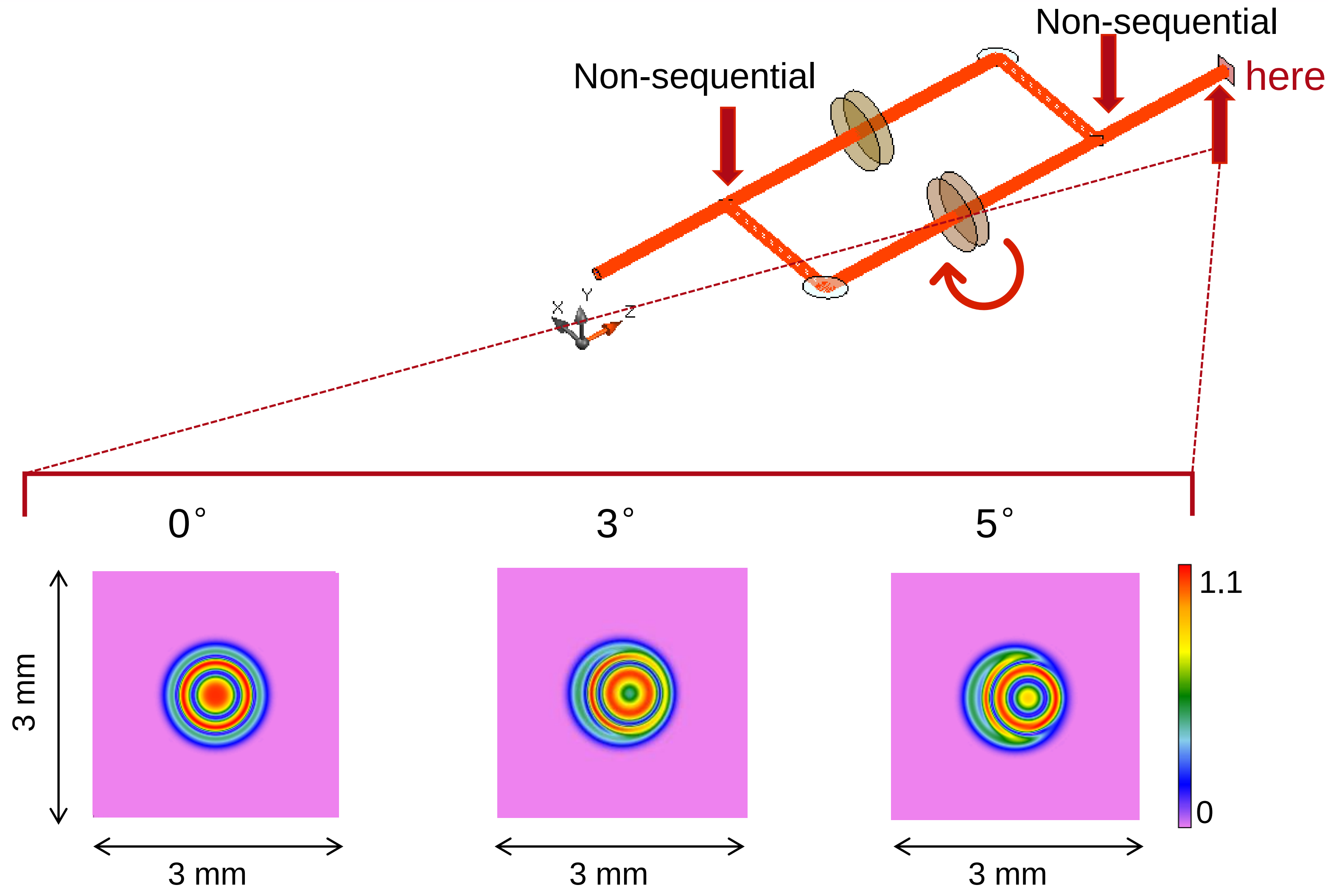

Results: Field Tracing Lateral Shift of the Object

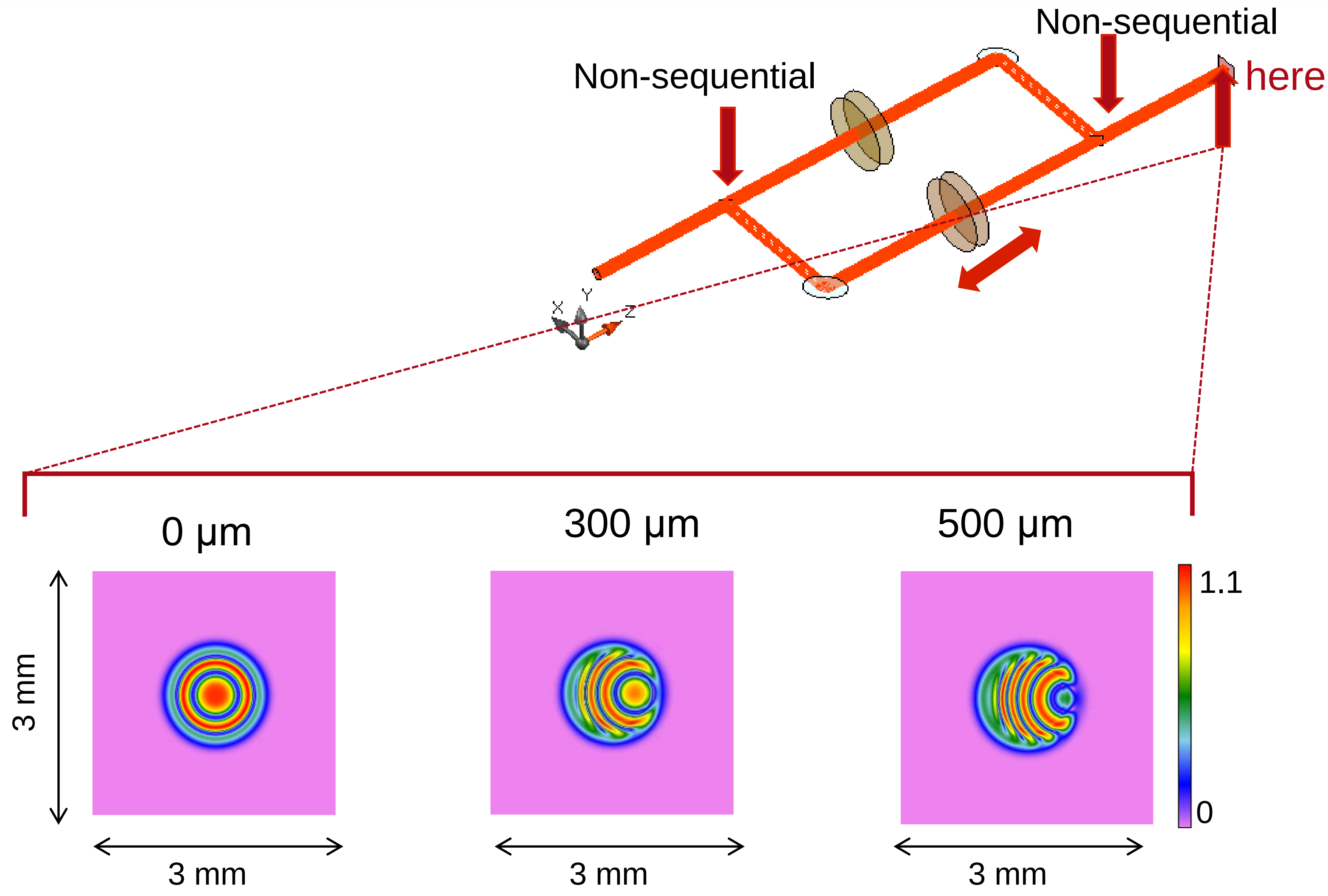

Interaction of Highly Focused Azimuthally polarized Field with Nano Particle

Task/System Illustration

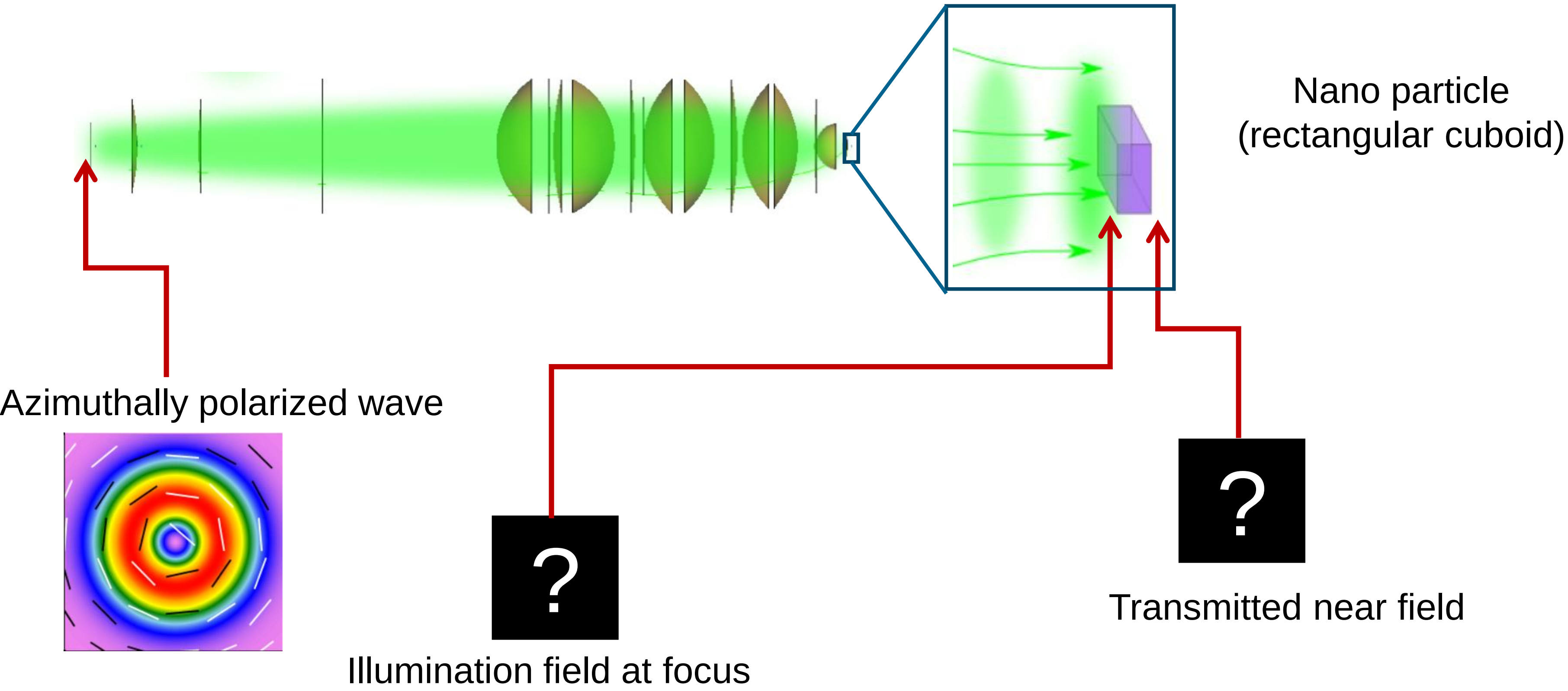

Dot Diagram at Focal Plane: NA=0.85

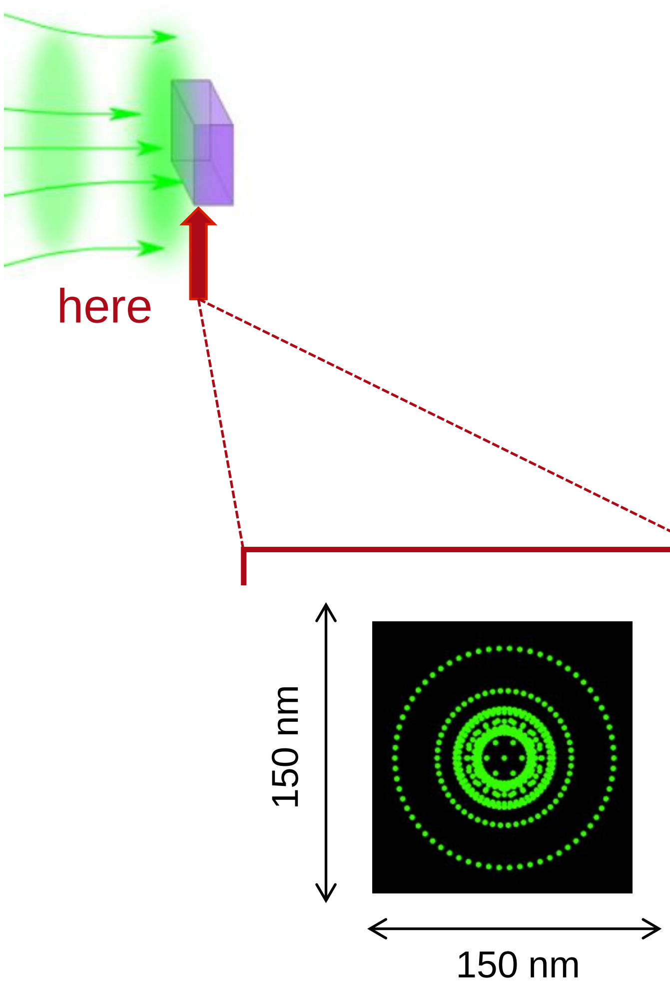

Field at Focal Plane: NA=0.85

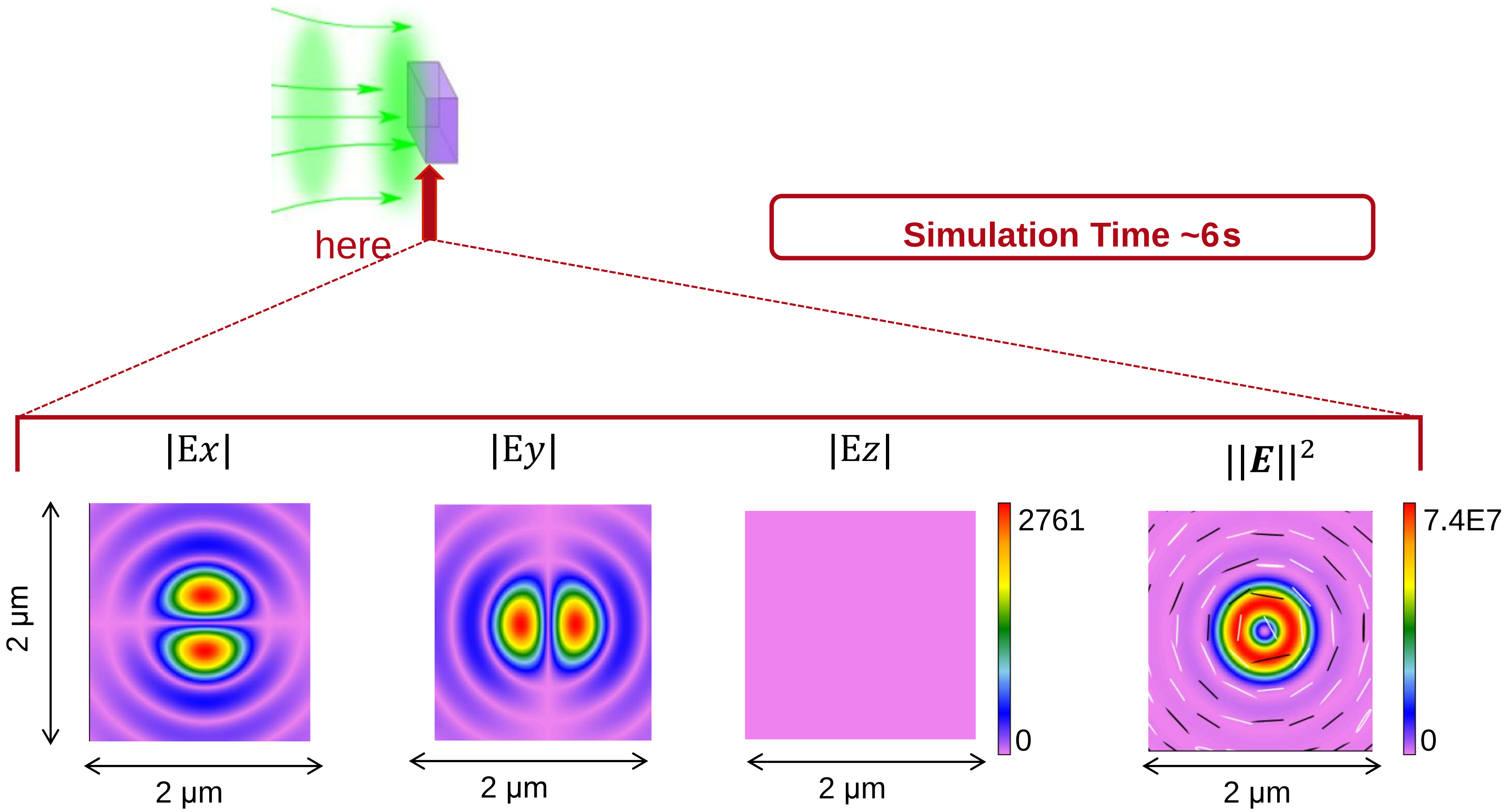

Transmitted Near Field

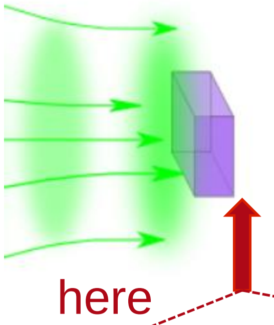

Size of particle: 900 nm × 600 nm × 300 nm

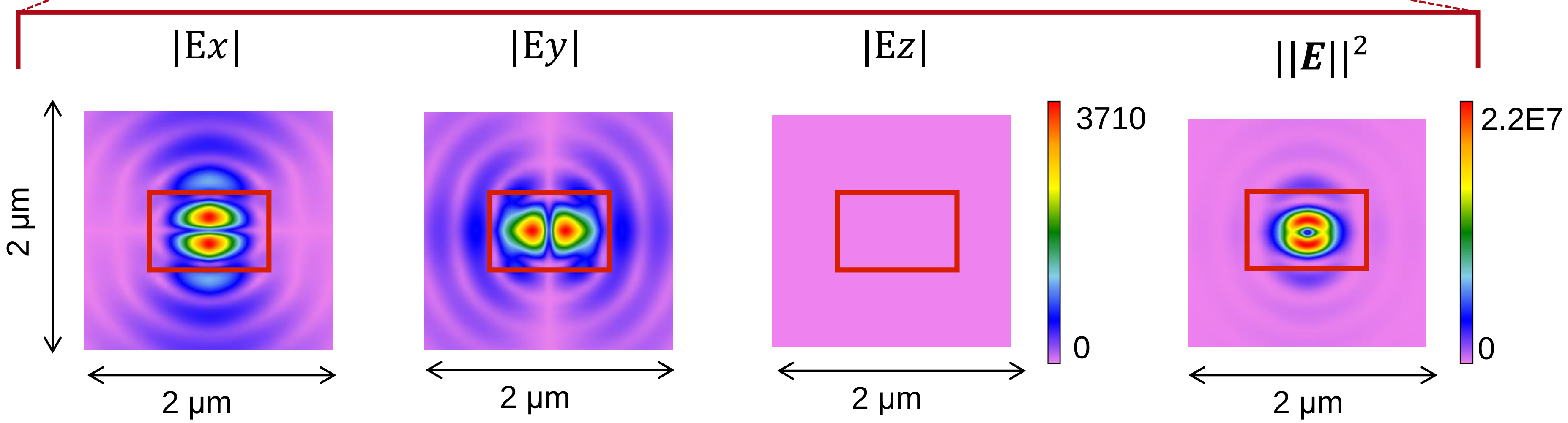

SHG

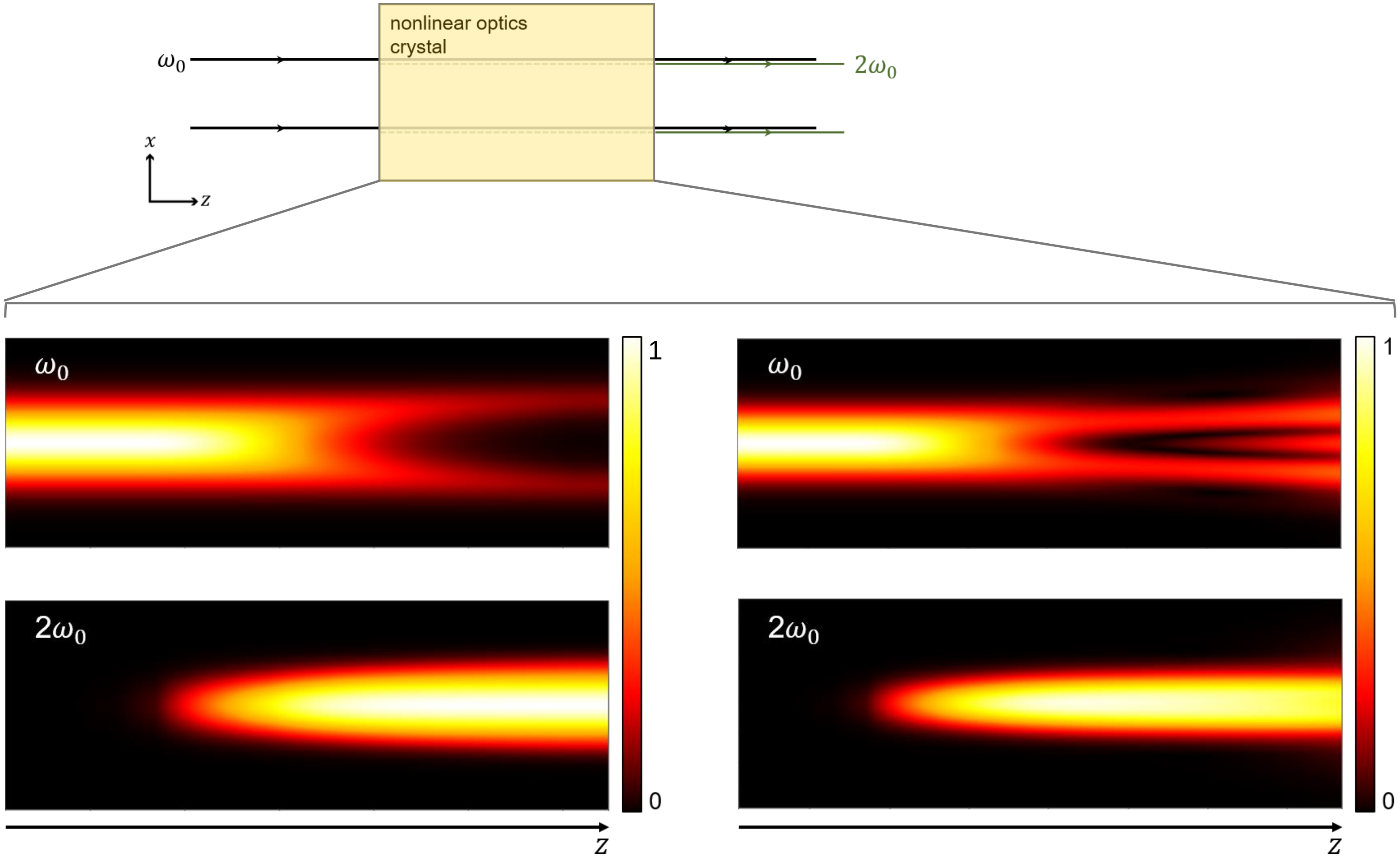

a) collimated input beam

b) divergent input beam

14:45-15:50

Light Shaping

Light shaping by inverse approach

Concept of amplitude matching and consequences

Inverse Design Concept: HOE and Freeform

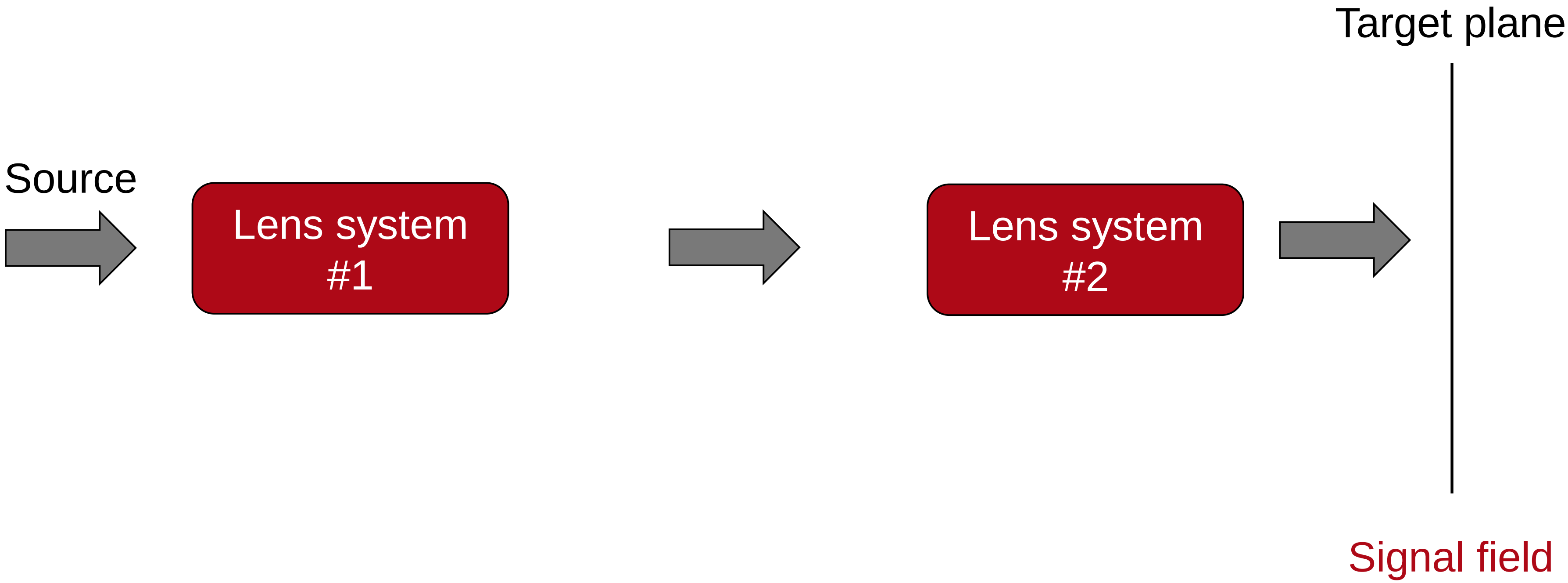

Inverse Design Concept: HOE and Freeform

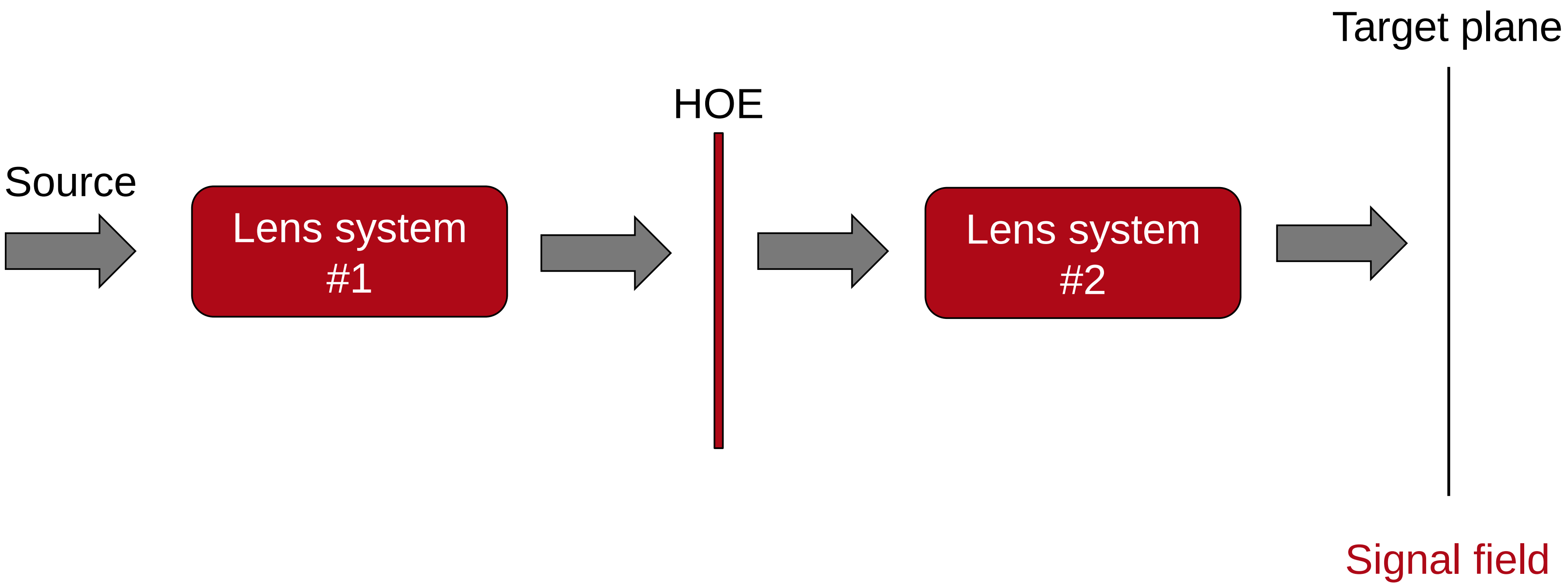

Inverse Design Concept: HOE and Freeform

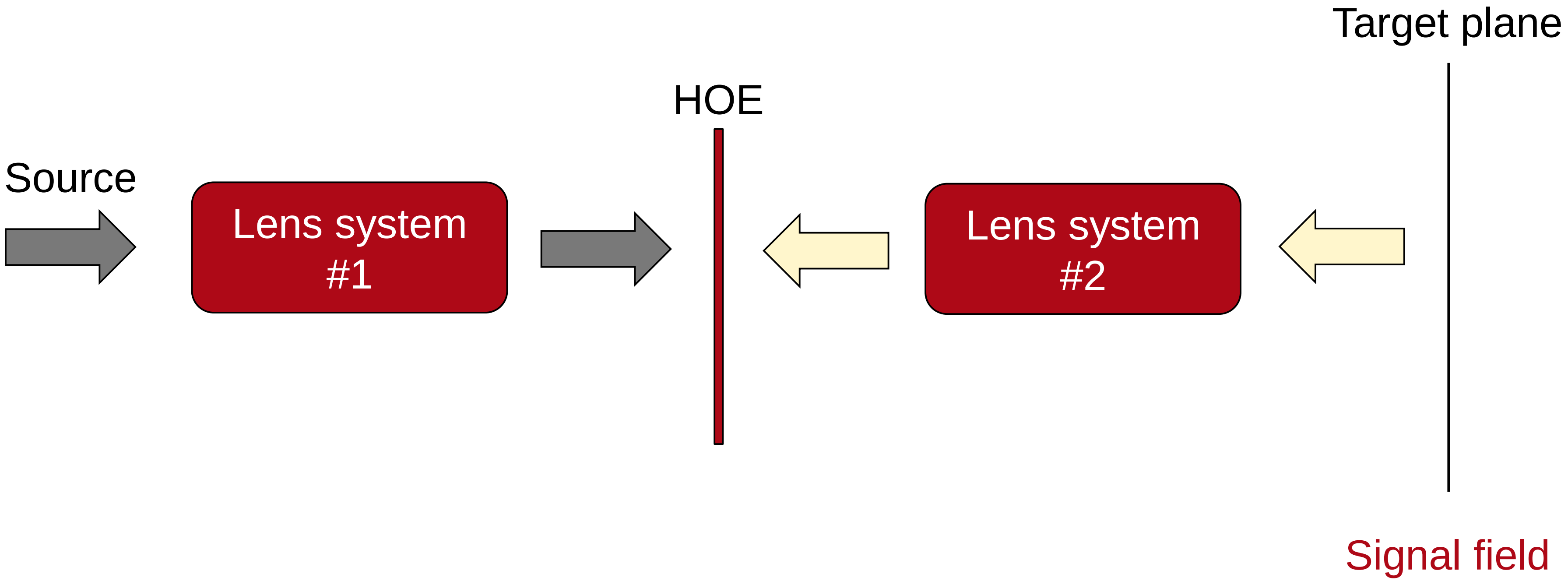

Inverse Design Concept: HOE and Freeform

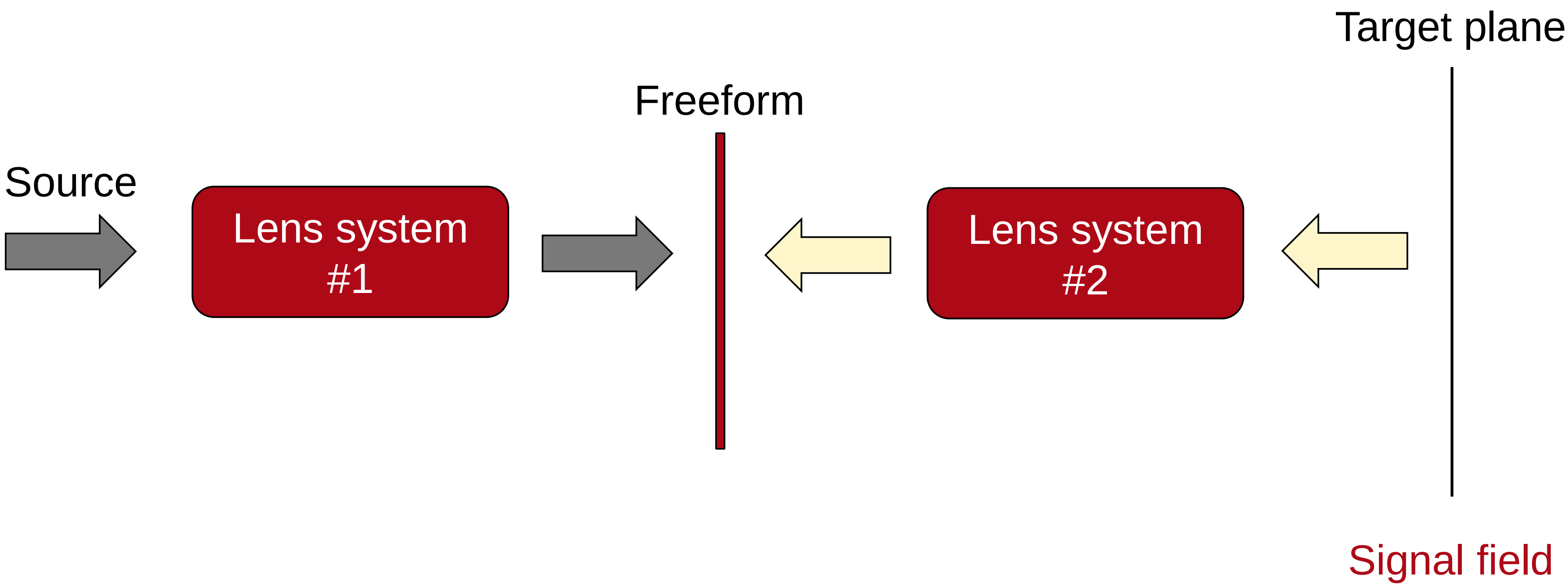

Inverse Design Concept: HOE and Freeform

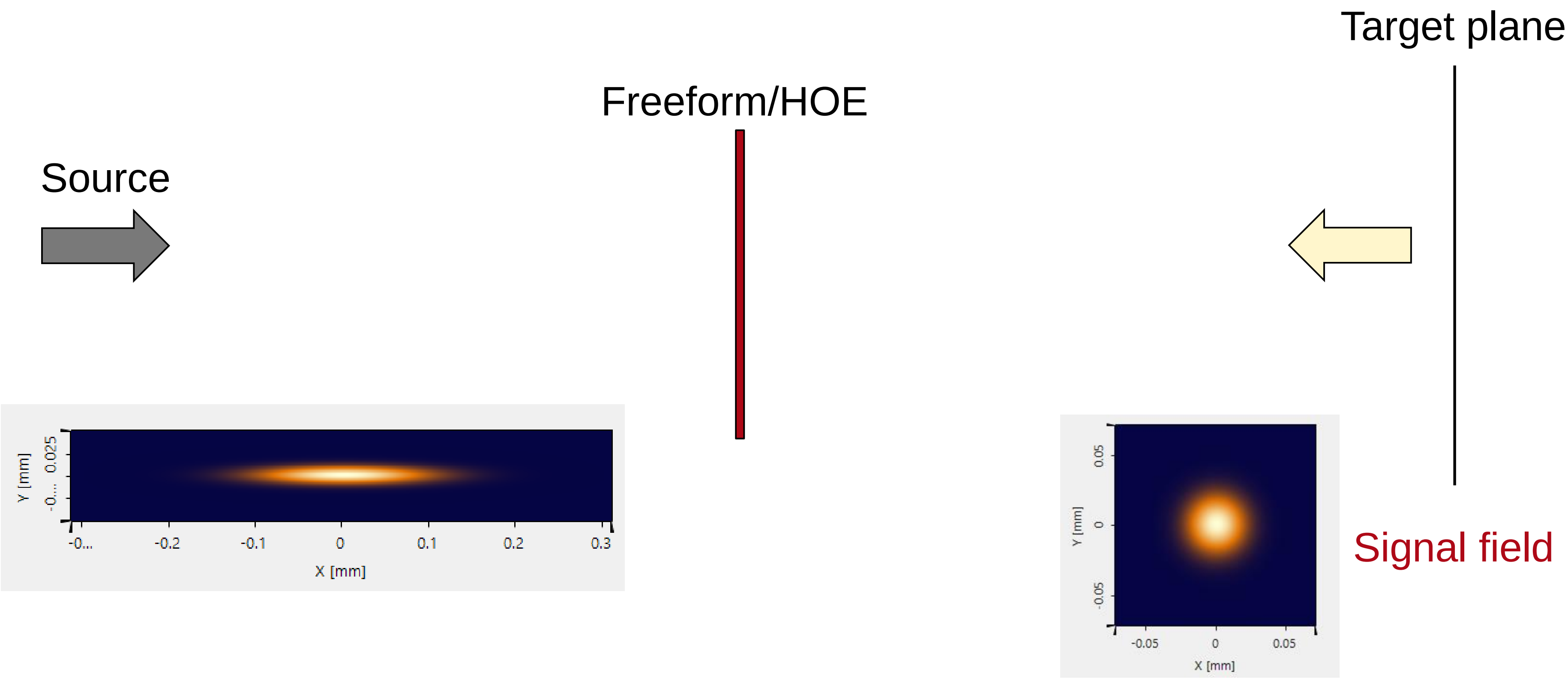

Inverse Design Concept: HOE and Freeform

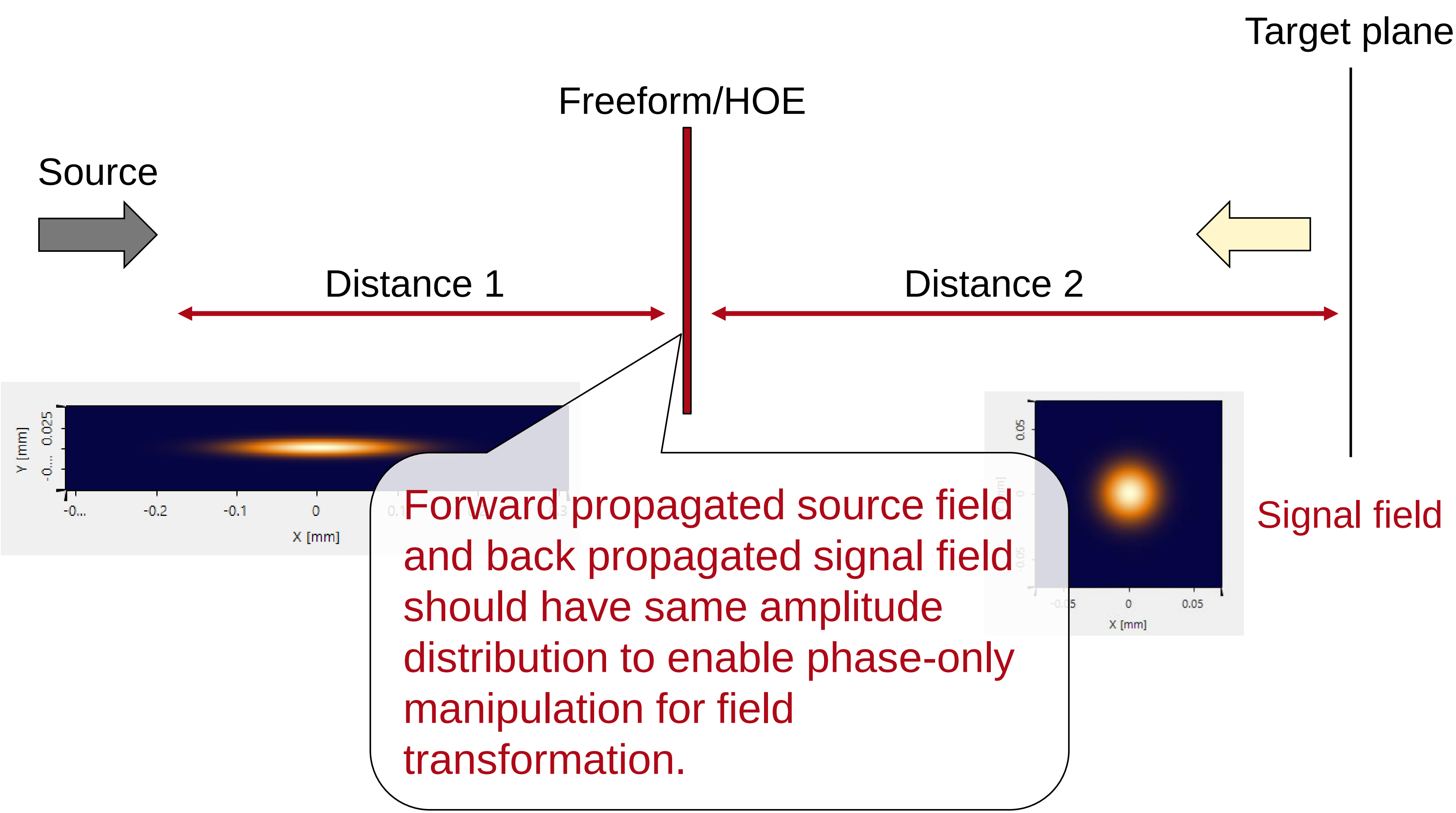

Inverse Design Concept: HOE and Freeform

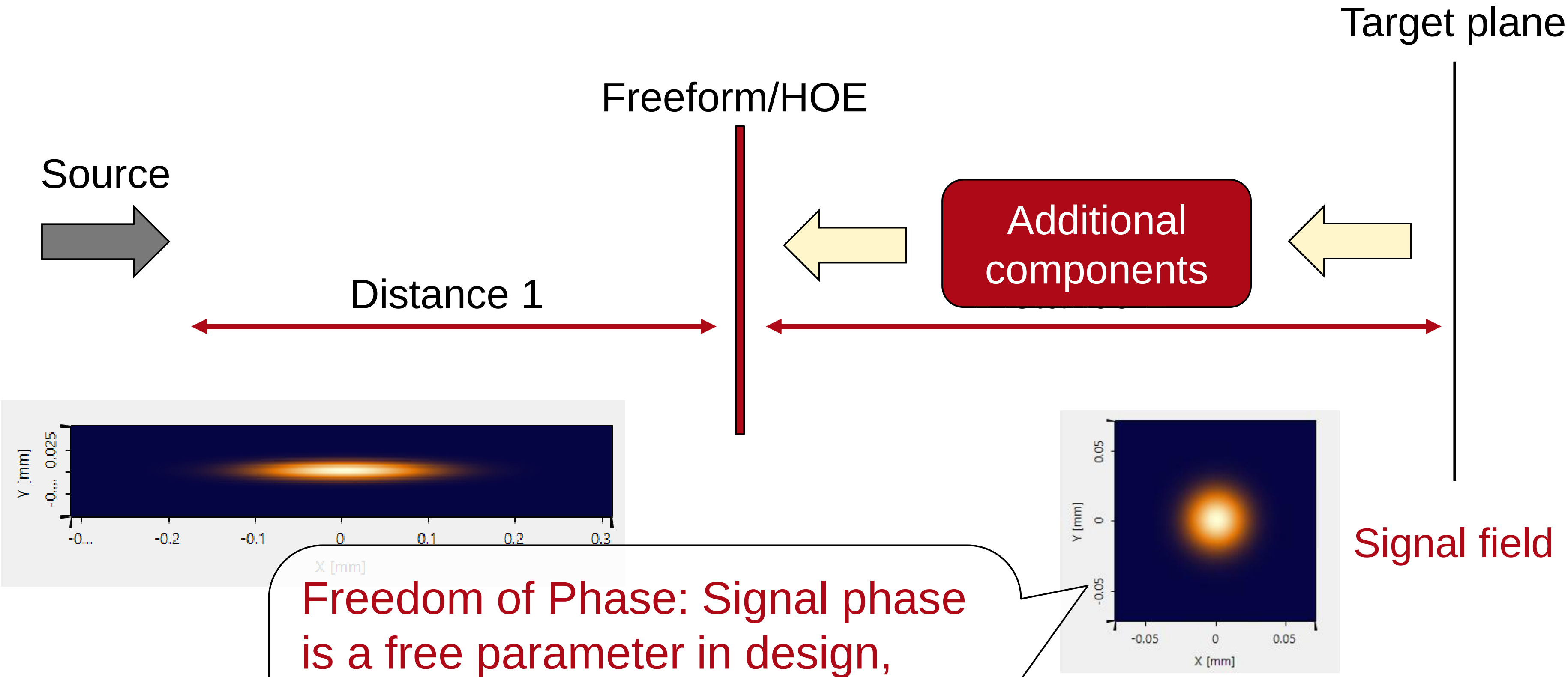

Freedom of Phase: Signal phase is a free parameter in design, when only the intensity is of concern. Comment: Phase affects the 3D signal behavior.

Inverse Design Concept: HOE and Freeform

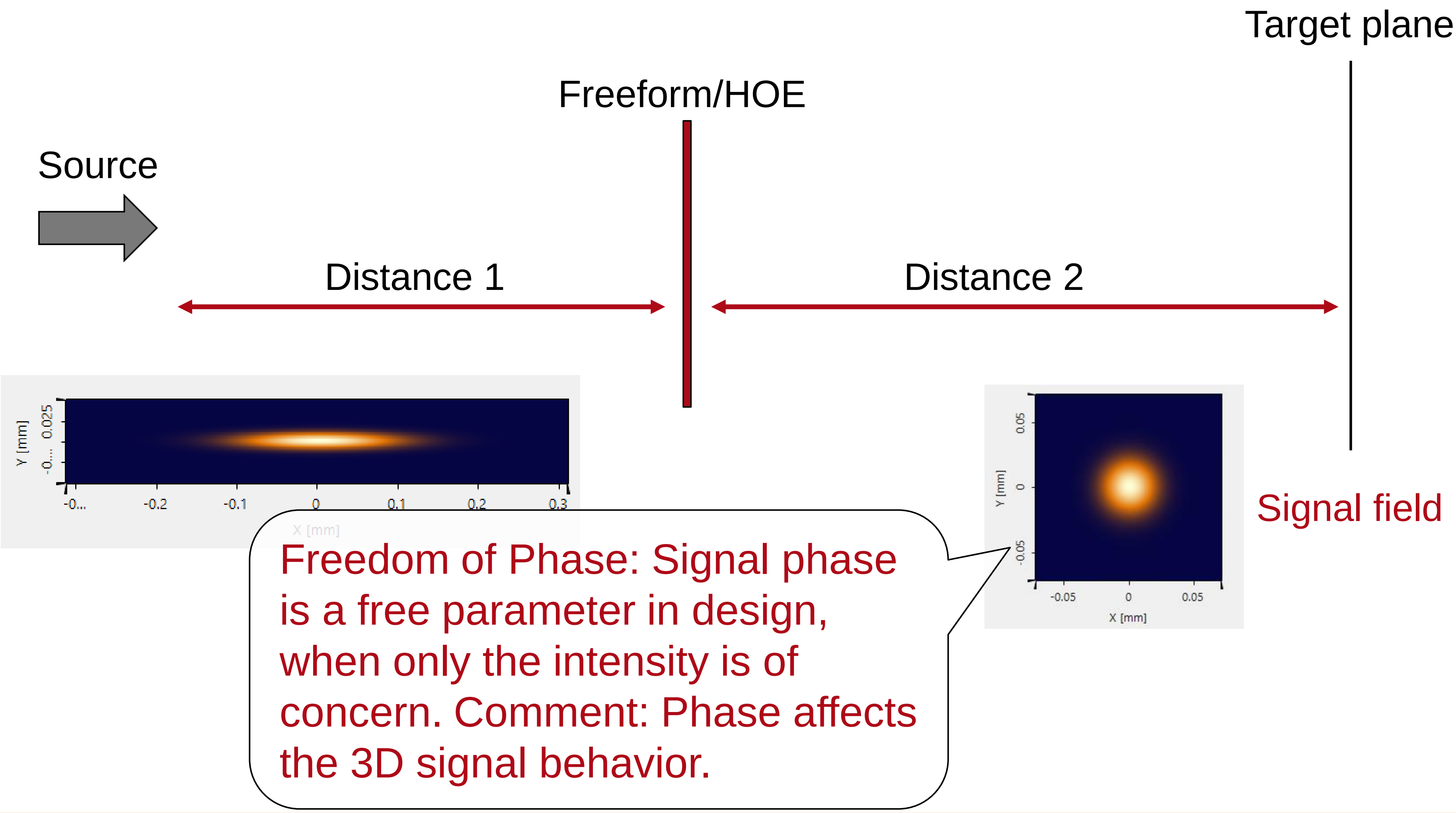

Light Shaping Concepts

- Tailored aberrations
- Stored scanning process
- Multichannel concept: Single Deflection
- Multichannel concept: General

Light Shaping Concepts

- Tailored aberrations
- Stored scanning process
- Multichannel concept: Single Deflection
- Multichannel concept: General

Light shaping by tailored aberrations

Refractive and diffractive optical elements

Beam Shaping: The Task

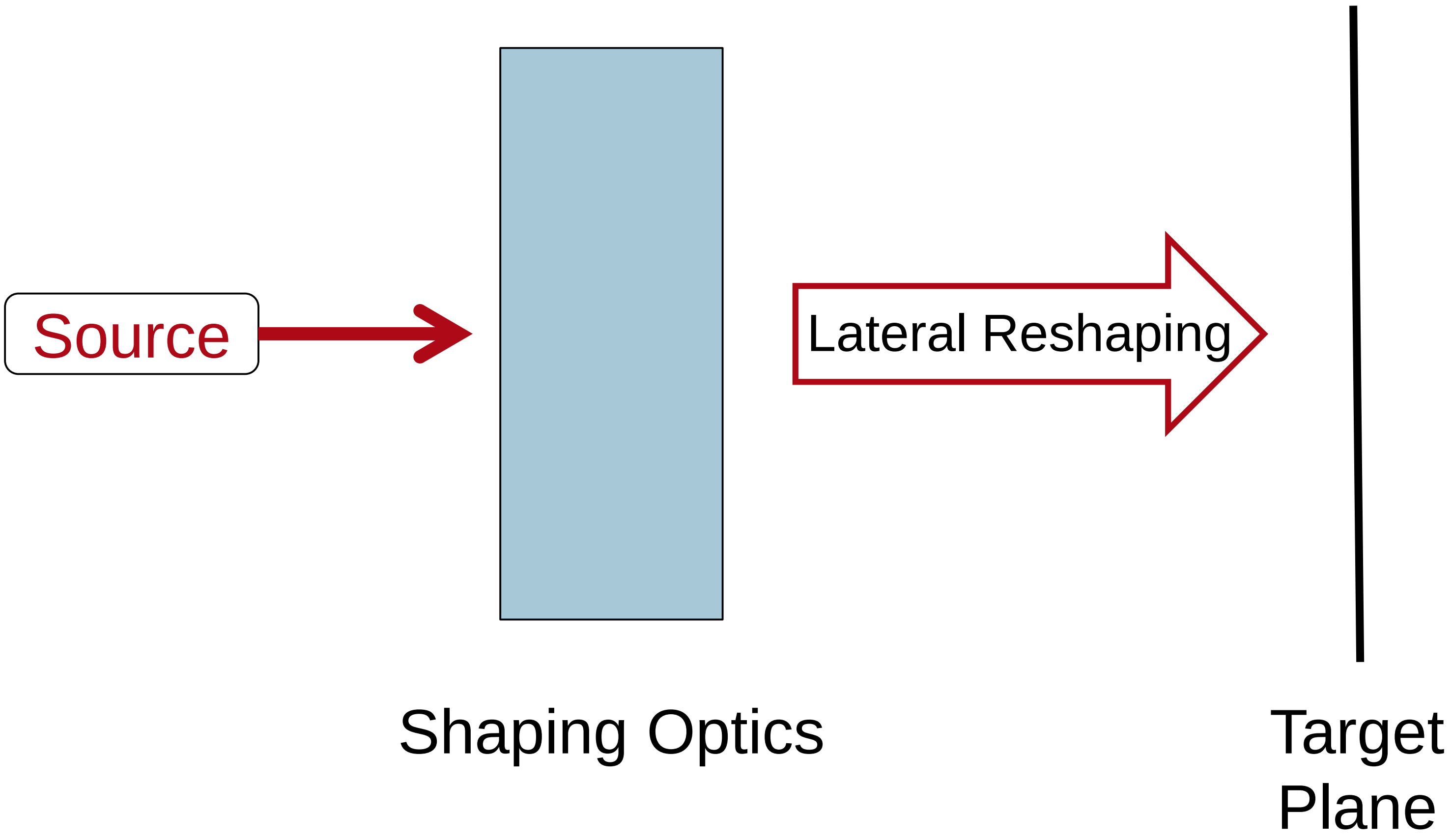

Beam Shaping: The Task

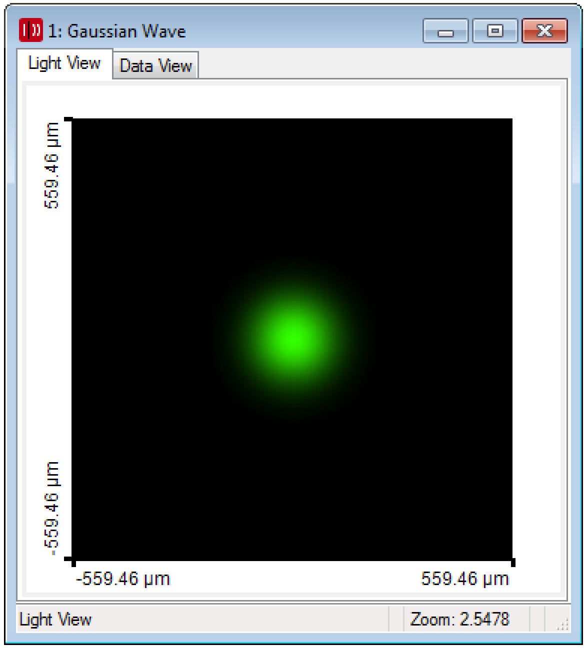

Lateral Reshaping

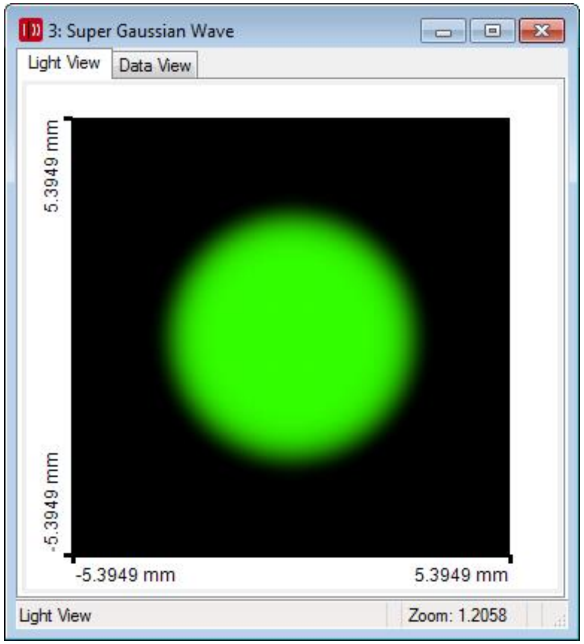

Beam Shaping: The Task

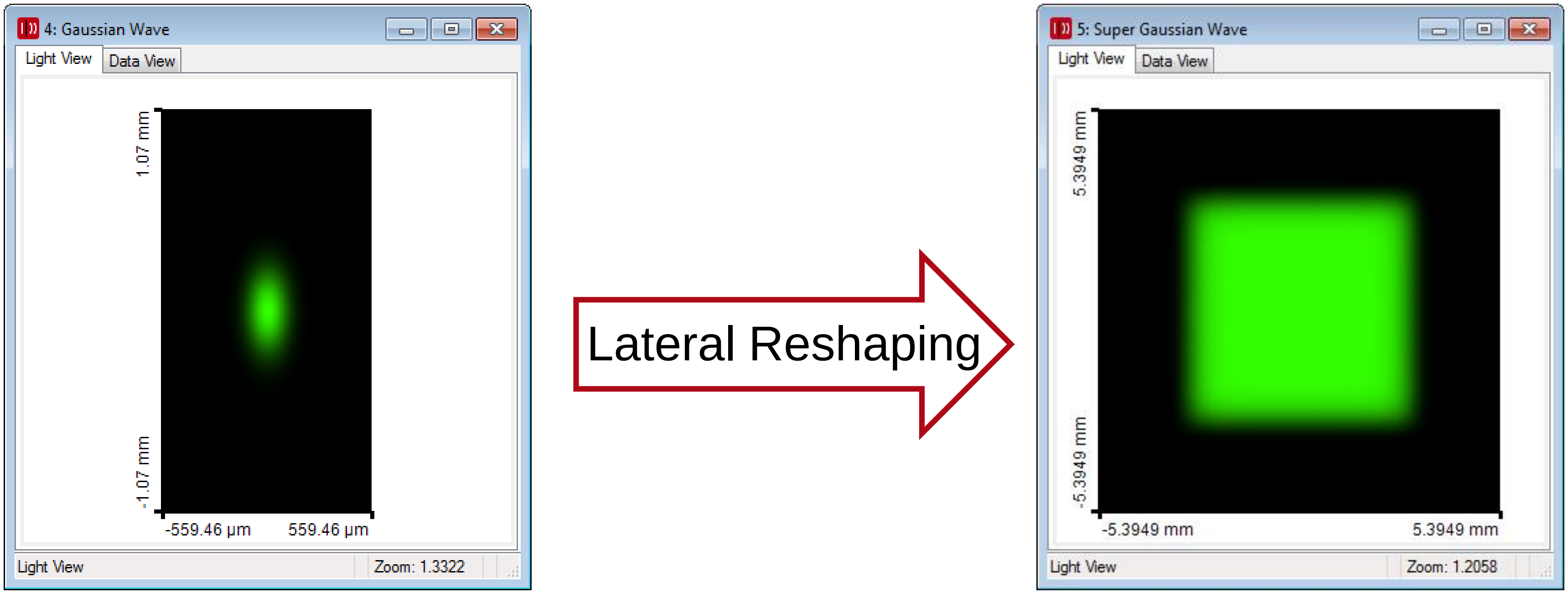

Beam Shaping: The Task

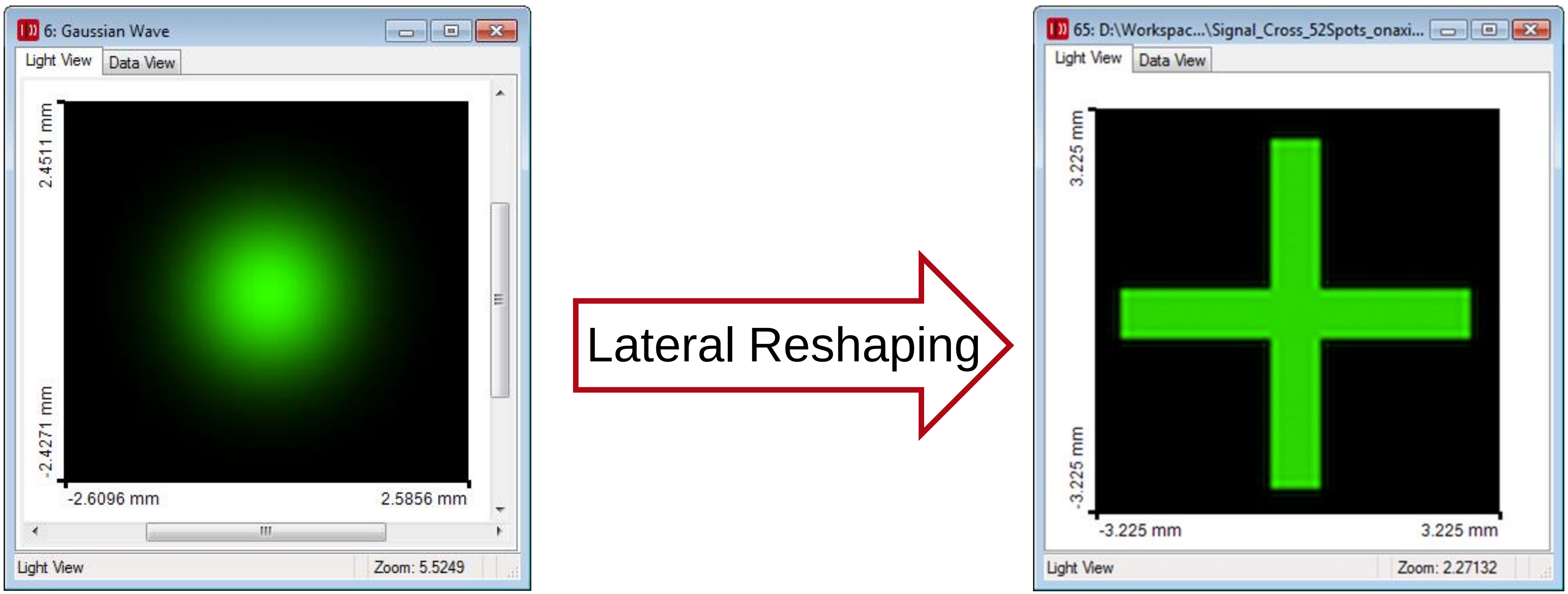

Basic „Beam Shaping“ Task: Focusing

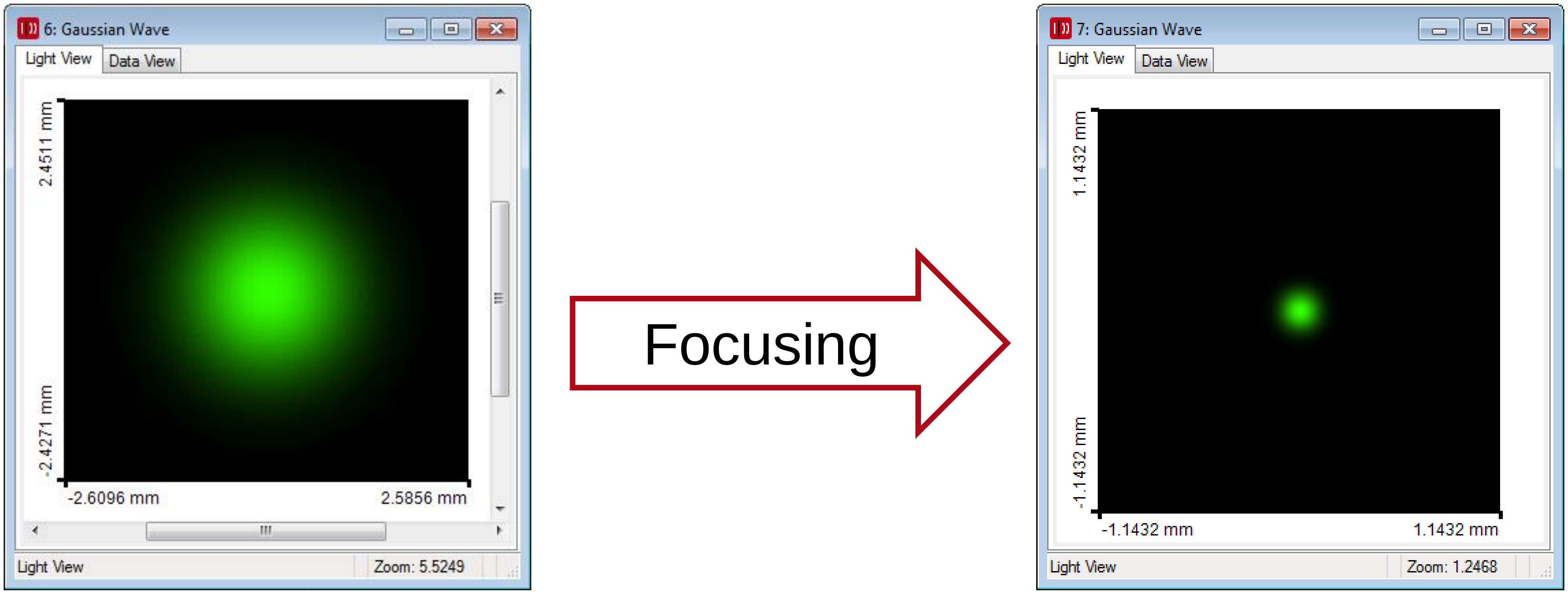

Basic „Beam Shaping“ Task: Focusing

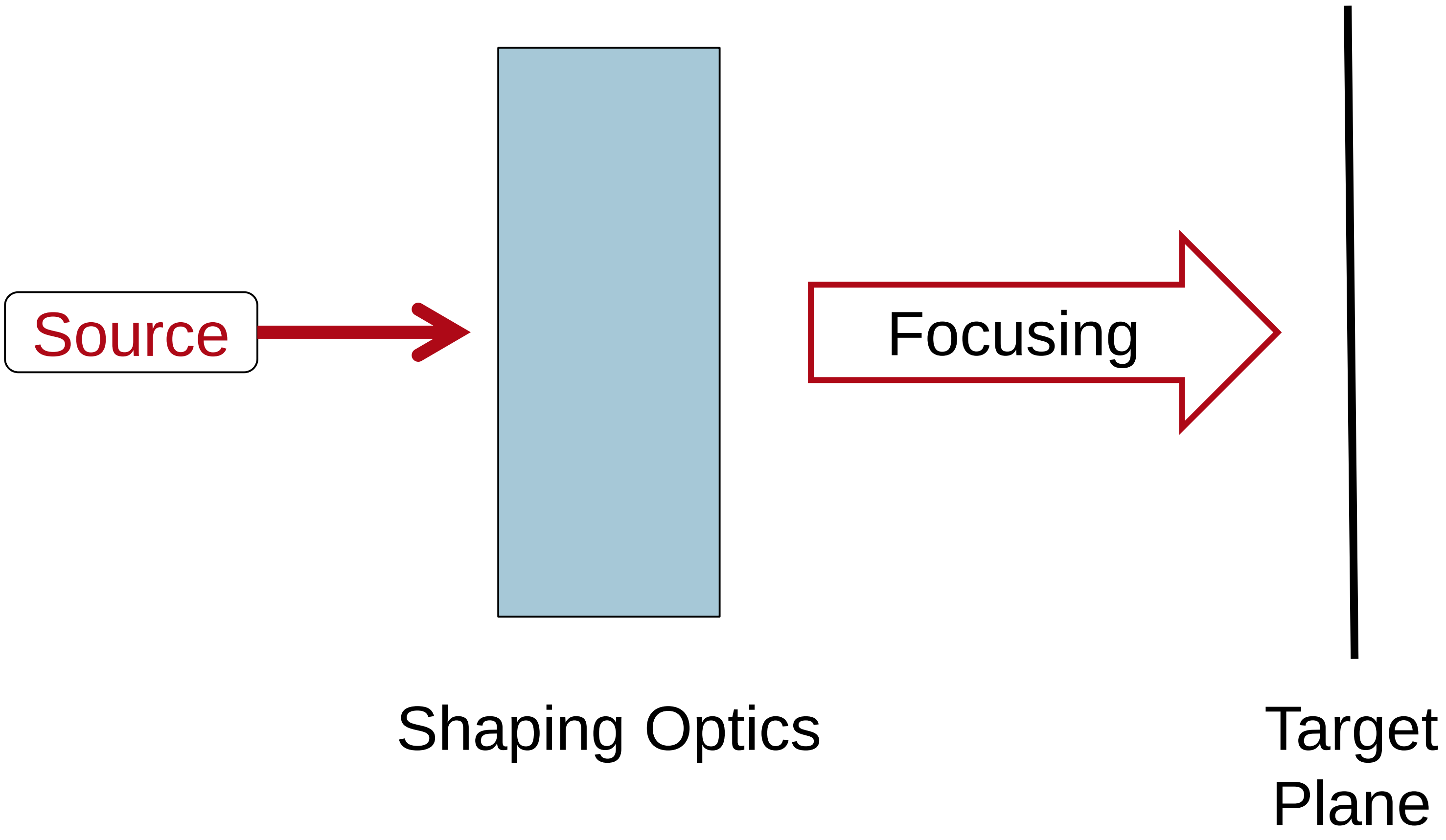

Basic „Beam Shaping“ Task: Focusing

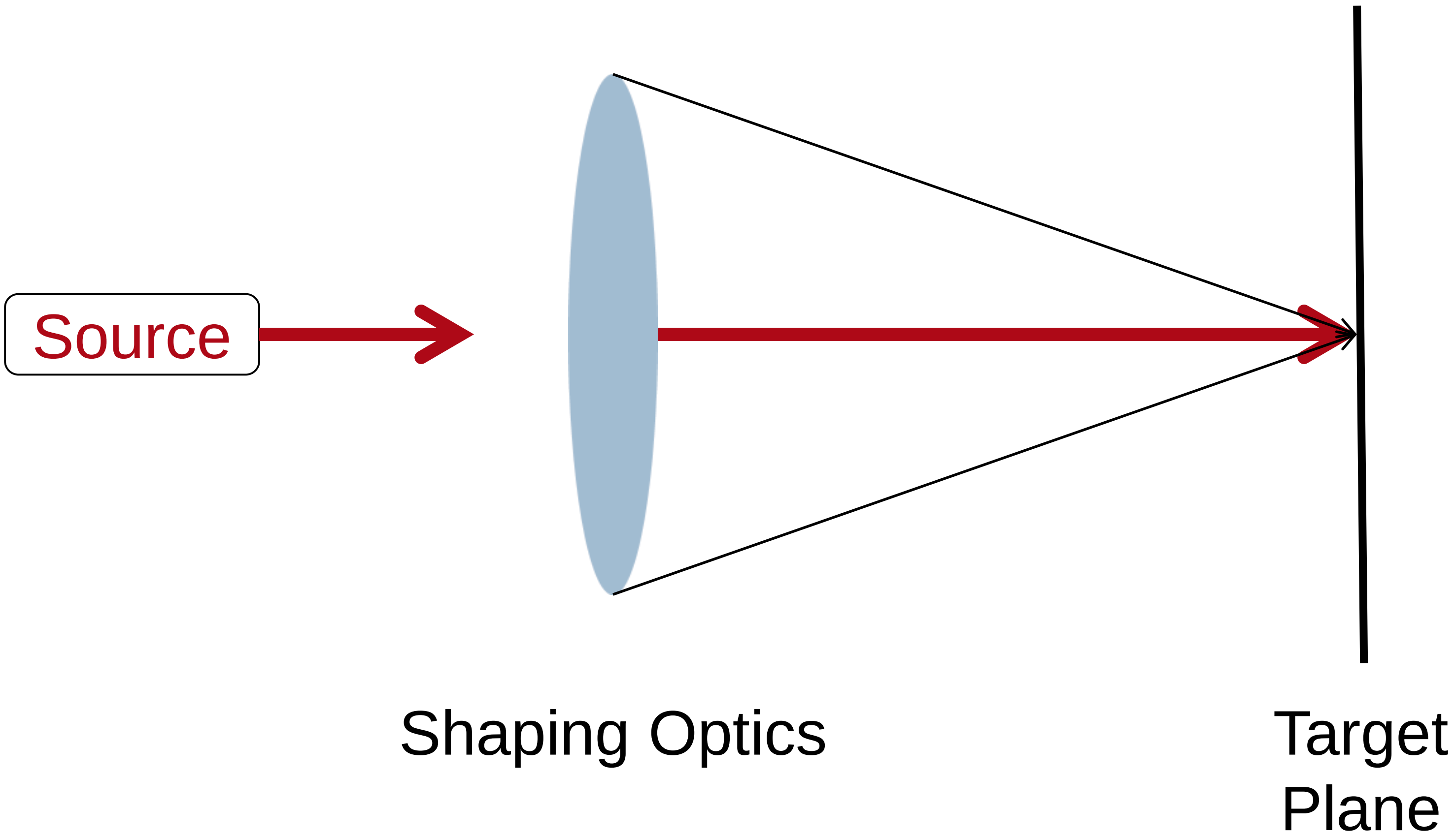

Basic „Beam Shaping“ Task: Focusing

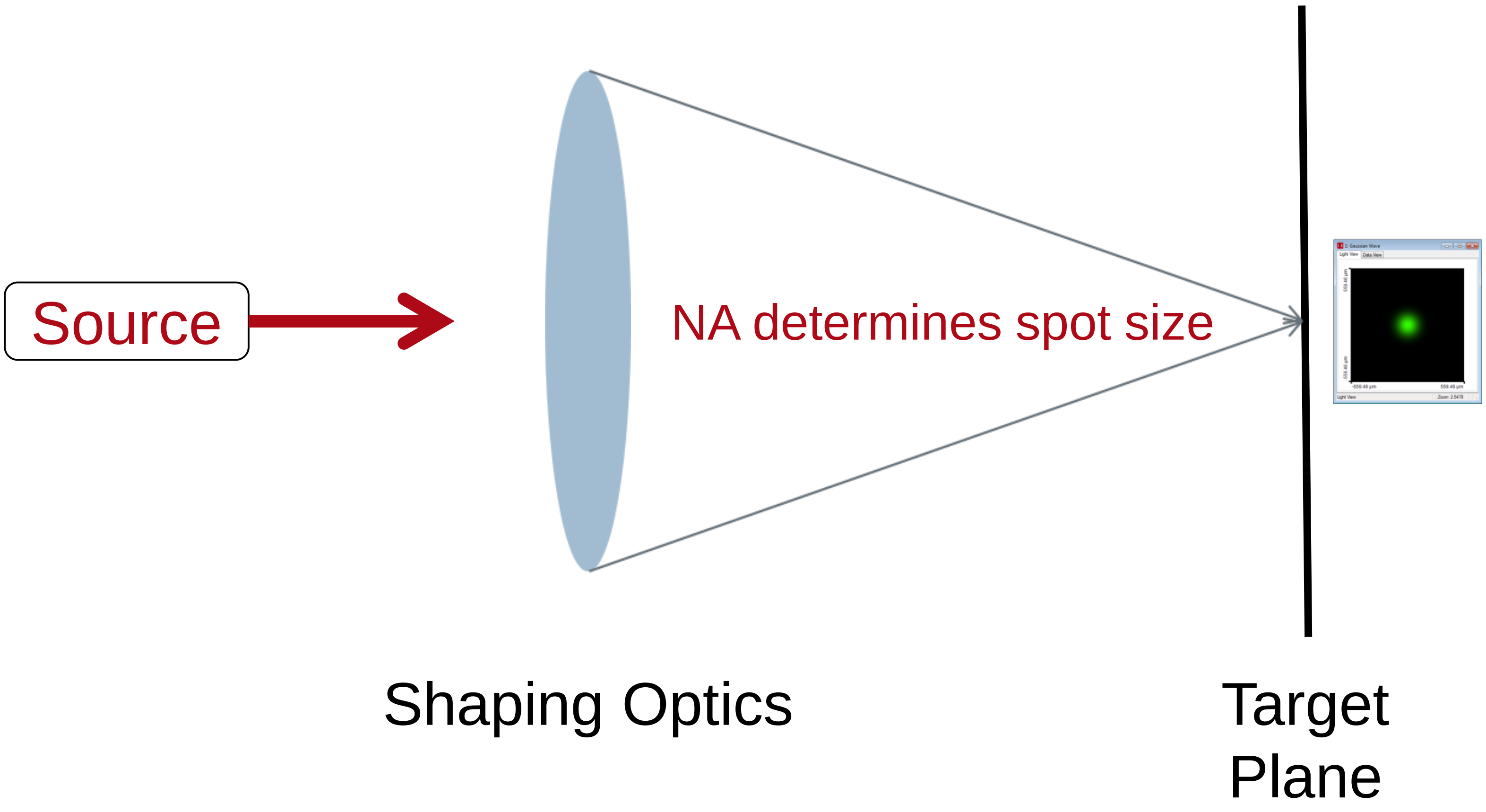

Light Shaping by Aberrations

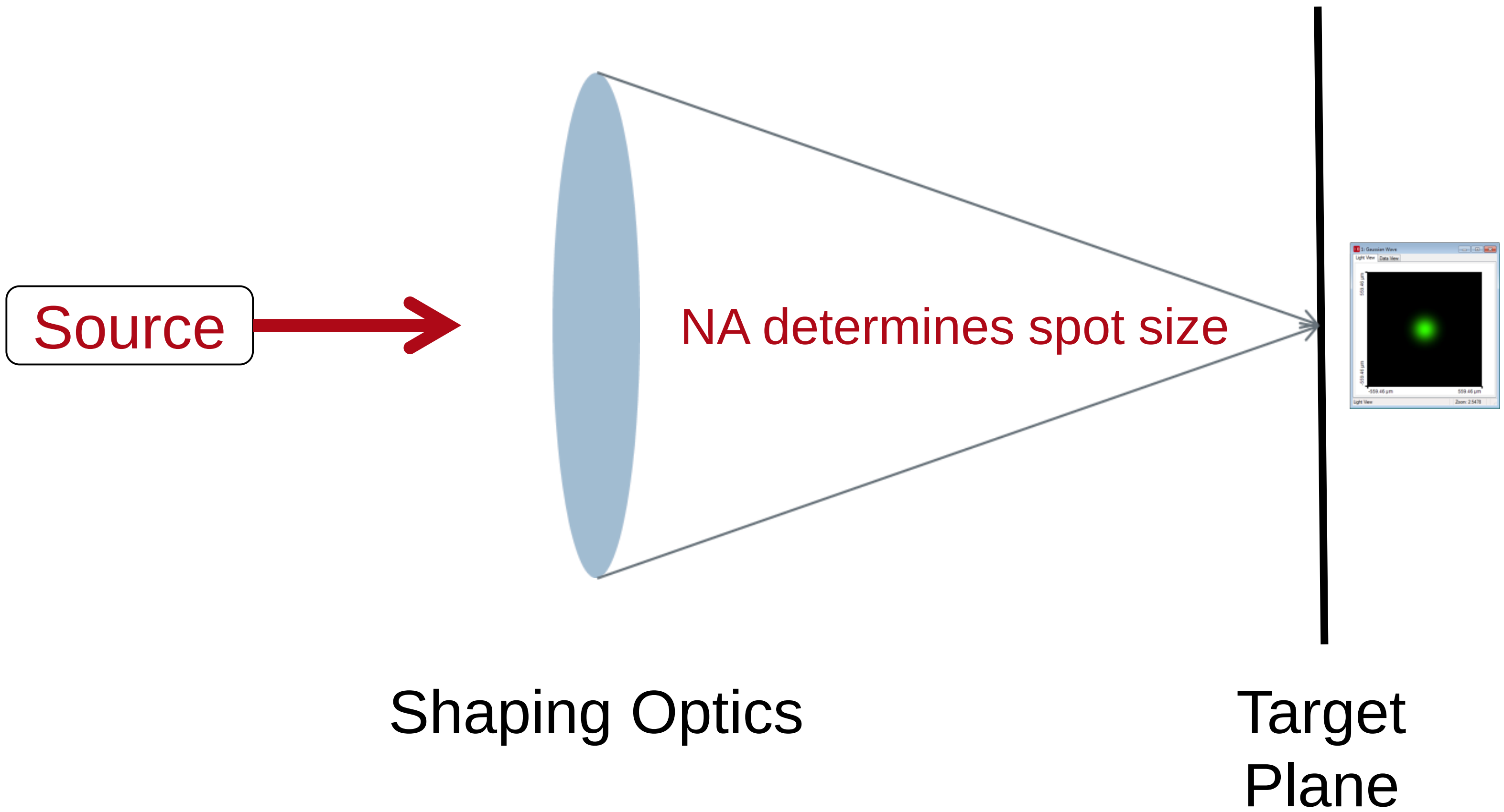

Beam shaping can be understood as the introduction of aberrations to shape the focus!

Ideal Lens vs. Spherical Aberrations

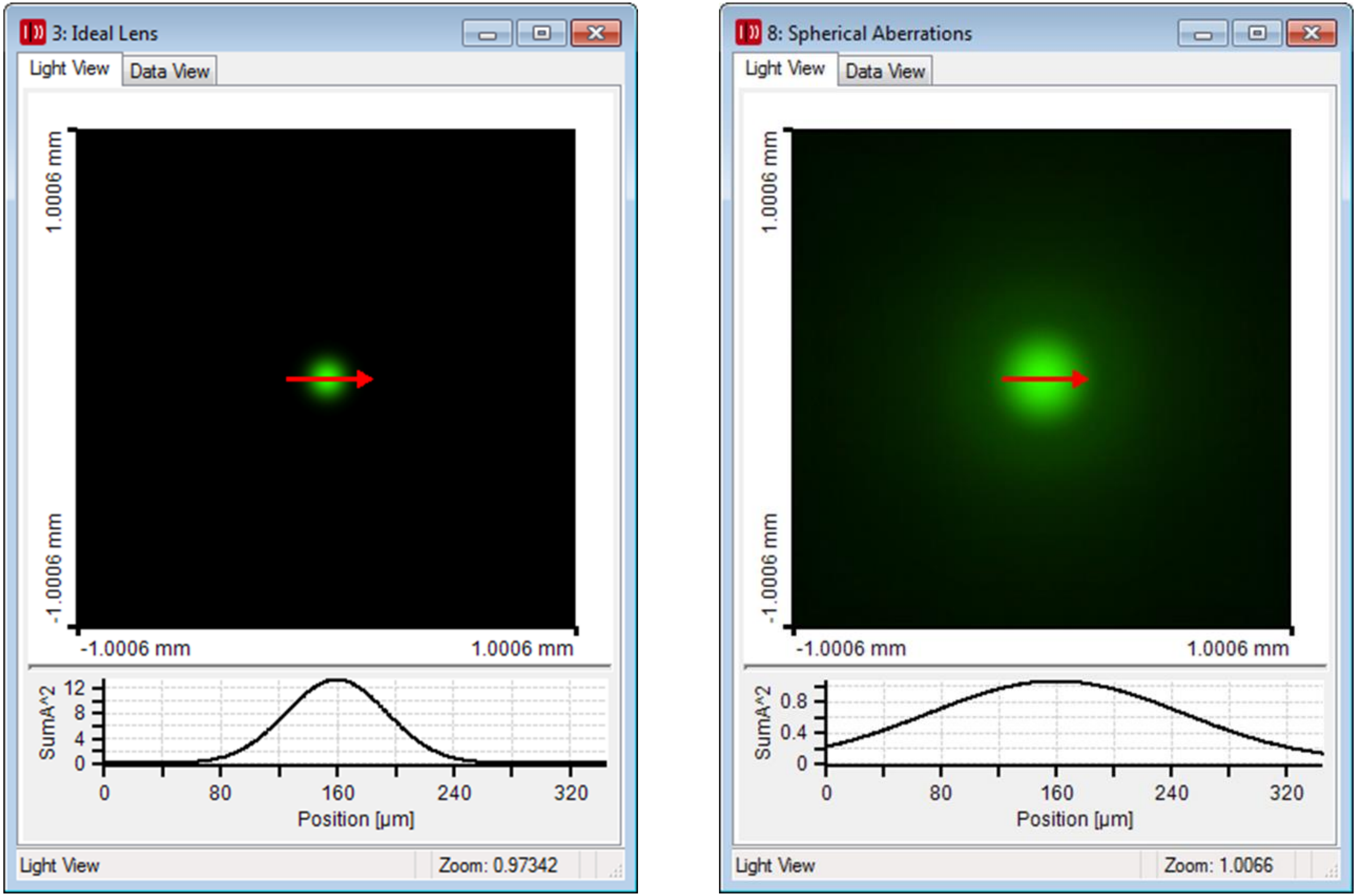

Ideal Lens vs. Astigmatism

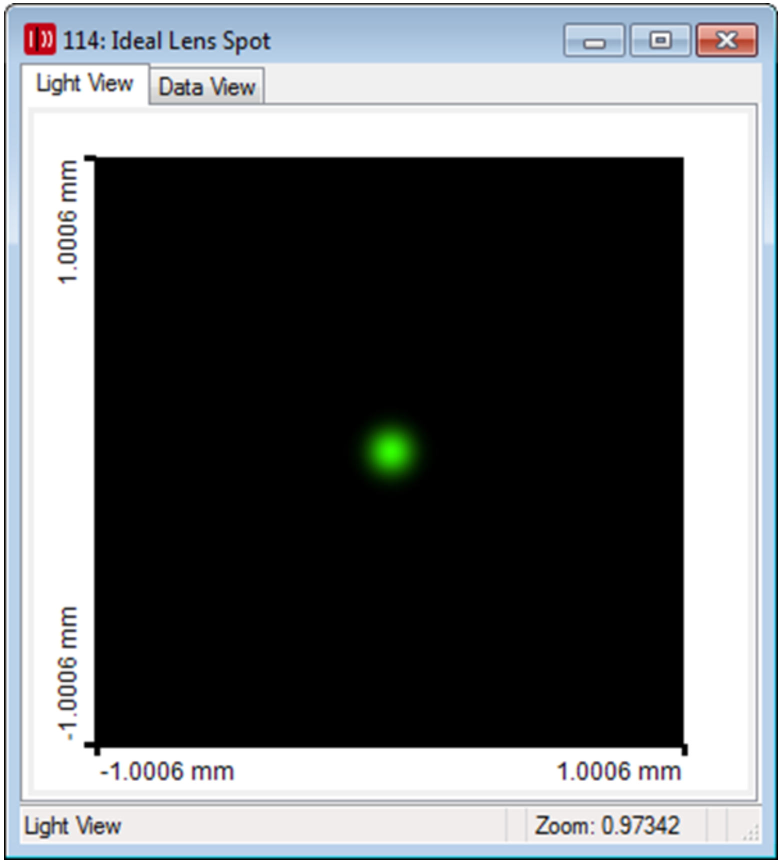

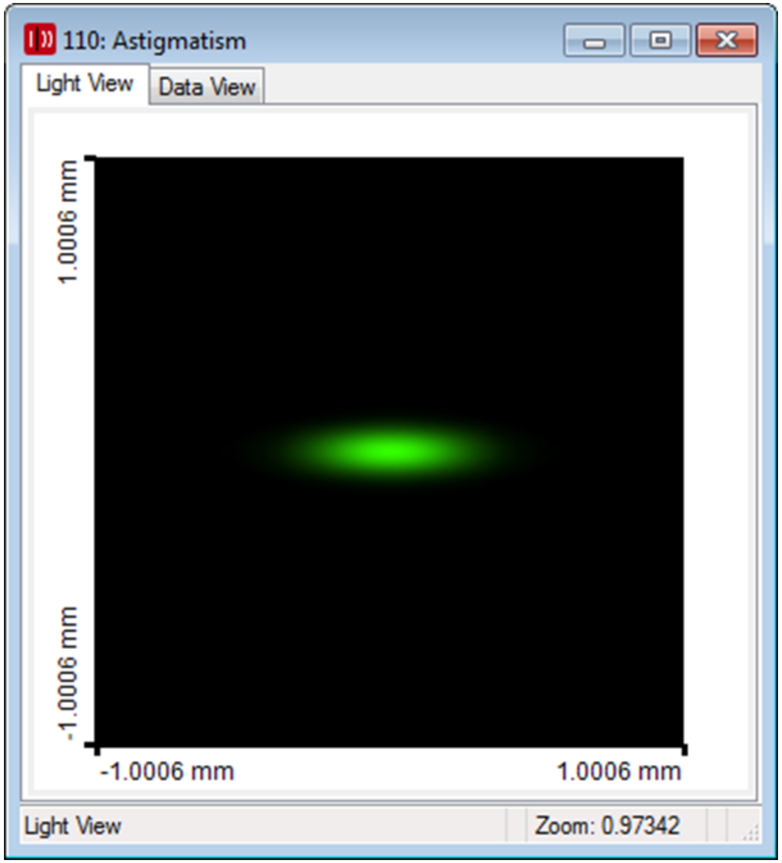

Ideal Lens vs. Coma

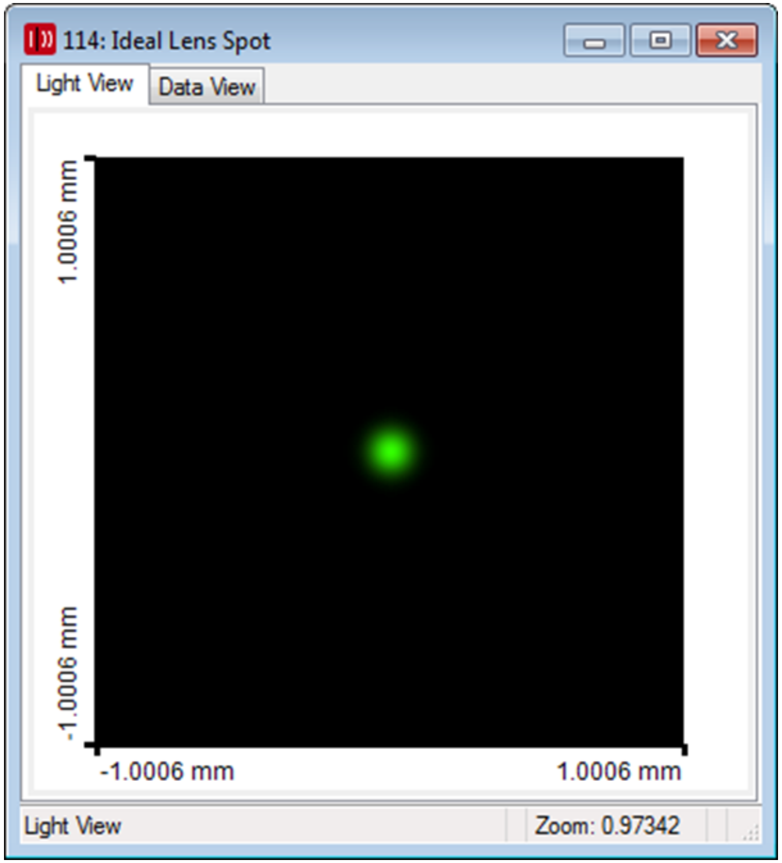

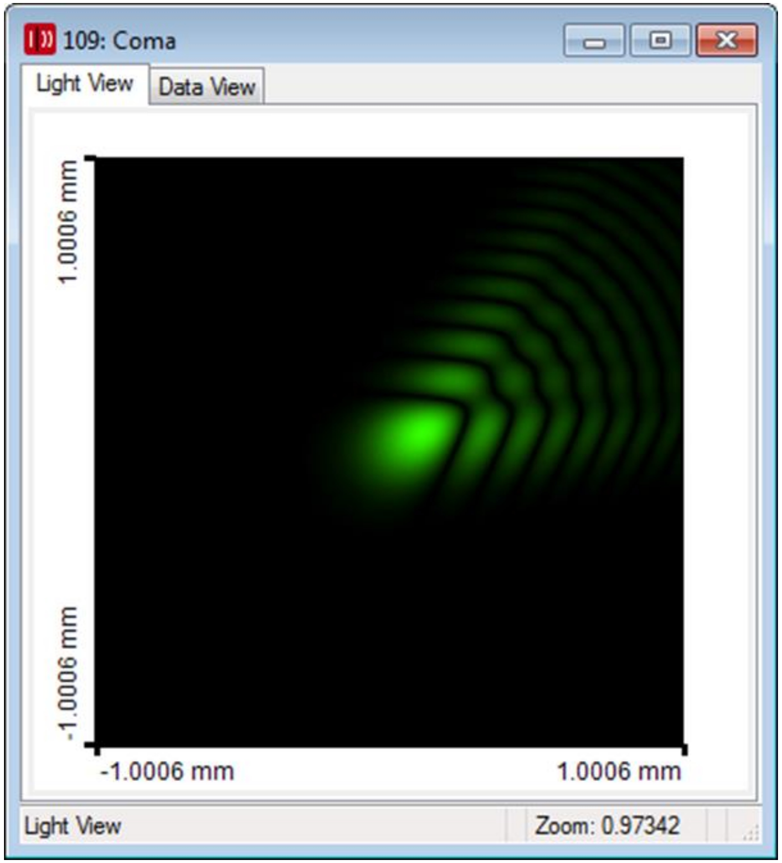

Ideal Lens vs. Mixed Aberration

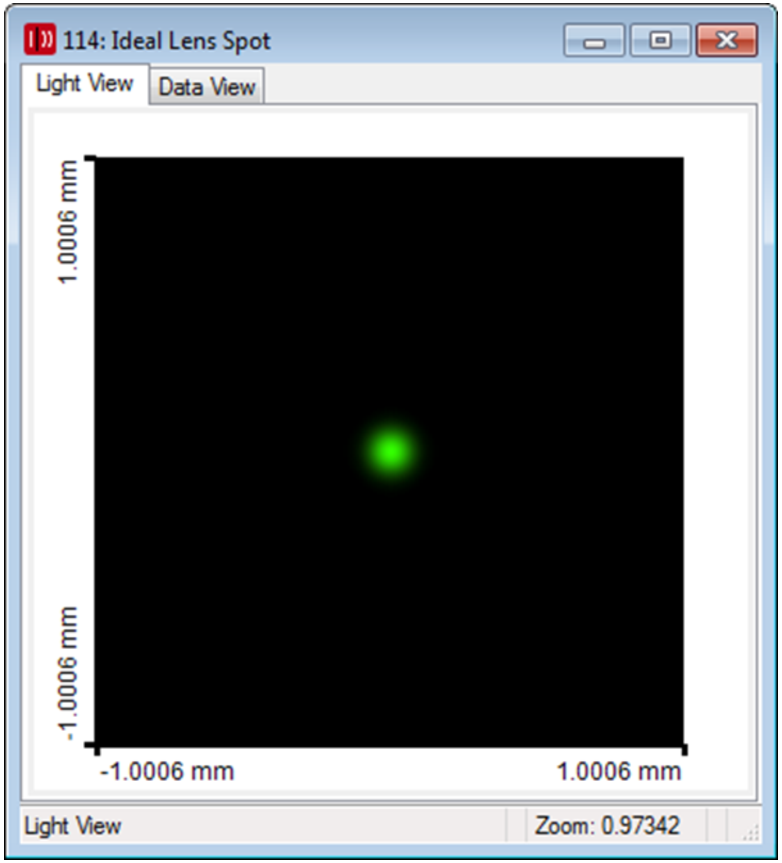

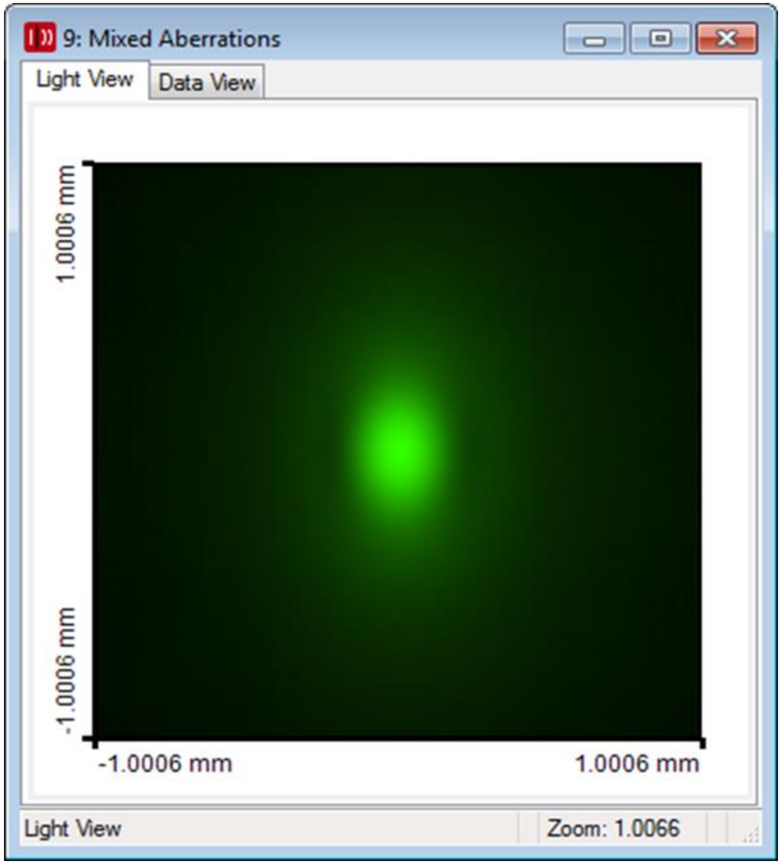

Conclusions for Beam Shaping

- Aberrations enlarge and reshape the focal spot of the ideal lens system

↓

- The focal spot of the ideal lens system must be
  - Smaller than the demanded shaped spot
  - Not bigger than the smallest feature in the shaped spot
- Designing a beam shaping system must always be started with selecting a lens system the NA of which enables the required focal spot size
- Remark: Aberrations of lens systems are allowed, because beam shaper can compensate that

Introduction of Aberrations

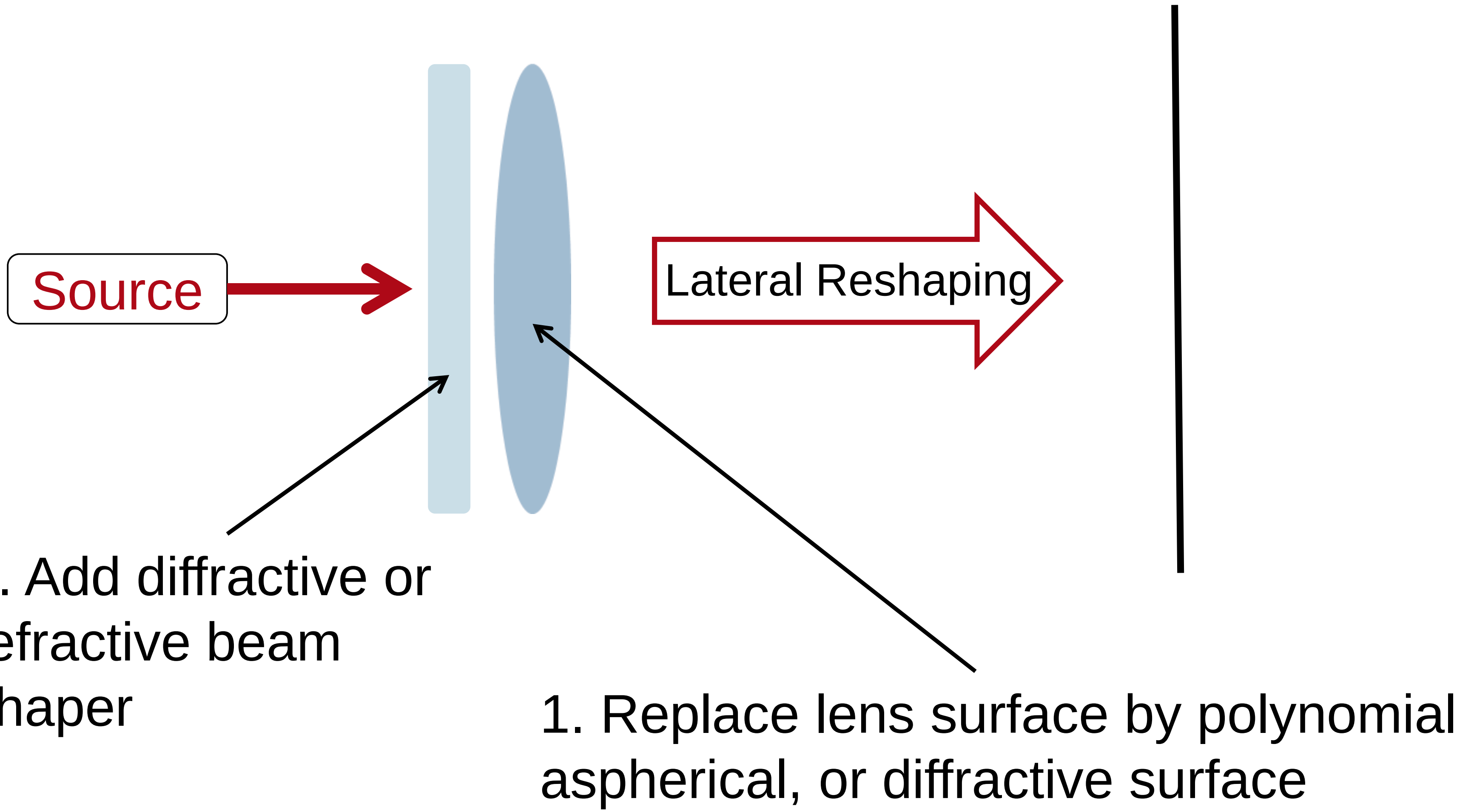

What Kind of Aberrations Are Needed?

- Dependent on the input beam and the required beam profile in the target plane aberrations must be introduced
- A basic approach to estimate the required aberrations for a given beam shaping problem is based on
  - Determination of geometrical distortion to redistribute energy
  - Calculation of phase function, which realizes the geometrical distortion

Geometrical Distortion Concept

Analytical beam shaping with application to laser-diode arrays

Harald Aagedal, Michael Schmid, Sebastian Egner, Jörn Müller-Quade, and Thomas Beth

Institut für Algorithmen und Kognitive Systeme, Universität Karlsruhe, Am Fasanengarten 5, D-76128 Karlsruhe, Germany

Frank Wyrowski

Institut für Angewandte Physik, Friedrich-Schiller-Universität, Max-Wien-Platz 1, D-07743 Jena, Germany

Vol. 14, No. 7/July 1997/J. Opt. Soc. Am. A 1549

Geometrical Distortion Concept

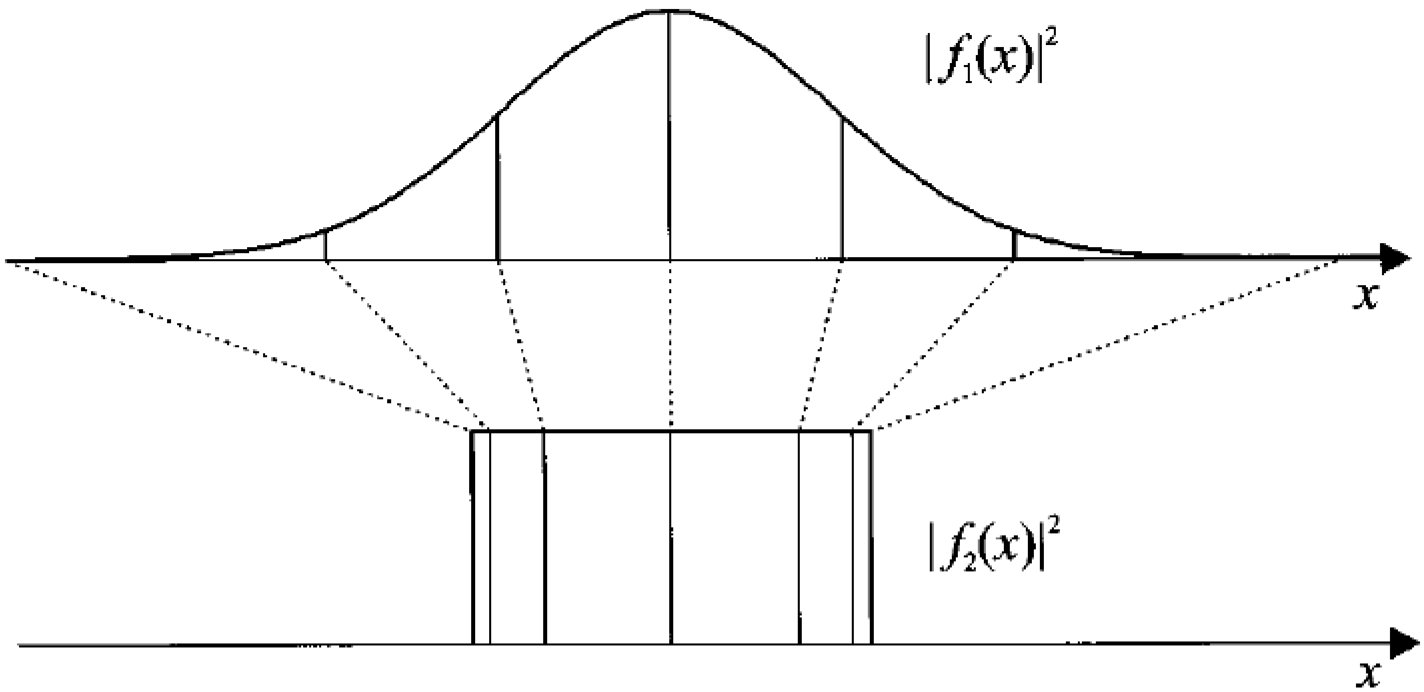

Fig. 1. Distortion transforming a Gaussian beam to a uniform distribution.

Vol. 14, No. 7/July 1997/J. Opt. Soc. Am. A 1549

Light Shaping > Refractive Optics

Design of a Refractive Beam Shaper to Generate a Circular Top-Hat

LightTrans International UG

Task Illustration

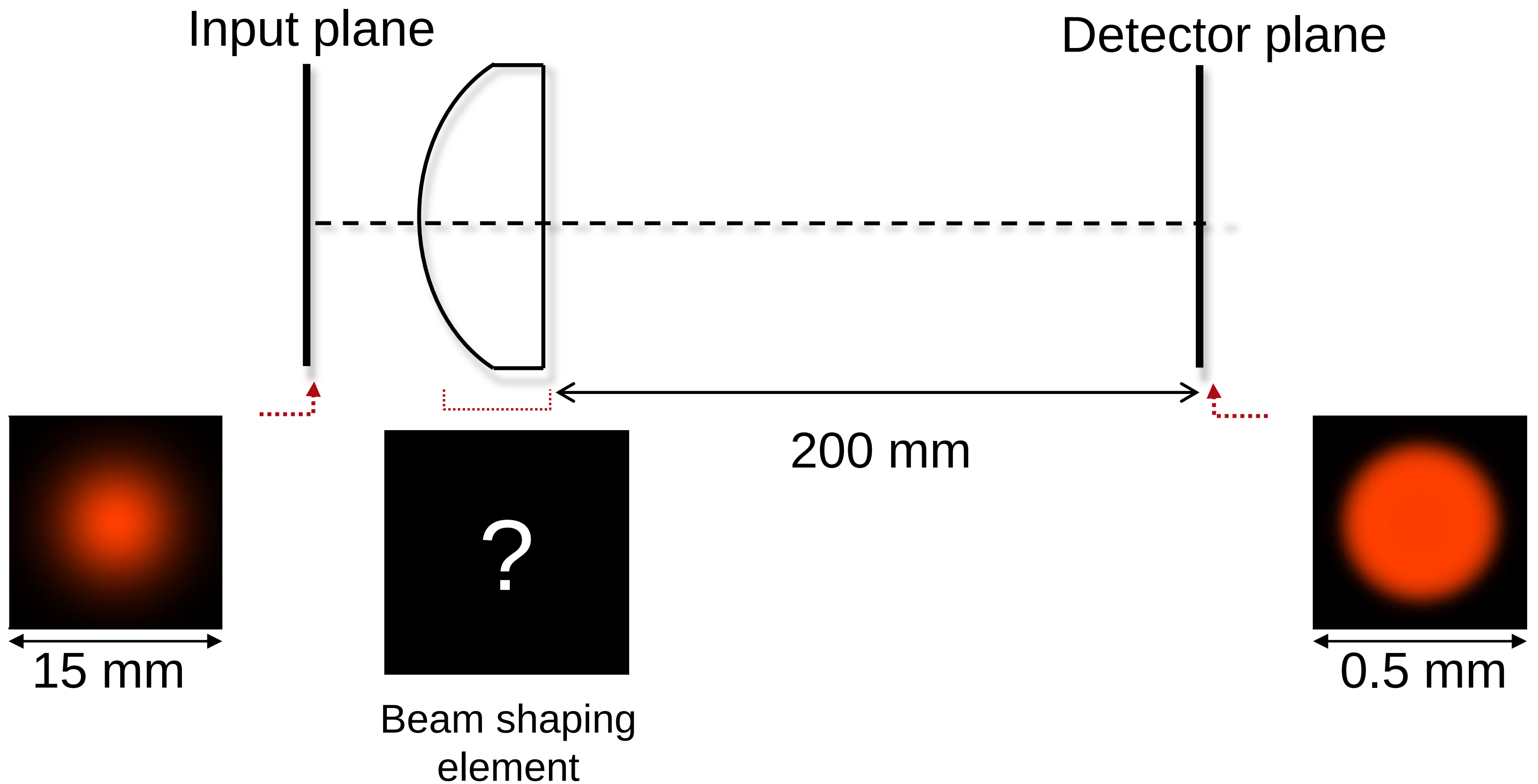

- Design a beam shaping element to shape a laser beam (fundamental mode) to a circular Top-Hat.

Specification: Light Source

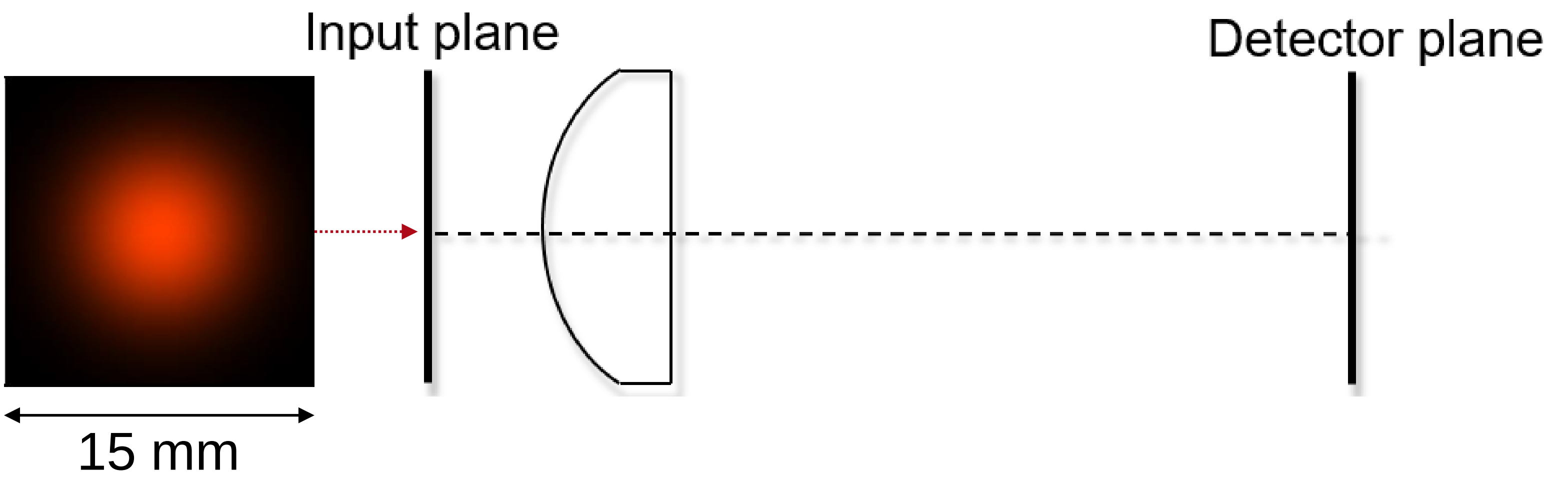

Parameter	Description / Value & Unit
type/number	Gaussian beam
coherence/mode	single Hermite Gaussian (0,0) mode
wavelength	632.8 nm
beam diameter ($1/e^2$)	8 mm x 8 mm

Specification: Beam Shaper Element

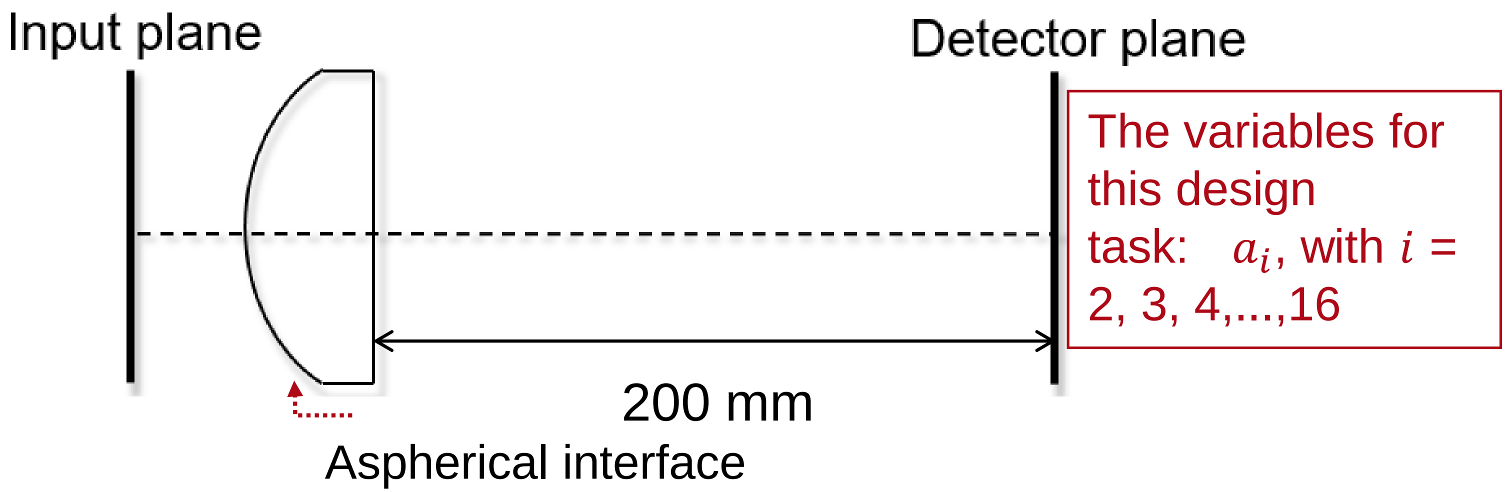

- Aspherical interface:

$$h(x, y) = \sum_i a_i r^i$$

with $r = \sqrt{x^2 + y^2}$ and i is polynormial order index

Parameter	Value & Unit
name/type	Aspherical lens
material	N-BK7
thickness	5 mm
size (diameter)	23 mm
Distance to detector	200 mm

Specification: Desired Pattern

Parameter	Description / Value & Unit
type/number	Top-Hat (Super-Gaussian Wave)
wavelength	632.8 nm
beam diameter ($1/e^2$)	400 µm x 400 µm
edge width	40 µm

Specifications: Merit Functions for Design

Parameter	Description / Value & Unit
conversion efficiency	> 90%
signal to Noise Radio (SNR)	> 22 dB
maximum relative intensity of stray light	< 10%

Specifications: Detector

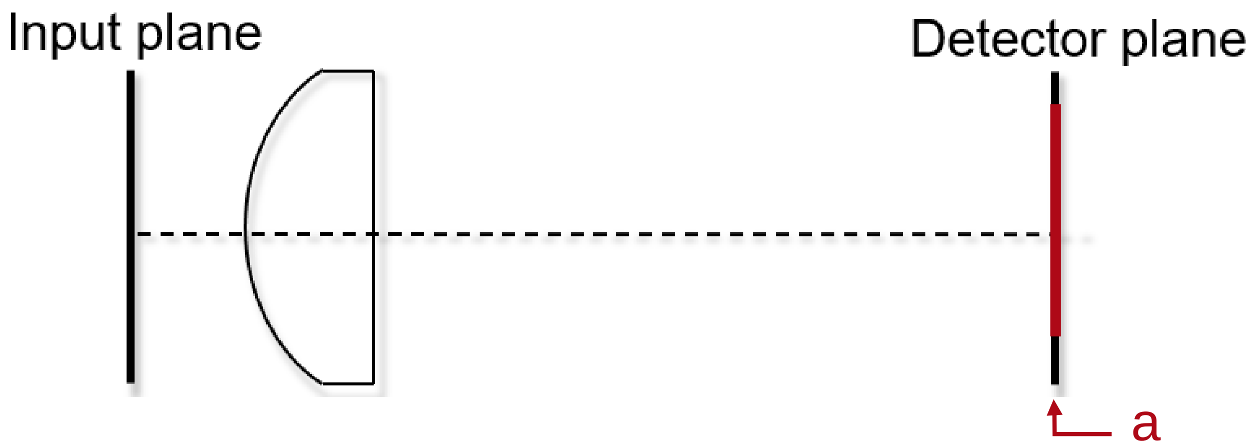

Position	Modeling Technique	Detector/Analyzer
a	field tracing	Intensity
b	field tracing	Value of merit functions

Optimization Process

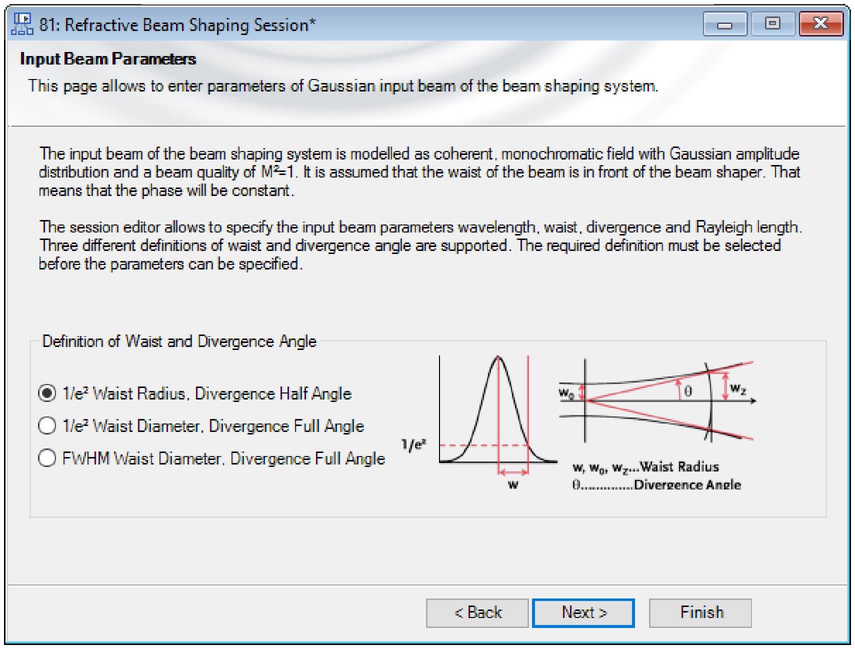

- Design Process is easily done by using the *Refractive Beam Shaping Session*.
  - Fill the parameters in illustration
  - Next!
- Click *Finish*, the beam shaper design is done immediately.

Design time → ~0.016 s !!!

* RO.0001_Refractive_Top_Hat_Beam_Shaper_Session_Editor.seditor

Results: Refractive Beam Shaper

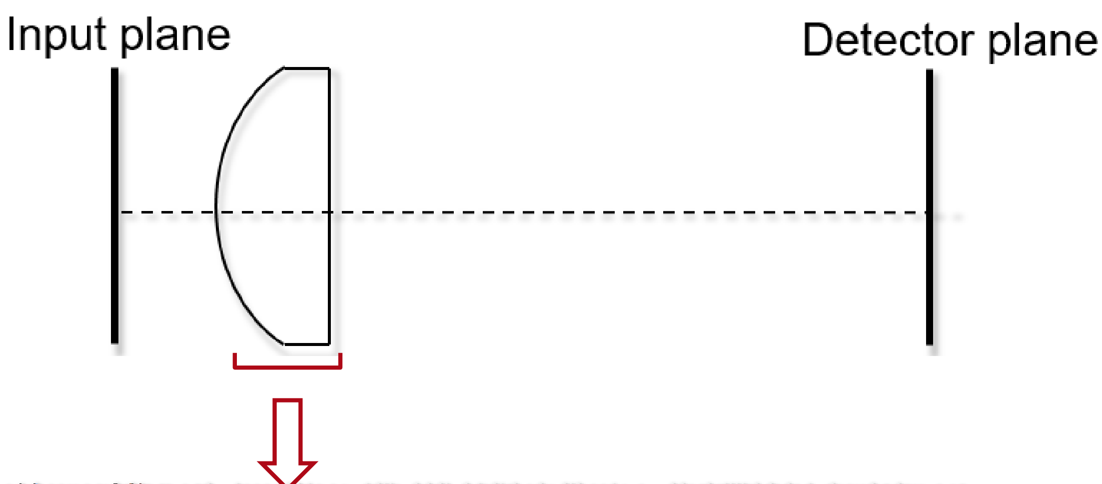

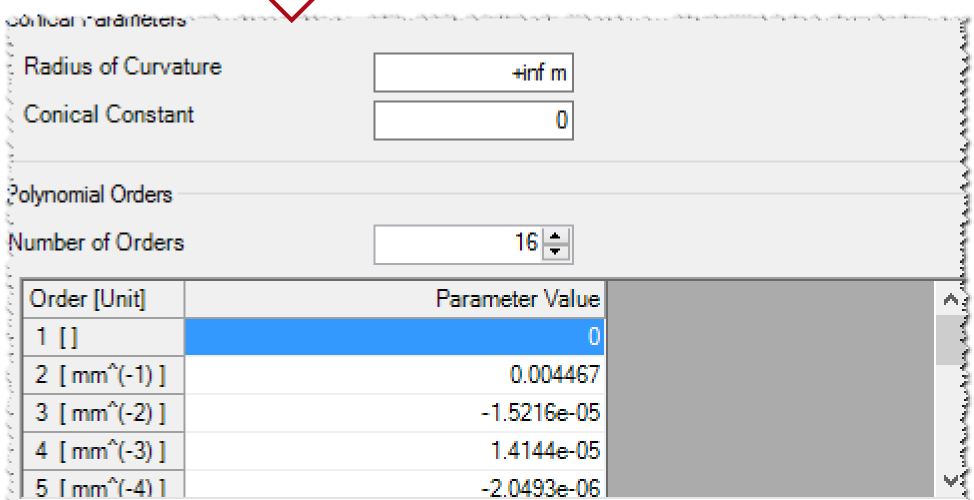

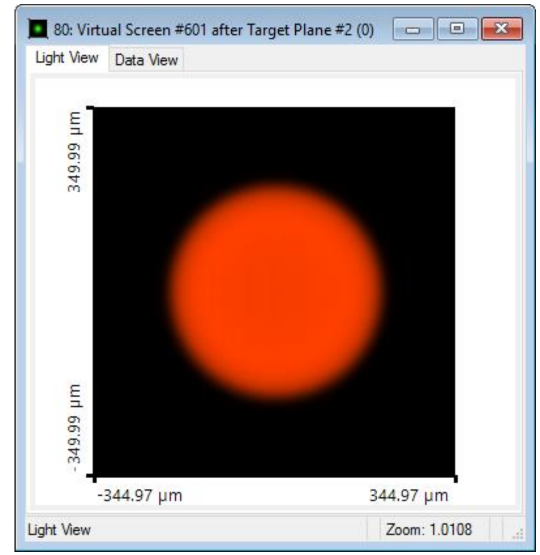

Parameter	Value & Unit
conversion efficiency	90.24%
SNR	22.353 dB
stray light	10.872%

*RO.0001_Refractive_Top_Hat_Beam_Shaper_LPD.lpd

Light Shaping > Refractive Optics

Modeling of a Refractive Beam Shaper with Measured Height Profile

LightTrans International UG

Task/System Illustration

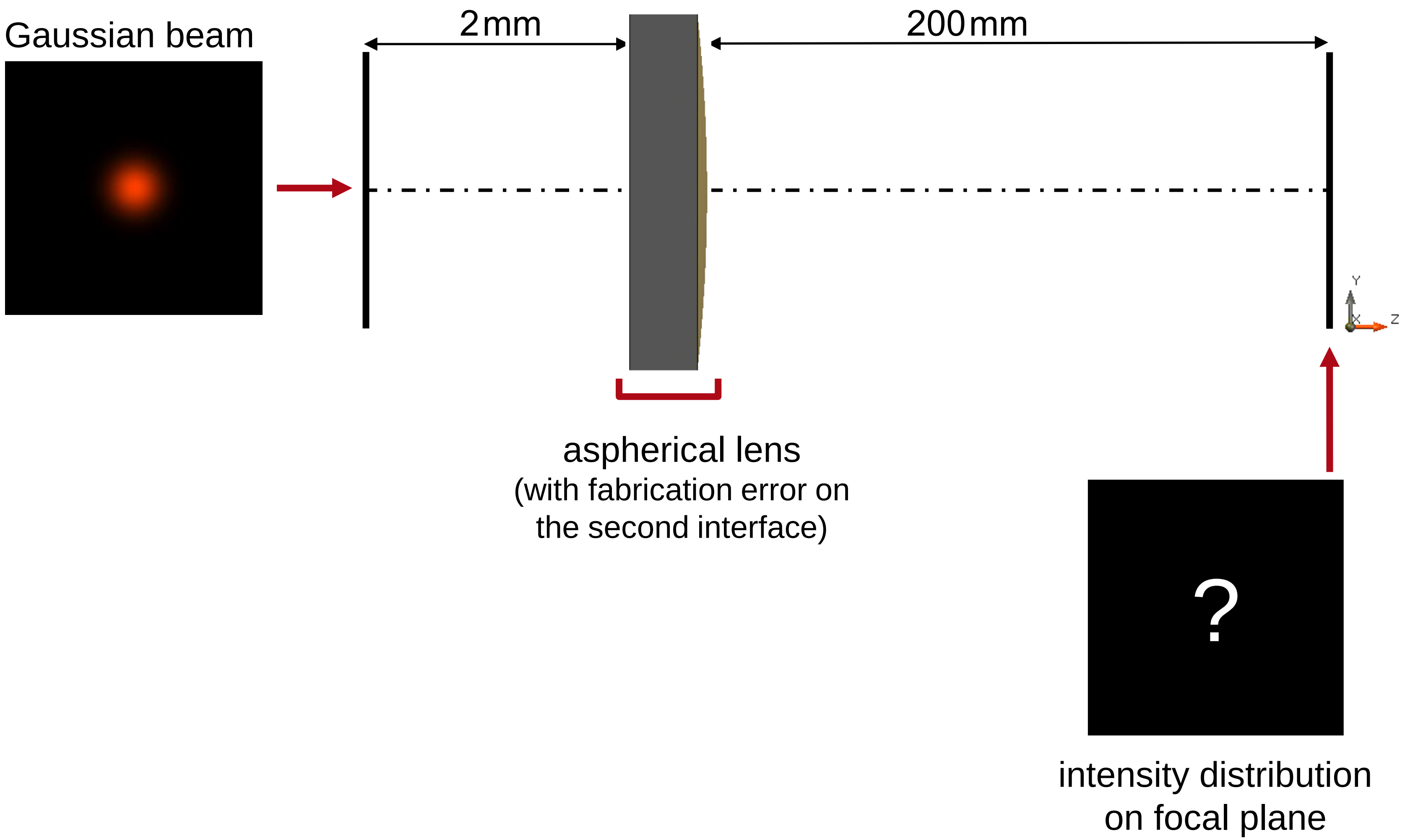

Highlights

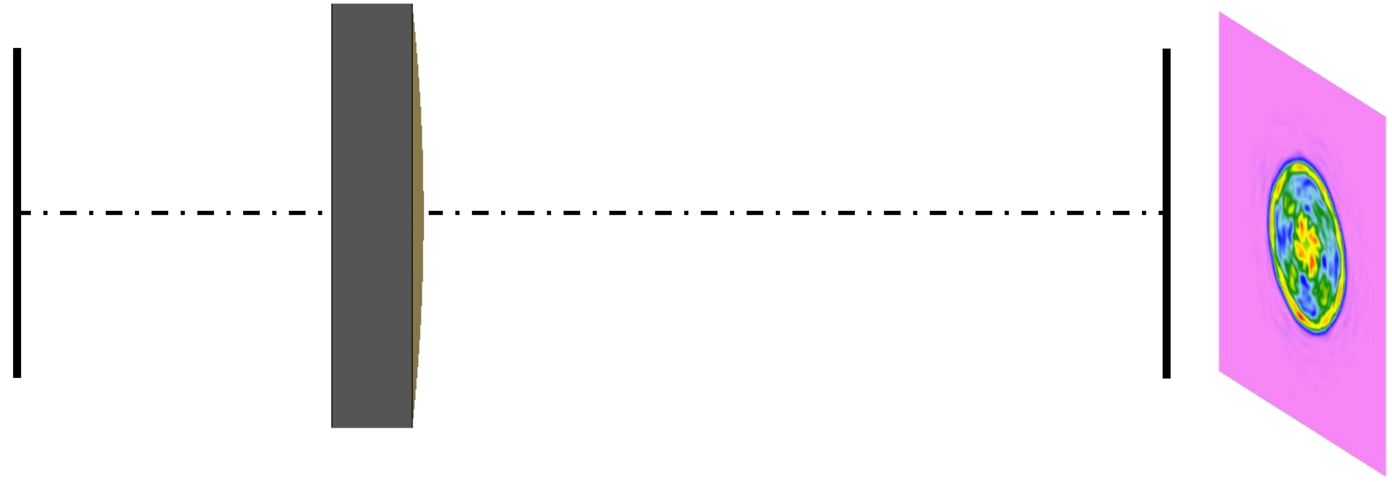

- simulation of fabrication tolerances by importing measurement data of height profiles

Specification: Light Source

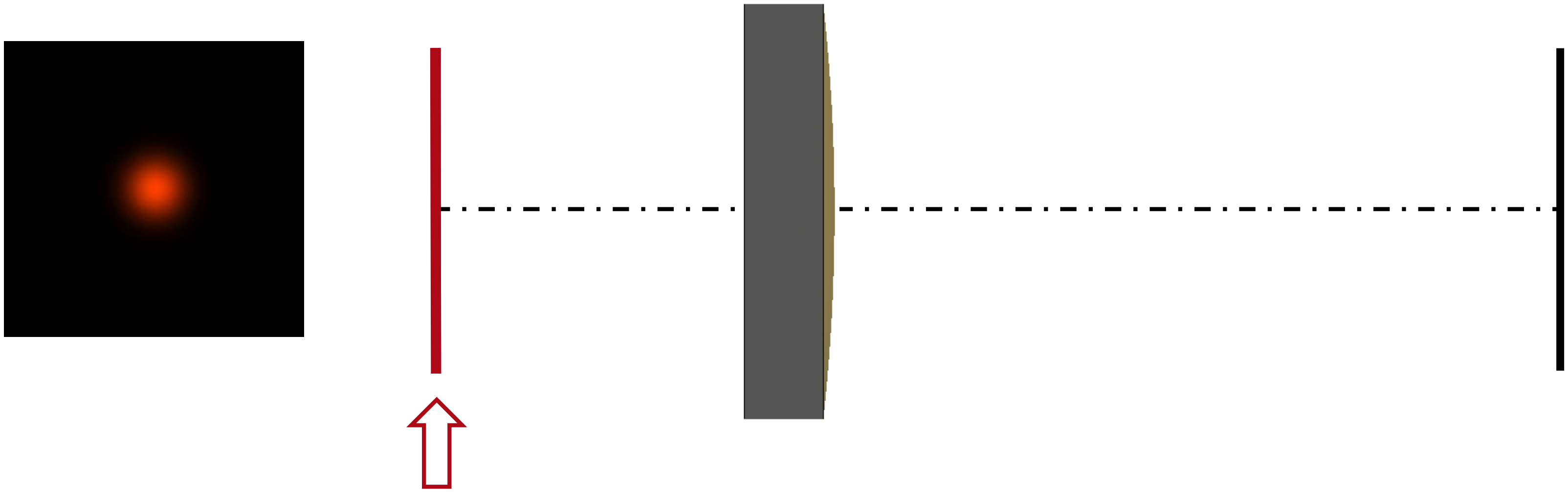

Parameter	Description / Value & Unit
type/number	Gaussian beam
coherence/mode	single Hermite Gaussian (0,0) mode
wavelength	632.8 nm
polarization	linear in x-direction (0°)
waist radius (1/e^2)	4 mm × 4 mm

Specification: Focusing Asphere

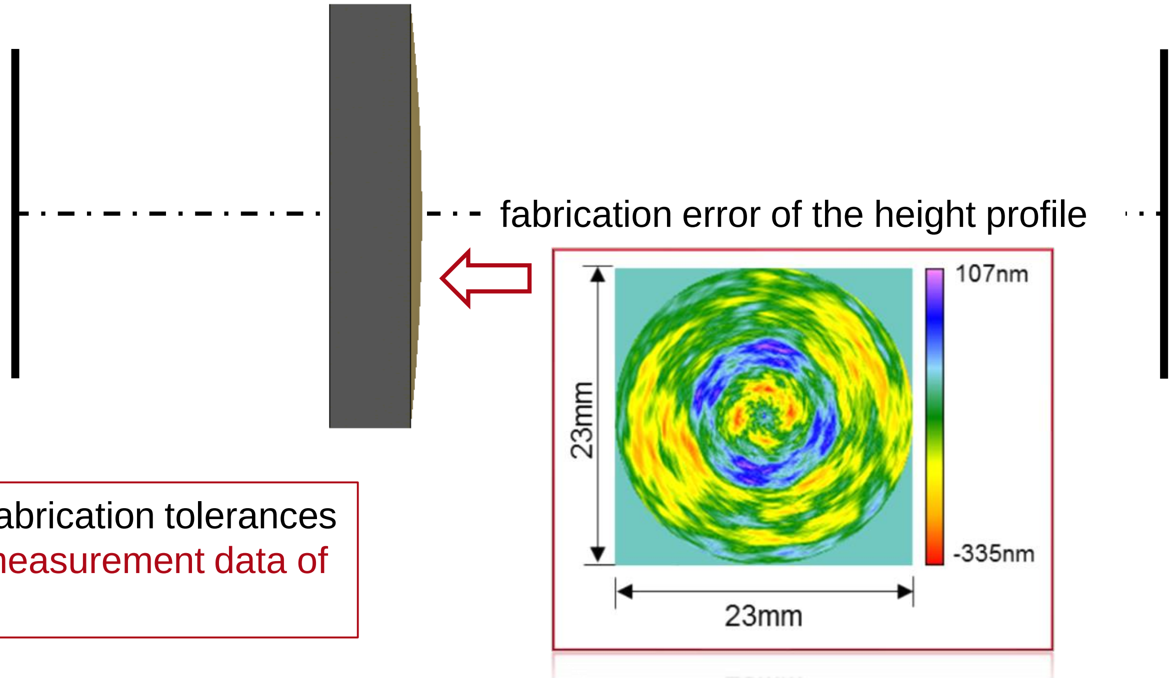

Highlights

- simulation of fabrication tolerances by importing measurement data of height profiles

Parameter	Value & Unit
name/type	convex-plano aspherical lens
first interface	plane interface
second interface	aspherical interface with measured height profile error
material (M)	N-BK7

Specification: Detectors

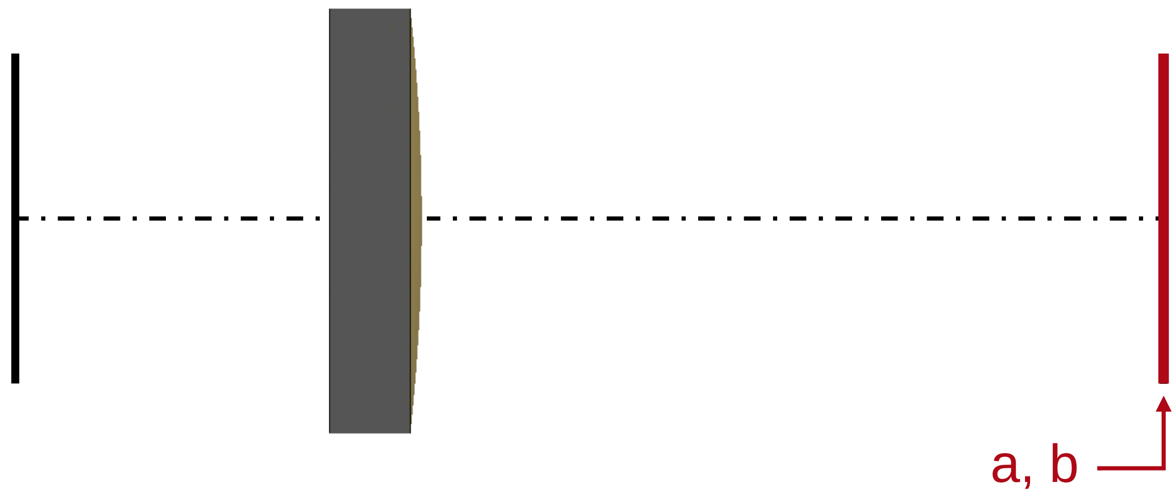

Position	Modeling Technique	Detector/Analyzer
a	field tracing	intensity distribution
b	field tracing	merit function detector

Results: Intensity Distribution

Highlights

- simulation of fabrication tolerances by importing measurement data of height profiles

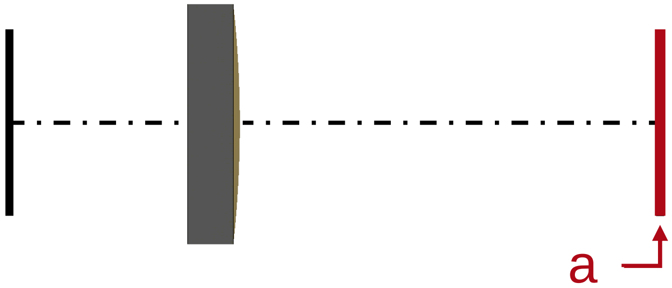

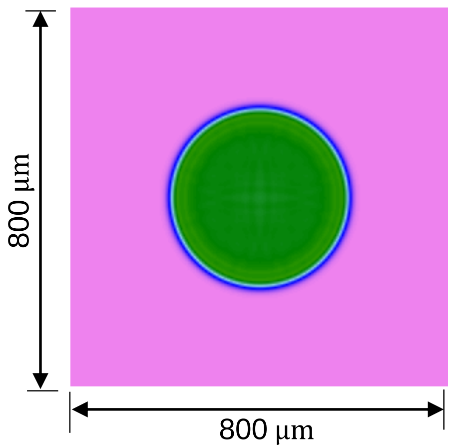

intensity of field at focal plane (without fabrication tolerances)

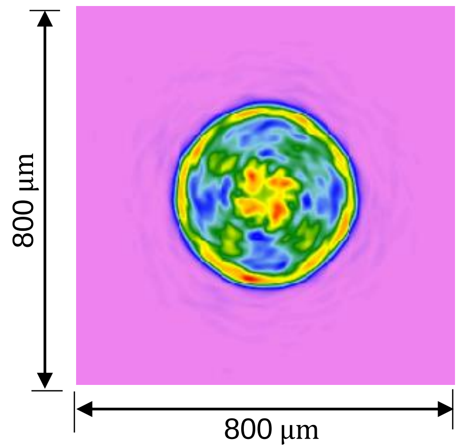

intensity of field at focal plane (with fabrication tolerances)

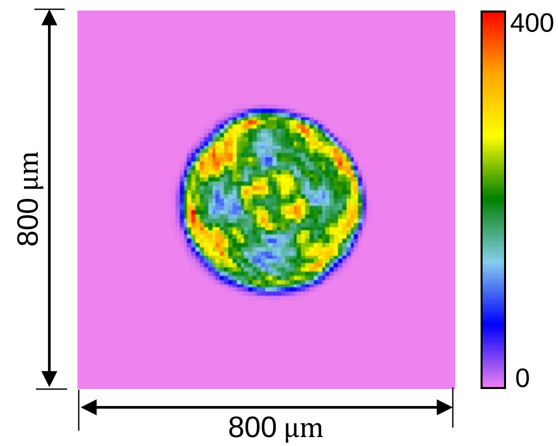

measured intensity at focal plane (with fabrication tolerances)

Results: Merit Function Detector

Highlights

- simulation of fabrication tolerances by importing measurement data of height profiles

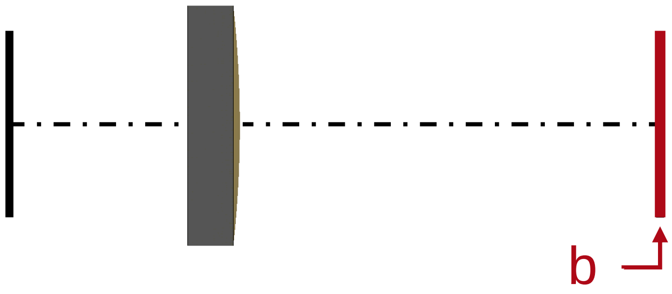

Detector/Analyzer	Result (without fabrication error)	Result (with fabrication error)
signal-to-noise ratio (SNR)	26.49 dB	14.66 dB
conversion efficiency	91.21%	87.15%
uniformity error	93.65%	99.73%

Modeling Task

Diffractive Beam shaper
Diameter: 2 × 2 mm
Phase Levels: 16

Target
Plane

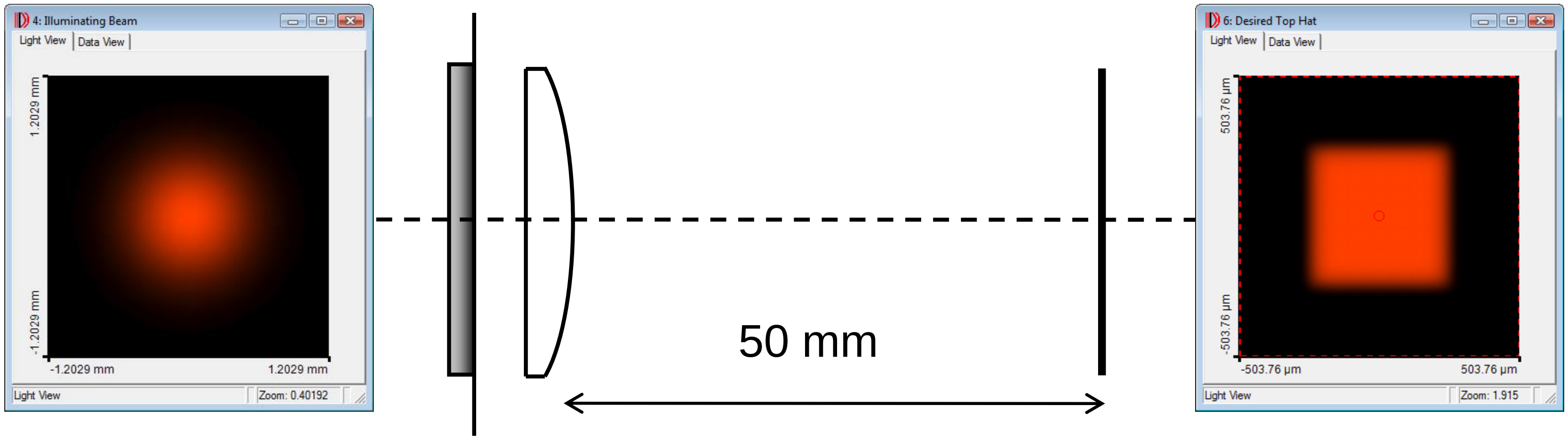

Illuminating Beam
Intensity

1f-Setup
Focal Length f=50 mm

Top Hat Intensity
(free of speckles)

Modeling Task

- The following tolerances of the system are to be analyzed.
- The ± tolerance values are regarded as 3-times ± the standard deviation σ.

Varied Parameters	**Value and Tolerances**
Waist Radius of Input Beam	(500 ± 25) µm
Etching Depths of all 4 Binary Masks	± 2 % of original height
x-Position of Beam Shaper	(0 ± 10) µm
y-Position of Beam Shaper	(0 ± 10) µm
Focal Length of Lens	(50 ± 0.5) mm

Simulation of Alignment Tolerances

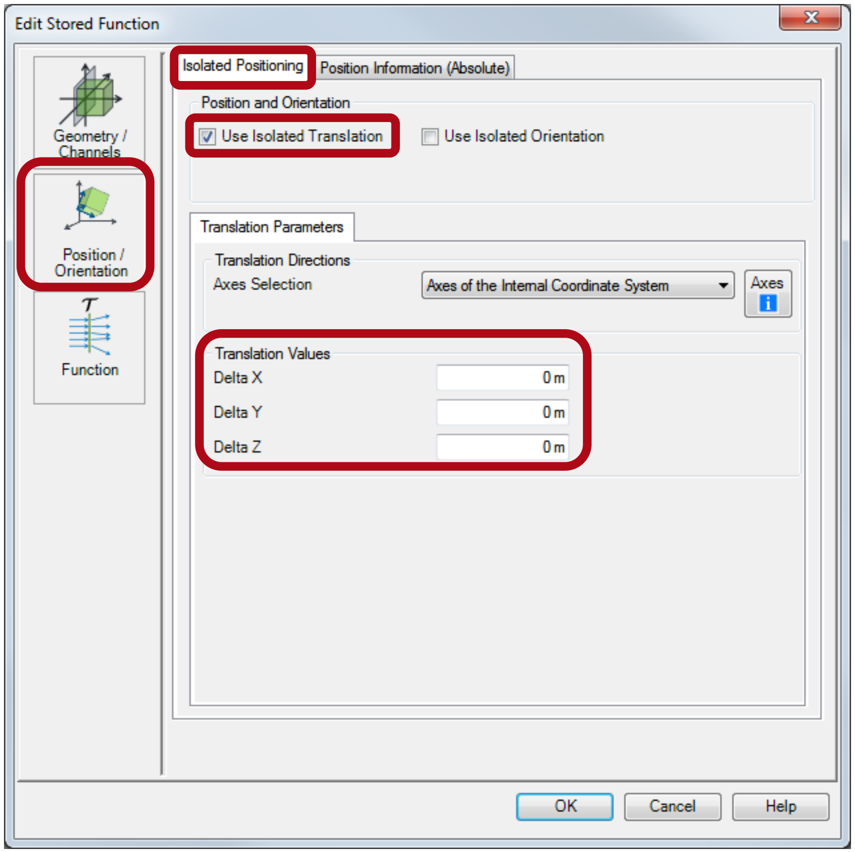

- Simulation of shift tolerances must be activated on *Tolerancing* page of *Stored Function* component and *Target Plane* component.
- Tolerance values are varied by *Parameter Run.* The values set in the component dialog are ignored.

Simulation of Etching Depth Tolerances

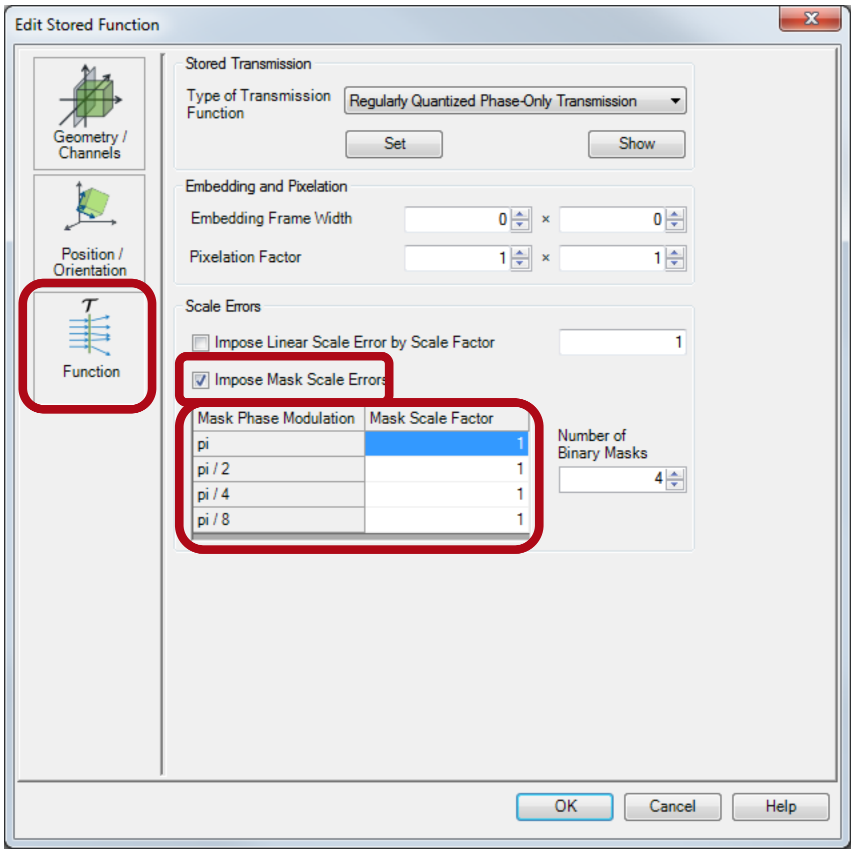

- Simulation of mask etching depth errors must be activated on *Function* page of *Stored Function* component.
- Tolerance values are varied by *Parameter Run*. The respective settings in the component dialog are ignored.
- A tolerance value of 1 represents an optimum etching depth.

Single Parameter Variation

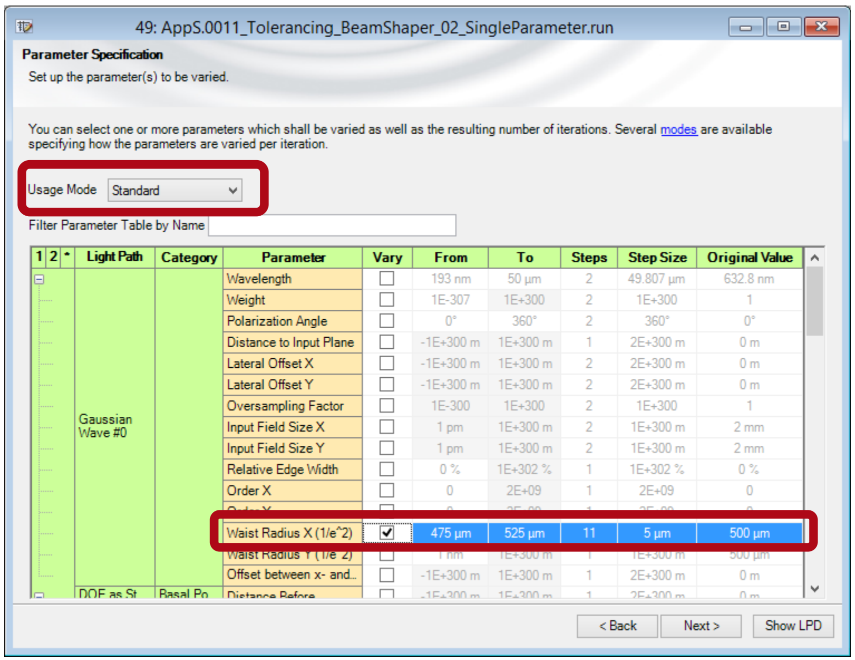

- The laser beam radius has typically a strong influence on the optical performance of a beam shaping system.
- The *Usage Mode: Standard* must be selected for the variation of a single parameter.
- *Waist Radius X* parameter must be selected.

Single Parameter Variation

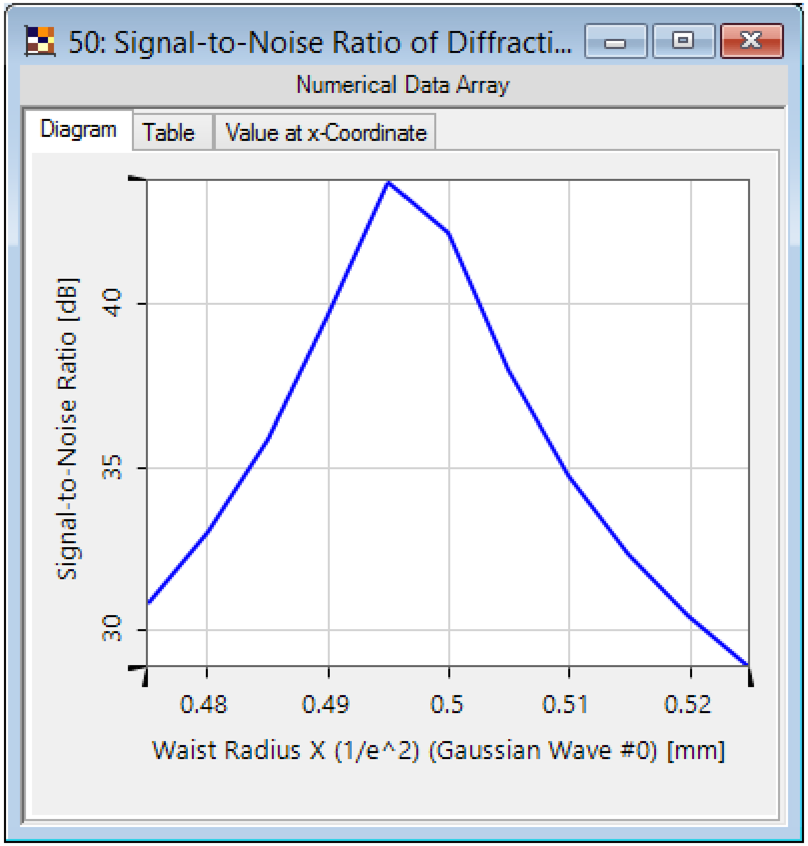

- The beam shaping system shows a strong sensitivity for a variation of the laser beam radius.
- The Signal to Noise Ratio (SNR) will drop to 28.8dB.

Monte-Carlo Simulation

Random mode for Monte Carlo simulation

Parameter Variation has a *Normal Distribution* with a certain standard deviation σ

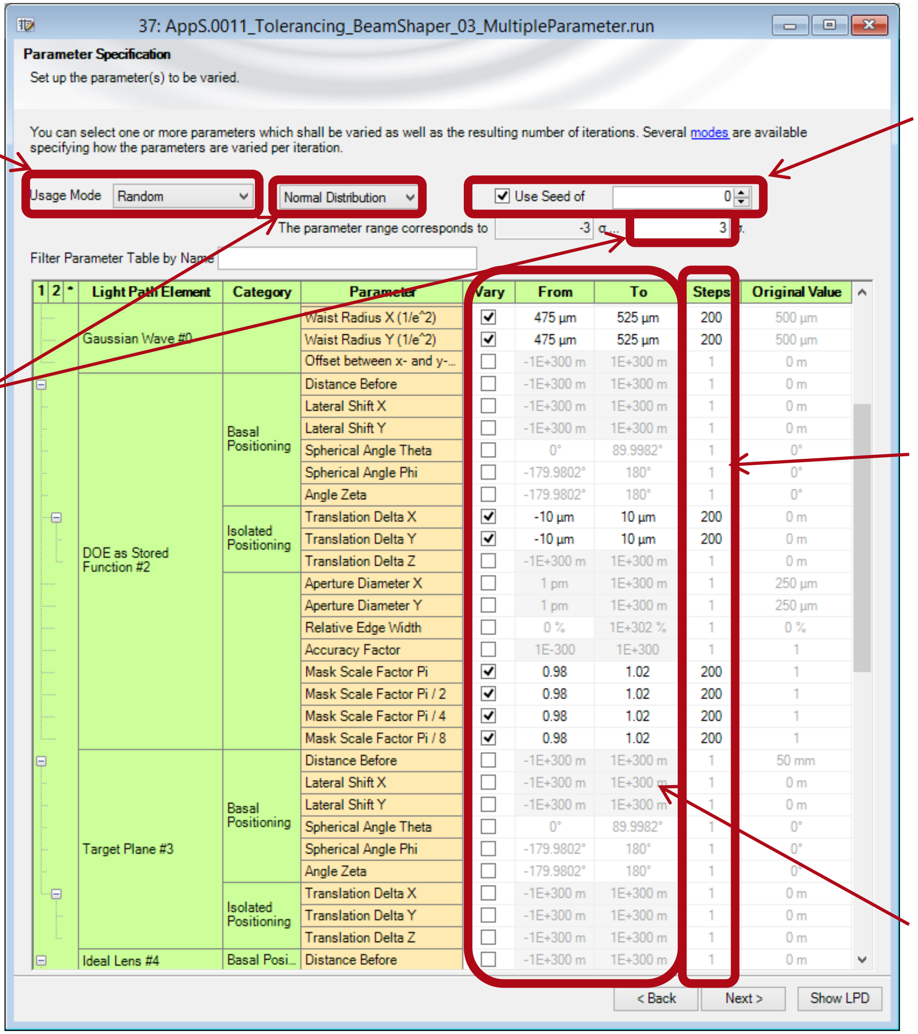

Light Path Element	Category	Parameter	Vary	From	To	Steps	Original Value
Gaussian Wave #0		Waist Radius X (1/e^2)	✓	475 µm	525 µm	200	500 µm
		Waist Radius Y (1/e^2)	✓	475 µm	525 µm	200	500 µm
		Offset between x- and y-...		-1E+300 m	1E+300 m	1	0 m
DOE as Stored Function #2	Basal Positioning	Distance Before		-1E+300 m	1E+300 m	1	0 m
		Lateral Shift X		-1E+300 m	1E+300 m	1	0 m
		Lateral Shift Y		-1E+300 m	1E+300 m	1	0 m
		Spherical Angle Theta		0°	89.9982°	1	0°
		Spherical Angle Phi		-179.9802°	180°	1	0°
		Angle Zeta		-179.9802°	180°	1	0°
	Isolated Positioning	Translation Delta X	✓	-10 µm	10 µm	200	0 m
		Translation Delta Y	✓	-10 µm	10 µm	200	0 m
		Translation Delta Z		-1E+300 m	1E+300 m	1	0 m
		Aperture Diameter X		1 pm	1E+300 m	1	250 µm
		Aperture Diameter Y		1 pm	1E+300 m	1	250 µm
		Relative Edge Width		0 %	1E+302 %	1	0 %
		Accuracy Factor		1E-300	1E+300	1	1
		Mask Scale Factor Pi	✓	0.98	1.02	200	1
		Mask Scale Factor Pi / 2	✓	0.98	1.02	200	1
		Mask Scale Factor Pi / 4	✓	0.98	1.02	200	1
		Mask Scale Factor Pi / 8	✓	0.98	1.02	200	1
Target Plane #3	Basal Positioning	Distance Before		-1E+300 m	1E+300 m	1	50 mm
		Lateral Shift X		-1E+300 m	1E+300 m	1	0 m
		Lateral Shift Y		-1E+300 m	1E+300 m	1	0 m
		Spherical Angle Theta		0°	89.9982°	1	0°
		Spherical Angle Phi		-179.9802°	180°	1	0°
		Angle Zeta		-179.9802°	180°	1	0°
	Isolated Positioning	Translation Delta X		-1E+300 m	1E+300 m	1	0 m
		Translation Delta Y		-1E+300 m	1E+300 m	1	0 m
		Translation Delta Z		-1E+300 m	1E+300 m	1	0 m
Ideal Lens #4	Basal Posi...	Distance Before		-1E+300 m	1E+300 m	1	0 m

A Seed can be used for reproducible results of the 'random' series.

Total number of variations

Minimum and maximum value of all tolerances defined by $\pm 3\sigma$

Monte-Carlo Simulation

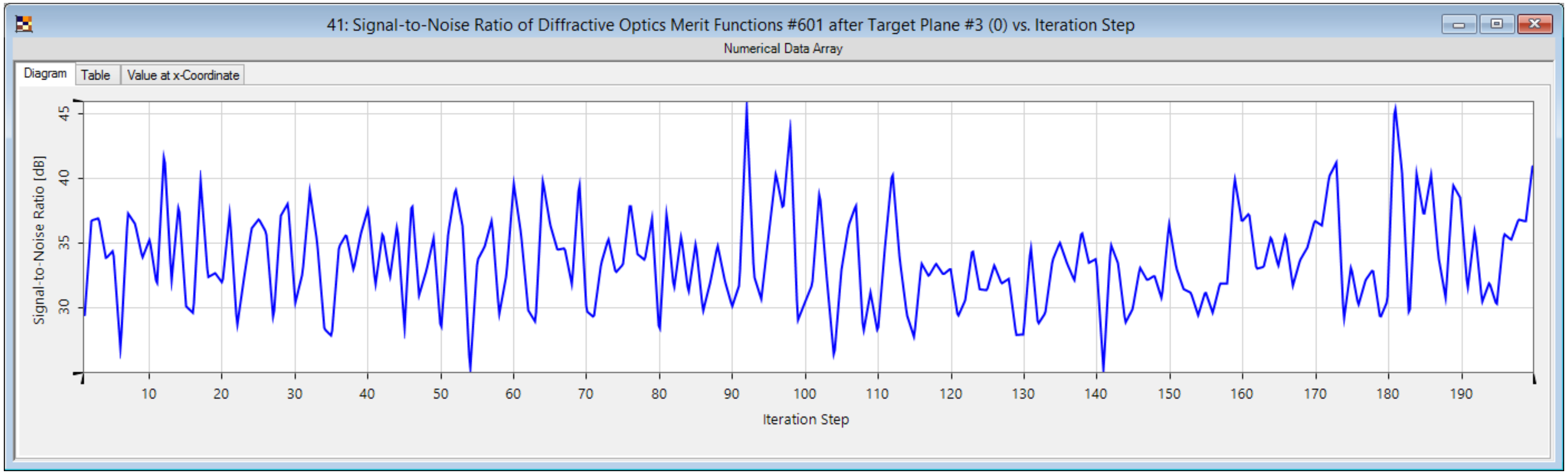

- Variation of the SNR depending on the random parameter set.
- The minimum SNR can be found from the diagram via the menu entry Detectors > Minimum.
- Minimum SNR: 24.9 dB
- Average SNR: 33.7 dB

Resulting Field Distributions

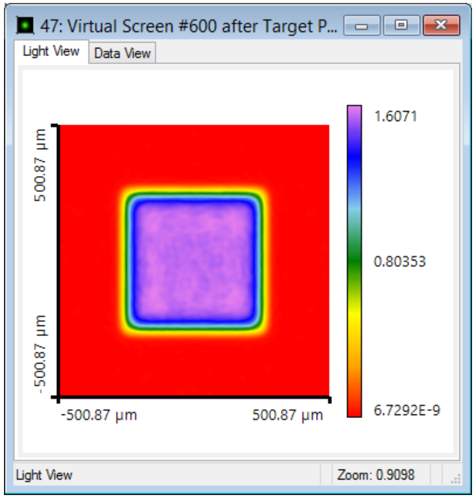

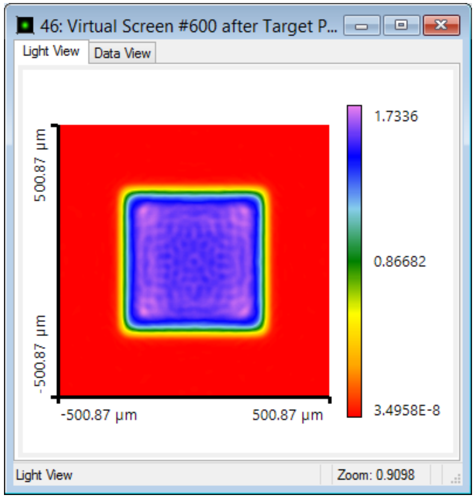

- Left: Ideal output intensity (SNR = 42.2 dB).
- Right: Light pattern with lowest SNR (SNR = 24.9 dB)
- Export of Monte-Carlo simulation results to external software (for example Microsoft Excel) allows further statistical evaluations.

Fast Physical Optics: Freeform Surfaces

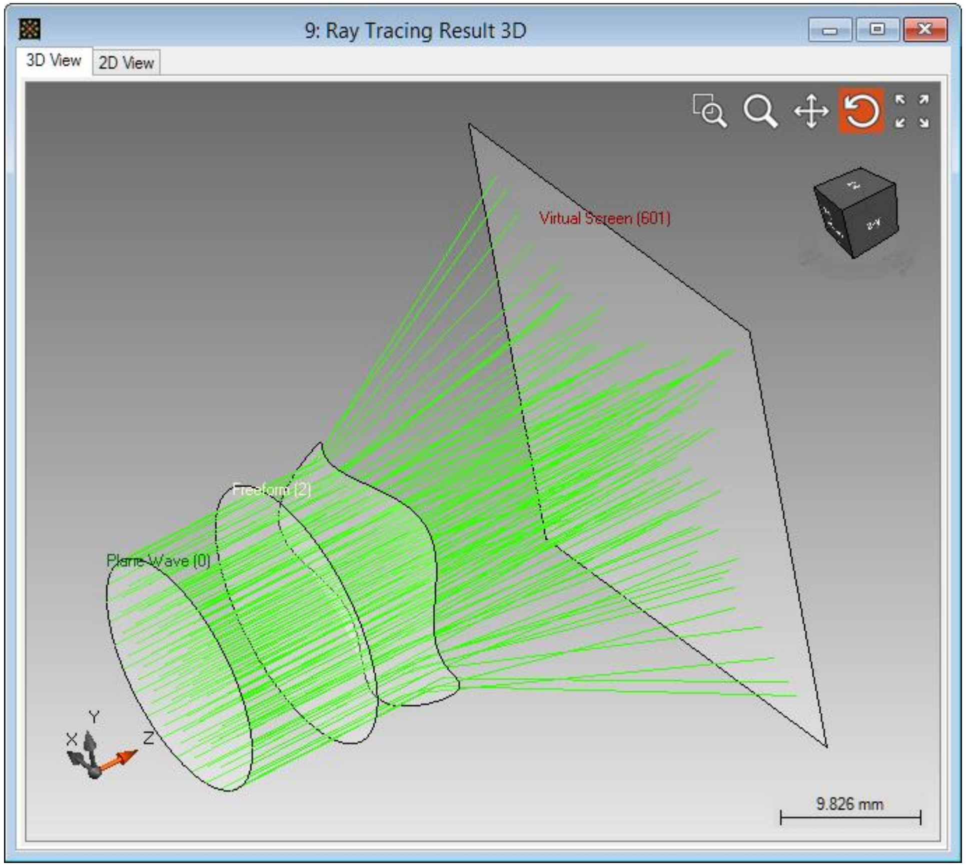

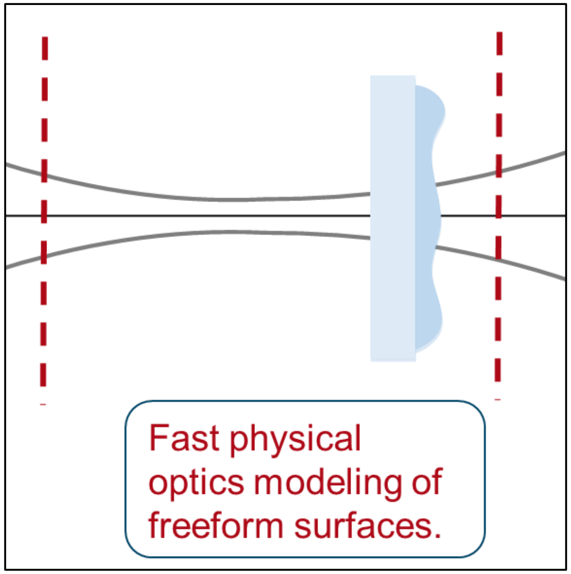

Fast Physical Optics: Freeform Surfaces

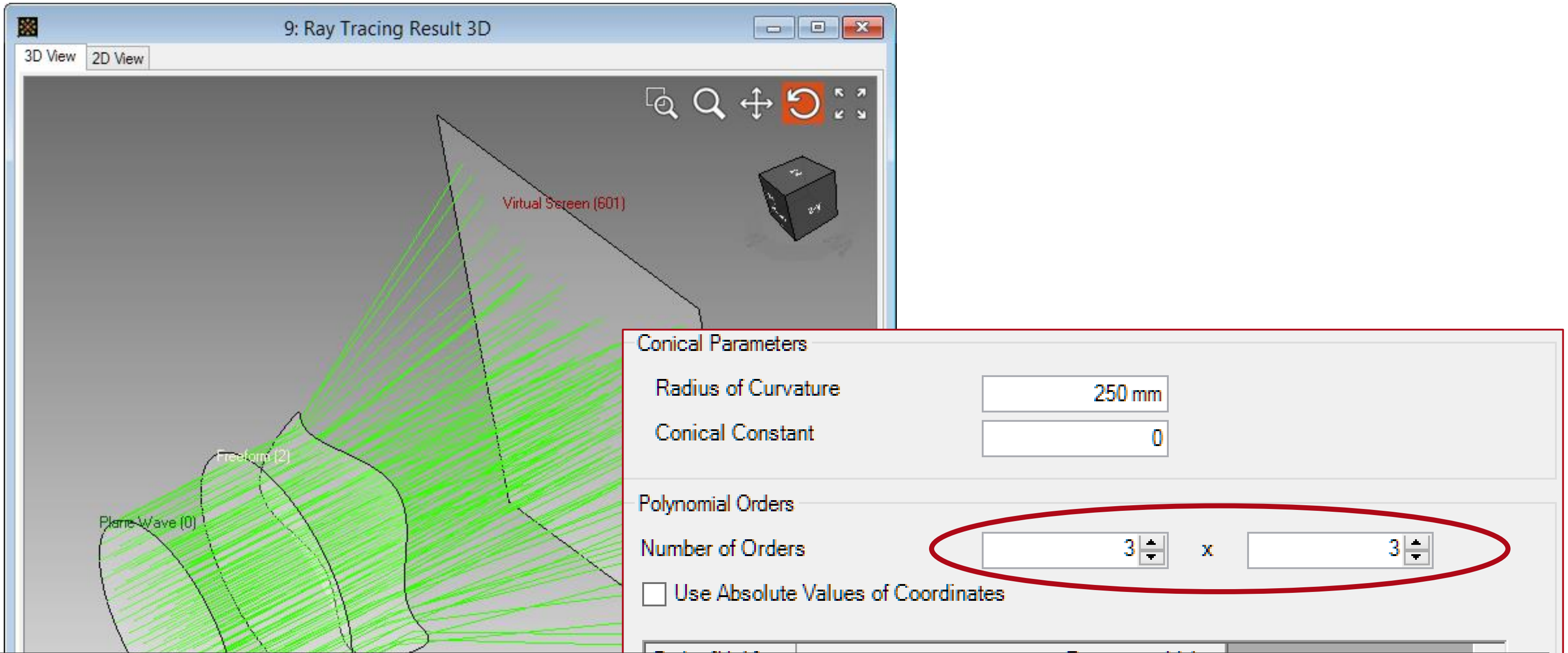

	Iteration Step	1	2	3	4	5	6	7
1	(2,0) [mm^(-1)] (Freeform #2 | Polynomial Interface #1)	0.0024274	0.0031541	0.0041695	0.00035002	0.003082	0.0024793	0.0025
2	(2,1) [mm^(-2)] (Freeform #2 | Polynomial Interface #1)	0.0013393	-0.0017223	0.0020993	0.0010653	-0.0014089	0.0017305	0.0007
3	(0,2) [mm^(-1)] (Freeform #2 | Polynomial Interface #1)	0.0027923	0.0029335	0.[illegible]	[illegible]	[illegible]	0.0020482	0.00016
4	(1,2) [mm^(-2)] (Freeform #2 | Polynomial Interface #1)	-0.00051556	-9.0126E-05	-0[illegible]	[illegible]	[illegible]	-0.0010599	-0.002
5	(2,2) [mm^(-3)] (Freeform #2 | Polynomial Interface #1)	0.00016179	0.00013574	0.00012223	0.00017955	0.00039437	4.0504E-05	0.0001
6	Distance Before (Virtual Screen #601 | Basal Positioning)	21.823 mm	25.564 mm	23.586 mm	23.353 mm	26.147 mm	29.382 mm	24.86

50 simulations

Fast Physical Optics: Freeform Surfaces

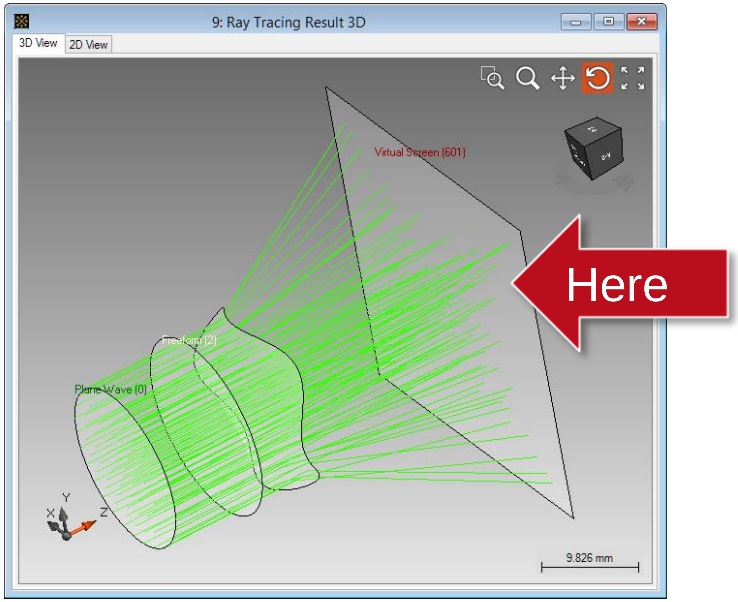

Amplitude $E_x(x,y)$

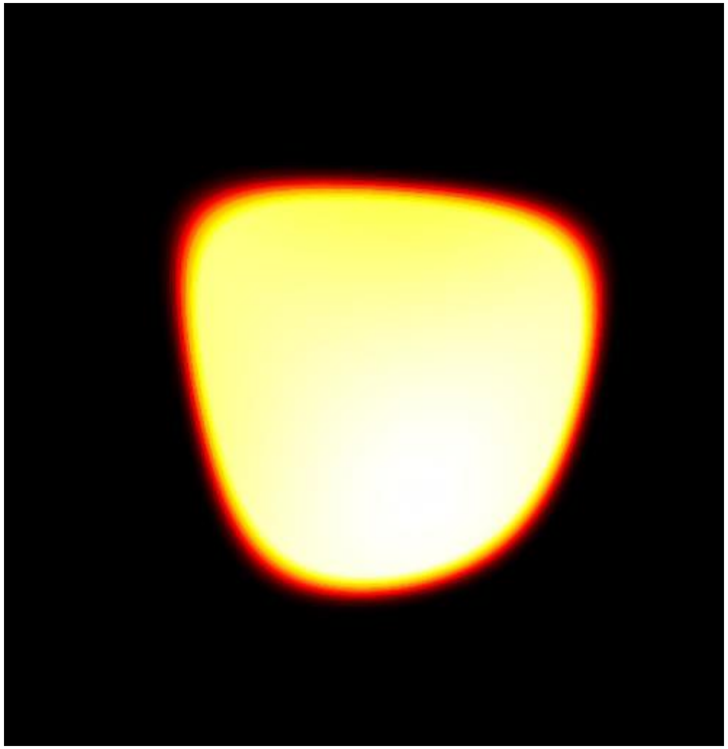

cpu time per simulation < 1 sec

Freeform: Field Tracing

Input: Gaussian beam
Diameter 10 mm

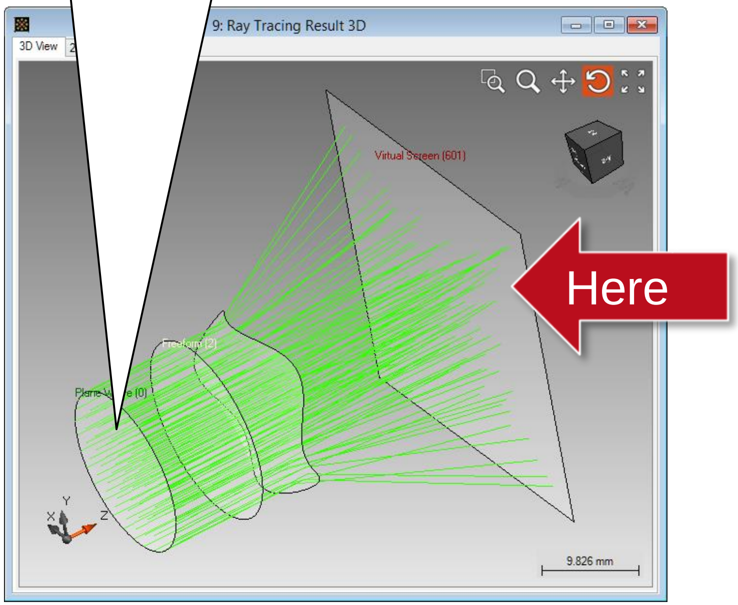

Amplitude $E_x(x,y)$

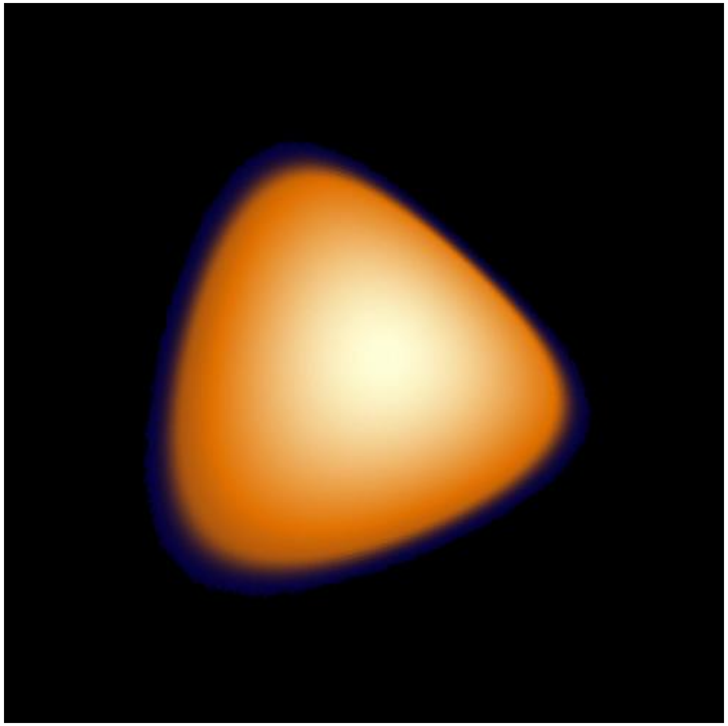

cpu time per simulation < 1 sec

Geometrical Distortion Concept

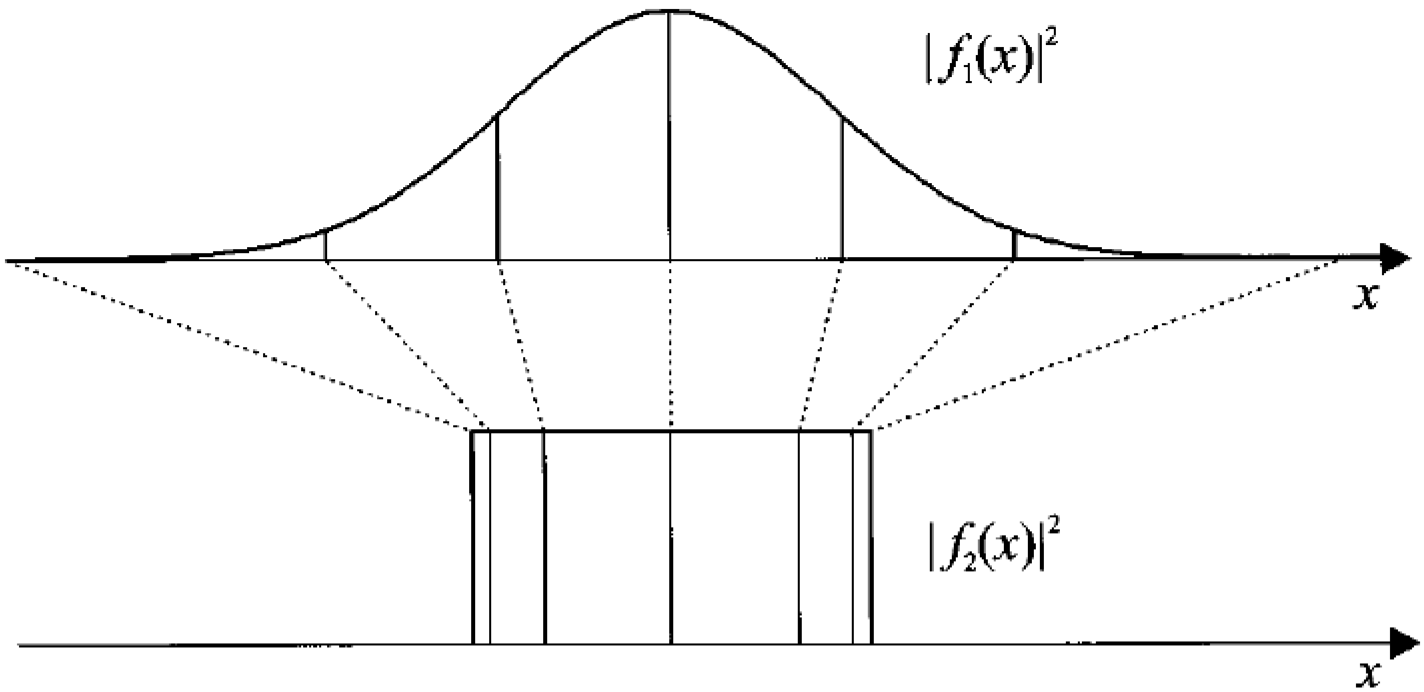

Fig. 1. Distortion transforming a Gaussian beam to a uniform distribution.

Vol. 14, No. 7/July 1997/J. Opt. Soc. Am. A 1549

Laser Beam Shaping: R&D

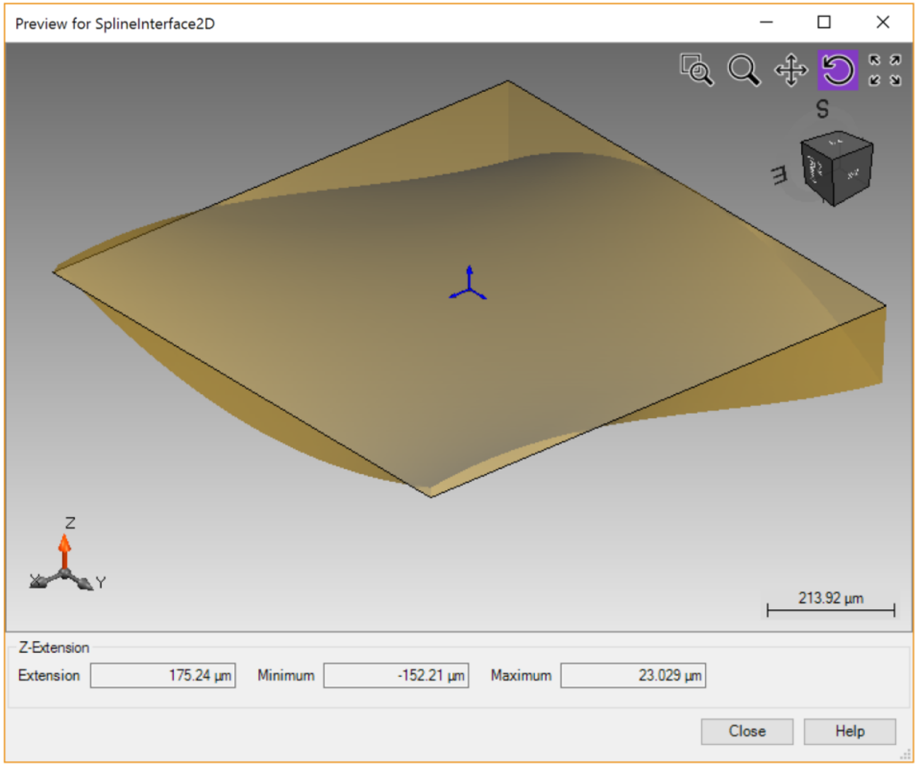

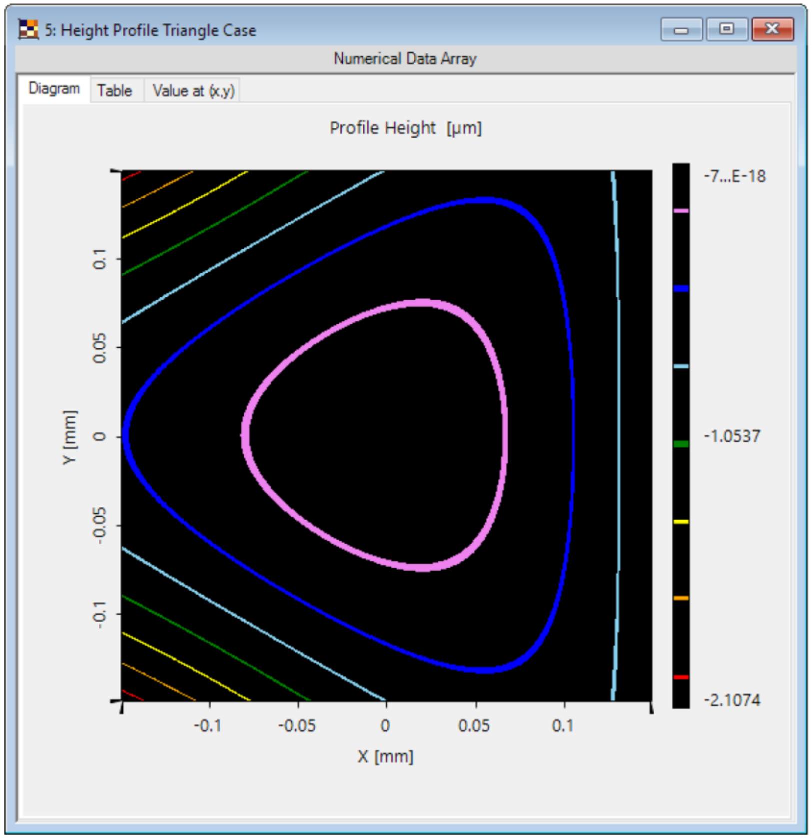

Laser Beam Shaping: R&D

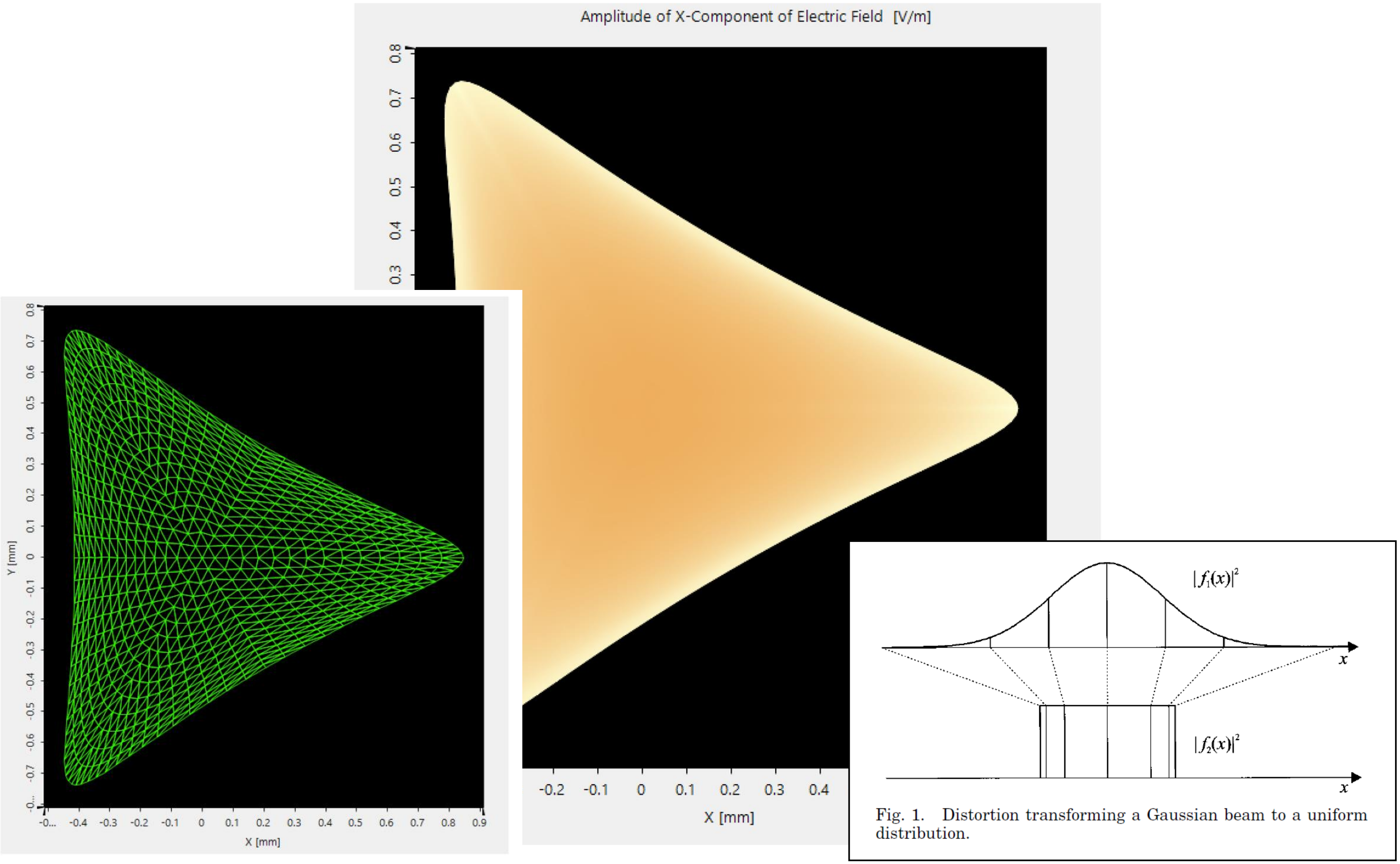

Fig. 1. Distortion transforming a Gaussian beam to a uniform distribution.

Light Shaping: R&D

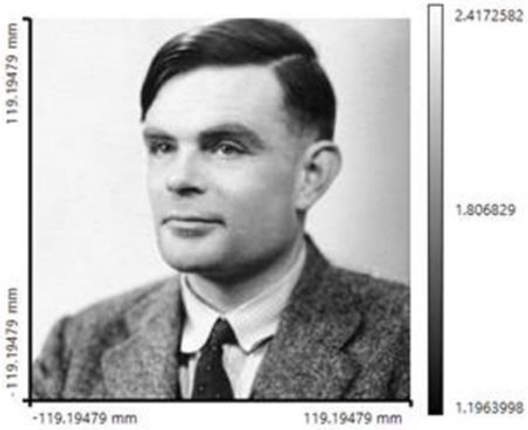

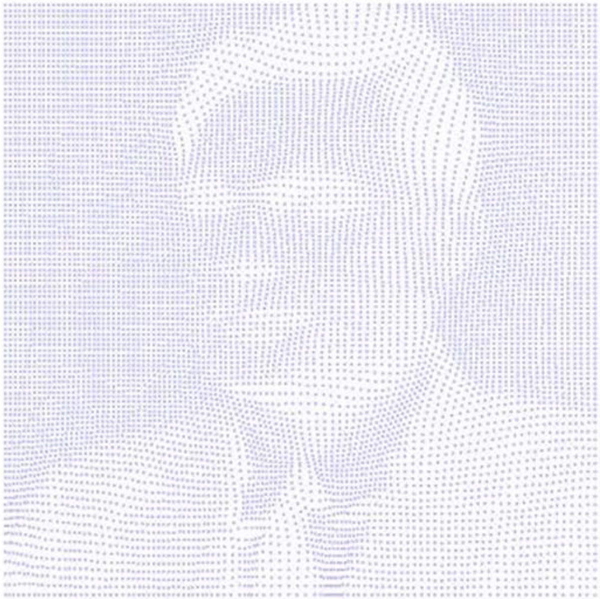

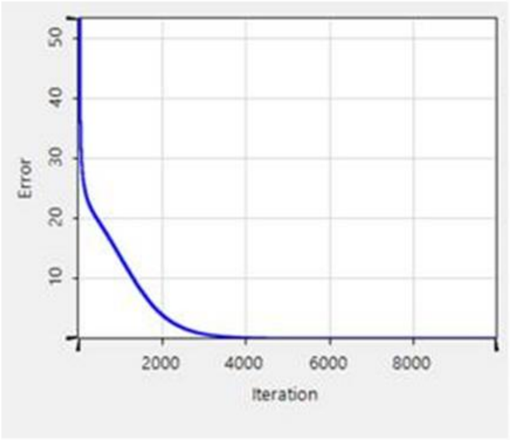

Light Shaping: R&D

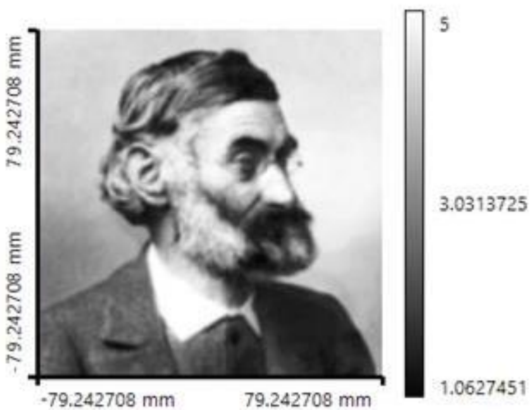

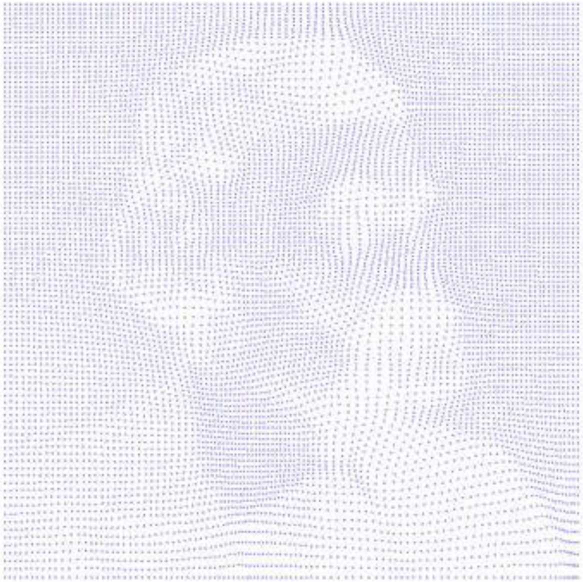

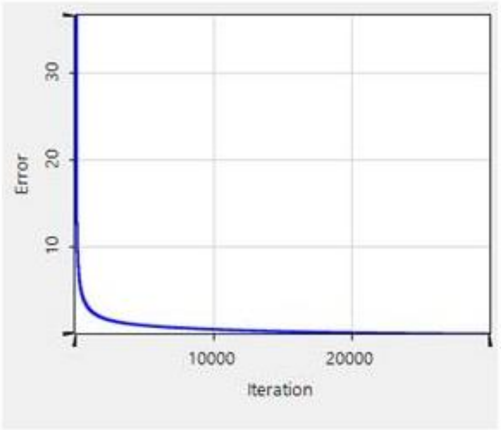

Light shaping by stored scanning process

Diffractive optical elements

Light Shaping Concepts

- Tailored aberrations
- Stored scanning process
- Multichannel concept: Single Deflection
- Multichannel concept: General

Light Shaping Concepts

- Tailored aberrations
- Stored scanning process
- Multichannel concept: Single Deflection
- Multichannel concept: General

Function Principle of DOE

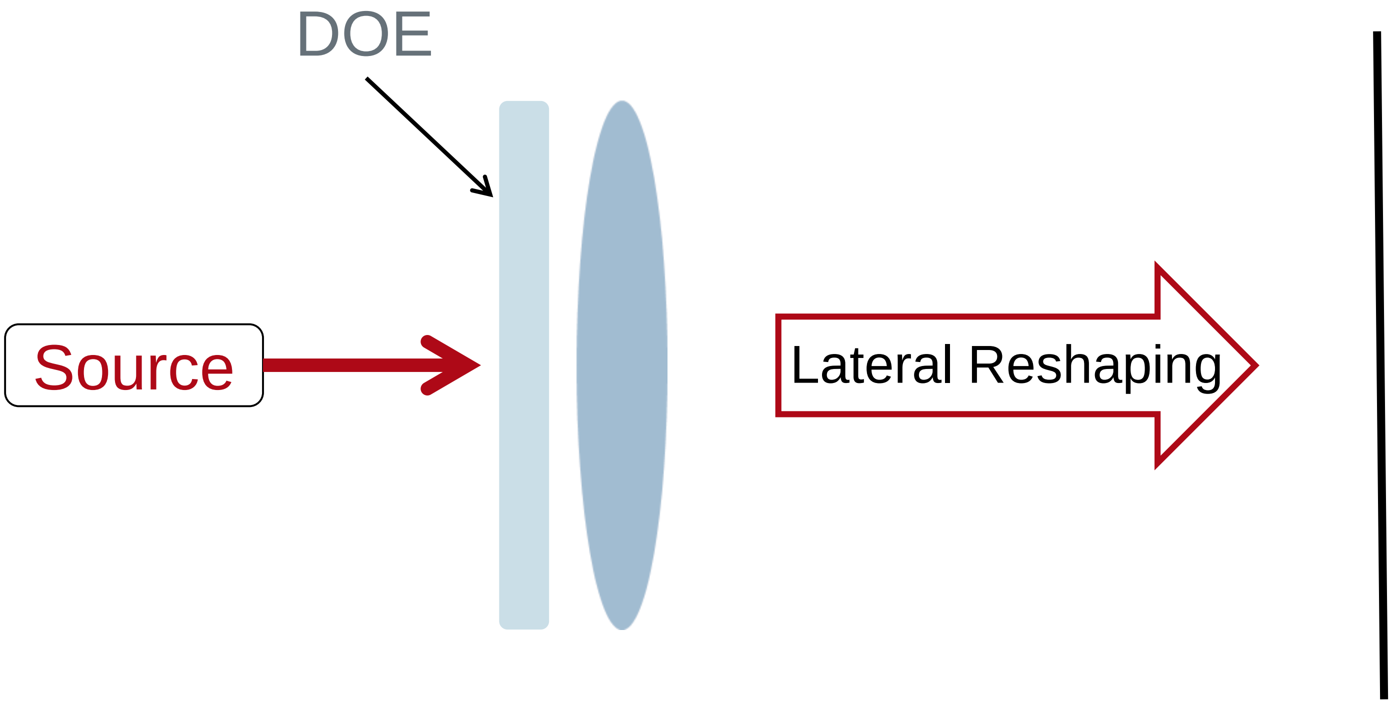

Illustration of Deflection

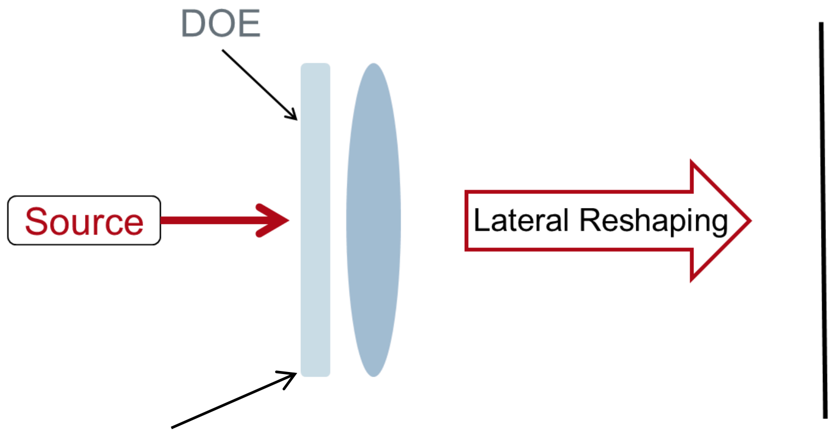

Phase of transmission

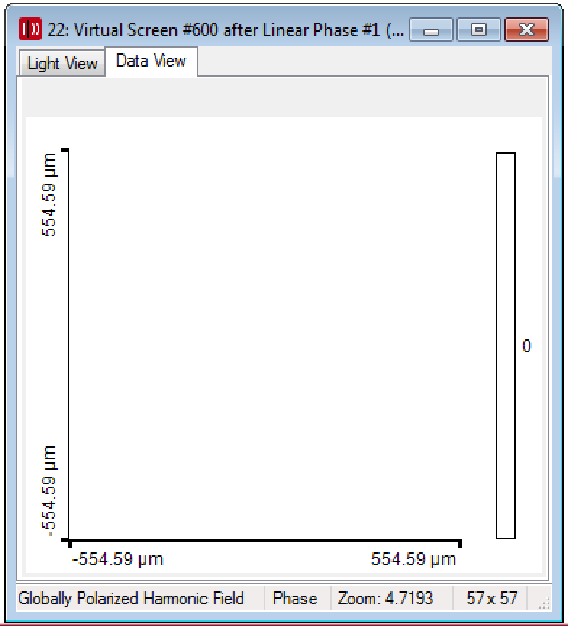

Intensity in target

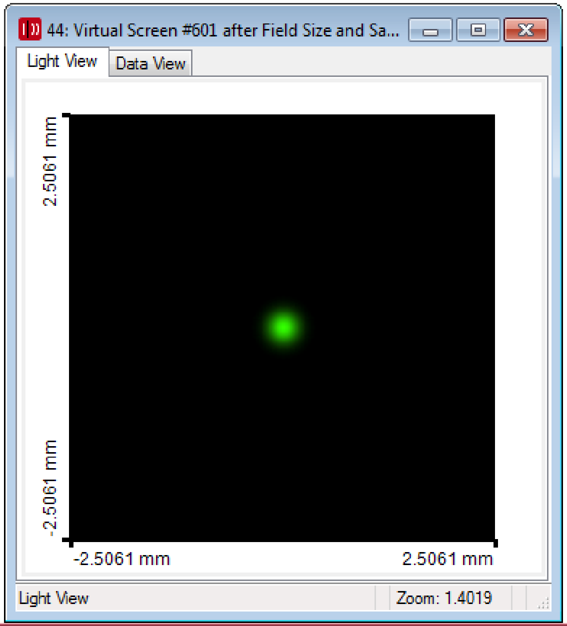

Illustration of Deflection

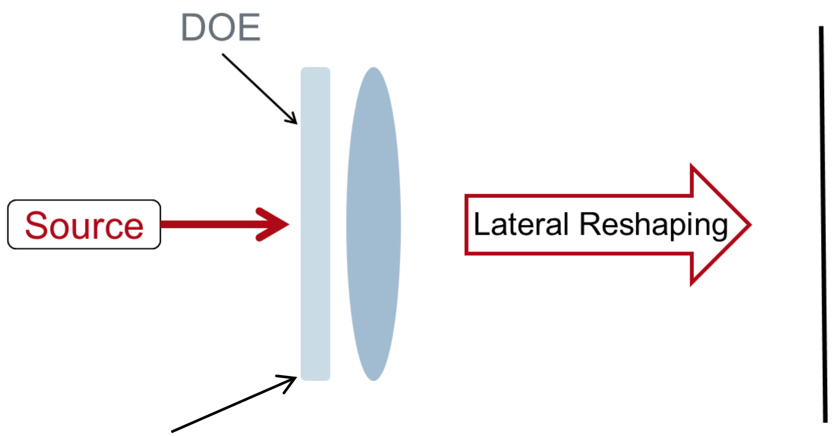

Phase of transmission

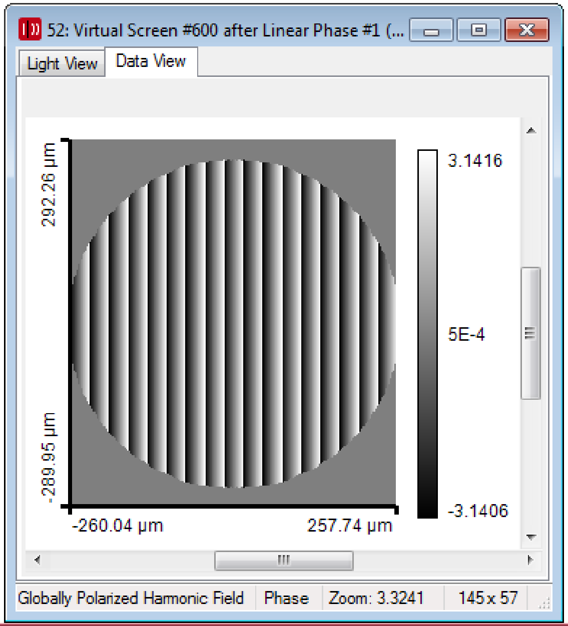

Intensity in target

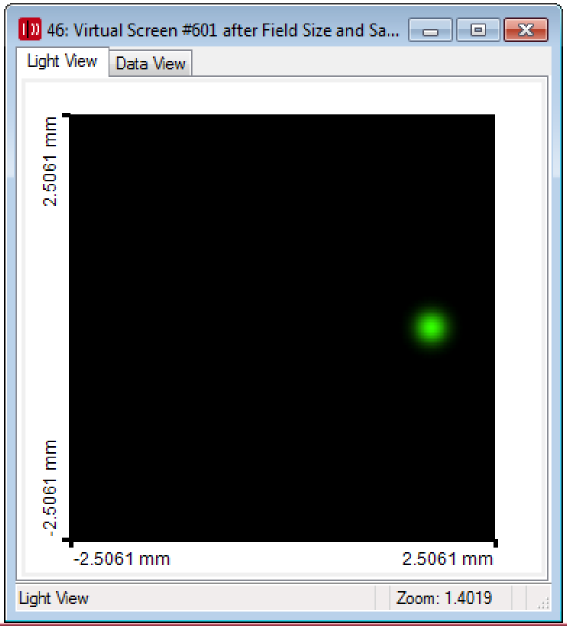

Illustration of Deflection

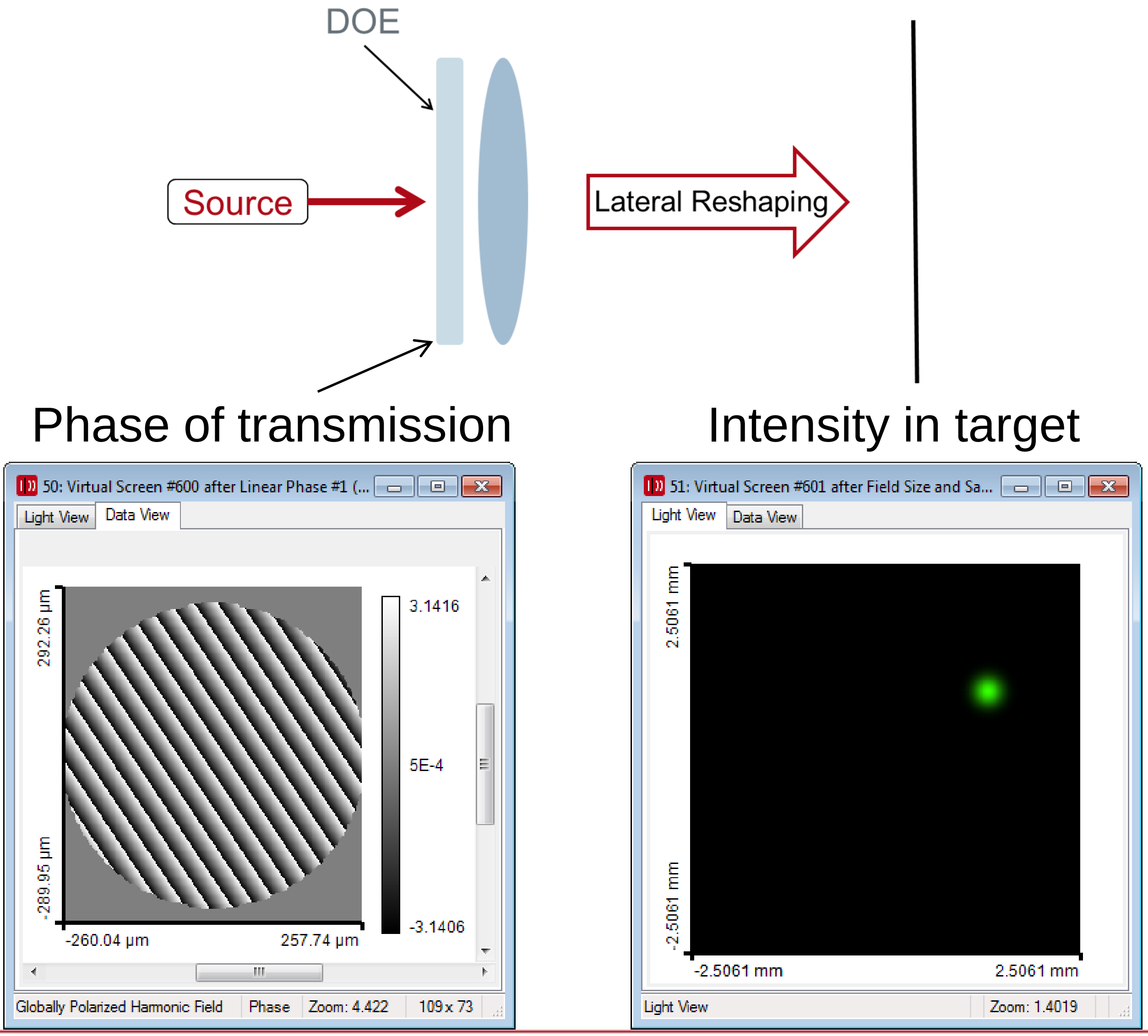

Illustration of Deflection

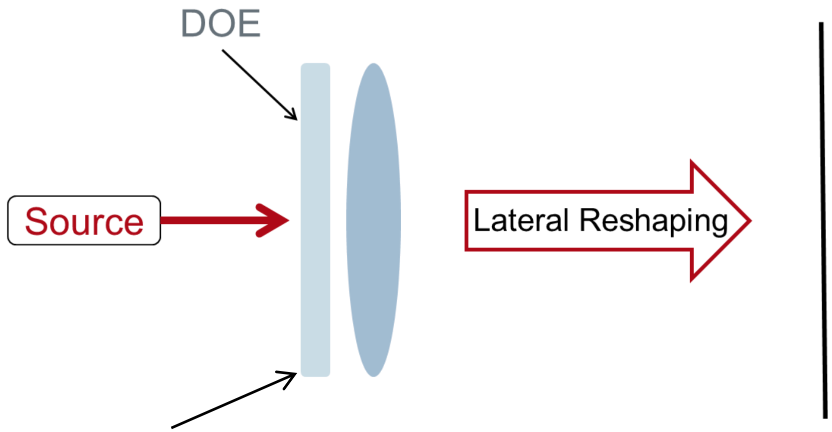

Phase of transmission

Intensity in target

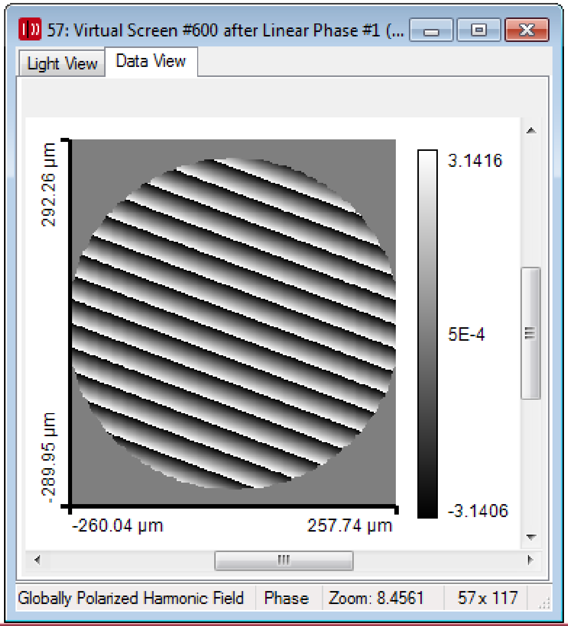

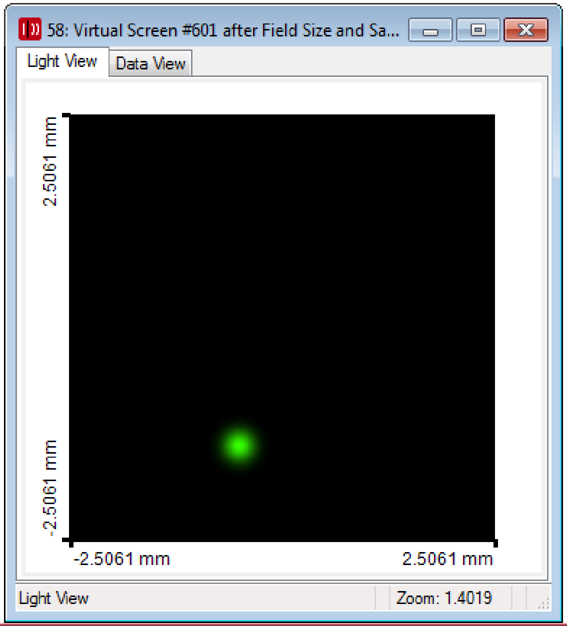

Illustration of Deflection

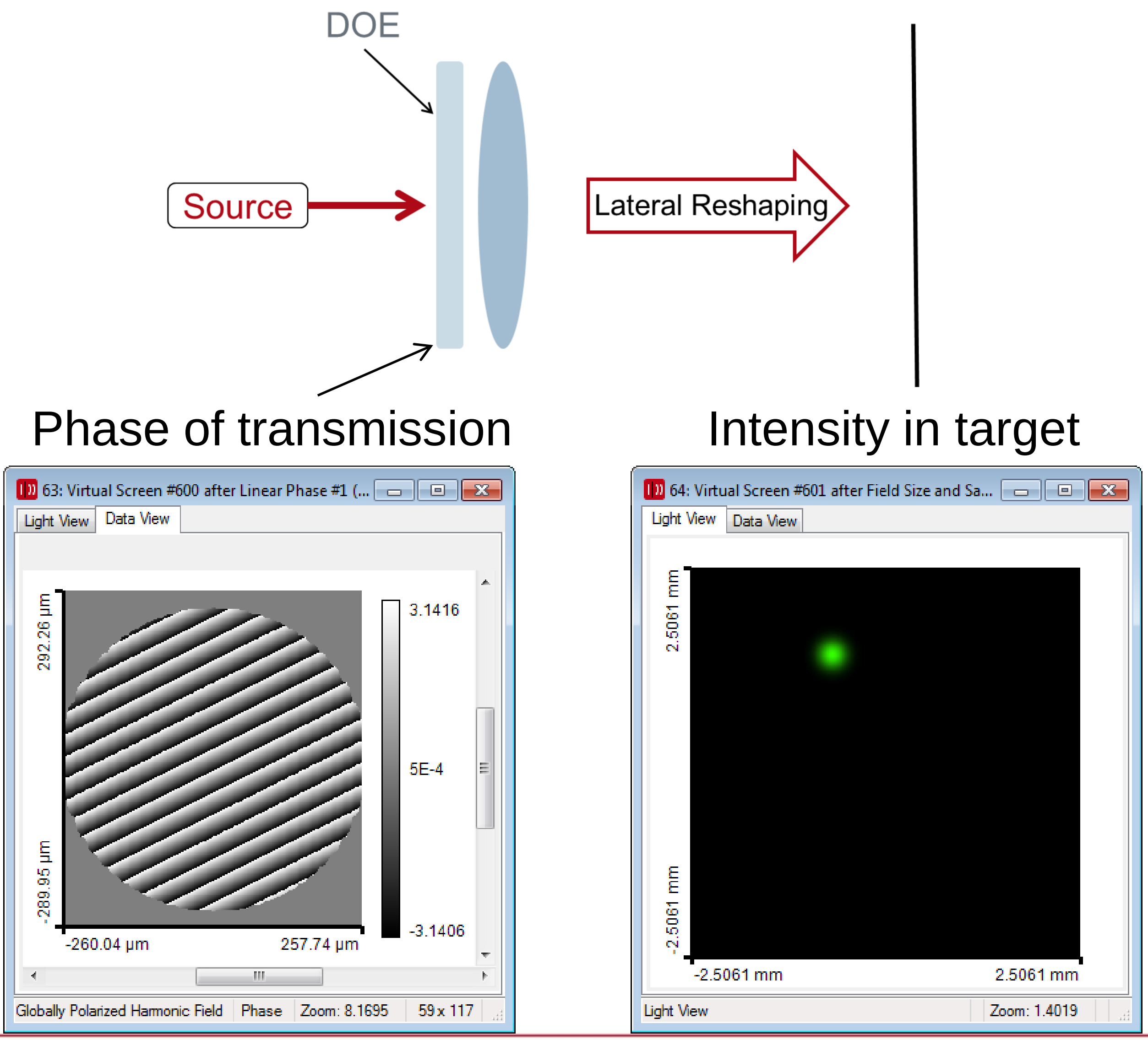

Illustration of Deflection: Sum

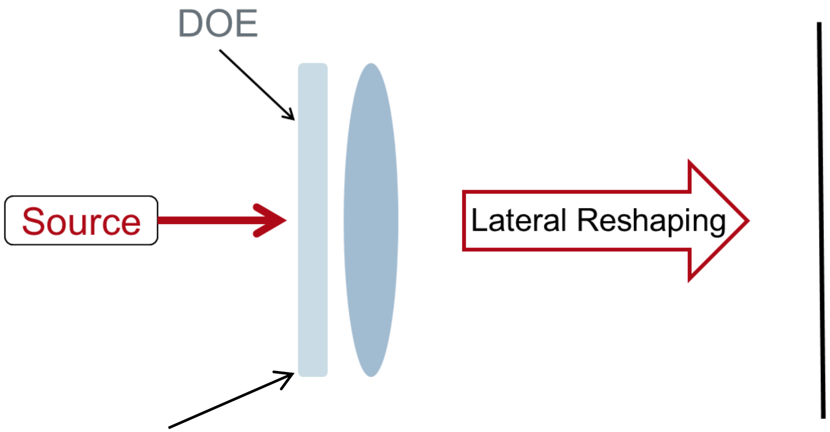

Phase of transmission

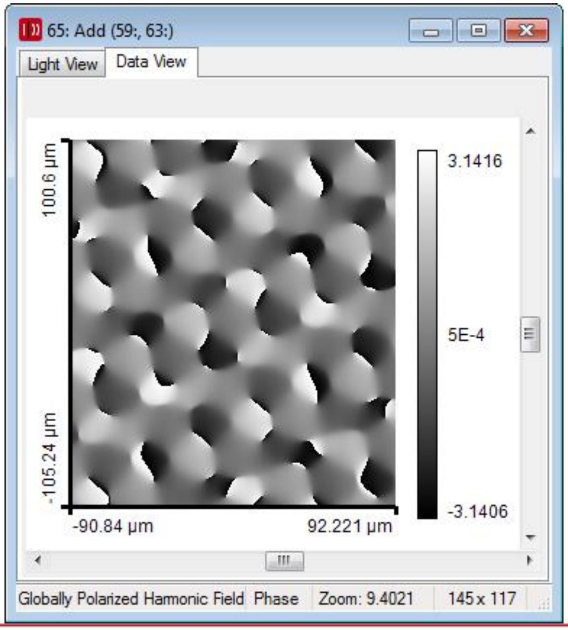

Intensity in target

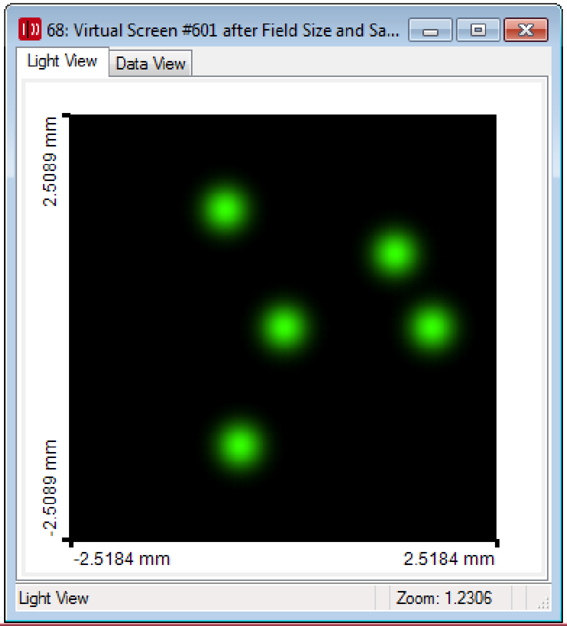

Basic Design Situations: Splitting

Diffractive Beam Splitting: Deflected output fields (beams) do not overlap

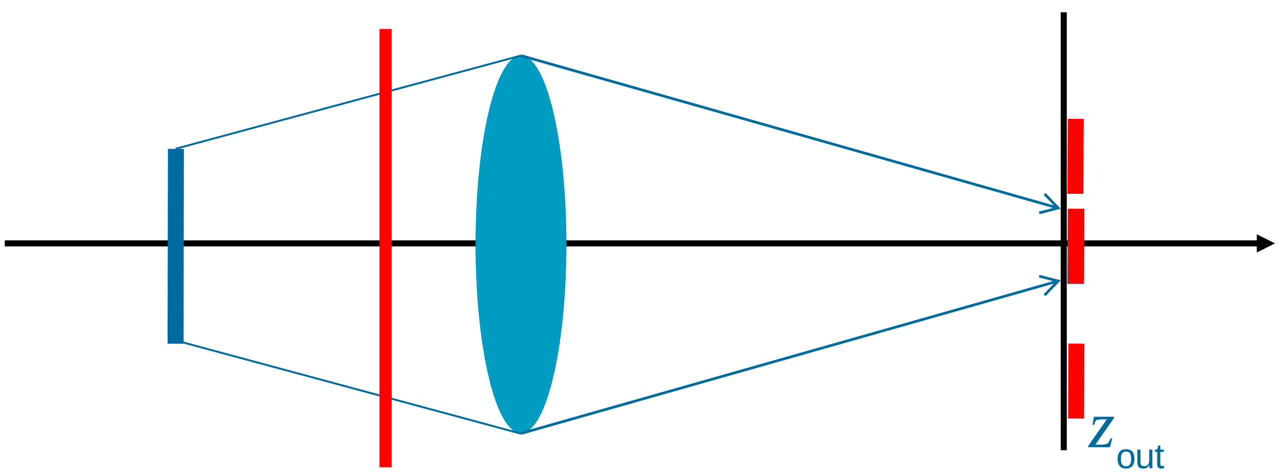

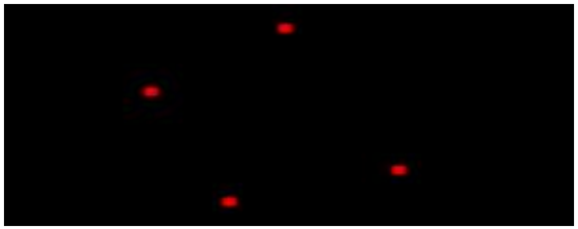

Basic Design Situations: Diffusing

Light Diffusing: Deflected output fields overlap and (partially) coherent interference is not controlled but speckle pattern appears

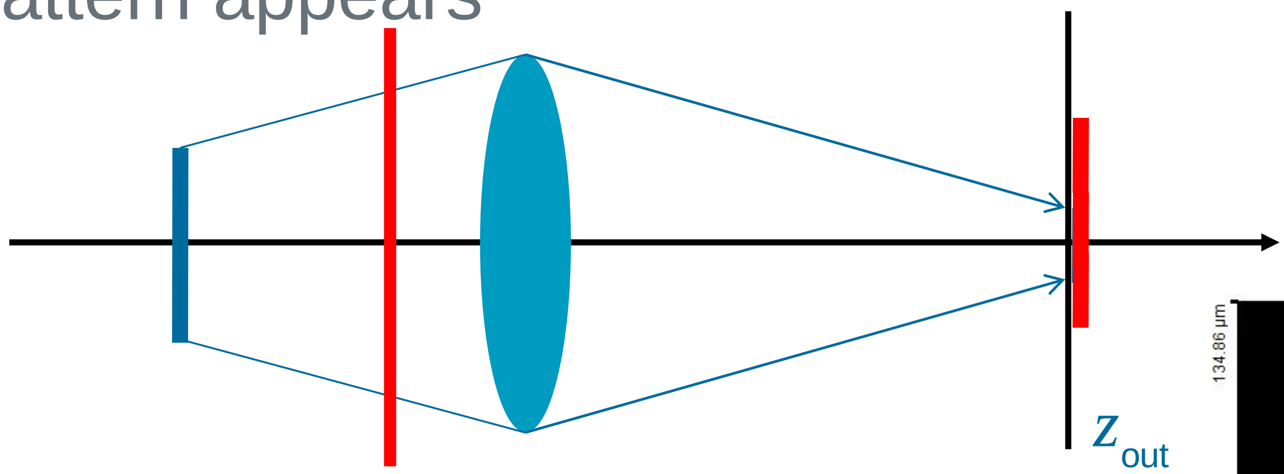

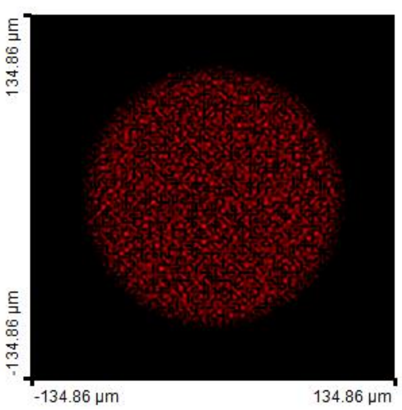

Basic Design Situations: Diffusing

Light Diffusing: D fields
overlap and rence
is not co ears.

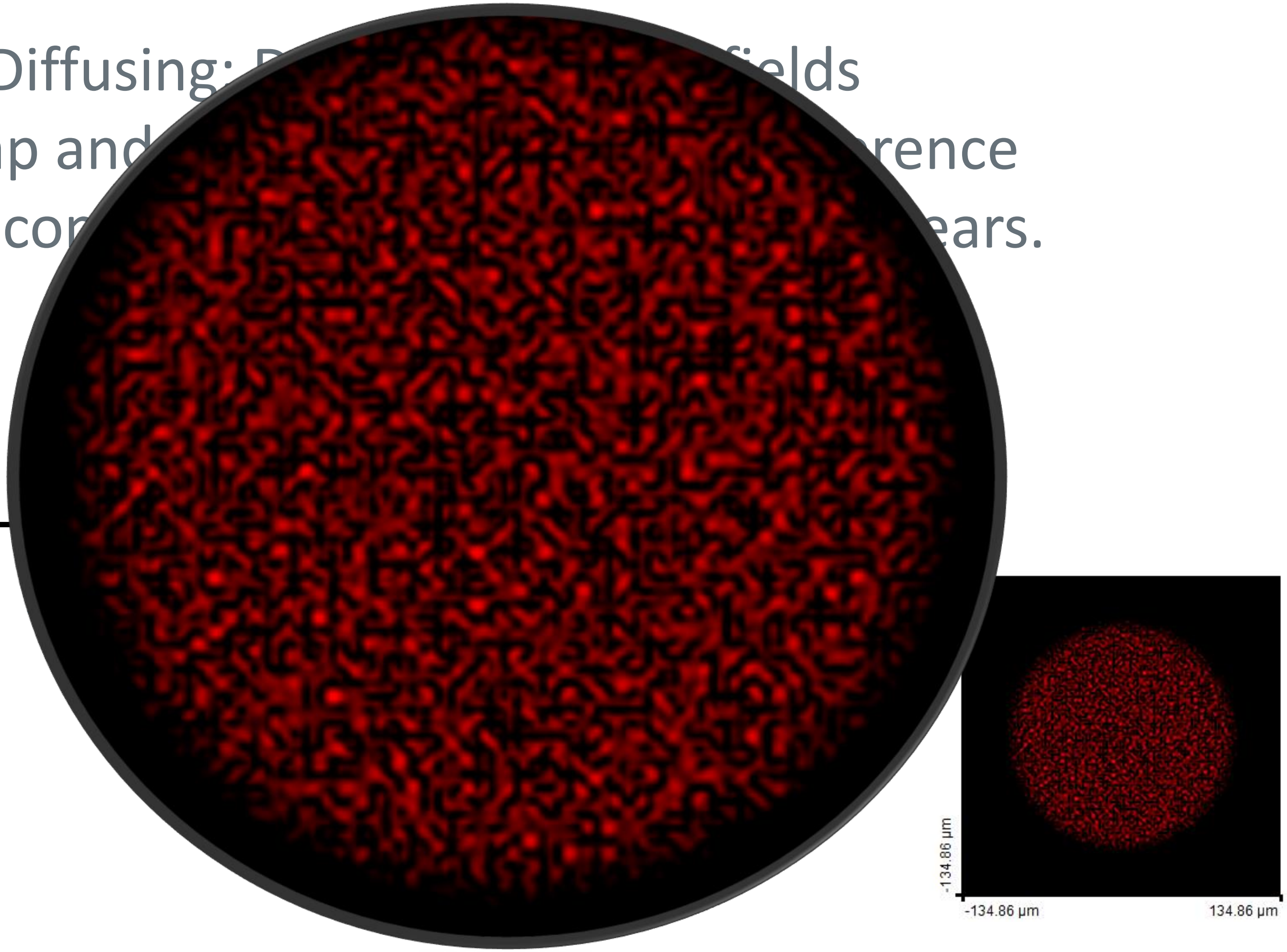

Illustration of Diffuser Concept

Phase

Amplitude

Intensity in Target Plane

Illustration of Diffuser Concept

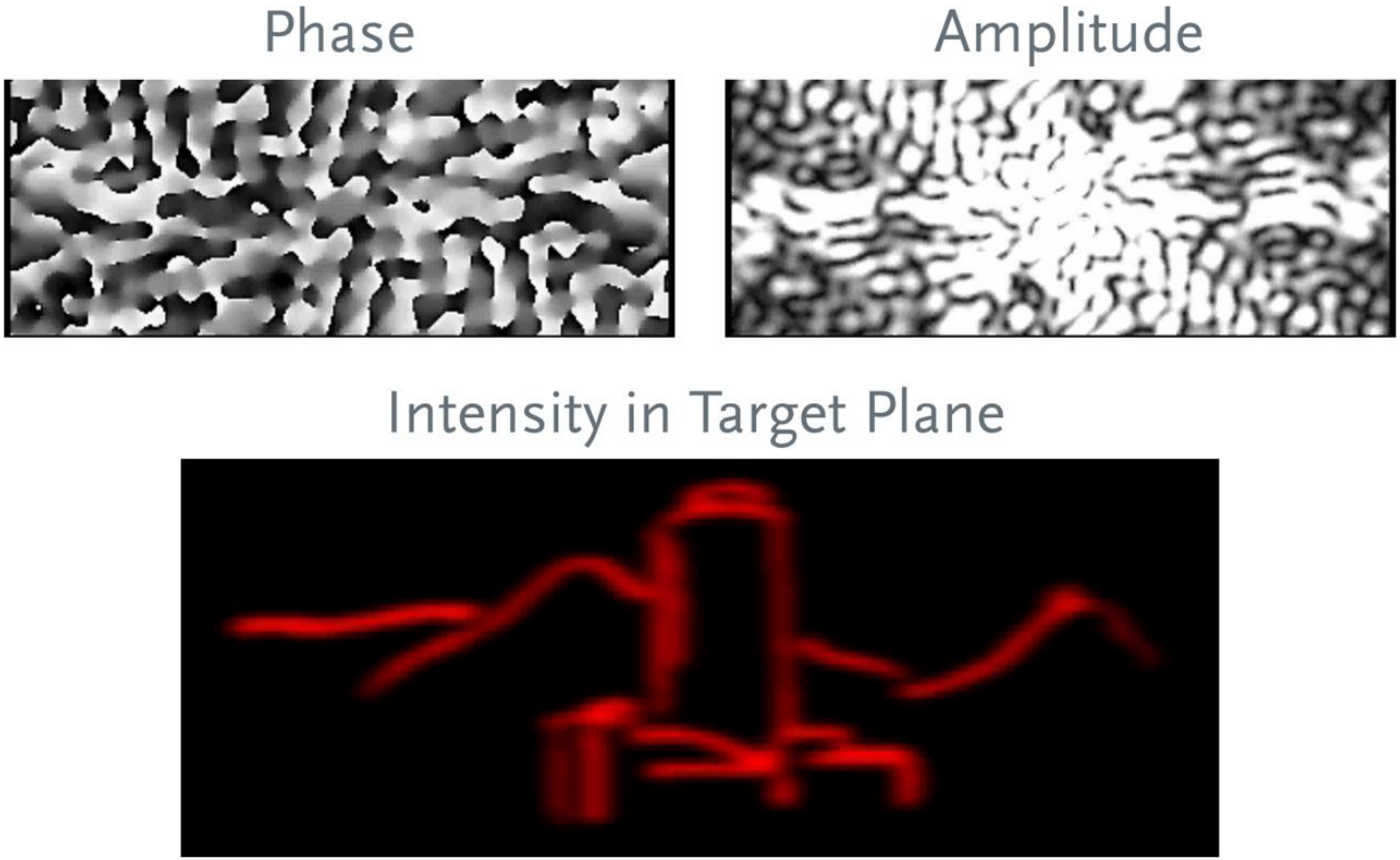

Light Diffusing

Amplitude

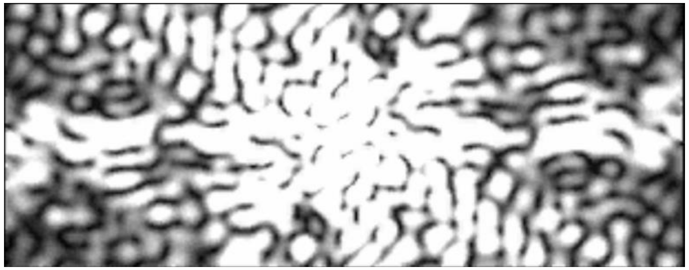

Phase

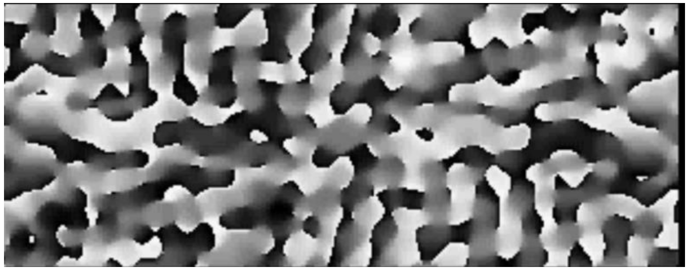

Advanced diffractive optics design techniques

Design technique (IFTA) implemented in VirtualLab™

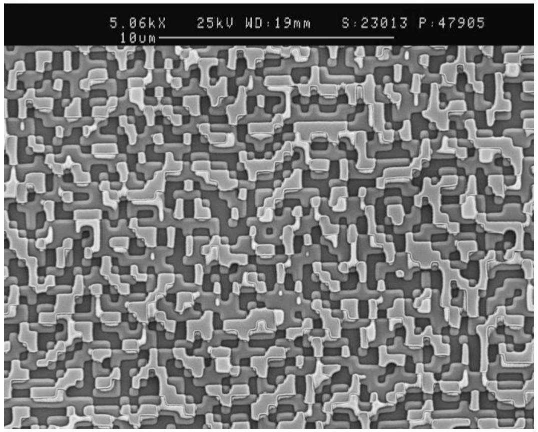

Micro-structured surface profile

Fabricated at IAP, University of Jena

Feature Sizes of Element

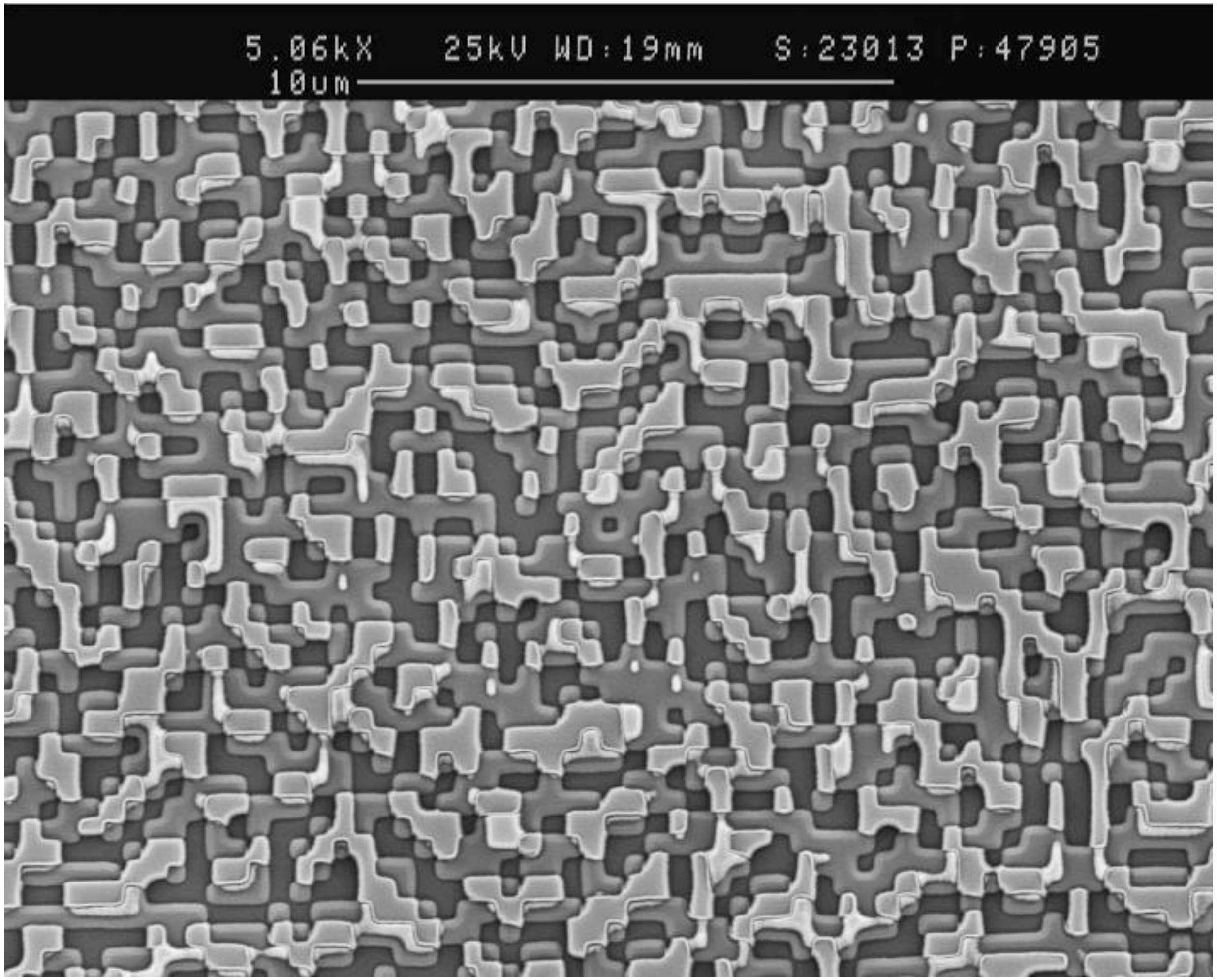

Feature size
about 400 nm

4 height levels

Optical Experiment

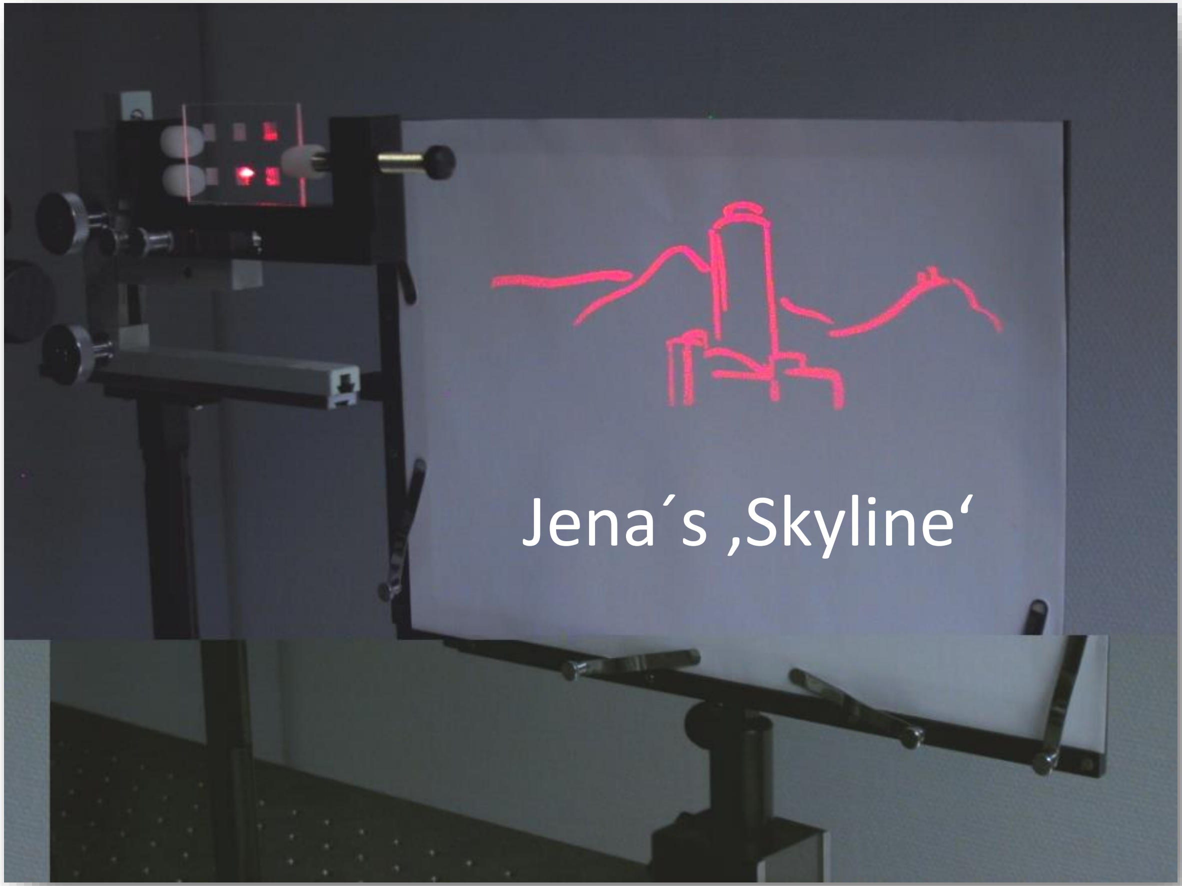

Show in VLF

Micro Optical Component

Modeling of Rounding of Pixels

Modeling of Rounding of Pixels

- Several micro structured surfaces consists of rectangular pixels.
- It is typically assumed that pixels have rectangular side walls and sharp edges.
- Exposure and etching processes during the fabrication of micro structured surfaces can lead to a rounding of pixel edges.
- The edge rounding can be modeled in a good approximation by convolution with a Gaussian beam.

Example with Data from Scenario 23.01

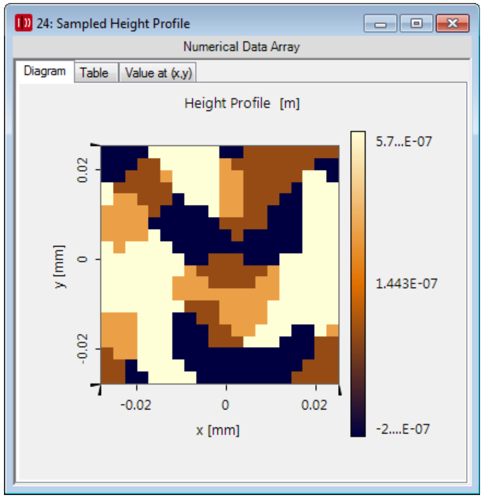

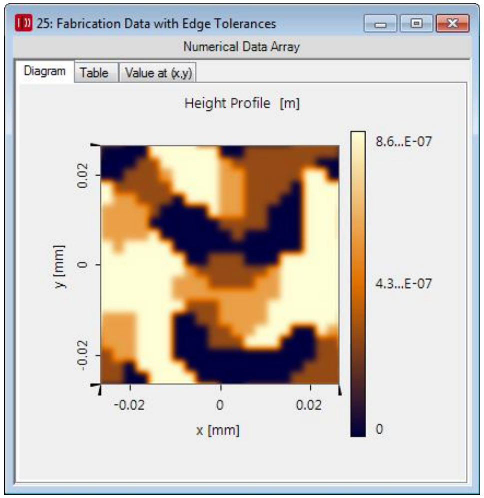

- VirtualLab Module **`Module_RoundedEdge_Tolerances.cs`** can be used to calculate from a perfect profile a profile with rounded edges.
- Calculation steps:
  - Get a *Data Array* with the perfect profile from the sampled interface.
  - Apply the module.
  - Set the *Data Array* with the modified profile into the sampled interface.
- Left side: edge rounding 2 µm, sampling distance 400 nm.

Results with 4x Increased Brightness

Simulation Result of Designed DOE

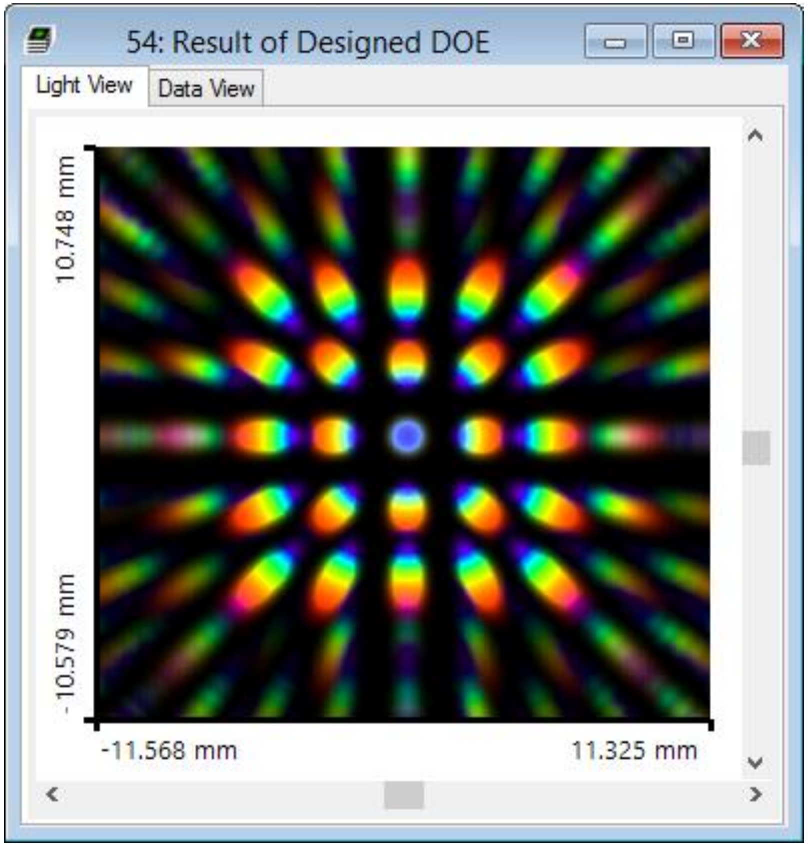

Simulation Result of DOE with Rounded Edges

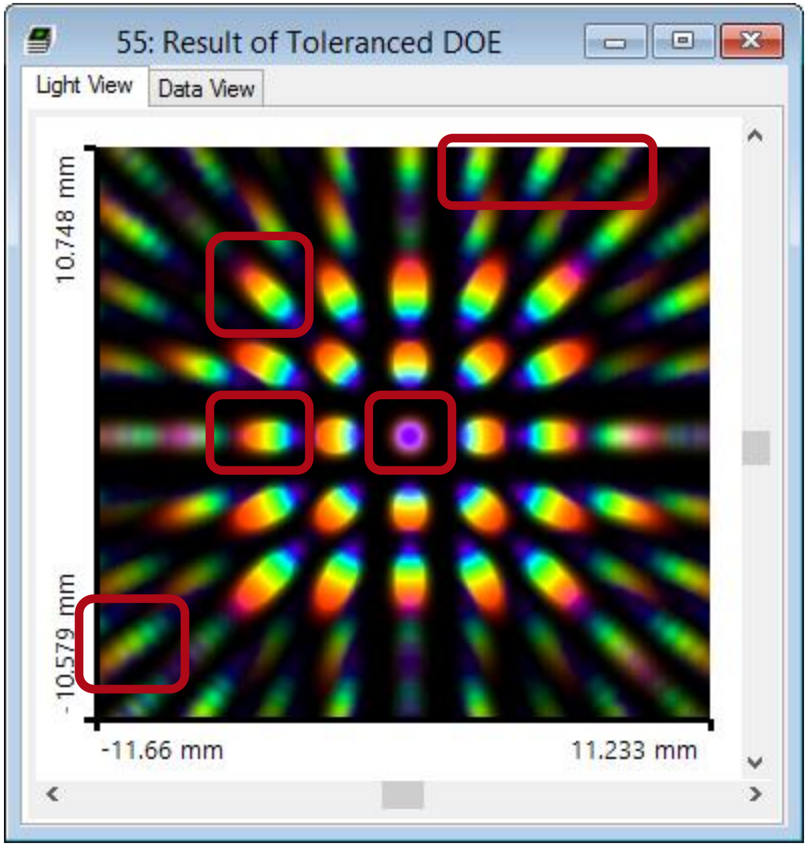

Comments on Diffuser Technology

- Very flexible in light pattern generation
- Robust against adjustment problems
- Coherent light leads to speckle pattern
- Size of speckle features can be adjusted by focusing system
- Diffusers work for partially coherent beams
- Partially coherent beams smooth the speckle pattern; effect can be simulated with VirtualLab™

Laser Show China

Spatial Light Modulator

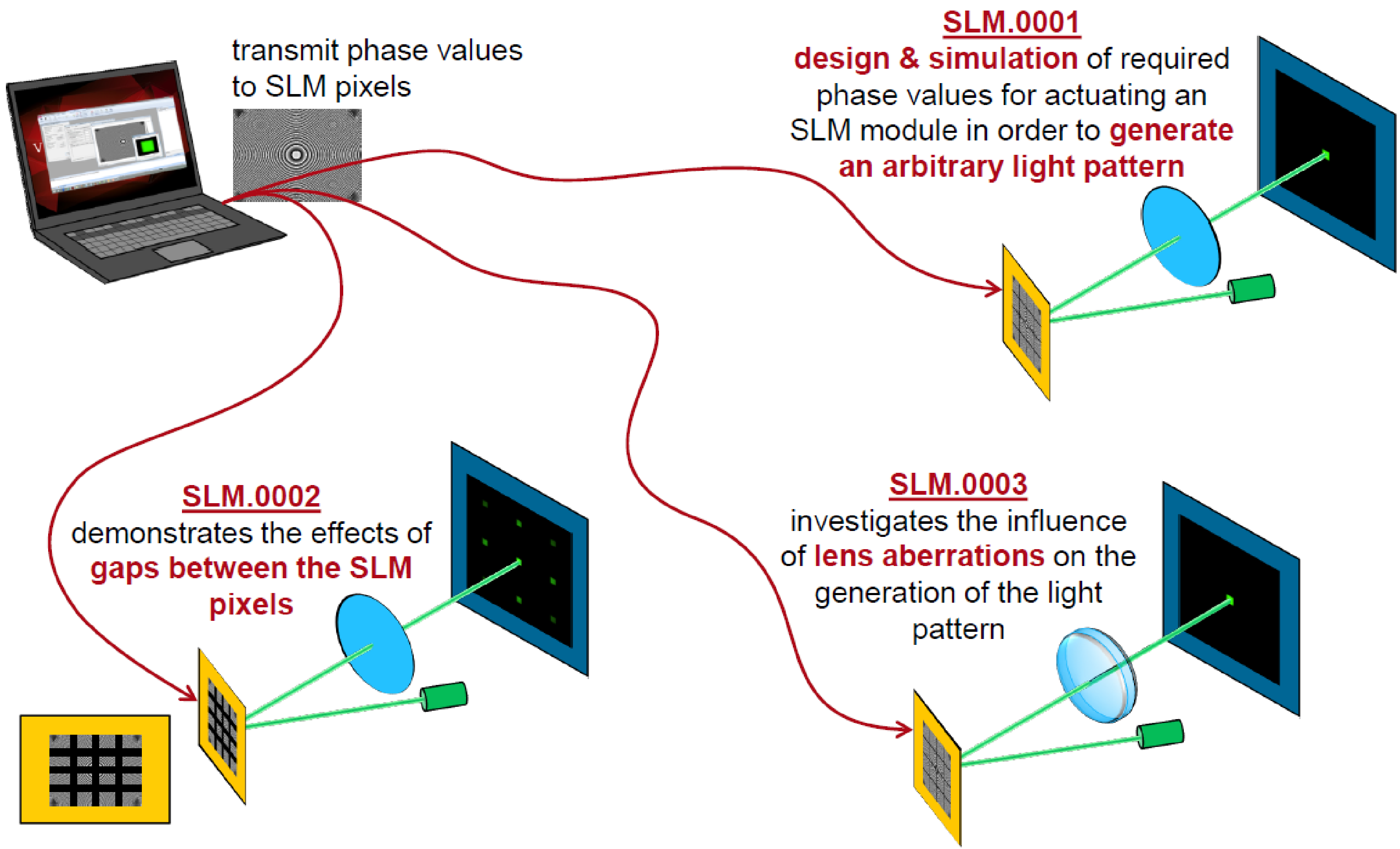

Spatial Light Modulator

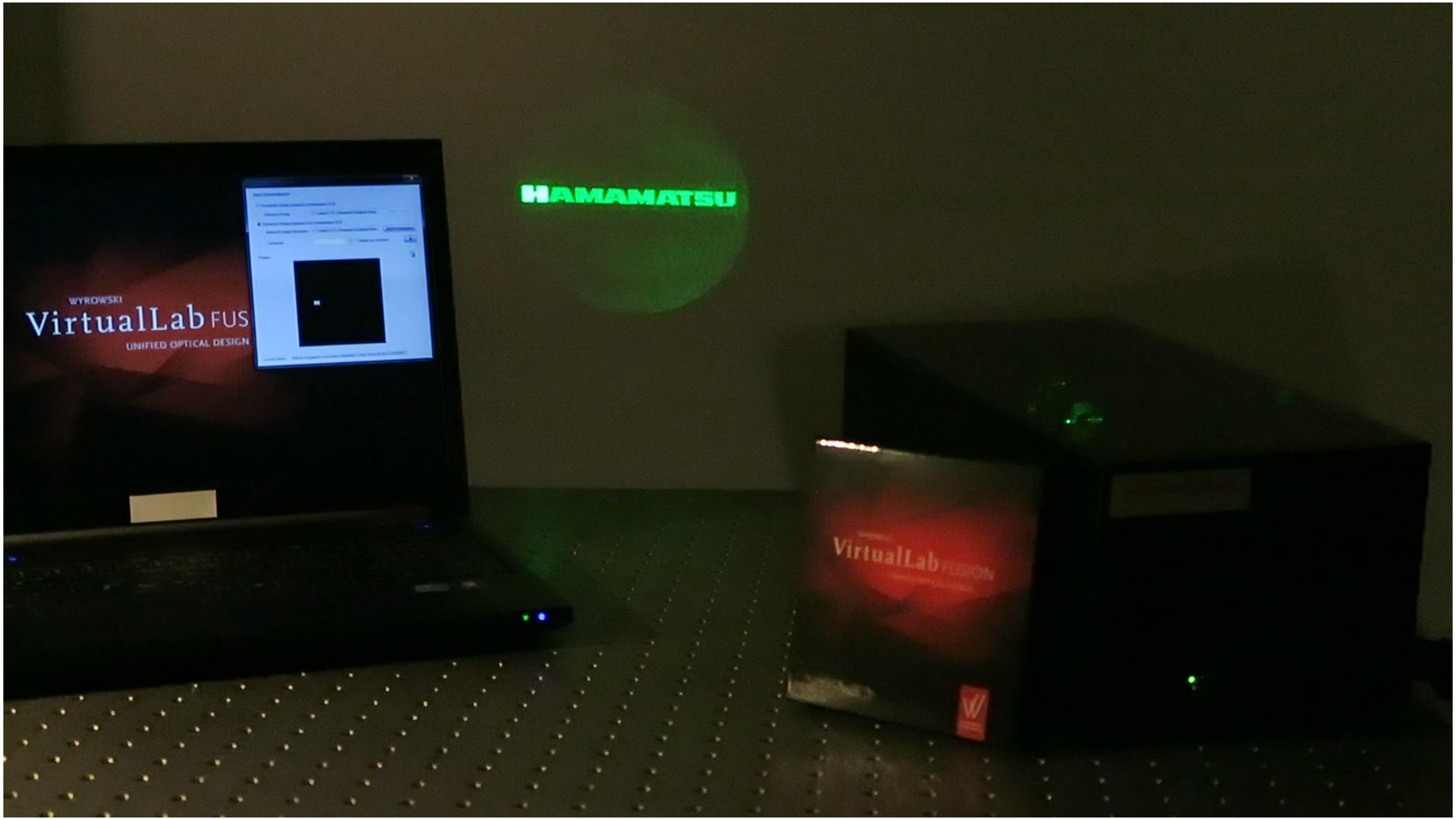

Light shaping by multichannel concept

Diffractive and refractive optical elements

Array of Deflectors

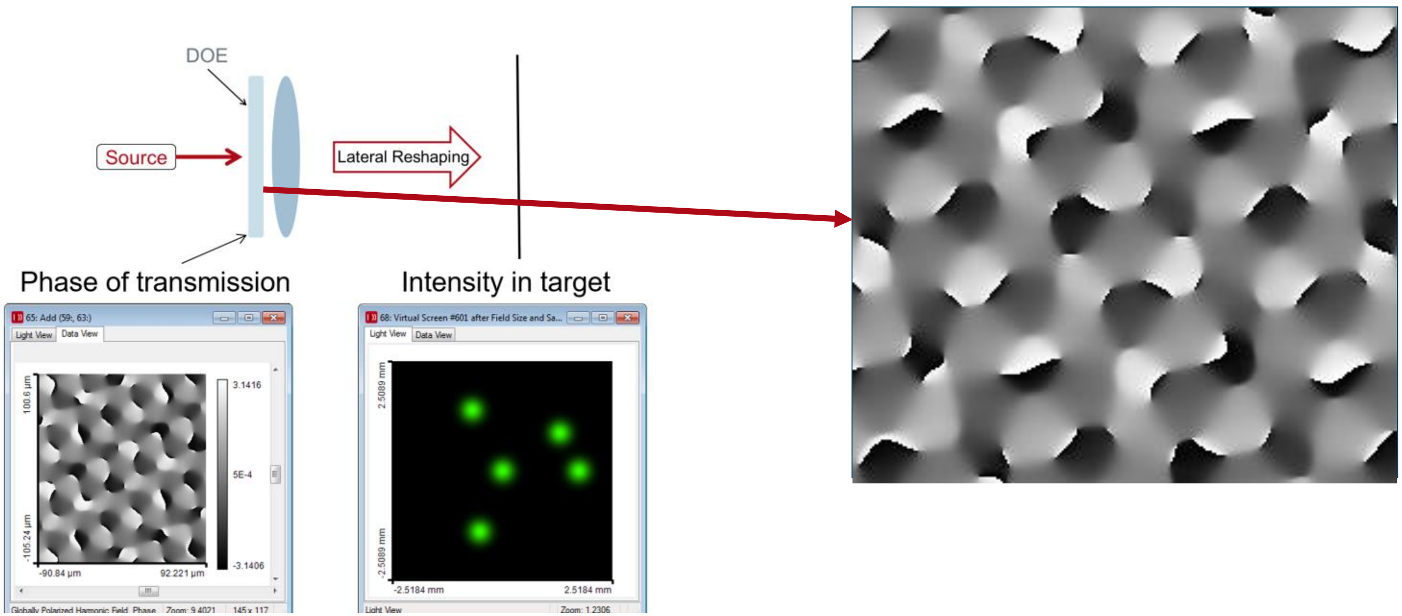

Array of Deflectors

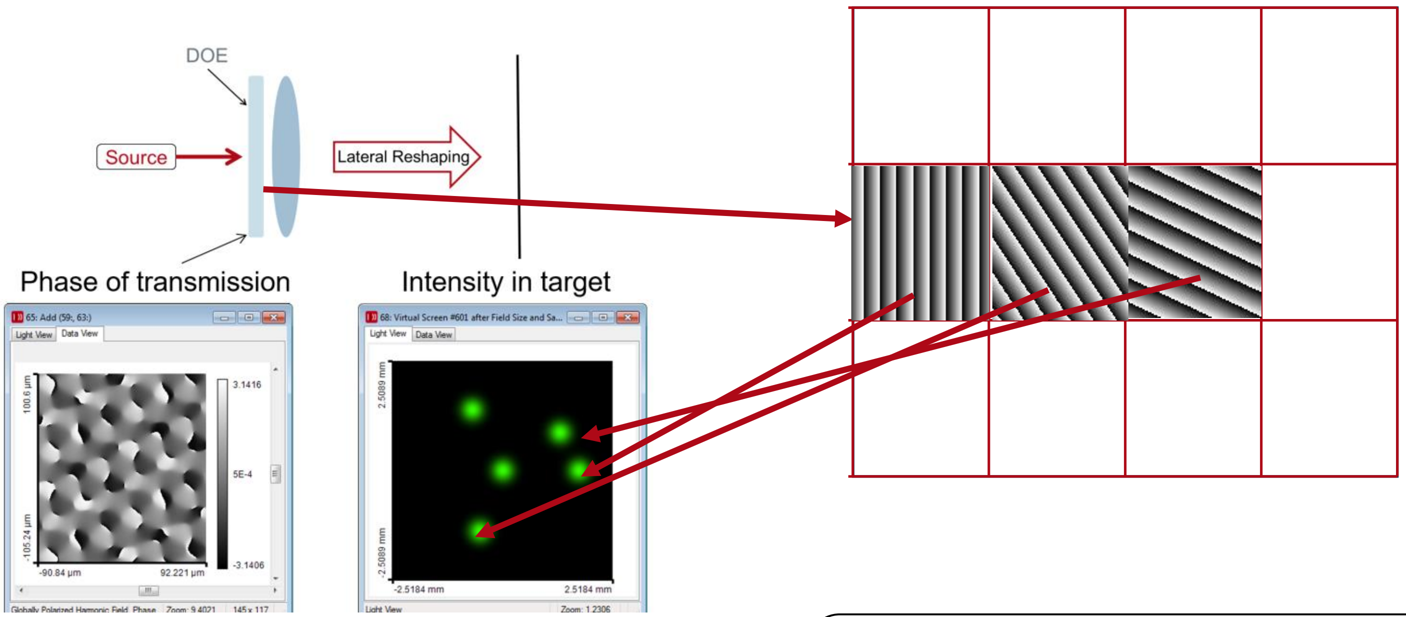

Deflection can be done by gratings, prisms, mirrors.

Task/System Illustration

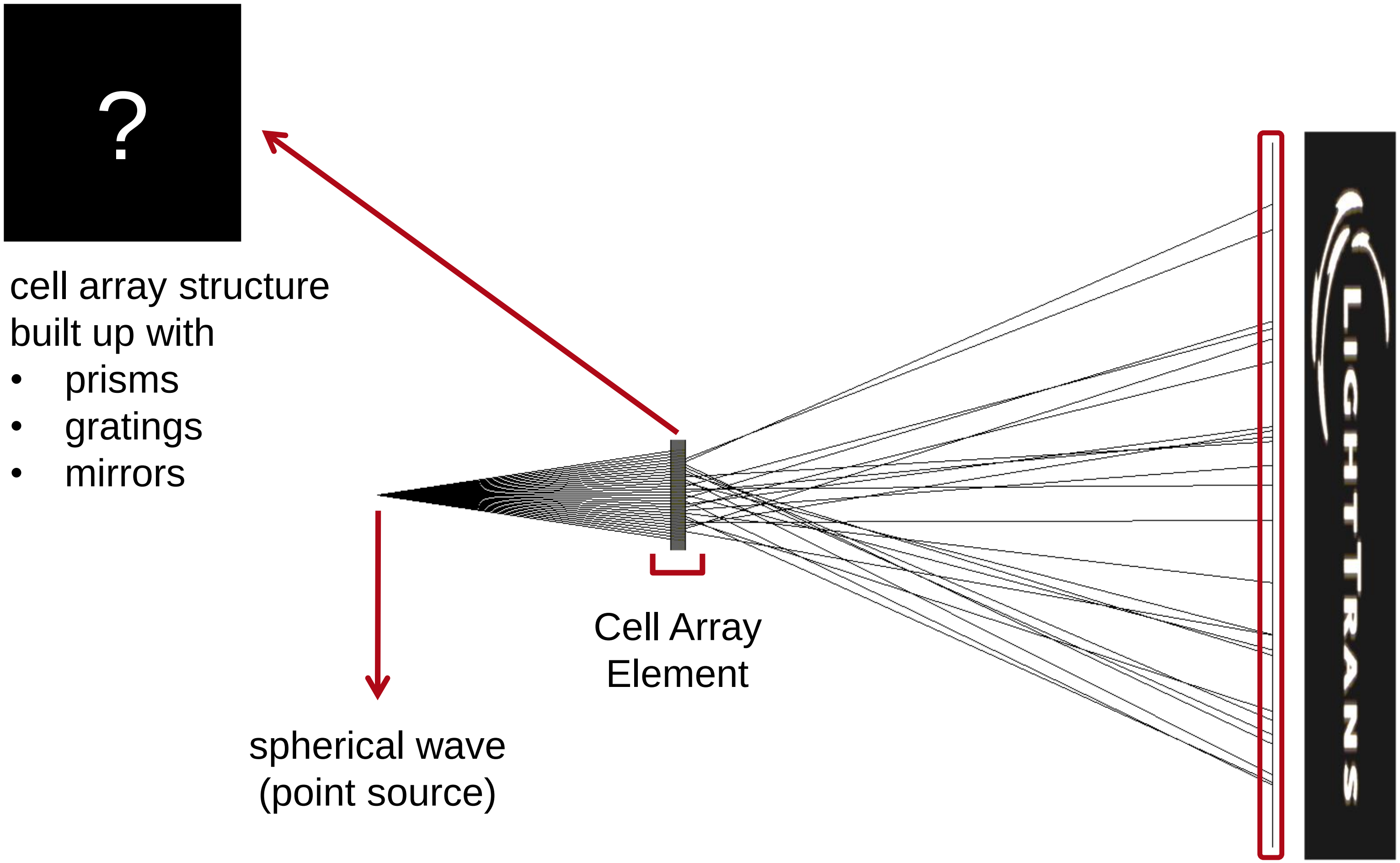

Specification: Light Source

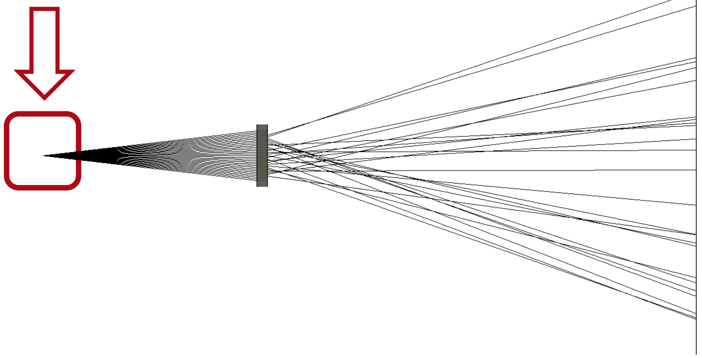

Parameter	Description / Value & Unit
type	RGB LED
emitter size	100 x 100 µm
wavelength	(473, 532, 635) nm
polarization	right circularly polarized light
number of lateral modes	3x3
Total number of lateral and spectral modes	27

Specification: Cell Array

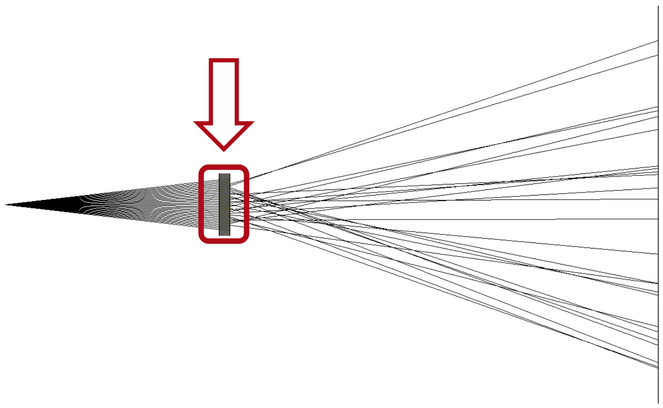

Parameter	Value & Unit
number of cells	100x100
cell size	125x125µm
array aperture	12.5x12.5mm

Results: 3D System Ray Tracing

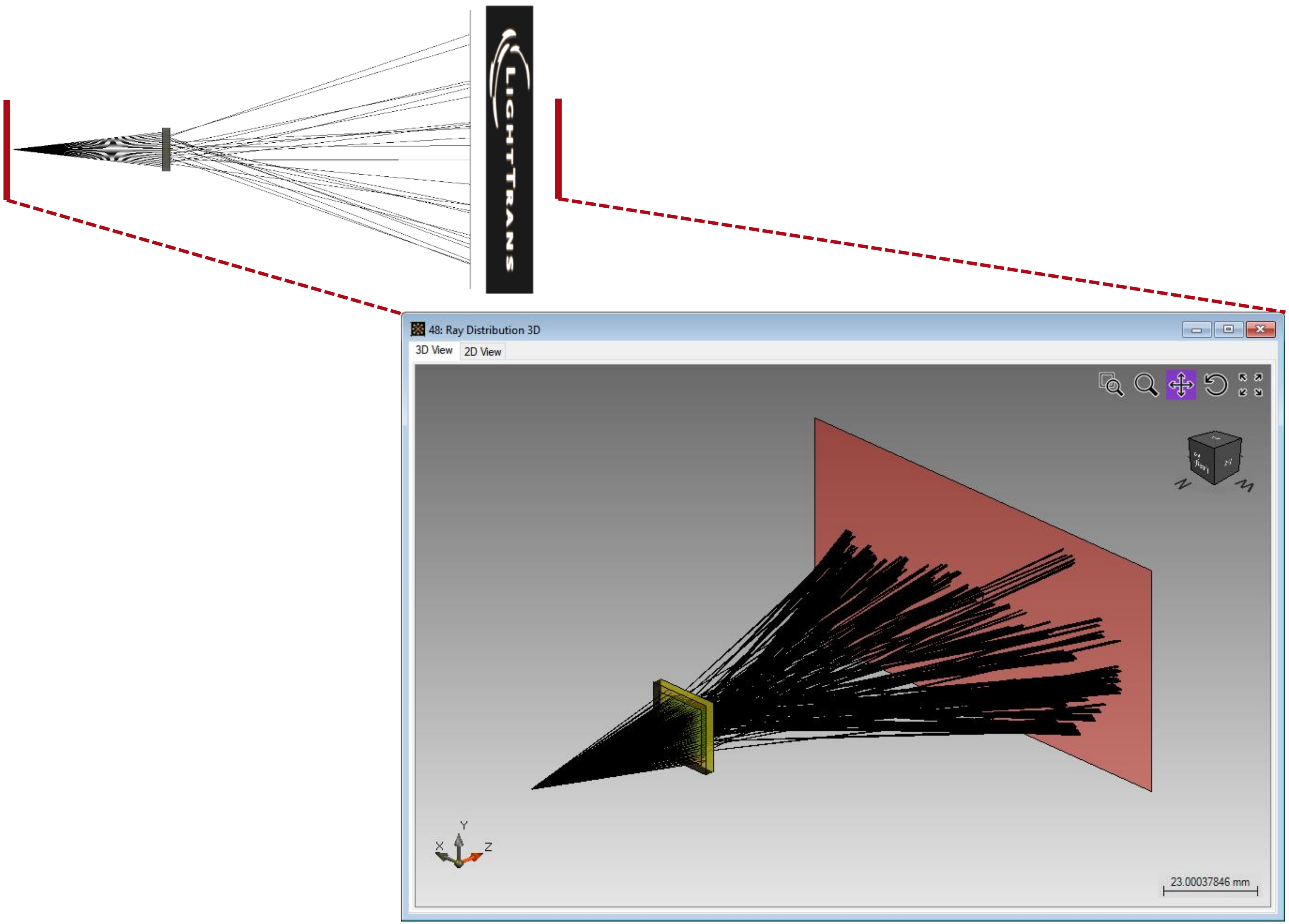

Results: Grating Cells Array

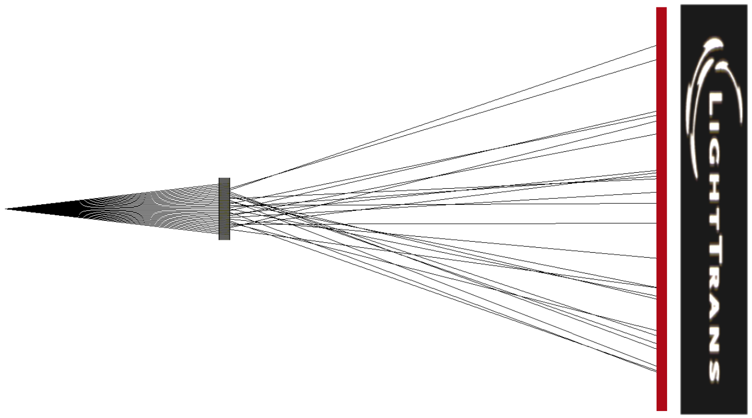

spot diagram

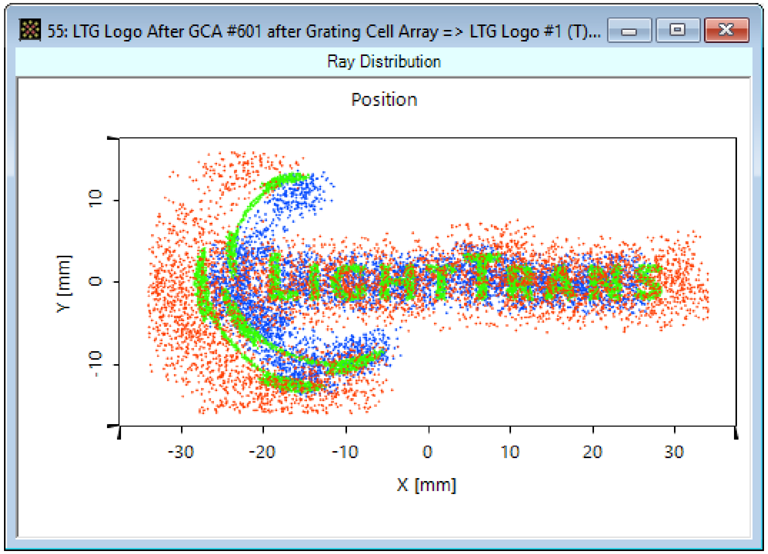

y pattern
lor view)

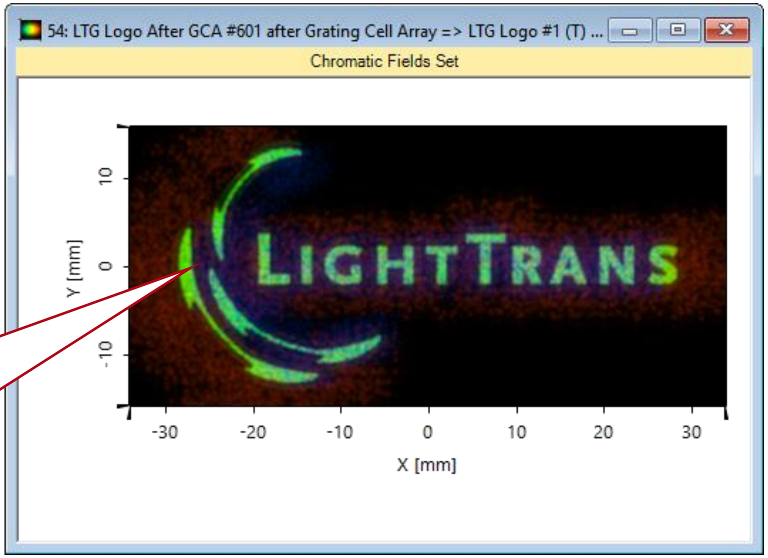

for grating cells array strong dispersion effects occur

Results: Prism Cells Array

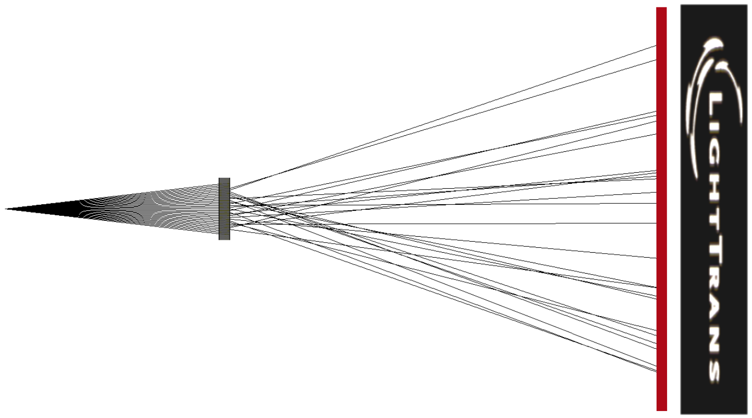

spot diagram

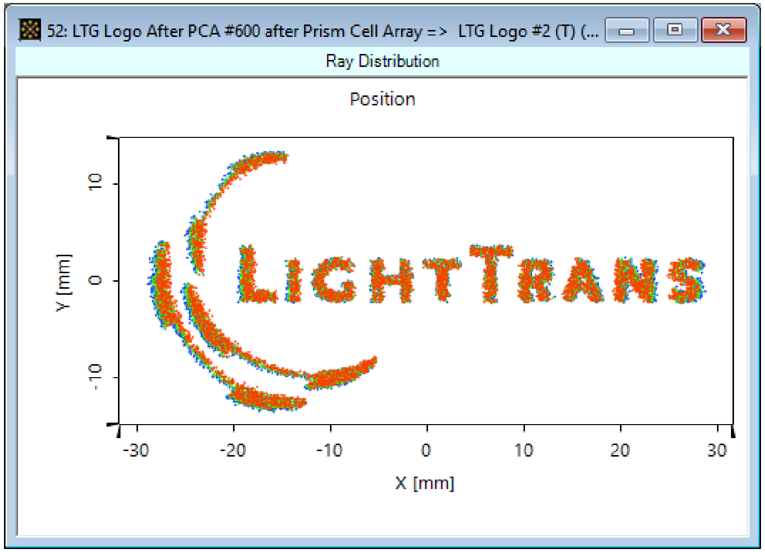

pattern

(real c lor view)

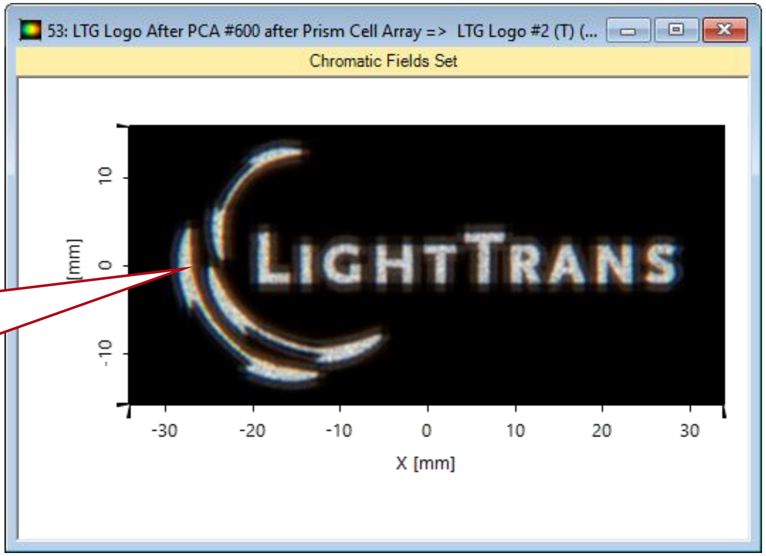

the dispersion is significantly reduced by using prisms

Results: Mirror Cells Array

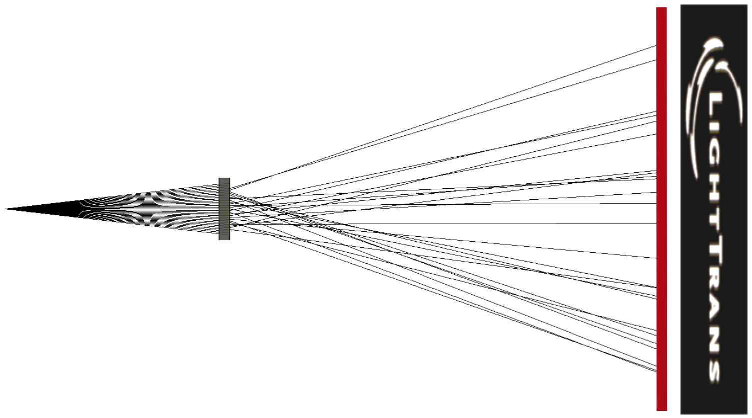

spot diagram

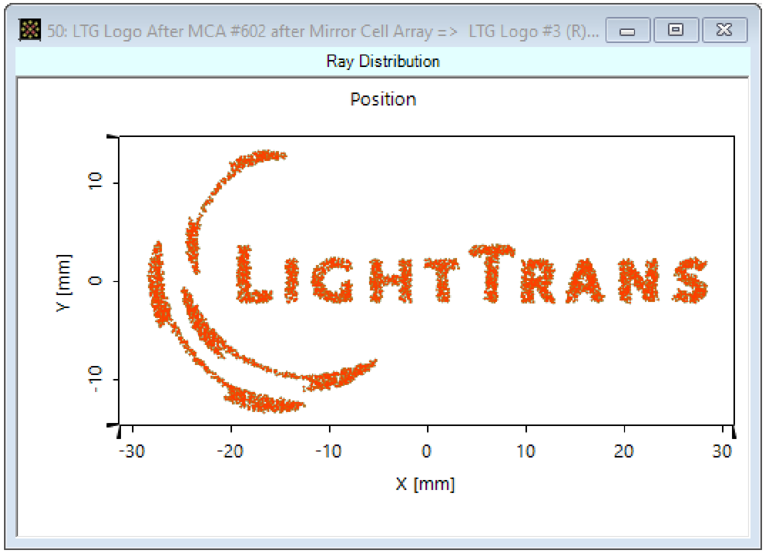

y pattern
(rea olor view)

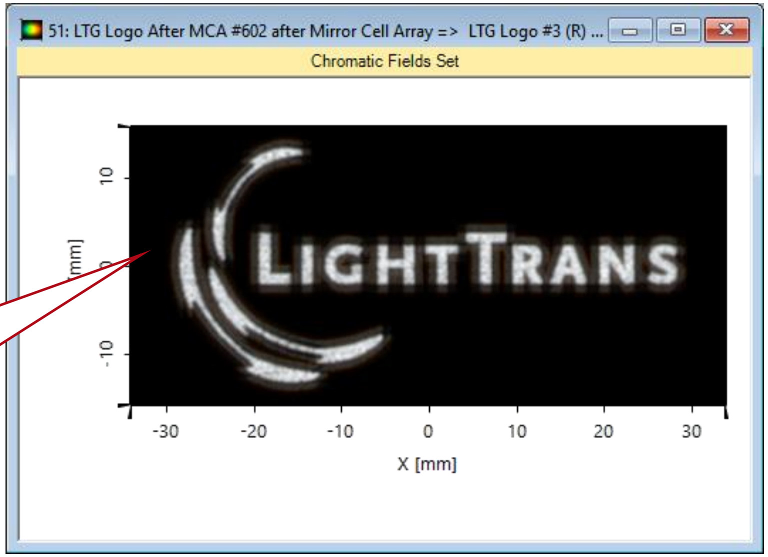

due to reflective approach no dispersion effects occur

Light shaping by arrays of microoptical components

Diffractive and refractive optical elements

Array of Microoptical Components

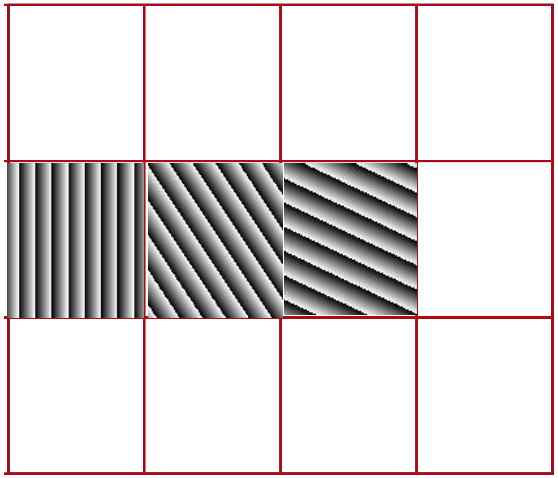

Array of Microoptical Components

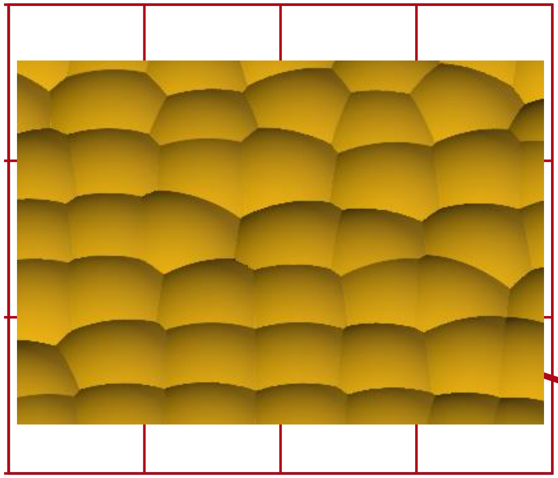

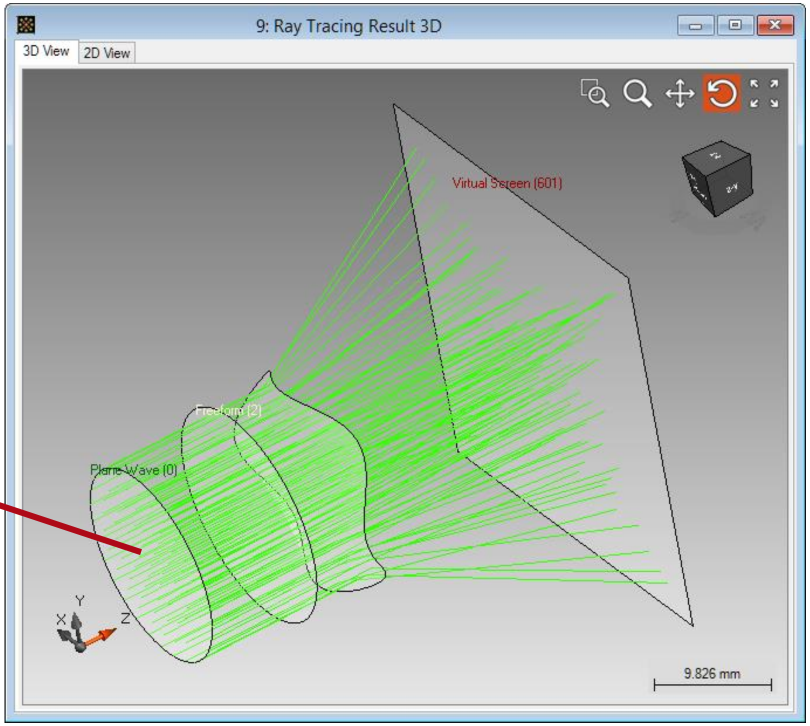

LED Top Hat Generation using Aperiodic Refractive Beam Shaper Array

Task/System Illustration

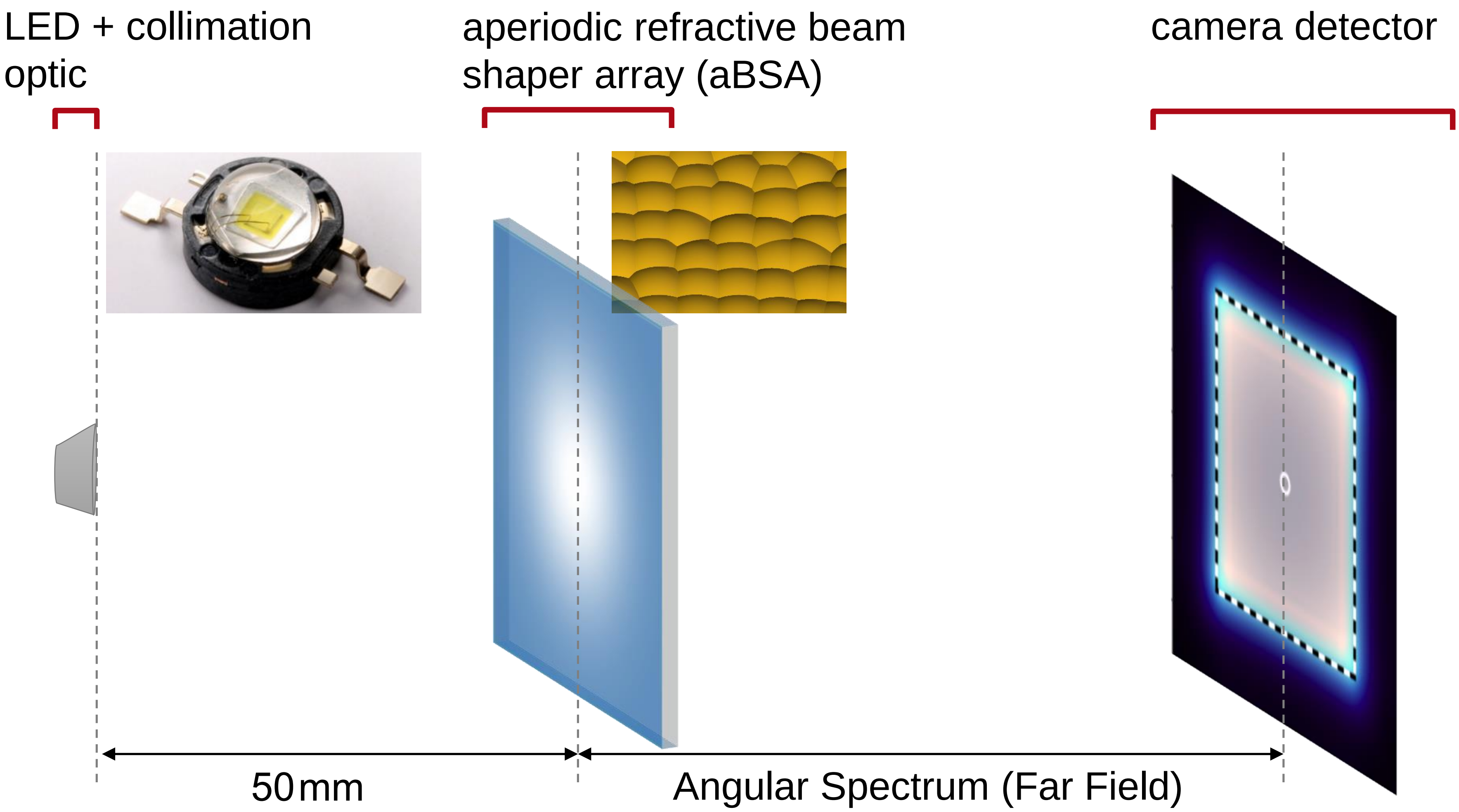

Specs: Light Source

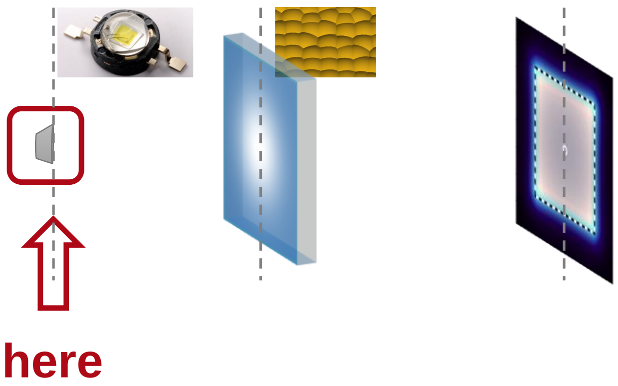

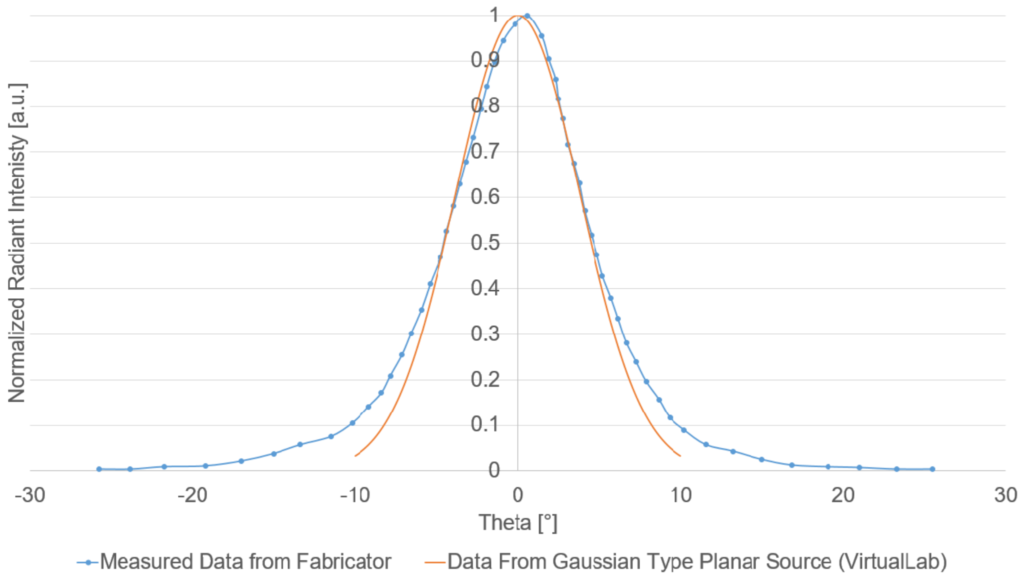

Parameter	Description / Value & Unit
name/type	Seoul Z-LED P4 from Seoul Semiconductors
partially coherent source type	Gaussian type planar source
collimation	TIR lens from Carclo Optics (part no. 10003)
spectrum	pure white light spectrum
FWHM radiant intensity	9°

Specs: Light Source

here

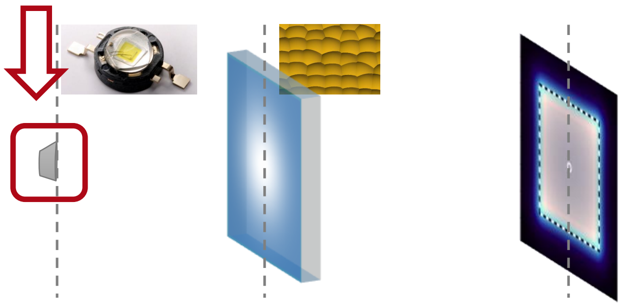

Highlights

- fast and accurate modeling of a white light LED
- design and analysis an aperiodic refractive beam shaper array to optimize a top hat intensity pattern

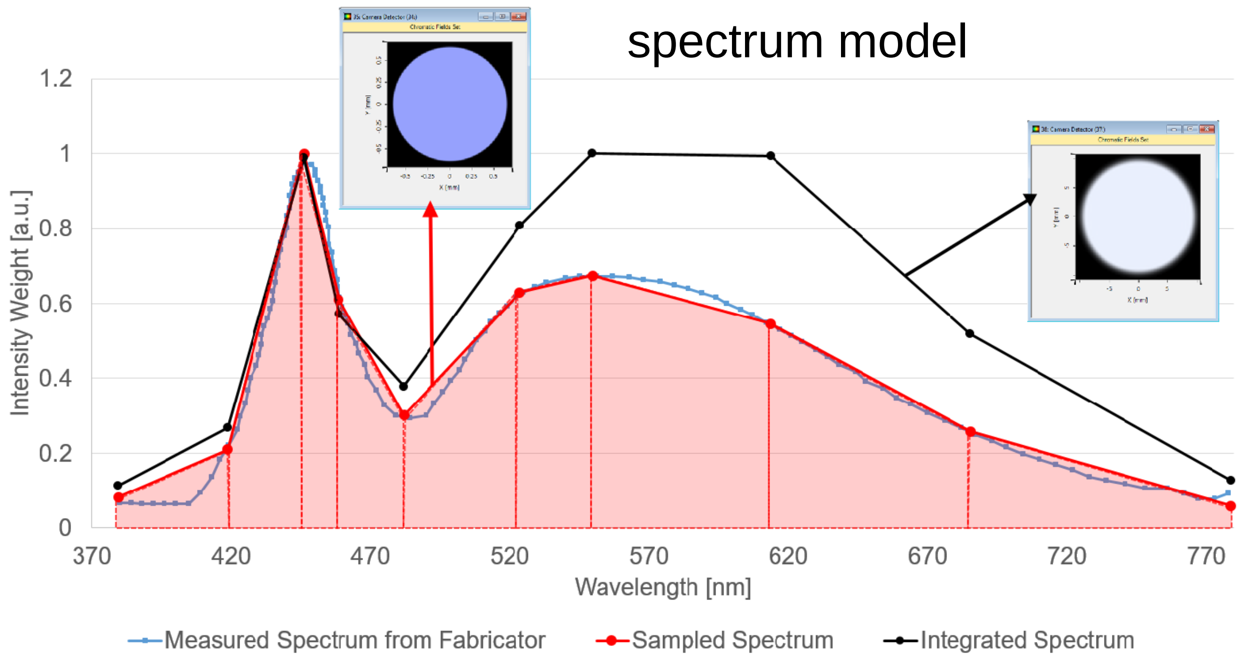

significant performance improvement
non-equidistant sampling of the spectrum

Specs: Aperiodic Refractive Beam Shaper Array

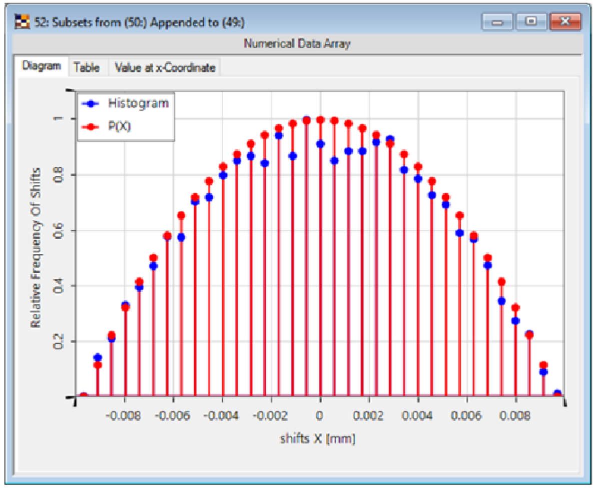

Histogram of Cell Distribution Function

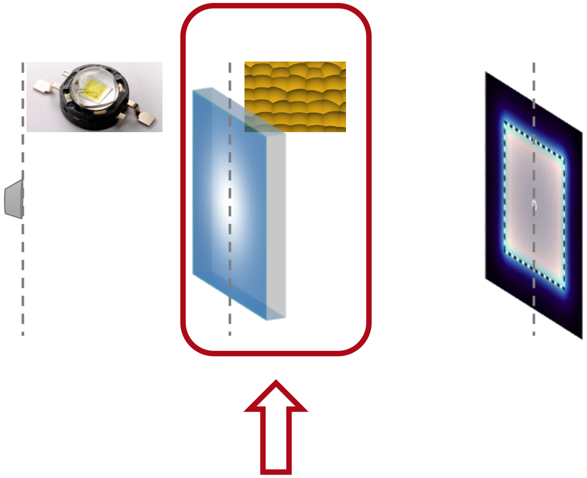

here

Highlights

- fast and accurate modeling of a white light LED
- design and analysis an aperiodic refractive beam shaper array to optimize a top hat intensity pattern

parametrization of the distribution function allows optimization regarding a desired target pattern

Parameter	Description / Value & Unit
cell array aperture	20x20mm
number of cells	124x124
cell distribution function	quadratic polynomial
substrate thickness	1mm
substrate material	fused silica

Specs: Evaluation

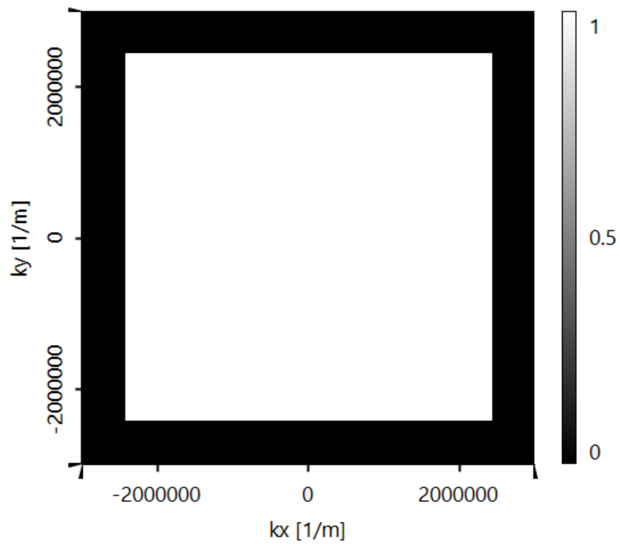

Desired Target Pattern

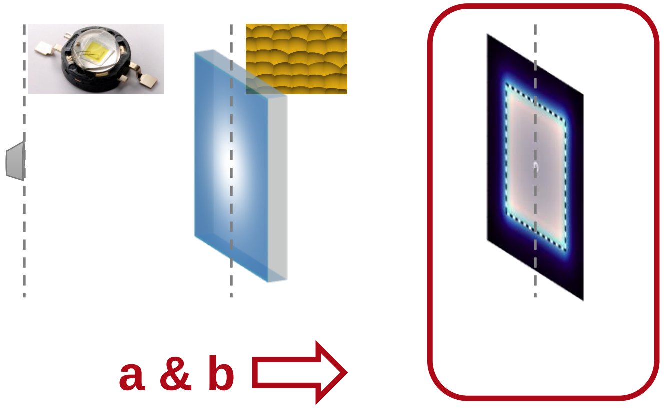

Position	Type of Evaluation	Description / Value & Unit
a	camera detector	evaluates intensity pattern
b	performance criteria evaluation	evaluates conversion & window efficiency and uniformity error regarding the desired target pattern

Results: Intensity Pattern (real color view)

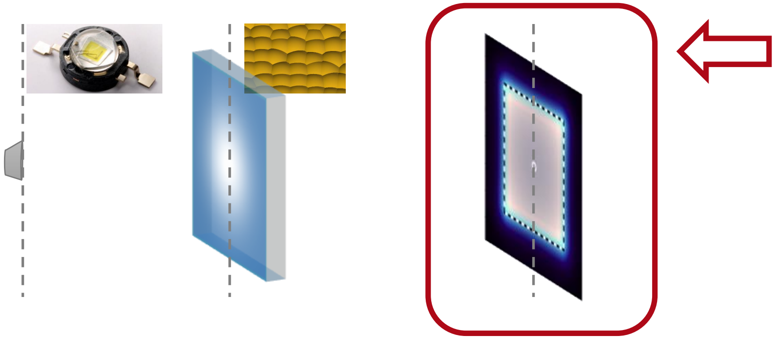

a

Highlights

- fast and accurate modeling of a white light LED
- design and analysis an aperiodic refractive beam shaper array to optimize a top hat intensity pattern

aperiodic beam shaper array

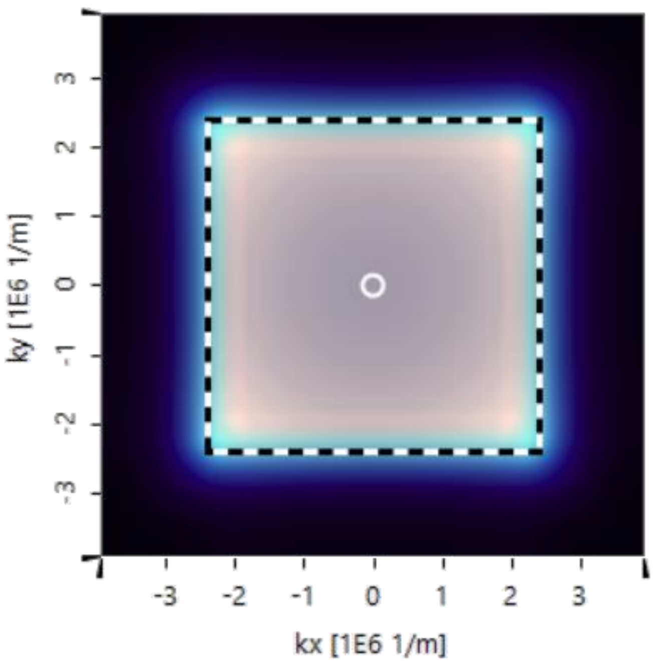

periodic microlens array

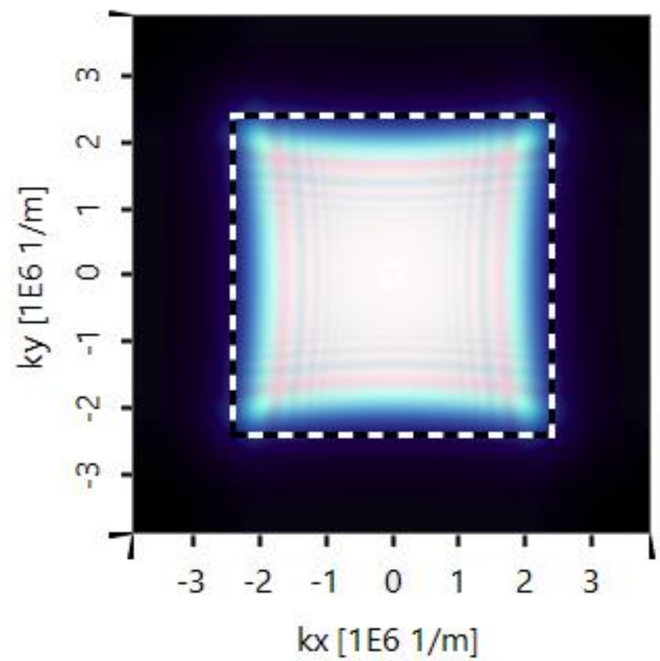

Results: Performance Criteria Evaluation

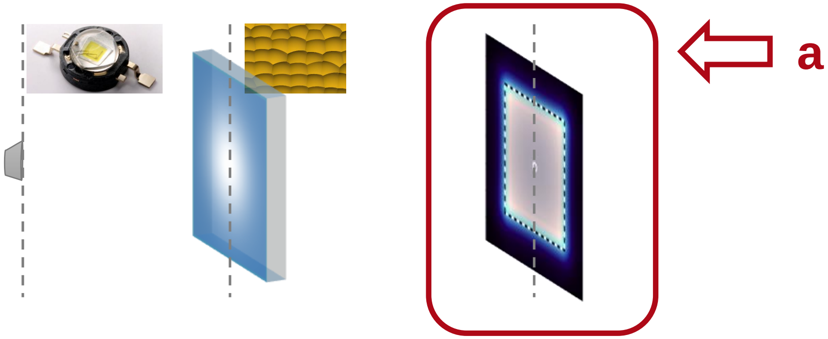

Highlights

- fast and accurate modeling of a white light LED
- design and analysis an aperiodic refractive beam shaper array to optimize a top hat intensity pattern

Parameter	Value & Unit Aperiodic Beam Shaper Array	Value & Unit Microlens Array
window efficiency	92.23 %	99.93 %
conversion efficiency	89.34 %	80.18 %
uniformity error	17.92 %	49.08 %

Virtual And Mixed Reality > Pattern Generation

High-NA Pattern Generation Using Two Beam Splitter Elements

LightTrans International UG

Specification: First Beam Splitter

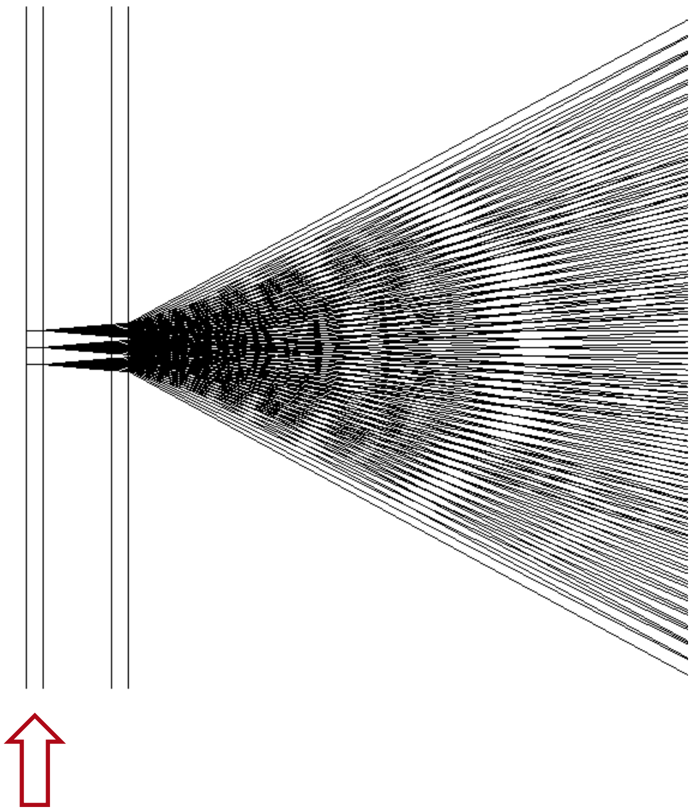

paraxial beam splitter

Parameter	Value & Unit
number of orders	11x11
order separation	1x1°
period	30.35x30.35 µm
pixel size	690x690 nm
discrete height levels	8
material	fused silica

surface profile

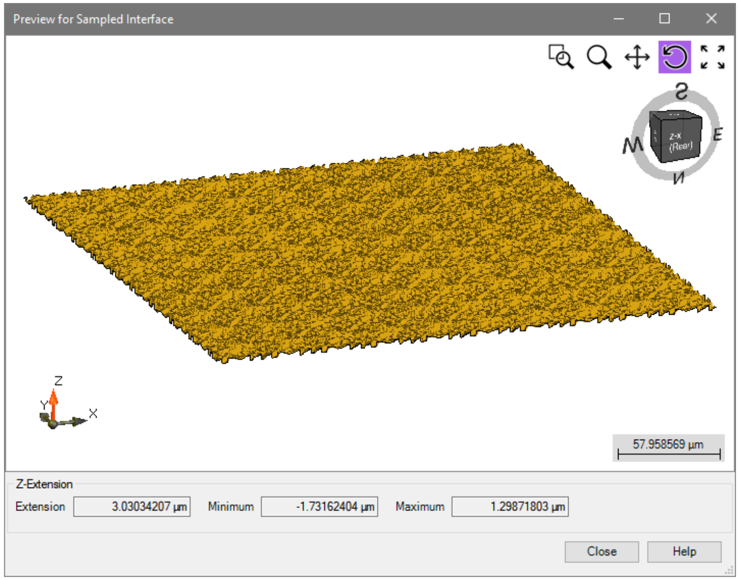

Specification: Second Beam Splitter

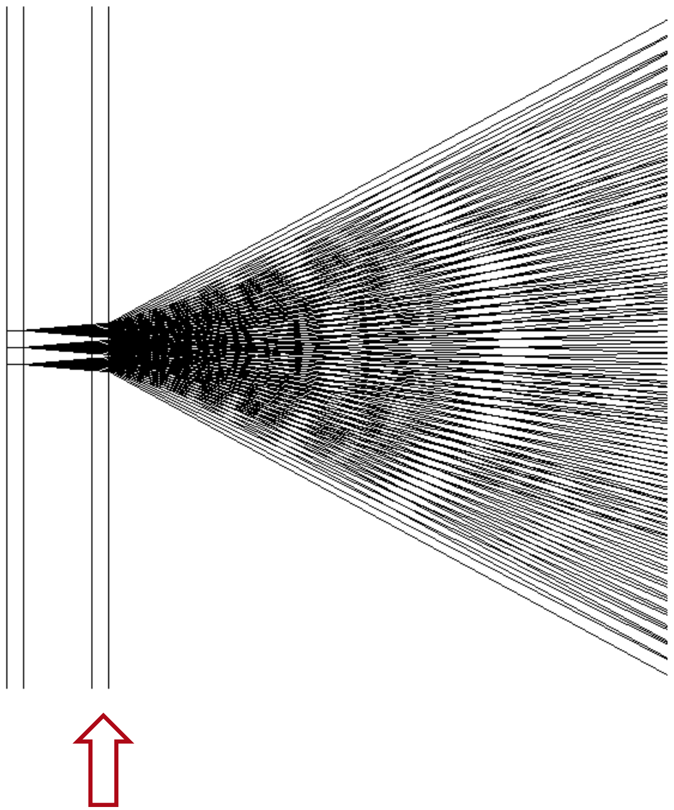

high-NA beam splitter

Parameter	Value & Unit
number of orders	5x5
order separation	11x11°
period	2.73x2.73μm
pixel size	130x130nm
discrete height levels	8
material	fused silica

surface profile

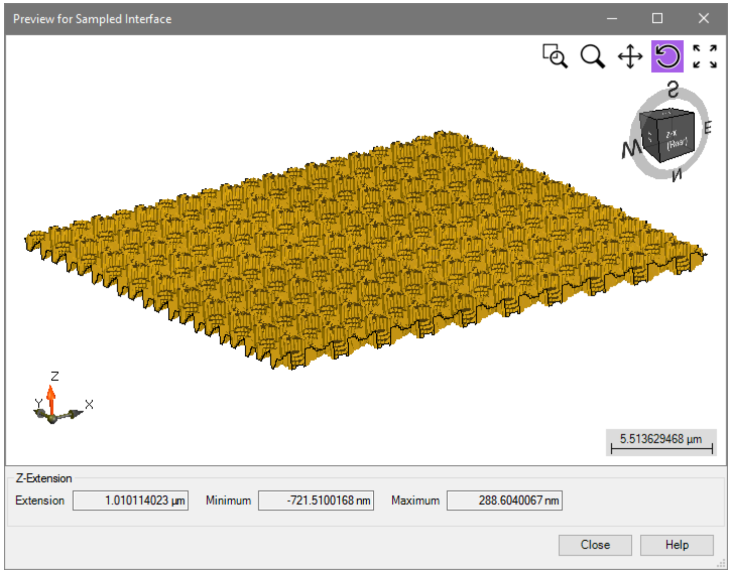

Results: Spot Diagram

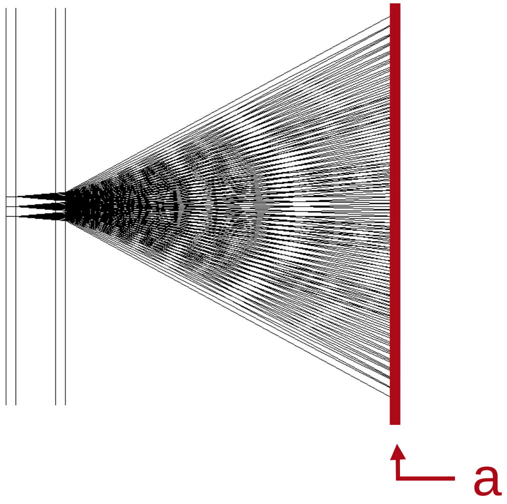

combination of both beam splitter generate **55x55 order** with **55x55° full opening spread**

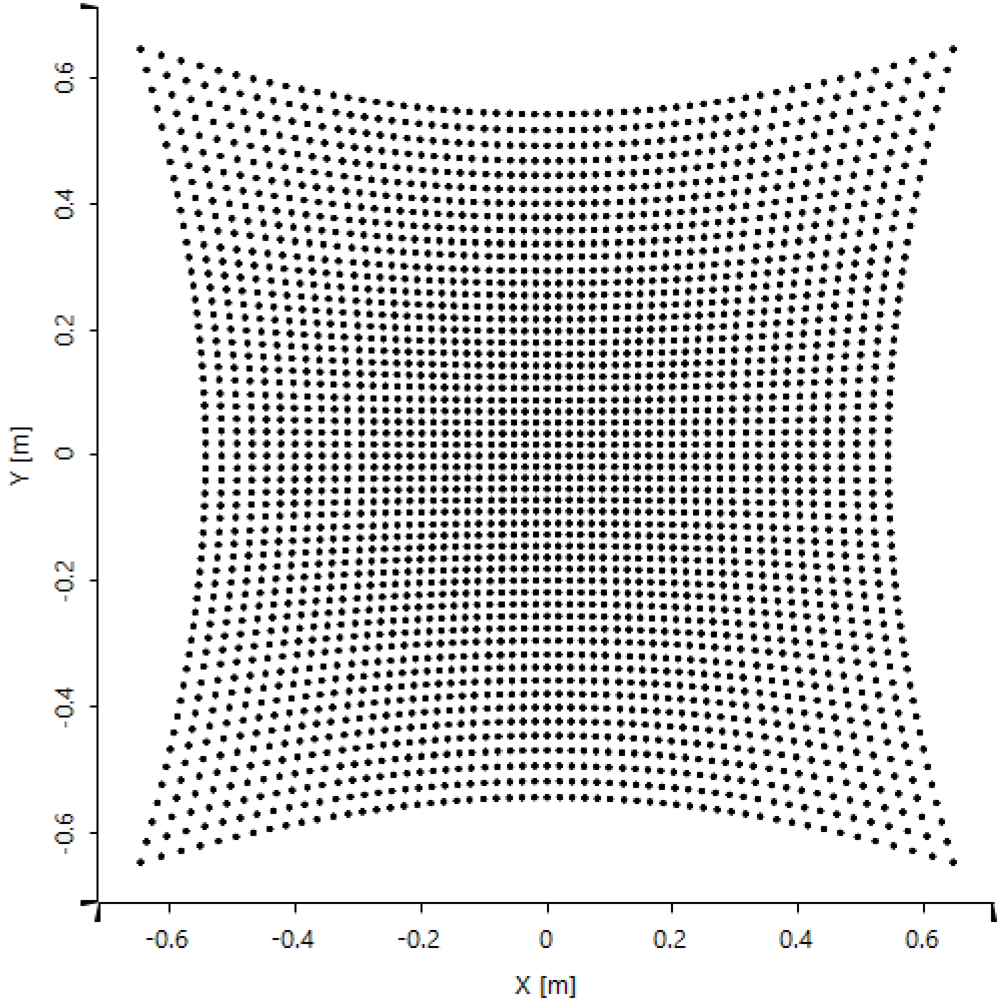

spot diagram

Results: Output Evaluation

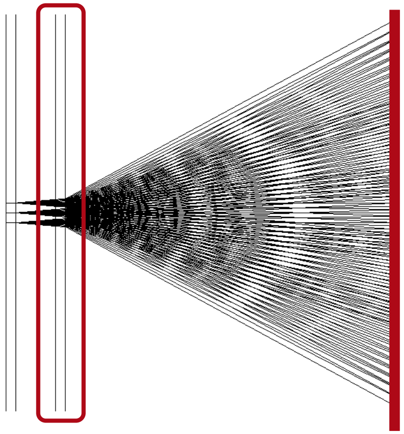

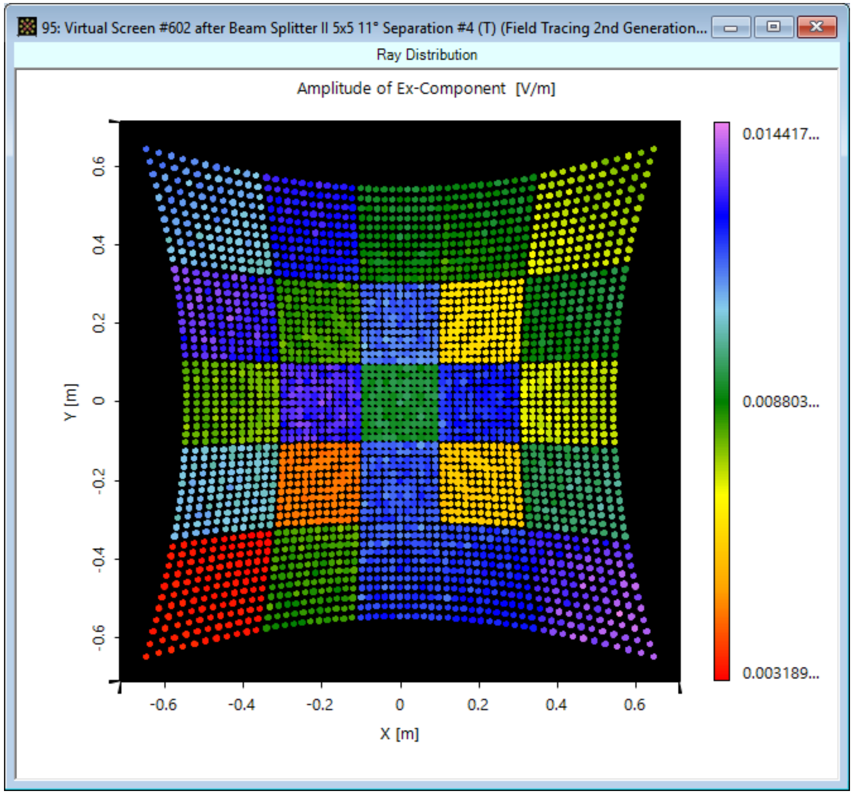

Light Shaping Concepts

- Tailored aberrations
- Stored scanning process
- Multichannel concept: Single Deflection
- Multichannel concept: General

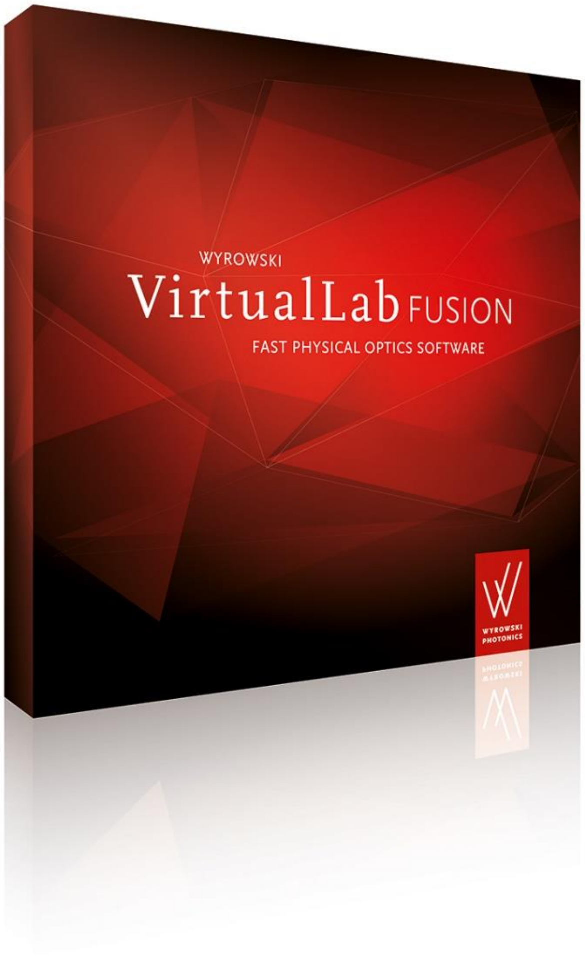

Final part

NED

Virtual and Mixed Reality: Imaging Systems



- VR/MR glasses are sophisticated imaging devices.
- Development of VR/MR glasses demands advanced modeling and design of imaging systems.
- What are the special challenges in the modeling?

Typical Imaging Quality Criteria

- Modeling of imaging quality criteria like
  - ➢ Wavefront error
  - ➢ PSF/MTF
- Criteria dependent on image point position on micro display: FOV

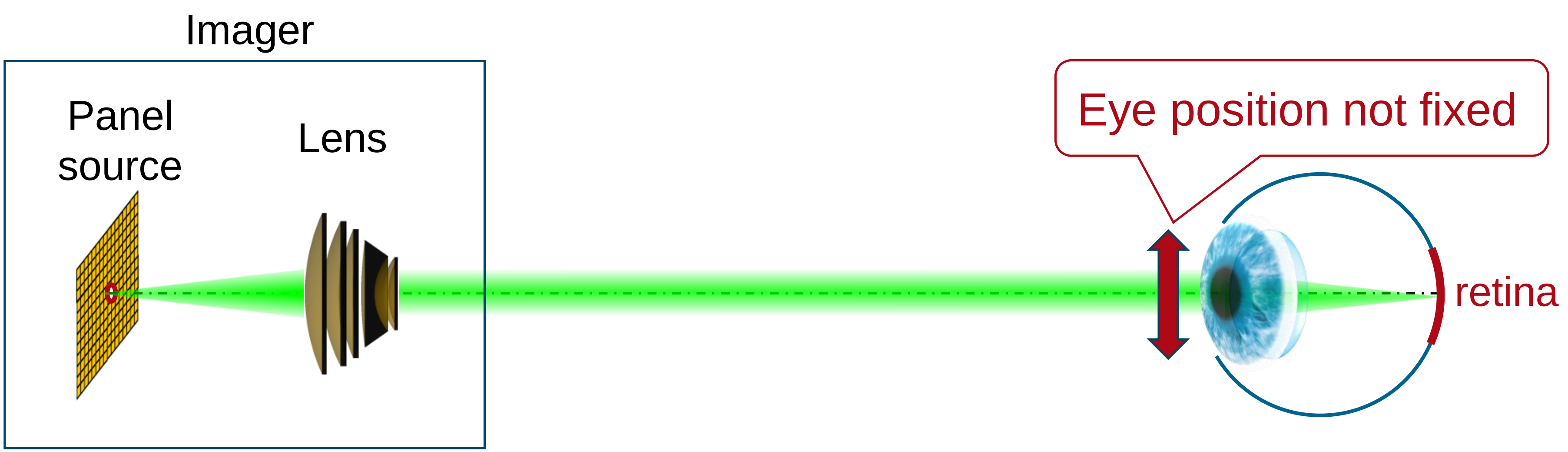

PSF Calculation: Partially Filled Pupil

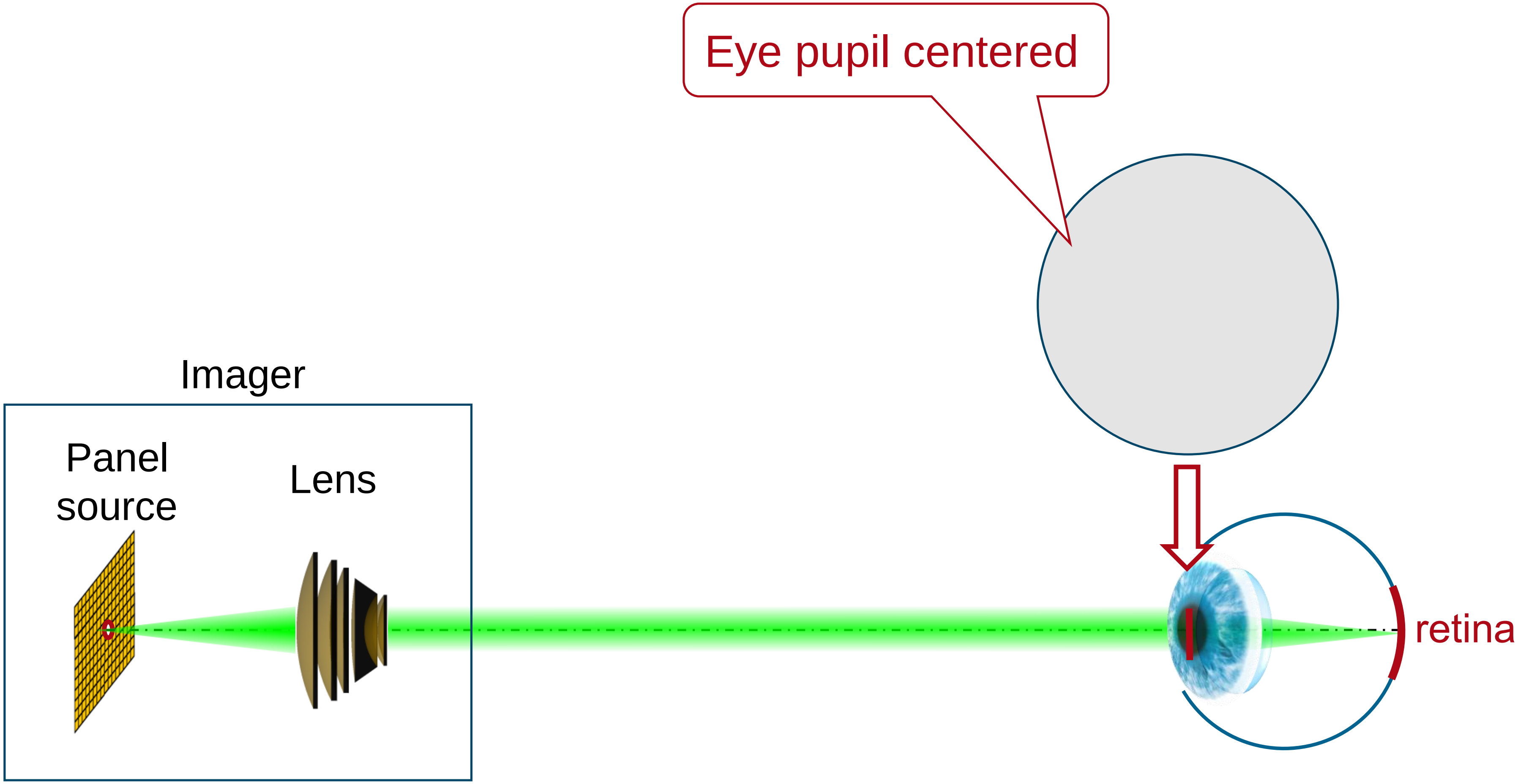

PSF Calculation: Partially Filled Pupil

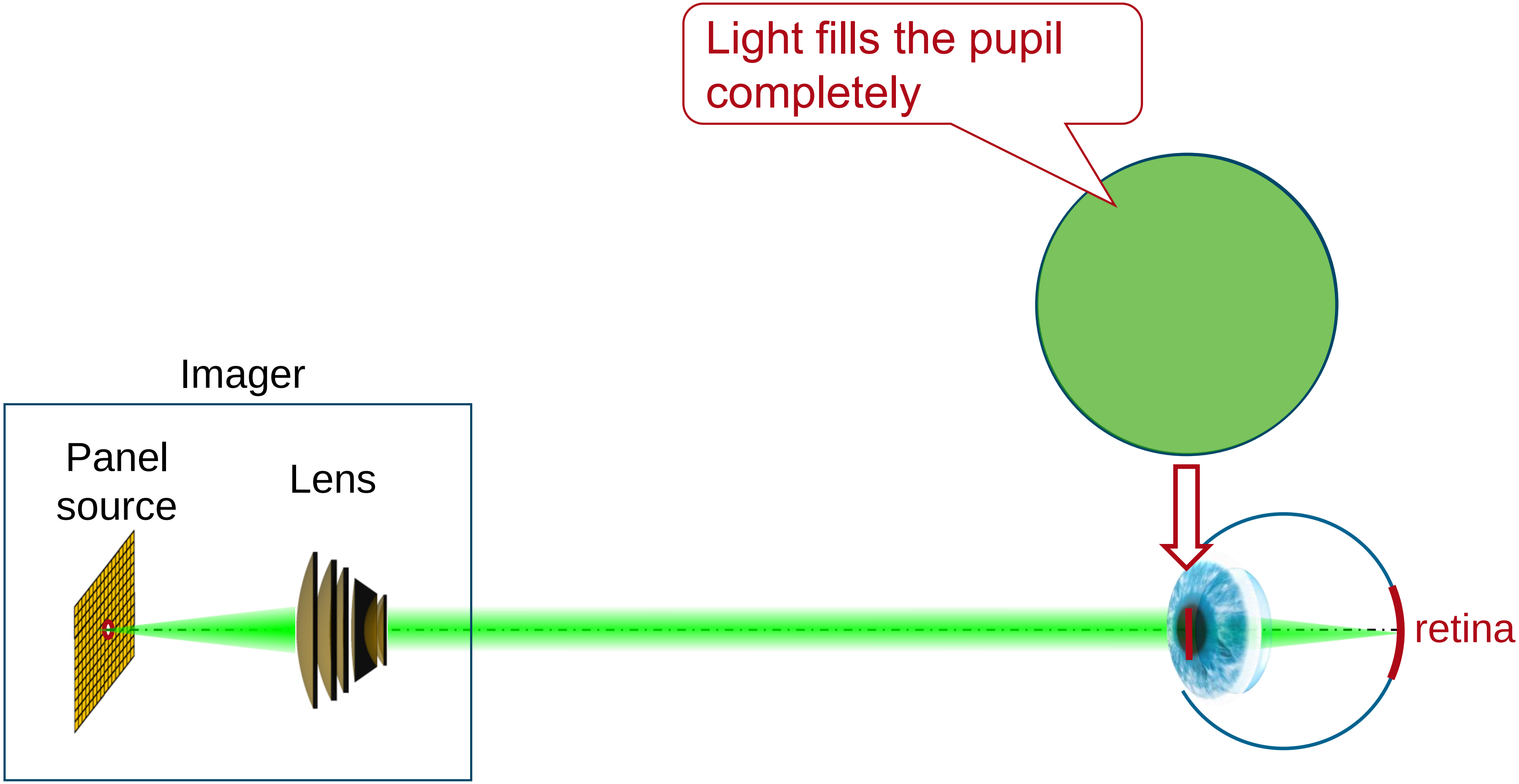

PSF Calculation: Partially Filled Pupil

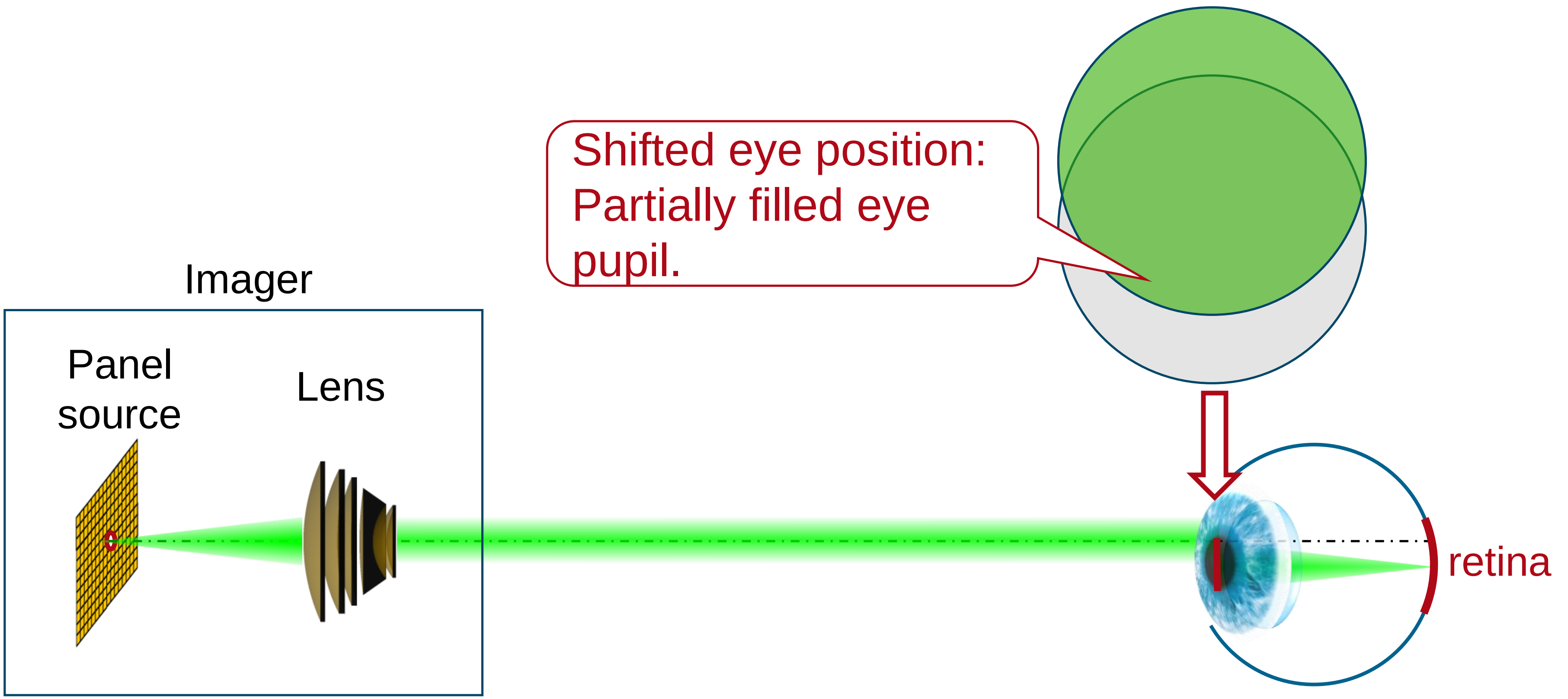

PSF Calculation: Partially Filled Pupil

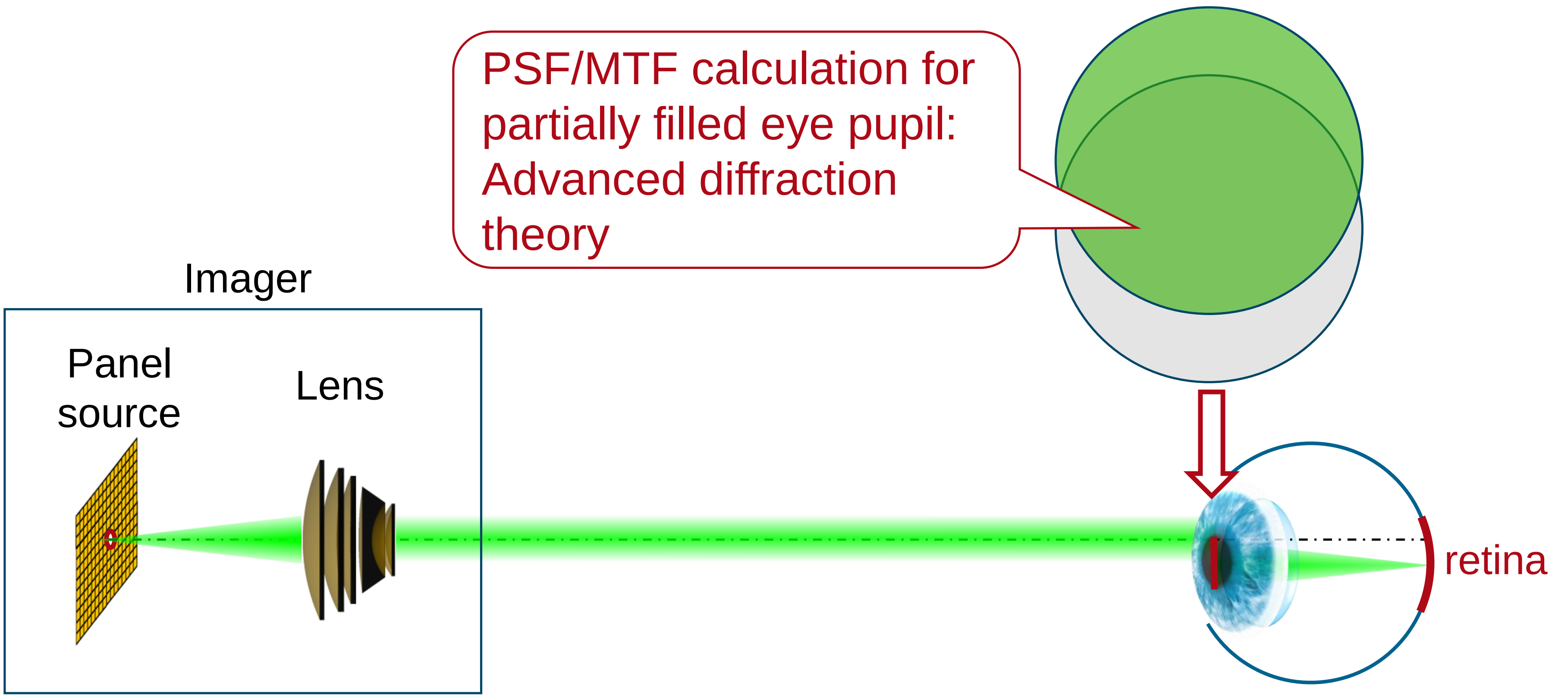

Challenges in Modeling of VR/MR

- PSF/MTF calculation for partially filled exit pupils

Results: 3D System Ray Tracing

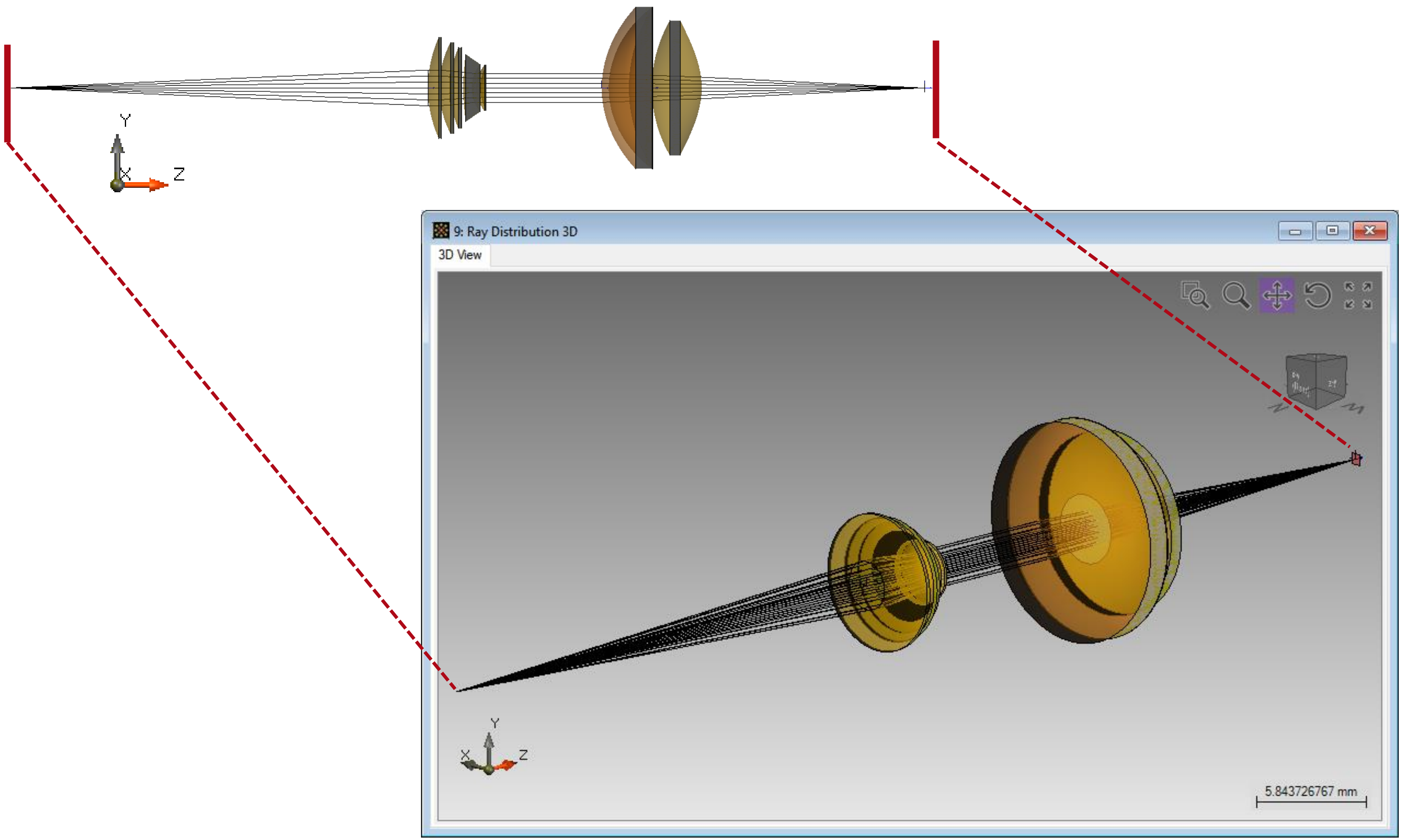

Results: Illumination of Pupil

Highlight

advanced PSF and MTF evaluation of fully or partly illuminated apertures

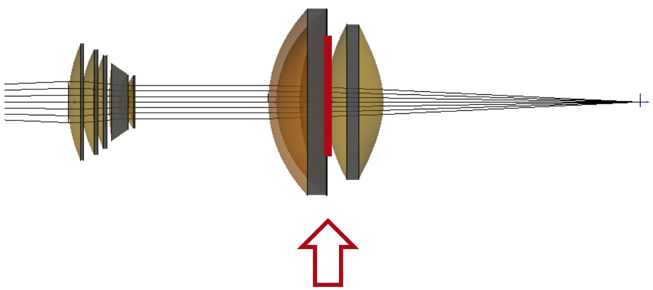

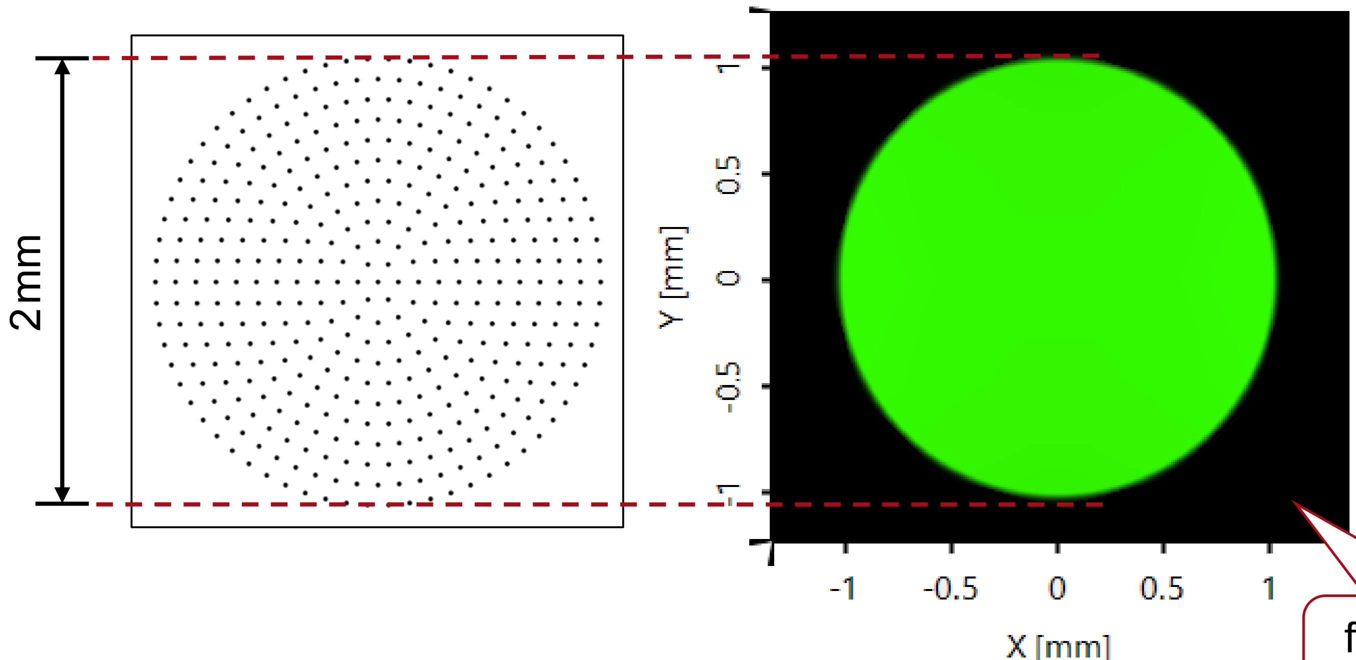

fully illuminated aperture

dot diagram of ray positions

intensity

Results: Illumination of Pupil

Highlight

advanced PSF and MTF evaluation of fully or partly illuminated apertures

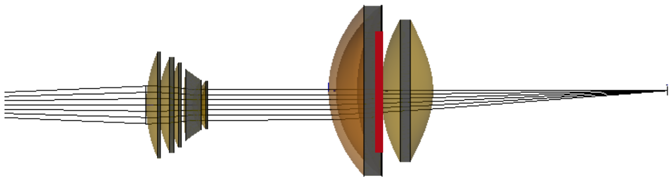

Boundary effect well-sampled.

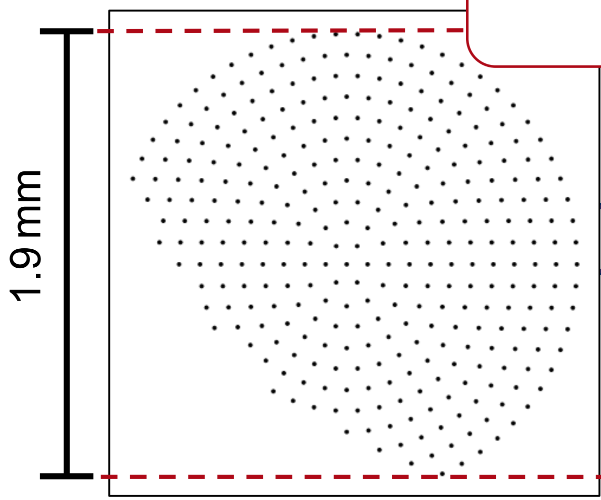

dot diagram of ray positions

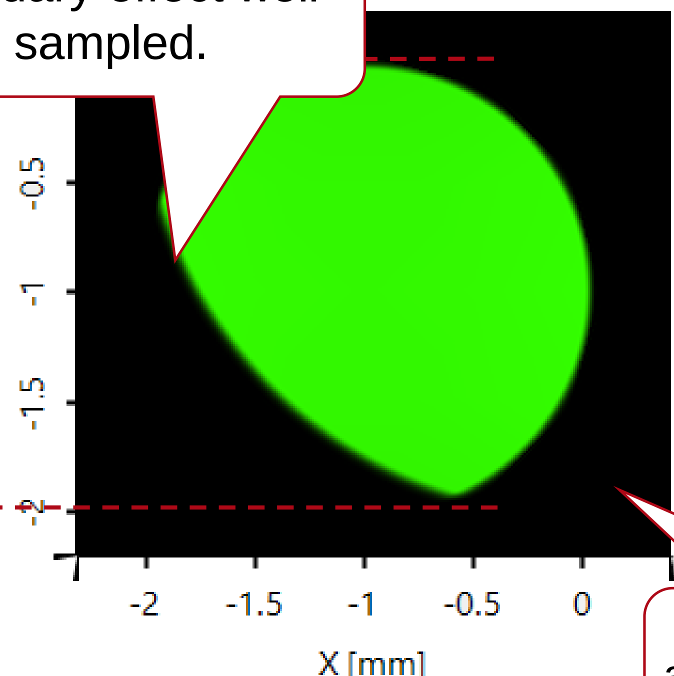

intensity

partly illuminated aperture by shifting eye to (1, 1)mm

Results: PSF & MTF

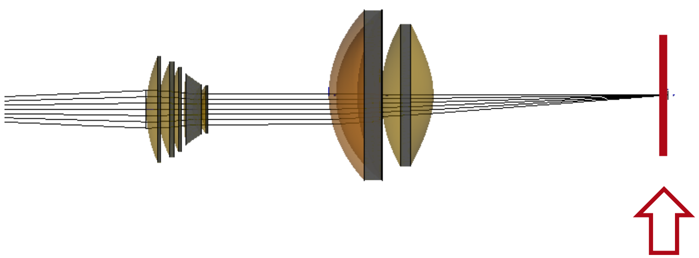

Highlight

advanced PSF and MTF evaluation of fully or partly illuminated apertures

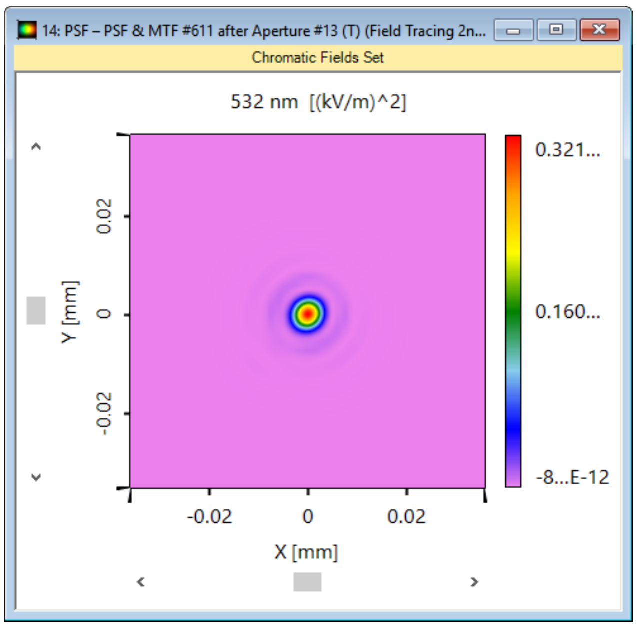

PSF

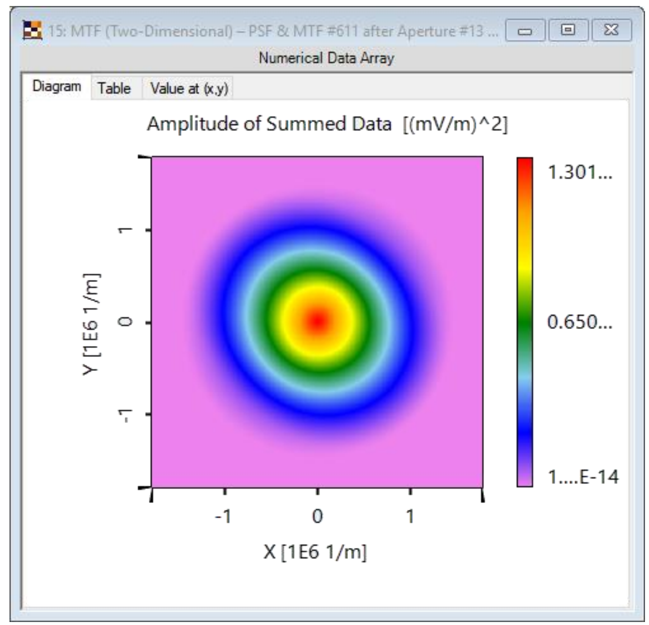

2D MTF

Simulation Time ~ few seconds

Results: PSF & MTF – Comparison

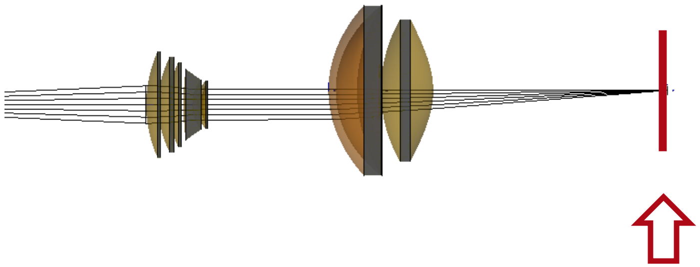

Highlight

advanced PSF and MTF evaluation of fully or partly illuminated apertures

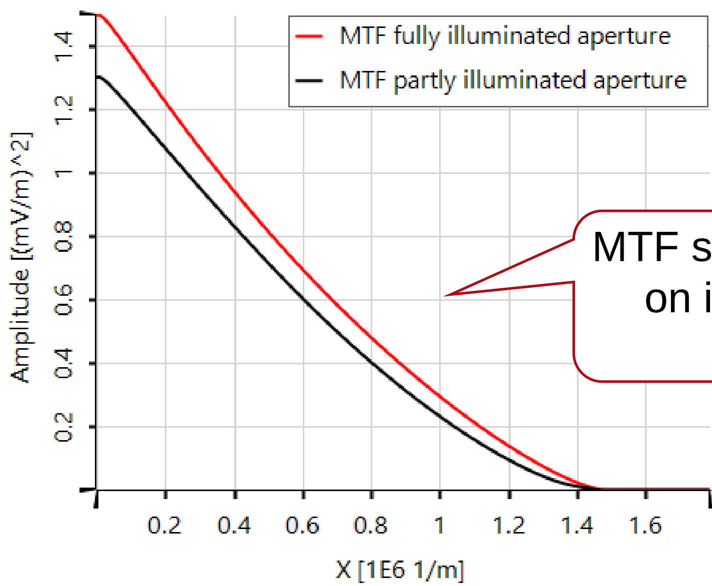

MTF strongly depends on illumination of aperture

MTF profile line

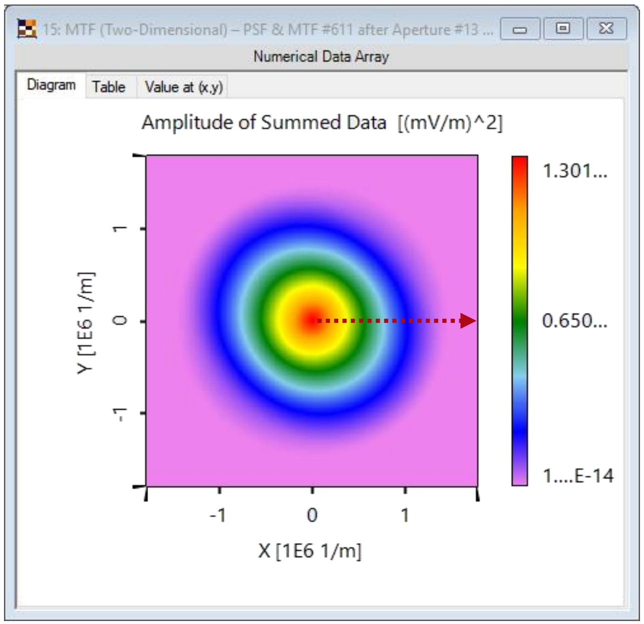

2D MTF
(from system with partly illuminated aperture)

Spatial Guiding of Imaging Channel

Spatial Guiding of Imaging Channel

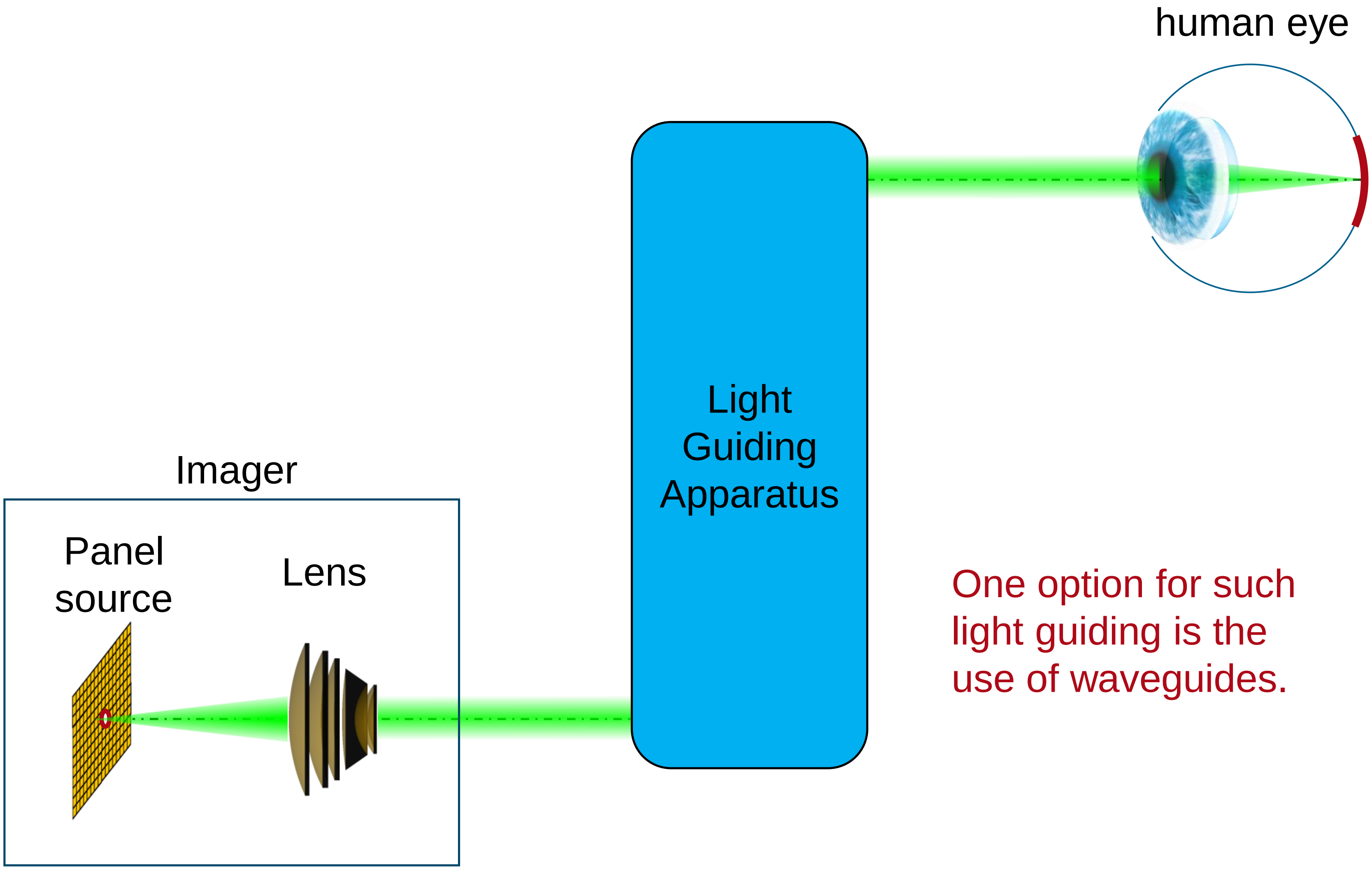

One option for such light guiding is the use of waveguides.

Spatial Guiding of Imaging Channel

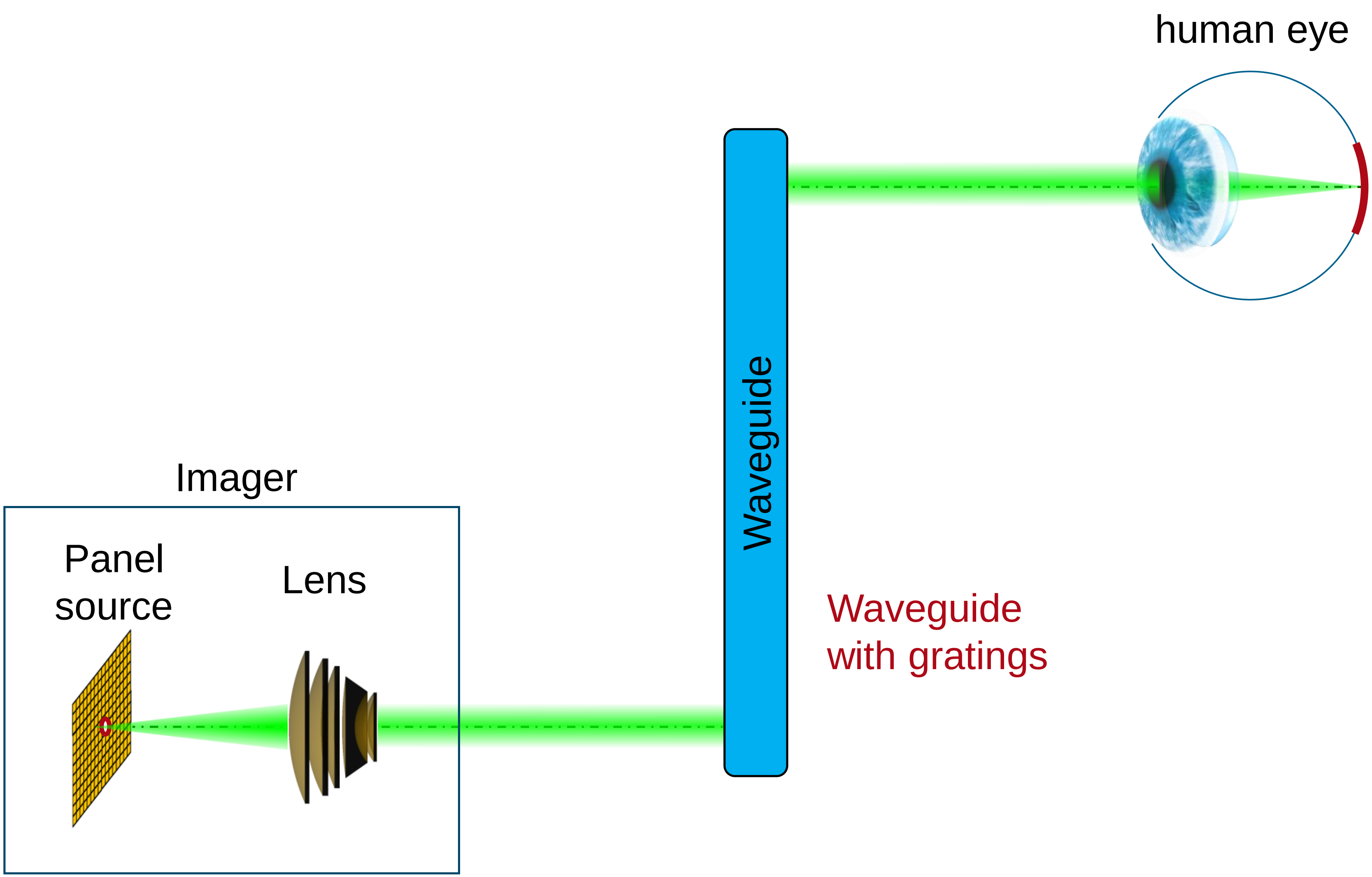

Gratings, Detrimental Orders and Ghost Images

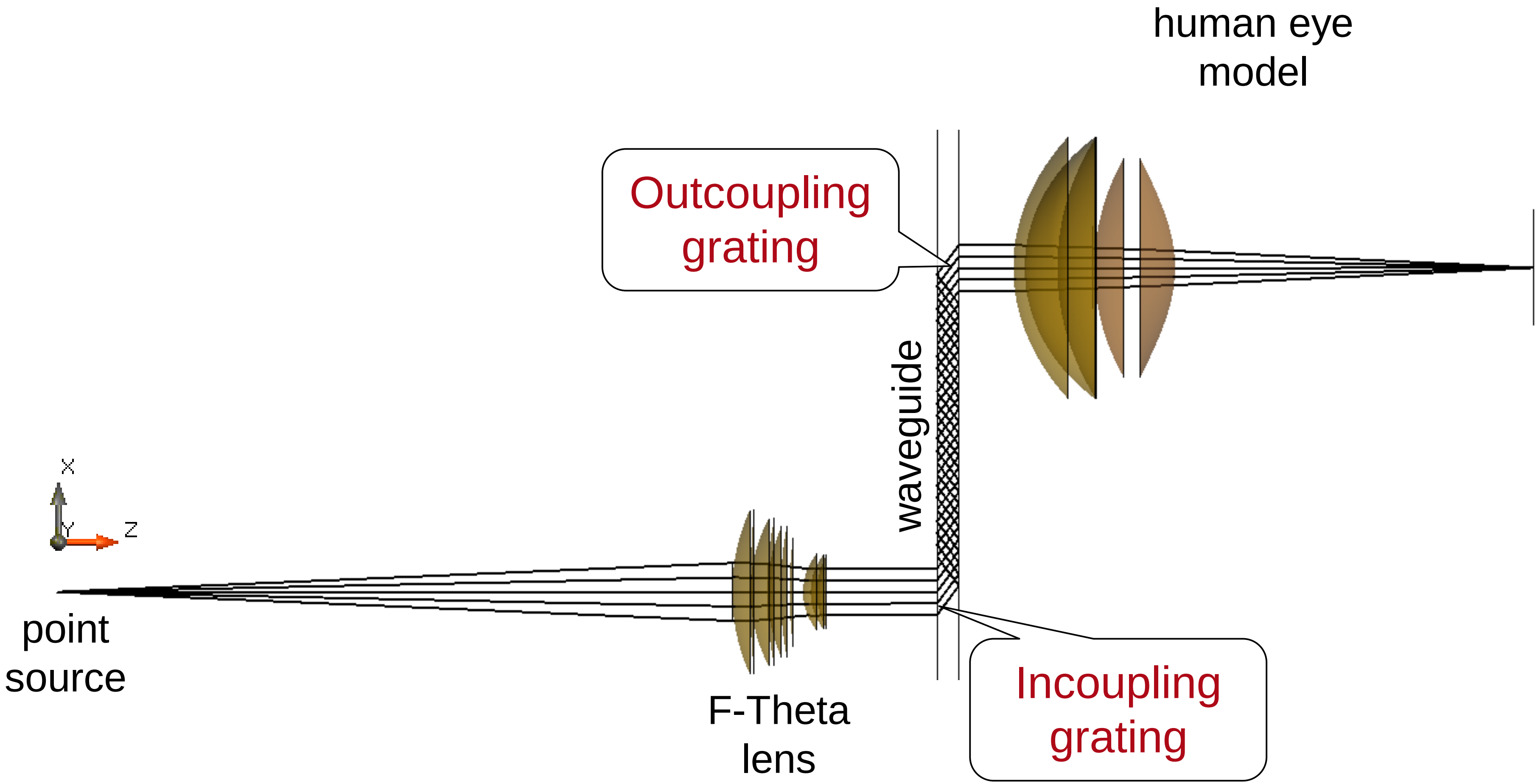

Gratings, Detrimental Orders and Ghost Images

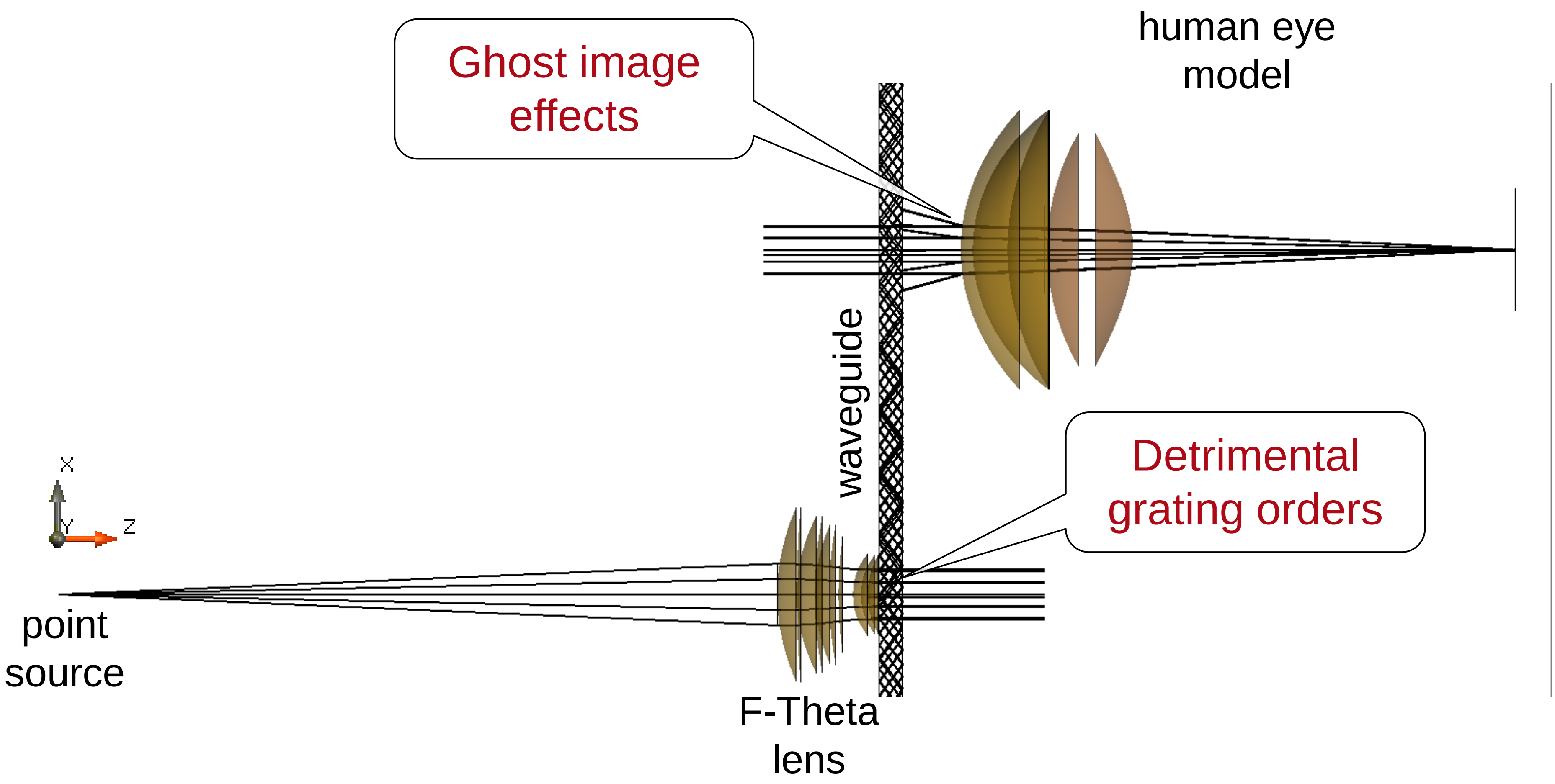

Challenges in Modeling of VR/MR

- PSF/MTF calculation for partially filled exit pupils
- Non-sequential modeling of imaging channels

Challenges in Modeling of VR/MR

- PSF/MTF calculation for partially filled exit pupils
- Non-sequential modeling of imaging channels
- Imaging channels with gratings
  - Non-sequential lightpath analysis including polarization dependent evaluation of grating effects
  - Inclusion of higher orders and straylight

Result: 3D Ray Tracing

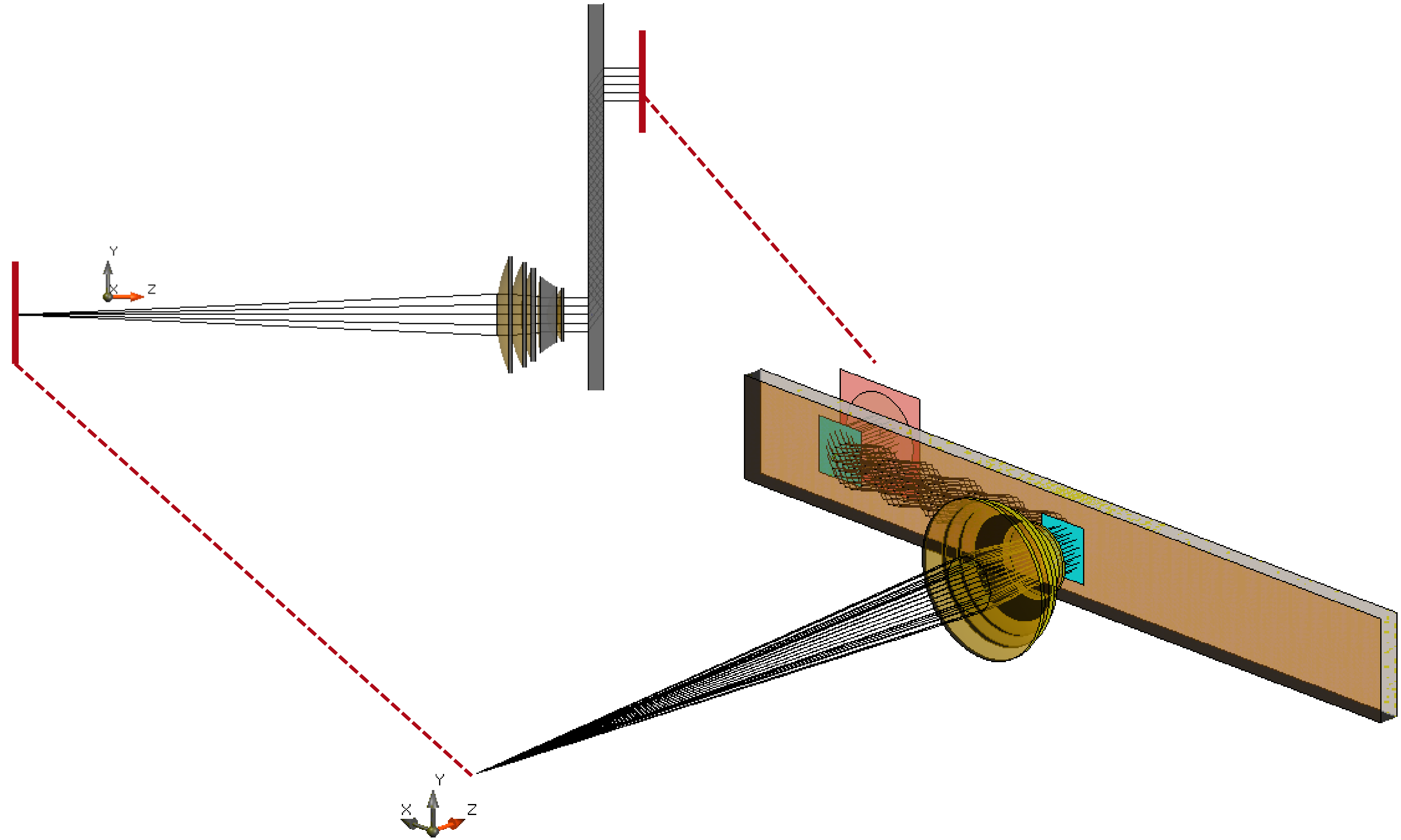

Result: 2D PSF & 2D MTF

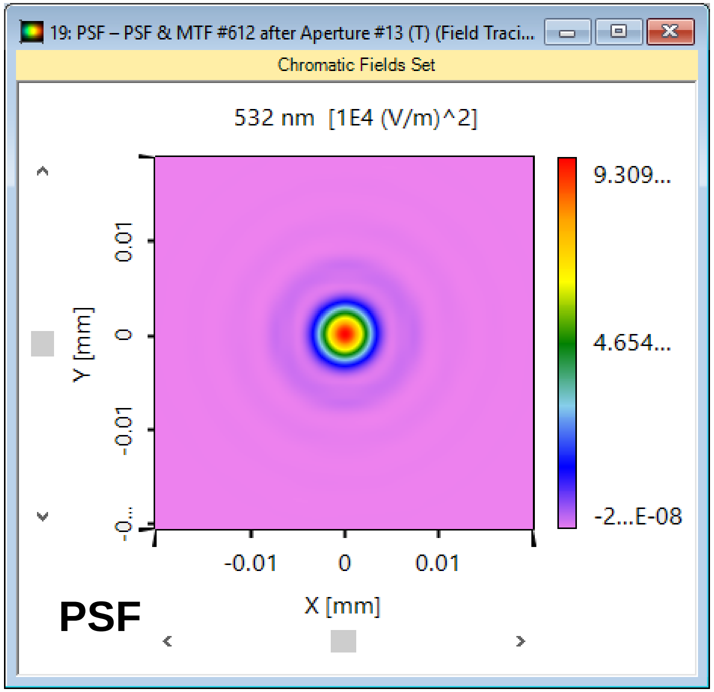

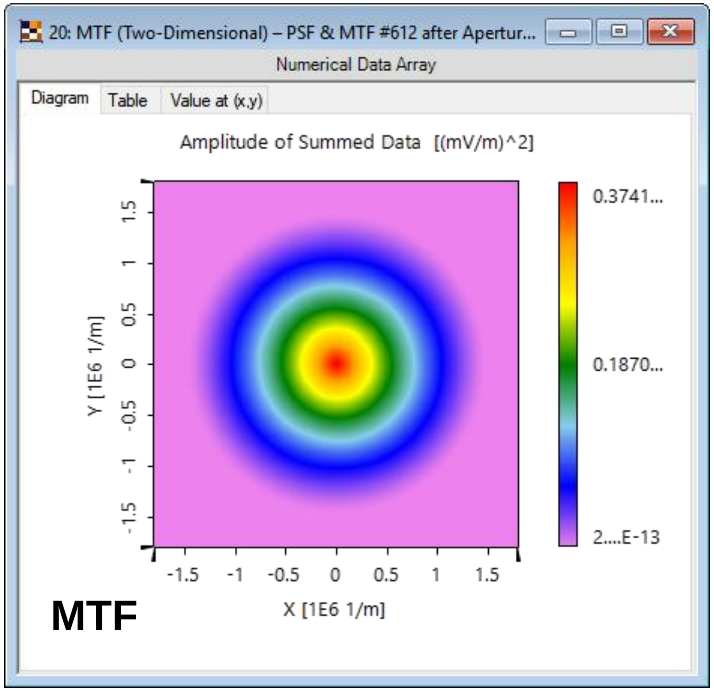

Highlights

- non-sequential analysis of propagation in the waveguide
- regard of wavefront aberrations for PSF and MTF calculation

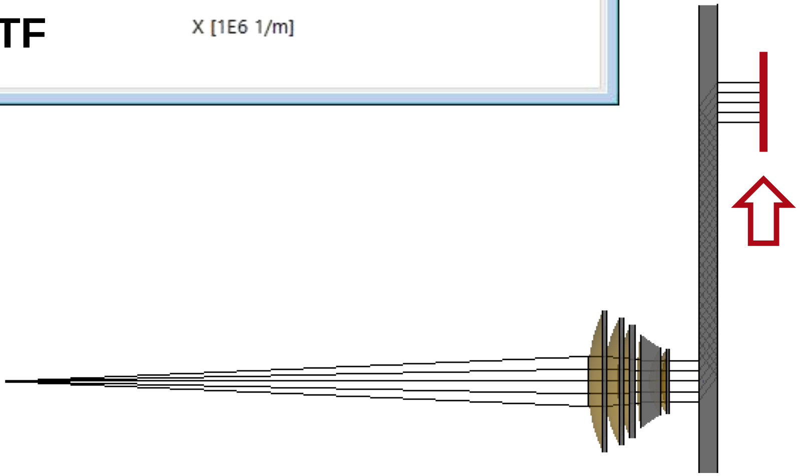

Simulation of Waveguide with Curved Surfaces

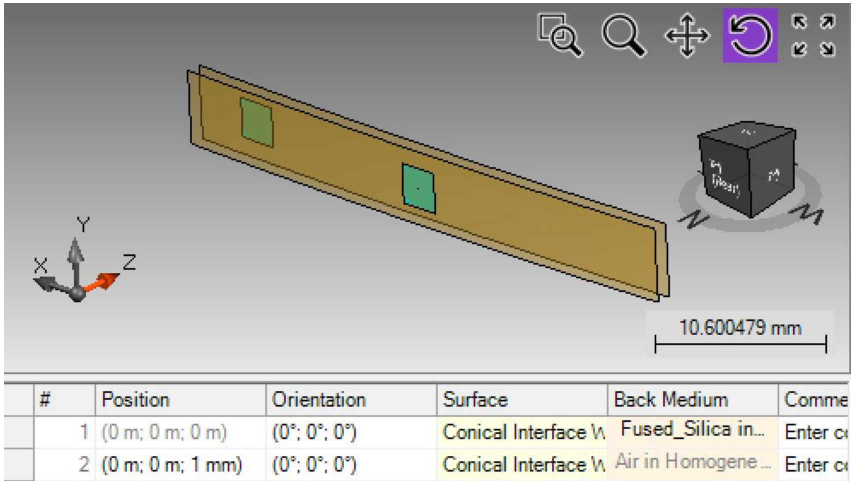

Parameter	Value & Unit
type surface(s)	conical
radius of curvature	500 mm
size of surface(s)	40 x 5 mm
total profile height	6.2500391 µm

- For waveguide applications it is very important to investigate the effect of surface deformations.
- Therefore we introduce curved surfaces instead of planar surfaces to describe the waveguide stack.

Result: 3D Ray Tracing

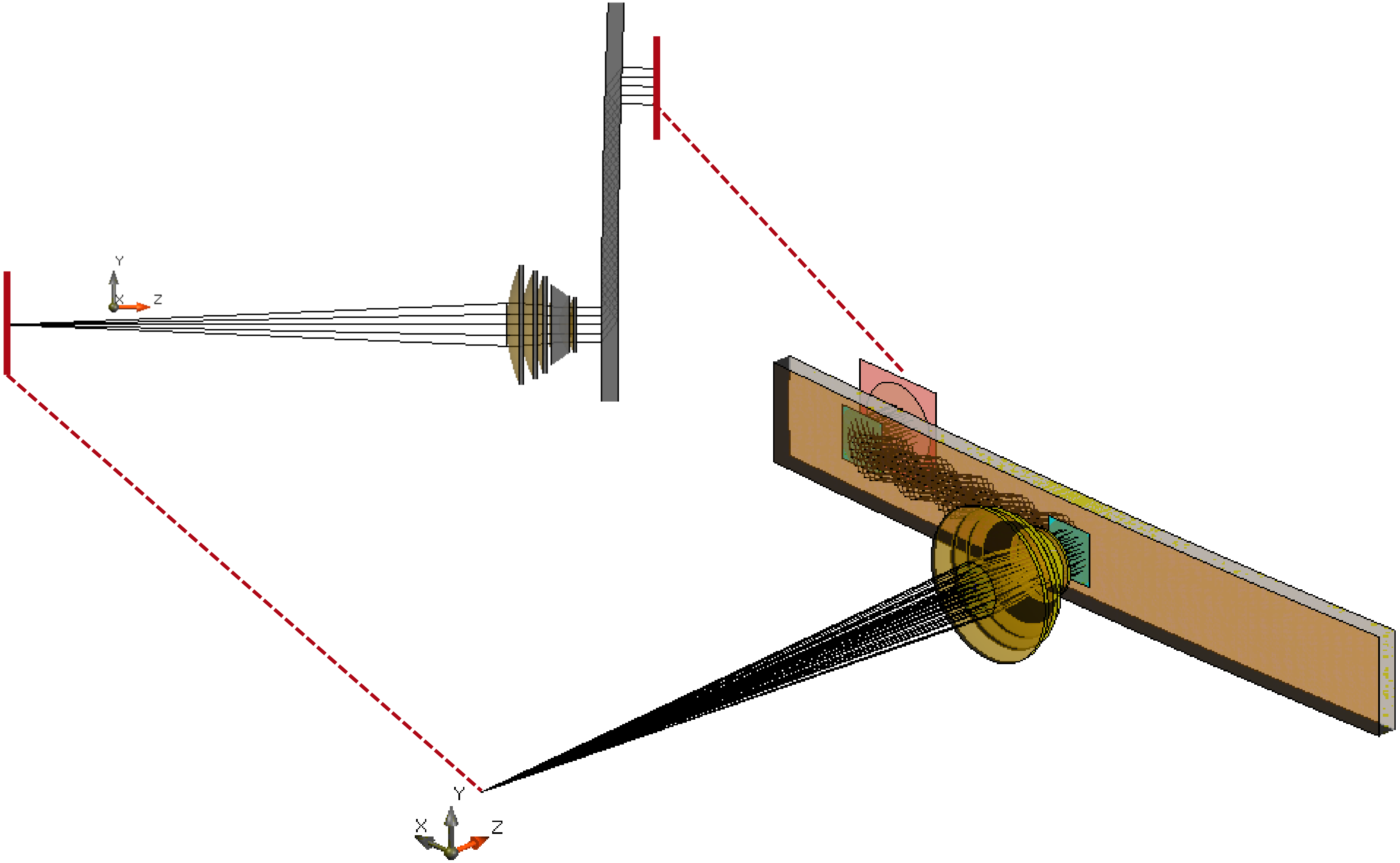

Result: 2D PSF & 2D MTF for Curved Surfaces

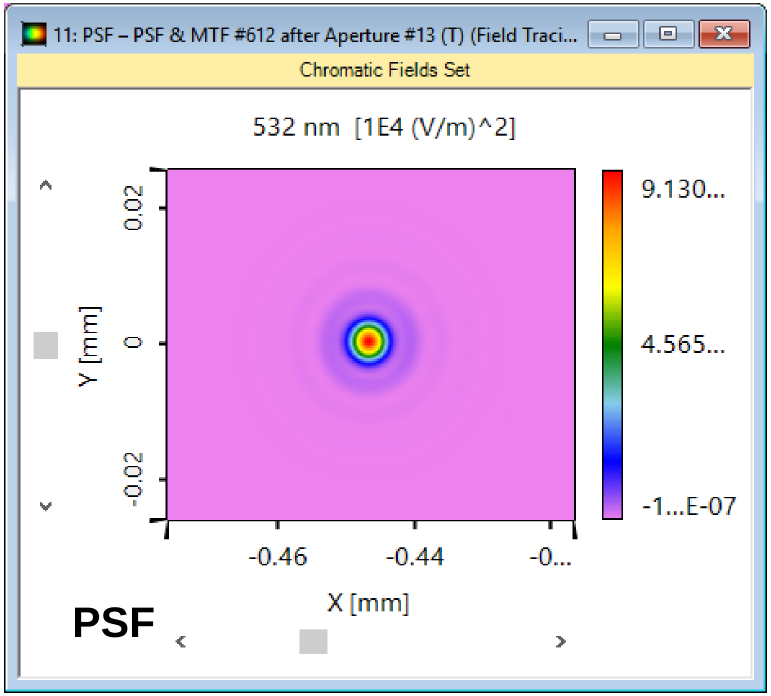

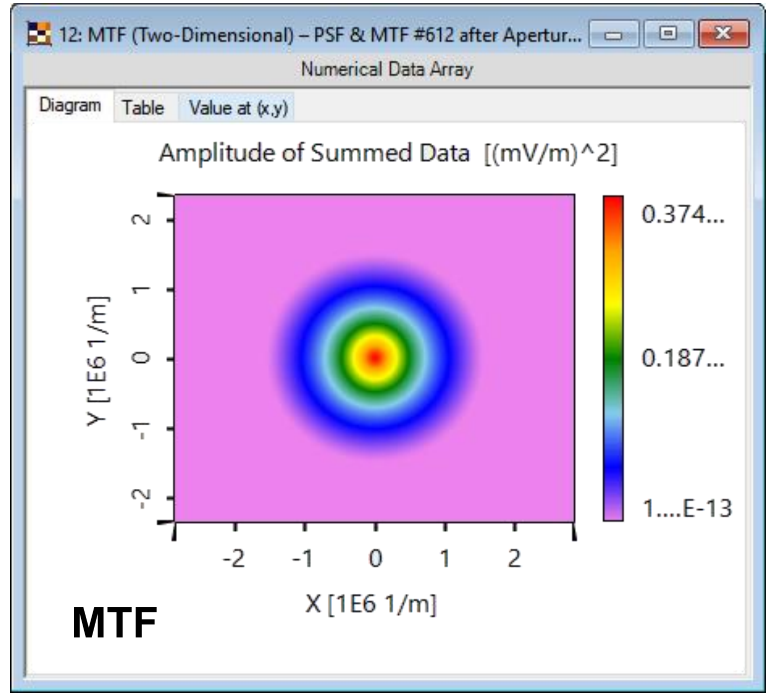

Highlights

- non-sequential analysis of propagation in the waveguide
- regard of wavefront aberrations for PSF and MTF calculation

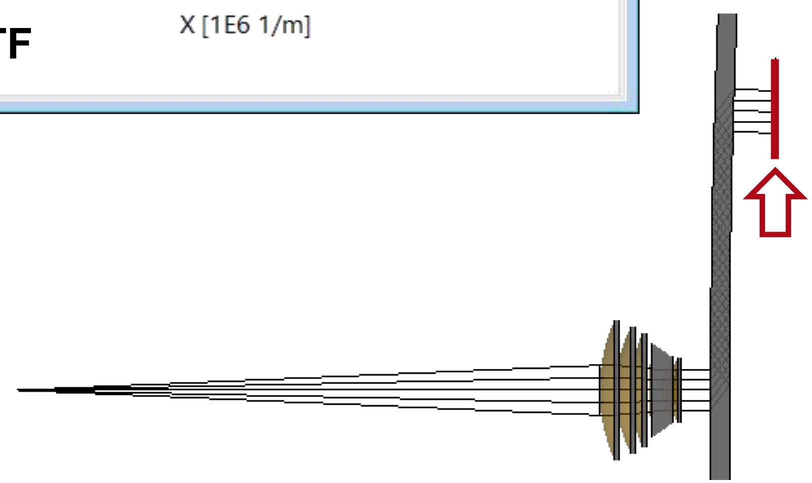

Result: 1D MTF Curved vs. Planar

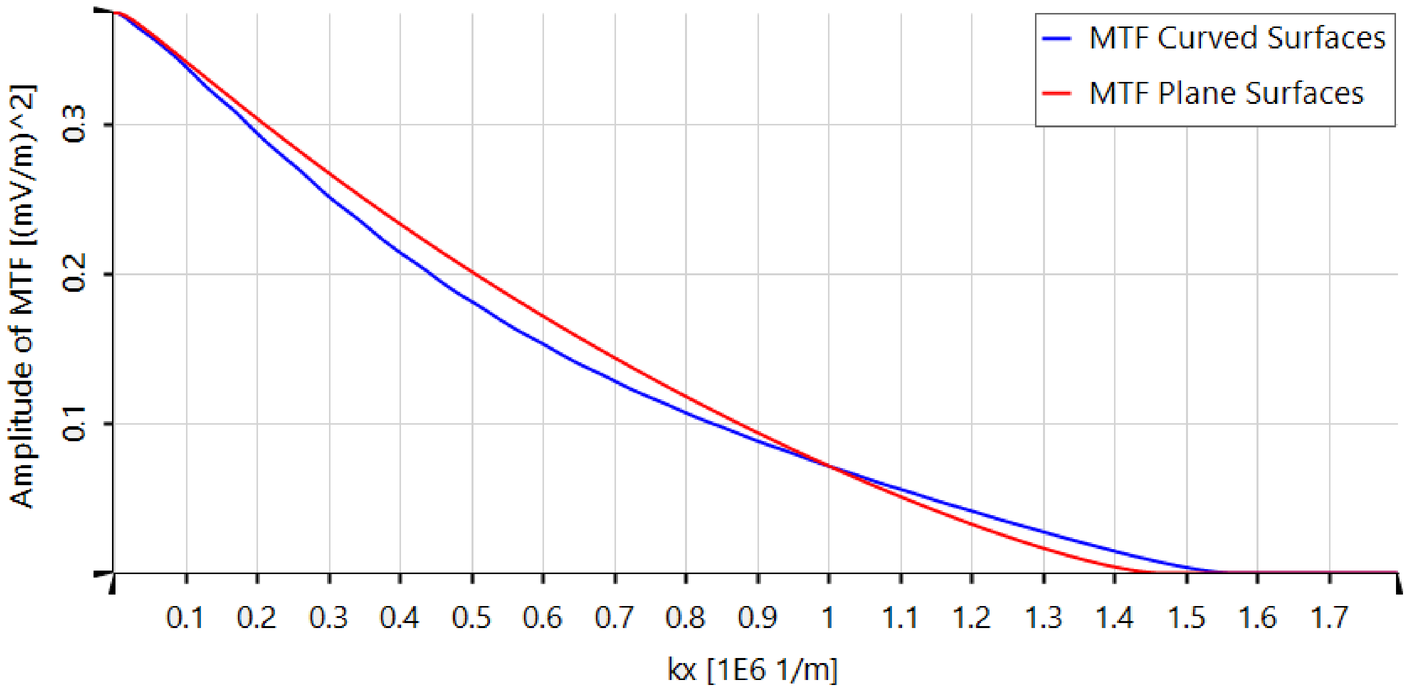

Highlights

- non-sequential analysis of propagation in the waveguide
- regard of wavefront aberrations for PSF and MTF calculation

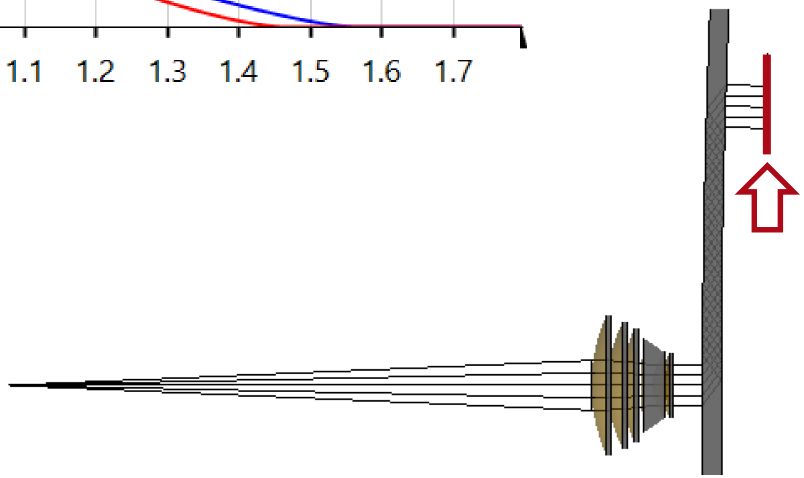

Evaluation of FOV Effects

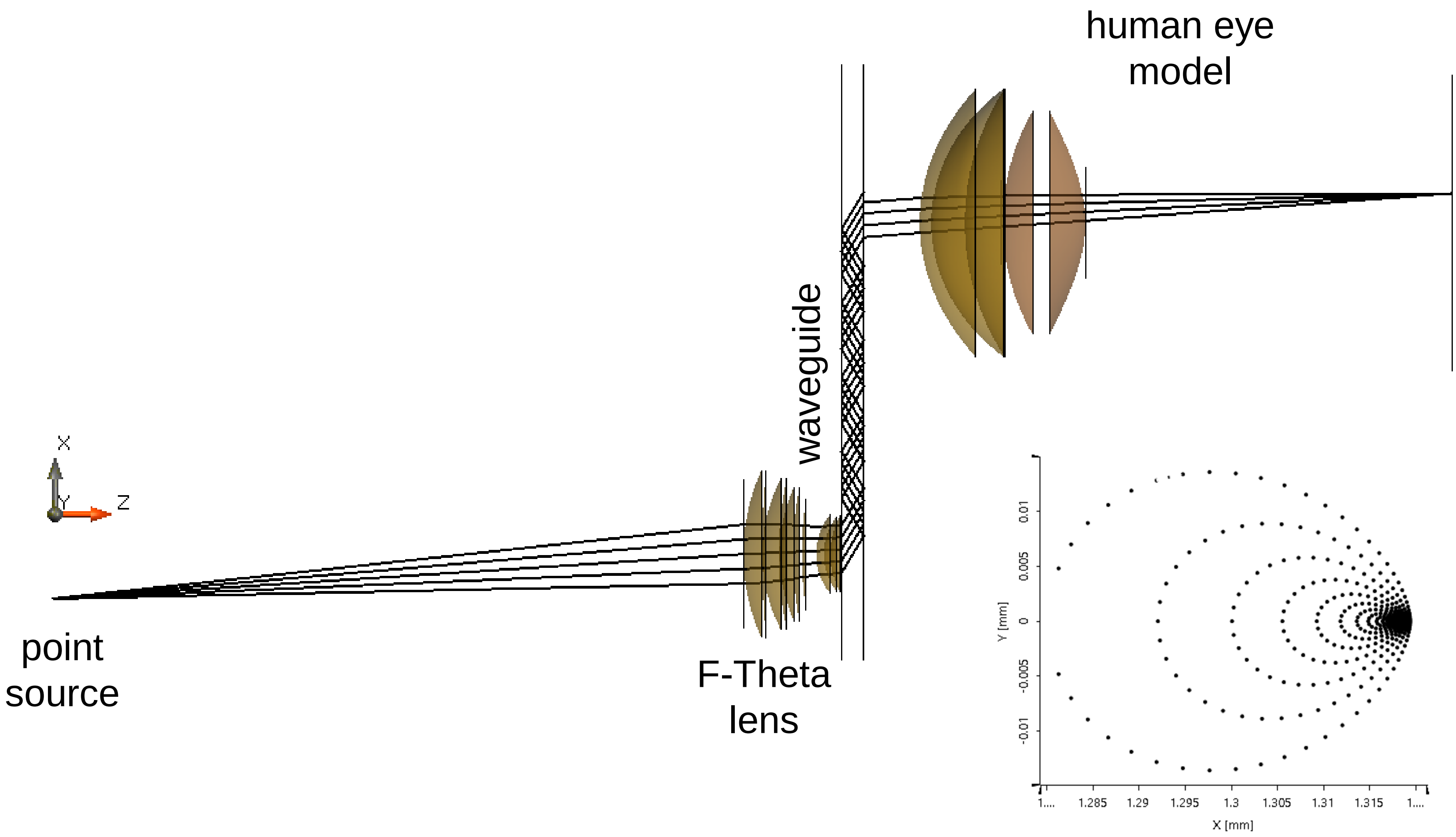

Evaluation in FOV Effects

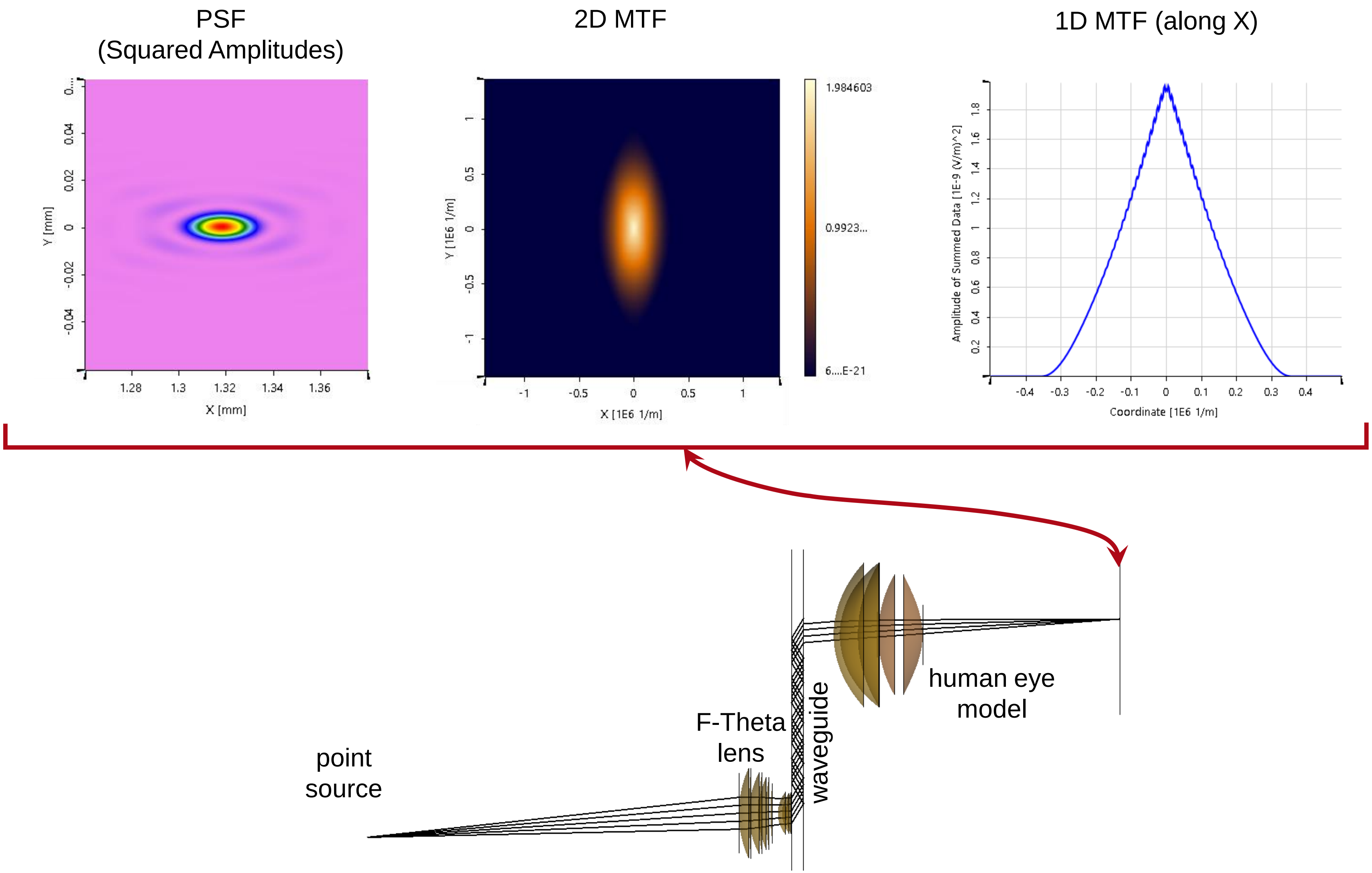

Challenges in Modeling of VR/MR

- PSF/MTF calculation for partially filled exit pupils
- Non-sequential modeling of imaging channels
- Imaging channels with gratings
  - Non-sequential lightpath analysis including polarization dependent evaluation of grating effects
  - Inclusion of higher orders and straylight

Results: 3D System Ray Tracing

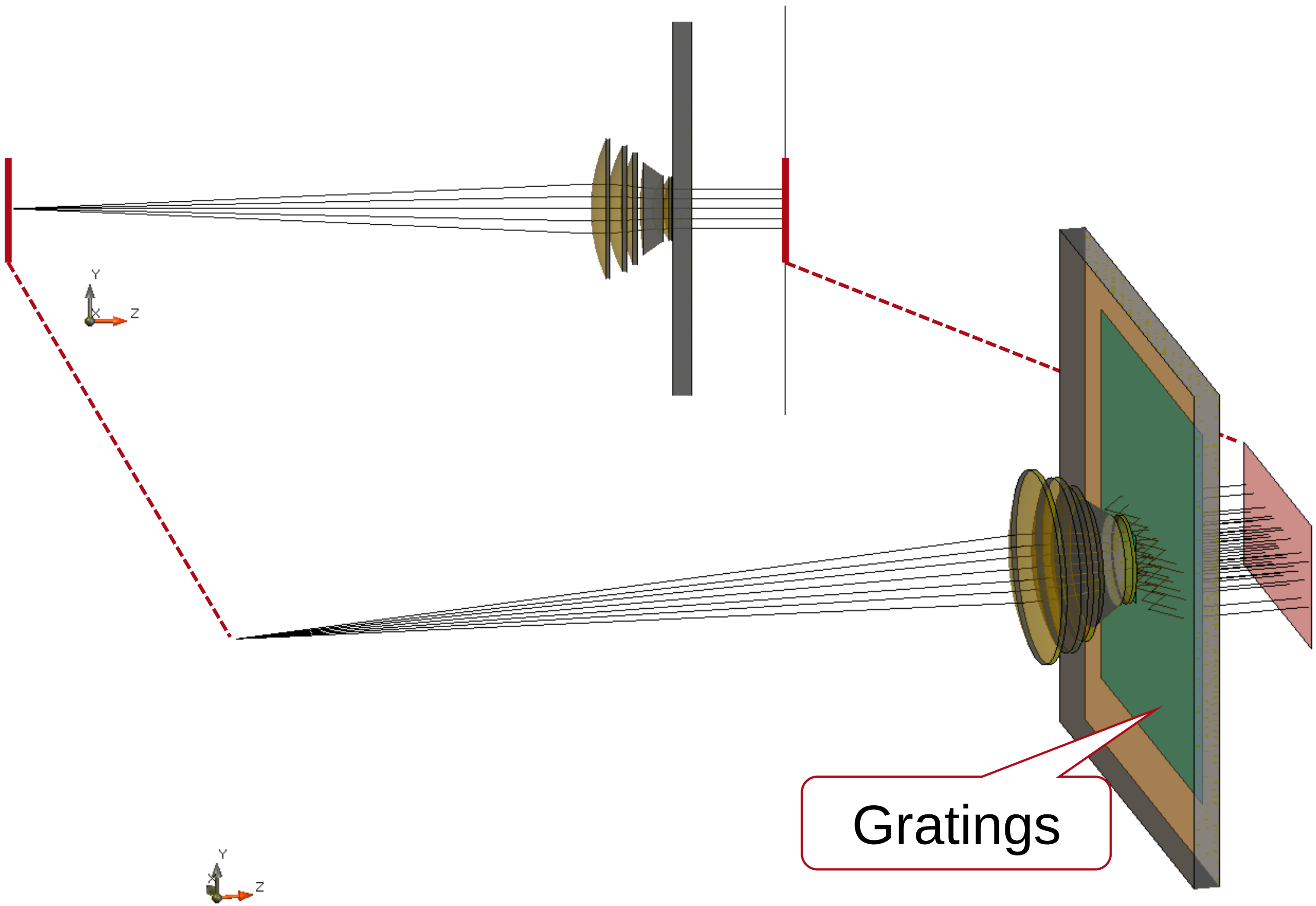

Result I: Only 0th Non-Reflected Orders

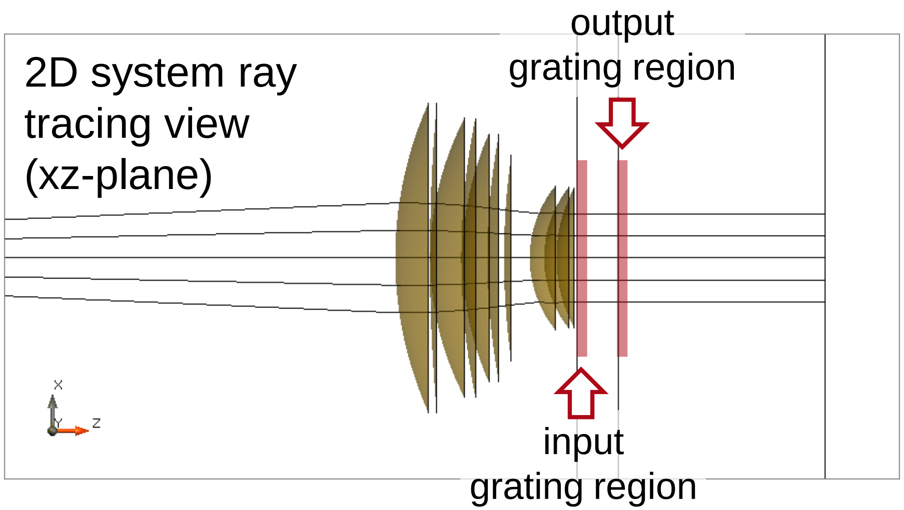

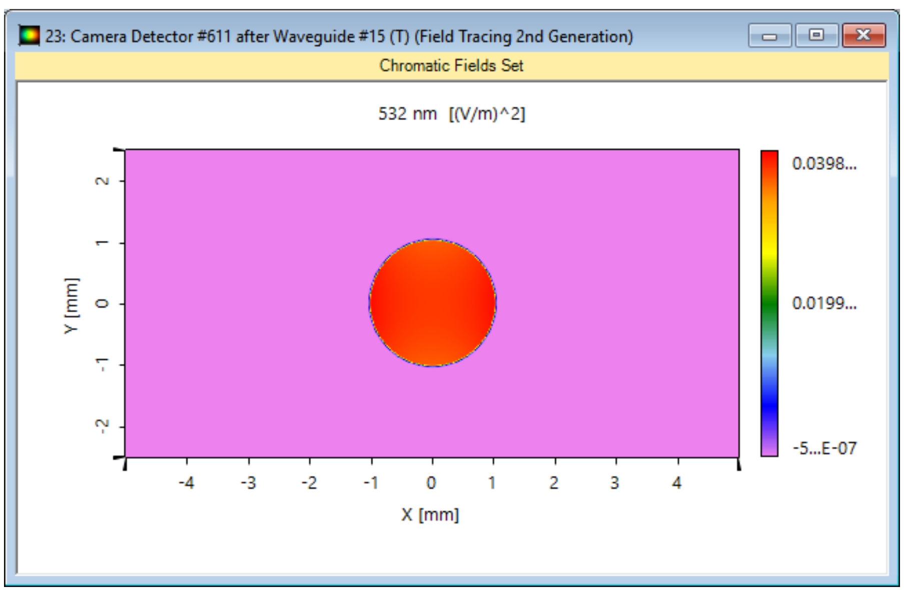

Highlights

tailored light guiding within a waveguide using surface gratings

Region	Channel	Order	Efficiency
input	forward	T0	20 %
output	forward	T0	20 %

individual specification option for simulated diffraction order for each region

intensity pattern (inverse rainbow colors) with modulation due to polarization effects from lens surfaces

Result II: Plus +1st Non-Reflected Orders

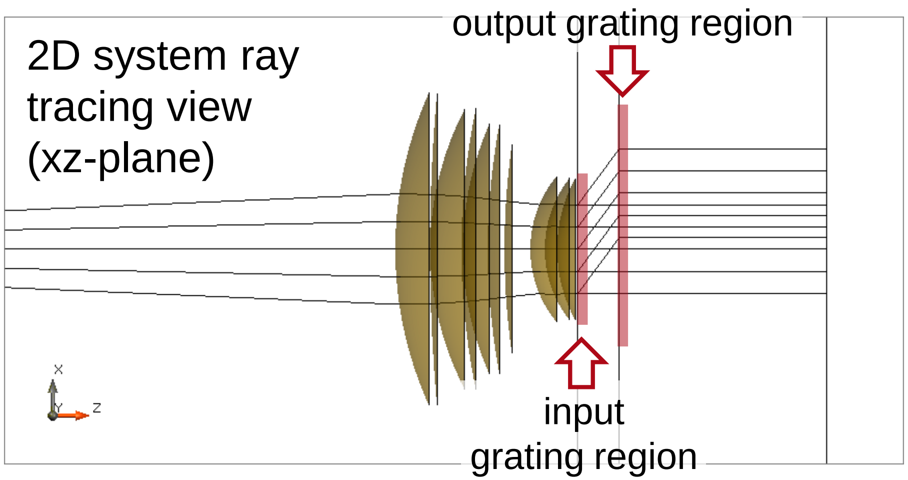

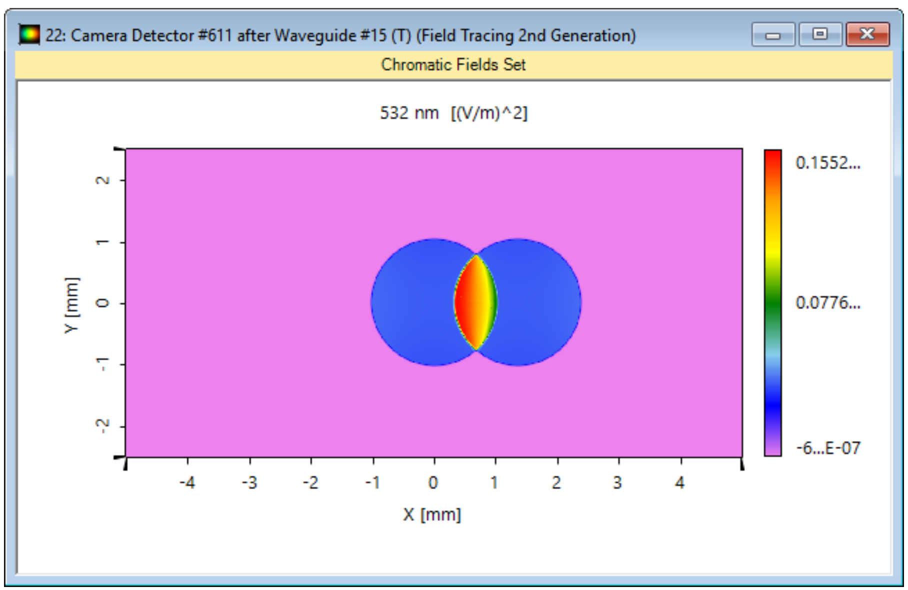

Highlights

tailored light guiding within a waveguide using surface gratings

Region	Channel	Order	Efficiency
input	forward	T0	20 %
input	forward	T+1	20 %
output	forward	T0	20 %
output	forward	T-1	20 %

intensity pattern (inverse rainbow colors)
different order modes are summed coherently

Result III: Plus Back Reflections

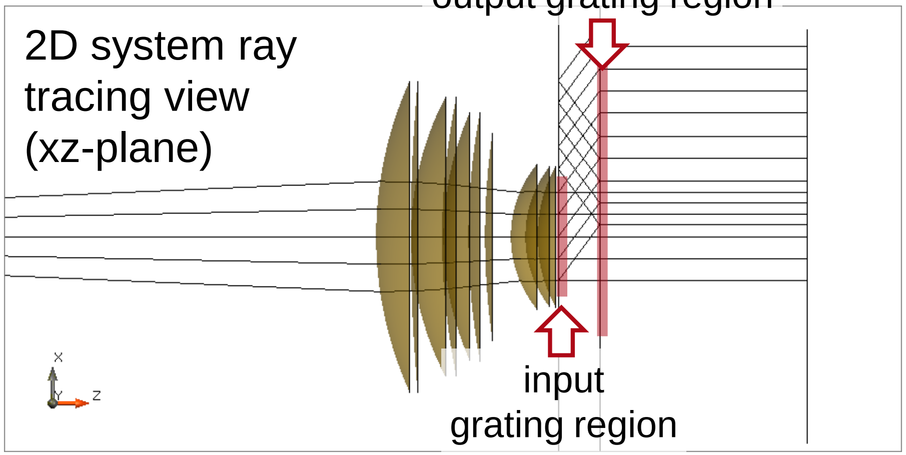

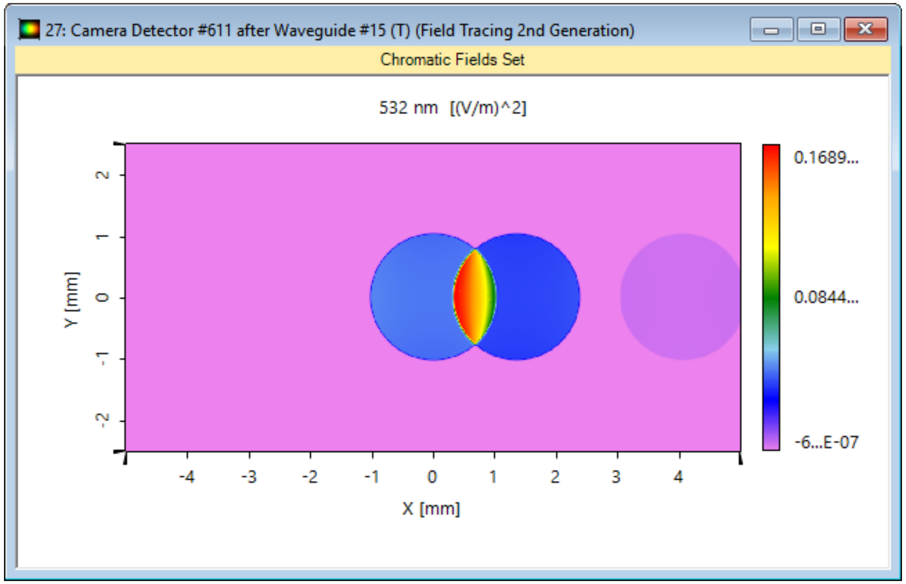

Highlights

tailored light guiding within a waveguide using surface gratings

Region	Channel	Order	Efficiency
input	forward	T0	20 %
input	forward	T+1	20 %
input	backward	R0	10 %
output	forward	T0	20 %
output	forward	R0	10 %
output	forward	T-1	20 %

intensity pattern (inverse rainbow colors) with multiple reflected light modes

Result IV: Further Multi-Reflected Orders

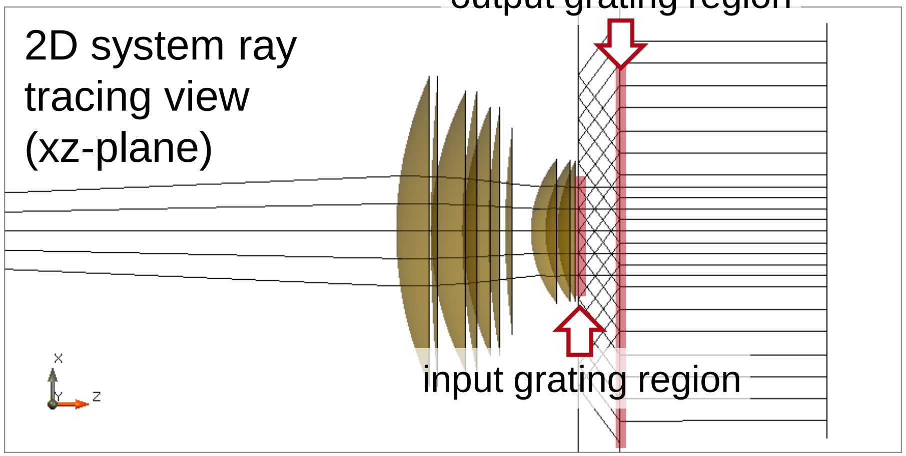

Highlights

tailored light guiding within a waveguide using surface gratings

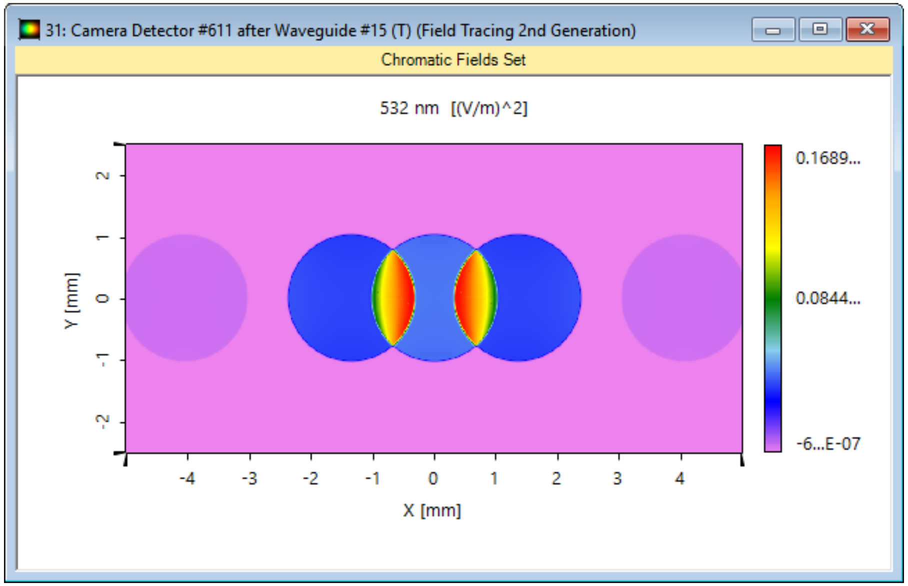

Region	Channel	Order	Efficiency
input	forward	T0	20%
input	forward	T+1	20%
input	forward	T-1	20%
input	backward	R0	10%
output	forward	T0	20%
output	forward	R0	10%
output	forward	T+1	20%
output	forward	T-1	20%

intensity pattern (inverse rainbow colors) with further multiple reflected light modes

Exit Pupil Expansion

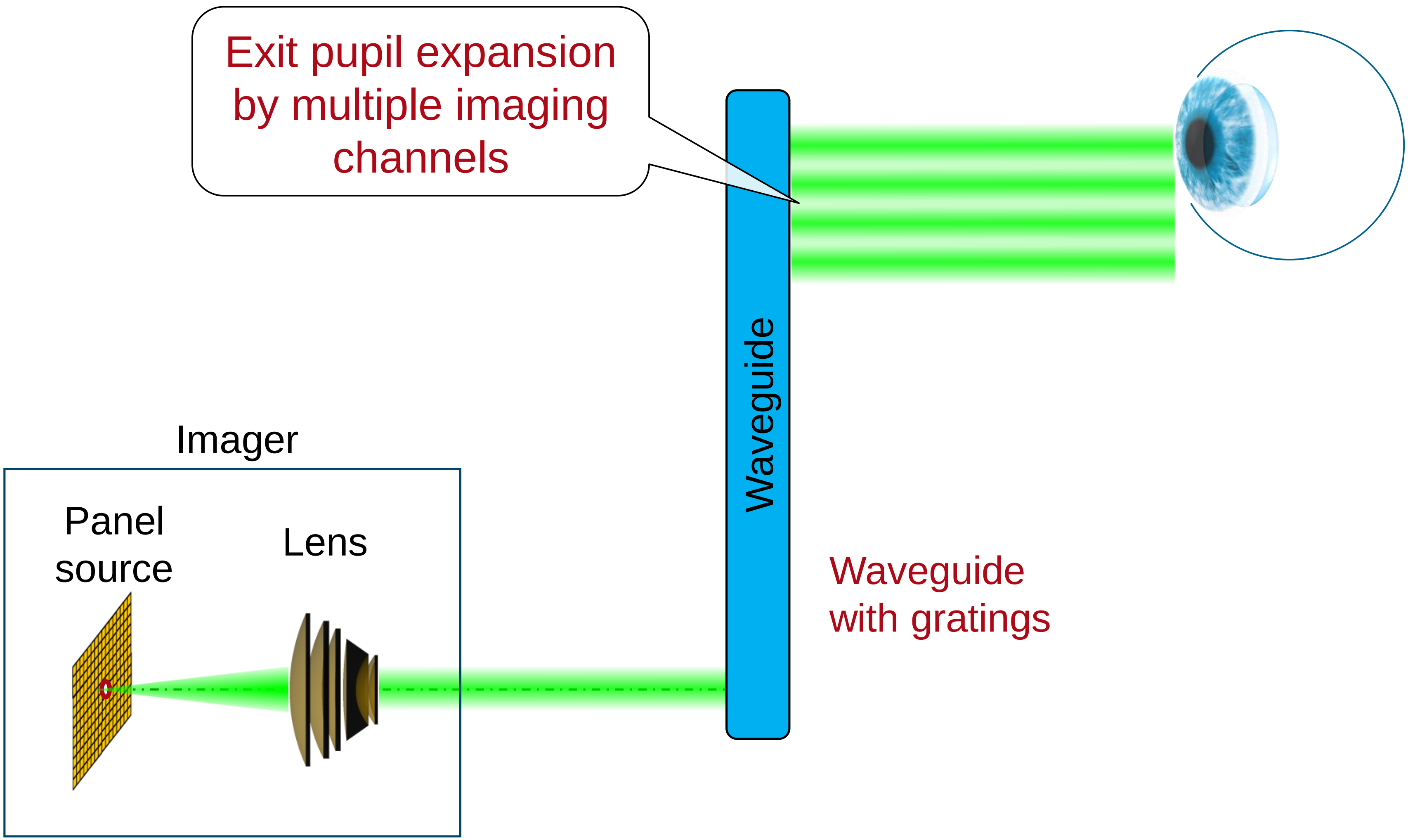

Exit Pupil Expansion

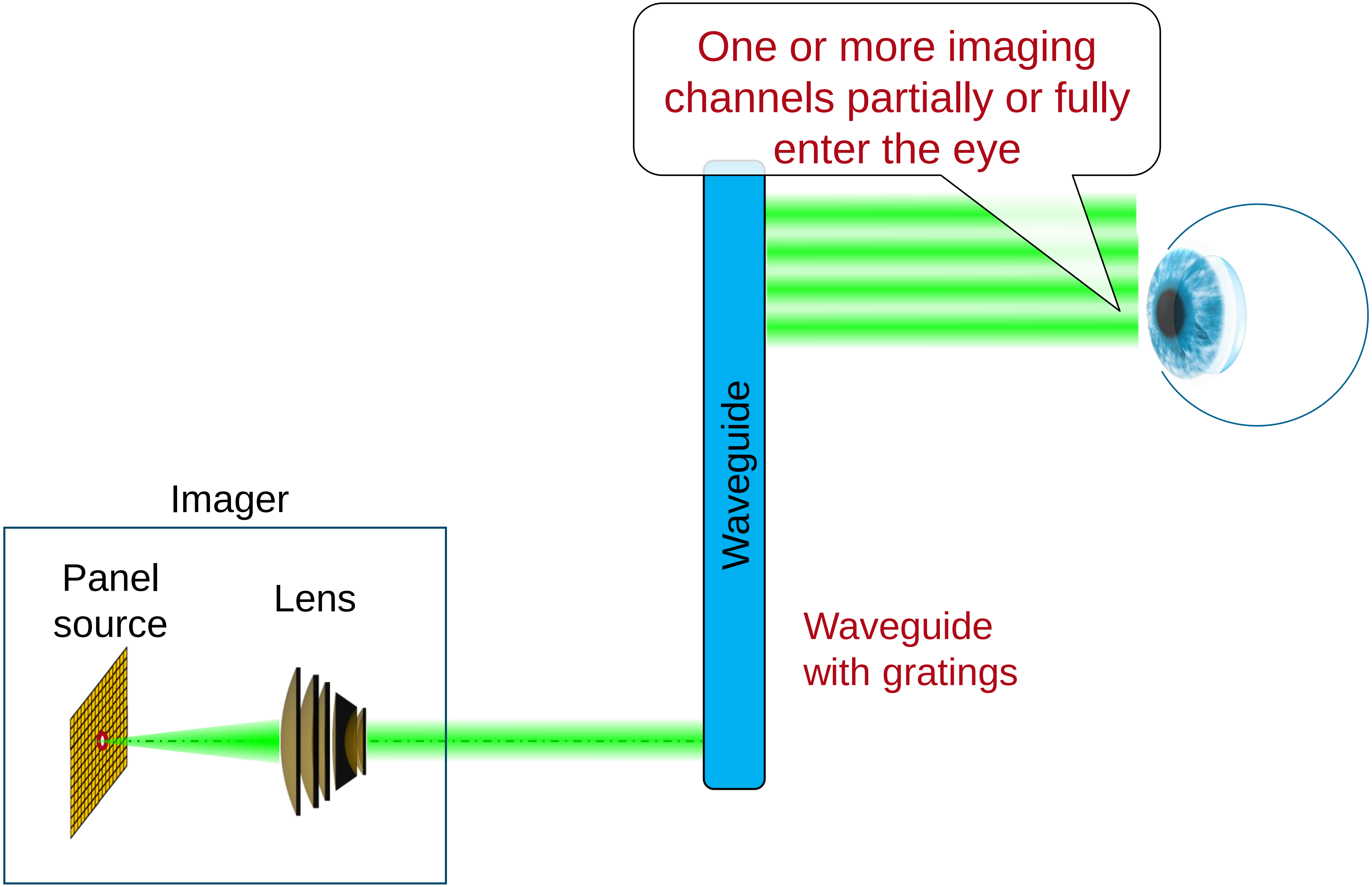

2D Exit Pupil Expansion (Levola)

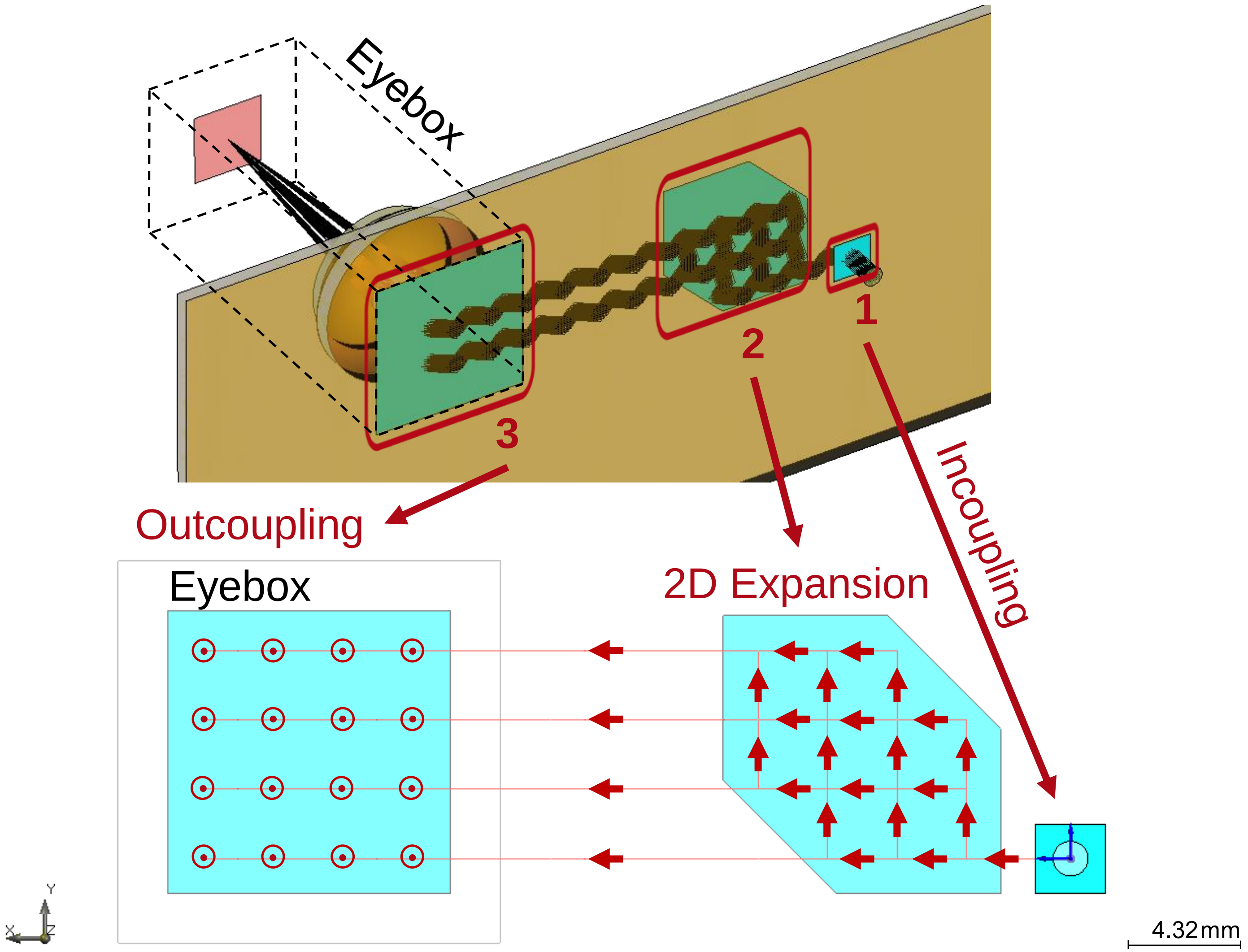

Challenges in Modeling of VR/MR

- PSF/MTF calculation for partially filled exit pupils
- Non-sequential modeling of imaging channels
- Imaging channels with gratings
  - Non-sequential lightpath analysis including polarization dependent evaluation of grating effects
  - Inclusion of higher orders and straylight
- Multichannel imaging system
  - Evaluation of channel distribution in eyebox

Modulated Grating Regions

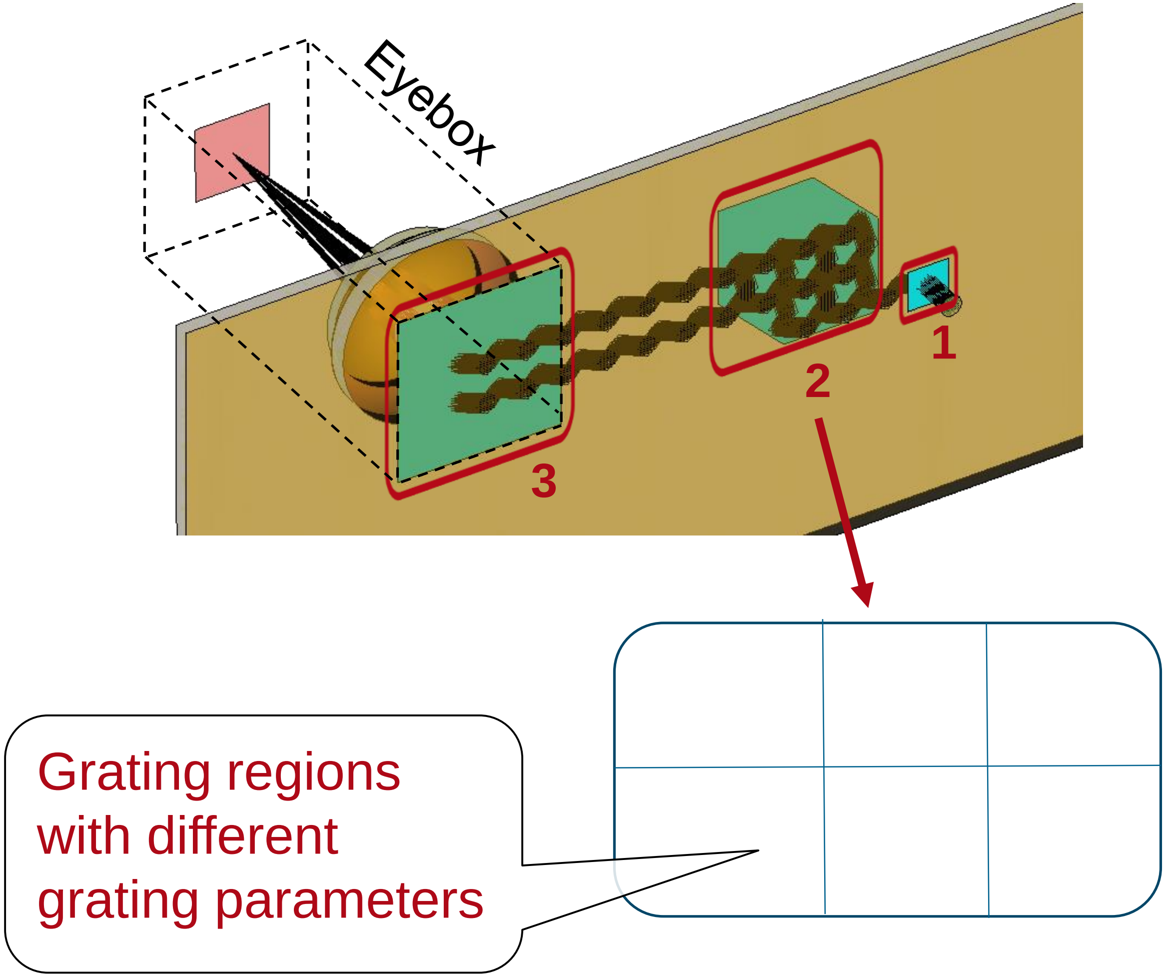

Aperture Effects at Region Boundaries

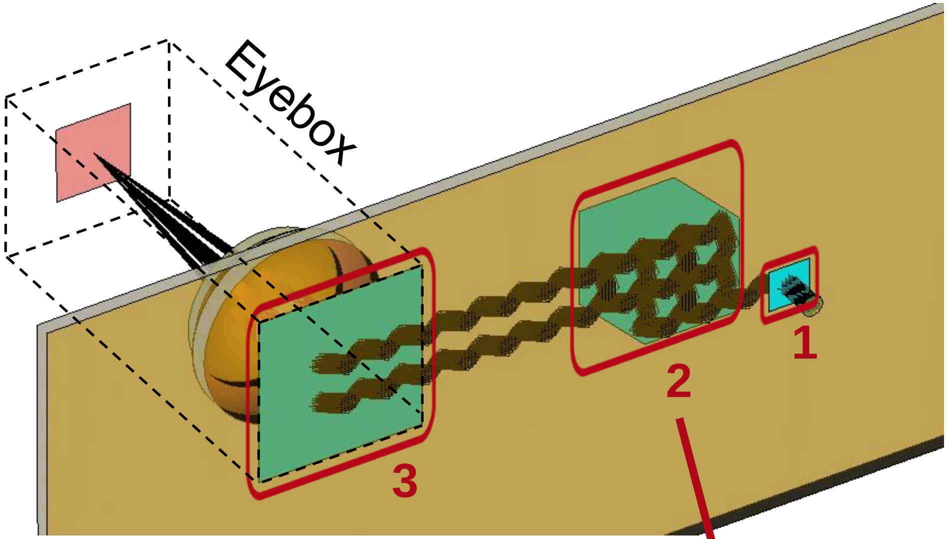

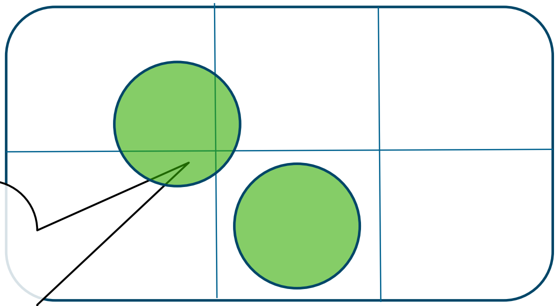

Fields do not necessarily hit one region only but can be split at region boundaries.

Challenges in Modeling of VR/MR

- PSF/MTF calculation for partially filled exit pupils
- Non-sequential modeling of imaging channels
- Imaging channels with gratings
  - Non-sequential lightpath analysis including polarization dependent evaluation of grating effects
  - Inclusion of higher orders and straylight
- Multichannel imaging system
  - Evaluation of channel distribution in eyebox
  - Multiple aperture effects along lightpath of each channel

Multiple Channels in Eye Pupil

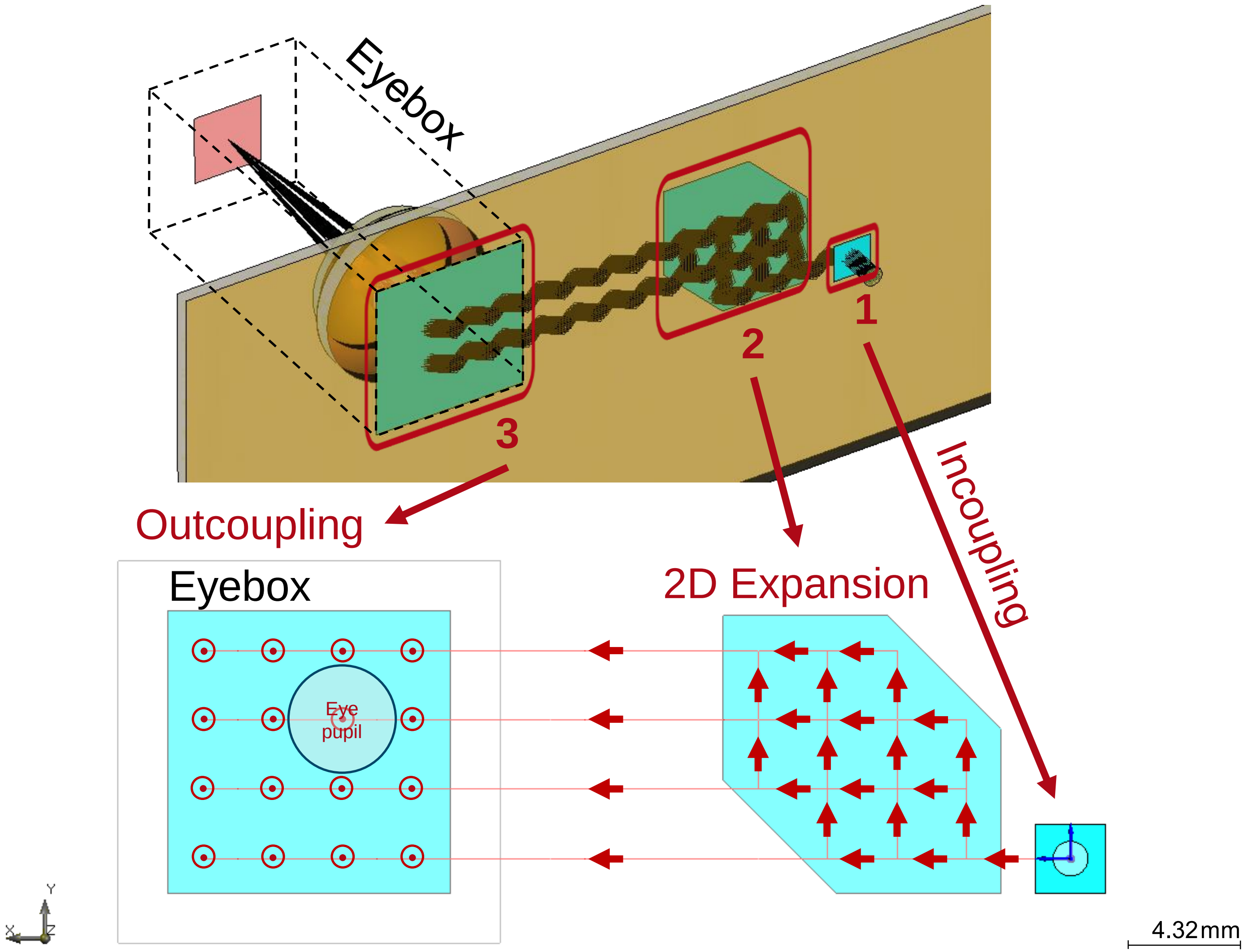

Multiple Channels in Eye Pupil

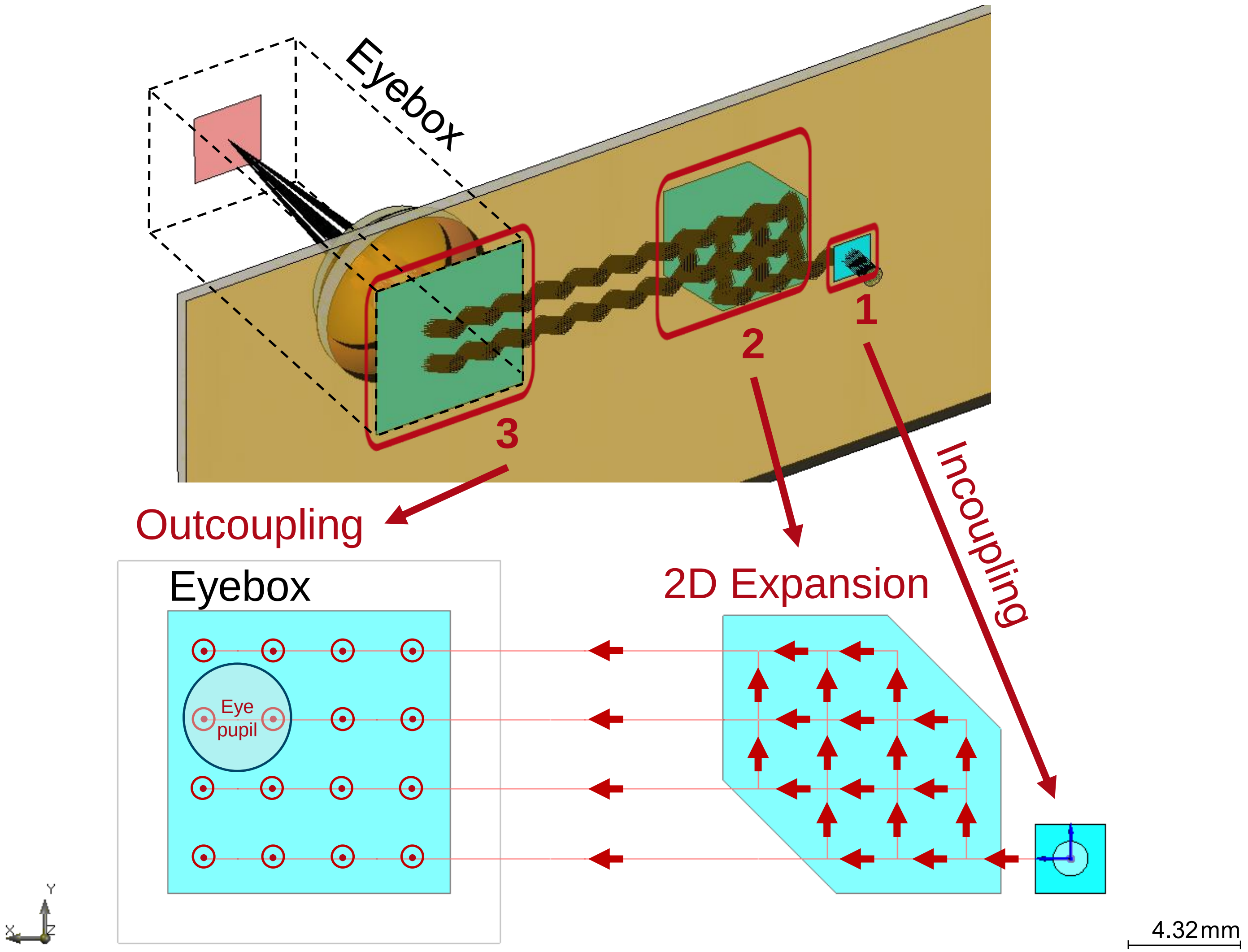

Multiple Channels in Eye Pupil

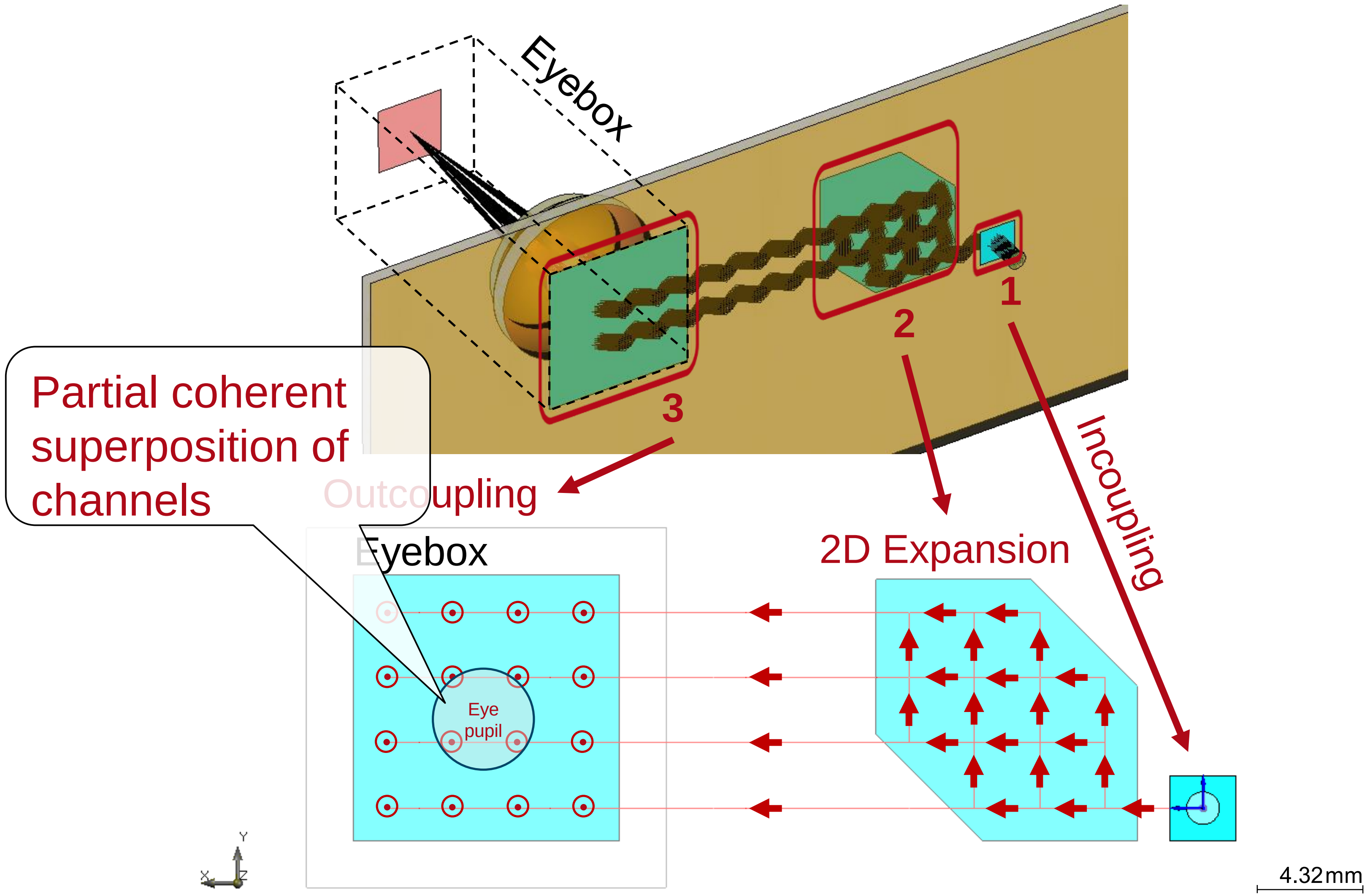

Results: 3D System Ray Tracing

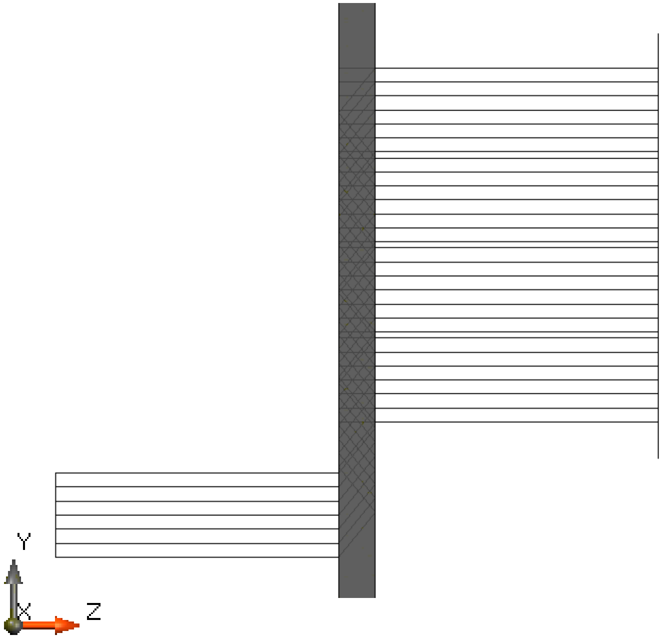

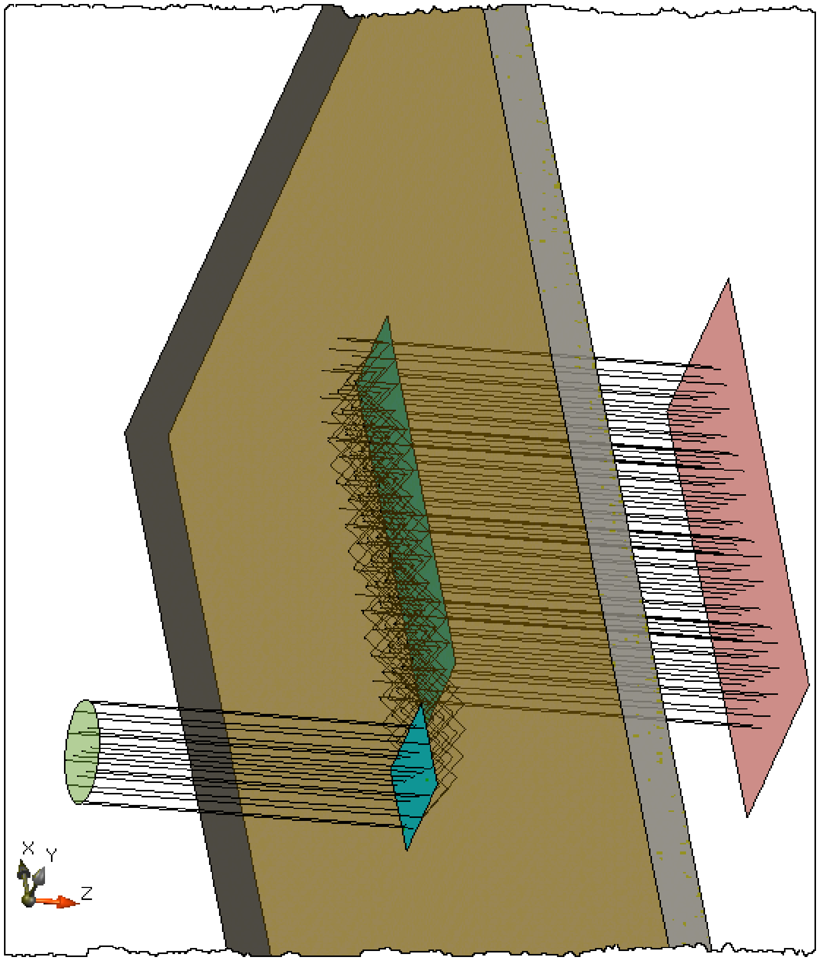

Results: One Outcoupling Grating

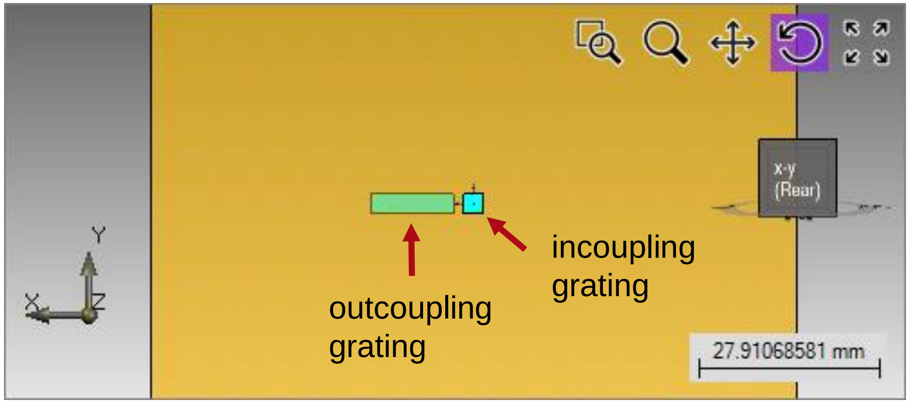

intensity pattern (false color view)

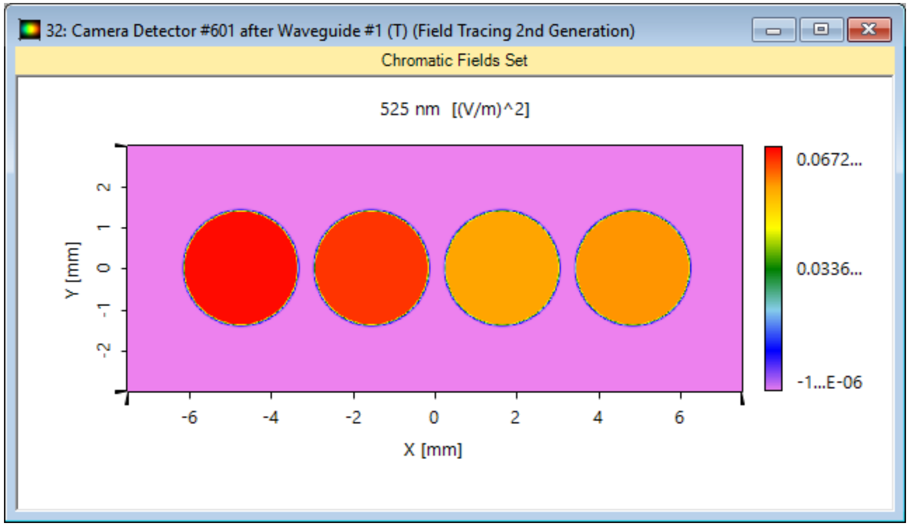

Highlights

- waveguide simulations including rigorously calculated efficiencies of sub-wavelength grating structures

Grating Parameter	Value & Unit
type	sawtooth grating
period	395 nm
height	140 nm

Results: Four Optimized Outcoupling Gratings

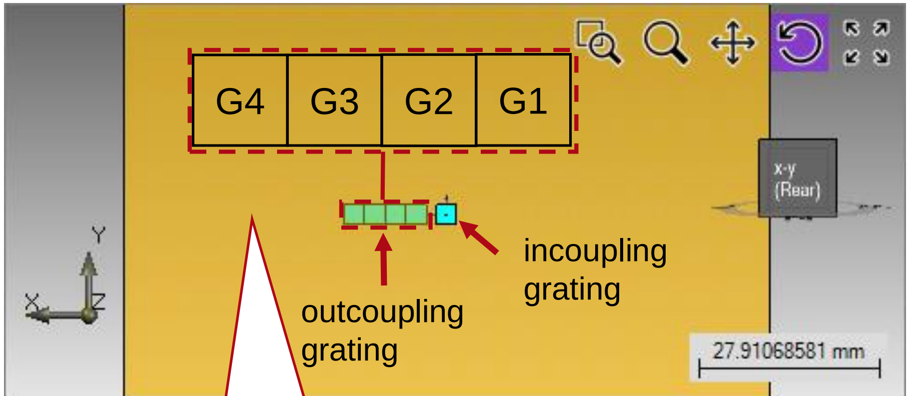

segmentation of outcoupling grating

different grating depths of each segment for optimized efficiencies

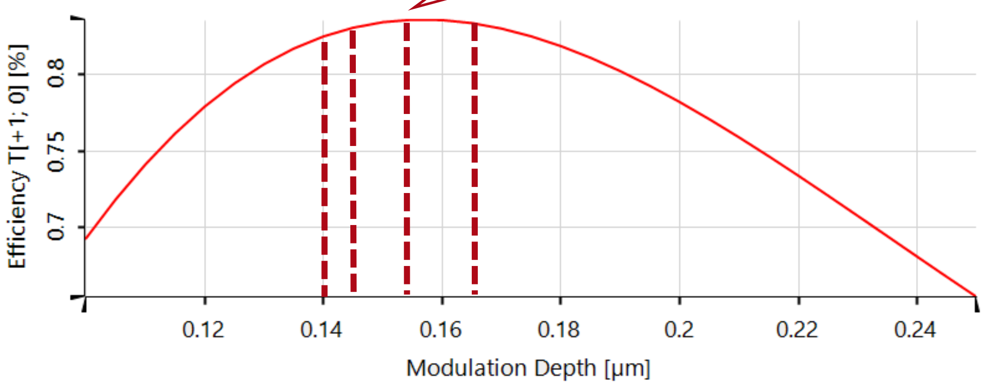

Highlights

- waveguide simulations including rigorously calculated efficiencies of sub-wavelength grating structures
- specification & optimization of multiple grating regions for tailored output generation

Grating Parameter	Value & Unit
type	sawtooth grating
period	395 nm
depth G1	140 nm
depth G2	145 nm
depth G3	155 nm
depth G4	165 nm

Results: Optimized Output Uniformity

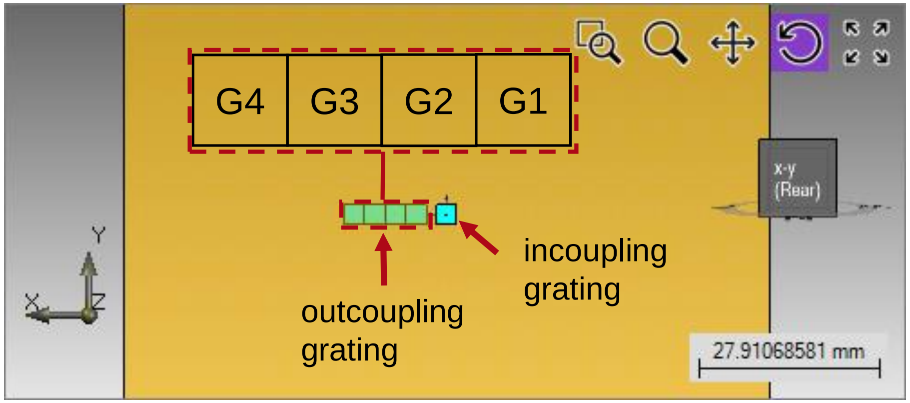

intensity pattern (false color view)

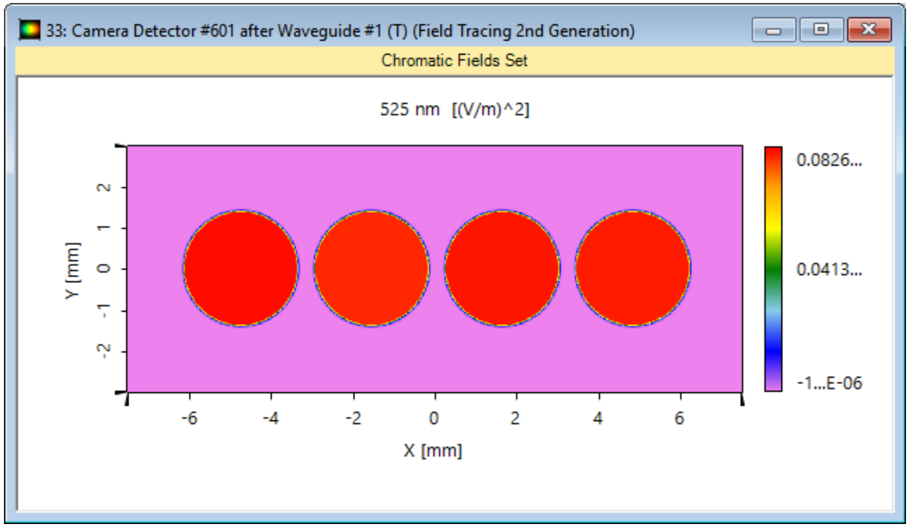

Highlights

- waveguide simulations including rigorously calculated efficiencies of sub-wavelength grating structures
- specification & optimization of multiple grating regions for tailored output generation

Grating Parameter	Value & Unit
type	sawtooth grating
period	395nm
depth G1	140nm
depth G2	145nm
depth G3	155 nm
depth G4	165 nm

Challenges in Modeling of VR/MR

- PSF/MTF calculation for partially filled exit pupils
- Non-sequential modeling of imaging channels
- Imaging channels with gratings
  - Non-sequential lightpath analysis including polarization dependent evaluation of grating effects
  - Inclusion of higher orders and straylight
- Multichannel imaging system
  - Evaluation of channel distribution in eyebox
  - Multiple aperture effects along lightpath of each channel
  - Partially coherent superposition of channels for PSF/MTF calculation

Multiple Channels in Eye Pupil

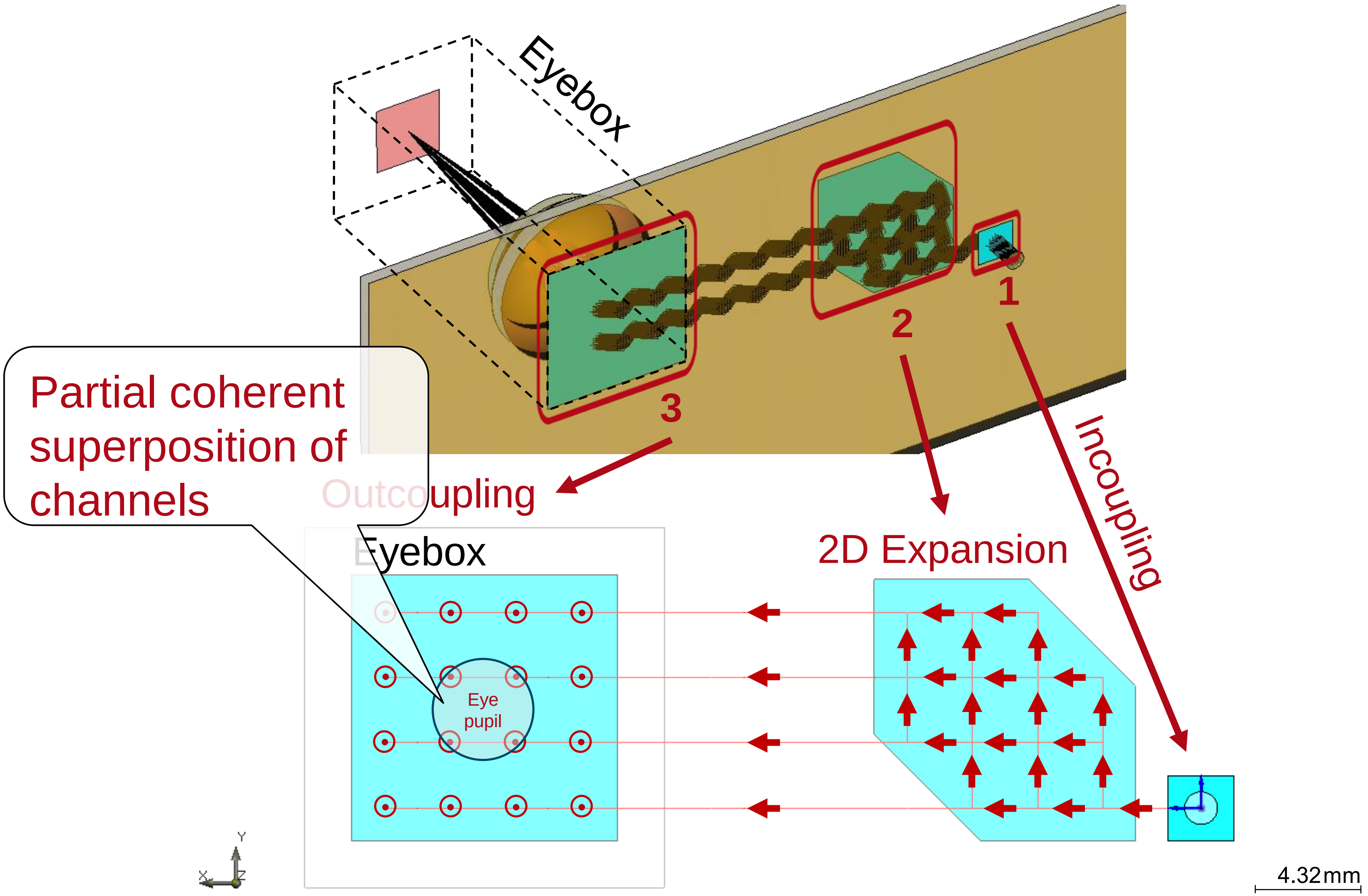

3D Ray Tracing Analyzer

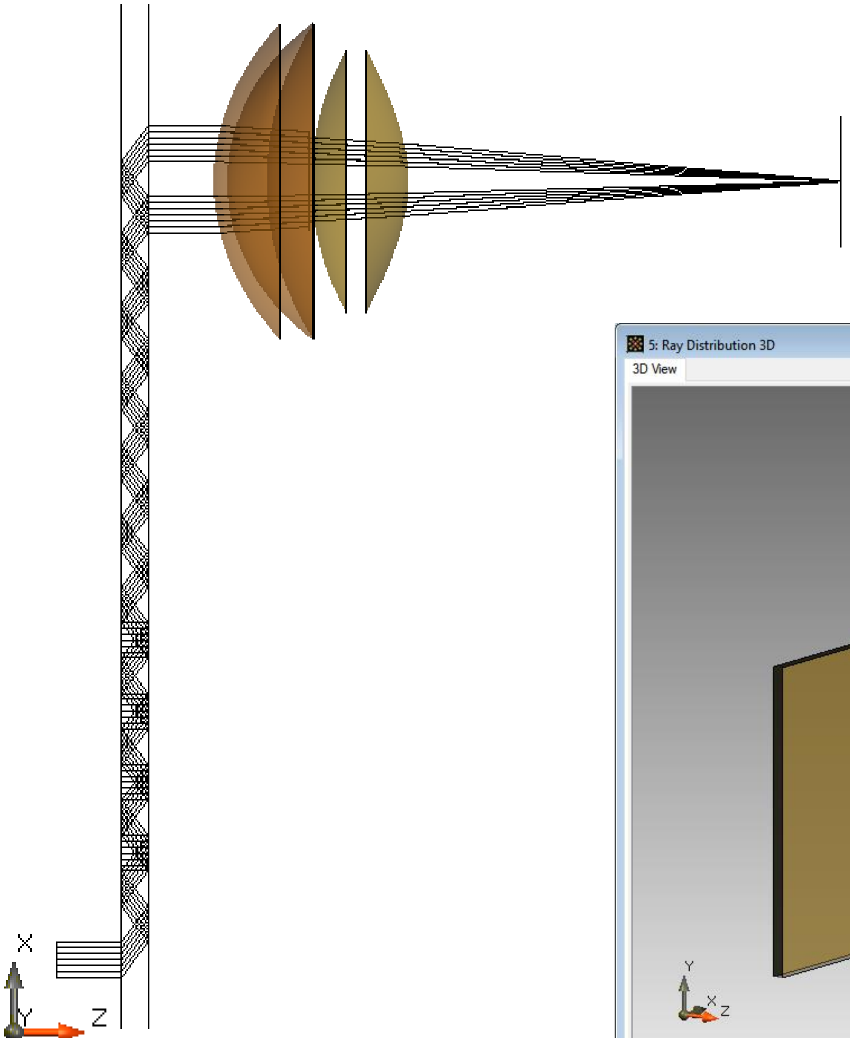

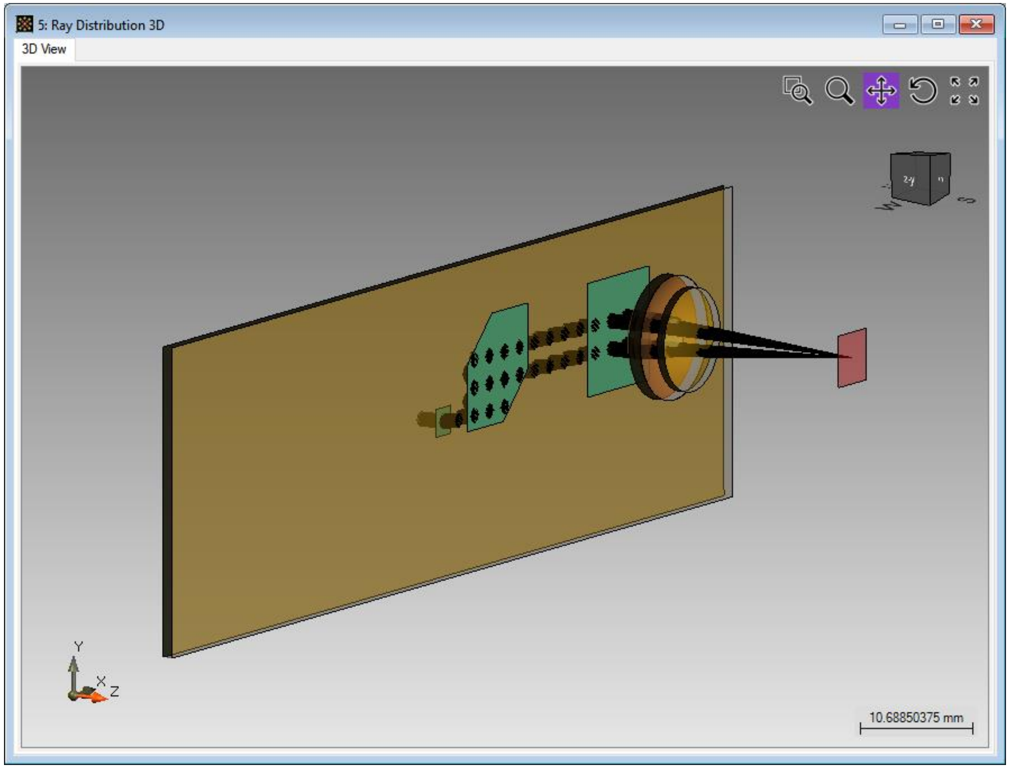

Result: Spots & Intensity at Pupil

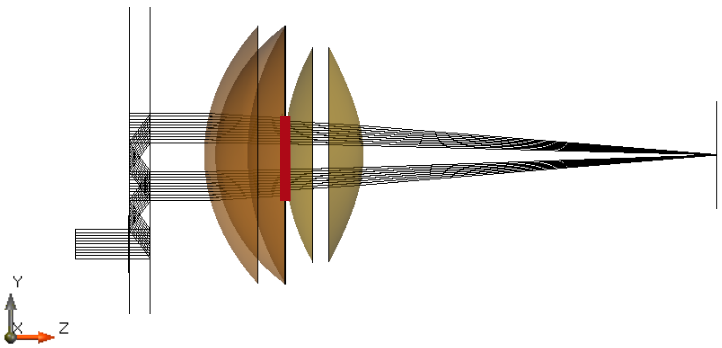

Highlights

- non-sequential ray and field tracing analysis of waveguide optics
- definition of arbitrary in- and outcoupling regions at the waveguide containing ideal or real grating surfaces

ray tracing spot diagram

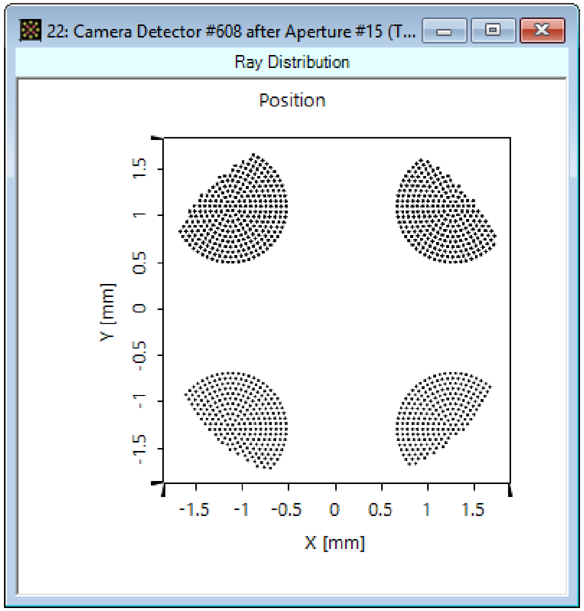

intensity
(real color view)

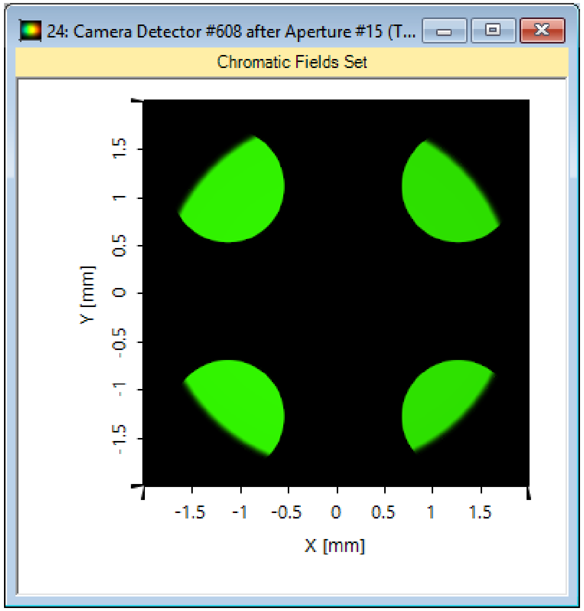

Result: PSF at Retina

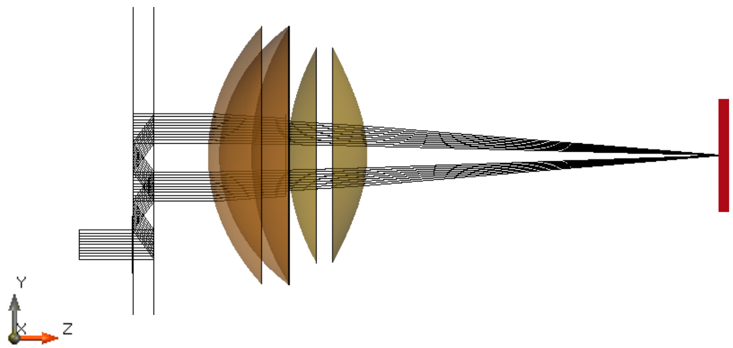

Highlights

- non-sequential ray and field tracing analysis of waveguide optics including **coherence**, polarization and energy effects
- calculation of **PSF** and MTF of arbitrary shaped and illuminated apertures

PSF coherent

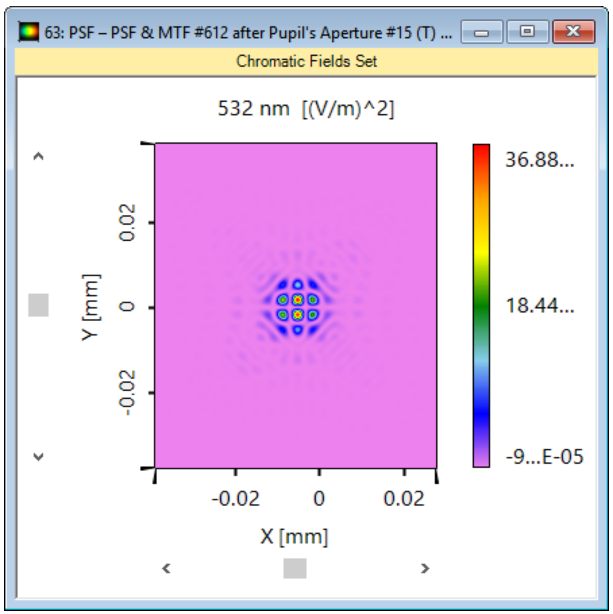

PSF incoherent

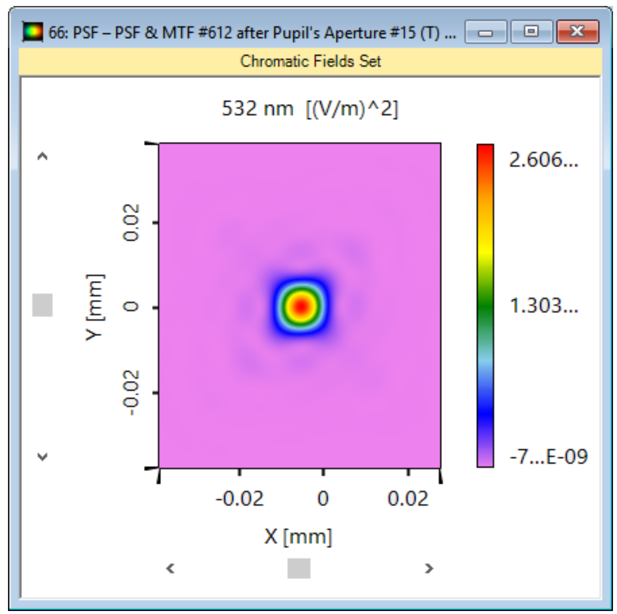

Result: MTF at Retina

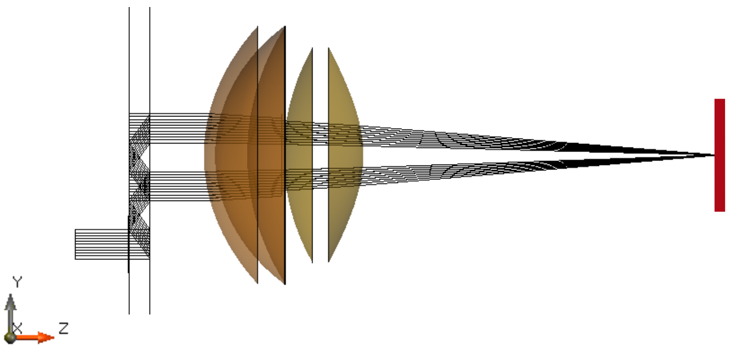

Highlights

- non-sequential ray and field tracing analysis of waveguide optics including coherence, polarization and energy effects
- calculation of PSF and MTF of arbitrary shaped and illuminated apertures

MTF coherent

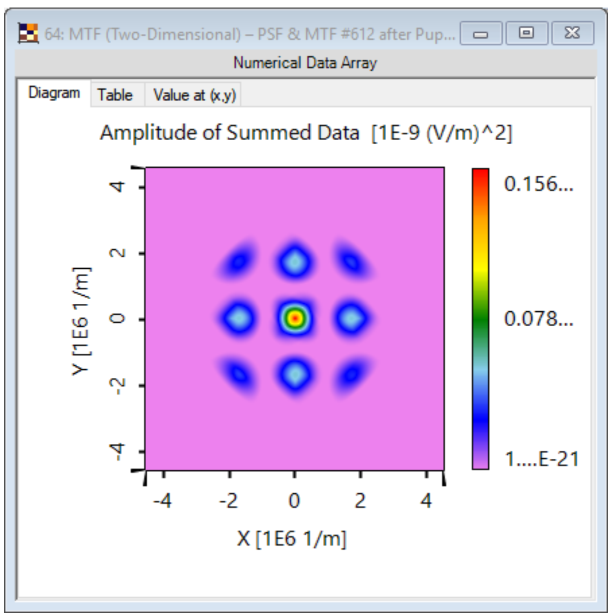

MTF incoherent

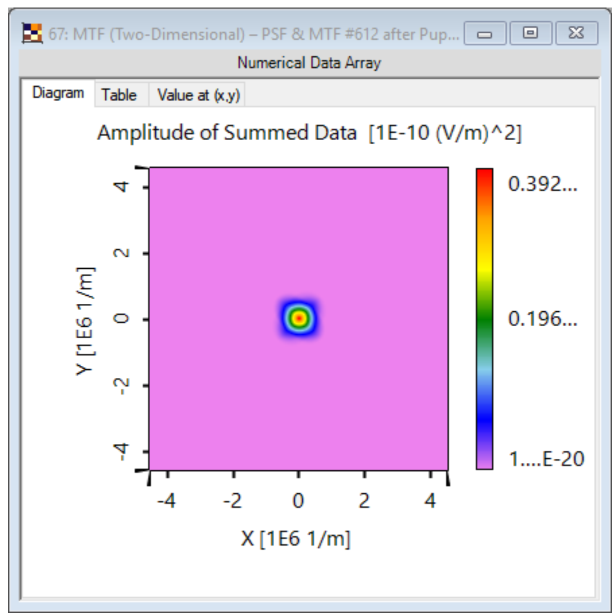

Result: MTF at Retina

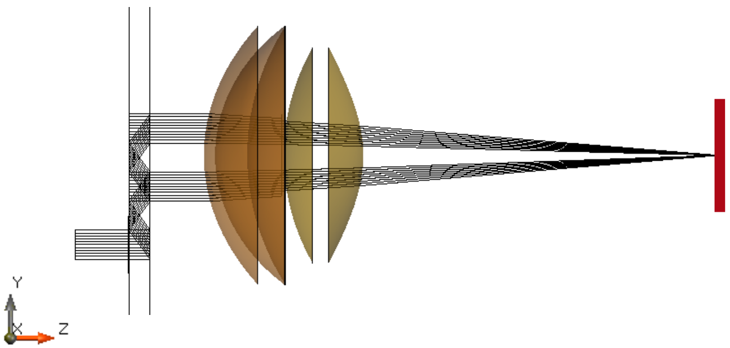

Highlights

- non-sequential ray and field tracing analysis of waveguide optics including coherence, polarization and energy effects
- calculation of PSF and MTF of arbitrary shaped and illuminated apertures

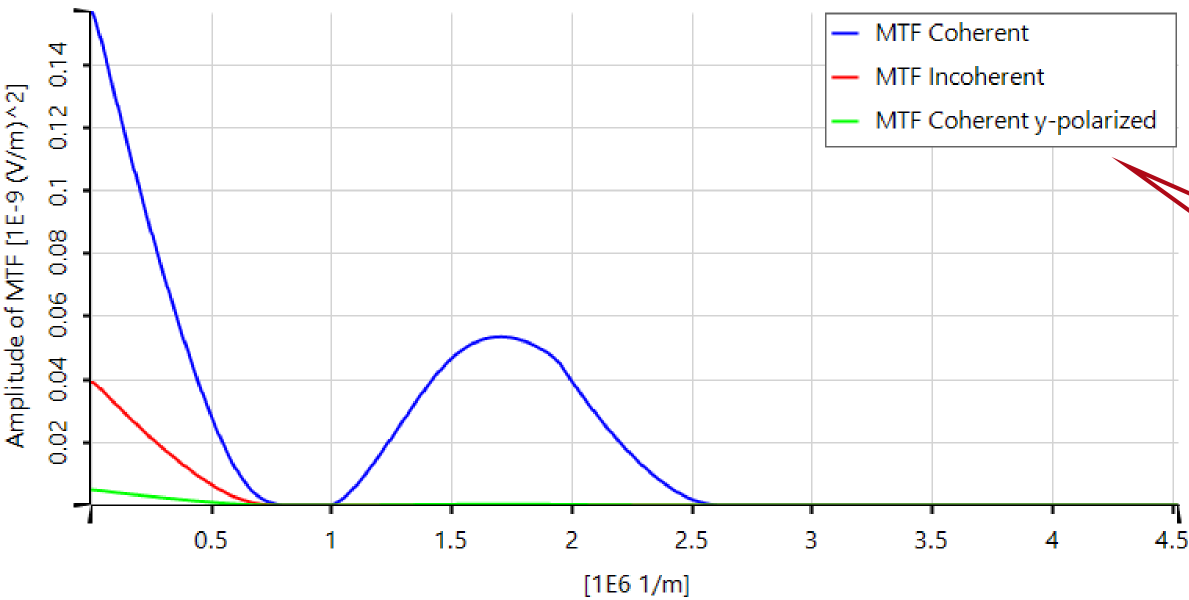

MTF strongly dependent on coherence and polarization effects

Waveguide Stack

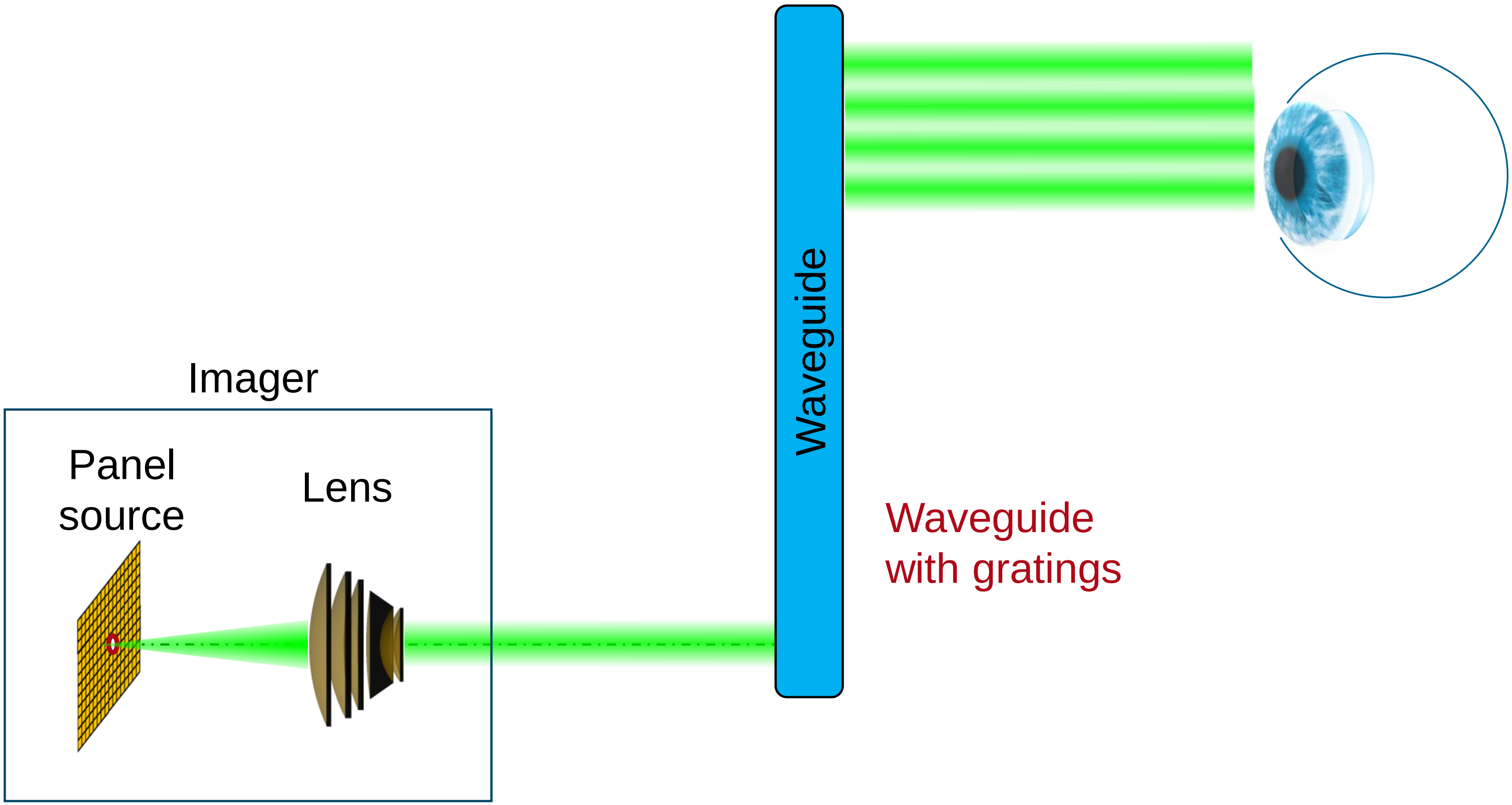

Waveguide Stack

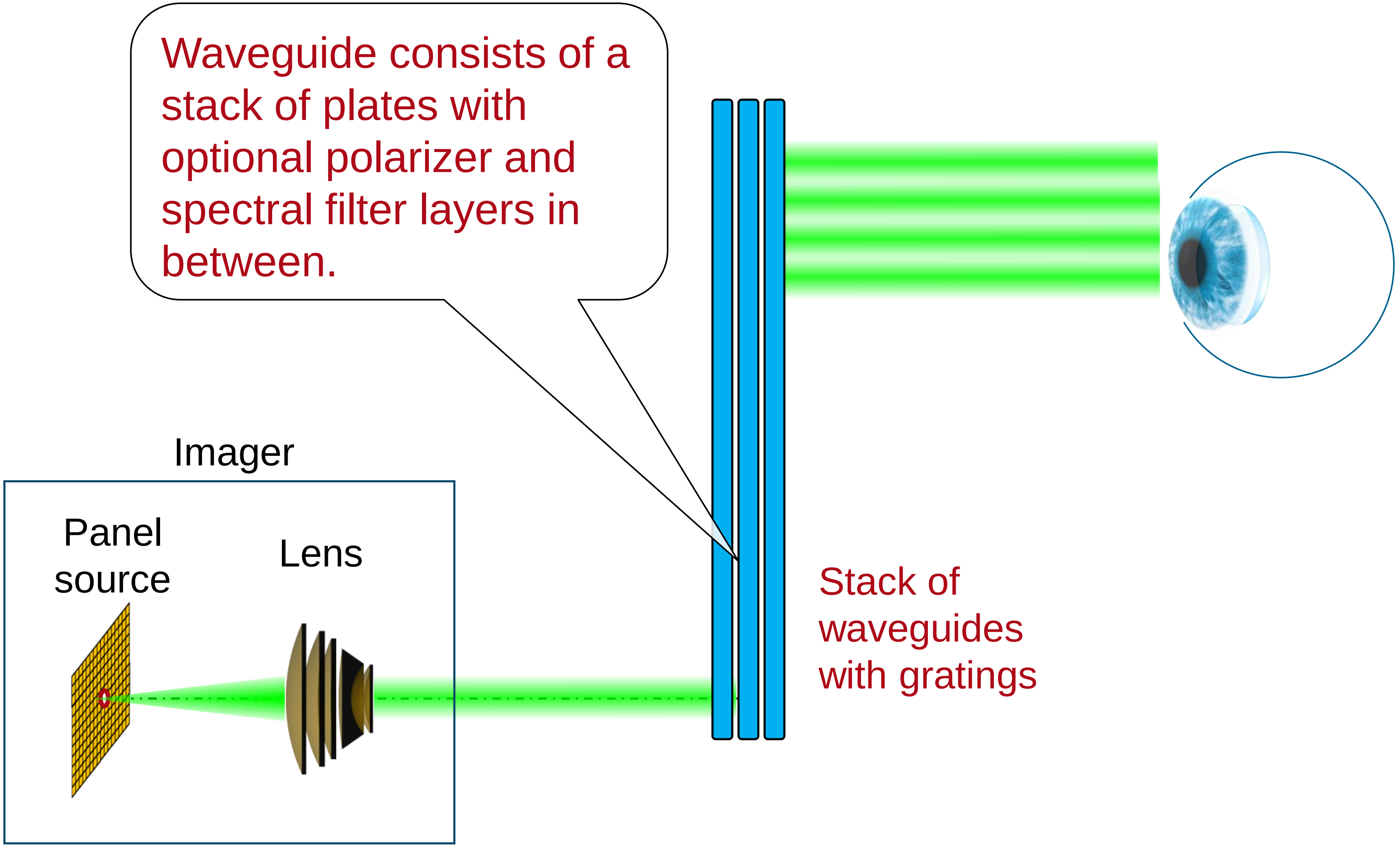

Challenges in Modeling of VR/MR

- PSF/MTF calculation for partially filled exit pupils
- Non-sequential modeling of imaging channels
- Imaging channels with gratings
  - Non-sequential lightpath analysis including polarization dependent evaluation of grating effects
  - Inclusion of higher orders and straylight
- Multichannel imaging system
  - Evaluation of channel distribution in eyebox
  - Multiple aperture effects along lightpath of each channel
  - Partially coherent superposition of channels for PSF/MTF calculation
- Multilayer stack with spectral filter and polarization layers

Challenges in Modeling of VR/MR

- PSF/MTF calculation for partially filled exit pupils
- Non-sequential modeling of imaging channels
- Imaging channels with gratings
  - Non-sequential lightpath analysis including polarization dependent evaluation of grating effects
  - Inclusion of higher orders and straylight
- Multichannel imaging system
  - Evaluation of channel distribution in eyebox
  - Multiple aperture effects along lightpath of each channel
  - Partially coherent superposition of channels for PSF/MTF calculation
- Multilayer stack with spectral filter and polarization layers

→ Modeling must be based on non-sequential physical optics to provide access to all merit functions and to ensure accurate modeling results.

Challenges in Modeling of VR/MR

- PSF/MTF calculation for partially filled exit pupils
- Non-sequential modeling of imaging channels
- Imaging channels with gratings
  - Non-sequential lightpath analysis including polarization dependent evaluation of grating effects
  - Inclusion of higher orders and straylight
- Multichannel imaging system
  - Evaluation of channel distribution in eyebox
  - Multiple aperture effects along lightpath of each channel
  - Partially coherent superposition of channels for PSF/MTF calculation
- Multilayer stack with spectral filter and polarization layers

→ The non-sequential physical optics modeling must be **fast** to enable practical work.

Efficiency Calculation in Optical Systems

Abstract

- In modern optical system design it is always important to evaluate the efficiency of the system.
- If the efficiency in the detector signals is significantly smaller than 100% it is also important for the optical engineer to understand where the rest of the light is going to.
- VirtualLab allow the automatic evaluation of the efficiency of an optical system.

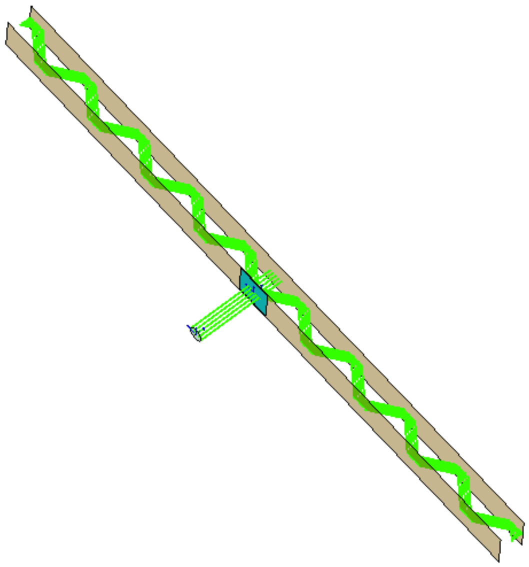

Modeling Task: Waveguiding without Outcoupling

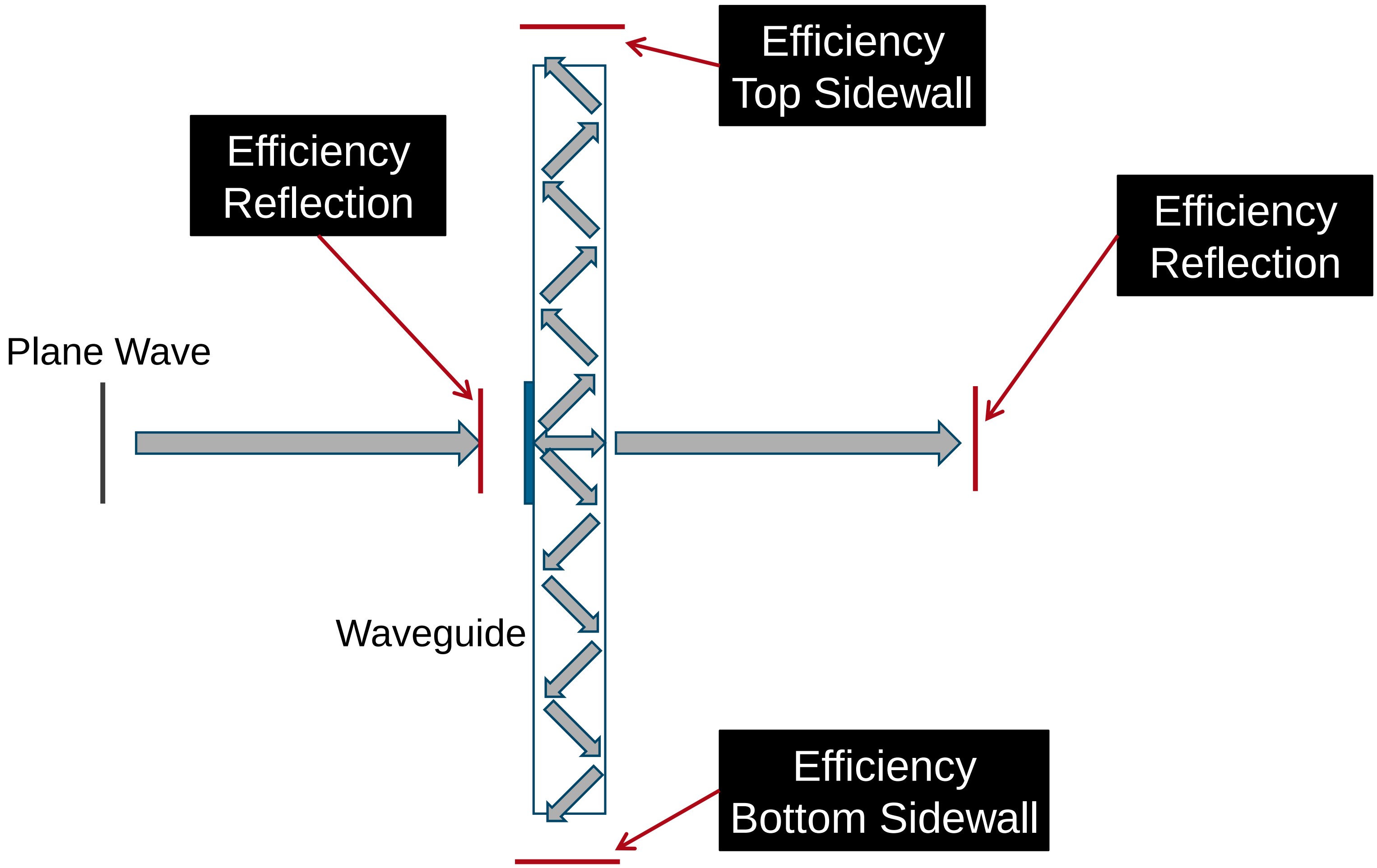

Simulation Results

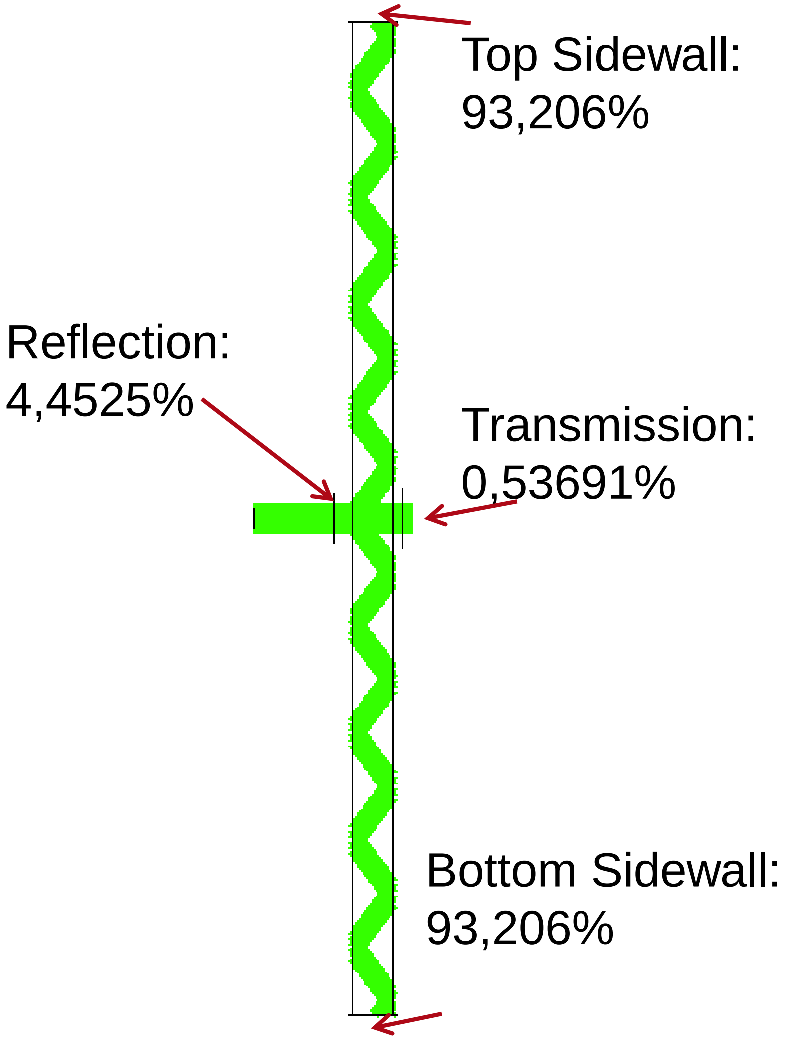

Detector	Efficiency
Transmission	0,53691%
Reflection	4,4525%
Top Sidewall	93,206%
Bottom Sidewall	1,7849%
Total	**99,981%**

Efficiency is calculated by building the ratio between the source flux and the flux at the detector.

Summation of all detector signal gives the efficiency of the complete system.

Some Info

- Webpages:
  - Applied Computational Optics Group (http://www.applied-computational-optics.org)
  - Wyrowski Photonics UG (www.wyrowski-photonics.com).
  - LightTrans (http://www.lighttrans.com/)

- Check the description box for instructions on how to get your trial version!